CHEMICAL & PHARMACEUTICAL BULLETIN

Vol. 35, No. 12 December 1987

Regular Articles

[Chem. Pharm. Bull. 35(12)4687—4694(1987)]

Adsorption of Cetylpyridinium and Cetyltrimethylammonium Ions on Hydroxyapatite and Concurrent Release of Phosphate and Calcium Ions from the Surface of Hydroxyapatite

SABURO SHIMABAYASHI,*[1] HIDEJI TANAKA, and MASAYUKI NAKAGAKI

Faculty of Pharmaceutical Sciences, Kyoto University, Yoshida-Shimoadachi-cho, Sakyo-ku, Kyoto 606, Japan

(Received April 27, 1987)

Concentrations of phosphate ion ($[Pi]_f$) and calcium ion ($[Ca^{2+}]_f$), liberated from the surface of synthetic hydroxyapatite ($Ca_{10}(PO_4)_6(OH)_2$; HAP) during the adsorption of cetylpyridinium ion (CP^+) or cetyltrimethylammonium ion (CTA^+), were determined as a function of the equilibrium concentrations of these surface active ions ($[CP^+]_f$ or $[CTA^+]_f$). A part of CP^+ or CTA^+ was adsorbed by ion-exchange with calcium ion (Ca^{2+}) on the surface of HAP, and the rest was adsorbed together with its counterion (Cl^- or Br^-). In the region below the critical micelle concentration (cmc), $[Ca^{2+}]_f$ increased with an increase in the adsorbed amount of the surface active ion. On the other hand, $[Pi]_f$ decreased with an increase in $[Ca^{2+}]_f$ to keep the solubility product of HAP (K_{sp}) constant. However, in the region above the cmc, $[Pi]_f$ increased with $[CP^+]_f$ or $[CTA^+]_f$ through the binding of phosphate ion (Pi) to the cationic micelles. The electroneutrality on the surface phase of HAP, the solubility product of HAP in the solution phase, and the counterion binding by micelles determined the relationship between $[Pi]_f$ and $[Ca^{2+}]_f$. The species of counterion of the surfactant (Cl^- or Br^-) affected the adsorbing and releasing behaviors: the release of Ca^{2+} due to the adsorption of CP^+ and the release of Pi through its binding to CP^+–micelles are more pronounced with cetylpyridinium chloride than with cetylpyridinium bromide. This result can be explained in terms of the affinity of the halide ion for CP^+ in the micellar and adsorbed phases ($Br^- > Cl^-$).

Keywords——hydroxyapatite; cetylpyridinium ion; cetyltrimethylammonium ion; adsorption; phosphate ion release; calcium ion release; ion-exchange; micelle; solubility product; counterion

Introduction

Hydroxyapatite ($Ca_{10}(PO_4)_6(OH)_2$; HAP) is a major inorganic constituent of mammalian hard tissues (teeth and bones) and a major or minor component of renal calculi. In the previous investigations,[2-4] the influence of surface active ions (dodecyl sulfate and dodecylammonium ions) on the surface properties of HAP was studied. It was found that calcium ion (Ca^{2+}) and/or phosphate ion (Pi) were released from the surface of HAP during the adsorption of the surface active ions. The ratio of these constituent ions released was nonstoichiometric (*i.e.*, $Ca^{2+}/Pi \neq 10/6$), and depended on various factors, such as the adsorbed amount and the concentration of the surface active ion, and the solubility product

(K_{sp}) for HAP. The releasing tendencies of Ca^{2+} and Pi were found to be mutually interchanged when the sign of the electric charge of the surface active ion was reversed.

However, as regards the competitive adsorption between Ca^{2+} and dodecylammonium ion (DA^+), the addition of the former caused a slight decrease of the adsorbed amount of the latter.[4] This fact is in contrast to the case of cetylpyridinium ion (CP^+).[5] That is, the adsorbed amount of CP^+ was greatly decreased by the added Ca^{2+} and the preferential adsorption of Ca^{2+} occurred. Roseman *et al.* found, in their kinetic study on the dissolution of HAP in the presence of cationic surfactant, that DA^+ was adsorbed more strongly than CP^+ on HAP.[6] The hemimicelle formation of DA^+ at the surface of HAP may be responsible for the high affinity of DA^+ to HAP.[7]

In the present work, the influence of CP^+ and cetyltrimethylammonium ion (CTA^+) on the surface properties of HAP was studied in order to obtain a clearer view of the influence of surface active cations. The amounts of Ca^{2+} and Pi liberated from the surface of HAP at a constant mixing ratio of HAP to the solution were determined as a function of the concentrations of these surface active ions in order to examine the relationships among them. Furthermore, the effect of the counterion (Cl^- and Br^-) on them was studied by comparing the results for cetylpyridinium chloride (CPC) with those for cetylpyridinium bromide (CPB).

Experimental

Materials——HAP was the same sample as that used in the previous studies.[2-4] CPC, CPB, and cetyltrimethylammonium chloride (CTAC), purchased from Tokyo Chemical Industry Co., Ltd., were of extra pure reagent grade. They were recrystallized twice from acetone for CPC and CPB, or from ethanol–acetone mixture (1 : 14) for CTAC.

Methods——HAP was suspended in a solution of a surfactant (CPC, CPB, or CTAC) of known concentration at 30 °C, and the suspension was shaken vigorously at frequent intervals. No buffer solutions were used in order to avoid the effects of buffering agents on the properties of the HAP surface and cationic micelles. After at least 14 d, which was sufficient to attain adsorption and dissolution equilibria, the suspension was filtered through a Millipore filter with a pore size of 0.1 μm, and the filtrate was used for chemical analysis. Prior to the filtration, the optical density of the suspension at 850 nm (OD_{850}) in the upper part of the test tube was measured on a Shimadzu model UV-180 spectrophotometer at 24 h after the last shaking. This is a convenient index of the stability of HAP suspension,[8] as a portion of the added HAP had already sedimented to the bottom and the rest remained in the aqueous phase. The higher the OD_{850}, the more stable the suspension.

The concentrations of CP^+ and CTA^+ were determined by the methylene blue diphasic titration method (Epton method) using a standard solution of sodium dodecyl sulfate (SDS).[9] The concentrations of Cl^- and Br^- were determined by the mercuric thiocyanate method.[10] Halide ion (Cl^- or Br^-) was allowed to react with mercuric thiocyanate in the presence of ferric nitrate to form mercuric chloride and thiocyanate ion. The latter product immediately combined with ferric ion to form the red ferric thiocyanate complex. Its absorbance was measured at 458 nm. It was confirmed that CP^+ and CTA^+ do not interfere with the determination. Calibration curves were obtained using aqueous solutions of NaCl and KBr. The adsorbed amounts of CP^+, CTA^+, Cl^- and Br^- were calculated from the differences of the concentrations before and after addition of HAP.

The concentration of Pi released from the surface of HAP was determined by the molybdenum blue method of Gee *et al.*[11] The phosphate ammonium molybdate complex formed was reduced with stannous chloride. The absorbance of the resulting color was measured at 720 nm after 15 min. Prior to the determination, a slight excess of SDS was added to the sample solutions in order to precipitate CP^+ or CTA^+. The precipitate was then removed with a Millipore filter (0.1 μm pore size), and the filtrate was used for the determination. A calibration curve was obtained by subjecting aqueous solutions of K_2HPO_4 to the same treatment as that for the sample solutions. The concentration of Ca^{2+} released was determined by ethylenediaminetetraacetic acid (EDTA) chelatometry with 1-(1-hydroxy-2-naphthylazo)-6-nitro-2-naphthol-4-sulfonic acid (BT indicator) at pH 10. Since CP^+ and CTA^+ interfere with the color change of the indicator, a slight excess of SDS was added to the sample solutions prior to the determination (it was not necessary to remove the precipitate). The pH of the filtrate was measured on a Toa HM-5ES pH meter.

It was confirmed that the adsorbed amounts of the surface active ion and its counterions, and the equilibrium concentrations of Pi and Ca^{2+}, were independent of the mixing order of water, adsorbate solution, and the HAP powder. A dilution experiment was carried out by adding water to the suspension after equilibria had been attained. The adsorbed amounts and the concentrations of the ions after re-equilibration were determined. These experiments showed that the adsorptions and liberations of the ions are reversible.

Henceforth, the symbol X_i represents the increment of species i at the surface of HAP, and was calculated by means of the following equation;

$$X_i = (\text{initial concentration of species i} - \text{equilibrium concentration of species i})/(\text{weight of HAP added}) \quad (1)$$

Therefore, X_{CP^+}, X_{CTA^+}, X_{Cl^-} and X_{Br^-} take zero or positive values (=the adsorbed amounts). On the other hand, the numerical values of X_{Pi} and $X_{Ca^{2+}}$ are negative, because the concentrations of Pi and Ca^{2+} were initially zero.

Results

Adsorption Isotherms of CP^+ and CTA^+ on HAP

Figure 1 shows the adsorption isotherms of CP^+ and CTA^+ on HAP from aqueous solutions of CPC, CPB and CTAC at a constant mixing ratio of HAP to the solution (solid/solution ratio). The adsorbed amount of CP^+ (X_{CP^+}) increased to a maximum, and then decreased slightly with an increase in the concentration of free CP^+ ($[CP^+]_f$). This result is in contrast to that with CTA^+: the adsorbed amount of CTA^+ (X_{CTA^+}) increased monotonously with an increase in the concentration of free CTA^+ ($[CTA^+]_f$). It was found that X_{CP^+} decreased with an increase in the solid/solution ratio (○, ◑ and ●) and that X_{CP^+} from the CPC solution was smaller than that from the CPB solution (compare ● and ▲).

Adsorption Isotherms of Cl^- and Br^- on HAP

The full lines in Fig. 2 show the adsorption isotherms of Cl^- and Br^- on HAP from aqueous solutions of CPC, CTAC and CPB. The adsorbed amounts of these ions (X_{Cl^-} and X_{Br^-}) increased monotonously with their concentrations ($[Cl^-]_f$ and $[Br^-]_f$). The dotted line on open squares shows the adsorption isotherm of Cl^- from an aqueous solution of KCl, an indifferent salt towards the HAP surface.[12] In this case, Cl^- was scarcely adsorbed on HAP. The adsorbed amount of Br^- from an aqueous solution of KBr is also plotted in this figure (indicated by open triangles); adsorption of Br^- was not detectable within the experimental error of the present work. These results lead to the conclusion that Cl^- and Br^- are adsorbed

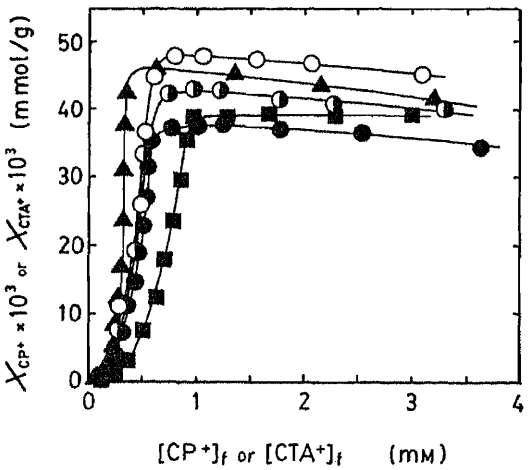

Fig. 1. Adsorption Isotherms of CP^+ and CTA^+ from Aqueous Solutions of CPC, CPB and CTAC at a Constant Mixing Ratio of HAP to the Solution

Surface active agent used: CPC (○, ◑, ●), CPB (▲), CTAC (■).
Solid/solution ratio (g/l): 20 (○), 30 (◑), 40 (●, ▲, ■).

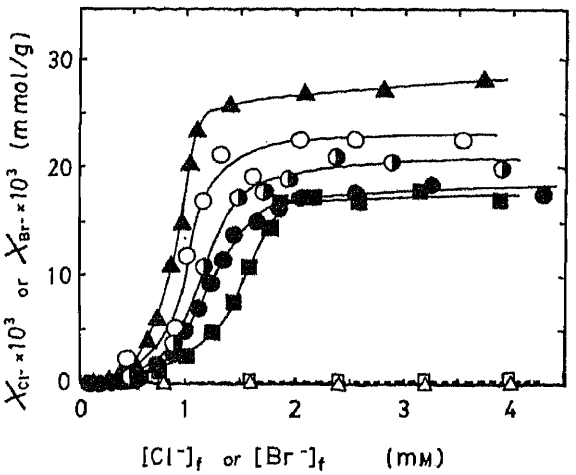

Fig. 2. Adsorption Isotherms of Cl^- and Br^- from Aqueous Solutions of CPC, CPB and CTAC at a Constant Mixing Ratio of HAP to the Solution

All the symbols and the experimental conditions are the same as those in Fig. 1. The adsorbed amounts of Cl^- and Br^- from aqueous solutions of KCl and KBr are also indicated in this figure by the symbols □ and △ (solid/solution ratio = 40 g/l).

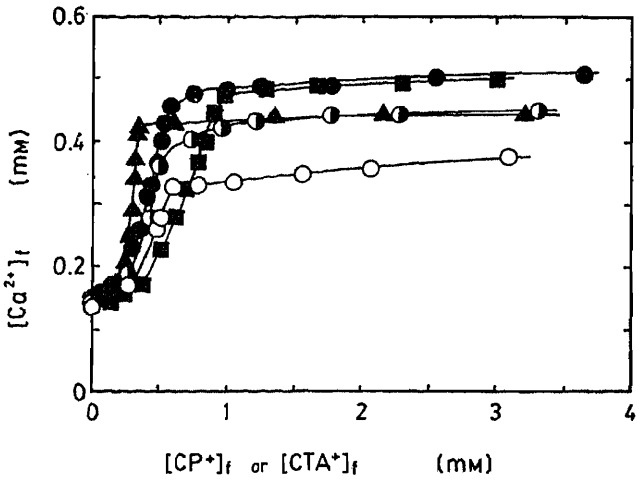

Fig. 3. Relationship between the Equilibrium Concentration of the Surface Active Ion and That of Calcium Ion Released from the Surface of HAP

All the symbols and the experimental conditions are the same as those in Fig. 1.

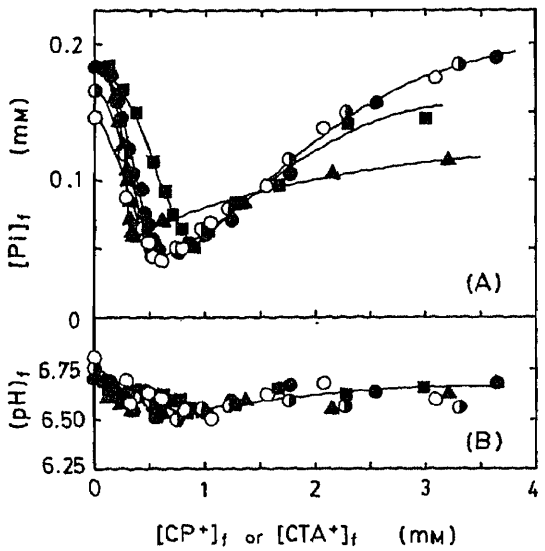

Fig. 4. Relationships between the Equilibrium Concentration of the Surface Active Ion and That of Phosphate Ion Released from the Surface of HAP (A) or the Equilibrium pH of the Solution (B)

All the symbols and the experimental conditions are the same as those in Fig. 1.

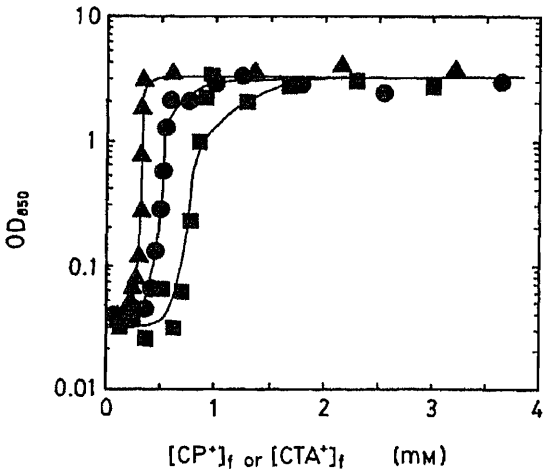

Fig. 5. Optical Density of the Suspension as a Function of the Equilibrium Concentration of the Surface Active Ion

The ordinate scale is logarithmic. All the symbols are the same as those in Fig. 1.

not by direct interaction with the HAP surface but by counterion binding with the surface active cation adsorbed on HAP.

Release of Calcium Ion from the Surface of HAP

It was found that Ca^{2+} was released from the surface of HAP during the adsorption of CP^+ and CTA^+ on HAP. The concentration of Ca^{2+} released, $[Ca^{2+}]_f$, is plotted against $[CP^+]_f$ or $[CTA^+]_f$ in Fig. 3. It shows that $[Ca^{2+}]_f$ increases with $[CP^+]_f$ or $[CTA^+]_f$, and with the surface area of HAP added, *i.e.*, with the solid/solution ratio (see ○, ◑ and ●).

Release of Phosphate Ion and the Equilibrium pH of the Solution

The concentration of Pi released ($[Pi]_f$) and the equilibrium pH of the solution ($(pH)_f$) are

plotted as a function of $[CP^+]_f$ or $[CTA^+]_f$ in Figs. 4A and B. It shows that both $[Pi]_f$ and $(pH)_f$ decrease to a minimum, and then increase with an increase in the concentration of the surface active ion. The concentrations of CP^+ and CTA^+ at which $[Pi]_f$ has a minimum value are 0.58, 0.34 and 0.91 mM for CPC, CPB and CTAC, respectively.

Optical Density of the HAP Suspension

It was found that the HAP powder sedimented rapidly and a clear interface between the sediment phase and the liquid phase was observed when the surfactant concentration was low. However, when the concentration became high enough, the suspension remained turbid even though 24 h had passed, due to the powder that had not sedimented. Figure 5 shows the relationships between OD_{850} and $[CP^+]_f$ or $[CTA^+]_f$. The curves increased sigmoidally in the same manner as those shown in Figs. 1 to 3. Therefore, it is reasonable to consider that the adsorption of the surface active ion is very closely related to the stability of the HAP suspension.

Discussion

The curves shown in Fig. 4A reverse their slopes from negative to positive at some concentration of surface active ions. This result suggests the existence of two distinct releasing mechanisms for Pi below and above this concentration. The values of $-\log(Ca^{2+})^{10}(PO_4^{3-})^6(OH^-)^2$, where ( ) means the activity of the ion in the parenthesis, were obtained according to the method mentioned previously[2,13,14] in the region of $[CP^+]_f$ and $[CTA^+]_f$ below the break points. The numerical values obtained were 113.1—116.0, 113.3—114.8, and 113.3—114.9 for CPC, CPB and CTAC, respectively. These values are within the range of the literature values of $-\log K_{sp}$ for HAP (108—125).[15] This result suggests that the decrease of $[Pi]_f$ in the region of concentration of CP^+ or CTA^+ lower than that at the break point was caused by the increase of $[Ca^{2+}]_f$ (Fig. 3) to maintain the solubility product for HAP, K_{sp}, constant. On the other hand, in the region of higher concentration of CP^+ or CTA^+, $[Pi]_f$ increased despite the increase in $[Ca^{2+}]_f$. As K_{sp} for HAP should be kept constant even in this region, it was concluded that the activity coefficient of PO_4^{3-} decreased with an increase in $[CP^+]_f$ or $[CTA^+]_f$ owing to the binding of Pi to the surface of micelles. Accordingly, the concentration of the surface active cation at which $[Pi]_f$ has a minimum value (0.58, 0.34 and 0.91 mM for CPC, CPB and CTAC, respectively) was identified as the critical micelle concentration (cmc) of the system.[2-4] This effect of micelles is more pronounced for CPC than for CPB (compare ● with ▲). This can be explained by the difference of the binding affinity of Cl^- and Br^- to cationic micelles. That is, as Cl^- is more weakly bound to cationic micelles than Br^-,[16-19] Pi was exchanged more easily with Cl^- than with Br^- at the micelle surface. Marra reported that Cl^- also has a lower affinity than Br^- to cationic monolayers.[20]

Figure 6 shows the relationship between the adsorbed amount of the surface active cation (X_{CP^+} or X_{CTA^+}, quoted from Fig. 1) and the increment of the released amount of Ca^{2+} ($-\Delta X_{Ca^{2+}}$) due to the addition of the surfactant in the region below the cmc. The latter values were obtained from the data shown in Fig. 3, according to the following equation;

$$-\Delta X_{Ca^{2+}} = ([Ca^{2+}]_f \text{ in the presence of the surfactant} - [Ca^{2+}]_f \text{ in the absence of the surfactant})/(\text{weight of HAP added}) \quad (2)$$

Although X_{CP^+} and $[Ca^{2+}]_f$ depended on the solid/solution ratio as shown in Figs. 1 and 3, all the experimental points for CPC thus plotted are roughly on one curve irrespective of the

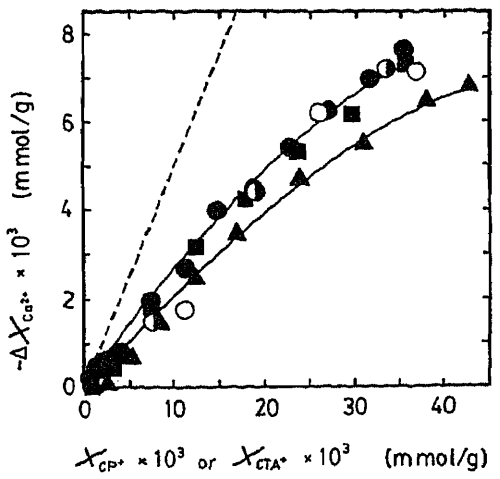

Fig. 6. Relationship between the Adsorbed Amount of the Surface Active Ion and the Amount of Ca^{2+} Released through the Adsorption of the Surface Active Ion in the Region below the cmc

All the symbols and the experimental conditions are the same as those in Fig. 1. The dotted line shows the hypothetical relationship of $-\Delta X_{Ca^{2+}}/X_{CP^+}$ and $-\Delta X_{Ca^{2+}}/X_{CTA^+} = 1/2$.

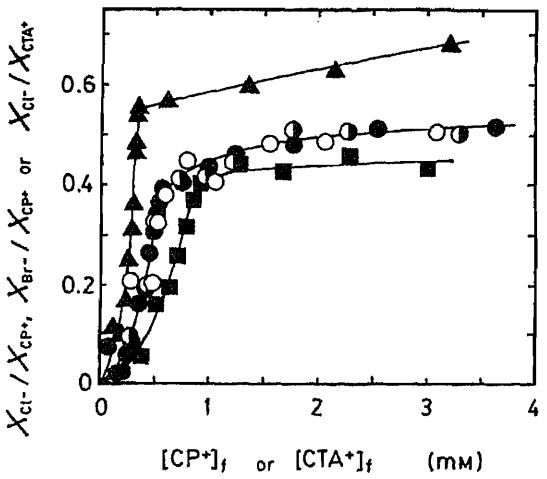

Fig. 7. Relationship between the Equilibrium Concentration of the Surface Active Ion and the Ratio of the Adsorbed Amount of the Counterion to That of the Surface Active Ion

All the symbols and the experimental conditions are the same as those in Fig. 1.

ratio. This result suggests that the increase of $[Ca^{2+}]_f$ with an increase in the concentration of the surface active ion in this region was caused by the mechanism of ion-exchange between Ca^{2+} on the surface of HAP and the surface active cation adsorbed on HAP. However, the size of the surfactant polar group is larger than that of Ca^{2+}.[21] The exchange, therefore, may occur owing to electrostatic repulsion between the adsorbed cationic head group of the surfactant and Ca^{2+} adjacent to the adsorption site. On the other hand, a part of CP^+ or CTA^+ was adsorbed on HAP together with Cl^- or Br^- as a counterion, as mentioned in Results. The ratio of the adsorbed amount of Cl^- to that of CP^+ (X_{Cl^-}/X_{CP^+}) is plotted against $[CP^+]_f$ in Fig. 7. The data for CPB (X_{Br^-}/X_{CP^+}) and CTAC (X_{Cl^-}/X_{CTA^+}) are also plotted in this figure as a function of $[CP^+]_f$ or $[CTA^+]_f$. It shows that the ratio increases with the concentration of the surface active ion. Therefore, the decrease of the Pi release in the region below the cmc (Fig. 4) and the increase of the simultaneous binding of Cl^- or Br^- as a counterion to the surface active cation (Fig. 2) depress the accumulation of formal positive charge on the HAP surface. These facts are responsible for the downward deviation of the curves from the dotted line (which shows the relationship of $-\Delta X_{Ca^{2+}}/X_{CP^+}$ and $-\Delta X_{Ca^{2+}}/X_{CTA^+} = 1/2$) in Fig. 6. The facts that the amount of Ca^{2+} expelled by CPB was smaller than that by CPC, and that X_{Br^-}/X_{CP^+} was larger than X_{Cl^-}/X_{CP^+} (compare ▲ with ● in Figs. 6 and 7), show that Br^- is more strongly bound to CP^+ in the adsorbed phase than Cl^-, in a similar manner to their binding to CP^+ micelles, as mentioned previously.

When the concentration of the surface active ion becomes higher than the cmc, Pi is captured by the cationic micelles as a counterion. Therefore, Ca^{2+} release still continues in this region to compensate for the positive charge remaining on the surface of HAP through the release of Pi. The decrease of X_{CP^+} in Fig. 1 may take part in this compensation in order to maintain the electroneutrality of the surface phase.

Figure 8 shows the relationship between the increase of positive charge and that of negative charge at the surface of HAP. The former values were obtained from the amounts of CP^+ or CTA^+ adsorption and Ca^{2+} release, and the latter ones from those of Cl^- or Br^-

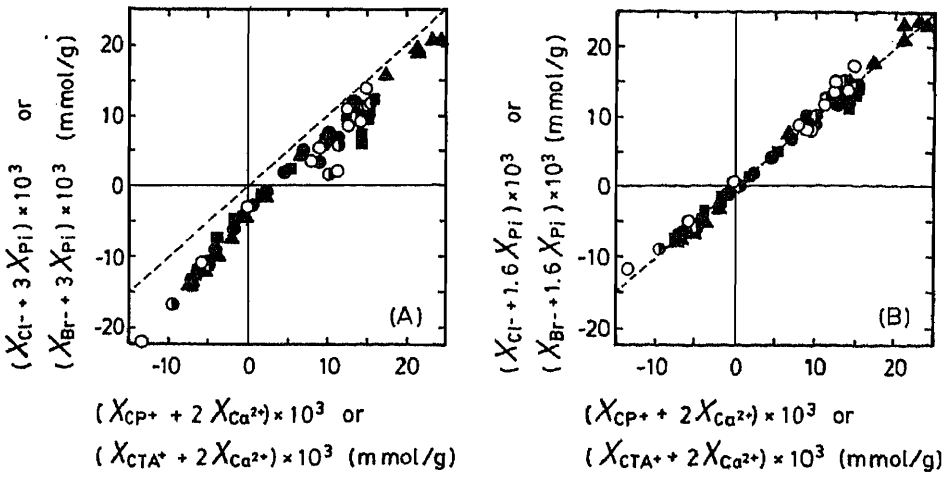

Fig. 8. Relationship between the Increment of Positive Charge and That of Negative Charge on the Surface of HAP at the Adsorption Equilibrium of the Cationic Surfactant

The apparent valency of Pi on the surface of HAP for the calculation is taken to be 3 (A) or 1.6 (B). All the symbols and the experimental conditions are the same as those in Fig. 1. The dotted line shows the condition of electroneutrality of the system at equilibrium.

adsorption and Pi release. When the valency of Pi on the surface of HAP was considered to be 3 (A), all the experimental points deviated downwards from the dotted line which indicates electroneutrality with respect to adsorption and desorption of the ions. On the other hand, when a value of 1.6 was adopted for the valency of Pi (B), they were almost on the dotted line. These results suggest that Pi on the surface of HAP is protonated and acts as an anion with a valency of 1.6. This protonated phosphate may be more easily liberated from the surface of HAP than PO_4^{3-}.[22] Another constituent anion, *i.e.*, OH^-, should be released from HAP. Therefore, the value of 1.6 is an apparent valency involving the contributions of H^+ bound to released Pi and OH^- released simultaneously.

Hanna and Saleeb reported that the zeta-potential of HAP powder is reversed from negative to positive as the adsorbed amount of CP^+ or CTA^+ increased.[21] The contact angle and the flotation recovery increased as the zeta-potential increased. Therefore, the increase of OD_{850} shown in Fig. 5 can be attributed to the increase of positive charge at the surface of HAP through the adsorption of surface active cations. This conclusion does not conflict with the requirement for electroneutrality of the surface phase of HAP discussed above for the following reason. That is, the obtained amounts of adsorption of Cl^- and Br^- after filtration are the sum of these ions located at the Stern layer and at the diffuse layer.[23] Consequently, the potential at just outside of the HAP surface is positive and the electrostatic repulsion between positive charges on the HAP powders make the suspension stable.

In conclusion, the amounts of Ca^{2+} and Pi released from the surface of HAP depended on the equilibrium concentrations of CP^+ and CTA^+, on the adsorbed amounts of these surface active ions, and on the species and affinity of the counterion for the surfactant. Moreover, the requirement of electroneutrality of the surface phase of HAP and the restriction of K_{sp} for HAP in the solution phase also affect the relationships among them.

References and Notes

1) Present address: *Faculty of Pharmaceutical Sciences, The University of Tokushima, Sho-machi, Tokushima 770, Japan.*
2) S. Shimabayashi, H. Tanaka, and M. Nakagaki, *Chem. Pharm. Bull.*, **34**, 4474 (1986).

3) S. Shimabayashi, H. Tanaka, and M. Nakagaki, *Chem. Pharm. Bull.*, **35**, 2171 (1987).
4) S. Shimabayashi, H. Tanaka, and M. Nakagaki, *Chem. Pharm. Bull.*, **35**, 3539 (1987).
5) S. Shimabayashi, C. Tamura, and M. Nakagaki, *Yakugaku Zasshi*, **102**, 137 (1982).
6) T. J. Roseman, W. I. Higuchi, B. Hodes, and J. J. Hefferren, *J. Dental Res.*, **48**, 509 (1969).
7) R. K. Mishra, S. Chander, and D. W. Fuerstenau, *Colloids and Surfaces*, **1**, 105 (1980).
8) S. Shimabayashi, S. Sumiya, T. Aoyama, and M. Nakagaki, *Chem. Pharm. Bull.*, **32**, 1279 (1984); S. Shimabayashi, S. Sumiya, and M. Nakagaki, *Yakugaku Zasshi*, **104**, 1024 (1984).
9) I. Nishi, T. Imai, and M. Kasai (eds.), "Kaimen-Kasseizai Binran (Handbook of Surface Active Agents)," Sangyo Tosho Publishing, Tokyo, 1960, pp. 831—832.
10) The Chemical Society of Japan (ed.), "Shin Zikken Kagaku Koza," Vol. 9, Maruzen, Tokyo, 1976, pp. 245—246, p. 250; S. Utsumi, *Nippon Kagaku Zasshi*, **73**, 835 (1952); A. Tomonari, *ibid.*, **83**, 693 (1952).
11) A. Gee, L. P. Domingues, and V. R. Deitz, *Anal. Chem.*, **26**, 1487 (1954).
12) M. Kukura, L. C. Bell, A. M. Posner, and J. P. Quirk, *J. Colloid Interface Sci.*, **76**, 900 (1972).
13) E. C. Moreno, T. M. Gregory, and W. E. Brown, *J. Res. Nat'l Bur. Std.*, **72(A)**, 773 (1968).
14) A. N. Smith, A. M. Posner, and J. P. Quirk, *J. Colloid Interface Sci.*, **54**, 176 (1976).
15) S. Chander and D. W. Fuerstenau, "Adsorption on and Surface Chemistry of Hydroxyapatite," ed. by D. W. Misra, Plenum Press, New York, 1984, pp. 29—49.
16) E. B. Abuin, E. Lissi, P. S. Araujo, R. M. V. Aleixo, H. Chaimovich, N. Bianchi, L. Miola, and F. H. Quina, *J. Colloid Interface Sci.*, **96**, 293 (1983); E. Abuin, E. Lissi, N. Bianchi, L. Miola, and F. H. Quina, *J. Phys. Chem.*, **83**, 5166 (1983); H. Chaimovich, J. B. S. Bonilha, M. J. Politi, and F. H. Quina, *ibid.*, **83**, 1851 (1979); J. B. S. Bonilha, G. Chiericato, Jr., S. M. Martins-Franchetti, E. J. Ribaldo, and F. H. Quina, *ibid.*, **86**, 4941 (1982).
17) D. Bartet, C. Gamboa, and L. Sepúlveda, *J. Phys. Chem.*, **84**, 272 (1980); C. Gamboa, L. Sepúlveda, and R. Soto, *ibid.*, **85**, 1429 (1981).
18) H. D. Burrows, S. J. Formosinho, M. Fernanda, J. R. Paiva, and E. J. Rasburn, *J. Chem. Soc., Faraday Trans. 2*, **76**, 685 (1980).
19) L. S. Romsted, *J. Phys. Chem.*, **89**, 5107, 5113 (1985).
20) J. Marra, *J. Phys. Chem.*, **90**, 2145 (1986).
21) H. S. Hanna and F. Z. Saleeb, *Colloids and Surfaces*, **1**, 295 (1980).
22) C. L. Kibby and W. K. Hall, "The Chemistry of Biosurfaces," Vol. 2, ed. by M. L. Hair, Marcel Dekker, Inc., New York, 1972, pp. 663—729.
23) M. Nakagaki and Y. Nakamura, *Yakugaku Zasshi*, **93**, 460 (1973).

[Chem. Pharm. Bull. 35(12)4695—4699(1987)]

N-Pyridoxylidenehydrazine-*N'*,*N'*-diacetic Acid. III.[1] Formation of Metal Chelates in Solution

YOSHIKAZU MATSUSHIMA,*[,a] YOSHIKO NAGATA,[a] YUKO TAMANO,[a] SETSURO SUGATA,[a] TADAO FUJIE,[a] YOSHIHARU KARUBE,[b] and AKIRA KONO[c]

Kyoritsu College of Pharmacy,[a] Shibakoen 1-5-30, Minatoku, Tokyo 105, Faculty of Pharmaceutical Sciences, Fukuoka University,[b] Nanakuma, Jonanku, Fukuoka 814-01, and Kyushu Cancer Center Research Institute,[c] Notame, Minamiku, Fukuoka 815, Japan

(Received May 6, 1987)

Metal chelate formation of *N*-pyridoxylidenehydrazine-*N'*,*N'*-diacetic acid (**1**) and related hydrazines in solution was studied by means of absorption spectroscopy. Compound **1** and *N*-pyridoxylidene-*N'*-methylhydrazine (**2**) in methanol formed Cu(II) chelates of the same spectral character, which indicated the chelation of the phenolate oxygen and the hydrazine nitrogen atoms to Cu(II). The compositions of the chelates were 1 : 1 for **1** and 1 : 2 for **2**, indicating that **1** acts as a tri- or tetradentate ligand. *N*-(3-Hydroxy-4-pyridylmethylene)hydrazine-*N'*,*N'*-diacetic acid formed a Cu(II) chelate similar to that of **1** but *N*-pyridoxylidene-*N'*,*N'*-dimethylhydrazine and *N*-pyridoxylidene-*N'*,*N'*-diphenylhydrazine did not form chelates under similar conditions. Addition of an equimolar or excess amount of Co(II), Ni(II), Zn(II), Cd(II) or La(III) salt to **1** in methanol gave rise to absorption assignable to the chelate of **1**, whereas **2** did not form metal chelates under the same conditions. It was concluded that the iminodiacetic acid moiety of **1** coordinated to the metal ions and enhanced the stability constant of the metal chelates.

Keywords——pyridoxal; hydrazine; hydrazone; methanol; iminodiacetic acid; *N*-pyridoxylidenehydrazine-*N'*,*N'*-diacetic acid; *N*-pyridoxylidene-*N'*-methylhydrazine; metal chelate; Cu(II); absorption spectrum

Preparation of *N*-pyridoxylidenehydrazine-*N'*,*N'*-diacetic acid (**1**) and related compounds and evaluation of their ^{99m}Tc complexes as hepatobiliary imaging agents were reported in the previous papers.[1] Compound **1** is the hydrazone of hydrazine-*N*,*N*-diacetic acid with pyridoxal (PL). Its molecular structure was designed on the basis of the following considerations.

The ^{99m}Tc complexes of a number of chelating ligands have been used as radiopharmaceuticals for hepatobiliary scintigraphy. The ligands currently used are classified into two groups of compounds. One group consists of derivatives of iminodiacetic acid (IDA), such as *N*-(2,6-diethylphenylcarbamoylmethyl)iminodiacetic acid (E-HIDA). Its ^{99m}Tc chelate is one of the most widely used hepatobiliary radiopharmaceuticals. The other group of the ligands consists of the Schiff bases of PL with amino acids. Compound **1** has two sets of chelating groups in the molecule, *i.e.* the IDA and PL Schiff base moieties, and was assumed to be a good model compound for studies of hepatobiliary imaging as well as metal chelation.

The results of biodistribution and scintigraphic studies in experimental animals showed that the ^{99m}Tc complexes of **1** and a related hydrazone, *N*-(3-hydroxy-4-pyridylmethylene)hydrazine-*N'*,*N'*-diacetic acid were good hepatobiliary tracers. The results also showed that considerable radioactivity was present in the liver and kidneys. Consequently, these compounds are not as satisfactory as E-HIDA as ligands of hepatobiliary radiopharmaceuticals. This was assumed to be due to the presence of polymeric forms of ^{99m}Tc. In an effort to avoid the polymerization of ^{99m}Tc and to improve the yield of the ^{99m}Tc chelate, metal chelation by **1** and related ligands was studied.

Since no stable nuclide of Tc exists, structural studies of Tc chelates by conventional chemical methods are impossible. However, studies of the complexes of other metals such as Cu(II) might improve our understanding of the Tc chelates. The present paper describes the results of spectrophotometric studies of the metal chelates of **1** and related hydrazones.

Results

The spectroscopic properties of the chromophores of PL, its analogs, their Schiff bases, metal chelates of the Schiff bases and other derivatives are sensitively dependent upon structural factors. Extensive studies have been made on the assignments of the spectral bands to specific species in solution and on the shift of the bands with changes in the structural features of the species.[1b,2-4] Interpretation of the spectra of the metal chelates of the PL hydrazones in the present study was assisted by the results of these studies.

The absorption spectra of methanolic and aqueous solutions of hydrazones and metal ions were measured under various conditions. The hydrazones studied were **1**, *N*-pyridoxylidene-*N'*-methylhydrazine (**2**), *N*-pyridoxylidene-*N'*,*N'*-dimethylhydrazine (**3**) and *N*-pyridoxylidene-*N'*,*N'*-diphenylhydrazine (**4**), which are the hydrazones of PL with hydrazine-*N*,*N*-diacetic acid, methylhydrazine, 1,1-dimethylhydrazine and 1,1-diphenylhydrazine, respectively. *N*-(3-Hydroxy-4-pyridylmethylene)hydrazine-*N'*,*N'*-diacetic acid (**5**) was also studied; it is the hydrazone of hydrazine-*N'*,*N'*-diacetic acid with 4-formyl-3-hydroxypyridine, a structural analog of PL. The structures of the hydrazines are shown in Chart 1.

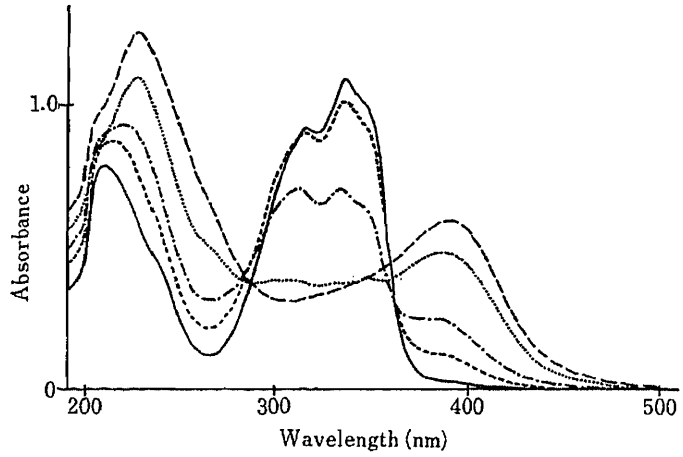

Fig. 1. Absorption Spectra of *N*-Pyridoxylidenehydrazine-*N'*,*N'*-diacetic Acid and Cu(II) in Methanol

Concentration of **1**: 6×10^{-5} M.
Concentrations of Cu(II): ——, 0; – – – –, 1.5×10^{-5} M; – – –, 3.0×10^{-5} M; ——, 6.0×10^{-5} M; — —, 1.2×10^{-4} M.

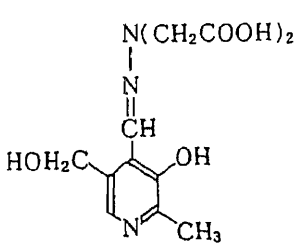

1

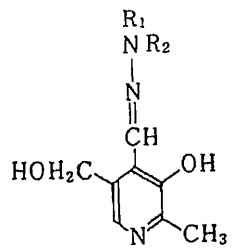

2: $R_1=CH_3$, $R_2=H$
3: $R_1=R_2=CH_3$
4: $R_1=R_2=C_6H_5$

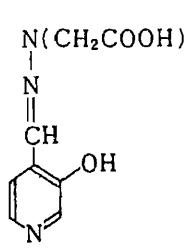

5

Chart 1

Cu(II) Chelates

Figure 1 shows the spectra of solutions containing 6.0×10^{-5} M **1** and various concentrations of Cu(II) perchlorate. With increase of the concentration of Cu(II), the absorption of the band at 336 nm decreased and the band at 389 nm appeared. The band at 336 nm was assigned as the π_1-band[5] of the nonpolar neutral species of **1**.[1b] The band at 389 nm was quite similar to the π_1-bands of the metal chelates of the aldimines formed from PL and amino acids.[2-4] The band can be assigned to the Cu(II) chelate of **1**, in which the phenolate oxygen and the hydrazine nitrogen atoms are chelated. The involvement of the IDA moiety is not clear from the spectra, since no significant effect on the spectra is expected upon chelation. The 389-nm band disappeared instantly on addition of a solution of tetrasodium ethylenediamine-*N*,*N*,*N'*,*N'*-tetraacetate.

The formation of the chelate was complete in the presence of two equivalents of Cu(II) to the ligand. The method of continuous variation[6] was applied for determining the composition of the metal chelate. As shown in Fig. 2A, the results (monitored at 389 nm) indicated the formation of the 1 : 1 chelate.

The spectral study of ligand **2** and Cu(II) gave results similar to those in the case of **1**. The π_1-bands assigned to the neutral species and Cu(II) chelate of **2** were at 299 nm and 366 nm, respectively. The continuous variation method (with monitoring at 360 nm) indicated that the composition of the chelate was 1 : 2 (metal : ligand), as shown in Fig. 2B. Compounds **3** and **4** did not form Cu(II) chelates in measurable amounts under the conditions employed.

Spectra similar to those shown in Fig. 1 were observed in aqueous solutions of **1** and Cu(II) at pH 9—10. The π_1-band of the Cu(II) chelate in aqueous solution appeared at around 380 nm, and was broader and weaker than in methanol. At the lower pH range, the band was observable only in the presence of excess amounts of Cu(II). The results indicated that the stability of the chelate was not as high as expected. The π_1-band of the Cu(II) chelate of **2** was found at around 360 nm in aqueous solution. The band was observed at pH 9—10 in the presence of an excess amount of Cu(II) over **2**, indicating that the stability of this chelate was lower than that of **1**.

No reliable values have been obtained yet for the stability constants of the Cu(II) chelates of **1** and **2** in aqueous solution by potentiometric measurements, because the values are so low. Attempts to isolate the chelates were unsuccessful.

Compound **5** formed the Cu(II) chelate in a similar manner to **1** in both methanol and

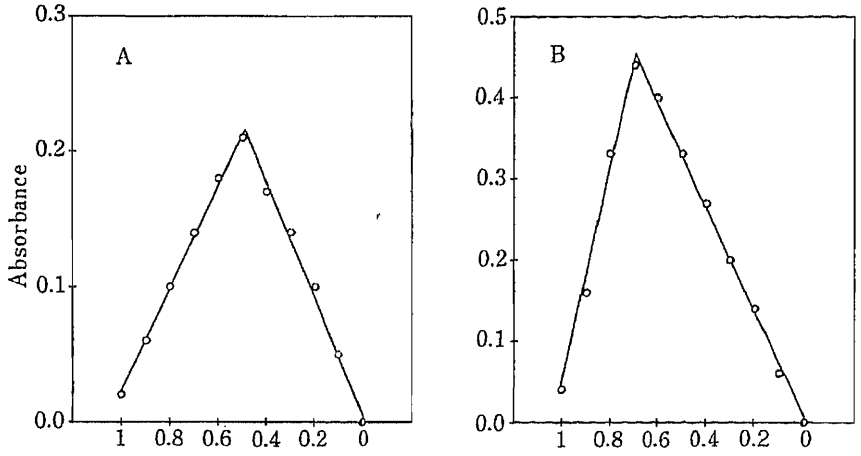

Fig. 2. The Method of Continuous Variation for Determining the Cu(II) Chelates of Hydrazines

The numbers on the abscissa indicate the ratio of the concentration of the hydrazine to the total concentration of the hydrazine and the Cu(II) salt, which was maintained at 6.0×10^{-6} M. A, the absorbance of the chelate of 1 monitored at 389 nm. B, the absorbance of the chelate of 2 monitored at 360 nm.

water. The π_1-band of the chelate was at 378 nm in methanol and at around 370 nm in water.

Chelates of Other Metals

Metal chelates of **1** with other divalent and trivalent metal ions were studied similarly.

Absorption spectra ascribed to the formation of Co(II) and Ni(II) chelates were obtained by addition of an equimolar amount of the metal perchlorate to **1** in methanol. On addition of equimolar Zn(II) or Cd(II) perchlorate to **1** in methanol, spectra assignable to the acidic forms of **1**[1b] were observed. The spectra of the chelates were obtained after addition of excess metal perchlorate and neutralization with alkali. They indicate the low stability of the Zn(II) and Cd(II) chelates.

The π_1-bands were found at 394, 410, 379 and 370 nm for the Co(II), Ni(II), Zn(II) and Cd(II) chelates of **1**, respectively. The composition of each of the four divalent metal chelates was shown to be 1 : 1 from the continuous variation study.

The La(III) chelate of **1** was formed in methanol under conditions similar to those used in the case of Cd(II). The absorption of the chelate was at around 360 nm. The partial overlap of the absorption with that of the ligand prevented us from obtaining reliable data on the composition of the chelate. The formation of the Al(III) chelate was not detected under the conditions used.

The formation of the metal chelates of **2** in methanol was examined by addition of 1—6 equivalents of Co(II), Ni(II), Zn(II), Cd(II), Al(III) and La(III) salts. No indication of the formation of metal chelates was obtained from the spectral study.

Discussion

N-Pyridoxylidenehydrazine-*N'*,*N'*-diacetic acid (**1**) and *N*-pyridoxylidene-*N'*-methylhydrazine (**2**) formed Cu(II) chelates of the same spectral character in methanol, though the compositions of the chelates were 1 : 1 and 1 : 2, respectively. The considerable spectral changes between the neutral species of the ligands and the metal chelates indicate that the phenolate oxygen and the hydrazine nitrogen atoms chelate Cu(II) ion. Since **2** is assumed to act as a bidentate ligand, the formation of the 1 : 2 (metal : ligand) chelate is reasonable. The chelation by the IDA moiety of **1** could not be determined, as chelation would not significantly change the spectra. The formation of the 1 : 1 chelate suggests that **1** acts as a tri- or tetradentate ligand. The stability constant of the Cu(II) chelate of **1** was larger than that of **2** in aqueous solution. This represents further support for the assumption that the IDA moiety coordinated Cu(II) in the 389-nm absorbing chelate.

The Co(II) and Ni(II) chelates of **1** were formed in methanol, as was the Cu(II) chelate. On the other hand, the formation of the Zn(II), Cd(II) and La(III) chelates was recognized only in the presence of a large excess of the metal salt. The possibility can not be excluded that the metal ions were chelated only by the IDA moiety in dilute solutions. The fact that **2** did not form chelates with these metal ions showed that the IDA moiety plays an important role in the chelation of **1**.

We conclude that the IDA moiety introduced into *N*-pyridoxylidenehydrazine coordinated metal ions and enhanced the stability of the metal chelates. However, the stability constants of **1** with Cu(II) and other di- and trivalent metals were not as high as we had expected. We assume that the ^{99m}Tc chelation of **1** was incomplete due to the low stability of the chelate under the conditions used in the previous study, resulting in the formation of polymeric forms of the radionuclide, which led to the accumulation of radioactivity in the liver and kidneys.

Experimental

The hydrazones used in the study were prepared according to the method described previously.[1] Other chemicals

and solvents were of reagent grade and were obtained from commercial sources.

The absorption spectra were recorded at room temperature with a Shimadzu UV-240 spectrophotometer. All spectral studies were carried out immediately after preparing sample solutions.

Acknowledgment This work was supported in part by Grants-in-Aid for Scientific Research from the Ministry of Education, Science and Culture, Japan and by The Science Research Promotion Fund of the Japan Private School Promotion Foundation.

References and Notes

1) *a*) Part I: Y. Matsushima, S. Mori, Y. Karube, S. Sugata, A. Kono, H. Kunitoku, Y. Yamamoto, Y. Miyake, and M. Kojima, *Chem. Pharm. Bull.*, **32**, 2262 (1984); *b*) Part II: Y. Matsushima, Y. Nagata, Y. Tamano, and S. Sugata, *Annual Report of Kyoritsu College of Pharmacy*, **30**, 1 (1985).
2) Y. Matsushima and A. E. Martell, *J. Am. Chem. Soc.*, **89**, 1322 (1967); E. E. Snell, P. M. Fasella, A. E. Braunstein, and A. Ross, eds., "Chemical and Biological Aspects of Pyridoxal Catalysis," Macmillan, New York, 1963.
3) Y. Matsushima, *Chem. Pharm. Bull.*, **16**, 2046 (1968); S. Matsumoto and Y. Matsushima, *J. Am. Chem. Soc.*, **96**, 5228 (1974); *idem*, *Chem. Pharm. Bull.*, **23**, 106 (1975); S. Matsumoto, Y. Karube, and Y. Matsushima, *ibid.*, **23**, 1852 (1975); Y. Karube and Y. Matsushima, *ibid.*, **25**, 2526 (1977); Y. Karube, Y. Ono, Y. Matsushima, and Y. Ueda, *ibid.*, **26**, 2642 (1978).
4) R. G. Kallen, T. Korpela, A. E. Martell, Y. Matsushima, C. M. Metzler, D. E. Metzler, Y. V. Morozov, I. M. Ralston, F. A. Savin, Y. M. Torchinsky, and H. Ueno, "Transaminases," ed. by P. Christen and D. E. Metzler, Wiley-Interscience, New York, 1985, Chapter 2, and references cited therein.
5) Of the two π–π^* absorption bands of pyridine and its derivatives in the ultraviolet and visible regions, the longer wavelength band has been named π_1, and the shorter one, π_2. See: K. Nakamoto and A. E. Martell, *J. Am. Chem. Soc.*, **81**, 5857 (1959) and references 2, 3.
6) P. Job, *Ann. Chim.*, **6**, 97 (1936).

[Chem. Pharm. Bull. 35(12)4700—4704(1987)]

Oxidation of Cycloalkan[*b*]indoles with Iodine Pentoxide (I_2O_5)

KIYOSHI YOSHIDA,*,[a] JIRO GOTO,[a] and YOSHIO BAN*,[b]

Faculty of Pharmaceutical Sciences, Hokkaido University,[a] Sapporo 060, Japan and School of Pharmaceutical Science, Toho University,[b] Miyama, 2-2-1, Funabashi, Chiba 274, Japan

(Received April 25, 1987)

Oxidation of cycloalkan[*b*]indoles (**3**) with iodine pentoxide (I_2O_5) in 80% aqueous tetrahydrofuran (THF) at room temperature regioselectively afforded 6-oxocycloalkan[*b*]indoles (**4**) in various yields. The yield of this oxidation depends on the size of the ring fused with the indole nucleus. The essential reaction species is I_2O_5, not HIO_3, which might be generated by hydrolysis of I_2O_5 in the aqueous reaction medium. Oxidation of 1-hydroxytetrahydrocarbazole (**5**) under the above conditions afforded spiro oxindoles **6** and **7** in 36 and 39% yields, respectively, accompanied with only a trace of 1-oxotetrahydrocarbazole (**4a**).

Keywords——indole oxidation; iodine pentoxide; cycloalkan[*b*]indole; 6-oxocycloalkan[*b*]-indole; 2-acylindole; 1-hydroxytetrahydrocarbazole; spiro oxindole

It has been shown[1] that 2,3-disubstituted indole derivatives react easily with various oxidants. Most oxidizing agents act as electrophiles and initially attack the C-3 position of the indole ring, leading to the formation of 2-acyl-[2-6] or 3-acylindoles,[7,8] and to the oxidative cleavage of the C-2, C-3 double bond.[9,10] We discovered that iodine pentoxide (I_2O_5), which had not been utilized in organic syntheses, oxidized the nine-membered amide (**1a**) to provide 2-acylindole (**2a**) in good yield. This reaction was successfully applied to the total synthesis of "strychnos" type indole alkaloids.[11]

In the present paper, we wish to describe an application of the I_2O_5 oxidation to cycloalkan[*b*]indoles (**3**) for a convenient and regioselective oxidation of the C-2 side chain of indoles.

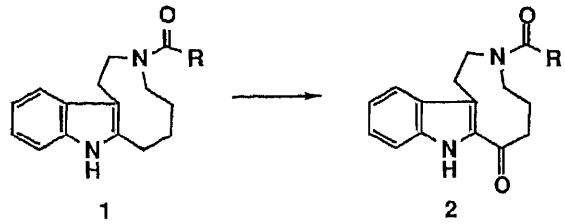

1 2

a: R=$CHClC_2H_5$ b: R=$CHBrC_2H_5$ c: R=CH_3

Chart 1

Cycloalkan[*b*]indoles (**3a—d**) were treated with 1.2 eq of I_2O_5 in 80% (v/v) aqueous tetrahydrofuran (THF) at room temperature to provide 6-oxocycloalkan[*b*]indoles (**4a—d**). The structures of the products were established by comparison of melting points and spectral data with the reported values.[2,12,13] In particular, the ultraviolet (UV) spectra[12] showed characteristic absorptions at about 240 and 310 nm due to $n\rightarrow\pi^*$ and $\pi\rightarrow\pi^*$, transitions respectively. It is interesting that the oxidation yield is strongly dependent on the size of the ring fused with the indole nucleus.[14] In the cases of **3b**[15] and **3d**, the reactions quite smoothly

TABLE I. Oxidation of Cycloalkan[*b*]indoles (3) with I_2O_5

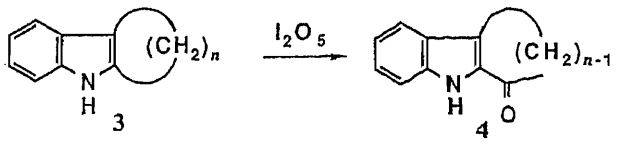

Substrate		Reaction time (h)	Product	Yield (%)
$n=4$	**3a**	0.5	**4a**	53
$n=5$	**3b**	2.0	**4b**	99
$n=6$	**3c**	2.0	**4c**	14
$n=10$	**3d**	2.0	**4d**	84

afforded products (**4b** and **4d**)[13] in 99 and 84% yields, respectively. In the oxidation of tetrahydrocarbazole (**3a**),[16] however, the starting material disappeared within 0.5 h and the product (**4a**)[12b] was obtained in 53% yield, while several unstable by-products were detected by thin-layer chromatography (TLC). Oxidation of **3c**[2] afforded the desired product (**4c**)[2] in 14% yield, accompanied with 6-(3-indolyl)hexanal as an unstable oil in 6.6% isolated yield. The latter was characterized on the basis of the spectral data. The reason why the oxidation yields of **3** vary widely may be differences in the ring strain of the intermediates (Chart 3). For comparative studies of this reagent with other known oxidants, **1c** was treated with I_2O_5 (1.2 eq) in 80% THF for 2 h to afford **2c** in 48% yield. This result might be compared with the previous report of the oxidation of **1c** with SeO_2[6] to give the same product in 26% yield. Oxidation of **1b** under the same conditions also proceeded smoothly to give **2b** in 87% yield. Other oxidants, for example, H_5IO_6[5] and MnO_2,[4] which oxidize cycloalkan[*b*]-indoles to 6-oxocycloalkan[*b*]indoles were not effective for **1b** and **1c**, and the starting materials were recovered.

To clarify the oxidation mechanism, the following experiments were carried out. Oxidation of **3b** with 0.5 eq of I_2O_5 for 3 h gave (**4b**) in 83% yield, whereas with less than 0.5 eq of the reagent, several spots were monitored on TLC together with those of **3b** and **4b**. On the other hand, compound **3b** when treated with 1.0 eq of iodic acid (HIO_3) provided **4b** in 81% yield as a single product. However, it took 4 h to complete the reaction. Reaction of compounds **3a** and **3c** with 1.2 eq of HIO_3 provided none of the desired products, but the starting materials were recovered. From these experiments, it is clear that I_2O_5 is the essential reaction species, and not HIO_3 which might be generated in the aqueous reaction medium. Exceptionally, the most oxidizable substrate (**3b**) reacted with HIO_3 slowly to give **4b**.

In order to determine whether 6-hydroxycycloalkan[*b*]indoles are intermediates of this reaction or not, 1-hydroxytetrahydrocarbazole (**5**)[17] was treated with 1.2 eq of I_2O_5 under the standard conditions. To our surprise, spiro oxindoles (**6** and **7**) were obtained in 36% and 39% yields, respectively,[18] accompanied with only a trace amount of 1-oxotetrahydrocarbazole (**4a**). The structures of the spiro oxindoles (**6** and **7**) were determined by the following chemical conversions. Compound **6**, which crystallized as a single isomer, though its stereochemistry was unknown, was oxidized with pyridinium chlorochromate (PCC) to give **8** in 80% yield. The infrared (IR) spectrum of **8** showed an absorption at 1755 cm^{-1}, which indicates the presence of a five-membered ketone. The unstable hemiacetal (**7**) of a mixture of the stereoisomers was oxidized with PCC to provide the lactone (**9**) in 67% yield.

From these experiments, 6-hydroxycycloalkan[*b*]indoles should not be intermediates. Although the mechanism of the I_2O_5 oxidation reaction has not yet been established, a possible mechanism is shown in Chart 3. Further mechanistic studies of the oxidation of

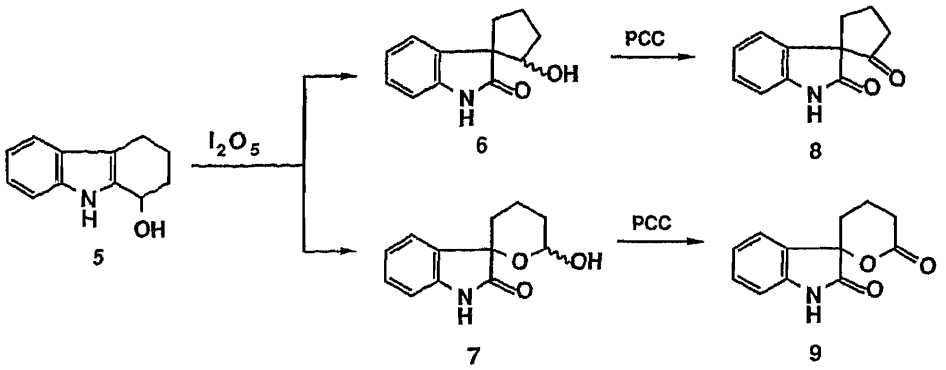

Chart 2

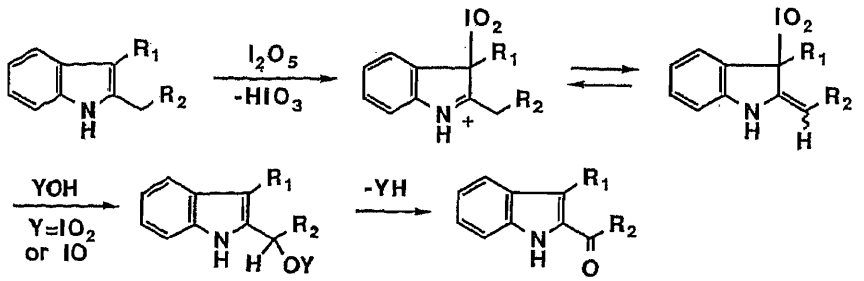

Chart 3

1-hydroxytetrahydrocarbazole (**5**) to the spiro oxindoles (**6** and **7**) are in progress.

It may be concluded that I_2O_5 effectively oxidizes the C-2 side chain of indoles under aqueous conditions at room temperature to provide 2-acylindoles regioselectively. It is advantageous that the reagent is a stable crystalline compound, commercially available, and inexpensive.

Experimental

Melting points were determined on a Yamato M-P melting point apparatus and are uncorrected. IR spectra were recorded on a JASCO A-302 spectrometer and UV spectra were measured on a Hitachi ESP-3T spectrophotometer. Mass spectra (MS) were taken on a JEOL D-300 spectrometer. Proton nuclear magnetic resonance (^{1}H-NMR) spectra were determined on a JEOL FX-100 spectrometer, and chemical shifts (δ) are given in parts per million (ppm) downfield from tetramethylsilane as an internal standard. Coupling constants, J, are given in hertz (Hz); s, d, t, m, and br indicate singlet, doublet, triplet, multiplet, and broad, respectively.

6,7,8,9,10,11,12,13,14,15-Decahydro-5*H*-cyclododec[*b*]indole (3d)——Freshly distilled phenylhydrazine (2.59 g, 24.0 mmol) was added to a solution of cyclododecanone (3.64 g, 20.0 mmol) in 20 ml of ethanol and the mixture was allowed to stand at room temperature for 0.5 h. After evaporation of the solvent, the crude phenylhydrazone was heated at reflux temperature in 100 ml of 10% H_2SO_4 for 1.5 h. The separated oil was extracted with CH_2Cl_2, then the extract was dried and concentrated to give a brown solid, which was recrystallized from hexane to afford colorless crystals (3.85 g, 75.5%); mp 97—99 °C. IR (Nujol): 3280 cm^{-1}. *Anal.* Calcd for $C_{18}H_{25}N$: C, 84.65; H, 9.87; N, 5.48. Found: C, 84.61; H, 9.93; N, 5.52.

General Procedure for the Iodine Pentoxide (I_2O_5) Oxidation of Cycloalkan[*b*]indoles (3)——Iodine pentoxide (400 mg, 1.20 mmol) was added to a solution of a cycloalkan[*b*]indole **3** (1.00 mmol) in 25 ml of 80% (v/v) aqueous THF. The mixture was stirred at room temperature, the solvent was evaporated off at room temperature and the residue was extracted with ethyl acetate. The extract was successively washed with water, 5%-$Na_2S_2O_3$, saturated $NaHCO_3$ and brine, and dried over Na_2SO_4. After evaporation of the solvent, the crude residue was purified by silica gel column chromatography to obtain the corresponding 6-oxocycloalkan[*b*]indole (**4**).

1-Oxo-1,2,3,4-tetrahydrocarbazole (4a)——mp 165—168 °C (from ethanol) [lit.[12b] 166—167 °C]. IR (Nujol): 3340, 1635 cm^{-1}.

6-Oxo-6,7,8,9,10-pentahydrocyclohept[*b*]indole (4b)——mp 147—148 °C (from ethyl acetate–hexane) [lit.[13] 148 °C]. IR (Nujol): 3300, 1640 cm^{-1}.

6-Oxo-6,7,8,9,10,11-hexahydro-5*H*-cycloct[*b*]indole (4c)——mp 183—184 °C (from methanol) [lit.[2] 185 °C]. IR (Nujol): 3300, 1630 cm^{-1}.

6-(3-Indolyl)hexanal——IR ($CHCl_3$): 3380, 2729, 1719 cm^{-1}. NMR (CCl_4) δ: 0.8—2.9 (6H, m), 2.28 (2H, t, J=7.0 Hz), 2.64 (2H, t, J=7.0 Hz), 6.9—7.7 (5H, m), 8.63 (1H, br), 9.77 (1H, t, J=2 Hz).

6-Oxo-6,7,8,9,10,11,12,13,14,15-decahydro-5*H*-cyclododec[*b*]indole (4d)——mp 217—220 °C (from ethanol). IR (Nujol): 3310, 1640 cm^{-1}. *Anal.* Calcd for $C_{18}H_{23}NO$: C, 80.25; H, 8.61; N, 5.20. Found: C, 80.36; H, 8.67; N, 5.08.

3-Acetyl-7-oxo-1,2,3,4,5,6,7,8-octahydroazonino[5,4-*b*]indole (2c)——Yield 48%; mp 208—210 °C [lit.[6] 209—210 °C]. IR (Nujol): 3250, 1625, 1575, 1530 cm^{-1}. UV λ_{max}^{EtOH} nm: 314, λ_{min}^{EtOH} nm: 269. *Anal.* Calcd for $C_{16}H_{18}N_2O_2$: C, 71.09; H, 6.71; N, 10.36. Found: C, 70.91; H, 6.64; N, 10.28.

3-(2-Bromobutyryl)-7-oxo-1,2,3,4,5,6,7,8-octahydroazonino[5,4-*b*]indole (2b)——Yield 87%; mp 203—204 °C (from ether–hexane). IR (Nujol): 3320, 1630, 1610 cm^{-1}. UV λ_{max}^{EtOH} nm: 238, 314. *Anal.* Calcd for $C_{18}H_{21}BrN_2O_2$: C, 57.30; H, 5.61; N, 7.43. Found: C, 57.46; H, 5.71; N, 7.48.

I_2O_5 Oxidation of 1-Hydroxy-1,2,3,4,-tetrahydrocarbazole (5)——Iodine pentoxide (800 mg, 2.40 mmol) was added to a solution of **5** (374 mg, 2.00 mmol) in 50 ml of 80% aqueous THF and the mixture was stirred at room temperature for 50 min. After general work up described above, the crude residue was purified by flash chromatography (ethyl acetate : benzene = 1 : 1) to obtain **7** (171 mg, 39%) as an unstable solid and **6** (145 mg, 36%); mp 147—148 °C (from ethyl acetate). IR ($CHCl_3$): 3340, 1710, 1620 cm^{-1}. MS *m/z*: 203 (M^+), 175, 146, 128. UV λ_{max}^{EtOH} nm: 253, 282; λ_{min}^{EtOH} nm: 228. NMR ($CDCl_3$) δ: 1.5—2.6 (6H, m), 4.4 (1H, m), 6.65—7.4 (4H, m), 8.24 (1H, br). *Anal.* Calcd for $C_{12}H_{13}NO_2$: C, 70.91; H, 6.45; N, 6.89. Found: C, 70.61; H, 6.44; N, 7.02.

The Spiroketone (8)——A solution of **6** (35 mg, 0.172 mmol) in 1 ml of CH_2Cl_2 was added dropwise to a suspension of PCC (185 mg, 0.86 mmol) and Celite (1.0 g) in 4 ml of dry CH_2Cl_2 and the reaction mixture was stirred for 4 h. The mixture was diluted with 5 ml of ether and filtered through a short column packed with silica gel. After concentration of the filtrate, the residue was purified by silica gel column chromatography (ethyl acetate : hexane = 2 : 3) to give **8** (28 mg, 80%) as colorless crystals; mp 165—167 °C (from ethyl acetate). IR ($CHCl_3$): 3450, 1775, 1710, 1620 cm^{-1}. MS *m/z*: 201 (M^+), 146. NMR ($CDCl_3$) δ: 2.00—2.86 (m, 6H), 6.82—7.36 (m, 4H), 7.80 (br, 1H). *Anal.* Calcd for $C_{12}H_{11}NO_2$: C, 71.62; H, 5.51; N, 6.96. Found: C, 71.71; H, 5.49; N, 6.98.

The Spirolactone (9)——The hemiacetal **7** (18 mg, 0.082 mmol) was treated with PCC (106 mg, 0.49 mmol) and Celite (1.2 g) in 4 ml of dry CH_2Cl_2 for 7 h. After work-up as described above, the crude residue was purified by silica gel preparative TLC (ethyl acetate : hexane = 1 : 1) to give the lactone **9** (12 mg, 67%); mp 134—135 °C (from ethyl acetate–hexane). IR ($CHCl_3$): 3440, 1740, 1625 cm^{-1}. MS *m/z*: 217 (M^+), 189, 161, 146, 133. *Anal.* Calcd for $C_{12}H_{11}NO_3$: C, 66.35; H, 5.10; N, 6.45. Found: C, 66.19; H, 5.11; N, 6.46.

Acknowledgment We gratefully acknowledge financial support for this work by a Grant-in-Aid for Special Project Research (No. 60119006, to Professor Michio Kobayashi) from the Ministry of Education, Science and Culture, Japan. We also thank Professors Osamu Yonemitsu and Masakatsu Shibasaki, and Dr. Takeshi Wakamatsu (Hokkaido University), for their encouragement and helpful suggestions.

References and Notes

1) R. J. Sundberg, "The Chemistry of Indoles," Academic Press, New York, 1979, pp. 282—315.
2) B. Witkop, J. B. Patrick, and M. Rosenblum, *J. Am. Chem. Soc.*, **73**, 2641 (1951).
3) F. Y. Chen and E. Leete, *Tetrahedron Lett.*, **1963**, 2013.
4) B. Hughes and H. Suschitzky, *J. Chem. Soc.*, **1965**, 875.
5) L. J. Dolby and D. L. Booth, *J. Am. Chem. Soc.*, **88**, 1049 (1966).
6) S. Sakai, A. Kubo, K. Katsuura, K. Mochinaga, and M. Ezaki, *Chem. Pharm. Bull.*, **20**, 76 (1972).
7) M. F. Bartlett, D. F. Dickel, and W. I. Taylor, *J. Am. Chem. Soc.*, **80**, 126 (1958).
8) Y. Oikawa and O. Yonemitsu, *J. Org. Chem.*, **42**, 1213 (1977).
9) B. Witkop and S. Goodwin, *J. Am. Chem. Soc.*, **75**, 3371 (1953) and references cited therein.
10) *a*) M. Nakagawa, S. Kato, S. Kataoka, and T. Hino, *J. Am. Chem. Soc.*, **101**, 3136 (1979); *b*) M. Nakagawa, S. Kato, S. Kataoka, S. Kadota, H. Watanabe, H. Okajima, T. Hino, and B. Witkop, *Chem. Pharm. Bull.*, **29**, 1013 (1981).
11) *a*) Y. Ban, K. Yoshida, J. Goto, and T. Oishi, *J. Am. Chem. Soc.*, **103**, 6990 (1981); *b*) Y. Ban, K. Yoshida, J. Goto, T. Oishi, and E. Ishigamori, *Tetrahedron*, **39**, 3657 (1983).
12) *a*) T. Shioiri, K. Ishizumi, and S. Yamada, *Chem. Pharm. Bull.*, **15**, 1010 (1967); *b*) K. Ishizumi, T. Shioiri, and S. Yamada, *ibid.*, **15**, 863 (1967).
13) M. Muhlstadt and W. Treibs, *Ann.*, **608**, 38 (1957).
14) Oxidation of cyclopent[*b*]indole immediately afforded a dark tar.
15) W. H. Perkin and S. G. P. Plant, *J. Chem. Soc.*, **1928**, 2583.

16) C. U. Rogers and B. B. Corson, "Organic Syntheses," Coll. Vol. IV, ed. by N. Rabjohn, John Wiley and Sons, Inc., New York, 1963, p. 884.
17) J. S. Beer, L. McGrath, and A. Robertson, *J. Chem. Soc.*, **1950**, 2118.
18) Dolby and Booth reported[5] that the oxidation of **3a** with H_5IO_6 afforded no 1-oxotetrahydrocarbazole (**4a**) although at that time they were not able to characterize the products. In our experiments, unstable products **6** and **7** were separated on TLC only when benzene–ethyl acetate was used as a developing solvent.

[Chem. Pharm. Bull. 35(12)4705—4710(1987)]

Reaction of 1,2,4-Triazines with *N*-Phenylmaleimide[1)]

MASAHARU OKI* and SADAKATSU SHIMADA

Production Technology Research Laboratories, Daiichi Seiyaku Co., Ltd., 16–13, Kitakasai, 1-chome, Edogawa-ku, Tokyo 134, Japan

(Received April 30, 1987)

Diels–Alder addition of *N*-phenylmaleimide (**2**) to 1,2,4-triazines (**1**) occurred across carbons 3 and 6 of the triazines to give 1 : 1 adducts. After losing nitrogen, they gave dihydropyridines, which underwent a variety of further reactions. Pyridine derivatives (**3**) and bis-adducts (**4**) containing a 2-azabicyclo[2.2.2]oct-2-ene residue were obtained.

Keywords——1,2,4-triazine; Diels–Alder reaction; 1*H*-pyrrolo[3,4-*c*]pyridine-1,3(2*H*)-dione; *N*-phenylmaleimide; azapentacyclo[5.5.2.0^{2,6}.0^{8,12}]tetradec-13-ene

Inverse electron demand Diels–Alder reactions of 1,2,4-triazines have been well documented by Neunhoeffer,[2)] and have been found to be useful synthetic routes to a variety of complex heterocyclic systems.[3)] However, there are few reports on the reaction of 1,2,4-triazines with electron-deficient dienophiles. Neunhoeffer *et al.*[4)] have reported the reaction of 1,2,4-triazines with dimethyl acetylenedicarboxylate (DMAD), an electron-

TABLE I. Reaction of 1,2,4-Triazines (**1**) with *N*-Phenylmaleimide (**2**)

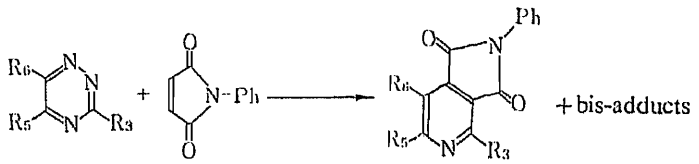

1 **2** **3** **4**

Compd. No.	Substituent			Molar ratio 2/1	Reaction temp. (°C)	Conditions time (h)	Yield (%)[a)]		Recovery (%)[a)]
	R_3	R_5	R_6				3	4	1
1a	SMe	H	H	1.8	140	120	38	—	—
1b	$N(Me)_2$	H	H	1.5	110	48	5	19	25
1c	OMe	H	H	1	140	72	8	2	—
1d	SMe	Me	Me	1.6	140	72	30	—	13
1e	$N(Me)_2$	Me	Me	1.5	110	72	5	47	26
1f	OMe	Me	Me	1.7	140	48	2	54	30
1g	SMe	Ph	Ph	1	140	72	12	—	88
1h	SMe	Ph	H	1	140	72	23	30	17
1i	$N(Me)_2$	Ph	H	1.8	140	72	7	18	25
1j	COOEt	H	H	1.5	140	12	20	7	40
1k	COOEt	Ph	Ph	1.9	140	54	41	—	40
1l	H	Me	OMe	1.5	140	64	Trace	—	—
1m	H	Ph	OMe	1.5	140	64	13	—	38
1n	$N(Me)_2$	Ph	Ph	1	140	120	—	—	100

a) Isolation yields.

TABLE II. 1*H*-Pyrrolo[3,4-*c*]pyridine-1,3(2*H*)-diones (3)

Compd. No.	mp (°C)	IR (KBr): cm^{-1}	Formula	Analysis (%) Calcd (Found)			
				C	H	N	S
3a	237—239	1770 1710	$C_{14}H_{10}N_2O_2S$	62.21 (62.30	3.73 3.86	10.36 10.41	11.86 11.88)
3b	179—180	1750 1710	$C_{15}H_{13}N_3O_2$	67.41 (67.04	4.90 4.98	15.72 15.34	— —)
3c	220—222	1770 1725	$C_{14}H_{10}N_2O_3$	66.14 (65.87	3.96 3.94	11.02 11.03	— —)
3d	233—234	1760 1710	$C_{16}H_{14}N_2O_2S$	64.41 (64.31	4.73 4.81	9.39 9.39	10.75 10.43)
3e	167—169	1750 1710	$C_{17}H_{17}N_3O_2$	69.14 (68.71	5.80 5.89	14.23 13.99	— —)
3f	289—241	1765 1720	$C_{16}H_{14}N_2O_3$	68.08 (68.09	5.00 5.14	9.92 9.89	— —)
3g	>290	1765 1710	$C_{26}H_{18}N_2O_2S$	73.91 (73.56	4.29 4.43	6.63 6.38	7.59 7.33)
3h	228—229	1775	$C_{20}H_{14}N_2O_2S$	69.35 (69.09	4.07 4.22	8.09 7.95	9.26 9.57)
3i	168—171	1755 1710	$C_{21}H_{17}N_3O_2$	73.46 (73.14	4.99 4.98	12.24 12.52	— —)
3j	148—150	1780 1730 1720	$C_{16}H_{12}N_2O_4$	64.86 (65.04	4.08 4.31	9.45 9.41	— —)
3k	202—204	1775 1740 1720	$C_{28}H_{21}N_2O_4$	74.82 (74.41	4.70 4.61	6.23 6.02	— —)
3m	178—182	1770 1720	$C_{20}H_{14}N_2O_3$	72.72 (72.36	4.27 4.34	8.48 8.36	— —)

Compd. No.	^{1}H-NMR ($CDCl_3$) J=Hz
3a	2.66 (3H, s), 7.43 (5H, brs), 7.47 (1H, d, J=5), 8.87 (1H, d, J=5)
3b	3.32 (6H, s), 7.05 (1H, d, J=5), 7.40 (5H, brs), 8.55 (1H, d, J=5)
3c	4.18 (3H, s), 7.42 (1H, d, J=5), 7.43 (5H, brs), 8.65 (1H, d, J=5)
3d	2.66 (3H, s), 3.65 (6H, s), 7.40 (5H, brs)
3e	2.50 (3H, s), 2.53 (3H, s), 3.25 (6H, s), 7.48 (5H, brs)
3f	2.57 (6H, s), 4.10 (3H, s), 7.39 (5H, brs)
3g	2.72 (3H, s), 7.2—7.5 (15H, m)
3h	2.79 (3H, s), 7.4—7.65 (8H, m), 7.92 (1H, s), 8.0—8.3 (2H, m)
3i	3.43 (6H, s), 7.3—7.6 (8H, m), 7.6 (1H, s), 8.0—8.25 (2H, m)
3j	1.48 (3H, t, J=7.5), 4.60 (2H, q, J=7.5), 7.4—7.7 (5H, m), 8.10 (1H, d, J=5), 9.22 (1H, d, J=5)
3k	1.49 (3H, t, J=7.5), 4.63 (2H, q, J=7.5), 7.2—7.65 (15H, m)
3l	2.65 (3H, s), 4.32 (3H, s), 7.43 (5H, brs), 8.70 (1H, s)
3m	4.20 (3H, s), 7.4—7.7 (8H, m), 7.8—8.2 (2H, m), 9.04 (1H, s)

deficient acetylenic dienophile, to obtain pyrimidine or pyridine derivatives through the Diels–Alder cycloaddition reaction only in the case of 1,2,4-triazines which have two or three dialkylamino substituents. The addition reaction of 1,2,4-triazines with electron-deficient

TABLE III. Physicochemical Data for the Bis-adducts (4)

Compd. No.	mp (°C)	IR (KBr): cm^{-1}	^{1}H-NMR ($CDCl_3$) J=Hz	Formula	Analysis (%) Calcd (Found)			
					C	H	N	S
4b	190—192	1775 1720	2.86 (6H, s), 3.08 (2H, dd, J=3, 9), 3.45 (2H, d, J=9), 3.90 (1H, m), 7.0—7.5 (10H, m), 8.25 (1H, d, J=3.5)	$C_{25}H_{22}N_4O_4$	*m/z* 443 (M+1)[a]			
4c	270—275	1775 1720	3.61 (2H, dd, J=9, 3), 3.67 (3H, s), 3.87 (2H, d, J=9), 4.07 (1H, m), 6.9—7.7 (10H, m), 8.40 (1H, d, J=3.5) (DMSO-d_6)	$C_{24}H_{19}N_3O_5$	*m/z* Calcd for M^+ 429.133 (Found: 429.131)[b]			
4e	165—207 (dec.)	1770 1720	2.04 (3H, s), 2.10 (3H, s), 2.85 (2H, d, J=9), 2.87 (6H, s), 3.47 (2H, d, J=9), 7.0—7.5 (10H, m)	$C_{27}H_{26}N_4O_4$	*m/z* Calcd for M^+ 470.195 (Found: 470.189)[b]			
4f	284—286	1775 1720	2.00 (3H, s), 2.07 (3H, s), 2.86 (2H, d, J=8.5), 3.47 (2H, d, J=8.5), 3.79 (3H, s), 7.0—7.5 (10H, m)	$C_{26}H_{23}N_3O_5$	68.26 (68.20	5.07 5.11	9.18 9.08	— —)
4h	>290	1775 1720	2.57 (3H, s), 3.48 (4H, m), 4.80 (1H, t, J=3), 6.9—7.1 (3H, m), 7.3—7.6 (10H, m), 7.9—8.0 (2H, m)	$C_{30}H_{23}N_3O_4S$	69.08 (68.92	4.44 4.55	8.06 8.04	6.15 6.51)
4i	170—175	1770 1715	3.02 (6H, s), 3.43 (2H, dd, J=3, 9), 3.73 (2H, d, J=9), 4.76 (1H, t, J=3), 6.8—7.1 (3H, m), 7.3—7.7 (10H, m), 7.9—8.1 (2H, m)	$C_{31}H_{26}N_4O_4$	*m/z* 519 (M+1)[a]			
4j	>290	1775 1750	1.46 (3H, t, J=7.5), 3.40 (2H, dd, J=3, 9), 3.88 (2H, d, J=9), 4.19 (1H, dd, J=3, 4), 4.57 (2H, q, J=7.5), 7.1—7.6 (10H, m), 8.56 (1H, d, J=4)	$C_{26}H_{21}N_3O_6$	66.24 (66.04	4.49 4.46	8.91 9.16	— —)

a) Fast atom bombardment mass spectrum. *b*) High-resolution mass spectrum.

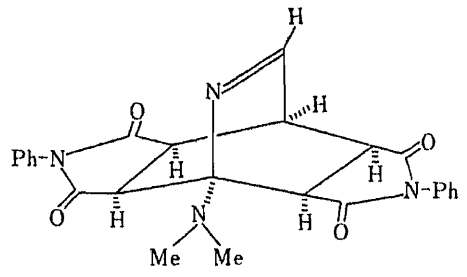

4b

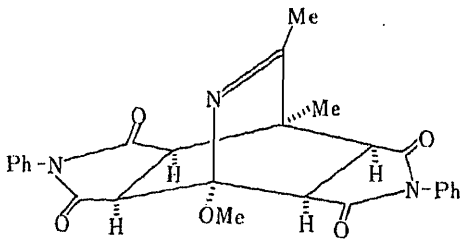

4f

Chart 1

olefins has not yet been reported. Here we wish to report the reaction of 1,2,4-triazines with *N*-phenylmaleimide, an electron-deficient olefinic dienophile.

Treatment of triazines (**1a—m**) with equimolar to two-fold molar excess of *N*-phenylmaleimide gave 1*H*-pyrrolo[3,4-*c*]pyridine-1,3(2*H*)-diones (**3a—m**) and the bis-adducts (**4b, c, e, f, h—j**). In the case of 3-dimethylamino-5,6-diphenyl-1,2,4-triazine (**1n**) no adduct was obtained, and the starting material was recovered quantitatively. These results are summarized in Table I.

The structure of the products were confirmed by their elemental analysis and spectral data. The infrared (IR) spectra of **3** and **4** showed characteristic absorptions between 1700—

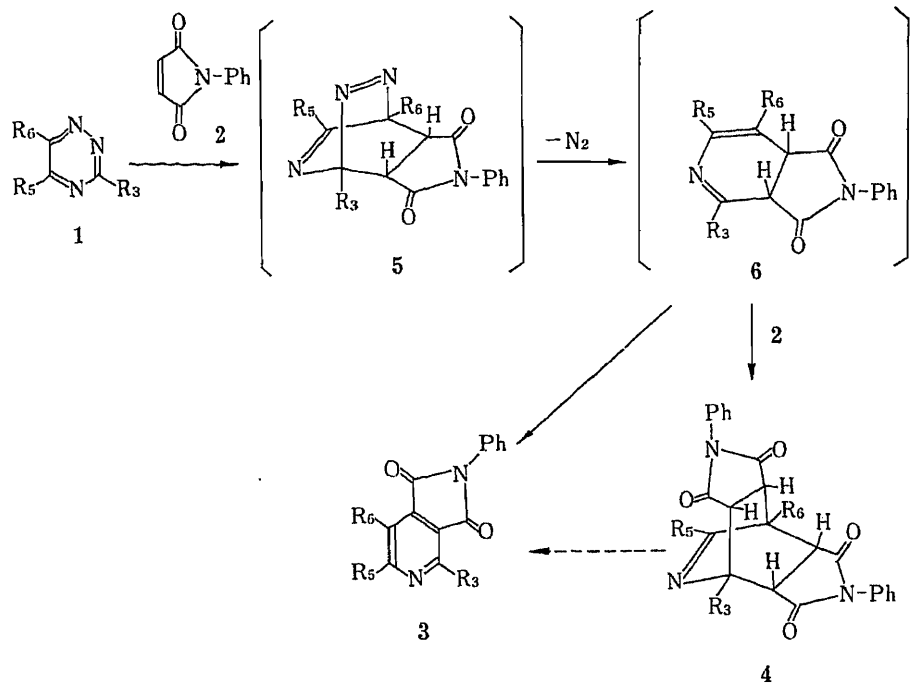

Chart 2

1780 cm^{-1} attributable to carbonyl groups. The proton nuclear magnetic resonance (^{1}H-NMR) spectra of all the products also showed signals consistent with the assigned structures. For example, that of **3a** showed signals of the pyridine ring protons at δ 7.47 (d, J=5 Hz) and 8.87 (d, J=5 Hz), methyl protons at δ 2.66 and phenyl protons at δ 7.43. The ^{1}H-NMR spectrum of **4b** showed signals of methyl protons at δ 2.86 (6H, s), azabicyclooctene residue protons at δ 3.08 (2H, dd, J=3, 9 Hz), 3.45 (2H, d, J=9 Hz), 3.90 (1H, dd, J=3, 3.5 Hz) and 8.25 (1H, d, J=3.5 Hz), and phenyl protons at δ 7.0—7.5 (10H, m).

The coupling constant (3 Hz) between the bridgehead proton and the vicinal proton suggests that their configuration is *cis*. The ^{13}C-NMR spectrum of **4f** showed signals at δ 16.0, 22.5, 42.8, 43.6, 46.6, 51.6, 91.7, 126.8, 128.5, 128.9, 131.9, 171.8, 174.1 and 174.5 (ppm). These signals were assigned by the use of off-resonance and/or complete decoupling techniques. The ^{1}H- and ^{13}C-NMR patterns, in addition to the coupling constants, indicate that **4b** and **4f** have the symmetrical structures shown in Chart 1. Other bis-adducts probably have similar structures.

It appeared that **4e** was converted to **3e** on reflux in xylene. Possibly the conversion proceeded *via* retro Diels–Alder reaction, although we did not test for the formation of *N*-phenylmaleimide. We had anticipated this conversion because **4e** melted over a wide range. In the case of **4f**, the conversion did not occur under the same conditions.

On the basis of these results, the reaction process may be as shown in Chart 2. The addition occurs across carbons 3 and 6 of the triazine to give **5** as an intermediate. After loss of nitrogen, the dihydropyridine **6** may be formed, and *endo* addition of *N*-phenylmaleimide (**2**) occurs to give the bis-adduct (**4**). On the other hand, the pyridine derivative (**3**) is provided by oxidation of **6**, and possibly also through **4**. It seems that the stability of 1,2,4-triazines and the steric constraints are important in the formation of these products, in addition with the electronic effect of the substituents. It is unexpected that addition products were obtained in the cases of **1j** and **1k**, but not in the case of **1n**. Neunhoeffer *et al.* reported no cycloaddition product in the case of **1c** and DMAD.[4a)]

In summary, we found that a number of 1,2,4-triazines afforded cycloaddition products

with *N*-phenylmaleimide. These are the first examples of Diels–Alder reaction of an electron-deficient olefin with 1,2,4-triazines. Further extensions of the cycloaddition of electron-deficient olefins with a variety of azines are under investigation.

Experimental

Melting points are uncorrected. IR spectra were recorded on a Hitachi model 260 spectrophotometer. NMR spectra were obtained on a JEOL model JNM-PMX 60 or a Hitachi R-20B at 60 MHz, or a Varian XL-200 spectrometer at 200 MHz. Chemical shifts are reported in δ (ppm) relative to tetramethylsilane as an internal standard. The following abbreviations are used: s=singlet, d=doublet, t=triplet, q=quartet, br=broad, and dd=double doublet. Mass spectra (MS) were recorded on a JEOL JMS-D300 or JEOL JMS-HX100 mass spectrometer. Column chromatography was performed on silica gel (Merck Kieselgel 60, 70—230 mesh).

Preparation of 1,2,4-Triazines (1)——3-Methylthio-, 3-dimethylamino-, and 3-methoxy-1,2,4-triazines (**1a—i, n**) were prepared from thiosemicarbazide (**7**), and 3-carboethoxy-1,2,4-triazines (**1j—k**) were prepared from ethyl thiooxalate (**8**) by a modification of the literature method.[5] 6-Methoxy-1,2,4-triazines (**1l, 1m**) were prepared following the procedure described later.[6] The structures of the products were confirmed largely on the basis of their ^{1}H-NMR data.

4,5-Dihydro-5-methyl-1,2,4-triazin-6(1*H*)-one (10a)——A solution of 5.0 g of hydrazine hydrate in 50 ml of ethanol was added dropwise to a solution of 14.5 g of *N*-formylalanine ethylester (**9a**) in 150 ml of ethanol. The mixture was stirred for 3 d at room temperature to afford 3.66 g of precipitate, which was filtered off, and the filtrate was evaporated to give a further 2.8 g. The combined precipitate was heated at 140 °C for 7 h, and the residue was recrystallized from methanol–chloroform to give 2.5 g of **10a** (28.6%), mp 136—139 °C. ^{1}H-NMR (DMSO-d_6) δ: 1.23 (3H, d, J=7 Hz), 3.88 (1H, q, J=7 Hz), 6.82 (1H, d, J=4.5 Hz), 7.00 (1H, br s), 10.0 (1H, br s).

4,5-Dihydro-5-phenyl-1,2,4-triazin-6(1*H*)-one (10b)——*N*-Formylphenylalanine ethylester (**9b**) (2.1 g) and P_2S_5 (0.5 g) were refluxed in toluene for 1 h. After decantation, 0.5 g of hydrazine hydrate in 5 ml of ethanol was added and the whole was refluxed for a further 2 h. After standing overnight, the solution was evaporated to dryness. The residue was recrystallized from $CHCl_3$ to afford 0.9 g of **10b** (51%). ^{1}H-NMR (DMSO-d_6) δ: 4.95 (1H, d, J=2 Hz), 7.05 (1H, d, J=5 Hz), 7.39 (5H, s), 7.60 (1H, br), 10.3 (1H, br).

5-Methyl-1,2,4-triazin-6(1*H*)-one (11a)——NaOAc (10 g) was added to a solution of 11.3 g of **10a** in $CHCl_3$ (200 ml) and methanol (200 ml). Then 12 g of Br_2 was added dropwise at −5 °C. After being neutralized by addition of Na_2CO_3 solution, the reaction mixture was extracted with $CHCl_3$. The organic layer was dried with Na_2SO_4 and evaporated to dryness, and the residue was purified by silica gel chromatography to give 5.8 g of **11a**, mp 98—100 °C. IR (KBr): 1670 cm^{-1}. ^{1}H-NMR ($CDCl_3$) δ: 2.60 (3H, s), 8.26 (1H, s), 11.5—12.5 (1H). MS *m/z*: 111 (M^+). (**11a** easily dimerized upon heating.)

5-Phenyl-1,2,4-triazin-6(1*H*)-one (11b)——Compound **10b** (1.75 g) was treated in a manner similar to that described above to give **11b**, mp 166—169 °C. *Anal.* Calcd for $C_9H_7N_3O$: C, 62.42; H, 4.07; N, 24.27. Found: C, 62.06; H, 4.25; N, 24.09. IR (KBr): 1650 cm^{-1}. ^{1}H-NMR ($CDCl_3$) δ: 7.5—7.8 (3H, m), 8.45 (1H, s), 8.6—8.85 (2H, m), 12.1—12.6 (1H).

6-Methoxy-5-methyl-1,2,4-triazine (1l)——Compound **11a** (2.5 g) was treated with CH_2N_2 in ether. After standing for 3 h at room temperature, the reaction mixture was concentrated. Separation of the residue by silica gel column chromatography gave a mixture (1 : 5) of **1l** and the *N*-methylated compound (**12**) (1.5 g). Recrystallization from hexane yielded 0.9 g of **12**, mp 49—50 °C. ^{1}H-NMR ($CDCl_3$) δ: 2.56 (3H, s), 3.78 (3H, s), 8.12 (1H, s). (**12** gave no reaction product with **2**.) The filtrate was evaporated to give a 1 : 1 mixture of **1l** and **12**. This mixture was used for the addition reaction with **2**. **1l**; ^{1}H-NMR ($CDCl_3$) δ: 2.53 (3H, s), 4.21 (3H, s), 9.17 (1H, s).

6-Methoxy-5-phenyl-1,2,4-triazine (1m)——A mixture of 1.0 g of **11b** and 1 ml of $POCl_3$ was refluxed for 15 min. The reaction mixture was concentrated *in vacuo*, and Na (260 mg) in 50 ml of methanol was added to the residue. After being refluxed for 5 min, the reaction mixture was evaporated to dryness and the residue was extracted with $CHCl_3$. The extract was dried over Na_2SO_4. Removal of the solvent by evaporation left the residue, which was chromatographed on silica gel to afford **1m** (0.85 g, 78%), mp 42—46 °C. ^{1}H-NMR ($CDCl_3$) δ: 4.32 (3H, s), 7.4—7.7 (3H, m), 8.2—8.5 (2H, m), 9.43 (1H, s).

Dimerization of 11a[7]——**11a** was heated at 100 °C on an oil bath. The solid residue showed a different character from that of **11a**, indicating that the compound was the dimer of **11a**. The data are shown below: MS *m/z*:222 (M^+), ^{1}H-NMR ($CDCl_3$) δ: 1.40 (3H, s), 3.07 (2H, d, J=3 Hz), 6.76 (1H, d, J=4 Hz), 7.05 (1H, d, J=4 Hz, disappeared with D_2O addition), 8.25 (1H, s), 10.2 (1H, s, disappeared with D_2O addition), 11.5—12.5 (1H, br).

Preparation of 3e from 4e——Compound **4e** (200 mg) was refluxed in xylene (30 ml) for 21 h, then the reaction mixture was concentrated *in vacuo*, and the residue was chromatographed on a silica gel column. Elution with $CHCl_3$ gave **3e** (50 mg, 40%).

Reaction of 1,2,4-Triazines (1) with *N*-Phenylmaleimide (2) (General Procedure)——A mixture of 400 mg of the 1,2,4-triazine **1a** and 1.0 g of *N*-phenylmaleimide (**2**) was refluxed in 60 ml of xylene for 120 h. The reaction mixture

was chromatographed on a silica gel column with chloroform–methanol to give 320 mg of **3a**. The starting material was seen on a thin layer chromatogram of the reaction mixture, but could not be separated in this case.

Similarly, each of **1b**—**n** was refluxed for a specified period with **2** in an appropriate solvent (benzene, toluene, xylene). The reaction mixture was treated according to the above procedure. A part of **4h** and **4j** appeared as a precipitate in the reaction mixture, and was filtered off before proceeding as noted above. These results are summarized in Table I. The data for **3** and **4** are given in Tables II and III.

Acknowledgements The authors wish to express their thanks to Prof. F. Yoneda, Faculty of Pharmaceutical Sciences of Kyoto University, for his encouragement. Thanks are also due to the members of the analytical section for elemental analysis and spectral measurements.

References and Notes

1) A part of this work was presented at The 101st Annual Meeting of the Pharmaceutical Society of Japan, Kumamoto, April 1981.
2) H. Neunhoeffer and P. F. Wiley, "Chemistry of 1,2,3-Triazines, Tetrazines and Pentazines," Vol. 33 in the series "The Chemistry of Heterocyclic Compounds," ed. by A. Weissberger and E. C. Taylor, Wiley-Interscience, New York, 1978, pp. 189—1072.
3) See, among others: *a*) D. L. Boger, J. S. Panek, and M. M. Meier, *J. Org. Chem.*, **47**, 895 (1982); *b*) E. C. Tailor and J. E. Macor, *Tetrahedron Lett.*, **26**, 2419 (1985); *c*) D. L. Boger, S. R. Duff, J. S. Panek, and M. Yasuda, *J. Org. Chem.*, **50**, 5782 (1985); *d*) L. Maggiora and M. P. Mertes, *ibid.*, **51**, 950 (1986).
4) *a*) H. Neunhoeffer and B. Lehmann, *Justus Liebigs Ann. Chem.*, **1977**, 1413; *b*) H. Neunhoeffer, B. Lehmann, and E. Ewald, *ibid.*, **1977**, 1421, 1718.
5) *a*) P. Schmidt and J. Druey, *Helv. Chim. Acta*, **38**, 1560 (1955); *b*) W. W. Paudler and J. H. Barton, *J. Org. Chem.*, **31**, 1720 (1966); *c*) H. Neunhoeffer, H. Hennig, H.-W. Frühauf, and M. Mutterrer, *Tetrahedron Lett.*, **1969**, 3147; *d*) W. W. Paudler and T.-K. Chen, *J. Heterocycl. Chem.*, 7, 767 (1970); *e*) H. Neunhoeffer and B. Lehmann, *Chem. Ber.*, **109**, 1113 (1976).
6) *a*) K. L. Leschinsky and J. P. Chupp, *J. Heterocycl. Chem.*, **17**, 1621 (1980); *b*) E. C. Tailor and J. E. Macor, *Tetrahedron Lett.*, **26**, 2415 (1985).
7) *a*) J. Adams and R. G. Shepherd, *Tetrahedron Lett.*, **1968**, 2747; *b*) D. K. Krass, T.-K. Chen, and W. W. Paudler, *J. Heterocycl. Chem.*, **10**, 343 (1973).

[Chem. Pharm. Bull. 35(12)4711—4716(1987)]

Reaction of Cyclic Phosphites with Haloacetones

IWAO MORITA,* MASAMI TSUDA, MASAHIRO KISE, and MAKOTO SUGIYAMA

Research Laboratories, Nippon Shinyaku Co., Ltd., Nishiohji-hachijo, Minami-ku, Kyoto 601, Japan

(Received May 12, 1987)

Treatment of various cyclic phosphites (**1**), *e.g.*, 2-methoxy-1,3,2-dioxaphosphorinane (**1a**), 2-methoxy-5,5-dimethyl-1,3,2-dioxaphosphorinane (**1b**) and 2-methoxy-1,3,2-dioxaphosphorane (**1c**), with haloacetones (**2**) gave cyclic Arbuzov products (**3**), cyclic Perkow products (**4**), cyclic methylphosphonates (**5**), and acyclic products (**6—8**). Compound **1a** gave all of the products (**3a**, **4a**, **5a**, **6ag**, **7ag**, **8ag**). However, cyclic phosphites with substituents in the ring (**1b**, **1d**) gave only the cyclic products (**3—5**). The five-membered ring phosphite (**1c**) yielded only the acyclic products (**6cg**, **7cg**). Treatment of **1a** with chloroacetone gave only the Perkow products (**4a**, **7ah**). Cyclic phosphite (**1f**) with a 2-benzyloxy substituent afforded simply the cyclic products (**3a**, **4a**, **9**). A mechanistic interpretation of these reactions is presented.

Keywords——cyclic phosphite; haloacetone; cyclic acetonylphosphonate; cyclic enol phosphate; Arbuzov reaction; Perkow reaction

In organophosphorus chemistry, it is well known that trialkyl phosphites react with α-halocarbonyl compounds to give enol phosphates (the Perkow reaction[1]) and/or 2-oxoalkylphosphonates (the Arbuzov reaction[2]). Both reactions depend on the nature of the compounds and the conditions employed. The 2-oxoalkylphosphonates obtained by means of the Arbuzov reaction can serve as useful synthetic intermediates for the synthesis of α,β-unsaturated ketones.[3] However, cyclic phosphites have not been reported to react with α-halocarbonyl compounds. We previously reported[4,5] syntheses of cyclic acetonylphosphonates which were key intermediates of 1,4-dihydropyridine-5-cyclic phosphonates with calcium antagonistic activity. We now describe the reaction of cyclic phosphites with α-haloacetones.

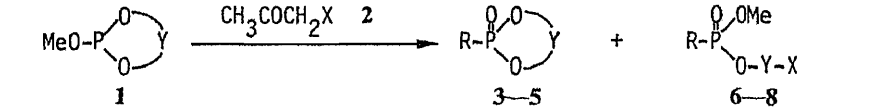

1: **1a**: Y = $-CH_2CH_2CH_2-$; **1b**: Y = $-CH_2C(Me)_2CH_2-$; **1c**: Y = $-CH_2CH_2-$; **1d**: Y = $-C(Me)_2-C(Me)_2-$; **1e**: Y = $-CH_2CH=CHCH_2-$

2: **2g**: X = Br; **2h**: X = Cl; **2i**: X = I

3—5: **3**: R = CH_3COCH_2-; **4**: R = $CH_2=C(Me)-O-$; **5**: R = Me

6—8: **6**: R = CH_3COCH_2-; **7**: R = $CH_2=C(Me)-O-$; **8**: R = Me

Chart 1

Results and Discussion

In the usual Arbuzov reaction, haloacetones are added to trialkyl phosphites heated to 80—120 °C. The reaction of the cyclic phosphite (**1a**) with bromoacetone was carried out under the same conditions (method A) to afford the cyclic methylphosphonate (**5a**), the acyclic products (**6ag**, **7ag**, **8ag**), which are not obtained from trialkyl phosphites, plus the acetonylphosphonate (**3a**) (an Arbuzov product) and the enol phosphate (**4a**) (a Perkow reaction product).

The cyclic phosphite (**1b**), with two methyl groups at the 5-position, yielded the cyclic methylphosphonate (**5b**), and other normal products but no acyclic products. In the reactions of cyclic phosphites with alkyl halides, the cyclic phosphites were less reactive than the acyclic phosphites.[6] The above results, however, suggest that the cyclic phosphites (**1**) are more reactive than the trialkyl phosphites, because **1** formed **5** and **8**. Therefore, to avoid the formation of **5**, the reaction was carried out at room temperature or below with a mixture of **1** and bromoacetone, in which an exothermic reaction occurred (method B). In method B, the yields of the acetonylphosphonates (**3**) and the enol phosphates (**4**) were increased about 1.2 and 1.6—1.7 times, respectively, but that of the methylphosphonates (**5**) was decreased to one-third. The yield of acyclic products was unaffected. In the same manner as in method B, the reaction of various cyclic phosphites (**1a—f**) with haloacetones (**2g—i**) was carried out. These results are summarized in Table I.

The reaction of 2-methoxy-1,3,2-dioxaphosphorane (**1c**) (five-membered ring) with bromoacetone afforded only the acyclic products (**6cg**, **7cg**); the cyclic acetonylphosphonate (**3c**) was not obtained, presumably because of the instability of its ring. However, 4,4,5,5-tetramethyl-1,3,2-dioxaphosphorane (**1d**) afforded the cyclic acetonylphosphonate (**3d**) in 53% yield, and no acyclic products were obtained. The phosphite (**1e**) (seven-membered ring) gave mainly the acyclic products (**6eg**, **7eg**), with acetonylphosphonate (**3e**) as a minor product (10%).

On the other hand, the reaction of **1a** with chloroacetone by method B gave mainly the enol phosphate (**4a**) in 70% yield; the acetonylphosphonate (**3a**) was scarcely detected. In the reaction with iodoacetone, **1a** yielded the same products as with bromoacetone, but in different ratios; that is, the yield of Arbuzov products was 50% more and that of the Perkow products was 29% (compared to method B) less than with bromoacetone.

When 2-benzyloxy-1,3,2-dioxaphosphorinane (**1f**) was used instead of **1a**, although

Table I. Products of the Reaction of Cyclic Phosphites with Haloacetones

Run	Phosphite 1	Haloacetone X	Method[a]	Product						
				3	4	5	6	7	8	9
1	**1a**	Br	A	27	24	25	11	3	8	
2	**1a**	Br	B	33	38	8	11	3	3	
3	**1b**	Br	A	45	20	22	—	—	—	
4	**1b**	Br	B	55	35	7	—	—	—	
5	**1c**	Br	B	—	—	—	42	18	—	
6	**1d**	Br	B	53	22	Trace	—	—	—	
7	**1e**	Br	B	10	—	—	17	3	—	
8	**1a**	Cl	B	—	70	—	—	8	—	
9	**1a**	I	B	51	9	15	8	—	1	
10	**1f**	Br	B	37	41					12

a) See Experimental.

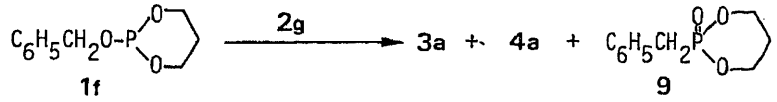

Chart 2

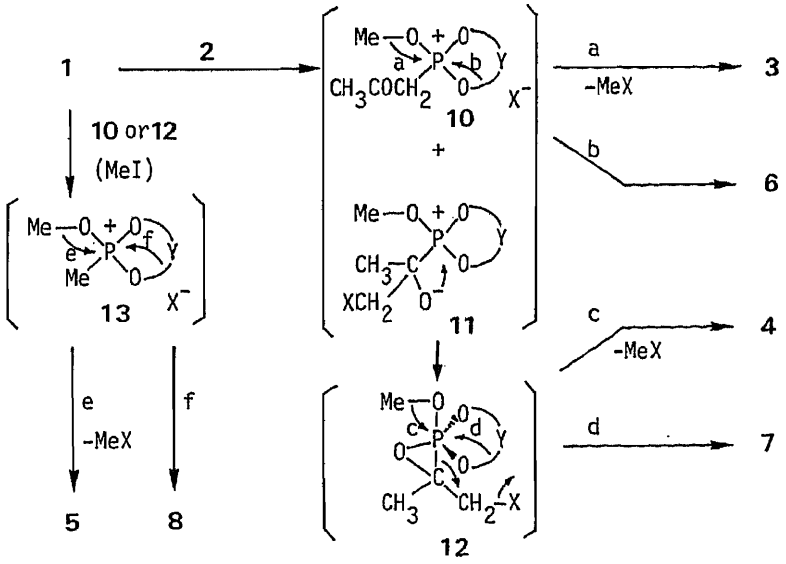

Chart 3

acyclic products were scarcely detected, the formation of **3a** was slightly increased because of the increase of the benzylphosphonate (**9**) and the decrease of the total yield.

Several mechanisms which would account for concomitant Arbuzov and Perkow reactions have been reported from a number of laboratories.[7-9] The mechanism of the Perkow reaction is especially complex, with more than one mechanism often being involved. Among the proposed mechanisms, we are interested in that suggested by Borowitz *et al.*,[8] which involves the initial attack of a phosphite on the carbonyl carbon followed by the formation of a three-membered-ring intermediate compound, and in that of Gillespie *et al.*,[9] which involves a penta-coordinate phosphepane intermediate. The reaction mechanism of the cyclic phosphites (**1**) with haloacetones may be represented by a modification of Borowitz's mechanism (Chart 3). The phosphonium salt (**10**) and/or the adduct (**11**) is first formed, then **10** gives the cyclic acetonylphosphonate (**3**) through path a and the acyclic product (**6**) through path b, and the phosphonium adduct (**11**) gives the enol phosphate (**4**) and the acyclic enol phosphate (**7**) *via* a quasi-three-membered-ring transition state (**12**).

The methylphosphonates (**5**, **8**) were supposed to be formed from the phosphonium salt (**13**), which in general could be obtained from the reaction of **1** with methyl halides. However, **1a** was recovered unchanged when a mixture of **1a** and excess methyl bromide was heated for a long time at atmospheric pressure. No formation of **5** or **8** was observed. This result suggests that **13** was not formed by the reaction with methyl bromide, but was formed by reaction with some other methylation agent, such as the intermediate (**10** or **12**).

In the reaction of **1a**, all the products in Chart 3 are formed. In the reaction of **1b**, the absence of the acyclic products (**6**, **7**, **8**) suggests that Br^- in the intermediates (**10**, **12**, **13**) does not attack a carbon atom in the ring because of steric hindrance by the substituent at the 5-position. The exclusive formation of the acyclic products (**6cg**, **7cg**) in the reaction of **1c** with bromoacetone suggests that the reaction proceeds through paths b and d because of the instability of the five-membered ring. The reason why **1d** does not yield acyclic products is

presumably the steric hindrance by the four methyl substituents. Compound **1e** with the seven-membered ring did not yield the enol phosphate (**4e**) during the reaction, suggesting that the intermediates (**11**, **12**) were not formed in considerable amounts in this case, although a small amount of **7eg** could be explained by the intermediary formation of **12**. More experiments are required to elucidate the mechanistic fearures of the reaction in detail.

The effect of the haloacetones differs with the halogen involved. Chloroacetone forms only the carbonyl adduct (**11**) because of the polarization induced on the carbonyl group by the electronegative Cl atom to give the Perkow products. With iodoacetone, the greater reactivity of I^- leads mainly to the formation of **10** rather than **11**; **5a** is also increased through **13**, which is formed by the reaction of **1a** with methyl iodide. It is known that the cyclic phosphites react with methyl iodide at room temperature.[6]

With a benzyloxy group substituted at the 2-position on the cyclic phosphite, the reaction proceeds through paths a and c because the dealkylation is much easier in this case than in the methyl derivative.

The effect of temperature on the Arbuzov and Perkow products was the same as in the acyclic phosphite reactions.[2]

Experimental

Melting points were determined with a Büchi melting point apparatus and are uncorrected. Infrared (IR) spectra were measured on a Hitachi IR-215 spectrophotometer. Mass spectra (MS) were measured on a Hitachi RMU-6M spectrometer (relative intensity %). Nuclear magnetic resonance (NMR) spectra were recorded on a Varian YX-200 spectrometer. Chemical shifts are given in δ (ppm) with tetramethylsilane as an internal standard. The following abbreviations are used: s = singlet, d = doublet, t = triplet, q = quartet, m = multiplet, br = broad. Column chromatography was performed by flash chromatography on Merck silica gel (Kieselgel F_{254} 60H).

Reaction of 2-Methoxy-1,3,2-dioxaphosphorinane (1a) with Bromoacetone——Method A: Bromoacetone (5.48 g, 0.04 mol) was added dropwise to the preheated (60 °C) phosphite **1a** (5.44 g, 0.04 mol) at a rate which kept the temperature at 120 °C without further heating, with stirring. The reaction mixture was stirred for 1 h at 70—80 °C and then cooled. The mixture was chromatographed on silica gel (hexane–AcOEt) to afford a mixture (3.39 g) of **3a** (27%) and **5a** (25%), **4a** (1.61 g, 24%), a mixture (1.78 g) of **6ag** (11%) and **8ag** (8%), and **7ag** (0.53 g, 3%). The yields (%) of mixture components were calculated from the NMR spectra (**3a**: CH_2COCH_3 and **5a**: CH_3. **6ag**: CH_2COCH_3 and **8ag**: CH_3).

Method B: A mixture of bromoacetone (5.48 g, 0.04 mol) and **1a** (5.44 g, 0.04 mol) was stirred at 10 °C, causing an exothermic reaction in which the temperature rose to 80 °C. When the evolution of methyl bromide gas had almost ceased, the mixture was kept at 60 °C for 1 h. The reaction mixture was chromatographed on silica gel (hexane–

2-Acetonyl-2-oxo-1,3,2-dioxaphosphorinane (**3a**)[4]: Distillation of the mixture of **3a** and **5a** obtained in method (3%), and **7ag** (0.50 g, 3%).

2-Acetonyl-1-oxo-1,3,2-dioxaphosphorinane (**3a**)[4]: Distillation of the mixture of **3a** and **5a** obtained in method B gave **3a** (2.3 g) as a second fraction [bp 158—160 °C (0.8 mmHg)].

2-Oxo-2-(2-propenyloxy)-1,3,2-dioxaphosphorinane (**4a**): bp 131—134 °C (0.3 mmHg), colorless oil. *Anal.* Calcd for $C_6H_{11}O_4P \cdot 1/2H_2O$: C, 38.49; H, 6.46. Found: C, 38.66; H, 6.06. MS *m/z* (%): 178 (M^+, 17), 139 (100). IR ν_{max}^{film} cm^{-1}: 1660, 1305, 1235, 1060, 1030. NMR ($CDCl_3$) δ: 1.70—1.86 (1H, m, C_5-H), 2.01 (3H, s, CH_3), 2.22—2.48 (1H, m, C_5-H), 4.35—4.60 (5H, m, $2\times OCH_2$, =CH), 4.81 (1H, t, J = 1 Hz, =CH).

2-Methyl-2-oxo-1,3,2-dioxaphosphorinane (**5a**): Distillation of the mixture of **3a** and **5a** obtained in method B gave **3a** (0.3 g) as a first fraction [bp 118—122 °C (0.8 mmHg)]. The oil obtained was crystallized from AcOEt, mp 98—99 °C. *Anal.* Calcd for $C_4H_9O_3P$: C, 35.30; H, 6.67. Found: C, 35.14; H, 7.02. MS *m/z* (%): 136 (M^+, 45), 80 (100). IR ν_{max}^{film} cm^{-1}: 1320, 1250, 1140, 1055. NMR ($CDCl_3$) δ: 1.58 (3H, d, J = 18 Hz, PCH_3), 1.90—2.22 (2H, m, CH_2), 4.12—4.32 (2H, m, OCH_2), 4.45—4.66 (2H, m, OCH_2).

3-Bromopropyl Methyl Acetonylphosphonate (**6ag**): Distillation of the mixture of **6ag** and **8ag** obtained in method A gave **6ag** (0.52 g) as a second fraction [bp 134—136 °C (0.5 mmHg)]. *Anal.* Calcd for $C_7H_{14}O_4P$: C, 30.79; H, 5.17. Found: C, 30.50; H, 5.44. MS *m/z* (%): 272 (M^+, 13), 193 (100). IR ν_{max}^{film} cm^{-1}: 1715, 1365, 1260, 1040, 1015. NMR ($CDCl_3$) δ: 2.21 (2H, q, J = 7 Hz, CH_2), 2.34 (3H, s, $COCH_3$), 3.12 (2H, d, J = 23 Hz, PCH_2), 3.50 (2H, t, J = 7 Hz, CH_2Br), 3.81 (3H, d, J = 11 Hz, $POCH_3$), 4.18—4.32 (2H, m, OCH_2).

3-Bromopropyl Methyl 2-Propenyl Phosphate (**7ag**): bp 120—123 °C (0.5 mmHg). *Anal.* Calcd for $C_7H_{14}BrO_4P$: C, 30.79; H, 5.17. Found: C, 29.38; H, 4.93. MS *m/z* (%): 273 (M^+, 0.9), 113 (100). IR ν_{max}^{film} cm^{-1}: 1660, 1280, 1250, 1030, 980. NMR ($CDCl_3$) δ: 1.97 (3H, s, CH_3), 2.23 (2H, q, J = 6 Hz, CH_2=), 3.52 (2H, t, J = 6 Hz, CH_2Br), 3.84 (3H,

d, J=11 Hz, OCH_3), 4.25 (2H, m, $POCH_2$); 4.54 (1H, s, =CH), 4.78 (1H, t, J=1 Hz, =CH).

3-Bromopropyl Methyl Methylphosphonate (**8ag**): **8ag** was not purified by the above distillation; therefore it was synthesized from **1a** by reaction with methyl bromide. **1a** (1.0 g) and methyl bromide (20 g) were heated in a sealed tube for 3 h at 100 °C. The reaction mixture was concentrated, and the residue was chromatographed on silica gel (hexane–AcOEt) to afford **8ag** (0.19 g, 11.2%), bp 113—115 °C (2 mmHg) as a colorless oil. *Anal.* Calcd for $C_5H_{12}BrO_3P$: C, 25.99; H, 5.24. Found: C, 25.43; H, 5.15. MS *m/z* (%): 151 (M−80; −HBr, 52.5), 111 (100). IR ν_{max}^{film} cm^{-1}: 1310, 1240, 1040, 1020. NMR ($CDCl_3$) δ: 1.50 (3H, d, J=18 Hz, PCH_3), 2.20 (2H, m, CH_2), 3.51 (2H, t, J=6 Hz, CH_2Br), 3.75 (3H, d, J=12 Hz, $POCH_3$), 4.11—4.25 (2H, m, $POCH_2$).

Reaction of 2-Methoxy-5,5-dimethyl-1,3,2-dioxaphosphorinane (1b) with Bromoacetone——Method A: Bromoacetone (5.48 g, 0.04 mol) was added dropwise to preheated (70 °C) **1b** (6.56 g, 0.04 mol) at a rate which kept the temperature at 120 °C without further heating, with stirring. The reaction mixture was stirred for 1 h at 70—80 °C and then cooled. The mixture was chromatographed on silica gel (hexane–AcOEt) to afford a mixture (5.16 g) of **3b** and **5b** (45% and 22%, respectively) and **4b** (1.65 g, 20%).

Method B: A mixture of bromoacetone (5.48 g, 0.04 mol) and **1b** (6.56 g, 0.04 mol) was stirred at 20 °C, causing an exothermic reaction in which the temperature rose to 120 °C. Work-up as for method B **1a** gave a mixture (4.96 g) of **3b** and **5b** (55% and 7%, respectively) and **4b** (2.32 g, 35%).

2-Acetonyl-5,5-dimethyl-2-oxo-1,3,2-dioxaphosphorinane (**3b**)[4]: Recrystallization of the above mixture (**3b** and **5b**; in method B) from ether gave **3b**, mp 91—92 °C.

5,5-Dimethyl-2-oxo-2-(2-propenyloxy)-1,3,2-dioxaphosphorinane (**4b**): mp 69—70 °C (recrystallization from iso-Pr_2O–ether). *Anal.* Calcd for $C_8H_{15}O_4P$: C, 46.60; H, 7.33. Found: C, 46.25; H, 7.14. MS *m/z* (%): 206 (M^+, 23), 99 (100). IR ν_{max}^{KBr} cm^{-1}: 1660, 1395, 1225, 1060, 1045, 1010. NMR ($CDCl_3$) δ: 0.90 (3H, s, CH_3), 1.30 (3H, s, CH_3), 2.00 (3H, d, J=1 Hz, =C–CH_3), 3.84—4.04 (2H, m, OCH_2), 4.14 (2H, d, J=10 Hz, OCH_2), 4.51—4.57 (1H, m, =CH), 4.79 (1H, t, J=1 Hz, =CH).

2,5,5-Trimethyl-2-oxo-1,3,2-dioxaphosphorinane (**5b**): The above mother liquid was concentrated and the residue was recrystallized from benzene–ether, mp 120—121 °C. *Anal.* Calcd for $C_6H_{13}O_3P$: C, 43.91; H, 7.98. Found: C, 43.66; H, 7.93. MS *m/z* (%): 164 (M^+, 2.3), 56 (100). IR ν_{max}^{KBr} cm^{-1}: 1475, 1320, 1255, 1050, 1010. NMR ($CDCl_3$) δ: 1.00 (3H, s, CH_3), 1.14 (3H, s, CH_3), 1.58 (3H, d, J=20 Hz, PCH_3), 3.77 (2H, dd, J=10, 15 Hz, OCH_2), 4.22 (2H, dd, J=8, 12 Hz, OCH_2).

Reaction of 2-Methoxy-1,3,2-dioxaphospholane (1c) with Bromoacetone——Method B: A mixture of bromoacetone (5.48 g, 0.04 mol) and **1c** (4.88 g, 0.04 mol) was stirred at room temperature, causing an exothermic reaction. After 20 min, the reaction mixture was heated at 60—70 °C for 1 h, then chromatographed on silica gel (hexane–AcOEt) to afford **4c** (1.15 g, 18%) and **6cg** (4.34 g, 42%) as an oil.

2-Bromoethyl Methyl Acetonylphosphonate (**6cg**): bp 135—140 °C (1 mmHg). *Anal.* Calcd for $C_6H_{12}BrO_4P \cdot 1/2H_2O$: C, 26.89; H, 4.89. Found: C, 26.80; H, 4.35. MS *m/z* (%): 259 (M^+, 0.9), 137 (100). IR ν_{max}^{film} cm^{-1}: 1710, 1255, NMR ($CDCl_3$) δ: 2.34 (3H, s, $COCH_3$), 3.15 (2H, d, J=23 Hz, PCH_2), 3.55 (2H, t, J=6 Hz, CH_2Br), 3.82 (3H, d, J=11 Hz, $POCH_3$), 4.31—4.46 (2H, m, $POCH_2$).

2-Bromoethyl Methyl 2-Propenyl Phosphate (**7cg**): bp 116—120 °C (1 mmHg). An analytical sample was not obtained. MS *m/z* (%): 259 (M^+, 3.3), 113 (100). IR ν_{max}^{film} cm^{-1}: 1660, 1280, 1230, 1030. NMR ($CDCl_3$) δ: 1.97 (3H, s, =–CH_3), 3.55 (2H, t, J=6 Hz, CH_2Br), 3.84 (3H, d, J=11 Hz, $POCH_3$), 4.29—4.44 (2H, m, $POCH_2$), 4.54 (1H, br s, =CH), 4.79 (1H, t, J=1 Hz, =CH).

Reaction of 2-Methoxy-4,4,5,5-tetramethyl-1,3,2-dioxaphospholane (1d) with Bromoacetone——A mixture of bromoacetone (4.11 g, 0.03 mol) and **1d** (5.34 g, 0.03 mol) was stirred at room temperature, causing an exothermic reaction. After 30 min, the reaction mixture was heated at 60 °C for 30 min, and the temperature then rose to 100 °C. When the evolution of methyl bromide gas had almost ceased, the mixture was kept at 60 °C for 30 min. The reaction mixture was chromatographed on silica gel (hexane–AcOEt) to afford **3d** (3.52 g, 53%) and **4d** (1.48 g, 22%) as oils.

2-Acetonyl-4,4,5,5-tetramethyl-2-oxo-1,3,2-dioxaphospholane (**3d**)[4]: bp 151—153 °C (0.5 mmHg), mp 54—56 °C (from iso-Pr_2O).

4,4,5,5-Tetramethyl-2-oxo-2-(2-propenyloxy)-1,3,2-dioxaphospholane (**4d**): bp 116—119 °C (1 mmHg), an unstable oil. *Anal.* Calcd for $C_9H_{17}O_4P \cdot 1/2H_2O$: C, 47.20; H, 7.92. Found: C, 47.23; H, 7.52. MS *m/z* (%): 220 (M^+, 9.8), 43 (100). IR ν_{max}^{film} cm^{-1}: 1660, 1295, 1145. NMR ($CDCl_3$) δ: 1.44 (6H, s, 2 × CH_3), 1.48 (6H, s, 2 × CH_3), 1.97 (3H, s, =–CH_3), 4.52 (1H, br s, =CH), 4.76 (1H, t-like, =CH).

Reaction of 2-Methoxy-4,7-dihydro-1,3,2-dioxaphosphepin (1e) with Bromoacetone——A mixture of bromoacetone (1.37 g, 0.01 mol) and **1e** (1.48 g, 0.01 mol) was stirred at 10 °C, causing an exothermic reaction. After 30 min the temperature rose to 100 °C. The mixture was kept at 60 °C for an additional 30 min. The reaction mixture was chromatographed on silica gel (hexane–AcOEt) to afford **3e** (0.37 g, 10%), **6eg** (0.99 g, 17%) and **7eg** (0.15 g, 3%) as an oil.

2-Acetonyl-2-oxo-4,7-dihydro-1,3,2-dioxaphosphepin (**3e**)[4]: bp 150—153 °C (0.5 mmHg).

4-Bromo-2-butenyl Methyl Acetonylphosphonate (**6eg**): bp 158—162 °C (0.6 mmHg); partial decomposition occurred when **6eg** was distilled, so no an analytical sample was obtained. MS *m/z* (%): 205 (65.2), 135 (100). IR ν_{max}^{film} cm^{-1}: 1710, 1350. NMR ($CDCl_3$) δ: 2.33 (3H, s, CH_3), 31.2 (2H, d, J=22 Hz, PCH_2), 3.79 (3H, d, J=11 Hz,

$POCH_3$), 4.01 (2H, d, J=8 Hz, CH_2Br), 4.68—4.78 (2H, m, OCH_2), 5.68—5.81 (1H, m, CH=), 5.90—6.07 (1H, m, CH=).

4-Bromo-2-butenyl Methyl 2-Propenyl Phosphate (**7eg**): MS *m/z* (%): 205 (12.9), 99 (100). IR ν_{max}^{film} cm^{-1}: 1650, 1280. NMR ($CDCl_3$) δ: 2.00 (3H, s, CH_3), 3.83 (3H, d, J=10 Hz, OCH_3), 4.50—4.88 (6H, m, $2\times CH_2+=CH_2$), 5.79 (2H, t, J=1.5 Hz, CH=CH).

Reaction of 1a with Chloroacetone——A mixture of chloroacetone (1.84 g, 0.02 mmol) and **1e** (2.72 g, 0.02 mol) was stirred at room temperature. The reaction mixture was heated at 70 °C for 2 h, then chromatographed on silica gel (hexane–AcOEt) to afford **4a** (2.50 g, 70%) and **7ag** (0.64 g, 14%).

3-Chloropropyl Methyl 2-Propenyl Phosphate (**7ah**): *Anal.* Calcd for $C_7H_{14}ClO_4P\cdot 1/2H_2O$: C, 35.38; H, 6.36. Found: C, 35.79; H, 6.03. MS *m/z* (%): 228 (M^+, 6.4), 113 (100). IR ν_{max}^{film} cm^{-1}: 1660, 1285. NMR ($CDCl_3$) δ: 1.96 (3H, s, $=C-CH_3$), 2.06—2.24 (2H, m, CH_2), 3.66 (2H, t, J=6 Hz, CH_2Cl), 3.83 (3H, d, J=11 Hz, $POCH_3$), 4.26 (2H, dd, J=6, 14 Hz, $POCH_2$), 4.52 (1H, s, =CH), 4.77 (1H, t, J=1 Hz, =CH).

Reaction of 1a with Iodoacetone——A mixture of iodoacetone (5.52 g, 0.03 mol) and **1a** (4.08 g, 0.03 mol) was stirred at 5 °C, causing an exothermic reaction; after 20 min the reaction temperature rose to 80 °C. The mixture was treated as described in method B. Chromatography gave a mixture (3.32 g) of **3a** and **5a** (51% and 15%, respectively) as an oil, **4a** (0.49 g, 9%) and a mixture (0.86 g) of **6ai** and **8ai** (8% and 1%, respectively).

3-Iodopropyl Methyl Acetonylphosphonate (**6ai**): bp 138—140 °C (0.5 mmHg). MS *m/z* (%): 320 (M^+, 0.7), 193 (100). IR ν_{max}^{film} cm^{-1}: 1710, 1355. NMR ($CDCl_3$) δ: 2.16 (2H, m, CH_2), 2.34 (3H, s, CH_3), 3.12 (2H, d, J=24 Hz, PCH_2), 3.26 (2H, t, J=7 Hz, CH_2I), 3.82 (3H, d, J=12 Hz, $POCH_3$), 4.18 (2H, m, OCH_2).

3-Iodopropyl Methyl Methylphosphonate (8ai)——A mixture of **1a** (1.36 g, 0.01 mol) and methyl iodide (2.8 g, 0.02 mol) was stirred for 2 h at room temperature, then refluxed for 2 h. The reaction mixture was concentrated, and the residue was crystallized from ether. The crystals (1.06 g, 88%: **5a**) were collected by filtration, and the filtrate was concentrated. The residue was chromatographed on silica gel to give **8ai** (0.218 g, 8%) as an oil. *Anal.* Calcd for $C_5H_{12}IO_3P$: C, 21.60; H, 4.35. Found: C, 21.45; H, 4.18. IR ν_{max}^{film} cm^{-1}: 1310, 1240, 1180, 1030. NMR ($CDCl_3$) δ: 1.50 (3H, d, J=18 Hz, CH_3), 2.08—2.25 (2H, m, CH_2), 3.75 (3H, d, J=11 Hz, $POCH_3$), 4.04—4.20 (2H, m, $POCH_2$).

Reaction of 2-Benzyloxy-1,3,2-dioxaphosphorinane (1f) with Bromoacetone——A mixture of bromoacetone (2.74 g, 0.02 mol) and **1f** (4.24 g, 0.02 mol) was stirred at room temperature; after 20 min the reaction temperature rose to 50 °C. The mixture was kept at 70 °C for 1 h and chromatographed on silica gel to give **4a** (1.47 g, 41%) and a mixture (1.84 g) of **3a** and **9** (37% and 12%, respectively). The mixture was crystallized from ether to give **9** (0.28 g, recrystallized from AcOEt).

2-Benzyloxy-2-oxo-1,3,2-dioxaphosphorinane (**9**): mp 136—138 °C. *Anal.* Calcd for $C_{10}H_{13}O_3P$: C, 56.60; H, 6.18. Found: C, 56.47; H, 6.30. IR ν_{max}^{KBr} cm^{-1}: 1495, 1290, 1050. NMR ($CDCl_3$) δ: 1.60—1.99 (2H, m, CH_2), 3.26 (2H, d, J=20 Hz, PCH_2), 3.94—4.18 (2H, m, $POCH_2$), 4.35—4.54 (2H, m, $POCH_2$), 7.20—7.40 (5H, m, ArH).

References

1) W. Perkow, K. Ullerich, and F. Meyer, *Naturwissenschaften*, **39**, 353 (1952) [*Chem. Abstr.*, **47**, 8248 (1953)]; F. W. Lichtenthaler, *Chem. Rev.*, **61**, 607 (1961).
2) A. E. Arbuzov, *J. Russ. Phys. Chem. Soc.*, **38**, 687 (1906); A. N. Pudovik, *Dokl. Akad. Nauk SSSR*, **105**, 735 (1955) [*Chem. Abstr.*, **50**, 4143*f* (1956)]; H. I. Jacobsen, M. J. Griffin, S. Preis, and E. V. Jensen, *J. Am. Chem. Soc.*, **79**, 1608 (1957); A. K. Bhattacharya and G. Thyagarajan, *Chem. Rev.*, **81**, 415 (1981).
3) L. Horner, H. Hoffmann, and H. G. Wippel, *Chem. Ber.*, **91**, 61 (1958); W. S. Wadsworth, *J. Am. Chem. Soc.*, **83**, 1733 (1961).
4) I. Morita, S. Tada, K. Kunimoto, M. Tsuda, M. Kise, and K. Kimura, *Chem. Pharm. Bull.*, **35**, 3898 (1987).
5) I. Morita, K. Kunimoto, M. Tsuda, S. Tada, M. Kise, and K. Kimura, *Chem. Pharm. Bull.*, **35**, 4144 (1987).
6) G. Aksnes and R. Erikson, *Acta Chem. Scand.*, **20**, 2463 (1966) [*Chem. Abstr.*, **67**, 21304*a* (1967)]; R. F. Hudson and R. Greenhalgh, *J. Chem. Soc., Chem. Commun.*, **1968**, 1300.
7) P. A. Chopard, V. M. Clark, R. F. Hudson, and A. J. Kirby, *Tetrahedron*, **21**, 1961 (1965) and references cited therein.
8) I. J. Borowitz, S. Firstenberg, G. B. Borowitz, and D. Schuessler, *J. Am. Chem. Soc.*, **94**, 1623 (1972).
9) P. Gillespie, F. Ramirez, I. Ugi, and D. Marquarding, *Angew. Chem., Int. Ed. Engl.*, **12**, 91 (1973).

[Chem. Pharm. Bull. 35(12)4717—4729(1987)]

Tannins and Related Compounds. LIX.[1] Aesculitannins, Novel Proanthocyanidins with Doubly-Bonded Structures from *Aesculus hippocastanum* L.

SATOSHI MORIMOTO, GEN-ICHIRO NONAKA, and ITSUO NISHIOKA*

Faculty of Pharmaceutical Sciences, Kyushu University 62, 3-1-1 Maidashi, Higashi-ku, Fukuoka 812, Japan

(Received May 14, 1987)

A chemical examination of the seed shells of *Aesculus hippocastanum* L. has led to the isolation of proanthocyanidins A-6 (**10**) and A-7 (**11**), and aesculitannins A (**12**), B (**13**), C (**14**), D (**15**), E (**16**), F (**17**) and G (**18**). On the basis of chemical and spectroscopic evidence, proanthocyanidins A-6 (**10**) and A-7 (**11**) have been determined to be A-type dimers each possessing a C-4, C-6 interflavanoid linkage, while aesculitannins A (**12**), B (**13**), C (**14**), D (**15**), E (**16**), F (**17**) and G (**18**) have been characterized as oligomeric proanthocyanidins possessing A-type unit(s) in each molecule. In addition, the presence of (−)-epicatechin (**1**), proanthocyanidins B-2 (**2**), B-5 (**3**), A-2 (**4**), A-4 (**5**) and C-1 (**6**), epicatechin-(4β→6)-epicatechin-(4β→6)-epicatechin (**7**), and cinnamtannins B_1 (**8**) and B_2 (**9**) was also demonstrated.

Keywords——*Aesculus hippocastanum*; Hippocastanaceae; aesculitannin; doubly-bonded proanthocyanidin; procyanidin; condensed tannin; flavan-3-ol; thiolytic degradation; epimerization; hydrogen peroxide oxidation

Proanthocyanidins, which occur mostly in plants of a woody habit, consist of flavan-3-ol units linked singly or doubly through interflavanoid linkages. Recently, a number of singly-linked proanthocyanidins have been isolated and their structures have been elucidated.[2—5] In contrast, proanthocyanidins possessing doubly-linked structures (the dimers belonging to this class are designated as A-type) are not so frequently found in nature, and their distribution is limited only to members of the families Ericaceae,[6] Hippocastanaceae,[7,8] Lauraceae,[3] Rosaceae,[5] *etc.* Among them, the horse chestnut tree, *Aesculus hippocastanum* L. (Hippocastanaecae), has long been known as a plant containing a large amount of the doubly-linked dimer, proanthocyanidin A-2.[7] Furthermore, along with five singly-linked procyanidins, two trimeric proanthocyanidins containing the A-2 unit in each molecule were obtained as an inseparable mixture.[8] As part of our chemical studies on tannins and related compounds, we have re-examined the seed shells of *Aesculus hippocastanum* L. and isolated two new dimers (**10** and **11**) (designated as proanthocyanidins A-6 and A-7), four trimers (**12**—**15**) (aesculitannins A, B, C and D) and three tetramers (**16**—**18**) (aesculitannins E, F and G), together with a flavan-3-ol (**1**) and several known proanthocyanidins (**2**—**9**). This paper describes the isolation and structure elucidation of these compounds.

The fresh seed shells of *Aesculus hippocastanum* L. were extracted with 80% aqueous acetone. The extract was subjected to a combination of Sephadex LH-20, MCI-gel CHP 20P and Bondapak C_{18}/Porasil B chromatographies with various solvent systems as described in the experimental section to give compounds **1**—**18**. Compounds **1**—**4**, **6** and **7** were identified as (−)-epicatechin,[3] procyanidins B-2,[3] B-5,[3] A-2[3] and C-1,[3] and epicatechin-(4β→6)-epicatechin-(4β→6)-epicatechin,[2] respectively, by comparisons of their physical and spectral data with those of authentic samples. Compound **5** was characterized as epicatechin-(4β→8, 2β→O→7)-entcatechin,[9] whose structural elucidation was previously reported.[10]

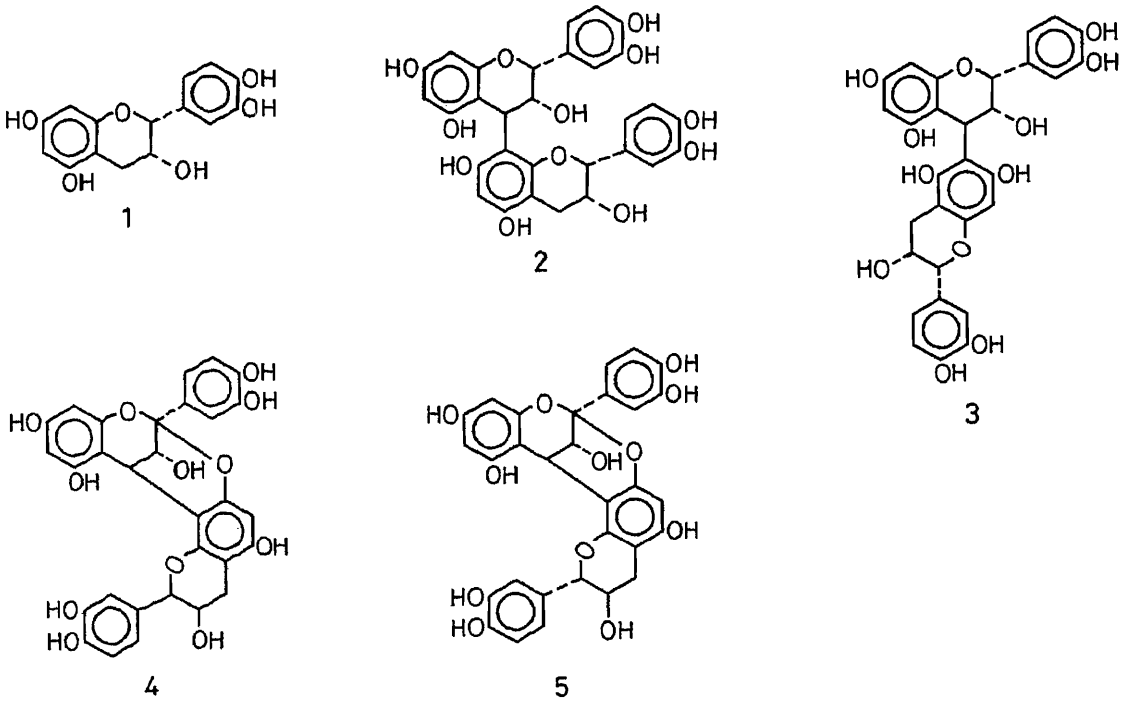

Chart 1

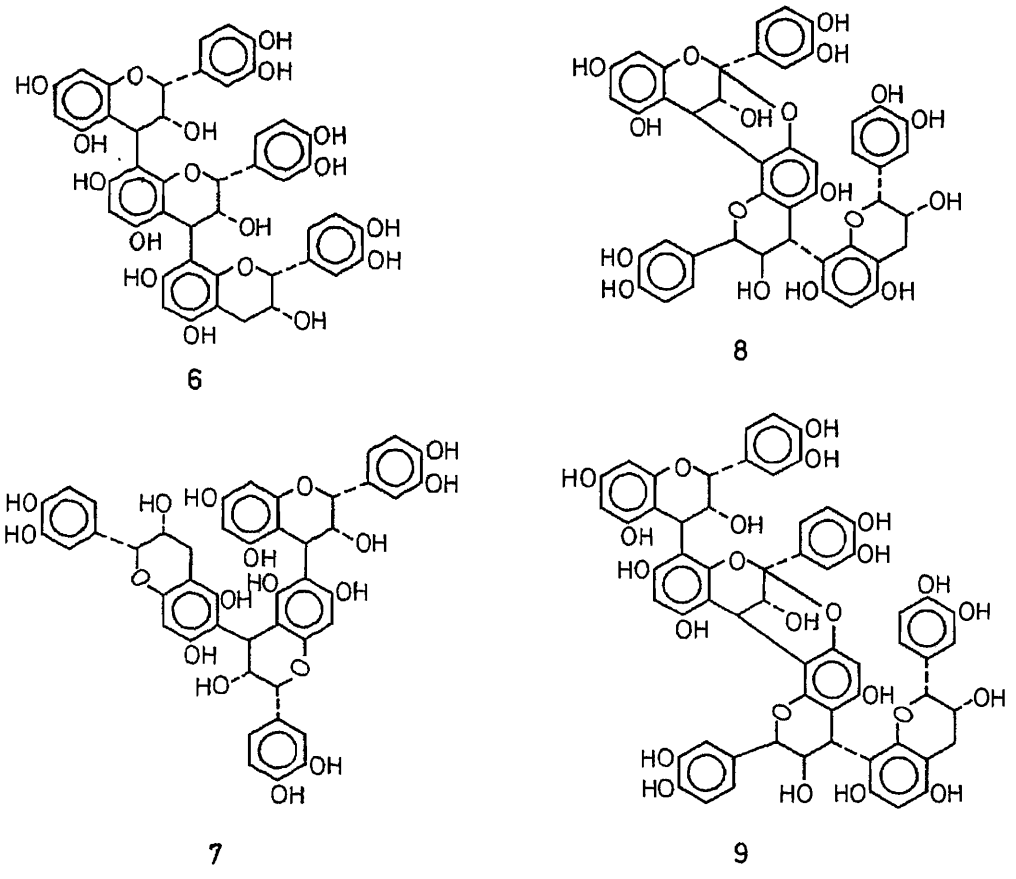

Chart 2

Compounds **8** and **9** were shown to be a trimer and a tetramer possessing an A-type unit in each molecule by ^{1}H- and ^{13}C-nuclear magnetic resonance (^{1}H- and ^{13}C-NMR) spectroscopy, and their physical and spectral data coincided with those of cinnamtannins B_1 and B_2,[11] respectively.

Proanthocyanidins A-6 (**10**) and A-7 (**11**) gave orange colorations (characteristic of proanthocyanidins) with the anisaldehyde-sulfuric acid reagent. The ^{13}C-NMR spectra of **10** and **11** were almost indistinguishable from each other, showing the presence of two flavan units in each molecule. The chemical shifts of the signals (δ 79.2 in **10** and δ 79.4 in **11**) due to the flavan C-2 carbon suggested the presence of an epicatechin unit in each case,[12] while those (δ 104.2 in **10** and δ 104.0 in **11**) assignable to ketal carbons were consistent with A-type proanthocyanidin structures.[8] Although these ^{13}C-NMR data were closely correlated with those of proanthocyanidin A-2, the ^{1}H-NMR spectra of **10** and **11** showed upfield shifts (δ 4.85 in **10** and 4.87 in **11**) of the lower flavan H-2 as compared with that (δ 5.00) of proanthocyanidin A-2 (**4**). In addition, the chemical shifts of these signals were rather similar to that (δ 4.84) found in 4,6-linked procyanidin B-5 (**3**), thus suggesting that the two flavan units in **10** and **11** are linked through the C-4 and C-6′ positions.[13]

Further confirmation of the position of the interflavanoid carbon-carbon linkage in **10** and **11** was obtained by oxidation of procyanidin B-5 (**3**) with hydrogen peroxide in the presence of sodium bicarbonate,[10] which afforded two proanthocyanidins identical with **10** and **11**, thus establishing unequivocally the position of the interflavanoid linkage to be C-4 and C-6′.

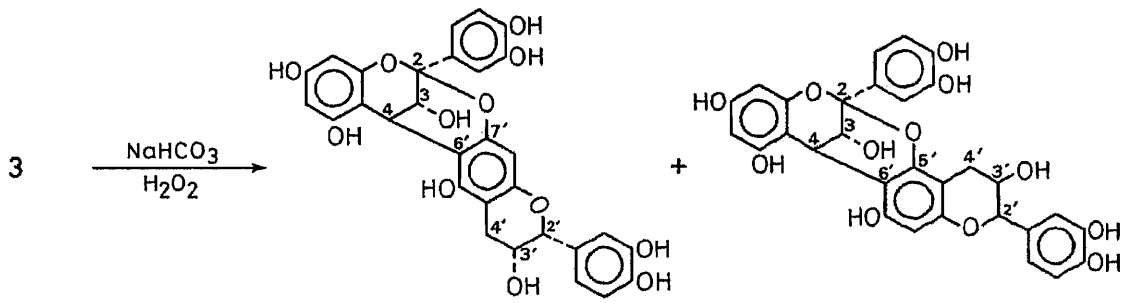

10 11

Chart 3

The location of the interflavanoid carbon-oxygen linkage in each compound was confirmed by nuclear Overhauser effect (NOE) experiments on the corresponding heptamethyl ethers **10a** and **11a**. In the ^{1}H-NMR spectrum of **10a**, irradiation at the methoxyl region (δ 3.70—4.00) caused a 10% enhancement of the integral intensity of the H-4′ methylene signals (δ 2.96, m), indicating that a methoxyl group is located at the C-5′ position, and consequently the ether linkage is between the C-2 and C-7′ positions. On the other hand, a similar NOE measurement in **11a** indicated that the two flavan units are connected through an ether linkage between the C-2 and C-5′ positions, since the integral intensity of the H-8′ signal (δ 6.20, s) was enhanced by 32% upon irradiation at the methoxyl region (δ 3.70—4.00).

On the basis of these chemical and spectral findings, proanthocyanidins A-6 and A-7 were characterized as epicatechin-(4β→6,2β→*O*→7)-epicatechin (**10**) and epicatechin-(4β→6,2β→*O*→5)-epicatechin (**11**), respectively.

Aesculitannin A (**12**) exhibited an $(M+H)^+$ ion peak at *m/z* 865 in its fast atom bombardment mass spectrum (FAB-MS), the molecular mass corresponding to a trimeric

constitution. The ^{13}C-NMR spectrum of **12** showed two signals at δ 81.5 and 76.7 attributable to flavan C-2 carbons. In addition, the appearance of a ketal carbon signal at δ 104.3 indicated that **12** possesses an A-type unit in the molecule. Acid-catalyzed degradation of **12** with benzylmercaptan[14] gave (−)-epicatechin 4-benzylthioether (**19**) (formed from the upper unit) and proanthocyanidin A-2 (**4**) (formed from the lower unit).

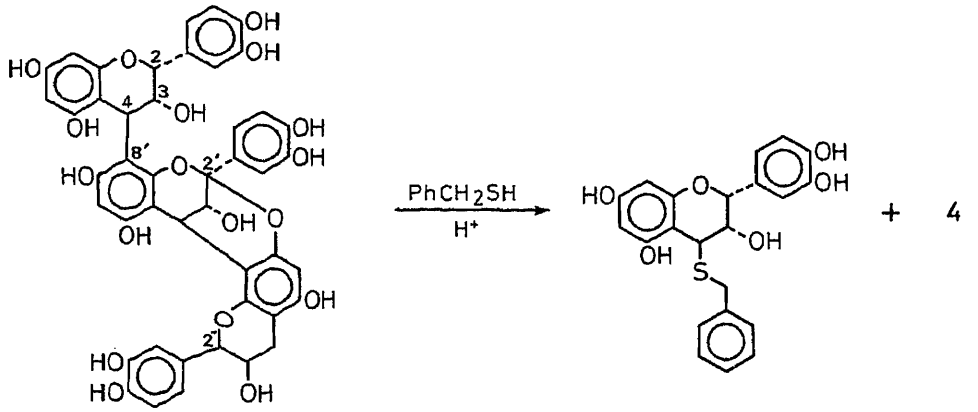

12 19

Chart 4

The location of the interflavanoid linkage between the epicatechin and A-2 units was assumed to be the C-4 and C-8′ positions, since in the ^{1}H-NMR spectrum of **12**, the chemical shifts of the signals assignable to H-2 (δ 4.96) and H-2″ (δ 5.19) were similar to those [δ 5.02 (H-2) and δ 5.16 (H-2″)] in procyanidin C-1 (**6**). Unequivocal confirmation of the location and the mode of the interflavanoid linkage was achieved by derivation of **12** from the tetrameric proanthocyanidin, cinnamtannin B_2 (**9**). On partial thiolytic degradation, **9** gave a trimeric proanthocyanidin 4″-benzylthioether (**20**), together with (−)-epicatechin 4-benzylthioether (**19**), proanthocyanidin A-2 4′-benzylthioether (**21**) and (−)-epicatechin (**1**).[11] The thioether (**20**), on desulfurization with Raney nickel, afforded a trimeric proanthocyanidin which was found to be identical with **12**.

Accordingly, aesculitannin A was concluded to be epicatechin-(4β→8)-epicatechin-(4β→8,2β→*O*→7)-epicatechin (**12**). This compound is probably identical with the trimeric proanthocyanidin D_1 or D_2[8] obtained as a mixture from this plant, although the location of each interflavanoid linkage has not been determined.

Aesculitannin B (**13**) showed the same $(M+H)^+$ ion peak at *m/z* 865 as that of **12** in the FAB-MS. The ^{13}C-NMR spectrum of **13** exhibited signals at δ 79.3 and 84.0 assignable to epicatechin and catechin C-2 carbons, respectively.[12] Furthermore, the presence of an A-type unit was revealed by a ketal resonance at δ 103.4. Similar thiolytic degradation of **13** gave (−)-epicatechin (**1**) and a dimeric proanthocyanidin benzylthioether (**22**). The thioether (**22**) was characterized as proanthocyanidin A-4 4′-benzylthioether by ^{1}H-NMR analysis and also by conversion with Raney nickel to proanthocyanidin A-4 (**5**).[10]

The location of the interflavanoid linkage between these component units was confirmed as follows. In the ^{1}H-NMR spectrum of **13**, the methine signal due to H-4 was observed at higher field [δ 3.44 (d, J=4 Hz)] than that [δ 4.32 (d, J=4 Hz)] of proanthocyanidin A-4 (**5**). This unusual upfield shift may be interpreted in terms of a through-space interaction of the B′-ring,[15] thus suggesting that the A-4 and (−)-epicatechin units are linked through the C-4′ and C-8″ positions. Furthermore, the structure of **13** was confirmed by epimerization[10] at the C-2′ position in cinnamtannin B_1 (**8**) with potassium carbonate in acetone, giving a trimeric proanthocyanidin identical with **13**.

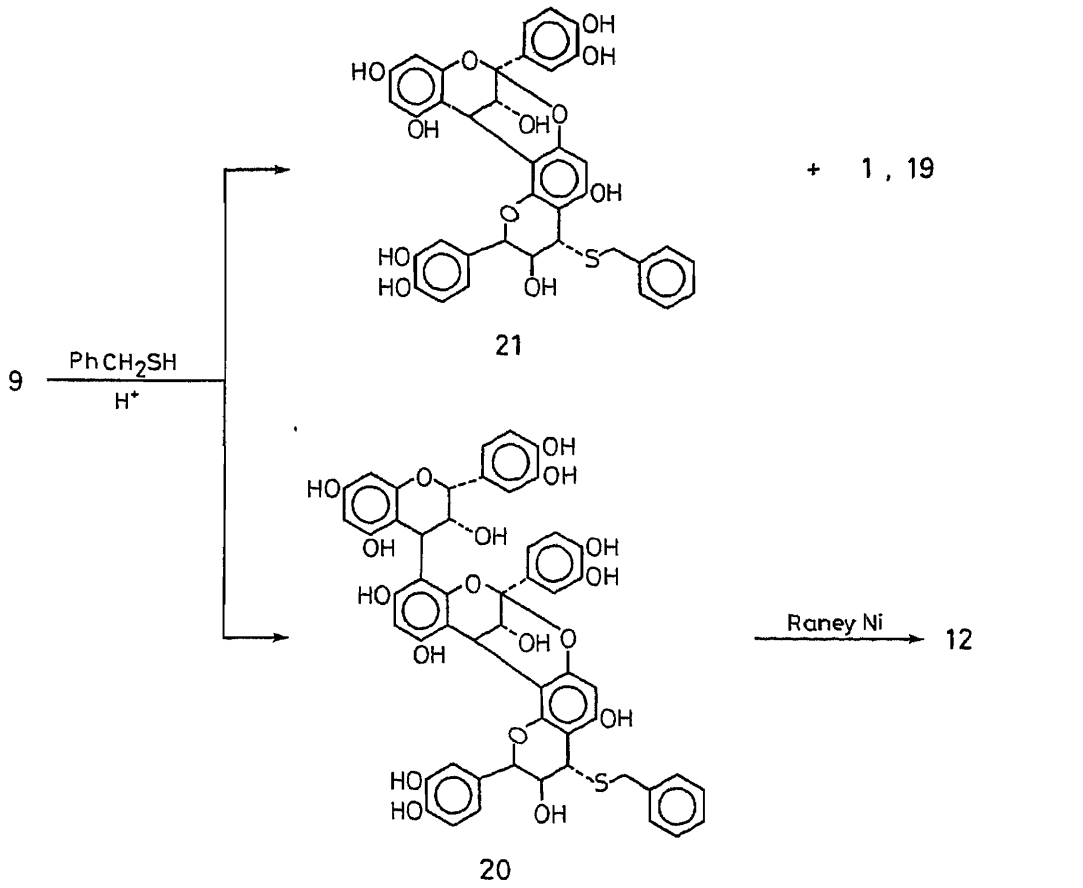

Chart 5

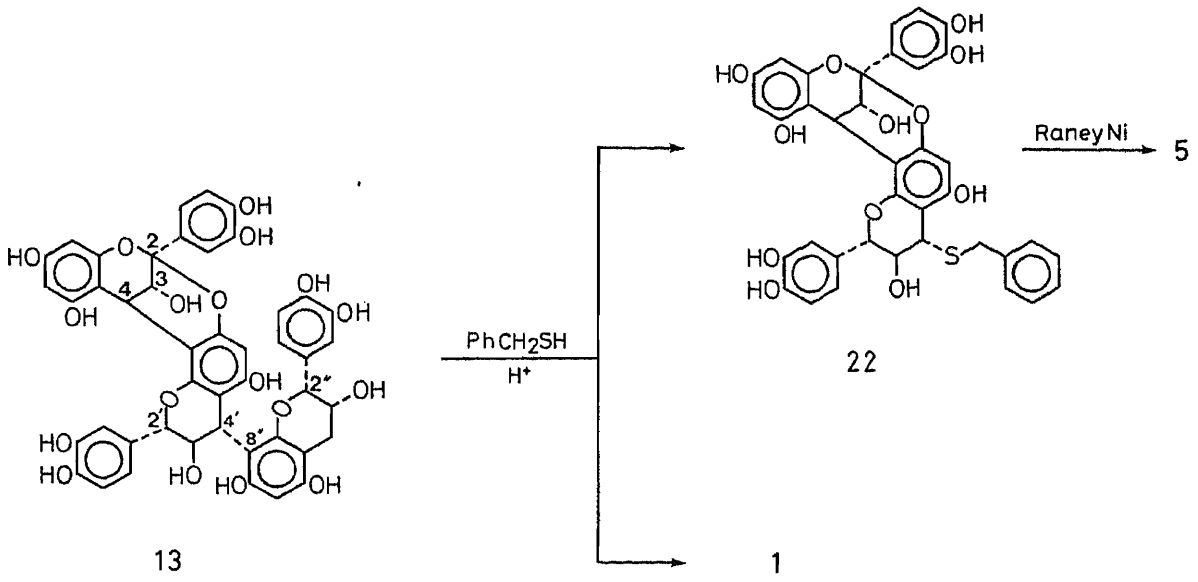

Chart 6

Thus, aesculitannin B was characterized as epicatechin-(4β→8,2β→O→7)-entcatechin-(4α→8)-epicatechin (**13**).

Aesculitannin C (**14**) afforded (−)-epicatechin (**1**) and several uncharacterized anthocyanidin pigments on degradation with ethanolic hydrochloric acid. The trimeric con-

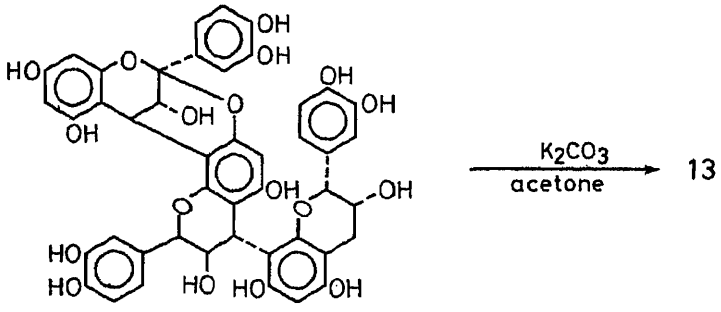

8

Chart 7

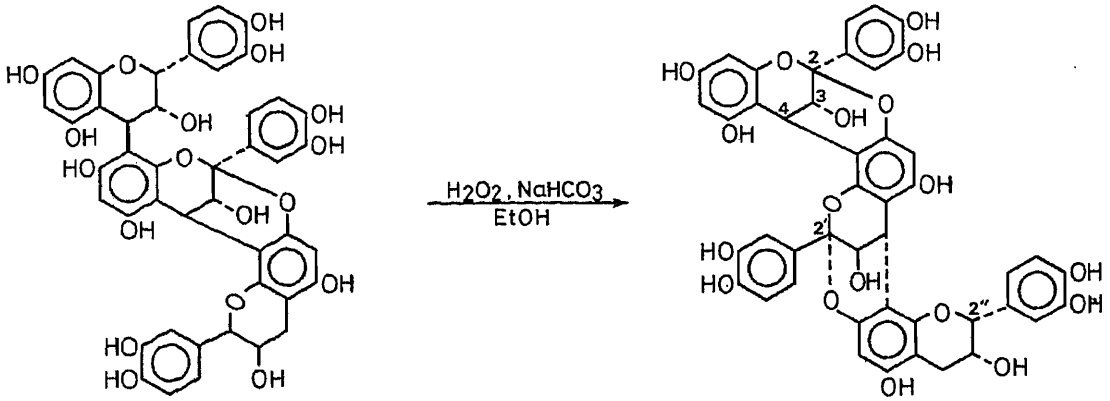

12 14

Chart 8

stitution was deduced from the FAB-MS data which showed the $(M+H)^+$ ion peak at m/z 863, though the molecular weight is two mass units less than those of **12** and **13**. The ^{13}C-NMR signal patterns arising from the C′,C″-rings were closely related to those found in **12** (Table I), suggesting that the lower two units possess an A-type structure similar to that of **12**. Furthermore, the absence of a C-2 methine signal and the appearance instead of a ketal carbon signal at δ 103.2 indicated that the upper two units are connected through C–C and C–O interflavanoid linkages.

On methylation with diazomethane, **14** yielded a decamethyl ether (**14a**). The ^1H-NMR spectrum of **14a** exhibited two upfield methoxyl signals (δ 3.39 and 3.52) assignable to the methoxyls at the C-5,5′ positions, along with eight methoxyl signals which lie in the normal region (δ 3.70—3.90). The upfield shifts of the two methoxyl groups implied the presence of a through-space interaction between these methoxyl groups and the B′,B″-rings,[8] suggesting that the locations of the two C–C interflavanoid linkages are C-4→C-8. From these spectral data, aesculitannin C is presumed to be formulated as **14**. The structure including the absolute stereochemistry was confirmed by derivation of this compound from aesculitannin A (**12**). Oxidation as described in the cases of proanthocyanidins A-6 (**10**) and A-7 (**11**) afforded a trimeric proanthocyanidin identical with aesculitannin C (**14**).

On the basis of these spectral and chemical data, aesculitannin C was established as the novel doubly-bonded proanthocyanidin, epicatechin-(4β→8,2β→O→7)-epicatechin-

TABLE I. ^{13}C-NMR Spectral Data for Compounds 4 and 10—18 (δ Value)[a]

	4	10	11	12	13	14	15	16	17	18
C-2	103.6	104.2	104.0	76.7	103.4	103.2[c]	103.1[c]	104.5	103.8	103.7[c]
C-3	67.1	67.1	67.0	72.5	66.8	67.0	67.5	66.3	66.3	67.0
C-4	29.9	—[b]	—[b]	36.7	—[b]	—[b]	—[b]	—[b]	—[b]	—[b]
C-2′	81.1	79.2	79.4	104.3	84.0	102.3[c]	102.9[c]	77.5	83.7	78.5
C-3′	65.7	66.9	66.3	66.8	73.6	67.9	68.0	72.7	73.6	71.4
C-4′	28.5	—[b]	—[b]	—[b]	38.6	—[b]	—[b]	38.6	38.8	38.9
C-2″				81.5	79.3	80.9	83.4	78.5	76.6	103.5[c]
C-3″				65.9	66.8	66.1	66.5	71.7	71.4	67.7
C-4″				—[b]	—[b]	—[b]	—[b]	37.3	37.3	—[b]
C-2‴								79.0	79.0	80.3
C-3‴								66.8	66.3	66.2
C-4‴								—[b]	—[b]	—[b]

a) Measured in acetone-d_6. b) Overlapped with solvent signals. c) Assignments may be interchanged.

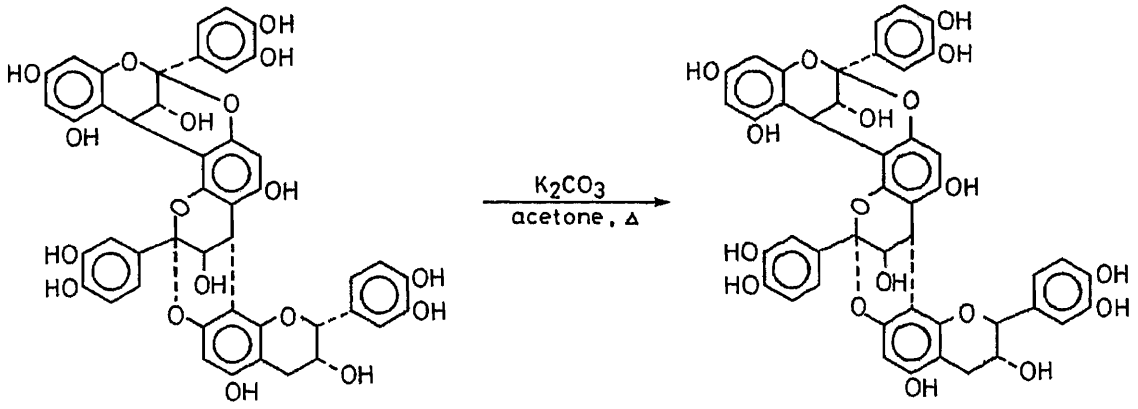

14 15

Chart 9

(4α→8,2α→O→7)-epicatechin (**14**).

Aesculitannin D (**15**) was shown to possess the same constitution as that of **14** by analysis of the FAB-MS [*m/z*: 863 $(M+H)^+$]. The ^{13}C-NMR spectrum of **15** was almost identical with that of **14**. The somewhat lowfield shift (δ 83.4) of the C-2″ carbon suggested that the lower terminal unit possesses catechin stereochemistry. This is supported by the result of acid-catalyzed degradation of **15**, which produced (−)-catechin (**23**) from the terminal unit. Accordingly, **15** was presumed to be the C-2″ epimer of aesculitannin C (**14**).

In order to confirm this structure, an attempt was made to prepare **15** from aesculitannin C (**14**). Alkaline treatment of **14** as described for aesculitannin A (**13**) furnished **15**. Thus, aesculitannin D was concluded to be epicatechin-(4β→8,2β→O→7)-epicatechin-(4α→8,2α→O→7)-entcatechin (**15**).

Aesculitannin E (**16**) showed in the FAB-MS the $(M+H)^+$ ion peak at *m/z* 1153, corresponding to a tetraflavanoid constitution. The ^{1}H-NMR spectrum measured at room temperature was complicated by conformational isomerism.[12] However, owing to the existence of unequal proportions of conformers, the ^{13}C-NMR signals arising from the major conformer could be assigned. The spectrum exhibited a signal at δ 104.5 due to a ketal carbon, along with signals at δ 77.5, 78.5 and 79.0, the chemical shifts of which were consistent with

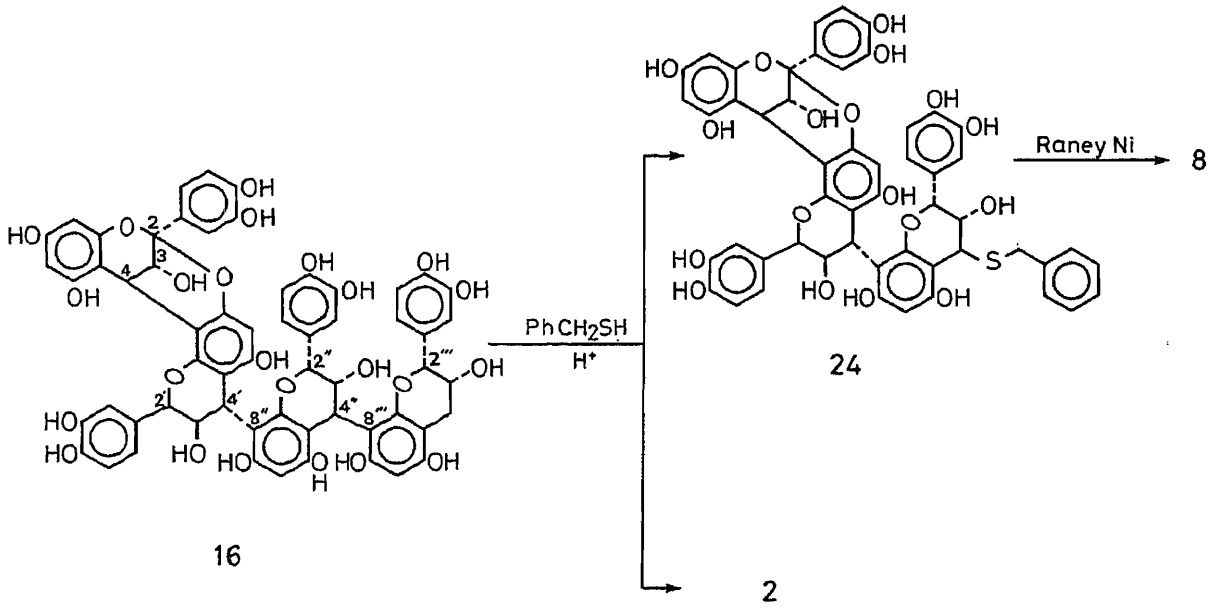

Chart 10

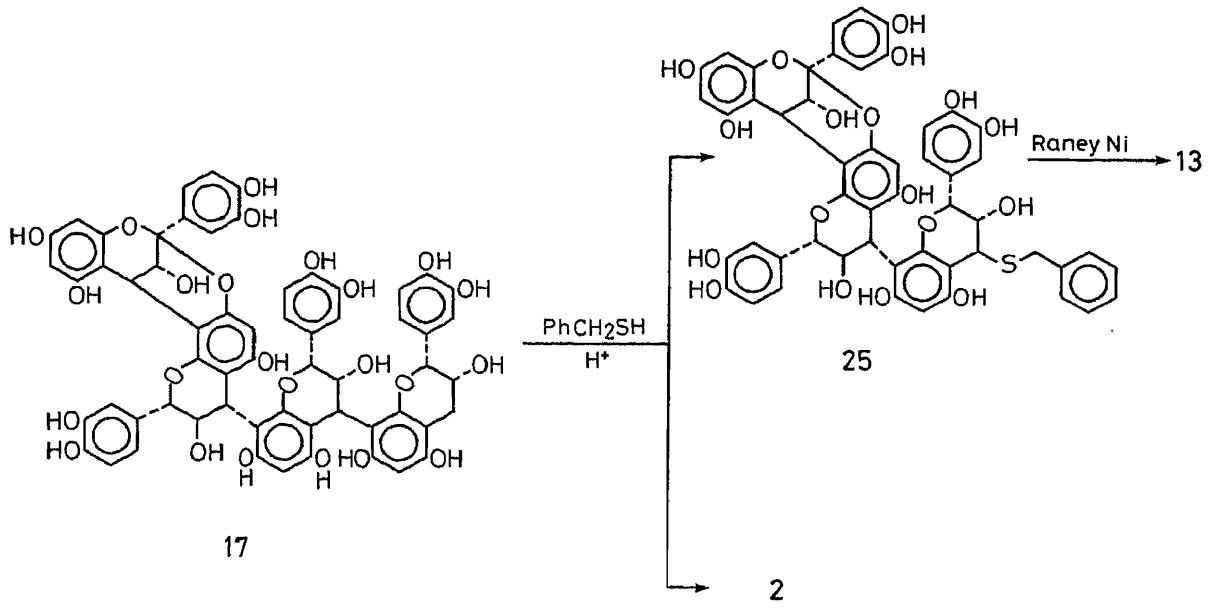

Chart 11

that of the epicatechin C-2 signal, thus suggesting that **16** consists of epicatechin and A-2 units. The structure of each component unit was established by thiolytic degradation of **16** to give proanthocyanidin A-2 4′-benzylthioether (**21**), (−)-epicatechin 4-benzylthioether (**19**), and (−)-epicatechin (**1**).

The locations and the modes of the interflavanoid linkages were confirmed as follows. Partial thiolytic degradation of **16** yielded, in addition to the above degradation products, procyanidin B-2 (**2**) and a trimeric proanthocyanidin benzylthioether. This thioether was characterized as cinnamtannin B_1 4″-benzylthioether (**24**) by desulfurization with Raney nickel to give cinnamtannin B_1 (**8**).

Based on these spectral and chemical data, aesculitannin E was characterized as

epicatechin-(4β→8,2β→O→7)-epicatechin-(4α→8)-epicatechin-(4β→8)-epicatechin (**16**).

Aesculitannin F (**17**) was shown to possess the same tetrameric constitution as that of **16** by FAB-MS analysis [*m/z*: 1153 $(M+H)^+$]. The ^{13}C-NMR spectrum of **17** was also complicated by conformational isomerism, but the major conformer showed a ketal carbon signal at δ 103.8 and three flavan C-2 signals at δ 76.6, 79.0 and 83.7, the former two C-2 signals being attributable to those in epicatechin units and the remaining one to a catechin unit.

To confirm the structure of **17**, partial thiolytic degradation was attempted. Compound **17** was degraded under conditions similar to those described in **16** to give proanthocyanidin A-4 4′-benzylthioether (**22**), procyanidin B-2 (**2**), (−)-epicatechin 4-benzylthioether (**19**), (−)-epicatechin (**1**) and a thioether (**25**). The thioether (**25**) was concluded to be the 4″-benzylthioether of aesculitannin B by spectral analysis and by conversion of **25** into aesculitannin B (**13**).

Accordingly, the structure of aesculitannin F was established as epicatechin-(4β→8,2β→O→7)-entcatechin-(4α→8)-epicatechin-(4β→8)-epicatechin (**17**).

The tetrameric constitution of aesculitannin G (**18**) was deduced from FAB-MS [*m/z*: 1151 $(M+H)^+$]. In the ^{13}C-NMR spectrum of **18**, the appearance of the signals at δ 78.5 and 80.3 implied the occurrence of two epicatechin units in the molecule. Furthermore, the presence of two A-type units was revealed by two ketal carbon resonances (δ 103.5 and 103.7). Similar thiolytic degradation led us to the assignment of the structures of the component units. That is, on treatment with acid in the presence of benzylmercaptan, **18** afforded proanthocyanidin A-2 4′-benzylthioether (**21**) and proanthocyanidin A-2 (**4**).

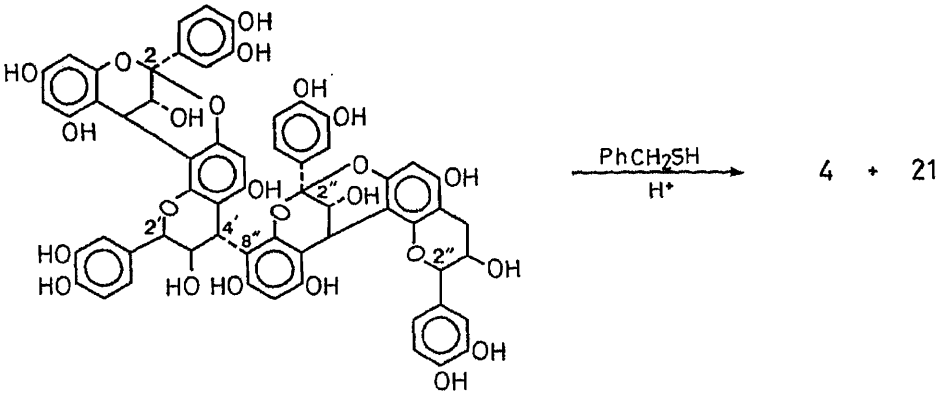

18

Chart 12

The position of the interflavanoid linkage between the two proanthocyanidin A-2 units was deduced by ^{1}H-NMR analysis. In the spectrum, the chemical shifts of the H-4 (δ 3.49) and H-2′ (δ 5.66) signals were quite different from those (H-4: δ 4.35; H-2′: δ 5.00) found in the case of proanthocyanidin A-2 (**4**). These unusual upfield and downfield shifts of H-4 and H-2′, respectively, were assumed to be caused by a through-space interaction between these protons and the B″-ring, thus suggesting the location of the interflavanoid linkage to be C-4′ and C-8″ positions. This was further supported by the fact that the ^{1}H-NMR chemical shifts of the H-4 and H-2′ signals are in good agreement with those (H-4: δ 3.41; H-2′: δ 5.72) of cinnamtannin B_1 (**8**). The configuration at C-4′ was concluded to be α on the basis of the coupling constant ($J \fallingdotseq 0$ Hz) of the H-4′ signal.

From these chemical and spectral data, aesculitannin G was characterized as epicatechin-(4β→8,2β→O→7)-epicatechin-(4α→8)-epicatechin-(4β→8,2β→O→7)-epicatechin (**18**).

In addition to the earlier findings by Mayer *et al.*[7] and Jacques and Haslam,[8] the seed

shells of *Aesculus hippocastanum* were found to contain a variety of doubly-linked proanthocyanidin dimers, trimers and tetramers. We have also recognized the presence of much higher oligomeric proanthocyanidins in this plant material, but the isolation of these compounds could not be done owing to their complex compositions and low yields. Proanthocyanidins A-6 (**10**) and A-7 (**11**) represent the first examples of A-type proanthocyanidins possessing a 4,6-interflavanoid linkage, and aesculitannins C (**14**) and D (**15**) are unique trimers in that they have rigid structures with two doubly-bonded interflavanoid linkages in each molecule.

It should be noted that aesculitannin A (**12**) dose not taste sweet (in fact, it is slightly astringent), whereas the structurally related trimers, cinnamtannins B_1 (**8**) and D_1 (**26**),[11] and aesculitannin B (**13**) have a strongly sweet taste.

Experimental

Melting points were determined on a Yanagimoto micromelting point apparatus and are uncorrected. Optical rotations were measured with a JASCO DIP-4 digital polarimeter. ^{1}H- and ^{13}C-NMR spectra were recorded on JEOL PS-100 and FX-100 spectrometers, respectively, using tetramethylsilane as an internal standard, and chemical shifts are given in δ (ppm). EI-MS were obtained with a JEOL D-300 instrument, and FD- and FAB-MS with a JEOL JMS DX-300 instrument. Column chromatography was carried out with Sephadex LH-20 (25—100 μ, Pharmacia Fine Chemical Co., Ltd.), MCI-gel CHP 20P (75—150 μ, Mitsubishi Chemical Industries, Ltd.), Bondapak C_{18}/Porasil B (35—75 μ, Waters Associates, Inc.) and Kieselgel 60 (230 mesh, Merck). Thin-layer chromatography (TLC) was conducted on precoated Kieselgel 60 F_{254} plates (0.2 mm, Merck), and spots were detected by ultraviolet (UV) illumination and by spraying ethanolic ferric chloride, 10% sulfuric acid and anisaldehyde-sulfuric acid reagents.

Isolation——The fresh seed shells (9.8 kg) of *Aesculus hippocastanum* were extracted three times with acetone–H_2O (4 : 1) at room temperature. The acetone was removed by evaporation *in vacuo*, and the aqueous solution was extracted with ether to remove waxes, *etc.* After concentration, the water solubles were chromatographed over MCI-gel CHP 20P with H_2O and then with MeOH. The MeOH eluate (541 g) was applied to a column of Sephadex LH-20, and elution with EtOH gave fractions 1 (17 g), 2 (106 g) and 3 (104 g). Fraction 1 was rechromatographed over MCI-gel CHP 20P with 30% aqueous MeOH to afford (−)-epicatechin (**1**) (8 g). Fraction 2 was further divided by Sephadex LH-20 chromatography with 60% aqueous MeOH into two fractions, 2-a (44 g) and 2-b (35 g). Fraction 2-a gave, on rechromatographies over MCI-gel CHP 20P (30% aqueous MeOH) and Bondapak C_{18} (20% aqueous MeOH), procyanidins B-2 (**2**) (6 g), B-5 (**3**) (2 g) and C-1 (**6**) (2 g), and cinnamtannin B_1 (**8**) (4 g). Repeated chromatographies of fraction 2-b on Sephadex LH-20 (EtOH), MCI-gel CHP 20P (30% aqueous MeOH) and Bondapak C_{18} (30% aqueous MeOH) furnished proanthocyanidins A-2 (**4**) (5 g), A-4 (**5**) (2 g), A-6 (**10**) (175 mg) and A-7 (**11**) (124 mg), and aesculitannins A (**12**) (1.2 g) and B (**13**) (1.3 g), and epicatechin-(4β→6)-epicatechin-(4β→6)-epicatechin (**7**) (254 mg). Sephadex LH-20 chromatography of fraction 3 with 80% aqueous MeOH afforded three fractions, 3-a (19 g), 3-b (25 g) and 3-c (22 g). Each fraction was repeatedly chromatographed over Sephadex LH-20 (60% aqueous MeOH), MCI-gel CHP 20P (30% aqueous MeOH) and Bondapak C_{18} (30% aqueous MeOH) to give cinnamtannin B_2 (**9**) (1.3 g) and aesculitannins C (**14**) (147 mg), D (**15**) (22 mg), E (**16**) (540 mg), F (**17**) (112 mg) and G (**18**) (172 mg).

Proanthocyanidin A-6 (10)——Colorless needles (H_2O), mp >300 °C, $[\alpha]_D^{21}$ +22.4° (c=1.2, acetone). *Anal.* Calcd for $C_{30}H_{24}O_{12}\cdot 2H_2O$: C, 58.82; H, 4.61. Found: C, 58.64; H, 4.49. FAB-MS *m/z*: 577 $(M+H)^+$. ^{1}H-NMR (acetone-d_6) δ: 2.85 (2H, m, H-4′), 4.14 (1H, d, J=4 Hz, H-3), 4.20 (1H, br s, H-3′), 4.34 (1H, d, J=4 Hz, H-4), 4.85 (1H, br s, H-2′), 6.05, 6.12 (3H, in total, A-ring H), 6.60—7.40 (6H in total, B-ring H).

Heptamethyl Ether (10a) of 10——**10** (43 mg) was methylated with ethereal diazomethane at room temperature for 24 h. Work-up was done as usual, and the product was purified by silica gel chromatography with benzene–acetone (4 : 1) to give the heptamethyl ether (**10a**) (30 mg). A white amorphous powder, $[\alpha]_D^{21}$ +22.7° (c=0.7, acetone). CD (c=0.038, MeOH) $[\theta]^{20}$ (nm): +113000 (240), 0 (254), −52300 (271). *Anal.* Calcd for $C_{37}H_{38}O_{12}$: C, 66.06; H, 5.39. Found: C, 65.78; H, 5.80. EI-MS *m/z*: 674 $(M)^+$. ^{1}H-NMR ($CDCl_3$) δ: 2.96 (2H, m, H-4′), 3.70—4.00 (21H in total, OMe×7), 4.00—4.30 (2H, m, H-3, 3′), 4.80 (1H, d, J=4 Hz, H-4), 4.85 (1H, s, H-2′), 6.13, 6.27 (each 1H, d, J=2 Hz, H-6, 8), 6.44 (1H, s, H-8′), 6.80—7.20 (6H in total, B-ring H).

Proanthocyanidin A-7 (11)——Colorless needles (H_2O), mp >300 °C, $[\alpha]_D^{21}$ +35.9° (c=1.2, acetone). *Anal.* Calcd for $C_{30}H_{24}O_{12}\cdot 5/2H_2O$: C, 57.97; H, 4.70. Found: C, 58.02; H, 4.50. FAB-MS *m/z*: 577 $(M+H)^+$. ^{1}H-NMR (acetone-d_6) δ: 2.70—3.20 (2H, m, H-4″), 4.15 (1H, d, J=4 Hz, H-3), 4.20 (1H, br s, H-3′), 4.30 (1H, d, J=4 Hz, H-4), 4.87 (1H, s, H-2′), 6.10, 6.12 (3H in total, A-ring H), 6.60—7.40 (6H in total, B-ring H).

Heptamethyl Ether (11a) of 11——**11** (25 mg) was methylated with ethereal diazomethane at room temperature. Work-up as described for **10** yielded the heptamethyl ether (**11a**) (30 mg). A white amorphous powder, $[\alpha]_D^{21}$ +41.2°

(c=0.7, acetone). CD (c=0.045, MeOH) $[\theta]^{20}$ (nm): +56000 (240). *Anal.* Calcd for $C_{37}H_{38}O_{12}\cdot 1/2H_2O$: C, 65.00; H, 5.75. Found: C, 65.35; H, 5.99. EI-MS m/z: 674 $(M)^+$. ^{1}H-NMR ($CDCl_3$) δ: 2.99 (2H, m, H-4'), 3.70—4.00 (21H in total, OMe×7), 4.20 (2H, m, H-3, 3'), 4.85 (1H, d, J=4 Hz, H-4), 4.88 (1H, s, H-2), 6.13, 6.27 (each 1H, d, J=2 Hz, H-6, 8), 6.20 (1H, s, H-8'), 6.80—7.20 (6H in total, B-ring H).

Derivation of 10 and 11 from 3——A mixture of **3** (1.5 g), sodium bicarbonate (300 mg) and hydrogen peroxide (1.5 ml) in EtOH (50 ml) was left at room temperature for 24 h. The reaction mixture was neutralized with Amberlite IR-120B (H^+ form), and the solvent was evaporated off *in vacuo*. The residue was subjected to Bondapak C_{18} chromatography (20% aqueous MeOH) to afford **10** (21 mg) and **11** (12 mg).

Aesculitannin A (12)——An off-white amorphous powder, $[\alpha]_D^{23}$ +133.6° (c=0.9, acetone). *Anal.* Calcd for $C_{45}H_{36}O_{18}\cdot 2H_2O$: C, 60.00; H, 4.47. Found: C, 60.09; H, 4.89. FAB-MS m/z: 865 $(M+H)^+$. ^{1}H-NMR (acetone-d_6) δ: 2.84 (2H, m, H-4''), 4.00 (1H, s, H-3), 4.12 (1H, d, J=4 Hz, H-3'), 4.30 (1H, br s, H-3''), 4.42 (1H, d, J=4 Hz, H-4'), 4.83 (1H, s, H-4), 4.96 (1H, s, H-2), 5.19 (1H, s, H-2''), 5.90—6.10 (4H in total, A-ring H), 6.60—7.40 (9H in total, B-ring H).

Thiolytic Degradation of 12——A mixture of **12** (100 mg), benzylmercaptan (2 ml) and acetic acid (2 ml) in EtOH (15 ml) was refluxed for 5 h with stirring. The reaction mixture was concentrated *in vacuo* to give an oily residue, which was chromatographed over Sephadex LH-20. Elution with EtOH afforded (−)-epicatechin 4-benzylthioether (**19**) (23 mg) and proanthocyanidin A-2 (**4**) (42 mg).

Partial Thiolytic Degradation of 9——A mixture of **9** (2 g), benzylmercaptan (4 ml) and acetic acid (3 ml) in EtOH (50 ml) was heated under reflux for 12 h. After concentration, the products were repeatedly chromatographed on Sephadex LH-20 using EtOH and 80% aqueous MeOH to give (−)-epicatechin (**1**) (32 mg), (−)-epicatechin 4-benzylthioether (**19**) (23 mg), proanthocyanidin A-2 4'-benzylthioether (**21**) (325 mg) and a trimeric proanthocyanidin 4''-benzylthioether (**20**) (32 mg). **20**: An off-white amorphous powder, $[\alpha]_D^{21}$ +33.5° (c=1.1, acetone). ^{1}H-NMR (acetone-d_6) δ: 3.25 (1H, d, J=4 Hz, H-3'), 4.40 (1H, d, J=4 Hz, H-4'), 4.76 (1H, s, H-4), 5.11 (1H, s, H-2), 5.27 (1H, s, H-2''), 5.80—6.20 (4H in total, A-ring H), 6.40—7.80 (14H in total, aromatic H).

Desulfurization of 20——The thioether (**20**) (30 mg) in EtOH–acetic acid (9:1) was shaken at 50 °C with Raney nickel (W-4) for 30 min. After removal of the catalyst by filtration, the filtrate was concentrated to dryness *in vacuo*. The residue was purified by Sephadex LH-20 chromatography (60% aqueous MeOH) to give **12** (12 mg).

Aesculitannin B (13)——An off-white amorphous powder, $[\alpha]_D^{21}$ +52.8° (c=1.2, acetone). *Anal.* Calcd for $C_{45}H_{36}O_{18}\cdot 2H_2O$: C, 60.00; H, 4.47. Found: C, 60.32; H, 4.44. FAB-MS m/z: 865 $(M+H)^+$. ^{1}H-NMR (acetone-d_6) δ: 2.84 (2H, m, H-4''), 3.44 (1H, d, J=4 Hz, H-4), 3.96 (1H, d, J=4 Hz, H-3), 4.04—5.00 (5H in total, m, H-2', 2'', 3', 3'', 4'), 5.70—6.20 (4H in total, A-ring H), 6.60—7.30 (9H in total, B-ring H).

Thiolytic Degradation of 13——A mixture of **13** (120 mg), benzylmercaptan (2 ml) and acetic acid (2 ml) in EtOH (10 ml) was treated as described for **12**, and similar separation afforded (−)-epicatechin (**1**) (12 mg) and a thioether (**22**) (48 mg). **22**: An off-white amorphous powder, $[\alpha]_D^{21}$ +27.1° (c=0.82, acetone). *Anal.* Calcd for $C_{37}H_{30}O_{12}S\cdot H_2O$: C, 62.00; H, 4.50. Found: C, 62.34; H, 4.89. ^{1}H-NMR (acetone-d_6) δ: 4.00—4.30 (4H, m, $-SCH_2-$, H-4', H-3'), 4.33 (1H, d, J=4 Hz, H-3), 4.44 (1H, d, J=4 Hz, H-4), 5.16 (1H, d, J=8 Hz, H-2'), 5.90—6.20 (3H in total, A-ring H), 6.60—7.60 (11H in total, aromatic H).

Desulfurization of 22——The thioether **22** (40 mg) in EtOH–acetic acid (9:1) (4 ml) was treated with Raney nickel at 50 °C for 10 min. The reaction mixture was worked up as before to furnish proanthocyanidin A-4 (**5**) (31 mg).

Epimerization of 8——A mixture of **8** (150 mg) and potassium carbonate (30 mg) in acetone (20 ml) was heated under reflux for 10 min. After removal of potassium carbonate by filtration, the filtrate was concentrated to dryness *in vacuo*. The residue was subjected to Bondapak C_{18} chromatography with 20% aqueous MeOH to give **13** (49 mg).

Aesculitannin C (14)——An off-white amorphous powder, $[\alpha]_D^{21}$ +39.5° (c=1.2, acetone). *Anal.* Calcd for $C_{45}H_{34}O_{18}\cdot 2H_2O$: C, 60.13; H, 4.26. Found: C, 60.32; H, 4.44. FAB-MS m/z: 863 $(M+H)^+$. ^{1}H-NMR (acetone-d_6) δ: 2.90 (2H, m, H-4''), 3.99 (1H, d, J=4 Hz, H-3), 4.30 (2H, m, H-3', 3''), 4.45, 4.58 (each 1H, d, J=4 Hz, H-4, 4'), 4.97 (1H, s, H-2''), 6.00—6.20 (4H in total, A-ring H), 6.60—7.60 (9H in total, B-ring H).

Decamethyl Ether (14a) of 14——**14** (30 mg) was methylated with ethereal diazomethane. Work-up as before yielded the decamethyl ether (**14a**) (16 mg). **14a**: A white amorphous powder, $[\alpha]_D^{21}$ +23.5° (c=0.7, acetone). CD (c=0.016, MeOH) $[\theta]^{20}$ (nm): +285000 (235), 0 (248), −87500 (270). *Anal.* Calcd for $C_{55}H_{54}O_{18}$: C, 65.86; H, 5.43. Found: C, 65.68; H, 5.80. FD-MS m/z: 1002 $(M)^+$. ^{1}H-NMR ($CDCl_3$) δ: 2.91 (2H, m, H-4''), 3.39, 3.52 (each 3H, s, OMe×2), 3.70—3.90 (24H in total, OMe×8), 4.19 (1H, d, J=3 Hz, H-3), 4.40—4.50 (2H, m, H-3', 3''), 4.95, 4.99 (each 1H, d, J=3 Hz, H-4', 4''), 4.97 (1H, s, H-2''), 6.10—6.40 (4H in total, A-ring H), 6.80—7.70 (9H in total, B-ring H).

Acid-Catalyzed Degradation of 14——A solution of **14** (50 mg) in 1 N ethanolic HCl (10 ml) was refluxed for 5 h with stirring. The solvent was evaporated off under reduced pressure, and the residue was chromatographed on Sephadex LH-20. Elution with 60% aqueous MeOH furnished (−)-epicatechin (**1**) (5 mg).

Derivation of 14 from 12——A mixture of **12** (600 mg), sodium bicarbonate (200 mg) and hydrogen peroxide (1 ml) in EtOH (25 ml) was left at room temperature for 12 h. Work-up as described for **10** and **11** yielded **14** (32 mg).

Aesculitannin D (15)——An off-white amorphous powder, $[\alpha]_D^{22}$ +55.1° (c=1.1, acetone). *Anal.* Calcd for

$C_{45}H_{34}O_{18}\cdot H_2O$: C, 61.36; H, 4.12. Found: C, 61.32; H, 4.44. FAB-MS *m/z*: 863 $(M+H)^+$. ^{1}H-NMR (acetone-d_6) δ: 2.58 (1H, dd, $J=16$, 8 Hz, H-4''), 2.90 (1H, dd, $J=16$, 6 Hz, H-4), 4.00 (1H, d, $J=4$ Hz, H-3), 4.24 (1H, m, H-3''), 4.36 (2H, s, H-3', 4'), 4.58 (1H, d, $J=4$ Hz, H-4), 4.82 (1H, d, $J=8$ Hz, H-2''), 6.00—6.20 (4H in total, A-ring H), 6.70—7.60 (9H in total, B-ring H).

Acid-Catalyzed Degradation of 15——A solution of **15** (60 mg) in 1 N ethanolic HCl (10 ml) was refluxed for 5 h with stirring. The reaction mixture was worked up as before to give (−)-catechin (**23**) (4 mg).

Epimerization of 14——A mixture of **14** (25 mg) and potassium carbonate (10 mg) in acetone (20 ml) was refluxed for 10 min. Work-up as described for **13** afforded **15** (18 mg).

Aesculitannin E (16)——An off-white amorphous powder, $[\alpha]_D^{21}$ +74.7° ($c=1.7$, acetone). *Anal.* Calcd for $C_{60}H_{48}O_{24}\cdot 3H_2O$: C, 59.70; H, 4.51. Found: C, 59.41; H, 4.38. FAB-MS *m/z*: 1153 $(M+H)^+$.

Thiolytic Degradation of 16——A mixture of **16** (200 mg) and benzylmercaptan (2 ml) in 0.1 N ethanolic HCl (20 ml) was refluxed for 2 h. The reaction mixture was treated as before to furnish proanthocyanidin A-2 4'-benzylthioether (**21**) (65 mg), (−)-epicatechin 4-benzylthioether (**19**) (30 mg) and (−)-epicatechin (**1**) (23 mg).

Partial Thiolytic Degradation of 16——A mixrure of **16** (600 mg) and benzylmercaptan (4 ml) in 0.05 N ethanolic HCl (40 ml) was heated under reflux for 2 h. The reaction mixture was concentrated to dryness *in vacuo*, and the oily residue was repeatedly chromatographed over Sephadex LH-20 (EtOH) and MCI-gel CHP 20P (60% aqueous MeOH) to give (−)-epicatechin (**1**) (10 mg), (−)-epicatechin 4-benzylthioether (**19**) (15 mg), proanthocyanidin A-2 4'-benzylthioether (**21**) (30 mg), procyanidin B-2 (**2**) (7 mg) and a thioether (**24**) (284 mg). **24**: An off-white amorphous powder, $[\alpha]_D^{22}$ +75.6° ($c=0.71$, acetone). *Anal.* Calcd for $C_{52}H_{42}O_{18}S\cdot 7/2H_2O$: C, 59.48; H, 4.76. Found: C, 59.45; H, 4.76. ^{13}C-NMR (acetone-d_6) δ: 37.3 ($-SCH_2-$), 38.1 (C-4'), 44.5 (C-4''), 66.1 (C-3), 70.4 (C-3''), 71.6 (C-3'), 75.5 (C-2''), 78.9 (C-2'), 95.9, 96.4, 98.4 (C-6, 8, 6', 6''), 104.0 (C-2).

Desulfurization of 24——A solution of **24** (150 mg) in acetic acid–EtOH (1 : 9) (5 ml) was treated with Raney nickel (W-4) at room temperature for 1 h. Work-up as before afforded cinnamtannin B_1 (**8**) (75 mg).

Aesculitannin F (17)——An off-white amorphous powder, $[\alpha]_D^{22}$ +108.9° ($c=0.7$, acetone). *Anal.* Calcd for $C_{60}H_{48}O_{24}\cdot H_2O$: C, 61.54; H, 4.30. Found: C, 61.29; H, 4.60. FAB-MS *m/z*: 1153 $(M+H)^+$.

Partial Thiolytic Degradation of 17——A mixture of **8** (300 mg) and benzylmercaptan (2 ml) in 0.05 N ethanolic HCl (20 ml) was treated as described for **16** to give proanthocyanidin A-4 4'-benzylthioether (**22**) (12 mg), (−)-epicatechin 4-benzylthioether (**19**) (8 mg), (−)-epicatechin (**1**) (5 mg), procyanidin B-2 (**2**) (16 mg) and a thioether (**25**) (152 mg). **25**: An off-white amorphous powder, $[\alpha]_D^{22}$ +127.6° ($c=0.7$, acetone). *Anal.* Calcd for $C_{52}H_{42}O_{18}S\cdot 3H_2O$: C, 59.99; H, 4.56. Found: C, 59.66; H, 4.56. ^{13}C-NMR (acetone-d_6) δ: 37.0 ($-SCH_2-$), 38.7 (C-4'), 43.9 (C-4''), 66.8 (C-3), 71.4 (C-3''), 73.8 (C-3'), 75.5 (C-2''), 83.7 (C-2'), 96.1, 96.7, 97.2, 97.4 (C-6, 8, 6', 6''), 103.7 (C-2).

Desulfurization of 25——A solution of **25** (120 mg) in acetic acid–EtOH (1 : 9) (5 ml) was treated with Raney nickel (W-4) at room temperature for 1 h. Work-up as before afforded **13** (60 mg).

Aesculitannin G (18)——An off-white amorphous powder, $[\alpha]_D^{22}$ +9.6° ($c=0.5$, acetone). *Anal.* Calcd for $C_{60}H_{46}O_{24}\cdot 5H_2O$: C, 58.06; H, 4.55. Found: C, 58.22; H, 4.55. FAB-MS *m/z*: 1151 $(M+H)^+$. ^{1}H-NMR (acetone-d_6) δ: 2.96 (2H, m, H-4'''), 3.49 (1H, d, $J=4$ Hz, H-4), 3.89 (1H, br s, H-3'''), 4.06 (1H, d, $J=4$ Hz, H-3), 4.20 (2H, s, H-3'', 4''), 4.55 (2H, s, H-4', 2'''), 5.66 (1H, s, H-2'), 5.90—6.40 (5H in total, A-ring H), 6.50—7.60 (12H in total, B-ring H).

Thiolytic Degradation of 18——A mixture of **18** (50 mg) and benzylmercaptan (1 ml) in 0.5 N ethanolic HCl (10 ml) was treated as before to give proanthocyanidin A-2 4'-benzylthioether (**21**) (5 mg) and proanthocyanidin A-2 (**4**) (10 mg).

Acknowledgements The authors are grateful to the Executive Board of the Fukuoka Botanic Garden for permission to collect plant materials. They are also indebted to Mr. Y. Tanaka, Miss K. Soeda and Mr. K. Isobe for measurements of ^{13}C-NMR spectra, ^{1}H-NMR spectra and MS, respectively.

References and Notes

1) Part LVIII: G. Nonaka, M. Ishimatsu, T. Tanaka, I. Nishioka, M. Nishizawa, and T. Yamagishi, *Chem. Pharm. Bull.*, **35**, 3127 (1987).
2) F.-L. Hsu, G. Nonaka, and I. Nishioka, *Chem. Pharm. Bull.*, **33**, 3142 (1985); *idem*, *ibid.*, **33**, 3293 (1985).
3) S. Morimoto, G. Nonaka, and I. Nishioka, *Chem. Pharm. Bull.*, **34**, 633 (1986).
4) Y. Kashiwada, G. Nonaka, and I. Nishioka, *Chem. Pharm. Bull.*, **34**, 4083 (1986).
5) E. Ezaki-Furuichi, G. Nonaka, I. Nishioka, and K. Hayashi, *Agric. Biol. Chem.*, **50**, 2061 (1986).
6) K. Weinges, W. Kaltenhäuser, H.-D. Marx, E. Nader, F. Nader, J. Perner, and D. Seiler, *Annalen*, **711**, 194 (1968).
7) W. Mayer, L. Göll, E. V. Ärndt, and Mannschreck, *Tetrahedron Lett.*, **1966**, 429.
8) D. Jacques and E. Haslam, *J. Chem. Soc., Perkin Trans. 1*, **1974**, 2663.
9) The name entcatechin was recently proposed for (−)-catechin.[16]

10) G. Nonaka, S. Morimoto, J. Kinjo, T. Nohara, and I. Nishioka, *Chem. Pharm. Bull.*, **35**, 149 (1987).
11) G. Nonaka, S. Morimoto, and I. Nishioka, *J. Chem. Soc., Perkin Trans. 1*, **1983**, 2139.
12) A. C. Fletcher, L. J. Porter, E. Haslam, and R. K. Gupta, *J. Chem. Soc., Perkin Trans. 1*, **1977**, 1682.
13) G. Nonaka, F.-L. Hsu, and I. Nishioka, *J. Chem. Soc., Chem. Commun.*, **1981**, 781.
14) R. S. Thompson, D. Jacques, E. Haslam, and R. J. N. Tanner, *J. Chem. Soc., Perkin Trans. 1*, **1972**, 1387.
15) Examination of the Dreiding model shows that in the case of the C-4 and C-8 linkage, the B'-ring is located sterically close to H-4.
16) R. W. Hemingway, L. Y. Foo, and L. J. Porter, *J. Chem. Soc., Perkin Trans. 1*, **1982**, 1209.

[Chem. Pharm. Bull. 35(12)4730—4735(1987)]

Dioxopyrrolines. XL.[1] Photocycloaddition Reaction of 4-Ethoxycarbonyl-5-phenyl-1*H*-pyrrole-2,3-dione to Dihydrofurans. Formation of a 2,4-Dioxa-10-azatricyclo[6.3.0.0^{3,7}]undecane Ring System

TAKEHIRO SANO,*[a] MIYUKI HIROSE,[a] YOSHIE HORIGUCHI,[a]
HIROAKI TAKAYANAGI,[b] HARUO OGURA,[b]
and YOSHISUKE TSUDA[c]

Showa College of Pharmaceutical Sciences,[a] Tsurumaki, Setagaya-ku, Tokyo 154, Japan, School of Pharmaceutical Sciences, Kitasato University,[b] Minato-ku, Tokyo 108, Japan, and Faculty of Pharmaceutical Sciences, Kanazawa University,[c] 13-1 Takara-machi, Kanazawa 920, Japan

(Received May 19, 1987)

Photocycloaddition of the dioxopyrroline **1** to 2,3-dihydrofurans gave dihydropyridones **7** and 2,4-dioxa-10-azatricyclo[6.3.0.0^{3,7}]undecanes **8**. The structure of **8a** was determined by X-ray crystallographic analysis. The mechanisms of formation of the adducts are discussed from stereochemical point of view.

Keywords——photocycloaddition; dioxopyrroline; 1*H*-pyrrole-2,3-dione; 2,3-dihydrofuran; dihydropyridone; 2,4-dioxa-10-azatricyclo[6.3.0.0^{3,7}]undecane; stereo-selection rule

Photocycloaddition of the dioxopyrroline **1** to olefins proceeds in a regio- and stereoselective manner to give usually one of the following three compounds as a major product; *exo*- and *endo*-substituted cyclobutanes **2** and **3**, and a dihydropyridone **4**.[2] The product in this reaction largely depends on the nature of the olefin. Acyclic olefins give a cyclobutane whose stereochemistry can be predicted by the stereo-selection rule proposed in the previous paper[3]; that is, alkoxyalkenes (they form a very polar enone–olefin pair) give an *endo*-isomer **3** as the major product as a result of [2s+2s] addition of the favored *endo*-π-complex, while alkenes and butadienes (they form a polar enone–olefin pair) produce an *exo* isomer **2** as the major product as a result of [2s+2a] addition of the favored *endo*-π-complex. Cycloalkenes such as cyclopentene give a dihydropyridone **5**.[4,5] This can be explained by [1, 3] rearrangement of the highly strained intermediary cyclobutane **6** *via* the lactim form, followed by cheletropic loss of carbon monoxide.[3,4]

As a part of our studies on the photocycloaddition of dioxopyrroline to olefins we wish to present the results of photoannulation of **1** to dihydrofurans (oxa-cycloolefins), yielding a new ring system.

Results and Discussion

Irradiation of a solution of **1** and 2,3-dihydrofuran in dimethoxyethane for 1 h with $\geqq$300 nm light gave two adducts **7a** and **8a** in yields of 24% and 9%. No cyclobutane derivative was isolated in this photocycloaddition. Similar irradiation of **1** and 5-methyl-2,3-dihydrofuran also afforded two adducts **7b** and **8b** in yields of 14% and 17%. In contrast, 2,5-dihydrofuran and furan did not give any cycloadduct on similar irradiation.

The structures of **7a** and **7b** were readily deduced from the spectral data. They have molecular formulae corresponding to the 1:1 adduct minus CO. The presence of the

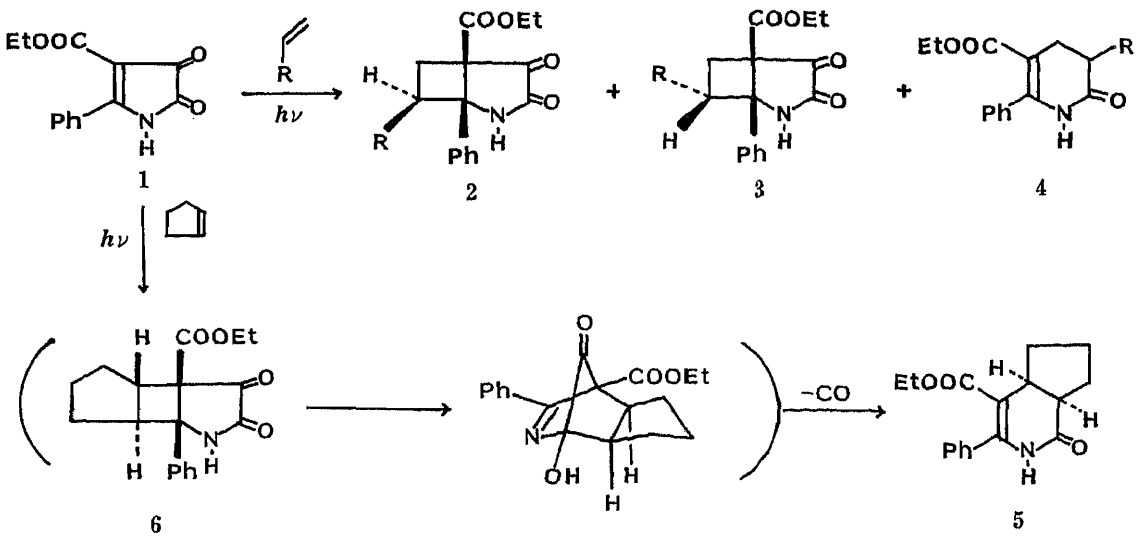

Chart 1

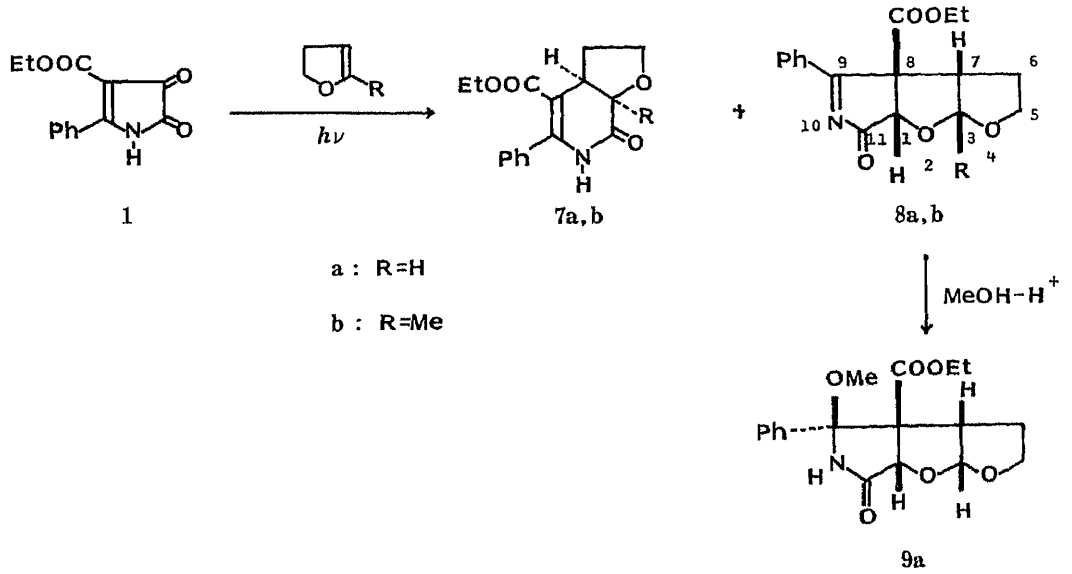

Chart 2

dihydropyridone moiety was established by the ultraviolet (UV) spectra (λ_{max}: 285 nm for **7a** and **7b**) and the infrared (IR) spectra (ν_{max}: 1660 cm^{-1} for **7a** and 1680 cm^{-1} for **7b**). These data are compatible with the reported spectral data for the dihydropyridone **5**.[4] The proton and carbon-13 nuclear magnetic resonance (^{1}H- and ^{13}C-NMR) spectra of **7a** and **7b** also supported the assigned structures.

The adducts **8a** and **8b** have the molecular formulae $C_{17}H_{17}NO_5$ and $C_{18}H_{19}NO_5$, respectively, as evidenced by the high-resolution mass spectra (HRMS) and elementary analyses, indicating that they are 1 : 1 adducts of the addends. However, the spectral data are not consistent with the expected cyclobutane structure. The adduct **8a** exhibited a strong UV absorption band at 278 nm (ε 19500) and the IR spectrum showed no signals due to an NH group. In addition to these data, the signal at δ 4.99 (1H) in the ^{1}H-NMR spectrum and the two signals at δ 114.8 and 189.1 in the ^{13}C-NMR spectrum were not consistent with the cyclobutane structure. The structure of **8a** was finally established by X-ray crystallographic

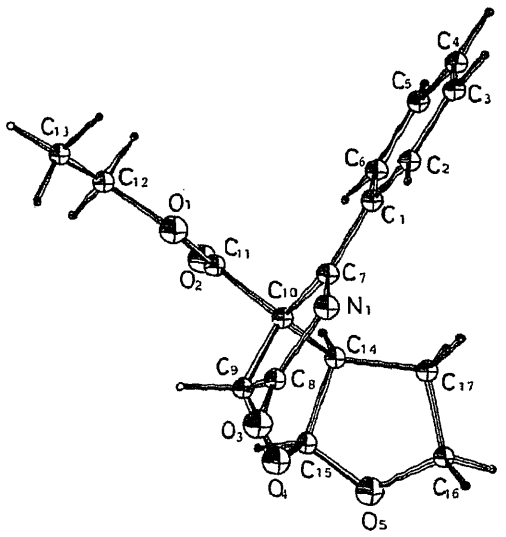

Fig. 1

TABLE I. Positional Parameters ($\times 10^4$) with Their Estimated Standard Deviations (in Parentheses) and Equivalent Isotropic Thermal Parameters (Å^2) of the Adduct **8a**

Atom	x	y	z	B_{eq}/B_{iso}
O1	1432 (2)	3017 (3)	4094 (2)	3.4
O2	2998 (2)	3536 (3)	4763 (2)	4.2
O3	860 (2)	−1630 (4)	2242 (2)	5.1
O4	2899 (2)	−691 (4)	2948 (2)	4.0
O5	4371 (2)	−1612 (4)	3915 (2)	4.6
N1	1118 (2)	−1135 (4)	4016 (2)	2.9
C1	1654 (3)	−102 (4)	5780 (3)	2.6
C2	2324 (3)	807 (6)	6538 (3)	4.0
C3	2252 (4)	885 (6)	7560 (3)	4.8
C4	1530 (3)	68 (5)	7811 (3)	4.1
C5	865 (3)	−836 (5)	7065 (3)	3.4
C6	919 (3)	−915 (5)	6040 (3)	2.9
C7	1702 (2)	−215 (4)	4698 (3)	2.5
C8	1311 (3)	−944 (5)	3030 (3)	3.1
C9	2140 (3)	234 (5)	3135 (3)	2.9
C10	2444 (3)	717 (4)	4318 (3)	2.5
C11	2350 (3)	2598 (5)	4432 (3)	3.2
C12	1214 (3)	4803 (5)	4096 (3)	4.0
C13	177 (4)	4992 (5)	3585 (4)	5.0
C14	3471 (3)	72 (5)	4737 (3)	3.2

$$B_{eq}=\frac{4}{3}\Sigma_i\Sigma_j\beta_{ij}a_ia_j$$

analysis, which indicated that it is a novel heterocyclic compound having the 2,4-dioxa-10-azatricyclo[6.3.0.0^{3,7}]undecane ring system with *cis-syn-cis* stereochemistry as shown in Fig. 1. The UV absorption band at 278 nm was thus attributed to the acylimino moiety conjugated with the phenyl group. Interestingly, the carbon signals due to the acylimino group were observed at fairly low field (δ 189.6 for C-9 and 191.4 for C-11).

In accordance with this acylimino structure, **8a** on treatment with methanol containing a catalytic amount of hydrochloric acid readily formed the methanol adduct **9a**. The structure of **9a** was confirmed by the disappearance of the UV absorption at 278 nm and by the appearance of two new carbon signals at δ 92.1 (C-9) and 175 (C-11). The stereochemistry of the methoxy group was deduced from the consideration that it should be introduced from the less-hindered convex face.

The adduct **8b** has similar spectral features (see Experimental) with those of **8a**, thus clarifying the structure.

The formation of **7** and **8** can be rationalized as follows. In the photocycloaddition of **1** and dihydrofuran, two transition states are possible, *i.e.*, an *endo*- and an *exo*-π-complex. The former transition state should be more favored than the latter, since the two addends are sufficiently planar, thus gaining a maximum overlap of orbitals in the former complex. If we assume that the dioxopyrroline–dihydrofuran pair is very polar, as is the dioxopyrroline–ethoxyethylene pair,[3] the stereo-selection rule[3] predicts that a [2s+2s] addition and a [2s+2a] addition are preferred in the favored transition and in the less favored one, respectively. Thus, the *endo*-π-complex gives the cyclobutane of *cis-syn-cis* configuration **10** as the major product, which has the stereochemistry favorable to [1, 3] rearrangement through a lactim form **11**. Subsequent cheletropic loss of CO gives the dihydropyridone **7a**.

TABLE II. Bond Lengths (Å) and Bond Angles (°) of **8a** with Their Estimated Standard Deviations (in Parentheses)

Atoms	Distance (Å)	Atoms	Distance (Å)	Atoms	Distance (Å)
O(1)–C(11)	1.337 (5)	O(1)–C(12)	1.473 (6)	C(16)–C(17)	1.506 (8)
O(2)–C(11)	1.196 (5)	O(3)–C(8)	1.201 (5)	O(4)–C(9)	1.426 (5)
O(4)–C(15)	1.447 (5)	O(5)–C(15)	1.382 (5)	O(5)–C(16)	1.442 (6)
C(1)–C(2)	1.396 (6)	N(1)–C(7)	1.288 (5)	N(1)–C(8)	1.436 (5)
C(2)–C(3)	1.402 (7)	C(1)–C(6)	1.393 (5)	C(1)–C(7)	1.470 (5)
C(5)–C(6)	1.397 (6)	C(4)–C(5)	1.381 (7)	C(3)–C(4)	1.373 (7)
C(7)–C(10)	1.531 (5)	C(8)–C(9)	1.520 (6)	C(9)–C(10)	1.559 (6)
C(12)–C(13)	1.487 (8)	C(10)–C(11)	1.532 (6)	C(10)–C(14)	1.541 (6)
C(14)–C(15)	1.543 (6)	C(14)–C(17)	1.551 (6)		

Atoms	Angle (°)	Atoms	Angle (°)
C(11)–O(1)–C(12)	116.4 (3)	C(1)–C(2)–C(3)	119.3 (4)
C(9)–O(4)–C(15)	108.5 (3)	C(2)–C(3)–C(4)	120.2 (5)
C(2)–C(1)–C(7)	121.1 (4)	C(3)–C(4)–C(5)	120.9 (5)
N(1)–C(7)–C(10)	116.2 (3)	C(4)–C(5)–C(6)	119.8 (4)
O(3)–C(8)–C(9)	126.1 (4)	C(1)–C(6)–C(5)	119.7 (4)
O(4)–C(9)–C(10)	107.5 (3)	N(1)–C(7)–C(1)	121.0 (3)
C(7)–C(10)–C(11)	110.9 (3)	O(3)–C(8)–N(1)	123.1 (4)
C(9)–C(10)–C(14)	104.0 (3)	O(4)–C(9)–C(8)	108.0 (3)
O(1)–C(11)–C(10)	109.2 (3)	C(8)–C(9)–C(10)	103.4 (3)
C(10)–C(14)–C(17)	117.9 (4)	C(7)–C(10)–C(9)	101.2 (3)
O(4)–C(15)–C(14)	104.7 (3)	C(9)–C(10)–C(11)	109.9 (3)
C(15)–O(5)–C(16)	109.0 (4)	O(1)–C(11)–O(2)	125.7 (4)
C(7)–N(1)–C(8)	108.4 (3)	O(1)–C(12)–C(13)	107.1 (4)
C(6)–C(1)–C(7)	118.8 (3)	C(10)–C(14)–C(15)	104.1 (3)
C(1)–C(7)–C(10)	122.9 (3)	C(15)–C(14)–C(17)	101.9 (3)
N(1)–C(8)–C(9)	110.7 (3)	O(4)–C(15)–O(5)	108.4 (3)
C(7)–C(10)–C(14)	115.8 (3)	O(5)–C(15)–C(14)	108.7 (3)
C(11)–C(10)–C(14)	113.9 (3)	O(5)–C(16)–C(17)	107.7 (4)
O(2)–C(11)–C(10)	125.1 (4)	C(14)–C(17)–C(16)	106.0 (4)
C(2)–C(1)–C(6)	120.1 (4)		

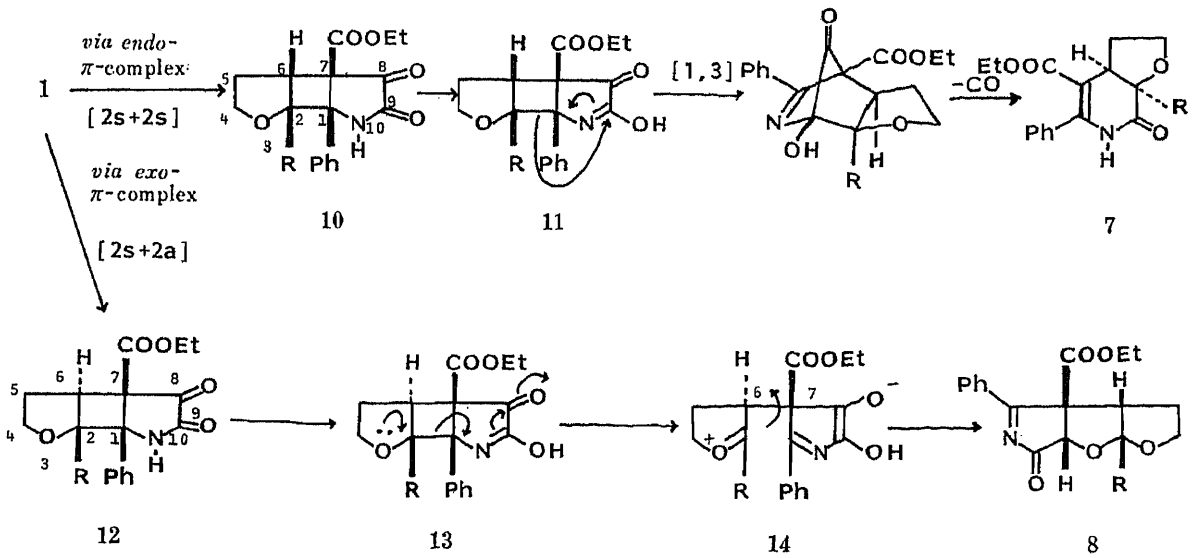

Chart 3

On the other hand, the less favored *exo*-π-complex gives the cyclobutane of *cis-anti-trans* configuration **12** as the major product. This highly strained intermediate would immediately decompose into **14** *via* the lactim form **13**, since a concerted [1, 3] rearrangement in this compound is impossible for steric reasons. The resulting zwitter-ion **14** cyclizes, with rotation of the C_6–C_7 bond and subsequent ketonization, to give the thermodynamically more stable *cis*-fused di-furano derivative **8a**. This mechanism well explains the stereochemistries at C-1, C-3, C-7, and C-8 in the product **8a**.

In the case of 5-methyl-2,3-dihydrofuran, the presence of the non-bonded interaction between the methyl and the phenyl groups in the *endo*-π-complex will destabilize this transition, thus decreasing its population and increasing the ratio of *exo*-π-complex. The results are reflected in the product formation; **7b** and **8b** were obtained in the ratio of *ca.* 1 : 1.

Experimental

Unless otherwise stated, the following procedures were adopted. Melting points were taken on a Yanagimoto micro hot-stage melting point apparatus, and are uncorrected. IR spectra were taken in Nujol mulls with a Hitachi 260-10 spectrophotometer and are given in cm^{-1}. UV spectra were recorded with a Hitachi 200-10 spectrophotometer. ^{1}H-NMR (100 MHz) and ^{13}C-NMR (25.0 MHz) spectra were taken in $CDCl_3$ solution with tetramethylsilane (TMS) as an internal standard on a JEOL FX-100 spectrometer. Chemical shifts are reported in ppm (δ), and signals are described as s (singlet), d (doublet), t (triplet), q (quartet), m (multiplet), or br (broad). HRMS were recorded on a JEOL JMS-D300 mass spectrometer. Thin layer chromatography (TLC) was performed on precoated Silica gel 60 F_{254} plates (Merck). Medium-pressure liquid chromatography (MPLC) was performed on Kusano CIC prepacked silica gel columns. The photolysis solution was irradiated internally using a 300 W high-pressure mercury lamp (Eikosha Halos PIH 300) with a Pyrex filter.

The Photocycloaddition of the Dioxopyrroline (1) to 2,3-Dihydrofuran——A solution of **1** (2 g, 8 mmol) and 2,3-dihydrofuran (4 g, 56 mmol) in dimethoxyethane (300 ml) was irradiated for 1 h at 0 °C. After removal of the solvent, the residue was dissolved in benzene and chromatographed over silica gel (Wako-gel C-200). Elution with benzene and crystallization of the eluate from MeOH–Et_2O–hexane gave (1*S**,3*R**,7*S**,8*R**)-8-ethoxycarbonyl-9-phenyl-2,4-dioxa-10-azatricyclo[6.3.0.0^{3,7}]undecan-9-en-11-one (**8a**, 230 mg, 9%) as pale yellow prisms, mp 126—127 °C. IR: 1750, 1730. UV $\lambda_{max}^{dioxane}$ nm (ε): 278 (19700). UV λ_{max}^{MeOH} nm (ε): 284 (20000). ^{1}H-NMR (270 MHz): 1.00 (3H, t, J=7 Hz, $COOCH_2C\underline{H}_3$), 1.50 (1H, m, C_6-H), 2.00 (1H, m, C_6-H), 3.89 (1H, dd, J=4, 9 Hz, C_5-H), 3.69 (1H, dd, J=5, 9 Hz, C_5-H), 3.97 (1H, ddd, J=4, 5, 10 Hz, C_7-H), 4.14 (2H, q, J=7 Hz, $COO\underline{C}H_2CH_3$), 4.99 (1H, s, C_1-H), 6.13 (1H, d, J=5 Hz, C_3-H), 7.6 (3H, m, Ar-H), 8.0 (2H, m, Ar-H). ^{13}C-NMR: 13.7 (q, $COOCH_2\underline{C}H_3$), 27.4 (t, C_6), 46.9 (d, C_7), 62.9 (t, C_5), 67.9 (s, C_8), 68.3 (t, $COO\underline{C}H_2CH_3$), 86.5 (d, C_1), 114.8 (d, C_3), 129.5 (d, 2C, Ph), 130.3 (d, 2C, Ph), 130.9 (s, Ph), 135.4 (d, Ph), 170.3 (s, $\underline{C}OOCH_2CH_3$), 189.6 (s, C_9), 191.4 (s, C_{11}). *Anal.* Calcd for $C_{17}H_{17}NO_5$: C, 64.75; H, 5.43; N, 4.44. HRMS *m/z*: 315.1107. Found: C, 64.36; H, 5.54; N, 4.35. HRMS *m/z*: 315.1112.

Further elution with benzene–CH_2Cl_2 (1 : 1) and crystallization of the product from CH_2Cl_2–Et_2O gave 4-ethoxycarbonyl-5-phenyl-2,3,3a,7a-tetrahydrofuro[2,3-*c*]pyridin-7(6*H*)-one (**7a**, 550 mg, 24%) as colorless needles, mp 156—157 °C. IR: 3260, 1720, 1660, 1600. UV $\lambda_{max}^{dioxane}$ nm (ε): 285 (10900). ^{1}H-NMR: 0.92 (3H, t, J=7 Hz, $COOCH_2C\underline{H}_3$), 1.7—2.1 (2H, m, C_5-H), 2.4—2.7 (1H, m, C_{4a}-H), 3.4—3.7 (1H, m, C_6-H), 3.95 (2H, q, J=7 Hz, $COO\underline{C}H_2CH_3$), 3.9—4.0 (1H, m, C_6-H), 4.64 (1H, d, J=9 Hz, C_{7a}-H), 7.3—7.45 (5H, m, Ar-H). ^{13}C-NMR: 13.6 (q, $COOCH_2\underline{C}H_3$), 32.6 (t, C_5), 39.7 (d, C_{4a}), 60.2 (t, C_6), 67.2 (t, $COO\underline{C}H_2CH_3$), 74.5 (d, C_{7a}), 106.2 (s, C_4), 127.6 (d, 2C, Ph), 128.4 (d, 2C, Ph), 129.5 (d, Ph), 135.4 (s, Ph), 144.2 (s, C_3), 166.6 (s, C_1), 169.0 (s, $\underline{C}OOCH_2CH_3$). *Anal.* Calcd for $C_{16}H_{17}NO_4$: C, 66.88; H, 5.96; N, 4.88. HRMS *m/z*: 287.1158. Found: C, 66.58; H, 6.08; N, 4.79. HRMS *m/z*: 287.1159.

The Photocycloaddition of 1 to 5-Methyl-2,3-dihydrofuran——A solution of **1** (3 g, 12 mmol) and 5-methyl-2,3-dihydrofuran (5 g, 60 mmol) in dimethoxyethane (300 ml) was irradiated for 1 h at 0 °C. After removal of the solvent, the residue was dissolved in benzene and chromatographed over silica gel (Wako-gel C-200). Elution with benzene and crystallization of the eluate from CH_2Cl_2–Et_2O gave (1*S**,3*R**,7*S**,8*R**)-8-ethoxycarbonyl-3-methyl-9-phenyl-2,4-dioxa-10-azatricyclo[6.3.0.0^{3,7}]undecan-9-en-11-one (**8b**, 690 mg, 17%) as colorless prisms, mp 90—92 °C. IR: 1760, 1730. UV $\lambda_{max}^{dioxane}$ nm (ε): 278 (20000). UV λ_{max}^{MeOH} nm (ε): 283 (18500). ^{1}H-NMR: 1.01 (3H, t, J=7 Hz, $COOCH_2C\underline{H}_3$), 1.4—1.6 (1H, m, C_6-H), 1.65 (3H, s, CH_3), 2.0—2.35 (1H, m, C_6-H), 3.5—3.9 (3H, m, C_5-H, C_7-H), 4.17 (2H, qd, J=1.5, 7 Hz, $COO\underline{C}H_2CH_3$), 4.96 (1H, s, C_1-H), 7.4—7.8 (3H, m, Ar-H), 8.0—8.1 (2H, m, Ar-H). ^{13}C-NMR: 13.7 (q, $COOCH_2\underline{C}H_3$), 23.2 (q, CH_3), 28.6 (t, C_6), 50.0 (d, C_7), 62.8 (t, C_5), 67.6 (t, $COO\underline{C}H_2CH_3$), 68.3 (s, C_8), 85.5 (d, C_1), 122.9 (s, C_3), 129.3 (d, 2C, Ph), 130.2 (d, 2C, Ph), 130.9 (s, Ph), 135.2 (d, Ph), 170.4 (s, $\underline{C}OOCH_2CH_3$), 189.8 (s, C_9), 191.5 (s, C_{11}). *Anal.* Calcd for $C_{18}H_{19}NO_5$: C, 65.64; H, 5.82; N, 4.25. HRMS *m/z*: 329.1261. Found: C, 65.52; H, 5.77; N, 4.29. HRMS *m/z*: 329.1260.

Further elution with CH_2Cl_2–benzene (1 : 1) gave a mixture of **1** and the adduct **7b**, which in CH_2Cl_2 was passed through a short column of alumina (Merck) to give a crude crystalline powder. This was purified by MPLC using hexane–AcOEt (3 : 1) as an eluent, followed by recrystallization from CH_2Cl_2–Et_2O to give 4-ethoxycarbonyl-7a-methyl-5-phenyl-2,3,3a,7a-tetrahydrofuro[2,3-*c*]pyridin-7(6*H*)-one (**7b**, 500 mg, 14%) as colorless needles, mp 138—142 °C. IR: 1710, 1680, 1640, 1600. UV $\lambda_{max}^{dioxane}$ nm (ε): 285 (10900). ^{1}H-NMR: 0.92 (3H, t, J=7 Hz, $COOCH_2CH_3$), 1.52 (3H, s, CH_3), 1.8—2.0 (1H, m, C_5-H), 1.4—1.7 (1H, m, C_5-H), 3.10 (1H, dd, J=8, 11 Hz, C_{4a}-H), 3.85—4.05 (2H, m, C_6-H), 3.95 (2H, q, J=7 Hz, $COOCH_2CH_3$), 7.07 (1H, br s, NH), 7.2—7.5 (5H, m, Ar-H). *Anal.* Calcd for $C_{17}H_{19}NO_4$: C, 67.76; H, 6.36; N, 4.65. HRMS *m/z*: 301.1314. Found: C, 67.81; H, 6.40; N, 4.70. HRMS *m/z*: 301.1299.

Methanolysis of 8a——**8a** (40 mg) was dissolved in 0.01% HCl–MeOH (10 ml) and stirred overnight at room temp. After dilution with CH_2Cl_2, the mixture was washed with water and dried over Na_2SO_4. The solvent was evaporated off and the residue in CH_2Cl_2 was passed through a column of silica gel (Wako-gel C-200). Crystallization of the eluate from Et_2O gave (1*S**,3*R**,7*S**,8*R**,9*S**)-8-ethoxycarbonyl-9-methoxy-9-phenyl-2,4-dioxa-10-azatricyclo[6.3.0.0^{3,7}]undecan-11-one (**9a**, 32 mg, 73%) as colorless prisms, mp 163—166 °C. IR: 3320, 1750, 1720. ^{1}H-NMR: 1.40 (3H, t, J=7 Hz, $COOCH_2CH_3$), 1.6—2.0 (2H, m, C_6-H), 2.95 (3H, s, OMe), 2.95—1.1 (1H, m, C_7-H), 3.74 (1H, m, C_5-H), 4.01 (1H, m, C_5-H), 4.40 (2H, q, J=7 Hz, $COOCH_2CH_3$), 5.51 (1H, s, C_1-H), 5.66 (1H, d, J=4 Hz, C_3-H), 7.35—7.45 (3H, m, Ar-H), 7.7—7.8 (2H, m, Ar-H). ^{13}C-NMR: 14.1 (q, $COOCH_2CH_3$), 25.5 (t, C_6), 49.3 (d, C_7), 50.3 (q, OCH_3), 62.3 (t, C_5), 68.0 (s, C_8), 69.3 (t, $COOCH_2CH_3$), 80.6 (d, C_1), 92.1 (s, C_9), 110.8 (d, C_3), 127.1 (d, 2C, Ph), 128.4 (d, 2C, Ph), 129.3 (d, Ph), 135.0 (s, Ph), 170.4 (s, $COOCH_2CH_3$), 175.8 (s, C_{11}). *Anal.* Calcd for $C_{18}H_{21}NO_6 \cdot 1/2\,H_2O$: C, 60.66; H, 6.22; N, 3.93. Found: C, 60.51; H, 6.01; N, 3.81. HRMS *m/z*: $M^+ - CH_3OH$ Calcd for $C_{17}H_{17}NO_5$ 315.1105. Found 315.1104.

Crystallographic Measurement——The crystal data were collected on a Rigaku Denki computer-controlled four-circle diffractometer using Cu-K_α radiation. The intensities of all the reflections with 2θ values up to 140° of (hkl), ($\bar{h}kl$), ($hk\bar{l}$) and ($\bar{h}k\bar{l}$) were measured by the $\omega-2\theta$ scanning technique at a scan rate of 8 per min. The backgrounds were measured at both ends of the scan range for 5.0 s. Three standard reflections were measured every 50 min, and showed no significant variation with time. The intensity data were corrected for the background count and for the usual Lorentz and polarization effects. In total, 2098 independent non-zero reflections were measured.

Crystal Data: $C_{17}H_{17}NO_5$. M_r=315.32. Monoclinic. a=14.736 (2), b=8.051 (1), c=13.358 (2) Å. β=107.14 (1). V=1514.4 Å^3, D_c=1.383 g/cm^3, z=4. Space group, $P2_1/n$. Crystal size, 0.3×0.4×0.3 mm.

Structure Analysis and Refinement——The structure was solved by the direct method using MULTAN and refined by the block-diagonal least-squares procedure with anisotropic factors, using 2098 reflections. The final R-value was 0.06. The atomic parameters, an ORTEP drawing of the molecule, bond lengths, and bond angles are given in Fig. 1 and Tables I and II, respectively.

References and Notes

1) Part XXXIX: T. Sano, J. Toda, N. Maehara, and Y. Tsuda, *Can. J. Chem.*, **65**, 94 (1987).
2) T. Sano, Y. Horiguchi, Y. Tsuda, K. Furuhata, H. Takayanagi, and H. Ogura, *Chem. Pharm. Bull.*, **35**, 9 (1987).
3) T. Sano, Y. Horiguchi, and Y. Tsuda, *Chem. Pharm. Bull.*, **35**, 23 (1987).
4) Y. Tsuda, M. Kaneda, Y. Itatani, T. Sano, H. Horiguchi, and Y. Iitaka, *Heterocycles*, **9**, 153 (1978).
5) T. Sano, Y. Horiguchi, Y. Tsuda, and Y. Itatani, *Heterocycles*, **9**, 161 (1978).

[Chem. Pharm. Bull. 35(12)4736—4746(1987)]

Asymmetric Synthesis Using Chiral Acetals: Studies on the Nucleophilic Addition of Organometallics to Chiral α-Keto Acetals in Open-Chain Systems

YASUMITSU TAMURA,* HIROKAZU ANNOURA, MASAHIRO FUJI, TAKAYUKI YOSHIDA, RITSUKO TAKEUCHI, and HIROMICHI FUJIOKA

Faculty of Pharmaceutical Sciences, Osaka University, 1-6, Yamada-oka, Suita, Osaka 565, Japan

(Received May 21, 1987)

Nucleophilic addition of organometallic reagents (Grignard reagents and organolithium reagents) to three chiral α-keto acetals (**1a**—**c**) in open-chain systems was studied. The reactions of the chiral α-keto acetals (**1a**, **1b**) having a chiral auxiliary as a ketone equivalent with Grignard reagents proceeded in a highly diastereoselective manner (>94% diastereomeric excess (de)). As an application of the reaction, the syntheses of the key intermediates (**6**, **8**) for (*R*)- and (*S*)-mevalolactone were achieved from the product obtained by the reaction of **1a** and vinylmagnesium bromide. On the other hand, in the reactions of the chiral α-keto acetal (**1c**) having a chiral auxiliary as an aldehyde equivalent, lower stereoselectivity was observed even when Grignard reagents were used as addends. The difference of stereoselectivity among the three chiral α-keto acetals (**1a**—**c**) is discussed.

Keywords——asymmetric synthesis; diastereoselective nucleophilic addition; chiral open-chain α-keto acetal; (−)-(2*S*,3*S*)-1,4-dimethoxy-2,3-butanediol; Grignard reagent; (*R*)-mevalolactone; (*S*)-mevalolactone

Development of stereocontrolled reactions in open-chain systems is one of the most attractive areas of organic synthesis. Many studies have been carried out on the stereocontrolled nucleophilic addition of organometallic reagents to open-chain ketones having chiral centers next to a carbonyl function.[1] Recently Eliel *et al.* and Mukaiyama *et al.* have achieved such stereocontrolled addition of organometallic reagents to chiral open-chain α-keto aldehyde derivatives (2-acyl-1,3-oxathiane,[2] α-keto aminal[3]) which have chiral auxiliaries next to the carbonyl function. However, their applications are limited to systems using chiral auxiliaries as aldehyde equivalents. Later, we reported that the nucleophilic addition of organometallic reagents to chiral α-keto acetals derived from (−)-(2*S*,3*S*)-1,4-dimethoxy-2,3-butanediol proceeds in a highly diastereoselective manner in open-chain systems as well as cyclic systems.[4] Thus, the nucleophilic addition of Grignard reagents to the acyclic α-keto acetals (**1a**, **1b**) proceeds in a highly stereoselective manner[5]; this is the first example of the use of a chiral acetal as a ketone equivalent in an open-chain system. Here we present a full account of the work and the results of an additional study on the nucleophilic addition of organometallic reagents to **1c** with a chiral auxiliary as an aldehyde equivalent.[6]

Results and Discussion

Syntheses of Chiral α-Keto Acetals (1a—c)

The chiral α-keto acetals (**1a**—**c**) were synthesized as shown in Chart 2. Transacetalization of α-hydroxydimethyl acetals (**2a**, **2b**)[7] with 1.2 mol eq of (−)-(2*S*,3*S*)-1,4-

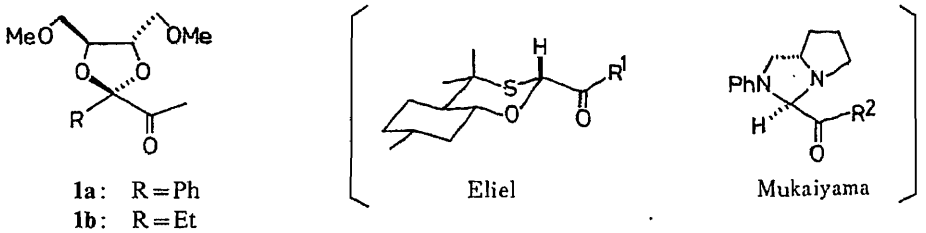

1a: R=Ph
1b: R=Et
1c: R=H

Chart 1

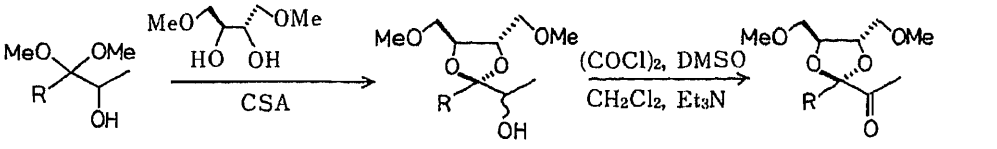

2a: R=Ph
2b: R=Et
2c: R=H

3a: R=Ph (80%)
3b: R=Et (64%)
3c: R=H (67%)

1a: R=Ph (98%)
1b: R=Et (95%)
1c: R=H (88%)

Chart 2

dimethoxy-2,3-butanediol in the presence of a catalytic amount of camphorsulfonic acid (CSA) proceeded smoothly under reduced pressure (0.5 mmHg) without any solvent to give α-hydroxy acetals (**3a**, **3b**, respectively) as an epimeric mixture at the secondary alcohol moiety. In the case of **2c**,[8] transacetalization was performed in dichloromethane (CH_2Cl_2). Oxidation of **3a**—**c** was achieved by Swern's procedure[9] to afford the desired α-keto acetals (**1a**—**c**).

Nucleophilic Addition of Organometallics to α-Keto Acetals (1a—c)

The results of the reactions of **1a**—**c** with organometallic reagents are summarized in Table I. In the reaction of **1a** with ethylmagnesium chloride (EtMgCl) in tetrahydrofuran (THF) at −78 °C, extremely high diastereoselectivity (>98% diastereomeric excess (de)) was obtained (run 1). It was also shown that THF is a slightly more effective solvent than ether (runs 1, 2), and a lower reaction temperature gives a better outcome (runs 1, 3, 4). In the reactions of **1b** and **1c** with EtMgCl in THF at −78 °C, similar high stereoselectivity (>98% de) was observed in the case of **1b** (run 10) but lower selectivity was obtained in the case of **1c** (run 16). The reactions of **1a**—**c** with other Grignard reagents showed the same tendency (extremely high stereoselectivity in runs 5—7 and 11—13; lower stereoselectivity in runs 17—19). The reactions of **1a**—**c** with organolithium reagents gave relatively poor stereoselectivity (runs 8, 9, 14, 15, 20).

The stereochemistries of the products were determined as follows. The absolute configuration of the tertiary alcohol of the product **4a**A (R=Ph, R′=vinyl; 96% de) formed from **1a** in run 5 was assigned as *S* by conversion into the diols (**6**, **8**),[10] key intermediates for (*R*)- and (*S*)-mevalolactone, whose stereochemistries were already established. Thus, hydroboration of **4a**A (R=Ph, R′=vinyl) followed by oxidative work-up afforded the 1,3-diol (**5**) accompanied with the 1,2-diol (**5′**).[11] Then, compound **5** was reductively deacetalized to give the 1,3-diol (**6**), which showed good agreement of the specific rotation with the reported value ($[\alpha]_D$ +1.76°, lit.[10] +1.77°). Compound **4a**A (R=Ph, R′=vinyl) was further converted into the diol **8** ($[\alpha]_D$ +17.3°, lit.[10] +17.3°) having a larger value of optical rotation by ozonolysis (reductive work-up) and successive deacetalization (Chart 3). The stereochemistries of the products in runs 1—4, 6, and 8 were assigned by correlation to the product in run 5. Thus, the product in run 1 was identical with the ethyl compound **4a**A (R=Ph, R′=Et)

TABLE I. Nucleophilic Addition of R′M to **1a—c**

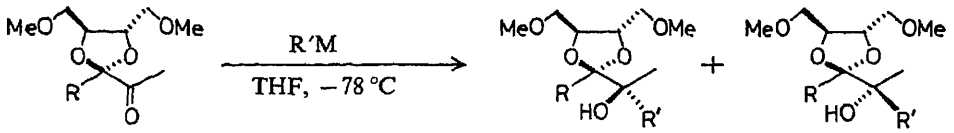

1a—c **4aA—4cA** **4aB—4cB**

Run	Substrate	R′M	Yield (%)	Ratio (A : B)
1	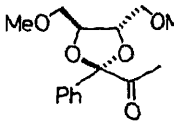 **1a**	EtMgCl	98	>99 : <1[a]
2		EtMgCl[f]	91	93 : 7[a]
3		EtMgCl[g]	95	93 : 7[a]
4		EtMgCl[h]	87	84 : 16[a]
5		 MgBr	90	98 : 2[b]
6		TMS–≡–MgCl	91	97 : 3[b]
7		PhMgBr	84	97 : 3[c]
8		TMS–≡–Li	90	55 : 45[d]
9		PhLi	80	33 : 67[c]
10	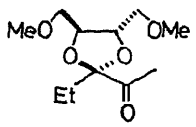 **1b**	EtMgCl	96	>99 : <1[c]
11		 MgBr	93	>99 : <1[e]
12		TMS–≡–MgCl	98	>99 : <1[c]
13		PhMgBr	81	98 : 2[c]
14		TMS–≡–Li	85	80 : 20[c]
15		PhLi	80	60 : 40[c]
16	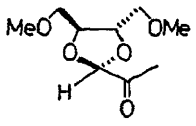 **1c**	EtMgCl	91	88 : 12[c]
17		 MgBr	85	62 : 38[c]
18		TMS–≡–MgCl	80	13 : 87[c]
19		PhMgBr	78	70 : 30[c]
20		TMS–≡–Li	69	60 : 40[c]

a) Determined by HPLC analysis. *b*) Determined by HPLC analysis of the ethyl compound (Chart 4). *c*) Determined by ^{1}H-NMR. *d*) Determined by separation. *e*) Determined by ^{1}H-NMR examination of the ethyl compound (Chart 4). *f*) The reaction was carried out in dry ether at −78 °C. *g*) The reaction was carried out at 0 °C. *h*) The reaction was carried out under reflux.

obtained by hydrogenation of the product in run 5. The products in runs 6 and 8 were converted to the corresponding ethyl compounds, **4a**A (R=Ph, R′=Et) and **4a**B (R=Ph, R′=Et), by hydrogenation after desilylation, and identified as shown in Chart 4 (**a** series). The stereochemistries of the products in runs 7 and 9 of the **a** series as well as those in runs 10—15 of the **b** series were tentatively assigned from the mechanistic analogy. The relationships of the stereochemistries of the products in runs 10, 11, 12, and 14 could also be determined from those of the enthyl compounds **4b**A (R=Et, R′=Et) and **4b**B (R=Et, R′=Et) (Chart 4, **b** series). The stereochemistry of the product **4c**A (R=H, R′=Et, 76% de) in run 16 was determined as shown in Chart 5. Compound **4c**A (R=H, R′=Et, 76% de) was transformed to 2-benzyloxy-2-methyl-butanal (**12**) by benzylation followed by acid hydrolysis. Since the specific rotation of **12** showed a negative value (−36°, lit.[12] −39° as 78% ee), the absolute configuration of the tertiary alcohol was determined to be *S*. The correlation of the stereochemistries of the products in runs 16, 17, 18, and 20 was achieved in the same way as used for the **a** and **b** series (Chart 4, **c** series).

As mentioned above, nucleophilic addition of Grignard reagents to the chiral α-keto acetals (**1a** and **1b**) proceeded with extremely high stereoselectivity to give the predominant products (**4a**A and **4b**A), which were formed by the attack of the reagents on the *si*-face of the

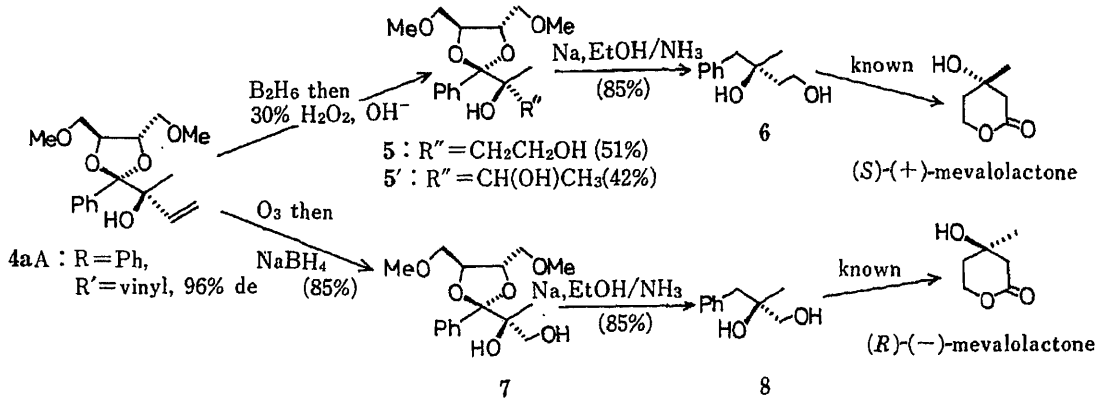

Chart 3

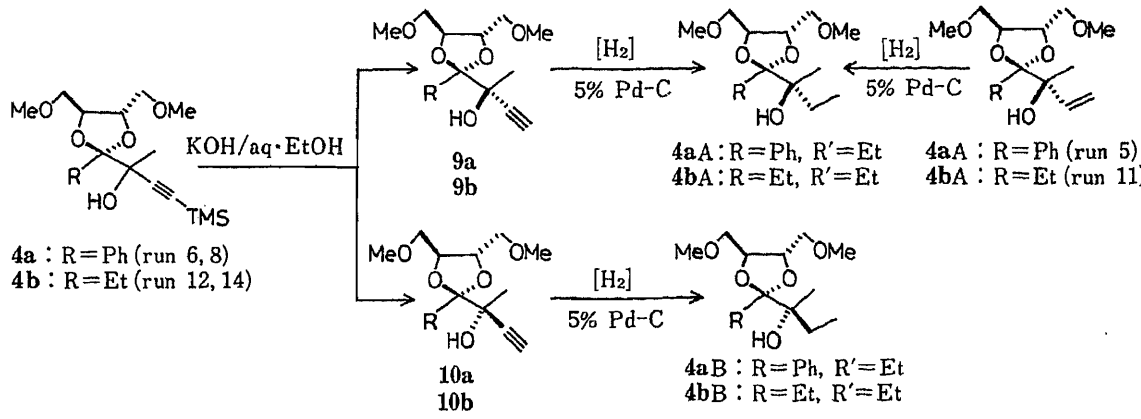

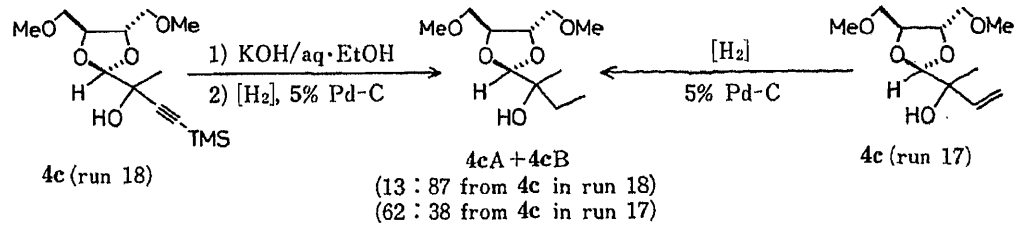

Chart 4

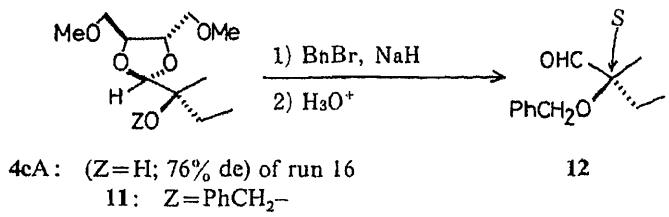

Chart 5

ketones. This result would suggest that the magnesium metal of the reagents chelates between the carbonyl oxygen atom, the methoxy oxygen atom, and one of the acetal oxygen atoms, leading to a rigid structure (A in Fig. 1) in the transition state of the reaction, then the alkyl group of the reagent attacks the *si*-face of the ketone. On the other hand, lower stereoselectivity was observed in the reactions of **1c** even when Grignard reagents were used as addends.

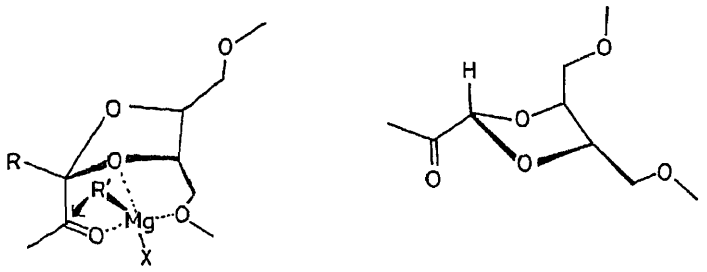

A: R=Et, Ph B

Fig. 1

This would suggest that the bulkiness of the R groups of **1a—c** plays an important role in fixing the conformation of the transition state. That is, **1c** would exist as conformer B as shown in Fig. 1, where the acetyl group occupies the quasi-equatorial position because of the smallness of R(=H), and the reaction would proceed without chelation or with only a weak chelation process. The reason for the poor stereoselectivity in the reactions of **1a—c** with organolithium reagents is still not clear.[13]

As shown in Chart 3, since compounds **6** and **8** are the key intermediates for (*R*)-(−)- and (*S*)-(+)-mevalolactone, this work provides a new asymmetric synthesis of optically active mevalolactone. The advantages of our asymmetric synthesis are (1) that a single diastereomer of the starting α-keto acetals is formed, (2) that the acetal, a widely used protecting group for the carbonyl group,[14] works as a chiral auxiliary, and (3) that the chiral diol is readily available in both enantiomers.[15]

Experimental

The following instruments were used to obtain physical data: specific rotation, Perkin-Elmer 241 polarimeter; infrared (IR) spectra, JASCO IRA-1 spectrometer; proton nuclear magnetic resonance (^{1}H-NMR) spectra, Hitachi R-22 (90 MHz), JEOL JNM-FX 90Q FT-NMR (90 MHz), or JEOL LNM-GX 500 FT-NMR (500 MHz) spectrometer (with tetramethylsilane as an internal standard); low- and high-resolution mass spectra (MS), JEOL JMS D-300 mass spectrometer (with a direct inlet system). A JASCO TRIROTAR-II high-pressure liquid chromatography (UV detector) was used for high-performance liquid chromatographic (HPLC) analysis. E. Merck silica gel (0.063—0.200 mm, 70—230 mesh ASTM) for column chromatography and E. Merck TLC plates pre-coated with Silica gel $60F_{254}$ for preparative thin layer chromatography (TLC) (0.5 mm) and TLC detection (0.2 mm) were used. Specific rotation was measured at 20 °C in $CHCl_3$, unless otherwise mentioned. All melting points are uncorrected.

Syntheses of the α-Hydroxy Acetals (3a—c)——General Procedure for **3a** and **3b**: One microspatula-full of CSA was added to a mixture of the α-hydroxydimethyl acetal **2a** (or **2b**)[7] (1 mmol) and (−)-(2*S*,3*S*)-1,4-dimethoxy-2,3-butanediol (**13**)[15] (1 mmol), and the resulting mixture was stirred overnight at room temperature under reduced pressure (0.5 mmHg). Then CH_2Cl_2 (5 ml) and K_2CO_3 (one microspatula-full) were added. The reaction mixture was stirred for 10 min, and the precipitate was filtered off. The filtrate was concentrated under reduced pressure. The residue was purified by column chromatography on silica gel using hexane–ether as an eluting solvent to give **3a** (or **3b**) as a diastereomeric mixture.

The α-hydroxy acetal **3a** (225 mg, 80%) was prepared from **2a** (200 mg, 1.02 mmol) and **13** (153 mg, 1.02 mmol). Colorless oil. IR $\nu_{max}^{CHCl_3}$ cm^{-1}: 3450, 1080. ^{1}H-NMR (10% solution in $CDCl_3$) δ: 1.02 and 1.04 (total 3H, each d, ratio 1:1, HOCHC$\underline{H}_3$), 3.26 and 3.33 (total 3H, both s, ratio 1:1, –OC$\underline{H}_3$), 3.44 (3H, s, –OC$\underline{H}_3$), 3.9—4.5 (7H, m, –C$\underline{H}_2$OCH$_3$ × 2 and –C$\underline{H}$–O × 3), 7.2—7.6 (5H, m, aromatic protons). *Anal.* Calcd for $C_{15}H_{22}O_5$: C, 63.81; H, 7.85. Found: C, 64.08; H, 8.03.

The α-hydroxy acetal **3b** (208 mg, 64%) was prepared from **2b** (206 mg, 1.39 mmol) and **13** (209 mg, 1.39 mmol). Colorless oil. IR $\nu_{max}^{CHCl_3}$ cm^{-1}: 3590, 3460, 1105. ^{1}H-NMR (10% solution in $CDCl_3$) δ: 0.92 (3H, t, J=7 Hz, –CH$_2$C$\underline{H}_3$), 1.21 (3H, d, J=6.6 Hz, HOCHC$\underline{H}_3$), 1.4—1.85 (2H, m, –C$\underline{H}_2$–), 2.78 (1H, d, J=7 Hz, –O$\underline{H}$), 3.39, 3.40, and 3.41 (total 6H, all s, ratio 1:1:2, –OC$\underline{H}_3$ × 2), 3.45—3.60 (4H, m, –C$\underline{H}_2$OCH$_3$ × 2), 3.70 (1H, m, –C$\underline{H}$–O), 3.90 (1H, m, –C$\underline{H}$–O), 4.1—4.5 (1H, m, –C$\underline{H}$–O). *Anal.* Calcd for $C_{11}H_{22}O_5$: C, 56.39; H, 9.46. Found: C, 56.37; H, 9.76.

The α-hydroxy acetal **3c** (653 mg, 67%) was prepared from **2c**[8] (565 mg, 4.7 mmol), **13** (710 mg, 4.7 mmol), and

one microspatula-full of CSA. The reaction was carried out in anhydrous CH_2Cl_2 (18 ml) at room temperature under a nitrogen atmosphere. After being stirred overnight, the resulting mixture was worked up in the same manner as described for **3a** and **3b**. Colorless oil. IR $\nu_{max}^{CHCl_3}$ cm^{-1}: 3450, 1095. ^{1}H-NMR (10% solution in $CDCl_3$) δ: 1.21 (3H, d, J=6.5 Hz, $HOCHCH_3$), 3.40 (6H, s, $-OCH_3 \times 2$), 3.47—3.60 (4H, m, $-CH_2OCH_3 \times 2$), 3.69—3.91 (1H, m, $-CH-OH$), 3.94—4.17 (2H, m, $-CH-O \times 2$), 4.91 and 4.94 (total 1H, both s, ratio 1 : 1, $O-CH-O$). *Anal.* Calcd for $C_9H_{18}O_5$: C, 52.41; H, 8.80. Found: C, 52.48; H, 9.13.

Syntheses of α-Keto Acetals (1a—c)——General Procedure: Dimethyl sulfoxide (DMSO) (0.42 ml) was added dropwise to a solution of oxalyl chloride $(COCl)_2$ (0.23 ml) in anhydrous CH_2Cl_2 (6.6 ml) at −78 °C. The resulting solution was stirred for 5 min and then **3** (1 mmol) in CH_2Cl_2 (2 ml) was added. After further stirring for 30 min, Et_3N (1.8 ml) was added to the reaction mixture. The resulting solution was stirred for 15 min and then treated with water. (The reaction was carried out at −60——70 °C under a nitrogen atmosphere.) The mixture was extracted with CH_2Cl_2. The organic layer was washed with aqueous 5% HCl, saturated aqueous $NaHCO_3$, and brine successively and then dried over $MgSO_4$. The solution was concentrated under reduced pressure. The residue was subjected to column chromatography on silica gel to give the α-keto acetal (**1**).

Compound **1a** (988 mg) was prepared from **3a** (1.01 g, 3.6 mmol) in 98% yield (eluent, benzene : ether = 8 : 1). **1a**: Colorless oil, $[\alpha]_D$ +65° (c=0.97). IR $\nu_{max}^{CHCl_3}$ cm^{-1}: 1725, 1085. ^{1}H-NMR (10% solution in $CDCl_3$) δ: 2.17 (3H, s, $-CH_3$), 3.34 and 3.41 (3H each, both s, $-OCH_3 \times 2$), 3.4—3.6 (4H, m, $-CH_2-OCH_3 \times 2$), 4.15 (2H center, m, $-O-CH- \times 2$), 7.2—7.6 (5H, m, aromatic protons). *Anal.* Calcd for $C_{15}H_{20}O_5$: C, 64.27; H, 7.19. Found: C, 64.19; H, 7.14.

Compound **1b** (429 mg) was prepared from **3b** (450 mg, 1.92 mmol) in 96% yield (eluent, hexane : ether = 2 : 1). **1b**: Colorless oil, $[\alpha]_D$ −6.1° (c=1.5). IR $\nu_{max}^{CHCl_3}$ cm^{-1}: 1728, 1073. ^{1}H-NMR (10% solution in $CDCl_3$) δ: 0.93 (3H, t, J=7.4 Hz, $-CH_2CH_3$), 1.81 (2H, q, J=7.4 Hz, $-CH_2CH_3$), 2.23 (3H, s, $-COCH_3$), 3.36 and 3.41 (3H each, both s, $-OCH_3 \times 2$), 3.4—3.6 (4H, m, $-CH_2-OCH_3 \times 2$), 4.0 (2H center, m, $-O-CH- \times 2$). *Anal.* Calcd for $C_{11}H_{18}O_5$: C, 56.88; H, 8.68. Found: C, 56.73; H, 8.91.

Compound **1c** (330 mg) was prepared from **3c** (380 mg, 1.84 mmol) in 88% yield (eluent, hexane : ether = 1 : 1). **1c**: Colorless oil, $[\alpha]_D$ −9.6° (c=1.3). IR $\nu_{max}^{CHCl_3}$ cm^{-1}: 1730, 1100. ^{1}H-NMR (10% solution in $CDCl_3$) δ: 2.22 (3H, s, $-COCH_3$), 3.40 (6H, s, $-OCH_3 \times 2$), 3.5—3.7 (4H, m, $-CH_2-OCH_3 \times 2$), 4.15 (2H center, m, $-O-CH- \times 2$), 5.09 (1H, s, $-O-CH-O-$). Exact MS Calcd for $C_9H_{16}O_5$: 204.0997. Found: 204.1002.

Nucleophilic Addition of Organometallics to α-Keto Acetals (1a—c)——General Procedure: An organometallic reagent (Grignard reagent or organolithium reagent, 5 mmol, 1—1.5 M THF solution) was added dropwise to a stirred solution of **1** (1 mmol) in anhydrous THF (10 ml). The mixture was stirred for 2—5 h at −78 °C under a nitrogen atmosphere (in the case of trimethylsilylethynylmagnesium chloride or trimethylsilylethynyllithium, the reaction was carried out at −78 °C for 1 h and then the mixture was allowed to warm to room temperature). The mixture was quenched with saturated aqueous NH_4Cl, allowed to warm to room temperature, and then extracted with ether. The organic layer was washed with brine, dried over $MgSO_4$, and concentrated under reduced pressure. The residue was subjected to column chromatography on silica gel to give **4**.

Run 1: The product [**4aA** (R′=Et), 30.4 mg] was prepared from **1a** (28 mg, 0.1 mmol) and EtMgCl in 98% yield (eluent, benzene : ether = 5 : 1). **4aA** (R′=Et): Colorless oil, $[\alpha]_D$ +9.1° (c=1.1). IR $\nu_{max}^{CHCl_3}$ cm^{-1}: 3450, 1600, 1450, 1090. ^{1}H-NMR (10% solution in $CDCl_3$) δ: 0.87 (3H, t, J=7.2 Hz, $-CH_2CH_3$), 1.13 (3H, s, $HO-C-CH_3$), 1.2—1.7 (2H, m, $-CH_2CH_3$), 3.28 and 3.43 (3H each, both s, $-OCH_3 \times 2$), 3.5—3.9 (4H, m, $-CH_2-OCH_3 \times 2$), 3.95—4.3 (2H, m, $-O-CH- \times 2$), 7.1—7.6 (5H, aromatic protons). *Anal.* Calcd for $C_{17}H_{26}O_5$: C, 65.78; H, 8.44. Found: C, 65.84; H, 8.73.

Runs 2—4: The products were prepared from **1a** and EtMgCl under the conditions shown in Table I. The ratios of the products were determined by HPLC analysis [Nucleosil 50-5 column; eluent, hexane : ethyl acetate = 4 : 1; flow rate 0.9 ml/min; retention time (t_R), **4aA** (R′=Et), 40.8 min, **4aB** (R′=Et), 38.6 min].

Run 5: The product [**4aA** (R′=vinyl), 96% de, 94.1 mg] was prepared from **1a** (95 mg, 0.34 mmol) and vinylmagnesium bromide in 90% yield (eluent, hexane : ethyl acetate = 2 : 1). **4aA** (R′=vinyl, 96% de): Colorless oil, $[\alpha]_D$ −1.08° (c=0.65). IR $\nu_{max}^{CHCl_3}$ cm^{-1}: 3454, 1450, 1090. ^{1}H-NMR (10% solution in $CDCl_3$) δ: 1.24 (3H, s, $-CH_3$), 3.28 and 3.44 (3H each, both s, $-OCH_3 \times 2$), 3.0—3.9 (5H, m, $-CH_2-OCH_3 \times 2$ and $-O-CH-$), 4.25 (1H center, m, $-O-CH-$), 4.9—5.3 (2H, AB in ABC, $-CH=CH_2$), 5.92 (1H, C in ABC, $-CH=CH_2$), 7.1—7.6 (5H, aromatic protons). *Anal.* Calcd for $C_{17}H_{24}O_5$: C, 66.21; H, 7.84. Found: C, 66.30; H, 8.06.

Run 6: Trimethylsilylethynylmagnesium chloride was prepared from trimethylsilylacetylene (0.26 ml) and EtMgCl (2.7 M THF solution, 0.55 ml) in anhydrous THF (7 ml) at room temperature. The product [**4aA** (R′=TMS−≡−), 94% de, 59 mg] was prepared from **1a** (46 mg, 0.164 mmol) and trimethylsilylethynylmagnesium chloride (5 ml) in 91% yield (eluent, hexane : ether = 2 : 1). **4aA** (R′=TMS−≡−, 94% de): Colorless oil, $[\alpha]_D$ +10.1° (c=0.91). IR $\nu_{max}^{CHCl_3}$ cm^{-1}: 3460, 3430, 2940, 1447, 1090. ^{1}H-NMR (10% solution in $CDCl_3$) δ: 0.13 (9H, s, $-SiMe_3$), 1.37 (3H, s, $-CH_3$), 3.30 and 3.45 (3H each, both s, $-OCH_3 \times 2$), 3.5—4.0 (4H, m, $-CH_2-OCH_3 \times 2$), 4.2—4.5 (2H, m, $-O-CH- \times 2$), 7.2—7.35 and 7.5—7.7 (5H, aromatic protons). *Anal.* Calcd for $C_{20}H_{30}O_5Si$: C, 63.46; H, 7.99. Found: C, 63.49; H, 8.04.

Run 7: The product [**4aA** (R′=Ph), 94% de, 19 mg] was prepared from **1a** (18 mg, 0.064 mmol) and PhMgBr in 84% yield (eluent, hexane : ether = 2 : 1). **4aA** (R′=Ph, 94% de): Colorless oil, $[\alpha]_D$ +16.8° (c=0.86). IR $\nu_{max}^{CHCl_3}$ cm^{-1}:

3469, 3000, 2848, 1452, 1094. ^{1}H-NMR (10% solution in $CDCl_3$) δ: 1.61 (3H, s, $-CH_3$), 3.06 (1H, dd, J=10, 5.7 Hz, $-CH_2OCH_3 \times 1/2$), 3.26 and 3.46 (3H each, both s, $-OCH_3 \times 2$), 3.4—3.6 (3H, m, $-CH_2OCH_3 \times 3/2$), 3.75 (1H center, m, –O–CH–), 4.10 (1H center, dt like, –O–CH–), 6.8—7.6 (10H, aromatic protons). *Anal.* Calcd for $C_{21}H_{26}O_5$: C, 70.37; H, 7.31. Found: C, 69.99; H, 7.43.

Run 8: Trimethylsilylethynyllithium was prepared from trimethylsilylacetylene (0.15 ml) and *n*-butyllithium (0.71 mmol in hexane) in THF (10 ml) at −40 °C. The product [**4a**A (R′=TMS–≡–): **4a**B (R′=TMS–≡–)=55:45, 24.3 mg] was prepared from **1a** (20 mg, 0.07 mmol) and trimethylsilylethynyllithium. Two components were separated by preparative TLC (benzene : ether=4:1, developed twice) to give **4a**A (R′=TMS–≡–, 13.3 mg, 49.5%), which was identical with the product of run 6, and **4a**B (R′=TMS–≡–, 10.9 mg, 40.5%). **4a**B (R′=TMS–≡–): Colorless oil, $[\alpha]_D$ +26.1° (c=0.83). IR $\nu_{max}^{CHCl_3}$ cm^{-1}: 3560, 2890, 1446, 1090. ^{1}H-NMR (10% solution in $CDCl_3$) δ: 0.14 (9H, s, $-SiMe_3$), 1.36 (3H, s, $-CH_3$), 3.29 and 3.43 (3H each, both s, $-OCH_3 \times 2$), 3.1—3.7 (4H, m, $-CH_2$–$OCH_3 \times 2$), 3.85 (1H center, m, –O–CH–), 4.25 (1H center, m, –O–CH–), 7.2—7.35 and 7.5—7.7 (5H, aromatic protons). *Anal.* Calcd for $C_{20}H_{30}O_5Si$: C, 63.46; H, 7.99. Found: C, 63.37; H, 8.19.

Run 9: The product [**4a**A (R′=Ph): **4a**B (R′=Ph)=33:67, 18.4 mg] was prepared from **1a** (18 mg, 0.064 mmol) and PhLi in 80% yield. Colorless oil. IR $\nu_{max}^{CHCl_3}$ cm^{-1}: 3450, 2990, 2890, 1443, 1090. ^{1}H-NMR (10% solution in $CDCl_3$) δ: 1.61 (3H, s, $-CH_3$), 3.26 (3H, s, $-OCH_3$), 3.43 and 3.46 (total 3H, both s, ratio 67:33, $-OCH_3$), 2.95—3.85 (5H, m, –OCH– and $-CH_2OCH_3 \times 2$), 4.1 (1H center, m, –O–CH–), 6.7—7.6 (10H, aromatic protons). *Anal.* Calcd for $C_{21}H_{26}O_5$: C, 70.37; H, 7.31. Found: C, 69.99; H, 7.43.

Run 10: The product [**4b**A (R′=Et), 78 mg] was prepared from **1b** (72 mg, 0.31 mmol) and EtMgCl in 96% yield (eluent, hexane : ether=2:1). **4b**A (R′=Et): Colorless oil, $[\alpha]_D$ −16° (c=2.6). IR $\nu_{max}^{CHCl_3}$ cm^{-1}: 3470, 1083. ^{1}H-NMR (10% solution in C_6D_6) δ: 1.01 (3H, t, J=7.0 Hz, $-CH_2CH_3$), 1.08 (3H, t, J=7.0 Hz, $-CH_2CH_3$), 1.31 (3H, s, HO–C–CH_3), 1.4—1.9 (4H, m, $-CH_2CH_3 \times 2$), 2.97 and 3.07 (3H each, both s, $-OCH_3 \times 2$), 3.1—3.6 (4H, m, $-CH_2OCH_3 \times 2$), 3.84 (1H, dt, J=9.0, 3.0 Hz, –O–CH–), 4.65 (1H, dt, J=9.0, 4.5 Hz, –O–CH–). *Anal.* Calcd for $C_{13}H_{26}O_5$: C, 59.52; H, 10.00. Found: C, 59.49; H, 9.73.

Run 11: The product [**4b**A (R′=vinyl), 11.5 mg] was prepared from **1b** (11 mg, 0.048 mmol) and vinylmagnesium bromide in 93% yield (eluent, hexane : ether=2:1). **4b**A (R′=vinyl): Colorless oil, $[\alpha]_D$ +16.5° (c=1.9). IR $\nu_{max}^{CHCl_3}$ cm^{-1}: 3445, 1097. ^{1}H-NMR (10% solution in C_6D_6) δ: 0.98 (3H, t, J=7.0 Hz, $-CH_2CH_3$), 1.45 (3H, s, HO–C–CH_3), 1.6—1.9 (2H, m, $-CH_2CH_3$), 2.98 and 3.06 (3H each, both s, $-OCH_3 \times 2$), 3.2—3.6 (2H, m, $-CH_2OCH_3$), 3.7—3.9 (3H, m, $-CH_2OCH_3$ and –O–CH–), 4.64 (1H, dt, J=7.5, 5.0 Hz, –O–CH–), 5.10 (1H, dd, J=10.0, 2.0 Hz, $^{H}\!>\!C\!=\!C\!<^{H}_{H}$), 5.41 (1H, dd, J=17.0, 2.0 Hz, $^{H}\!>\!C\!=\!C\!<^{H}_{H}$), 6.22 (1H, dd, J=17.0, 10.0 Hz, $-HC\!=\!CH_2$).

Anal. Calcd for $C_{13}H_{24}O_5$: C, 59.98; H, 9.29. Found: C, 60.17; H, 9.45.

Run 12: The product [**4b**A (R′=TMS–≡–), 30.7 mg] was prepared from **1b** (22 mg, 0.095 mmol) and trimethylsilylethynylmagnesium chloride (3 ml, prepared in the same manner as in the case of run 6) in 98% yield (eluent, hexane : ether=3:1). **4b**A: Colorless oil, $[\alpha]_D$ +50° (c=0.6). IR $\nu_{max}^{CHCl_3}$ cm^{-1}: 3430, 2160, 1105. ^{1}H-NMR (10% solution in C_6D_6) δ: 0.14 (9H, s, $-SiMe_3$), 1.06 (3H, t, J=7.2 Hz, $-CH_2CH_3$), 1.76 (3H, s, HO–C–CH_3), 1.90 and 2.30 (1H each, m, $-CH_2CH_3$), 2.86 and 3.02 (3H each, both s, $-OCH_3 \times 2$), 3.1—3.6 (4H, m, $-CH_2OCH_3 \times 2$), 3.81 (1H, ddd, J=8.2, 3.6, 1.8 Hz, –O–CH–), 4.63 (1H, br s, –OH), 4.75 (1H, dt, J=8.2, 3.6 Hz, –O–CH–). *Anal.* Calcd for $C_{16}H_{30}O_5Si$: C, 58.15; H, 9.15. Found: C, 58.18; H, 9.35.

Run 13: The product [**4b**A (R′=Ph), 96% de, 22.1 mg] was prepared from **1b** (20 mg, 0.086 mmol) and PhMgBr in 81% yield (eluent, benzene : ether=4:1). **4b**A (R′=Ph, 96% de): Colorless oil, $[\alpha]_D$ +51° (c=2.1). IR $\nu_{max}^{CHCl_3}$ cm^{-1}: 3445, 1080, 695. ^{1}H-NMR (10% solution in $CDCl_3$) δ: 0.80 (3H, t, J=7.0 Hz, $-CH_2CH_3$), 1.4—1.7 (2H, m, $-CH_2CH_3$), 1.64 (3H, s, HO–C–CH_3), 3.39 and 3.49 (3H each, both s, $-OCH_3 \times 2$), 3.4—4.1 (5H, m, $-CH_2OCH_3 \times 2$ and –O–CH–), 4.2—4.4 (2H, m, –O–CH– and –OH), 7.2—7.6 (5H, aromatic protons). *Anal.* Calcd for $C_{17}H_{26}O_5$: C, 65.78; H, 8.44. Found: C, 65.70; H, 8.53.

Run 14: The product [**4b**A (R′=TMS–≡–): **4b**B (R′=TMS–≡–)=80:20, 18.2 mg] was prepared from **1b** (15 mg, 0.065 mmol) and trimethylsilylethynyllithium (prepared in the same manner as in the case of run 7) in 85% yield. IR $\nu_{max}^{CHCl_3}$ cm^{-1}: 3575, 3425, 2160. ^{1}H-NMR (10% solution in C_6D_6) δ: 0.14 (9H, s, $-SiMe_3$), 1.04 and 1.06 (total 3H, each t, $-CH_2CH_3$), 1.90 and 2.30 (1H each, m, $-CH_2CH_3$), 2.88 and 3.04 (total 3H, both s, ratio 8:2, $-OCH_3$), 3.03 (3H, s, $-OCH_3$), 3.1—3.6 (4H, m, $-CH_2OCH_3 \times 2$), 3.81 and 4.02 (total 1H, m, ratio 8:2, –O–CH–), 4.6 (1H, br s, –OH), 4.75 (1H, dt, J=8.2, 3.6 Hz, –O–CH–). *Anal.* Calcd for $C_{16}H_{30}O_5Si$: C, 58.15; H, 9.15. Found: C, 58.20; H, 9.36.

Run 15: The product [**4b**A (R′=Ph): **4b**B (R′=Ph)=60:40, 21.3 mg] was prepared from **1b** (20 mg, 0.086 mmol) and PhLi in 80% yield. Colorless oil. IR $\nu_{max}^{CHCl_3}$ cm^{-1}: 3445, 1080, 695. ^{1}H-NMR (10% solution in $CDCl_3$) δ: 0.8 (3H, t, J=7.0 Hz, $-CH_2CH_3$), 1.4—1.7 (2H, m, $-CH_2CH_3$), 1.62 and 1.64 (total 3H, both s, ratio 6:4, HO–C–CH_3), 3.36, 3.39, 3.42 and 3.49 (total 6H, all s, ratio 4:6:4:6, $-OCH_3 \times 2$), 3.4—4.4 (6H, m, $-CH_2OCH_3 \times 2$ and O–CH– $\times 2$), 6.7—7.6 (5H, aromatic protons). *Anal.* Calcd for $C_{17}H_{26}O_5$: C, 65.78; H, 8.44. Found: C, 65.61; H, 8.62.

Run 16: The product [**4c**A (R′=Et): **4c**B (R′=Et)=88:12, 55 mg] was prepared from **1c** (53 mg, 0.26 mmol) and EtMgCl in 91% yield (eluent, hexane : ether=2:3). Colorless oil. IR $\nu_{max}^{CHCl_3}$ cm^{-1}: 3597, 3467, 1100. ^{1}H-NMR (10% solution in C_6D_6) δ: 1.01 and 1.02 (total 3H, each t, J=7.3 Hz, ratio 88:12, $-CH_2CH_3$), 1.23 and 1.25 (total 3H, both

s, ratio 12:88, HO–C(–CH$_3$)–, 1.5—1.8 (2H, m, –CH$_2$CH$_3$), 3.03 and 3.06 (3H each, both s, –OCH$_3$ × 2), 3.2—3.4 (4H, m, –CH$_2$OCH$_3$ × 2), 3.96—4.12 (2H, m, –O–CH– × 2), 4.97 and 4.98 (total 1H, both s, ratio 12:88, –O–CH–O–). *Anal.* Calcd for $C_{11}H_{22}O_5$: C, 56.39; H, 9.46. Found: C, 56.18; H, 9.75.

Run 17: The product [**4cA** (R′ = vinyl) : **4cB** (R′ = vinyl) = 62:38, 18 mg] was prepared from **1c** (20 mg, 0.098 mmol) and vinylmagnesium bromide in 78% yield (eluent; hexane : ethyl acetate = 2:1). Colorless oil. IR $\nu_{max}^{CHCl_3}$ cm^{-1}: 3583, 3430, 1095. ^{1}H-NMR (10% solution in $CDCl_3$) δ: 1.28 (3H, s, HO–C(–CH$_3$)–), 3.39 and 3.41 (3H each, both s, –OCH$_3$ × 2), 3.44—3.64 (4H, m, –CH$_2$OCH$_3$ × 2), 3.9—4.3 (2H, m, –O–CH– × 2), 4.93 and 4.96 (total 1H, both s, ratio 4:6 –O–CH–O–), 5.0—5.5 (2H, m, –CH=CH$_2$), 5.97 (1H, dd, J = 10.6, 16.8 Hz, –CH=CH$_2$). *Anal.* Calcd for $C_{11}H_{20}O_5$: C, 56.88; H, 8.68. Found: C, 56.85; H, 8.86.

Run 18: The product [**4cA** (R′ = TMS–≡–) : **4cB** (R′ = TMS–≡–) = 13:87, 60 mg] was prepared from **1c** (51 mg, 0.25 mmol) and trimethylsilylethynylmagnesium chloride (prepared in the same manner as in the case of run 6) in 80% yield (eluent, hexane : ethyl acetate = 3:1). Colorless oil. IR $\nu_{max}^{CHCl_3}$ cm^{-1}: 3563, 3410, 2160, 1095. ^{1}H-NMR (10% solution in $CDCl_3$) δ: 0.17 (9H, s, –SiMe$_3$), 1.46 (3H, s, HO–C(–CH$_3$)–), 3.41 (6H, s, –OCH$_3$ × 2), 3.4—3.7 (4H, m, –CH$_2$OCH$_3$ × 2), 3.96—4.3 (2H, m, –O–CH– × 2), 5.00 and 5.02 (total 1H, both s, ratio 87:13, –O–CH–O–). *Anal.* Calcd for $C_{14}H_{26}O_5Si$: C, 55.60; H, 8.66. Found: C, 55.44; H, 8.94.

Run 19: The product [**4cA** (R′ = Ph) : **4cB** (R′ = Ph) = 70:30, 38 mg] was prepared from **1c** (35 mg, 0.17 mmol) and PhMgBr in 78% yield. Colorless oil. IR $\nu_{max}^{CHCl_3}$ cm^{-1}: 3448, 3010, 1100, ^{1}H-NMR (10% solution in $CDCl_3$) δ: 1.54 (3H, s, HO–C(–CH$_3$)–), 3.33, 3.38, 3.39 and 3.41 (total 6H, all s, ratio 3:7:3:7, –OCH$_3$ × 2), 3.45—3.8 (4H, m, –CH$_2$OCH$_3$ × 2), 3.8—4.3 (2H, m, –O–CH– × 2), 5.21 and 5.30 (total 1H, both s, ratio 3:7, –O–CH–O–), 7.1—7.6 (5H, m, aromatic protons). *Anal.* Calcd for $C_{15}H_{22}O_5$: C, 63.81; H, 7.85. Found: C, 63.64; H, 8.07.

Run 20: The product [**4cA** (R′ = TMS–≡–) : **4cB** (R′ = TMS–≡–) = 60:40, 52 mg] was prepared from **1c** (51 mg, 0.25 mmol) and trimethylsilylethynyllithium (prepared in the same manner as in the case of run 7) in 69% yield.

Conversion of 4aA (R′ = vinyl) to the Diols 6 and 8——The 1,3-Diol **5**: A solution of B_2H_6 in THF (1 M solution, 0.195 ml) was added dropwise to a stirred solution of **4aA** (R′ = vinyl, 30 mg) in anhydrous THF (0.25 ml) at 0 °C under a nitrogen atmosphere. The mixture was stirred overnight at 0 °C and treated with water until the evolution of hydrogen ceased. Stirring was continued for 40 min at room temperature, then aqueous 3 M NaOH (0.15 ml) and aqueous 30% H_2O_2 (0.017 ml) were added dropwise to the resulting solution successively at 0 °C. The solution was stirred for 1 h at 40 °C and extracted with CH_2Cl_2. The organic layer was washed with aqueous 5% $Na_2S_2O_3$, dried over $MgSO_4$, and concentrated under reduced pressure. The residue was purified by preparative TLC (chloroform : ethyl acetate = 1:1) to give the 1,3-diol **5** (16.2 mg, 51%) and the 1,2-diol **5′** (13.3 mg, 41%). **5**: Colorless oil $[\alpha]_D$ +8.4° (c = 1.4). IR $\nu_{max}^{CHCl_3}$ cm^{-1}: 3450, 3000, 2932, 1092. ^{1}H-NMR (10% solution in $CDCl_3$) δ: 1.25 (3H, s, HO–C(–CH$_3$)–), 1.4 and 2.05 (1H each, m, –CH$_2$CH$_2$OH), 2.9—3.9 and 4.2 (8H, m, –O–CH– × 2 and –CH$_2$OCH$_3$ × 2 and –CH$_2$OH), 3.27 and 3.44 (3H each, both s, –OCH$_3$ × 2), 7.2—7.6 (5H, aromatic protons). *Anal.* Calcd for $C_{17}H_{26}O_6$: C, 62.56; H, 8.03. Found: C, 62.69; H, 8.26. **5′**: Colorless oil, $[\alpha]_D$ +15.3° (c = 0.34). IR $\nu_{max}^{CHCl_3}$ cm^{-1}: 3520, 1090. ^{1}H-NMR (10% solution in $CDCl_3$) δ: 1.07 (3H, s, HO–C(–CH$_3$)–), 1.21 (3H, d, J = 6.5 Hz, HO–CH–CH$_3$), 2.9—4.4 (7H, m, –O–CH–CH$_3$ and –CH$_2$OCH$_3$ × 2 and –O–CH– × 2), 3.27 and 3.44 (3H each, both s, –OCH$_3$ × 2), 7.2—7.6 (5H, aromatic protons). *Anal.* Calcd for $C_{17}H_{26}O_6$: C, 62.56; H, 8.03. Found: C, 62.53; H, 8.30.

The 1,3-Diol **6**: A solution of **5** (28 mg) and absolute EtOH (25 μl) in anhydrous THF (1.3 ml) was added dropwise to a stirred solution of Na metal (10 mg) in liquid NH_3 (7 ml) at −78 °C. After 2 min, the reaction was quenched by the addition of saturated aqueous NH_4Cl and allowed to warm to room temperature to remove NH_3. The residue was dissolved in water and extracted with ether. The ether layer was washed with brine, dried over $MgSO_4$, and concentrated under reduced pressure. The crude product was purified by silica gel column chromatography (dichloromethane : ethyl acetate = 5:1) to give **6** (13.5 mg, 88%), which was identical with an authentic sample in terms of IR and ^{1}H-NMR data and $[\alpha]_D$ +1.76° (c = 0.51, 95% EtOH): lit.[10] +1.77°.

The 1,2-Diol **7**: A solution of **4aA** (R′ = vinyl, 51 mg) in MeOH (5.5 ml) was treated with ozone at −78 °C. The completion of the reaction was checked by TLC. Excess ozone was removed by bubbling nitrogen gas through the solution and then one microspatula-full of $NaBH_4$ was added. The mixture was stirred for 30 min at room temperature, then water (5 ml) was added and the MeOH was evaporated off under reduced pressure. The aqueous solution was extracted with CH_2Cl_2. The organic layer was washed with brine, dried over $MgSO_4$, and concentrated under reduced pressure. The residue was purified on a silica gel column (hexane : ethyl acetate = 1:2) to give **7** (44 mg, 85%). **7**: Colorless oil, $[\alpha]_D$ +27° (c = 0.44). IR $\nu_{max}^{CHCl_3}$ cm^{-1}: 3475, 2900, 2875, 1095. ^{1}H-NMR (10% solution in $CDCl_3$) δ: 1.10 (3H, s, HO–C(–CH$_3$)–), 2.8—4.5 (8H, m, –CH$_2$OCH$_3$ × 2, –O–CH– × 2, and –CH$_2$OH), 3.25 and 3.43 (3H each, both s, –OCH$_3$ × 2), 7.2—7.5 (5H, aromatic protons). *Anal.* Calcd for $C_{12}H_{24}O_6$: C, 61.52; H, 7.75. Found: C, 61.24; H, 8.07.

The 1,2-Diol **8**: A solution of **7** (20 mg) and EtOH (20 μl) in anhydrous THF (1 ml) was added to a solution of Na metal (7.4 mg) in liquid NH_3 (7 ml) at −78 °C. The mixture was stirred for 3 min, then the reaction was quenched by the addition of aqueous NH_4Cl. The mixture was worked up in a usual way. The crude product was purified on a silica gel column (hexane : ethyl acetate = 1:1) to give the 1,2-diol **8** (8.6 mg, 85%), which was identical with an authentic sample on the basis of IR and ^{1}H-NMR comparisons and the following data. **8**: Colorless needless (hexane–ether), mp 66—67 °C, $[\alpha]_D$ +17.3° (c = 0.2, 95% EtOH) (lit.[10] mp 66.5—67.5 °C, $[\alpha]_D$ +17.3°).

4aA (R=Ph, R′=Et) from 4aA (R=Ph, R′=vinyl)——**4aA** (R=Ph, R′=vinyl) (10 mg) from run 5 was dissolved in ethyl acetate (1 ml) and hydrogenated in the presence of a catalytic amount of 5% Pd–C under atmospheric pressure at room temperature. After the completion of the reaction (checked by TLC), the catalyst was removed by filtration, and the filtrate was concentrated under reduced pressure. The residue was subjected to column chromatography on silica gel using benzene–ether (2:1) as an eluting solvent to give **4aA** (R=Ph, R′=Et) (10 mg), which was identical with **4aA** (R=Ph, R′=Et) from run 1 (^{1}H-NMR comparison and HPLC analysis).

4aA (R=Ph, R′=Et) and 4aB (R=Ph, R′=Et) from the Products Obtained in Runs 6 and 8——A solution of the product (19 mg) of run 8 in 0.85% KOH in aqueous 50% EtOH (1 ml) was refluxed for 15 min, then evaporated under reduced pressure to remove EtOH, and the residue was extracted with CH_2Cl_2. The organic layer was washed with brine, dried over $MgSO_4$, and concentrated under reduced pressure. The residue was separated by preparative TLC (benzene : ether=2:1, developed twice) to give **9a** (R=Ph) (8 mg, 53%) and **10a** (R=Ph) (6.4 mg, 42%). The product (7 mg) of run 6 was treated in the same manner as described above to give **9a** (R=Ph, 5.4 mg, 96%). **9a**: Colorless oil, $[\alpha]_D$ +7.4° (c=0.69). IR $\nu_{max}^{CHCl_3}$ cm^{-1}: 3420 (br), 3288, 3008, 1450, 1090. ^{1}H-NMR (10% solution in $CDCl_3$) δ: 1.41 (3H, s, HO–C(CH$_3$)–), 2.40 (1H, s, –C≡CH), 3.29 and 3.45 (3H each, both s, –OCH$_3$ ×2), 3.5—4.0 (4H, m, –CH$_2$OCH$_3$ ×2), 4.1—4.6 (2H, m, –O–CH– ×2), 7.2—7.7 (5H, aromatic protons). *Anal.* Calcd for $C_{17}H_{22}O_5$: C, 66.65; H, 7.24. Found: C, 66.64; H, 7.44. **10a** (R=Ph): Colorless oil, $[\alpha]_D$ +26.7° (c=0.4). IR $\nu_{max}^{CHCl_3}$ cm^{-1}: 3430 (br), 3228, 2960, 1450, 1090. ^{1}H-NMR (10% solution in $CDCl_3$) δ: 1.39 (3H, s, HO–C(CH$_3$)–), 2.40 (1H, s, –C≡CH), 3.28 and 3.42 (3H each, both s, –OCH$_3$ ×2), 3.5—4.0 (4H, m, –CH$_2$OCH$_3$ ×2), 4.1—4.5 (2H, m, –O–CH– ×2), 7.1—7.7 (5H, aromatic protons). *Anal.* Calcd for $C_{17}H_{22}O_5$: C, 66.65; H, 7.24. Found: C, 66.48; H, 7.42.

The acetylene compounds **9a** and **10a** were hydrogenated in the same manner as described for **4aA** (R=Ph, R′=vinyl). Purification was carried out on a silica gel column (benzene : ether=2:1). **9a** was converted into **4aA** (R=Ph, R′=Et) in 99% yield; this product was shown to be identical with **4aA** (R=Ph, R′=Et) from run 1 by ^{1}H-NMR comparison and HPLC analysis. **10a** was converted into **4aB** (R=Ph, R′=Et) in 99% yield. **4aB** (R=Ph, R′=Et): Colorless oil, $[\alpha]_D$ +28.3° (c=0.3). IR $\nu_{max}^{CHCl_3}$ cm^{-1}: 3000, 2960, 1454, 1090. ^{1}H-NMR (10% solution in $CDCl_3$) δ: 0.88 (3H, t, J=7.2 Hz, –CH$_2$CH$_3$), 1.13 (3H, s, HO–C(CH$_3$)–), 1.3—1.9 (2H, m, –CH$_2$CH$_3$), 3.28 and 3.43 (3H each, both s, –OCH$_3$ ×2), 3.5—3.9 (4H, m, –CH$_2$OCH$_3$ ×2), 4.0—4.4 (2H, m, –O–CH– ×2), 7.1—7.6 (5H, aromatic protons). *Anal.* Calcd for $C_{17}H_{26}O_5$: C, 65.78; H, 8.44. Found: C, 65.47; H, 8.57.

4bA (R=Et, R′=Et) from 4bA (R=Et, R′=vinyl)——**4bA** (R=Et, R′=vinyl) from run 11 was hydrogenated in the same manner as described for **4aA** (R=Ph, R′=vinyl). The product, **4bA** (R=Et, R′=Et), was shown to be identical with **4bA** (R=Et, R′=Et) from run 10 by ^{1}H-NMR (500 MHz, 10% solution in $CDCl_3$).

4bA (R=Et, R′=Et) and 4bB (R=Et, R′=Et) from the Products Obtained in Runs 12 and 14——The products of runs 12 and 14 were converted into **9b** and **10b** in the same manner as adopted for **9a** and **10a**. **9b** and **10b** were obtained in 75% and 19% yields, respectively, from the product of run 14 (TLC separation, hexane : ether=1:1, developed three times). In the case of the product of run 12, only **9b** was obtained in 95% yield. **9b**: Colorless oil, $[\alpha]_D$ +34.8° (c=0.7). IR $\nu_{max}^{CHCl_3}$ cm^{-1}: 3420, 3310, 1100. ^{1}H-NMR (10% solution in C_6D_6) δ: 1.02 (3H, t, J=7.0 Hz, –CH$_2$CH$_3$), 1.70 (3H, s, HO–C(CH$_3$)–), 1.7 and 2.3 (1H each, m, –CH$_2$CH$_3$), 2.10 (1H, s, –C≡CH), 2.87 and 3.02 (3H each, both s, –OCH$_3$ ×2), 3.1—3.9 and 4.6—4.9 (6H, m, –CH$_2$OCH$_3$ ×2 and –O–CH– ×2). *Anal.* Calcd for $C_{13}H_{22}O_5$: C, 60.45; H, 8.58. Found: 60.31; H, 8.64. **10b**: Colorless oil, $[\alpha]_D$ −23.1° (c=0.2). IR $\nu_{max}^{CHCl_3}$ cm^{-1}: 3395, 3300, 1098. ^{1}H-NMR (10% solution in C_6D_6) δ: 1.02 (3H, t, J=7.2 Hz, –CH$_2$CH$_3$), 1.63 (3H, s, HO–C(CH$_3$)–), 1.7—2.3 (2H, m, –CH$_2$CH$_3$), 2.03 (1H, s, –C≡CH), 2.97 and 3.03 (3H each, both s, –OCH$_3$ ×2), 3.2—3.6 (4H, m, –CH$_2$OCH$_3$ ×2), 3.97 (1H, dt, J=8.6, 3.7 Hz, –O–CH–), 4.6 (1H, dt, J=8.6, 5 Hz, –O–CH–). *Anal.* Calcd for $C_{13}H_{22}O_5$: C, 60.45; H, 8.58. Found: C, 60.57; H, 8.81.

Compounds **9b** and **10b** were hydrogenated in quantitative yield in a usual manner. **9b** was converted to **4bA** (R=Et, R′=Et), which was shown to be identical with **4bA** (R=Et, R′=Et) from run 11 by ^{1}H-NMR (500 MHz, 10% solution in $CDCl_3$). **10b** was converted to **4bB** (R=Et, R′=Et). **4bB**: Colorless oil, $[\alpha]_D$ +1.9° (c=0.11). IR $\nu_{max}^{CHCl_3}$ cm^{-1}: 3445, 1105. ^{1}H-NMR (10% solution in $CDCl_3$) δ: 0.92 (3H, t, J=6.8 Hz, –CH$_2$CH$_3$), 0.95 (3H, t, J=7.3 Hz, –CH$_2$CH$_3$), 1.15 (3H, s, HO–C(CH$_3$)–), 1.3—2.0 (4H, m, –CH$_2$–CH$_3$ ×2), 2.20 (1H, br s, –OH), 3.39 and 4.13 (3H each, both s, –OCH$_3$ ×2), 3.45—3.6 (4H, m, –CH$_2$OCH$_3$ ×2), 3.65—4.05 (1H, m, –O–CH–), 4.3—4.55 (1H, m, –O–CH–). *Anal.* Calcd for $C_{13}H_{26}O_5$: C, 59.52; H, 10.00. Found: C, 59.61; H, 9.70.

4cA (R′=Et) and 4cB (R′=Et) from the Product of Run 17——The product (10 mg) of run 17 was hydrogenated in quantitative yield in a usual manner to give the ethyl compounds [**4cA** (R′=Et) : **4cB** (R′=Et)=60:40, 10 mg], which were correlated with the product of run 16 by ^{1}H-NMR (500 MHz, C_6D_6) comparison.

4cA (R′=Et) and 4cB (R′=Et) from the Products Obtained in Runs 18 and 20——The product (27 mg) of run 18 was desilylated in a usual manner (see for **9** and **10**) to give a mixture of two acetylene compounds, which were not separable from each other and then used in a subsequent reaction without separation. Hydrogenation of the mixture of the above acetylene compounds in a usual manner afforded the ethyl compounds [**4cA** (R′=Et) : **4cB** (R′=Et)=13:87, 20.3 mg, 97% yield], which were correlated with the product of run 16 by ^{1}H-NMR (500 MHz, C_6D_6) comparison.

The product (33 mg) of run 20 was converted to the ethyl compounds [**4cA** (R′=Et) : **4cB** (R′=Et)=60:40, 25 mg, 98% yield] in the same manner as described above. Correlation of the ethyl compounds obtained here with the

product of run 16 was achieved by ^{1}H-NMR (500 MHz, C_6D_6) comparison.

Benzylation of 4cA (R = H, R′ = Et, 76% de) from Run 16——Sodium hydride (79 mg, 1.97 mmol) was added to a solution of **4cA** (R = H, R′ = Et; 76% de, 115 mg, 0.49 mmol) from run 16 in anhydrous THF (4 ml) and dimethylformamide (DMF) (1 ml) at 0 °C. The mixture was stirred for 1 h at 0 °C, then $PhCH_2Br$ (0.25 ml, 1.97 mmol) was added to the reaction mixture. The resulting solution was stirred for 12 h (overnight) at room temperature. Saturated aqueous NH_4Cl (5 ml) was added to the mixture and the solution was extracted with CH_2Cl_2. The organic layer was washed with brine, dried over $MgSO_4$, and evaporated under reduced pressure. The residue was subjected to column chromatography on silica gel using hexane–ether (3 : 1) as an eluting solvent to give **11** (158 mg, 99%). Colorless oil. IR $\nu_{max}^{CHCl_3}$ cm^{-1}: 1095. ^{1}H-NMR (10% solution in C_6D_6) δ: 1.04 (3H, t, J=6.7 Hz, $-CH_2CH_3$), 1.31 (3H, s, HO–C(–)–CH_3), 3.06 and 3.08 (3H each, both s, $-OCH_3 \times 2$), 3.14—3.4 (4H, m, $-CH_2OCH_3 \times 2$), 3.8—4.1 (2H, m, –O–CH–×2), 4.67 (2H, s, $-OCH_2Ph$), 5.14 and 5.16 (total 1H, both s, ratio 9 : 1, –O–CH–O–), 7.0—7.5 (5H, m, aromatic protons). *Anal.* Calcd for $C_{18}H_{28}O_5$: C, 66.64; H, 8.70. Found: C, 66.71; H, 8.99.

(*S*)-(−)-2-Benzyloxy-2-methylbutanal (12)——A solution of **11** (20 mg, 0.062 mmol) in concentrated H_2SO_4–AcOH–H_2O (1 : 50 : 50, 3 ml) was refluxed for 24 h. The resulting solution was neutralized with saturated aqueous $NaHCO_3$, and then extracted with CH_2Cl_2. The organic layer was washed with brine, dried over $MgSO_4$, and evaporated under reduced pressure. The residue was purified by preparative TLC (hexane : ether = 3 : 1) to give **12** (7.7 mg, 65%). Colorless oil. $[\alpha]_D$ −36° (c=0.5, C_6H_6); lit.[12] −39° (c=1.002, C_6H_6) as 78% ee. IR $\nu_{max}^{CHCl_3}$ cm^{-1}: 1730. ^{1}H-NMR (10% solution in $CDCl_3$) δ: 0.94 (3H, t, J=7.0 Hz, $-CH_2CH_3$), 1.32 (3H, s, HO–C(–)–CH_3), 1.63—1.95 (2H, m, $-CH_2CH_3$), 4.46 (2H, s, $-OCH_2Ph$), 7.34 (5H, s, aromatic protons), 9.65 (1H, s, –CHO). Elemental analysis was carried out on the 2,4-dinitrophenylhydrazone (mp 68 °C) (*Anal.* Calcd for $C_{18}H_{20}N_4O_5$: C, 58.06; H, 5.41; N, 15.05. Found: C, 57.94; H, 5.33; N, 15.05).

References and Notes

1) For a recent review, see: E. L. Eliel, "Asymmetric Synthesis," Vol. 2, ed. by J. D. Morrison, Academic Press, New York, 1983, pp. 125—155.
2) S. V. Frye and E. L. Eliel, *Tetrahedron Lett.*, **26**, 3907 (1985); J. E. Lynch and E. L. Eliel, *J. Am. Chem. Soc.*, **106**, 2943 (1984) and references cited therein; S. V. Frye and E. L. Eliel, *Tetrahedron Lett.*, **27**, 3223 (1986); M. Ohwa, T. Kogure, and E. L. Eliel, *J. Org. Chem.*, **51**, 2599 (1986).
3) T. Mukaiyama, Y. Sakito, and M. Asami, *Chem. Lett.*, **1978**, 1253; M. Asami and T. Mukaiyama, *ibid.*, **1983**, 93 and references cited therein.
4) Y. Tamura, H. Kondo, H. Annoura, R. Takeuchi, and H. Fujioka, *Tetrahedron Lett.*, **27**, 81 (1986); Y. Tamura, H. Annoura, H. Kondo, M. Fuji, T. Yoshida, and H. Fujioka, *Chem. Pharm. Bull.*, **25**, 2305 (1987).
For other asymmetric syntheses using chiral C_2-symmetrical acetals, see: W. S. Johnson, J. D. Elliott, and G. J. Hanson, *J. Am. Chem. Soc.*, **106**, 1138 (1984) and references cited therein; W. S. Johnson, C. Edington, J. D. Elliott, and I. R. Silverman, *ibid.*, **106**, 7588 (1984) and references cited therein; W. S. Johnson and M. F. Chan, *J. Org. Chem.*, **50**, 2598 (1985); J. D. Elliott, J. Steele, and W. S. Johnson, *Tetrahedron Lett.*, **26**, 2535 (1985); T. Hiyama, K. Saito, K. Sato, N. Wakasa, and M. Inoue, *Chem. Lett.*, **1986**, 1471; A. Alexakis, P. Mangeney, and J. F. Normant, *Tetrahedron Lett.*, **26**, 4197 (1985); P. Mangeney, A. Alexakis, and J. F. Normant, *ibid.*, **27**, 3143 (1986) and references cited therein; J. Fujiwara, Y. Fukutani, M. Hasegawa, K. Maruoka, and H. Yamamoto, *J. Am. Chem. Soc.*, **106**, 5004 (1984) and references cited therein; A. Mori and H. Yamamoto, *J. Org. Chem.*, **50**, 5444 (1985); K. Ishihara, A. Mori, I. Arai, and H. Yamamoto, *Tetrahedron Lett.*, **27**, 983 (1986); A. Mori, K. Ishihara, and H. Yamamoto, *ibid.*, **27**, 987 (1986) and references cited therein; Y. Naruse and H. Yamamoto, *ibid.*, **27**, 1363 (1986); I. Dyong and R. Wiemann, *Chem. Ber.*, **113**, 1592 (1980); M. Suzuki, Y. Kimura, and S. Terashima, *Tetrahedron Lett.*, **26**, 6481 (1985) and references cited therein; T. Matsumoto, F. Matsuda, K. Hasegawa, and M. Yanagiya, *Tetrahedron*, **40**, 2337 (1984); I. Arai, A. Mori, and H. Yamamoto, *J. Am. Chem. Soc.*, **107**, 8254 (1985); E. A. Mash and K. A. Nelson, *ibid.*, **107**, 8256 (1985); *idem*, *Tetrahedron Lett.*, **27**, 1441 (1986); G. Castalidi, S. Cavicchioli, C. Giordano, and F. Uggeri, *Angew. Chem., Int. Ed. Engl.*, **25**; 259 (1986); M. Utaka, Y. Fujii, and A. Takeda, *Chem. Lett.*, **1986**, 1103.
5) Y. Tamura, T. Ko, H. Kondo, H. Annoura, M. Fuji, R. Takeuchi, and H. Fujioka, *Tetrahedron Lett.*, **27**, 2117 (1986).
6) After our communication (ref. 5), a very similar study on the diastereoselective addition of organometallics to a chiral monoacetal of glyoxal was reported by French chemists [M. P. Heits, F. Gellibert, and C. Miskowski, *Tetrahedron Lett.*, **27**, 3859 (1986)].
7) R. M. Moriarty and K.-C. Hou, *Tetrahedron Lett.*, **25**, 691 (1984).
8) Compound **2c** was prepared from commercially available pyruvic aldehyde dimethyl acetal (Aldrich) by $LiAlH_4$ reduction.
9) A. J. Mancuso, S.-L. Huang, and D. Swern, *J. Org. Chem.*, **43**, 2480 (1978).
10) S. V. Frye and E. L. Eliel, *J. Org. Chem.*, **50**, 3402 (1985).
11) Compound **5′** is a single compound. The stereochemistry of the secondary alcohol was not determined.

12) T. Mukaiyama, Y. Sakito, and M. Asami, *Chem. Lett.*, **1979**, 705.
13) A similar result, that Grignard reagents are more selective as addends than organolithium reagents, was observed in our study on the nucleophilic addition to α-keto acetals in cyclic systems (ref. 4). See also W. C. Still and J. H. McDonald III, *Tetrahedron Lett.*, **21**, 1031 (1980).
14) J. F. W. McOmie, "Protective Groups in Organic Chemistry," Plenum Press, New York, 1973; T. W. Greene, "Protective Groups in Organic Synthesis," Wiley, New York, 1981.
15) (−)-(2*S*,3*S*)-1,4-Dimethoxy-2,3-butanediol can be readily prepared from L-(+)-tartaric acid in four steps: (1) $Me_2C(OMe)_2$/MeOH/*p*-TsOH/cyclohexane/*Δ* [M. Carmack and C. J. Kelley, *J. Org. Chem.*, **33**, 2171 (1968)]; (2) $LiAlH_4/Et_2O$/reflux; (3) MeI/KOH/DMSO; (4) 95% EtOH/*p*-TsOH/reflux. The (+)-enantiomer is available from D-mannitol (A. H. Haines and C. S. P. Jenkins, *J. Chem. Soc., Perkin Trans. 1*, **1972**, 273).

[Chem. Pharm. Bull. 35(12)4747—4756(1987)]

Cyclophanes. I. Preparations and Conformational Properties of Dioxazolo[3²]metacyclophane and Related Compounds

HIDEAKI SASAKI* and TOKUJIRO KITAGAWA

Faculty of Pharmaceutical Sciences, Kobe Gakuin University, Ikawadani, Nishi-ku, Kobe 673, Japan

(Received May 25, 1987)

The one-pot coupling reactions of bis(2-isocyano-2-tosylethyl)benzenes (**5**) with phthalaldehydes (**11**) afforded dioxazolo[3²]cyclophanes (**12a**, **12d**, **12e**, **12f**, and **12h**), bis(naphth[2,1-*d*]-oxazol-4-yl)benzenes (**13a**—**c**), and tetraoxazolo[3⁴]parametacyclophane (**14**) as 1 : 1, 1 : 2, and 2 : 2 adducts, respectively. On the basis of the variable-temperature nuclear magnetic resonance (VT-NMR) spectra of dioxazolo[3²]metacyclophane (**12e**), **12e** in solution at room temperature exists in a *syn* form and the energy barrier to the conformational change ($\Delta G^{\ddagger}$) at the coalescence temperature ($T_c = 38\,^{\circ}C$) is determined to be 64.5 kJ/mol, which is higher than that of parent [3²]metacyclophane (**1**). Therefore, it was suggested that the annelations of two oxazole rings to the two methylene bridges of **1** significantly affected the mobility of the benzene rings of **12e**.

Keywords——[3²]metacyclophane; cyclophane; conformational analysis; VT-NMR; COSY; oxazole; cyclization; isocyanide; tosylmethyl isocyanide; phthalaldehyde

In the past decade, the [3²]metacyclophane ring has been constructed by several methods, that is, ring expansion,[1] ring contraction,[2] cyclizations of bifunctional reactants, *i.e.*, malonic ester derivatives (**4**)[3] or 1,3-bis(2-isocyano-2-tosylethyl)benzene (**5b**)[4] with α,α′-dibromo-*m*-xylene (**6**), and cyclodimerization,[5] as shown in Chart 1. Moreover, the conformation of parent [3²]metacyclophane (**1**) both in solution and in the solid state has been assigned as a *syn* form on the basis of the variable-temperature nuclear magnetic resonance (VT-NMR) and X-ray studies.[5]

In the previous communication,[6] we presented a novel method for the preparation of [3²]metacyclophane derivative (**12e**) by cyclization of **5b** with isophthalaldehyde (**11b**). This method allows very convenient one-pot syntheses of [3²]metacyclophane derivative (**12e**) annelated with two oxazole rings to the two methylene bridges of **1**. This introduction of unsaturated systems into **1** makes it possible in principle to produce an extended conjugated system over three aromatic rings, that is, oxazole, benzene, and oxazole.[7] Therefore, it is very interesting to investigate whether or not the introduced conjugated system affects the conformation and the conformational change of [3²]metacyclophane derivative (**12e**).

In this paper, we wish to describe facile preparations of dioxazolo[3²]cyclophanes (**12**)[8] and bis(naphth[2,1-*d*]oxazol-4-yl)benzenes (**13**) as outlined in Chart 2 and the conformational properties of **12** on the basis of VT-NMR and ultraviolet (UV) spectra.

Synthesis

The results of the preparations are summarized in Table I. Thus, the one-pot coupling reaction of **5b** with **11b** in the presence of sodium ethoxide (EtONa) in refluxing ethanol (EtOH) afforded dioxazolo[3²]metacyclophane (**12e**) as an 1 : 1 adduct in 77% yield. The analogous reactions of 1,2- and 1,4-bis(2-isocyano-2-tosylethyl)benzenes (**5a** and **5c**) with **11b** gave dioxazolo[3²]orthometacyclophane (**12d**) in 84% yield and dioxazolo[3²]parametacyclophane (**12f**) in 15% yield, along with tetraoxazolo[3⁴]parametacyclophane (**14**) as

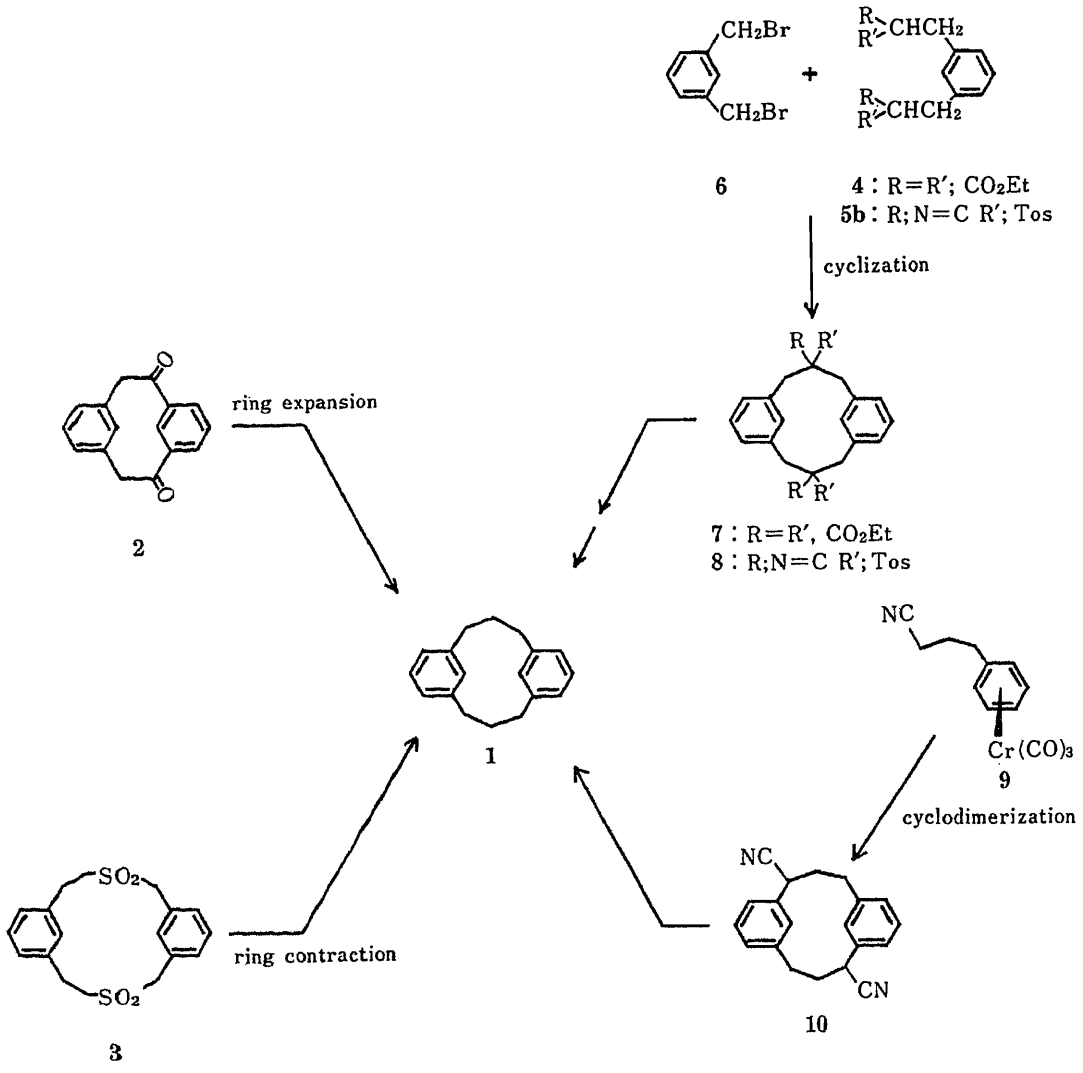

Chart 1

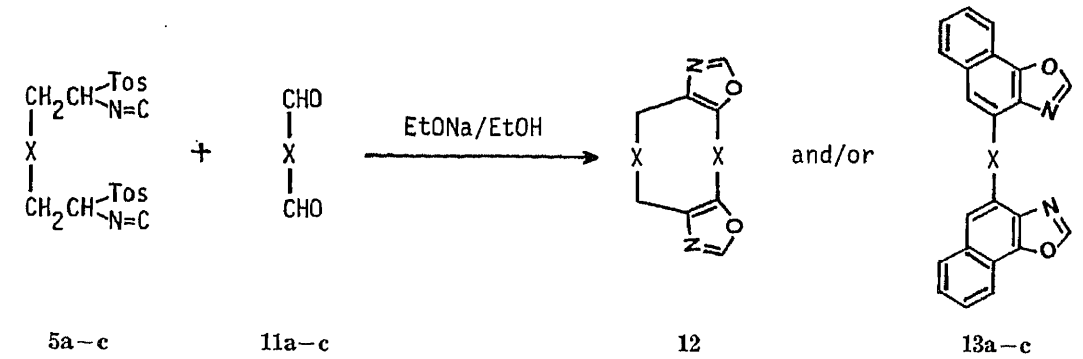

X;

5, 11, and 13
a : *ortho*
b : *meta*
c : *para*

Chart 2

TABLE I. Prepared Dioxazolo[3²]cyclophanes (**12a**, **12d**, **12e**, **12f**, and **12h**) and Bis(naphth[2,1-*d*]oxazol-4-yl)benzenes (**13a—c**)

	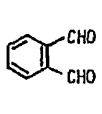 **11a**		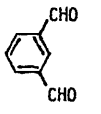 **11b**	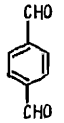 **11c**
	5:**11a**=1:1 adduct	**5**:**11a**=1:2 adduct	**5**:**11b**=1:1 adduct	**5**:**11c**=1:1 adduct
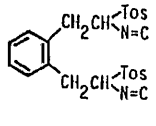 **5a**	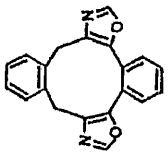 **12a** (2%)	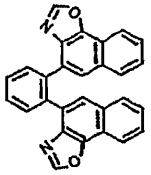 **13a** (0.8%)	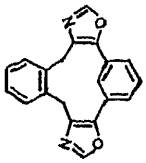 **12d** (84%)	[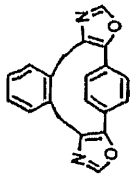] **12g**[a]
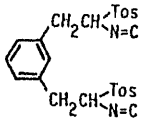 **5b**	[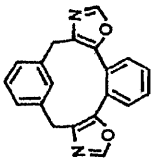] **12b**[a]	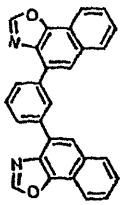 **13b** (74%)	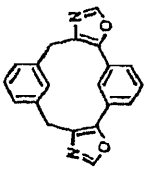 **12e** (77%)	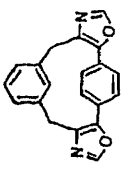 **12h** (85%)
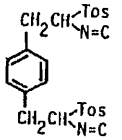 **5c**	[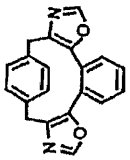] **12c**[a]	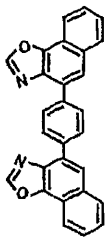 **13c** (84%)	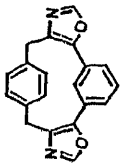 **12f** (15%)[b]	[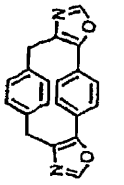] **12i**[a]

a) These cyclophanes could not be detected. *b*) The structure of tetraoxazolo[3⁴]parametacyclophane (**14**), afforded as a 2:2 adduct in 52% yield, is shown on the right.

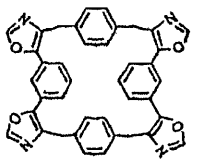

14

a 2:2 adduct in 52% yield. Subsequently, the treatment of **5a** with phthalaldehyde (**11a**) afforded dioxazolo[3²]orthocyclophane (**12a**) in 2% yield, along with 1,2-bis(naphth[2,1-*d*]-oxazol-4-yl)benzene (**13a**) as an 1:2 adduct in 0.8% yield. A similar treatment of **5b** and **5c** with **11a** gave no cyclophanes (**12b** and **12c**) but provided bis(naphth[2,1-*d*]oxazol-4-yl)benzenes (**13b** and **13c**) in 74% and 84% yields, respectively. On the other hand, the reaction of **5b** with terephthalaldehyde (**11c**) yielded the corresponding dioxazolo[3²]meta-paracyclophane (**12h**) in 85% yield, whereas the cyclophanes (**12g** and **12i**) were not obtained by the reactions of **5a** and **5c** with **11c**.

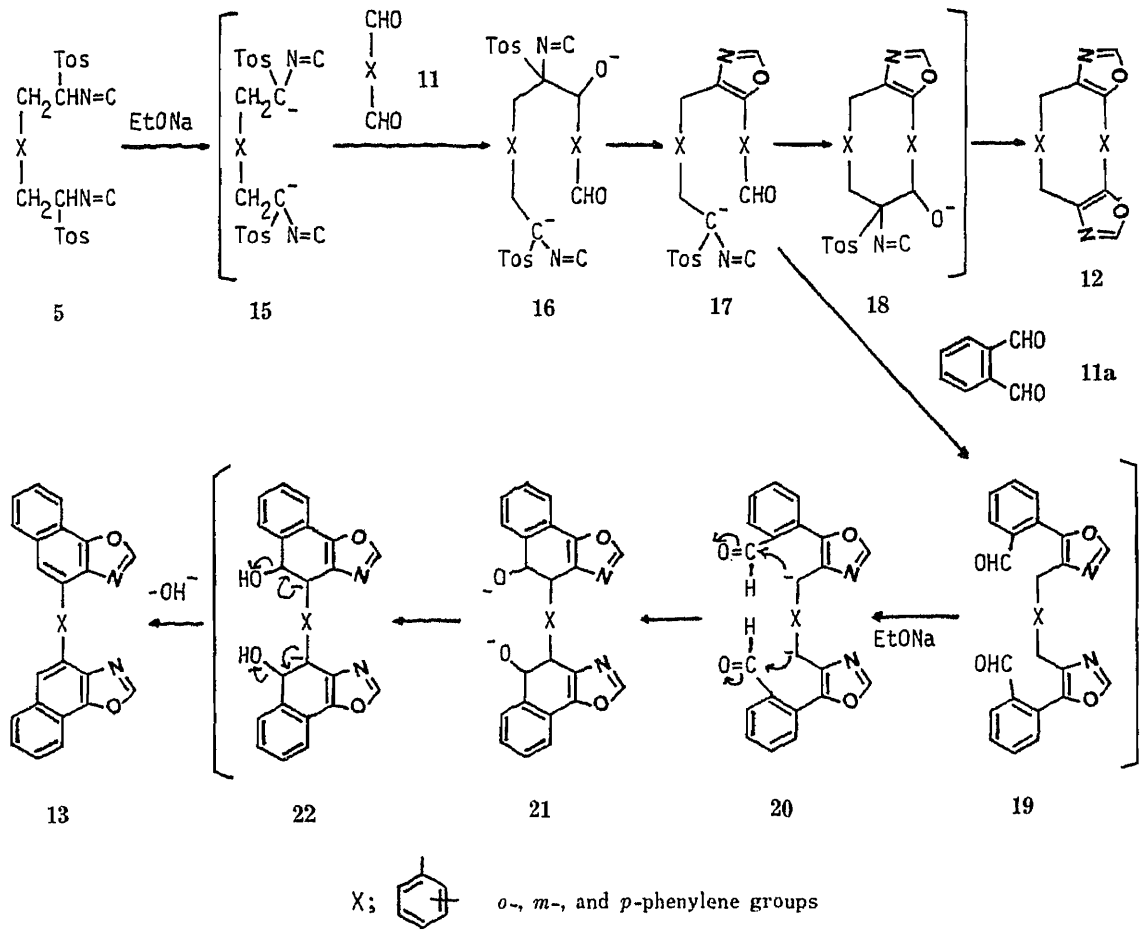

Chart 3

The coupling reaction pathway for the formations of **12** and **13** can be rationalized as follows: the intermediate (**16**) is formed by the nucleophilic attack of the dicarbanion (**15**) on one of carbonyl carbon atoms of **11**. Ring closure to the oxazole ring in **16** occurs to give **17** and then **12** is formed by the intramolecular cyclization of **17** to give the [3²]cyclophane ring, followed by ring closure to another oxazole ring in **18**. When **11a** is used as a carbonyl component, **17** can predominantly react with another **11a** to give **19** instead of intramolecular ring closure of **17**. Subsequently, the dianion (**21**) is produced by the intramolecular cyclization of **20** formed by loss of protons from **19**, and then **13** is produced by 1,3-proton shift in the dianion (**21**) following elimination of hydroxide anions from **22**.

The structures of dioxazolo[3²]cyclophanes (**12**), bis(naphth[2,1-*d*]oxazol-4-yl)benzenes (**13**), and tetraoxazolo[3⁴]parametacyclophane (**14**) were confirmed by the spectroscopic properties and analytical data. The infrared (IR) spectra show the characteristic absorptions of oxazole $\nu_{C2\text{-}H}$ around 3125 cm^{-1},[9] and the mass spectra (MS) show the molecular ion (M^+). The assignment of the ^{1}H-NMR signals of **12e** was achieved on the basis of the two-dimensional proton-proton chemical shift correlation (COSY) spectrum in dimethylsulfoxide-d_6 (DMSO-d_6) (Fig. 1). Although in $CDCl_3$ a part of the benzene proton signals of **12e** overlapped each other, the signals in $CDCl_3$ were readily assigned by changing the solvent composition stepwise from DMSO-d_6 to $CDCl_3$, as illustrated in Fig. 2. The ^{1}H-NMR spectra of the other dioxazolo[3²]cyclophanes (**12a**, **12d**, **12f**, and **12h**) and **14** in $CDCl_3$ were readily assigned from the coupling pattern and intensity of signals and by comparison with those of acyclic reference compounds (**24a**—**c**) as mentioned below.

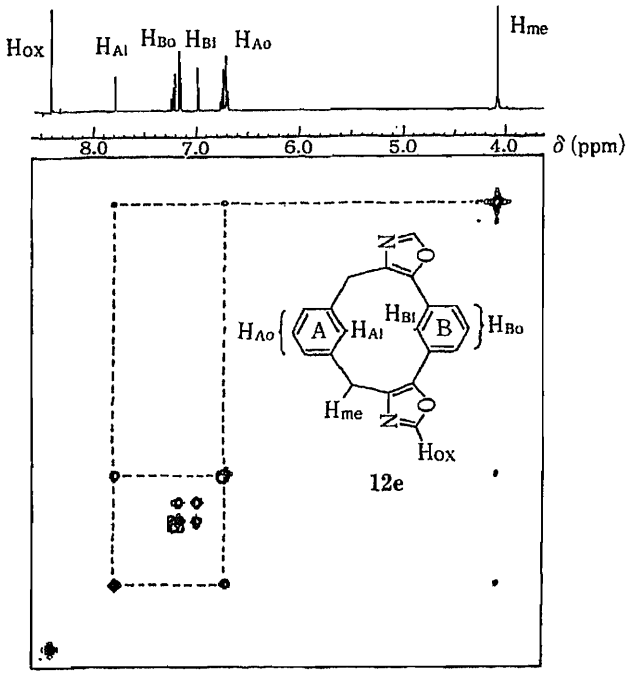

Fig. 1. COSY Spectrum of **12e** in DMSO-d_6

The benzene protons of the A ring were assigned on the basis of the observation of benzyl coupling with benzylic methylene protons.

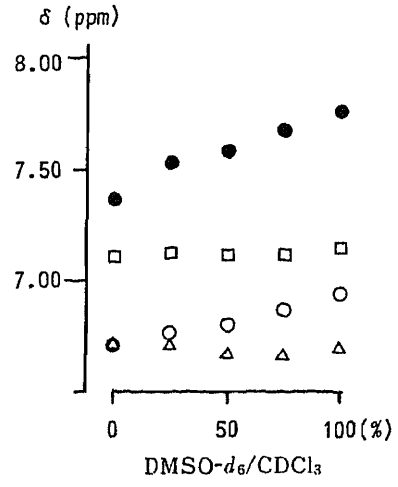

Fig. 2. Benzene Proton Signals of **12e** in $CDCl_3$ and DMSO-d_6 at Various Ratios

H_{Ai} (●), H_{Ao} (△), H_{Bi} (○), and H_{Bo} (□).

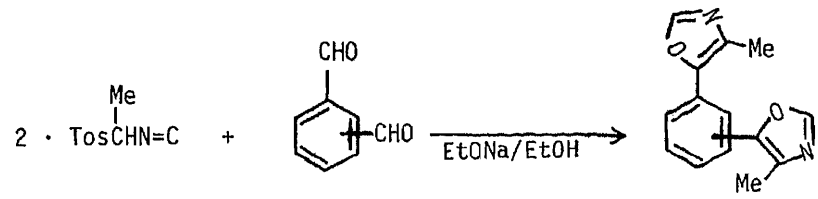

23 **11a—c** **24a—c**

Chart 4

Acyclic reference compounds (**24a—c**) were prepared by the reactions of 2 eq of 1-tosylethyl isocyanide (**23**)[10] with **11a—c** in the presence of EtONa, as outlined in Chart 4. The ^{1}H-NMR spectral data for **24a—c** in $CDCl_3$ are summarized in Table III.

Conformational Properties

The cyclophane **12e** undergoes conformational change in solution at room temperature, because the methylene signal of **12e** appears as a singlet. The observation of high-field shifts of inner aryl protons is generally useful for determination of preferred conformation of metacyclophanes, but it was suggested that the corresponding protons (H_{Ai} and H_{Bi}) of **12e** were strongly affected by both the anisotropic effect of the oxazole rings and the electrostatic effect of the oxygen atoms of the oxazole rings. As shown in Table II, H_{Ao} of **12e**, which was little affected by these effects, was observed at higher field than that of the corresponding protons of *m*-xylene (δ 6.88—7.05).[11] This fact suggests that H_{Ao} is affected by the shielding effect of the opposite benzene ring. Therefore, the preferred conformation of **12e** in solution at room temperature can be assigned as a *syn* form. Figure 3 shows the ^{1}H-NMR spectra of the methylene protons of **12e** in $CDCl_3$ at various temperatures between −29 and 48 °C. Since the T_c of the methylene signal is 38 °C, the $\Delta G^{\ddagger}$ value for conformational flipping is calculated to

TABLE II. ^{1}H-NMR Spectral Data for Dioxazolo[3^2]cyclophanes (**12a**, **12d**, **12e**, **12f**, and **12h**) and Tetraoxazolo[3^4]parametacyclophane (**14**) ($CDCl_3$, 90 MHz)

Compd. No.	Structure	$-CH_2-$	Aromatic-H	Oxazole C2-H
12a	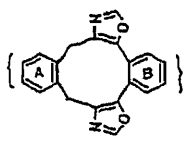	3.95 (4H, s)	6.70—7.00 (4H, m, H_A) 7.00—7.30 (4H, m, H_B)	7.70 (2H, s)
12d	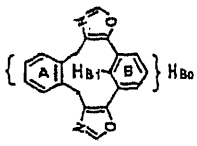	4.17 (2H, d, J=15 Hz) 4.35 (2H, d, J=15 Hz)	7.00—7.50 (4H, m, H_A) 7.79 (1H, brs, H_{Bi}), 7.30—7.50 (3H, m, H_{Bo})	7.88 (2H, s)
12e	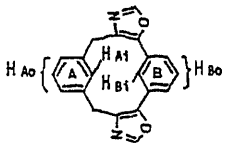	4.16 (4H, brs)	7.46 (1H, brs, H_{Ai}), 6.70—6.80 (3H, m, H_{Ao}) 6.75 (1H, brs, H_{Bi}), 7.05—7.15 (3H, m, H_{Bo})	7.86 (2H, s)
12f	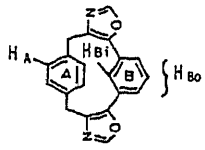	4.02 (4H, s)	6.90 (4H, s, H_A) 5.33 (1H, brs, H_{Bi}), 7.05—7.40 (3H, m, H_{Bo})	7.80 (2H, s)
12h	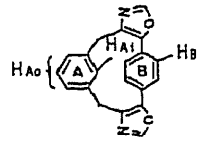	3.73 (4H, s)	6.07 (1H, brs, H_{Ai}), 6.65—6.90 (3H, m, H_{Ao}) 6.93 (4H, s, H_B)	7.82 (2H, s)
14[a]	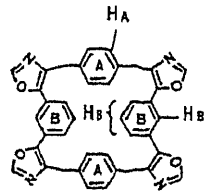	3.71 (8H, s)	6.99 (8H, s, H_A) 7.43—7.80 (8H, m, H_B)	7.84 (4H, s)

a) 100 MHz.

TABLE III. ^{1}H-NMR Spectral Data for Bis(4-methyl-5-oxazolyl)benzenes (**24a—c**) ($CDCl_3$, 90 MHz)

Compd. No.	Me	Aromatic-H	Oxazole C2-H
24a	1.96 (6H, s)	7.46 (4H, s)	7.80 (2H, s)
24b	2.46 (6H, s)	7.46—7.60 (3H, m), 7.81 (1H, brs)	7.81 (2H, s)
24c	2.46 (6H, s)	7.67 (4H, s)	7.82 (2H, s)

be 64.5 kJ/mol (15.4 kcal/mol),[12] which is higher than that of parent [3^2]metacyclophane (**1**) [T_c = −29 °C, $\Delta G^{\ddagger}$ = 48.1 kJ/mol (11.5 kcal/mol)].[5] Thus, it is considered that **12e** is more rigid than **1**, probably because of the annelations of two oxazole rings to the two methylene bridges of **1**.

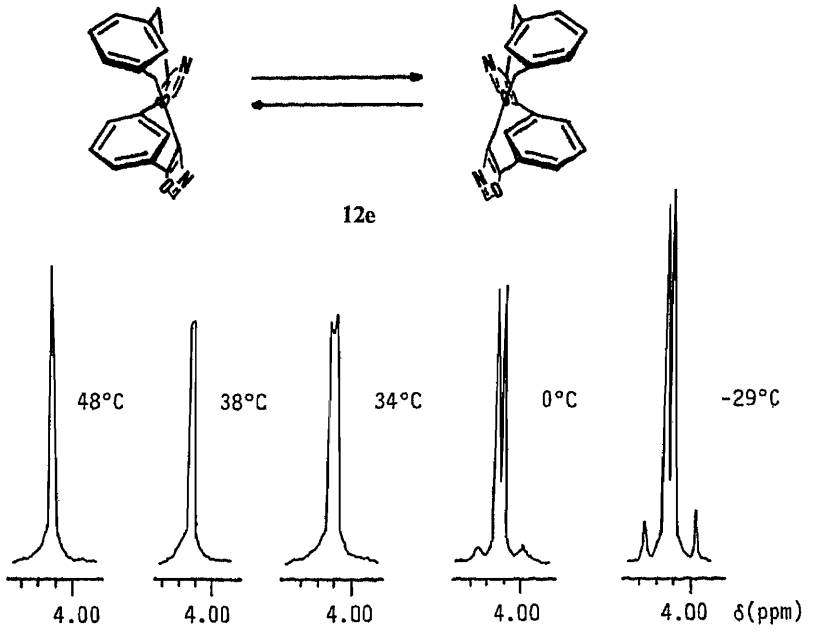

Fig. 3. VT-NMR Spectra and Conformational Flipping of **12e**

The UV spectra of cyclophanes (**12d**, **12e**, and **12f**) *meta*-substituted on the benzene ring by two oxazole rings and **24b** in EtOH are shown in Fig. 4. Compound **24b** shows a broad absorption around 265 nm ($\log \varepsilon = 4.02$) because of the presence of an extended conjugated system over three aromatic rings, *i.e.*, oxazole, benzene, and oxazole.[7] Since the absorption bands of **12e** exhibit significant hypsochromic shifts as compared with those of **24b**, the three aromatic rings of **12e** are suggested to be less coplanar than those of **24b**. The absorption bands of cyclophanes (**12d**—**f**) have a tendency to show bathocromic shifts with decreasing ring size. This finding suggests that the extension of the conjugated system over the three aromatic rings increase with decreasing size. Furthermore, the methylene signals of **12d**—**f** at room temperature appear as a sharp singlet (**12f**), a broad singlet (**12e**), and two doublets of AB type (**12d**), respectively. Thus, rigidity of cyclophanes of type **12d**—**f** is attributed to the extension of the conjugated system. Incidentally, the conformation of **12f** is not frozen even at −80 °C because of the appearance of the methylene and the *para*-substituted benzene proton signals as singlets (Fig. 5).

Since the methylene and the *para*-substituted benzene proton signals of **12h** as well as those of **12f** are observed as sharp singlets (Table II), **12h** undergoes rapid conformational change in solution at room temperature. Figure 6 shows the VT-NMR signals of the methylene protons of **12h** in $CDCl_3$ at various temperatures between −80 and −54 °C. The T_c of the methylene signal of **12h** is −62 °C and the $\Delta G^{\ddagger}$ value for conformational flipping is determined to be 47.7 kJ/mol (11.4 kcal/mol).[12]

As shown in Fig. 7, **24c** shows a broad and high intensity absorption around 300 nm ($\log \varepsilon = 4.20$), but the absorption bands of **12h** exhibit significant hypsochromic shifts and reduction of intensity in the region above 270 nm as compared with those of **24c** in the corresponding region. A similar tendency for the UV spectra of **12a** and **24a** was observed. Therefore, it is suggested that the three aromatic rings, *i.e.*, oxazole, benzene, and oxazole, in cyclophanes of type **12** are considerably displaced from planarity as contrasted with those of acyclic reference compounds (**24**).

In conclusion, facile preparations of novel [3^2]cyclophane derivatives (**12**) fused with two oxazole rings were accomplished by the one-pot cyclization of bis(2-isocyano-2-

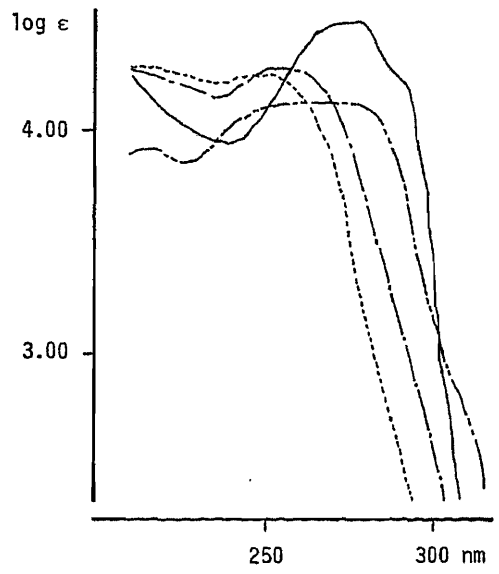

Fig. 4. UV Spectra of **12d** (——), **12e** (— — —), **12f** (------), and **24b** (— — —) in EtOH

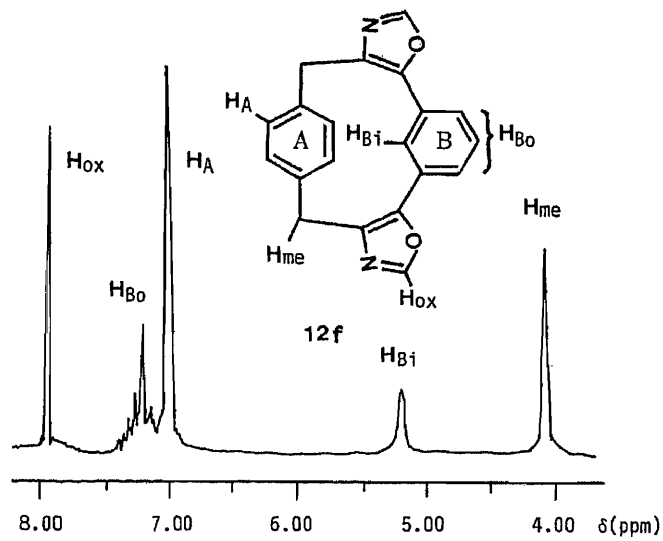

Fig. 5. ^{1}H-NMR Spectrum of **12f** at −80 °C

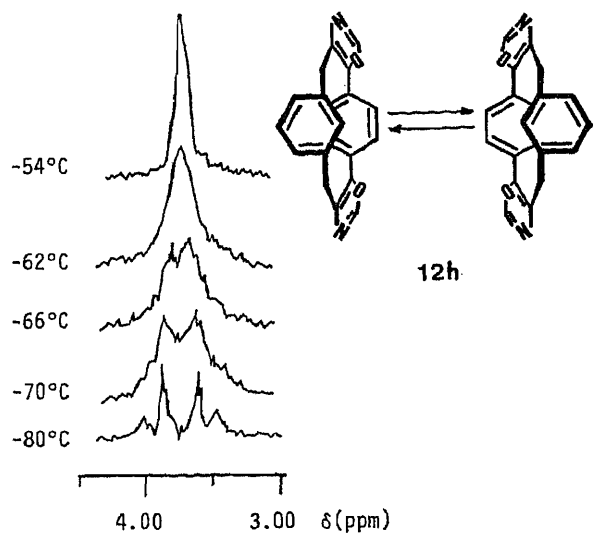

Fig. 6. VT-NMR Spectra and Conformational Flipping of **12h**

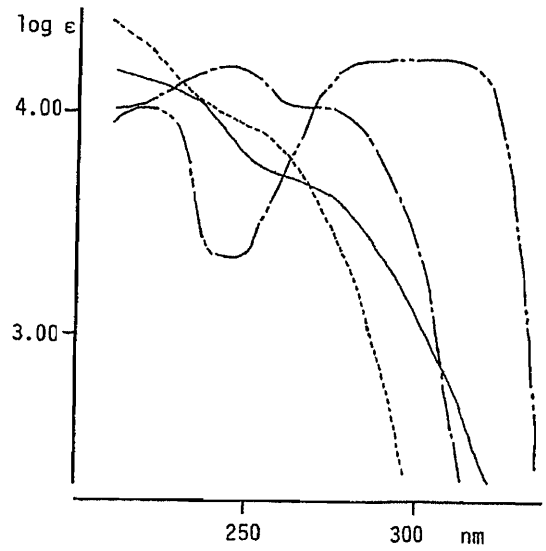

Fig. 7. UV Spectra of **12a** (------), **12h** (——), **24a** (— — —), and **24c** (— — —) in EtOH

tosylethyl)benzenes (**5**) with phthalaldehydes (**11**). Furthermore, it is demonstrated that in solution at room temperature the preferred conformation of dioxazolo[3^2]metacyclophane (**12e**) as well as that of parent [3^2]metacyclophane (**1**) can be assigned as a *syn* form and the increase of rigidity of **12e** with respect to the rigidity of **1** can be attributed to the annelations of two oxazole rings to the two methylene bridges of **1**.

Experimental

All melting points were taken on a Yanagimoto micro melting point determination apparatus and are uncorrected. IR spectra were recorded on a Hitachi model 260-30 infrared spectrophotometer. ^{1}H-NMR spectra were measured on a Bruker AM-400 (400 MHz) instrument and a Hitachi R-22 spectrometer (90 MHz) using tetramethyl-

silane as an internal reference. VT-NMR spectra were measured on a Nihondenshi JNM-FX 100 spectrometer (100 MHz). MS were measured on a Hitachi mass spectrometer, model RMU-6MG. UV spectra were measured on a Hitachi 323 spectrometer.

Dioxazolo[3²]orthocyclophane (12a) and 1,2-Bis(naphth[2,1-*d*]oxazol-4-yl)benzene (13a)——A solution of phthalaldehyde (**11a**) (1.34 g, 10 mmol) in EtOH (50 ml) was added dropwise to a stirred suspension of 1,2-bis(2-isocyano-2-tosylethyl)benzene (**5a**) (4.92 g, 10 mmol) and EtONa (Na; 0.46 g, 20 mmol) in EtOH (550 ml). After the mixture had been refluxed for 2 h, the solvent was removed under reduced pressure, and then a mixture of AcOEt (200 ml) and water (50 ml) was poured onto the residue. The organic layer was separated, washed with three 50 ml portions of water, and then dried over anhydrous $MgSO_4$. The solvent was evaporated off, and the residue was chromatographed on silica gel with (i) a mixture of benzene–AcOEt (9 : 1) and (ii) AcOEt. (i) Concentration of the benzene–AcOEt eluate gave a crude product, which was recrystallized from $CHCl_3$ to yield 17 mg (0.8%) of **13a**, colorless prisms. mp 214—216 °C. IR (KBr): 3130 (oxazole $\nu_{C2\text{-}H}$) cm^{-1}. ^1H-NMR (90 MHz, $CDCl_3$) δ: 7.30—8.20 (14H, m, aromatic-H), 7.95 (2H, s, oxazole C2-H). MS *m/z*: 412 (M^+). (ii) Concentration of the AcOEt eluate gave a crude product, which was recrystallized from benzene to yield 63 mg (2%) of **12a**, colorless prisms. mp 205—206 °C. *Anal.* Calcd for $C_{20}H_{14}N_2O_2$: C, 76.42; H, 4.49; N, 8.91. Found: C, 76.51; H, 4.58; N, 8.82. IR (KBr): 3115 (oxazole $\nu_{C2\text{-}H}$) cm^{-1}. MS *m/z*: 314 (M^+).

Dioxazolo[3²]orthometacyclophane (12d)——A solution of isophthalaldehyde (**11b**) (0.67 g, 5 mmol) in EtOH (25 ml) was added dropwise to a stirred suspension of **5a** (2.46 g, 5 mmol) and EtONa (Na; 0.23 g, 10 mmol) in EtOH (275 ml). After the mixture had been refluxed for 2 h, the solvent was removed under reduced pressure, and then a mixture of AcOEt (100 ml) and water (30 ml) was poured onto the residue. The organic layer was separated, washed with three 50 ml portions of water, and dried over anhydrous $MgSO_4$. The organic solvent was evaporated off to afford a crude product, which was recrystallized from CH_2Cl_2 to yield 1.32 g (84%) of **12d**, colorless prisms. mp 263—264 °C. *Anal.* Calcd for $C_{20}H_{14}N_2O_2$: C, 76.42; H, 4.49; N, 8.91. Found: C, 76.14; H, 4.49; N, 8.79. IR (KBr): 3125 (oxazole $\nu_{C2\text{-}H}$) cm^{-1}. MS *m/z*: 314 (M^+).

Dioxazolo[3²]metacyclophane (12e)——According to the same procedure as described above for the preparation of **12d**, the reaction of **11b** (1.34 g, 10 mmol) with 1,3-bis(2-isocyano-2-tosylethyl)benzene (**5b**) (4.92 g, 10 mmol) and EtONa (Na; 0.46 g, 10 mmol) in refluxing EtOH (600 ml) for 2 h gave a crude product, which was recrystallized from benzene to yield 2.43 g (77%) of **12e**, colorless prisms. mp 195—196 °C. *Anal.* Calcd for $C_{20}H_{14}N_2O_2$: C, 76.42; H, 4.49; N, 8.91. Found: C, 76.70; H, 4.52; N, 9.03. IR (KBr): 3140 (oxazole $\nu_{C2\text{-}H}$) cm^{-1}. MS *m/z*: 314 (M^+).

Dioxazolo[3²]parametacyclophane (12f) and Tetraoxazolo[3⁴]parametacyclophane (14)——A solution of **11b** (1.34 g, 10 mmol) in EtOH (50 ml) was added dropwise to a stirred suspension of 1,4-bis(2-isocyano-2-tosylethyl)benzene (**5c**) (4.92 g, 10 mmol) and EtONa (Na; 0.46 g, 20 mmol) in EtOH (550 ml). After the mixture had been refluxed for 2 h, the resulting mixture was cooled to 5 °C, and filtered with suction to collect a yellowish precipitate. Then, the precipitate was recrystallized from $CHCl_3$ to yield 1.63 g (52%) of **14**, pale yellow prisms. mp >300 °C. *Anal.* Calcd for $C_{40}H_{28}N_4O_4$: C, 76.42; H, 4.49; N, 8.91. Found: C, 75.96; H, 4.55; N, 8.77. IR (KBr): 3140 (oxazole $\nu_{C2\text{-}H}$) cm^{-1}. MS *m/z*: 628 (M^+). The filtrate was concentrated under reduced pressure, and a mixture of AcOEt (200 ml) and water (50 ml) was poured onto the residue. The organic layer was separated, washed with three 50 ml portions of water, and then dried over anhydrous $MgSO_4$. The solvent was evaporated off, and the residue was chromatographed on silica gel with AcOEt to give a crude product, which was recrystallized from CH_2Cl_2 to yield 0.47 g (15%) of **12f**, colorless needles. mp 190—192 °C. *Anal.* Calcd for $C_{20}H_{14}N_2O_2$: C, 76.42; H, 4.49; N, 8.91. Found: C, 76.52; H, 4.32; N, 8.69. IR (KBr): 3120 (oxazole $\nu_{C2\text{-}H}$) cm^{-1}. MS *m/z*: 314 (M^+).

Dioxazolo[3²]metaparacyclophane (12h)——According to the same procedure as described above for the preparation of **12d**, the reaction of terephthalaldehyde (**11c**) (1.34 g, 10 mmol) with **5b** (4.92 g, 10 mmol) and EtONa (Na; 0.46 g, 20 mmol) in refluxing EtOH (600 ml) for 2 h gave a crude product, which was recrystallized from CH_2Cl_2 to yield 2.70 g (85%) of **12h**, colorless needles. mp 246—248 °C. *Anal.* Calcd for $C_{20}H_{14}N_2O_2$: C, 76.42; H, 4.49; N, 8.91. Found: C, 76.58; H, 4.39; N, 8.85. IR (KBr): 3125 (oxazole $\nu_{C2\text{-}H}$) cm^{-1}. MS *m/z*: 314 (M^+).

1,3-Bis(naphth[2,1-*d*]oxazol-4-yl)benzene (13b)——A solution of **11a** (1.34 g, 10 mmol) in EtOH (50 ml) was added dropwise to a stirred suspension of **5b** (2.46 g, 5 mmol) and EtONa (Na; 0.23 g, 10 mmol) in EtOH (550 ml). After the mixture had been refluxed for 2 h, the resulting mixture was cooled to 5 °C, and filtered with suction to collect a yellowish precipitate. Then, the precipitate was recrystallized from $CHCl_3$ to yield 1.52 g (74%) of **13b**, pale yellow needles. mp 262—264 °C. *Anal.* Calcd for $C_{28}H_{16}N_2O_2$: C, 81.54; H, 3.91; N, 6.79. Found: C, 81.61; H, 3.76; N, 6.68. ^1H-NMR (90 MHz, $CDCl_3$) δ: 7.50—8.20 (14H, m, aromatic-H), 8.24 (2H, s, oxazole C2-H). IR (KBr): 3130 (oxazole $\nu_{C2\text{-}H}$) cm^{-1}. MS *m/z*: 412 (M^+).

1,4-Bis(naphth[2,1-*d*]oxazol-4-yl)benzene (13c)——According to the same procedure as mentioned above for the preparation of **13b**, the reaction of **11a** (1.34 g, 10 mmol) with **5c** (2.46 g, 5 mmol) and EtONa (Na; 0.23 g, 10 mmol) in refluxing EtOH (600 ml) for 2 h gave a crude product, which was recrystallized from $CHCl_3$ to yield 1.73 g (84%) of **13c**, orange prisms. mp 288—290 °C. *Anal.* Calcd for $C_{28}H_{16}N_2O_2$: C, 81.54; H, 3.91; N, 6.79. Found: C, 81.78; H, 3.89; N, 6.63. ^1H-NMR (90 MHz, $CDCl_3$) δ: 7.50—8.25 (14H, m, aromatic-H), 8.27 (2H, s, oxazole C2-H). IR (KBr): 3130 (oxazole $\nu_{C2\text{-}H}$) cm^{-1}. MS *m/z*: 412 (M^+).

1,2-Bis(4-methyl-5-oxazolyl)benzene (24a)——A solution of **11a** (2.01 g, 15 mmol) in EtOH (50 ml) was added

dropwise to a stirred solution of 1-tosylethyl isocyanide (**23**) (6.28 g, 30 mmol) and EtONa (Na; 0.69 g, 30 mmol) in EtOH (250 ml). After the mixture had been refluxed for 2 h, the solvent was removed under reduced pressure, and then a mixture of AcOEt (200 ml) and water (100 ml) was poured onto the residue. The organic layer was separated, washed with three 50 ml portions of water, and then dried over anhydrous $MgSO_4$. The solvent was evaporated off, and the residue was recrystallized from benzene to yield 2.06 g (57%) of **24a**, colorless prisms. mp 135—137 °C. *Anal.* Calcd for $C_{14}H_{12}N_2O_2$: C, 69.99; H, 5.03; N, 11.66. Found: C, 70.15; H, 4.90; N, 11.53. IR (KBr): 3145 (oxazole $\nu_{C2\text{-}H}$) cm^{-1}. MS *m/z*: 240 (M^+).

1,3-Bis(4-methyl-5-oxazolyl)benzene (24b)——According to the same procedure as described above for the preparation of **24a**, the reaction of **11b** (2.01 g, 15 mmol) with **23** (6.28 g, 30 mmol) and EtONa (Na; 0.69 g, 30 mmol) in refluxing EtOH (300 ml) for 2 h gave an oily product. The oily product was chromatographed on silica gel with benzene–AcOEt (1 : 1) to afford a crude solid, which was recrystallized from benzene to yield 1.64 g (45%) of **24b**, colorless needles. mp 202—204 °C. *Anal.* Calcd for $C_{14}H_{12}N_2O_2$: C, 69.99; H, 5.03; N, 11.66. Found: C, 69.82; H, 4.84; N, 11.57. IR (KBr): 3140 (oxazole $\nu_{C2\text{-}H}$) cm^{-1}. MS *m/z*: 240 (M^+).

1,4-Bis(4-methyl-5-oxazolyl)benzene (24c)——According to the same procedure as described above for the preparation of **24a**, the reaction of **11c** (2.01 g, 15 mmol) with **23** (6.28 g, 30 mmol) and EtONa (Na; 0.69 g, 30 mmol) in refluxing EtOH (300 ml) gave a crude product, which was recrystallized from CH_2Cl_2 to yield 1.19 g (33%) of **24c**, colorless needles. mp 203—205 °C. *Anal.* Calcd for $C_{14}H_{12}N_2O_2$: C, 69.99; H, 5.03; N, 11.66. Found: C, 70.09; H, 5.09; N, 11.74. IR (KBr): 3145 (oxazole $\nu_{C2\text{-}H}$) cm^{-1}. MS *m/z*: 240 (M^+).

Acknowledgment The authors are indebted to the Instrument Center, the Institute for Molecular Science, for assistance in obtaining the low temperature spectra.

References and Notes

1) D. Krois and H. Lehner, *J. Chem. Soc., Perkin Trans. 1*, **1982**, 477.
2) T. Otsubo, M. Kitasawa, and S. Misumi, *Bull. Chem. Soc. Jpn.*, **52**, 1515 (1979).
3) T. Shinmyozu, K. Kumada, T. Inazu, and T. Yoshino, *Chem. Lett.*, **1976**, 1405.
4) K. Kurosawa, M. Suenaga, T. Inazu, and T. Yoshino, *Tetrahedron Lett.*, **23**, 5335 (1982); H. Sasaki and T. Kitagawa, *Chem. Pharm. Bull.*, **31**, 2868 (1983).
5) M. F. Semmelhack, J. J. Harrison, D. C. Young, A. Gutierrez, S. Rafii, and J. Clardy, *J. Am. Chem. Soc.*, **107**, 7508 (1985).
6) H. Sasaki and T. Kitagawa, *Chem. Pharm. Bull.*, **31**, 756 (1983).
7) It has been reported that 5-phenyl and 4-methyl-5-phenyl substitution of oxazole caused a marked bathochromic shift and an increase in the intensity of the bands of the parent molecule. See: H. Bredereck, R. Gompper, and F. Reich, *Chem. Ber.*, **93**, 1389 (1960).
8) The cyclophane **12e**, for example, is termed dioxazolo[3^2]metacyclophane owing to the characteristic structure possessing two oxazole rings fused on the two methylene bridges in the [3^2]metacyclophane ring. Since the cyclophanes (**12f** and **12h**) have the same [3^2]metaparacyclophane ring, they are also termed for convenience dioxazolo[3^2]parametacyclophane (**12f**) and dioxazolo[3^2]metaparacyclophane (**12h**) in order to distinguish between them. According to the "Phane Nomenclature," **12e** is [1]metacyclo[1](4,5)oxazolo[0]metacyclo[0](5,4)oxazolophane. See: F. Vögtle and P. Neumann, *Tetrahedron*, **26**, 5847 (1970).
9) A. R. Katrizky and A. J. Boulton, "Advances in Heterocyclic Chemistry," Vol. 17, Academic Press, New York, 1974, p. 163.
10) A. M. van Leusen, R. J. Bouma, and O. Possel, *Tetrahedron Lett.*, **1975**, 3487.
11) W. Brügel, "Handbook of NMR Spectral Parameters," Vol. 1, Heyden and Son Ltd., London, 1979, p. 42.
12) Calculations were based on the following equations:

$$k_c = (\pi/\sqrt{2})[(\nu_A + \nu_B)^2 + 6J^2]^{1/2}$$

$$\Delta G^{\ddagger} = 2.303 \times 8.314 T_c (10.319 - \log k_c + \log T_c) .$$

See: P. M. Keehn and S. M. Rosenfeld (ed.), "Cyclophanes: Organic Chemistry, A Series of Monographs," Vol. 45-I, Academic Press, New York, 1983, p. 265.

[Chem. Pharm. Bull. 35(12)4757—4762(1987)]

Chemical and Chemotaxonomical Studies of Ferns. LXXIII.[1] New Flavonoids with Modified B-Ring from the Genus Pseudophegopteris (Thelypteridaceae)

HIROSHI WADA,[a] HIROYUKI FUJITA,[a] TAKAO MURAKAMI,*,[a] YASUHISA SAIKI[b] and CHIU-MING CHEN[c]

Faculty of Pharmaceutical Sciences, Science University of Tokyo,[a] Funakawara-machi, Shinjuku-ku, Tokyo 162, Japan, Department of Pharmaceutical Sciences, Kobe Gakuin University,[b] Arise Igawatani-machi, Nishi-ku, Kobe 673, Japan and Department of Chemistry, National Tsing Hua University,[c] Kuang Fu Road, Hsinchu, Taiwan, China

(Received May 25, 1987)

Chemical studies of three representatives of the genus Pseudophegopteris (Thelypteridaceae) revealed that the genus is characterized by the occurrence of unusual flavonoids with a modified B-ring related to protogenkwanin (VII). From *P. hirtirachis* HOLTT., three novel compounds, protogenkwanone (I), tetrahydroprotogenkwanone (II) and tetrahydroprotogenkwanin (III), were isolated, along with protogenkwanin 4′-*O*-*β*-D-glucoside (VI). From *P. subaurita* CHING, two new acylated glucosides of protogenkwanin, protogenkwanin 4′-*O*-(2-*O*-acetyl)-*β*-D-glucoside (IV) and 4′-*O*-(6-*O*-acetyl)-*β*-D-glucoside (V), were obtained, together with I, II and VI. From *P. bukoensis* HOLTT., IV, V and VI were isolated, in addition to apigenin 7-*O*-*α*-L-rhamnoside and kaempferol. The structures of the new compounds were determined by means of spectroscopic methods and chemical transformations.

Keywords——*Pseudophegopteris hirtirachis*; *Pseudophegopteris subaurita*; *Pseudophegopteris bukoensis*; Thelypteridaceae; protogenkwanin-type flavonoid; protogenkwanin; acylated glycoside; fern; chemotaxonomy; ^{13}C-NMR

As a continuation of our chemical and chemotaxonomical studies of ferns, we have investigated the constituents of three representatives of the genus Pseudophegopteris[2] (Thelypteridaceae). From *P. hirtirachis* HOLTT. (Japanese name: niitakawarabi) three novel flavonoids with a modified B-ring, protogenkwanone (I), tetrahydroprotogenkwanone (II) and tetrahydroprotogenkwanin (III), were isolated along with protogenkwanin 4′-*O*-*β*-D-glucoside (VI).[3] From *P. subaurita* CHING (Japanese name: mimigatashida), two new acylated glucosides of protogenkwanin (VII),[3] protogenkwanin 4′-*O*-(2-*O*-acetyl)-*β*-D-glucoside (IV) and 4′-*O*-(6-*O*-acetyl)-*β*-D-glucoside (V), were obtained, together with I, II and VI. From *P. bukoensis* HOLTT. (Japanese name: tachihimewarabi), IV, V and VI were isolated, in addition to apigenin 7-*O*-*α*-L-rhamnoside and kaempferol. In this paper, we describe the structural elucidation of these new compounds.

Compound I, $C_{16}H_{12}O_6$, pale yellow needles, mp 188—190 °C, showed ultraviolet (UV) spectra with shift reagents similar to those of VII (see Experimental). The proton nuclear magnetic resonance (^{1}H-NMR) spectrum of I showed signals assignable to a chelated hydroxyl proton at δ 12.6 (1H, s), *m*-coupled aromatic protons at δ 6.44 and 6.33 (each 1H, d, J=2.5 Hz), an olefinic proton at δ 6.53 (1H, s) and aromatic methoxyl protons at δ 3.81 (3H, s), indicating that compound I contains a 5-hydroxy-7-methoxychromone chromophore, as in the case of VII. Furthermore, a pair of doublets due to magnetically equivalent protons of *cis*-disubstituted olefins was observed at δ 6.97 and 6.32 (each 2H, d, J=10 Hz). The carbon-13 nuclear magnetic resonance (^{13}C-NMR) spectral data for the chromone moiety of I were in

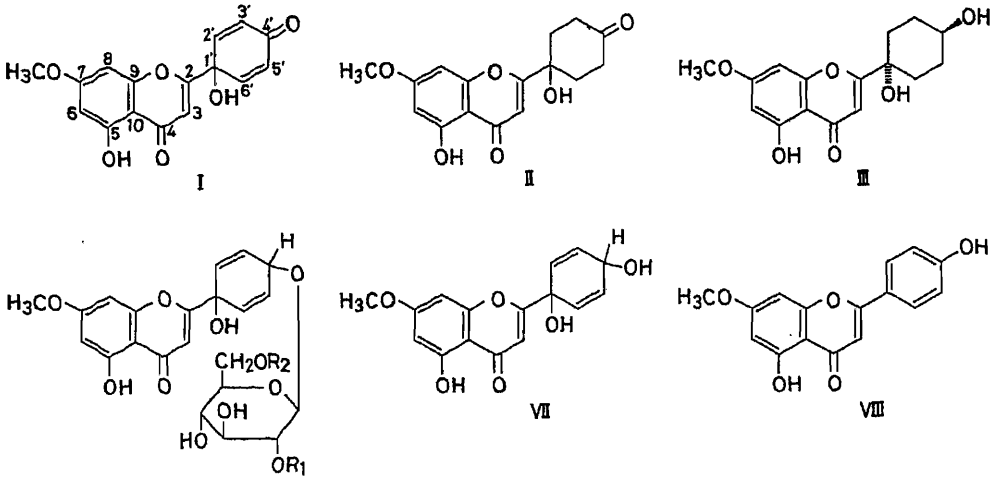

Fig. 1

TABLE I. ^{13}C Chemical Shifts (δ in C_5D_5N) of I—VI

C-Atom	I	II	III	IV	V	VI
2	168.3	175.4	177.3	171.8	171.9	171.9
3	107.7	105.8	105.5	106.8	106.8	106.8
4	182.9	183.3	183.5	183.3	183.2	183.2
5	162.6	162.6	162.6	162.4	162.5	162.5
6	98.9	98.8	98.6	99.3	99.0	98.9
7	166.2	166.1	165.9	166.1	165.9	166.0
8	93.0	92.8	92.6	92.5	92.7	92.8
9	158.3	158.4	158.5	158.8	158.5	158.6
10	106.1	105.8	105.9	106.1	106.0	106.0
1′	69.8	71.3	72.5	68.3	68.2	69.3
2′	148.1	37.0[a]	30.1[a]	132.6	132.0	131.8
3′	129.5	35.5[a]	29.0[a]	132.4	132.0	131.8
5′	129.5	35.5[b]	29.0[b]	130.4	131.3	131.5
6′	148.1	37.0[b]	30.1[b]	129.4	130.2	130.2
4′	185.0	209.3	64.5	69.3	69.6	68.3
7-OCH_3	56.0	56.1	55.9	56.2	56.0	56.0
Glc						
1				100.9	103.4	103.4
2				75.2	74.9	75.0
3				76.1	78.3	78.5[a]
4				71.7	71.4	71.8
5				78.9	75.2	78.2[a]
6				62.5	64.6	62.9
$\underline{C}OCH_3$				170.1	170.7	
$CO\underline{C}H_3$				21.1	20.7	

a, b) Assignments with the same superscripts for each compound may be interchanged.

good agreement with those of VI[4]) and the signals due to *cis*-disubstituted olefins appeared at δ 148.1 and 129.5 (each d). The further signals at δ 185.0 and 69.8 (s) were ascribed to a carbonyl carbon and a tertiary carbinyl carbon, respectively. Based on all these data, the remaining structure unit, $C_6H_5O_2$, was assigned as 1-hydroxy-4-oxo-2,5-cyclohexadiene.

Hence, compound I was assumed to be a 4′-dehydro derivative of VII. To confirm the structure, compound I was converted into genkwanin (apigenin 7-*O*-methyl ether) (VIII) by treatment with Zn powder in ethanolic H_2SO_4 solution. Thus, the structure of I was established to be 5-hydroxy-2-(1-hydroxy-4-oxo-2,5-cyclohexadienyl)-7-methoxychromone, and this compound was named protogenkwanone.

Compound II, $C_{16}H_{16}O_6$, colorless needles, mp 219—220 °C, contained the same chromone chromophore as that of I, as indicated by the UV, ^{1}H- and ^{13}C-NMR spectral data. Methylene proton signals were observed at δ 2.0—3.3 (8H) in the ^{1}H-NMR spectrum and the corresponding carbon signals at δ 37.0 (t) and 35.5 (t) in the ^{13}C-NMR spectrum (see Experimental and Table I). The ^{13}C-NMR spectrum further showed signals at δ 209.3 (s) and 71.3 (s) due to a carbonyl carbon and a tertiary carbinyl carbon, respectively. These data indicated that compound II was a tetrahydro derivative of I. On catalytic reduction of I using Pd–C, II was obtained. Thus, the structure of II was determined as 5-hydroxy-2-(1-hydroxy-4-oxocyclohexyl)-7-methoxychromone and the compound was named tetrahydroprotogenkwanone.

Compound III, $C_{16}H_{18}O_6$, colorless needles, mp 211—212 °C, has the same chromone chromophore as that of I. The ^{1}H-NMR spectrum is similar to that of II except for an additional signal of a secondary carbinyl proton at δ 4.38 (1H, broad s). Comparison of the ^{13}C-NMR spectral data of III with those of II revealed that the signal due to the 4′-ketone of II (δ 209.3) was replaced by a signal at δ 64.5 (d) due to a secondary carbinyl carbon (see Table I). These findings showed the presence of a 1,4-dihydroxycyclohexyl moiety in III. Accordingly, III was assumed to be a tetrahydro derivative of VII. The structure was confirmed by oxidative transformation of III with CrO_3–pyridine complex into II. The coupling patterns of the proton signals in the B-ring indicate that the B-ring adopts a chair conformation and the 4′-hydroxy group is axially oriented (see Table II). On comparing the ^{1}H-NMR spectrum of III in C_5D_5N with that in $CDCl_3$, a marked downfield shift (0.47 ppm) was observed for both axial protons at C-2′ and C-6′ which were *syn*-oriented with respect to the 4′-hydroxy group (pyridine-induced solvent effect[5]). A similar downfield shift (0.35 ppm) was also observed for the axial protons at C-3′ and C-5′. Consequently, the 1′-hydroxy

Table II. ^{1}H Chemical Shifts for the B-Ring Protons of Tetrahydroprotogenkwanin(III) in $CDCl_3$ and C_5D_5N (400 MHz)

Proton	Multiplicity (coupling constants in Hz)	δ_{CDCl_3}	$\delta_{C_5D_5N}$
2′,6′-$H_{ax.}$	ddd (13.3, 13.2, 3.9)	2.39	2.86
2′,6′-$H_{eq.}$	m (13.2, 3.9, *a*))	1.62	1.89
3′,5′-$H_{ax.}$	dddd (13.7, 13.2, 3.9, 2.9)	2.03	2.38
3′,5′-$H_{eq.}$	m (13.7, 3.9, *a*))	1.75	2.01
4′-H	brs	4.16	4.38

a) The other coupling constants could not be read.

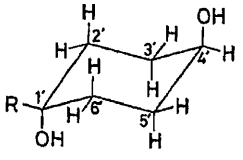

group should have an axial configuration. Thus, the structure of III was assigned as 2-(*trans*-1,4-dihydroxycyclohexyl)-5-hydroxy-7-methoxychromone and III was named tetrahydroprotogenkwanin.

Compound IV, $C_{24}H_{26}O_{12}$, was obtained as a colorless syrup, $[\alpha]_D^{18}$ $-51°$ ($c=2.2$, MeOH). The ^{1}H-NMR spectrum was similar to that of protogenkwanin 4′-*O*-*β*-D-glucoside (VI) except for an additional signal of an acetyl group at δ2.03 (3H, s). The ^{13}C-NMR spectrum exhibited the corresponding carbon signals at δ170.1 (s) and 21.1 (q). Alkaline hydrolysis of IV yielded VI. These findings showed that IV was an acetyl derivative of VI. In the ^{13}C-NMR spectrum of IV, the signals due to C-1 and C-3 of the glucose moiety were shifted upfield by 2.5 and 2.1 ppm, respectively, compared with those of VI. These acylation shifts indicated that the hydroxy group at C-2 of the glucose moiety was acetylated.[6] Therefore, the structure of IV was determined as protogenkwanin 4′-*O*-(2-*O*-acetyl)-*β*-D-glucoside.

Compound V, $C_{24}H_{26}O_{12}$, was isolated as a colorless syrup, $[\alpha]_D^{18}$ $-22°$ ($c=1.7$, MeOH). The ^{1}H- and ^{13}C-NMR spectra are quite similar to those of IV except for shifts of the sugar signals. Alkaline hydrolysis of V gave VI. The acetylation shifts in the ^{13}C-NMR spectrum showed that the acetyl group was located at C-6[6] in the glucose moiety. Thus, the structure of V was established to be protogenkwanin 4′-*O*-(6-*O*-acetyl)-*β*-D-glucoside.

The relative configuration of the hydroxy groups at C-1′ and C-4′ of compounds IV, V and VI remains undecided.[3]

Experimental

The ^{1}H-NMR spectra at 400 MHz were measured with a JNM-GX400 spectrometer using tetramethylsilane as an internal standard (s, singlet; d, doublet; m, multiplet; br s, broad singlet). The IR spectra were recorded on a Shimadzu 460 spectrometer. Sephadex LH-20 (Pharmacia) was used for column chromatography. The other instruments, materials and experimental conditions were the same as described in Part LXI[7] in this series.

Isolation Procedure——(1) *Pseudophegopteris hirtirachis* Holtt.: The air-dried fronds (380 g) of *P. hirtirachis*, collected in Renlun, Nantou, Taiwan, in December, were extracted three times with 3 l of MeOH under reflux for 6 h. The combined extracts (9 l) were passed through an activated charcoal column (40 g, 7 cm diameter) and the column was subsequently eluted with 10 l of MeOH. The combined eluates were concentrated to a syrup under reduced pressure. The syrup was adsorbed on silica gel (30 g) and applied to a silica gel column (90 g, 7 cm diameter). The column was eluted successively with $CHCl_3$ (1.2 l, frac. 1), 5% MeOH in $CHCl_3$ (800 ml, frac. 2), 10% MeOH in $CHCl_3$ (800 ml), 20% MeOH in $CHCl_3$ (800 ml, frac. 3) and 30% MeOH in $CHCl_3$ (800 ml, frac. 4). Rechromatography of frac. 1 on silica gel (eluent: $CHCl_3$–Et_2O mixtures) gave protogenkwanone (I, 60 mg) and tetrahydroprotogenkwanone (II, 60 mg). Evaporation of frac. 2 under reduced pressure followed by crystallization of the residue from a mixture of EtOH and *n*-hexane gave tetrahydroprotogenkwanin (III, 250 mg). Next, frac. 3 and frac. 4 were combined and evaporated to dryness under reduced pressure, and the residue was partitioned between the upper and lower layers of a mixture of $CHCl_3$ (28 ml), MeOH (28 ml) and H_2O (21 ml). The upper layer was concentrated to a syrup under reduced pressure and the residue was chromatographed on Sephadex LH-20 (eluent: 20% H_2O in MeOH) to yield protogenkwanin 4′-*O*-*β*-D-glucoside (VI, 55 mg).

(2) *Pseudophegopteris subaurita* Ching: The air-dried fronds (50 g) of *P. subaurita*, collected around Fenqihu (Chiayi) in Taiwan in December, were extracted three times with 1 l of MeOH under reflux for 6 h. The combined extracts (3 l) were passed through an activated charcoal column (50 g, 4 cm diameter) and the column was subsequently eluted with 3 l of MeOH. The combined eluates were concentrated to a syrup under reduced pressure. The syrup was adsorbed on silica gel (20 g) and applied to a silica gel column (90 g, 5 cm diameter). The column was eluted successively with $CHCl_3$ (300 ml, frac. 1), 5% MeOH in $CHCl_3$ (300 ml, frac. 2), 10% MeOH in $CHCl_3$ (300 ml, frac. 3) and 20% MeOH in $CHCl_3$ (300 ml, frac. 4). Rechromatography of frac. 1 and frac. 2 on silica gel (eluent: $CHCl_3$–Et_2O mixtures) afforded compounds I (200 mg) and II (40 mg), respectively. On the other hand, frac. 3 was rechromatographed on Sephadex LH-20 (eluent: 20% H_2O in MeOH) and further on silica gel (eluent: $CHCl_3$–MeOH mixtures) to yield protogenkwanin 4′-*O*-(2-*O*-acetyl)-*β*-D-glucoside (IV, 45 mg) and protogenkwanin 4′-*O*-(6-*O*-acetyl)-*β*-D-glucoside (V, 50 mg). Rechromatography of frac. 4 on Sephadex LH-20 (eluent: 20% H_2O in MeOH) gave compound VI (30 mg).

(3) *Pseudophegopteris bukoensis* Holtt.: The air-dried fronds (580 g) of *P. bukoensis*, collected on Sugadaira Heights (Nagano Prefecture) in Japan in September, were extracted three times with 3 l of MeOH under reflux for 6 h.

The combined extracts (9 l) were passed through an activated charcoal column (50 g, 7 cm diameter) and the column was subsequently eluted with 11 l of MeOH. The combined eluates were concentrated to a syrup under reduced pressure. The syrup was adsorbed on silica gel (100 g) and applied to a silica gel column (260 g, 7 cm diameter). The column was eluted successively with $CHCl_3$ (900 ml), 5% MeOH in $CHCl_3$ (900 ml), 10% MeOH in $CHCl_3$ (900 ml, frac. 1), 20% MeOH in $CHCl_3$ (900 ml, frac. 2) and 30% MeOH in $CHCl_3$ (900 ml, frac. 3). Rechromatography of frac. 1 on silica gel (eluent: $CHCl_3$–Et_2O and Et_2O–MeOH mixtures) gave kaempferol (35 mg) and a mixture of compounds IV and V. The mixture was rechromatographed on Sephadex LH-20 (eluent: 30% H_2O in MeOH) and further on silica gel (eluent: $CHCl_3$–MeOH mixtures) to afford compounds IV (45 mg) and V (35 mg). Next, frac. 2 was rechromatographed on silica gel (eluent: $CHCl_3$–MeOH mixtures) and further on Sephadex LH-20 (eluent: 20% H_2O in MeOH) to give compound VI (160 mg). From frac. 3, apigenin 7-*O*-α-L-rhamnoside (75 mg) was obtained.

Compound I [Protogenkwanone]——Pale yellow needles from EtOH, mp 188—190 °C. UV λ_{max}^{MeOH} nm (log ε): 232 (4.51), 249 sh (4.43), 258 sh (4.38), 299 (3.98), 325 sh (3.78), $\lambda_{max}^{MeOH+NaOAc}$ nm: 250 sh, 258 sh, 297 sh, $\lambda_{max}^{MeOH+AlCl_3+HCl}$ nm: 258, 269 sh, 314, 380. IR ν_{max}^{KBr} cm^{-1}: 3490, 3210, 1665, 1620, 1500, 1450, 1155. MS *m/z*: 300.0664 (M^+, Calcd for $C_{16}H_{12}O_6$: 300.0633), 284, 243, 192, 167, 135, 109. ^{1}H-NMR (100 MHz, in DMSO-d_6) δ: 12.6 (1H, s, 5-OH), 7.14 (1H, s, 1′-OH), 6.97 (2H, d, *J*=10 Hz, 2′,6′-H_2), 6.53 (1H, s, 3-H), 6.44 (1H, d, *J*=2.5 Hz, 8-H), 6.33 (1H, d, *J*=2.5 Hz, 6-H), 6.32 (2H, d, *J*=10 Hz, 3′,5′-H_2), 3.81 (3H, s, 7-OCH_3). ^{13}C-NMR (in DMSO-d_6) δ: 184.6 (s), 181.8 (s), 167.8 (s), 165.5 (s), 161.1 (s), 157.4 (s), 147.3 (d) × 2, 128.8 (d) × 2, 106.8 (d), 104.9 (s), 98.4 (d), 92.4 (d), 68.9 (s), 56.1 (q); δ in C_5D_5N: see Table I.

Compound II [Tetrahydroprotogenkwanone]——Colorless needles from EtOH, mp 219—220 °C. UV λ_{max}^{MeOH} nm (log ε): 232 (4.29), 251 (4.34), 257 (4.33), 295 (3.97), 317 sh (3.79), $\lambda_{max}^{MeOH+NaOAc}$ nm: 251 sh, 257, 292, 317 sh, $\lambda_{max}^{MeOH+AlCl_3+HCl}$ nm: 258, 264 sh, 310, 373. IR ν_{max}^{KBr} cm^{-1}: 3320, 1710, 1660, 1620, 1500, 1445, 1160. MS *m/z*: 304.0942 (M^+, Calcd for $C_{16}H_{16}O_6$: 304.0945), 234, 219, 191, 167, 135. ^{1}H-NMR (100 MHz, in C_5D_5N) δ: 6.95 (1H, s, 3-H), 6.61 (1H, d, *J*=2.5 Hz, 8-H), 6.54 (1H, d, *J*=2.5 Hz, 6-H), 3.80 (3H, s, 7-OCH_3), 2.8—3.3 (2H, m), 2.0—2.6 (6H, m). ^{13}C-NMR: see Table I.

Compound III [Tetrahydroprotogenkwanin]——Colorless needles from a mixture of EtOH and *n*-hexane, mp 211—212 °C. UV λ_{max}^{MeOH} nm (log ε): 232 (4.22), 250 (4.28), 257 (4.25), 293 (3.87), 317 sh (3.67), $\lambda_{max}^{MeOH+NaOAc}$ nm: 250, 257, 292, 317 sh, $\lambda_{max}^{MeOH+AlCl_3+HCl}$ nm: 257, 309, 370. IR ν_{max}^{KBr} cm^{-1}: 3400, 1660, 1620, 1510, 1440, 1160. MS *m/z*: 306.1110 (M^+, Calcd for $C_{16}H_{18}O_6$: 306.1102), 248, 219, 193, 167, 135. ^{1}H-NMR (400 MHz, in C_5D_5N) δ: 7.01 (1H, s, 3-H), 6.55 (1H, d, *J*=2.5 Hz, 8-H), 6.46 (1H, d, *J*=2.5 Hz, 6-H), 4.38 (1H, br s, $W_{1/2}$=9 Hz, 4′-H), 2.86 (2H, ddd, *J*=13.3, 13.2, 3.9 Hz, 2′,6′-axial-H_2), 2.38 (2H, dddd, *J*=13.7, 13.2, 3.9, 2.9 Hz, 3′,5′-axial-H_2), 2.01 (2H, m, *J*=13.7, 3.9 Hz,*) 3′,5′-equatorial-H_2), 1.89 (2H, m, *J*=13.2, 3.9 Hz,*) 2′,6′-equatorial-H_2); δ in $CDCl_3$: 6.42 (1H, d, *J*=2.5 Hz, 8-H), 6.41 (1H, s, 3-H), 6.35 (1H, d, *J*=2.5 Hz, 6-H), 4.16 (1H, br s, $W_{1/2}$=9 Hz, 4′-H), 2.39 (2H, ddd, *J*=13.3, 13.2, 3.9 Hz, 2′,6′-axial-H_2), 2.03 (2H, dddd, *J*=13.7, 13.2, 3.9, 2.9 Hz, 3′,5′-axial-H_2), 1.75 (2H, m, *J*=13.7, 3.9 Hz,*) 3′,5′-equatorial-H_2), 1.62 (2H, m, *J*=13.2, 3.9 Hz,*) 2′,6′-equatorial-H_2). *: The coupling constants could not be read. ^{13}C-NMR: see Table I.

Compound IV [Protogenkwanin 4′-*O*-(2-*O*-acetyl)-β-D-glucoside]——Colorless syrup, $[\alpha]_D^{18}$ −51° (*c*=2.2, MeOH). UV λ_{max}^{MeOH} nm (log ε): 233 (3.88), 252 (3.90), 259 sh (3.87), 296 (3.52), 319 (3.35), $\lambda_{max}^{MeOH+NaOAc}$ nm: 258 sh, 296, 319 sh, $\lambda_{max}^{MeOH+AlCl_3+HCl}$ nm: 231 sh, 251.5 sh, 257.5, 263 sh, 311, 364. IR ν_{max}^{KBr} cm^{-1}: 3380, 1740, 1660, 1620, 1505, 1435, 1160. ^{1}H-NMR (100 MHz, in CD_3OD) δ: 6.49 (1H, d, *J*=2 Hz, 8-H), 6.36 (1H, s, 3-H), 6.27 (2H, dd, *J*=10.5, 4 Hz, 3′,5′-H_2), 6.24 (1H, d, *J*=2 Hz, 6-H), 5.93 (2H, dd, *J*=10.5, 1.5 Hz, 2′,6′-H_2), 4.69 (1H, m, 4′-H), 4.68 (1H, d, *J*=8 Hz, anomeric-H), 3.3—4.2 (6H, m, sugar-H), 3.87 (3H, s, $-OCH_3$), 2.06 (3H, s, $-COCH_3$). ^{13}C-NMR: see Table I. *Anal.* Calcd for $C_{24}H_{26}O_{12}$: C, 56.91; H, 5.17. Found: C, 56.83; H, 5.29.

Compound V [Protogenkwanin 4′-*O*-(6-*O*-acetyl)-β-D-glucoside]——Colorless syrup, $[\alpha]_D^{18}$ −22° (*c*=1.7, MeOH). UV λ_{max}^{MeOH} nm (log ε): 233 (3.93), 252 (3.96), 258 sh (3.93), 296 (3.56), 318 sh (3.40), $\lambda_{max}^{MeOH+NaOAc}$ nm: 258 sh, 292, 317 sh, $\lambda_{max}^{MeOH+AlCl_3+HCl}$ nm: 231 sh, 252 sh, 258, 263 sh, 312, 364. IR ν_{max}^{KBr} cm^{-1}: 3400, 1720, 1660, 1620, 1505, 1435, 1160. ^{1}H-NMR (100 MHz, in CD_3OD) δ: 6.46 (1H, d, *J*=2 Hz, 8-H), 6.36 (1H, s, 3-H), 6.29 (2H, dd, *J*=10.5, 4 Hz, 3′,5′-H_2), 6.25 (1H, d, *J*=2 Hz, 6-H), 5.99 (2H, dd, *J*=10.5, 1.5 Hz, 2′,6′-H_2), 4.57 (1H, br s, 4′-H), 4.49 (1H, d, *J*=7 Hz, anomeric-H), 3.85 (3H, s, $-OCH_3$), 3.2—4.4 (6H, m, sugar-H), 2.10 (3H, s, $-COCH_3$). ^{13}C-NMR: see Table I. *Anal.* Calcd for $C_{24}H_{26}O_{12}$: C, 56.91; H, 5.17. Found: C, 56.82; H, 5.33.

Protogenkwanin 4′-*O*-β-D-Glucoside (VI)——Colorless needles from MeOH, mp 129—131 °C, $[\alpha]_D^{18}$ −40° (*c*=1.0, C_5H_5N). UV λ_{max}^{MeOH} nm (log ε): 233 (4.25), 252 (4.29), 258 sh (4.25), 296 (3.89), 330 (3.58), $\lambda_{max}^{MeOH+NaOAc}$ nm: 251 sh, 259 sh, 294, 332 sh, $\lambda_{max}^{MeOH+AlCl_3+HCl}$ nm: 237 sh, 251 sh, 258, 264 sh, 273 sh, 310, 374. IR ν_{max}^{KBr} cm^{-1}: 3420, 1670, 1620, 1580, 1505, 1435, 1160. ^{1}H-NMR (100 MHz, in DMSO-d_6) δ: 6.46 (1H, d, *J*=2.5 Hz, 8-H), 6.37 (1H, s, 3-H), 6.31 (1H, d, *J*=2.5 Hz, 6-H), 6.25 (2H, dd, *J*=10.5, 4 Hz, 3′,5′-H_2), 5.92 (2H, d, *J*=10.5 Hz, 2′,6′-H_2), 4.39 (1H, d, *J*=7 Hz, anomeric-H), 3.0—4.0 (6H, m, sugar-H), 3.83 (3H, s, $-OCH_3$). ^{13}C-NMR: see Table I. The physical and spectral data were in good agreement with those reported.[3,4]

Apigenin 7-*O*-α-L-Rhamnoside——Pale yellow needles from MeOH, mp 198—200 °C, $[\alpha]_D^{18}$ −94° (*c*=1.0, C_5H_5N). UV λ_{max}^{MeOH} nm (log ε): 269.5 (4.28), 336 (4.33). IR ν_{max}^{KBr} cm^{-1}: 3410, 1660, 1606, 1247, 1170, 1135, 1070. ^{1}H-NMR (60 MHz, in CD_3OD) δ: 7.76 (2H, d, *J*=8 Hz), 6.85 (2H, d, *J*=8 Hz), 6.67 (1H, d, *J*=2 Hz), 6.55 (1H, s), 6.38 (1H, d, *J*=2 Hz), 5.38 (1H, d, *J*=2 Hz), 3.2—4.0 (4H, m), 1.31 (3H, d, *J*=7 Hz). This compound was identified by

direct comparison (IR and mixed fusion) with an authentic sample.

Kaempferol——Yellow needles from MeOH, mp 285—286 °C. UV λ_{max}^{MeOH} nm (log ε): 224 sh (4.28), 268 (4.22), 294 sh (3.93), 322 sh (4.02), 369 (4.28). IR ν_{max}^{KBr} cm^{-1}: 3420, 1660, 1610, 1510, 1380, 1305, 1180. ^{1}H-NMR (60 MHz, in C_5D_5N) δ: 8.48 (2H, d, J=8 Hz), 7.26 (2H, d, J=8 Hz), 6.80 (1H, d, J=2.5 Hz), 6.70 (1H, d, J=2.5 Hz). This compound was identified by direct comparison (IR and mixed fusion) with an authentic sample.

Conversion of I into Genkwanin (VIII)——Compound I (15 mg) was dissolved in 3 ml of 5% H_2SO_4 in EtOH and then 10 mg of Zn powder was added. The mixture was stirred at 70 °C for a few minutes on a water bath, then allowed to cool. The precipitate was filtered off, washed with water, and taken up in an excess of MeOH, then the Zn powder was removed by filtration. The filtrate was concentrated, followed by recrystallization of the residue from MeOH to yield VIII (6 mg).

VIII [Genkwanin]——Pale yellow needles, mp 287—289 °C. UV λ_{max}^{MeOH} nm (log ε): 270 (4.31), 335 (4.39), $\lambda_{max}^{MeOH+NaOAc}$ nm: 270, 297 sh, 392. MS m/z: 284.0677 (M^+, Calcd for $C_{16}H_{12}O_5$: 284.0683), 255, 241, 167, 166, 138. The physical data were in good agreement with those reported.[3,8]

Catalytic Reduction of I——Compound I (20 mg) dissolved in 16 ml of EtOH was hydrogenated with Pd–C (20 mg) for 2 h at room temperature. The catalyst was filtered off, and the filtrate was evaporated to dryness followed by crystallization from EtOH to afford tetrahydroprotogenkwanone (II, 12 mg). It was identified by direct comparison (TLC, ^{1}H-NMR, IR and mixed fusion) with the natural product (II).

Pyridine–CrO_3 Complex Oxidation of III——Compound III (20 mg) dissolved in 1 ml of pyridine was added to a solution of CrO_3 (100 mg) in 1 ml of pyridine. The mixture was allowed to stand at room temperature for 16 h and then poured into ice-water. The product was extracted with EtOAc. The EtOAc layer was washed with water, dried over anhydrous $MgSO_4$ and evaporated to dryness. The residue was crystallized from EtOH to yield tetrahydroprotogenkwanone (II, 10 mg). It was identified by direct comparison (TLC, ^{1}H-NMR, IR and mixed fusion) with the natural product (II).

Alkaline Hydrolysis of IV——Compound IV (16 mg) was hydrolyzed with 4 ml of 1% KOH in EtOH at room temperature for 5 min. The reaction mixture was acidified with 3% HCl followed by removal of EtOH under reduced pressure to afford protogenkwanin 4′-*O*-*β*-D-glucoside (VI, 6 mg). It was identified by direct comparison (TLC, IR and mixed fusion) with an authentic sample.

Alkaline Hydrolysis of V——Compound V (24 mg) was hydrolyzed in the same way as described for compound IV to yield protogenkwanin 4′-*O*-*β*-D-glucoside (VI, 10 mg). It was identified by direct comparison (TLC, IR and mixed fusion) with an authentic sample.

References and Notes

1) Part LXXII: K. Hori, T. Satake, H. Yamaguchi, Y. Saiki, T. Murakami and C.-M. Chen, *Yakugaku Zasshi*, **107**, 774 (1987).
2) R.-C. Ching, *Acta Phytotaxonomica Sinica*, **8**, 289 (1963); *idem*, *ibid.*, **16**, 1 (1978).
3) M. Hauteville, J. Chopin, H. Geiger and L. Schuler, *Tetrahedron*, **37**, 377 (1981); *idem*, *Tetrahedron Lett.*, **1980**, 1227.
4) J. B. Harborne and T. J. Mabry (eds.), "The Flavonoids: Advances in Research," Chapman and Hall, London, New York, 1982, p. 128.
5) P. V. Demarco, E. Farcas, D. Doddrell, B. L. Mylari and E. Wenkert, *J. Am. Chem. Soc.*, **90**, 5480 (1968).
6) K. Yoshimoto, Y. Itatani and Y. Tsuda, *Chem. Pharm. Bull.*, **28**, 2065 (1980).
7) N. Tanaka, T. Murakami, H. Wada, A. B. Gutierrez, Y. Saiki and C.-M. Chen, *Chem. Pharm. Bull.*, **33**, 5231 (1985).
8) M. Nakao and K.-F. Tseng, *J. Pharm. Soc. Jpn.*, **52**, 148 (1932).

[Chem. Pharm. Bull. 35(12)4763—4768(1987)]

Stereospecific 1,2-Hydride Shift in the Rearrangement of 16β-Hydroxy-17-oxo Steroids to 17β-Hydroxy-16-ones with Acid and Base[1)]

MITSUTERU NUMAZAWA,* MASAO NAGAOKA, and AYAKO MUTSUMI

Tohoku College of Pharmacy, 4-1 Komatsushima-4-chome, Sendai 983, Japan

(Received May 25, 1987)

When 16β-hydroxy-5α-androstan-17-one (**2a**) and its 16α-deuterio derivative (**2a**-*16-d*) were separately treated with H_2SO_4 or NaOH, compound **2a** was rearranged to the 17β-hydroxy-16-oxo isomer (**3a**) with a marked kinetic deuterium isotope effect at the 16-position ($k_H/k_D=4.5$ or 3.0). The product **3a** obtained from compound **2a**-*16-d* retained deuterium at C-17 to the extent of 16—65% while no significant loss of the isotope from the substrate was observed during the reaction. Isotope-labeling experiments showed that the intramolecular 1,2-hydride shift is principally involved in the ketol rearrangement, and that the 16-oxo function of compound **3a** enolizes preferentially toward the C-17 position rather than the C-15 position under the above conditions.

Keywords——3,16β-dihydroxy-5α-androstan-17-one; [16α-^{2}H]3β,16β-dihydroxy-5α-androstan-17-one; 3β,17β-dihydroxy-5α-androstan-16-one; ketol rearrangement; isotope effect; 1,2-hydride shift; enolization

Previous studies on the relative stability[2)] of the four isomeric 16,17-ketols of steroids of the 14α-series have demonstrated that the most unstable ketols, 16β-hydroxy-17-ones, readily isomerize to the most stable ones, 17β-hydroxy-16-ones, in basic or acidic medium. Two mechanisms are feasible for the rearrangement. One is the conventional enolization mechanism[2b,c)] where the 17-oxo function of the 16β-alcohol can give the ene-diol intermediate, and ketonization may then give either the original or rearranged ketol (mechanism A, Fig. 1). In this mechanism, the equilibrium will be strongly displaced toward the 16-ketones, which are more thermodynamically stable.[2c)] The alternative mechanism, proposed for the acid-catalyzed rearrangement by Johnson *et al.*,[3)] proceeds through a sequence involving a reversible stereospecific 1,2-hydride shift in the protonated form (mechanism B). Loss of a proton from the intermediate finally affords the 16-ketones, which predominate at equilibrium. However, to date, there is no direct evidence for this mechanism. Thus, to reach an unambiguous decision as to whether or not the alternative sequence is operative in the

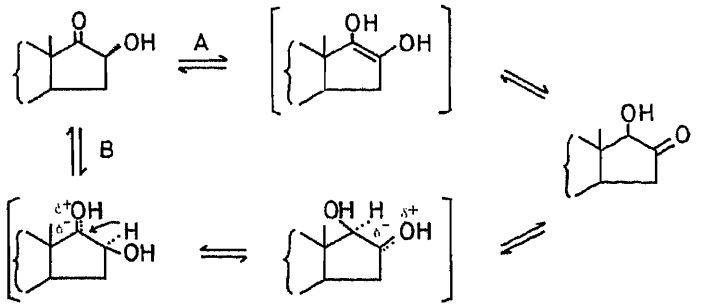

Fig. 1. Mechanisms Proposed for Rearrangement of 16β-Hydroxy-17-oxo Steroids under Basic and Acidic Conditions

rearrangement, we synthesized 16α-deuterio-16β-hydroxy-17-one **2a**-*16-d* and explored its conversion into the 17β-hydroxy-16-oxo derivative **3a** with H_2SO_4 and NaOH. The isotope-labeling experiments definitely demonstrated that stereospecific 1,2-hydride shift of the 16α-proton is actually involved in both acid- and base-catalyzed rearrangements.

Results and Discussion

Treatment of 3β-hydroxy-5α-androstan-17-one (**1**) with NaOD in D_2O–MeOD[4] gave its 16,16-dideuterated form, which was subsequently converted into [16α-^{2}H]3β,16β-dihydroxy-5α-androstan-17-one (**2a**-*16-d*)[3] *via* the 16β-acetoxy-17-oxo derivative **2b**-*16-d* essentially according to the methods reported previously.[5]

Dynamic aspects of rearrangement of the 16β-hydroxy-17-one **2a** to the 17β-hydroxy-16-oxo derivative **3a** with H_2SO_4 and NaOH were initially explored, especially in view of the deuterium isotope effect at the 16-position on the conversion of the deuterium-labeled substrate **2a**-*16-d*. The proton nuclear magnetic resonance (^{1}H-NMR) spectra of the ketols **2a** and **3a** proved to be useful for the quantitative analysis of the reaction mixtures without isolation. The signals at δ 0.93 (s, 3H) and 3.93 (m, 1H) due to the 16β-alcohol **2a**, and 0.73 (s, 3H) and 3.73 (s, 1H) due to the 17β-alcohol **3a** are those of the proton at the C-18 angular methyl and the proton at C-16 or C-17, respectively. When the 16β-alcohol **2a** and its 16-deuterio derivative **2a**-*16-d* were separately treated with 3 M H_2SO_4 in 75% MeOH at room temperature, the substrates slowly rearranged to the 17β-alcohol **3a**. As shown in Fig. 2, the rearrangement occurs with a marked kinetic deuterium isotope effect at the 16-position. The reaction time needed for the 50% conversion was about 2.5 d for compound **2a** and about 14 d

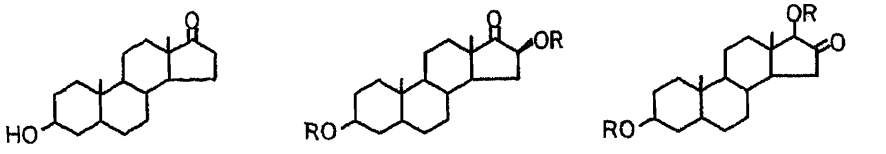

1

2a: R=H
2b: R=COCH$_3$

3a: R=H
3b: R=COCH$_3$

Chart 1

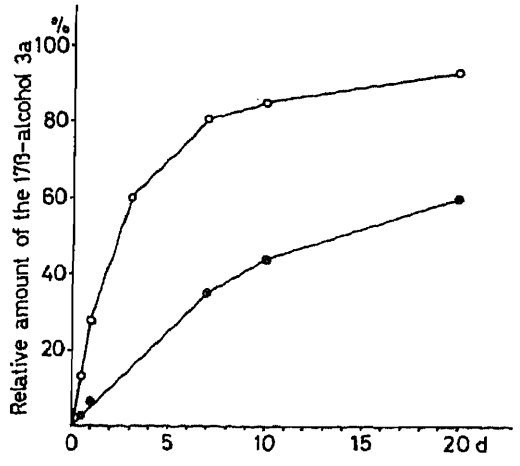

Fig. 2. Conversion of the 16β-Hydroxy-17-one **2a** (○) and Its 16α-Deuterio Derivative **2a**-*16-d* (●) to the 17β-Hydroxy-16-one **3a** with 3 M H_2SO_4

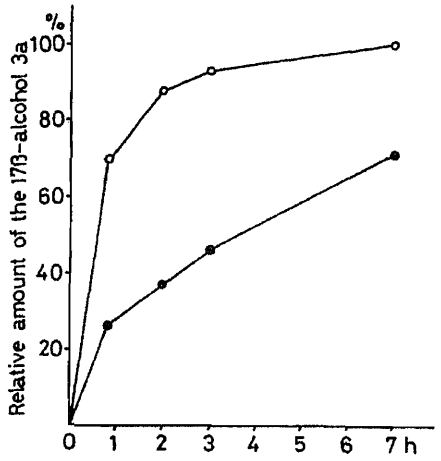

Fig. 3. Conversion of the 16β-Hydroxy-17-one **2a** (○) and Its 16α-Deuterio Derivative **2a**-*16-d* (●) to the 17β-Hydroxy-16-one **3a** with NaOH

for its deuterio derivative **2a**-*16-d*. The apparent isotope effect[6] observed in experiments using a one-day reaction time was about 4.5.

Conversion of the 16β-alcohol **2a** to the isomeric 17β-alcohol **3a** was smoothly catalyzed by 0.025 M NaOH in 75% MeOH, and 7-h reaction time was enough for almost complete rearrangement. The deuterium isotope effect at the 16-position in the conversion was about 3.0 (at 1 h) (Fig. 3). The k_H/k_D value was slightly different from that in the case of acid treatment (3.0 *vs.* 4.5). The results demonstrated that the breaking of the C–H bond at the C-16 position is involved in the rate expression[3a] of the rearrangement with both acid and base.

The deuterium contents of the recovered and rearranged ketols **2a** and **3a** obtained by treatment of the deuterated substrate **2a**-*16-d* with H_2SO_4 and NaOH were analyzed by mass (MS) and ^{1}H-NMR spectroscopies (Table I). We reasoned that the primary product **3a** produced through the 1,2-hydride shift process would retain deuterium at C-17 to the same extent as the starting material, and that the product **3a** formed through the conventional enolization mechanism would not be labeled with deuterium at C-17. These spectra showed 16—65% deuterium-labeling at the 17α-position of the ketol **3a**, while the isotope was completely retained in the recovered substrate **2a**. The isotope content of compound **3a** produced in experiments using a prolonged reaction time or drastic conditions was lower as compared to that with a short time or mild conditions. Furthermore, when the 17α-deuterio derivative of compound **3a** (57 atom%), obtained by the reaction of the 16β-alcohol **2a**-*16-d* with 0.025 M NaOH (Table I), was treated with NaOH or H_2SO_4 under the conditions employed in the rearrangement experiment, about 30 or 20% of the deuterium was lost from the labeled substrate **3a**-*17-d* (Table II). On the other hand, treatment of the 17β-alcohol **3a** with the deuterated acid or base efficiently introduced the isotope at C-17 of the 17β-alcohol **3a** (83 or more than 98 atom%), as shown in Table II.

From the results obtained above, it is concluded that the intramolecular 1,2-hydride shift mechanism is principally operative in the rearrangement of 16β-hydroxy-17-ones to 17β-hydroxy-16-ones with base and acid, and that the enolization process accounts for only a minor fraction even if it is operative (Fig. 4). It is well known that with acid only 16β-hydroxy-

TABLE I. Analysis of Deuterium Content of the Ketols **2a** and **3a** Obtained by Treatment of the Deuterated Ketol **2**-*16-d* with NaOH and H_2SO_4

Conditions Base or acid[c]	Time	Relative amounts of products[a] (%)		^{2}H-Content[b] (atom%)	
		2a	**3a**	**2a**	**3a**
Substrate: **2a**-*16-d* (90 atom%)					
3 M H_2SO_4	10 d	58	42	91	63
3 M H_2SO_4	20 d	40	60	90	36
0.025 M NaOH	1 h	74	26	89	65
0.025 M NaOH	7 h	30	70	—	57
1 M NaOH	1 h	0	100	—	46
1 M NaOH	3 h	0	100	—	16
Substrate: **2b**-*16-d* (90 atom%)[d]					
3 M H_2SO_4	25 d	37	63	—	31
1 M NaOH	1 h	0	100	—	50

a) The relative amounts of products were determined by measuring the peak height of the C-18 angular methyl resonance in the ^{1}H-NMR spectrum of the reaction mixtures without isolation. *b*) The deuterium content was determined by MS analysis (*m/z* 306 and 307, M^+) and the location of the isotope was found by ^{1}H-NMR analysis. *c*) For this treatment, 3 M H_2SO_4 (6 ml) was added to a solution of the substrate (0.35 mmol) in 14 ml of MeOH, or 0.025 or 1 M NaOH (4 ml) was added to that in 40 ml of 60% aqueous MeOH. *d*) The relative amounts of products and ^{2}H-contents were determined after derivatization of the products to the acetates **2b** and **3b**. MS: M^+ *m/z* 390 and 391.

TABLE II. Enolization of the Ketol **3a** with NaOD and D_2SO_4

Substrate	Conditions Base or acid[a)]	Time	^{2}H-Content at C-17 of **3a** atom% (^{2}H-distribution)
3a	3 M D_2SO_4[b)]	15 d	83[c)] (13% d_0, 46% d_1, 41% d_2)
3a	1 M NaOD[b)]	1 h	98[c)] (5% d_2, 95% d_3)
3a-*17-d*	3 M H_2SO_4[d)]	7 d	46[e)] (54% d_0, 46% d_1)
3a-*17-d*	1 M NaOD[d)]	1 h	40[e)] (60% d_0, 40% d_1)

a) For this treatment, 3 M D_2SO_4 or 1 M NaOD was added to the reaction mixture using deuterated solvents as described in Table I. *b*) The ketol **3a** was treated with the deuterated acid or base under the rearrangement conditions using D_2O and MeOD as solvents. *c*) ^{2}H-Content was determined by ^{1}H-NMR analysis. *d*) The ketol **3a**-*16-d* (57 atom%) was exposed to the rearrangement conditions. *e*) ^{2}H-Content was determined by MS analysis.

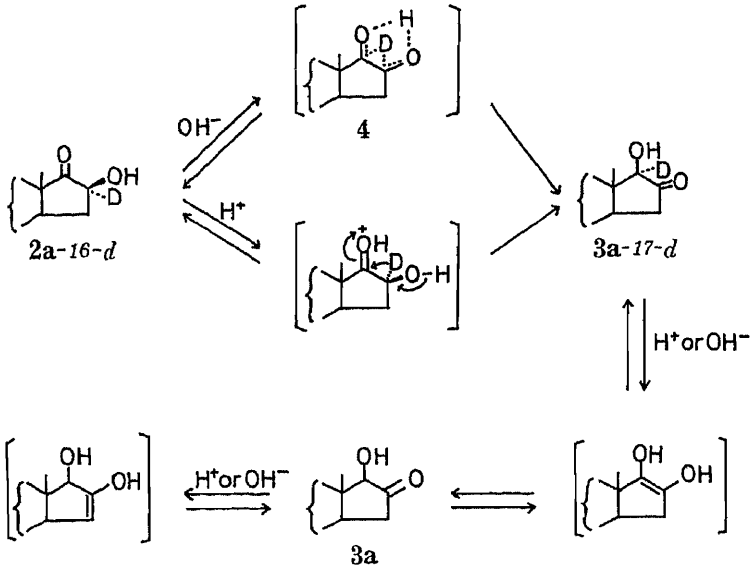

Fig. 4

17-ones are isomerized to 17β-hydroxy-16-ones, while the 16α-isomers are unchanged.[2c,3a)] To account for such a difference in the isomerization, the hydride shift mechanism was proposed for acid-catalyzed rearrangement.[3a)] The present results showed that the mechanism is operative in both acid- and base-catalyzed reactions. The reaction with an acid may principally proceed through a protonated form, as shown in Fig. 1, whereas with a base, it may proceed through transition state represented diagrammatically by **4** in Fig. 4 rather than the protonated form.

To our knowledge, no detailed study of enolization of the 16-oxo function of 17β-hydroxy-16-ones has previously been reported. Treatment of the 16-oxo derivative **3a** with the D_2O/NaOD/MeOD or D_2O/D_2SO_4/MeOD system led to the introduction of deuterium at C-17 at a rate greater than that at C-15 in each experiment (Table II), in accordance with the previous results[7)] on 17-unsubstituted 16-oxo steroids. Johnson *et al.*[3a)] assumed the 1,2-hydride shift process to be reversible. We could detect only enolization of the 16-oxo function of the ketol **3a**; hence there may be no apparent reversible reaction under the conditions employed.

When a deuterated 16β-acetoxy-17-one **2b**-*16-d* was treated with H_2SO_4 and NaOH as above, the rearranged product **3a** retained deuterium at C-17 to almost the same extent as the

16β-alcohol **2a** (Table I). It has been reported that α-acetoxyketone may rearrange during chromatography on alumina to give more stable isomers[3b,8] through an *ortho*-ester of the ene-diol. The present results show that this process involves first hydrolysis of the acetoxy group leading to the 16β-alcohol **2a**, followed by ketol rearrangement principally through the 1,2-hydride shift process as described above.

Recently we[9] proposed a new hydration–dehydration mechanism for the rearrangement of 16α-hydroxy-17-ones to 17β-hydroxy-16-ones with base. The case for the enolization mechanism, if not invalidated, is also weakened in that reaction. The present results along with the our previous findings[9] suggest that rearrangement of steroidal D-ring ketols has interesting theoretical implications. Further studies on the ketol rearrangement are in progress in this laboratory.

Experimental

Melting points were measured on a Yanagimoto melting point apparatus. ^{1}H-NMR spectra were obtained on a JEOL PMX 60 spectrometer with tetramethylsilane as an internal standard. Mass spectra were measured on a Hitachi RMU-7 spectrometer.

[16,16-$^2H_2$]3β-Hydroxy-5α-androstan-17-one (1-*16,16-d*$_2$)——A mixture of **1** (1.0 g, 3.45 mmol) was heated under reflux for 4 h with 20 ml of CH_3OD, 1.0 g (43.5 mmol) of Na metal and 3 ml of D_2O essentially according to the method reported by Tokes *et al.*[4] After this time, the reaction mixture was poured into 100 ml of chilled 6 M HCl solution. The precipitate was collected by filtration, washed with water and recrystallized from acetone to give the desired material **1**-*16,16-d*$_2$ (96%) as colorless needles, mp 173—174 °C (lit.[10] 172—174 °C, reported for non-labeled **1**), which consisted of the following mixture as determined by MS using the M^+ ion peak: 3% d_0, 6% d_1, 91% d_2.

[16α-^{2}H]3β,16β-Diacetoxy-5α-androstan-17-one (2b-*16-d*)——The deuterated compound **1**-*16,16-d*$_2$ (900 mg, 3.10 mmol) was converted to **2b**-*16-d* (36%) according to the previously reported method,[3a] mp 154—156 °C (lit.[3a] 153—155.5 °C, reported for non-labeled **2b**). 10% d_0 and 90% d_1 by MS. ^{1}H-NMR ($CDCl_3$) δ: 0.97 (3H, s, 19-Me), 0.93 (3H, s, 18-Me), 2.00 (3H, s, 3β-OAc), 2.10 (3H, s, 16β-OAc), 4.67 (1H, br m, 3α-H).

[16β-^{2}H]3β,16β-Dihydroxy-5α-androstan-17-one (2a-*16-d*)——The diacetate **2b**-*16-d* (600 mg, 1.61 mmol) was hydrolyzed with H_2SO_4 to yield **2a**-*16-d* (45%) according to the method previously reported by Kincl,[5] mp 181—183 °C (acetone) (lit.[4] 195—200 °C ($CHCl_3$–ether), reported for non-labeled **2a**). 10% d_0 and 90% d_1 by MS. ^{1}H-NMR ($CDCl_3$) δ: 0.87 (3H, s, 19-Me), 0.93 (3H, s, 18-Me), 3.50 (1H, br m, 3α-H).

Rearrangement Experiments——(A) Acid Catalysis: Compound **2a** or **2**-*16-d* (0.35 mmol) was dissolved in 14 ml of MeOH, then 6 ml of 3 M H_2SO_4 was added. The solution was allowed to stand at room temperature for an appropriate time and then neutralized with 5% $NaHCO_3$ solution. After removal of most of MeOH under reduced pressure at below 30 °C, the product was extracted with AcOEt (100 ml × 3). The organic layer was washed with water and dried (Na_2SO_4). After evaporation of the solvent, the residue (75—90 mg) was submitted to ^{1}H-NMR analysis and then purified by fractional crystallization from aqueous MeOH to give pure **2a** and **3a**. **2a**: mp 180—182 °C. ^{1}H-NMR ($CDCl_3$) δ: 3.93 (1H, m, 16α-H). **3a**: mp 200—203 °C (lit.[4] 202—205 °C). ^{1}H-NMR ($CDCl_3$) δ: 0.73 (3H, s, 18-Me), 0.83 (3H, s, 19-Me), 3.53 (1H, br m, 3α-H), 3.73 (1H, s, 17α-H).

(B) Base Catalysis: Solutions of **2a** and **2**-*16-d* (0.35 mmol) in 40 ml of 60% aqueous MeOH were each admixed with 4 ml of NaOH solution and then allowed to stand at room temperature for an appropriate time. Acidification with 5% HCl solution was followed by extraction with AcOEt and the usual work-up. The crude residue (83—92 mg) obtained was submitted to ^{1}H-NMR analysis and fractional crystallization as above. When **2b**-*16-d* was used as a substrate, the crude residue was acetylated with pyridine (1 ml)–Ac_2O (0.5 ml). The crude acetate obtained by evaporation of the solvent under reduced pressure was purified by fractional crystallization from acetone–water to give pure **2b** and **3b**. **3b**: mp 181—183 °C (lit.[2b] 179—181 °C). ^{1}H-NMR ($CDCl_3$) δ: 0.82 (3H, s, 18-Me), 0.87 (3H, s, 19-Me), 2.03 (3H, s, 3β-OAc), 2.17 (3H, s, 16β-OAc), 4.83 (1H, br m, 3α-H), 5.00 (1H, s, 17α-H).

Treatment of the 17β-Hydroxy-16-ones 3a and 3a-*16-d* with Acid or Base——The 17β-alcohol **3a** (20 mg, 0.71 mmol) was treated with 3 M D_2SO_4 (15 d) or 1 M NaOD (1 h) under the above rearrangement conditions using deuterated solvents (MeOD and D_2O). After work-up as above, the deuterated compound **3a** was quantitatively recovered in each experiment. D_2SO_4 treatment: **3a** (mp 201—203 °C) consisted of 13% d_0, 46% d_1 and 41% d_2 by MS; the ^{1}H-NMR spectrum showed that the 17α-H/17α-D ratio was about 17/83. NaOD treatment: **3a** (mp 200—202 °C) consisted of 5% d_2 and 95% d_3 by MS; the ^{1}H-NMR spectrum demonstrated that 17α-H of **3a** was almost completely exchanged for deuterium (more than 98%).

The 17β-alcohol **3a**-*16-d* (43% d_0 and 57% d_1), which was obtained by the rearrangement experiment using **2a**-*16-d* and H_2SO_4, was similarly treated with 3 M H_2SO_4 (7 d) and 1 M NaOH (1 h). The recovered **3a** was submitted to MS analysis. The 3 M H_2SO_4 treatment: **3a** (mp 199—203 °C) consisted of 54% d_0 and 46% d_1. The 1 M NaOH

treatment: **3a** (mp 200—203 °C) consisted of 60% d_0 and 40% d_1.

Acknowledgment We thank Professor Toshio Nambara and Dr. Kadzutake Shimada of Tohoku University for MS analysis.

References and Notes

1) A preliminary note was published in *J. Chem. Soc., Chem. Commun.*, **1982**, 530.
2) *a*) M. N. Huhman and M. H. Lott, *J. Am. Chem. Soc.*, **71**, 719 (1949); *b*) N. S. Leeds, D. K. Fukushima, and T. F. Gallagher, *ibid.*, **76**, 2943 (1954); *c*) J. Fishman, *ibid.*, **82**, 6143 (1960); *d*) S. Bernstein and E. W. Cantrall, *J. Org. Chem.*, **26**, 3560 (1961).
3) *a*) W. S. Johnson, B. Gastambide, and R. Pappo, *J. Am. Chem. Soc.*, **79**, 1957 (1957); *b*) D. N. Kirk and M. P. Hartshorn, "Steroid Reaction Mechanisms," Elsevier Publishing Co., Amsterdam, 1968, p. 388.
4) L. Tokes, R. L. LaLonde, and C. Djerassi, *J. Org. Chem.*, **32**, 1012 (1967).
5) F. A. Kincl, *J. Steroid Biochem.*, **7**, 419 (1976).
6) The k_H/k_D value shown in the text is not exact, because the deuterium content at C-16 of the ketol **2a**-*16-d* is not 100 atom% but 90 atom%. However, the value is assumed to be almost the same as that obtained using 100 atom%-labeled substrate.
7) J. Fishman, *J. Org. Chem.*, **27**, 1745 (1962).
8) L. F. Fieser and R. Stevenson, *J. Am. Chem. Soc.*, **76**, 1728 (1954); K. L. Williamson and W. S. Johnson, *J. Org. Chem.*, **26**, 4563 (1961); H. B. Henbest, D. N. Jones, and G. P. Slater, *J. Chem. Soc.*, **1961**, 4472.
9) M. Numazawa, M. Nagaoka, and Y. Osawa, *J. Org. Chem.*, **47**, 4024 (1982).
10) E. Elisberg, H. Vanderhaeghe, and T. F. Gallagher, *J. Am. Chem. Soc.*, **74**, 2814 (1962).

[Chem. Pharm. Bull. 35(12)4769—4776(1987)]

Studies on Peptides. CLVI.[1,2] Synthesis of Second Human Calcitonin Gene-Related Peptide (β-hCGRP) by Application of a New Disulfide-Bonding Reaction with Thallium(III) Trifluoroacetate

NOBUTAKA FUJII,[a] TOSHIHIRO WATANABE,[a] AKIRA OTAKA,[a] KIYOSHI BESSHO,[a] ITSUO YAMAMOTO,[b] TOSHIHARU NODA,[c] and HARUAKI YAJIMA*,[a]

Faculty of Pharmaceutical Sciences, Kyoto University,[a] Faculty of Medicine, Kyoto University,[b] Sakyo-ku, Kyoto 606, Japan and Research Laboratory, Toyo Jozo Co., Ltd.,[c] Ohito, Shizuoka 410-23, Japan

(Received May 27, 1987)

A 37-residue peptide corresponding to the entire amino acid sequence of second human calcitonin gene-related peptide (β-hCGRP) was synthesized by assembling seven peptide fragments, followed by two successive treatments; *i.e.*, first with thallium(III) trifluoroacetate to establish the disulfide bond between two Cys(Ad) residues and then with 1 M trimethylsilyl trifluoromethanesulfonate/trifluoroacetic acid in the presence of diphenyl sulfide and ammonium iodide to remove all protecting groups employed and at the same time to reduce Met(O) to Met. The result was compared with that obtained by the usual air-oxidation procedure.

Synthetic β-hCGRP exhibited a weak inhibitory action against bone Ca-resorption stimulated by [1—34]-parathyroid hormone *in vitro* and lowered the Ca and Pi levels in rat serum.

Keywords——second human calcitonin gene-related peptide synthesis; new disulfide bonding reaction; thallium trifluoroacetate oxidation; air-oxidized disulfide bonding reaction; Met(O) reduction; ammonium iodide; trimethylsilyl trifluoromethanesulfonate deprotection; hard-acid deprotection; soft base; diphenyl sulfide; inhibitory bone calcium resorption; lowering serum calcium; lowering serum phosphate ion

Following the structural elucidations of rat and human calcitonin gene-related peptides (rCGRP[3] and hCGRP[4]), Steenbergh *et al.*[5] screened a cDNA library of human medullary thyroid carcinoma mRNA with a genomic hCGRP-specific probe and presented evidence for the existence in the human genome of a second calcitonin gene, which encodes a second human CGRP (β-hCGRP). This peptide differs from hCGRP (named α-hCGRP) in three of the 37 amino acid residues, *i.e.*, Asp, Val and Asn (positions 3, 22 and 25) of hCGRP are replaced by Asn, Met and Ser respectively.

Following the synthesis of α-hCGRP,[6] we wish to report the synthesis of a 37-residue peptide corresponding to the entire amino acid sequence of β-hCGRP, for which a new disulfide bonding reaction with thallium(III) trifluoroacetate [$(CF_3COO)_3Tl$][7] was employed. Unlike α-hCGRP, this peptide possesses a Met residue. Thus, Met(O)[8] employed was reduced back to Met by treatment with NH_4I[9] without affecting the disulfide bond. The result was compared with that obtained by the usual air-oxidation procedure.

Protected β-hCGRP was prepared by assembling seven peptide fragments as shown in Fig. 1. Of these, four fragments, [3], [4], [5] and [6], are those employed for our previous synthesis of α-hCGRP. Thus, three fragments, [1], [2] and [7], which cover the areas of sequence variation, were newly synthesized. In the final step of the synthesis, the disulfide bond was first established between two Cys(Ad) residues[10] (positions 2 and 7) by treatment with $(CF_3COO)_3Tl$ in TFA. Next, all protecting groups employed, O-Bzl, N^G-Mts,[11] and N^ε-Z, were cleaved by treatment with 1 M TMSOTf/TFA[12] in the presence of PhSPh and at the

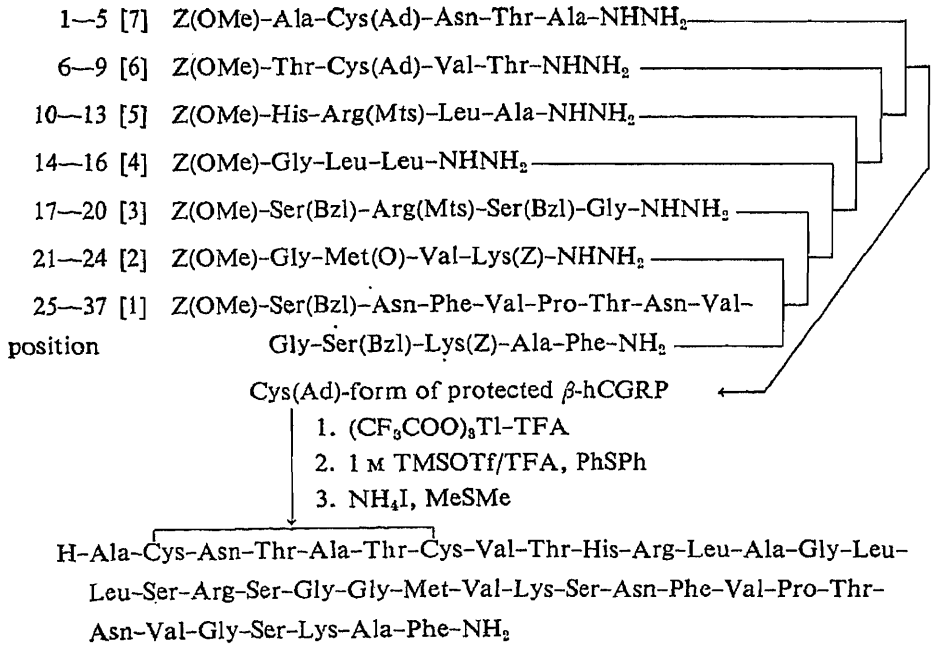

Fig. 1. Synthetic Route to β-Human Calcitonin Gene-Related Peptide (β-hCGRP)

same time, Met(O) was reduced back to Met by addition of NH_4I. As examined previously, the use of PhSPh as a soft base, rather than thioanisole, was desirable when the cleaving reaction was performed in the presence of the disulfide bond.[13] As also reported, NH_4I, with the aid of MeSMe, was found to be effective to reduce Met(O), without affecting the disulfide bond, while PhSPh was ineffective as an additive in the reduction of Met(O).[13]

Fragment [1], Z(OMe)–Ser(Bzl)–Asn–Phe–Val–Pro–Thr–Asn–Val–Gly–Ser(Bzl)–Lys-(Z)–Ala–Phe–NH_2, was prepared by the Su condensation[14] of Z(OMe)–Ser(Bzl)–OH with a TFA-treated sample of the available dodecapeptide amide used for the previous synthesis of α-hCGRP, Z(OMe)–Asn–Phe–Val–Pro–Thr–Asn–Val–Gly–Ser(Bzl)–Lys(Z)–Ala–Phe–NH_2.[6] This amino component was less soluble in DMF, thus, the reaction was performed in a mixture of DMSO–DMF–HMPA. The product was purified by precipitation from DMSO with MeOH and its purity was ascertained by thin layer chromatography (TLC), elemental analysis and amino acid analysis after 6 N HCl hydrolysis, as was done with other fragments.

Fragment [2], Z(OMe)–Gly–Met(O)–Val–Lys(Z)–$NHNH_2$, was synthesized in a stepwise manner starting from H-Val–Lys(Z)–OMe by the active ester procedures, *i.e.*, the Tcp ester[15] for the Met(O) residue and the Su ester for the Gly residue. The resulting protected tetrapeptide ester was converted to [2] by the usual hydrazine treatment.

Fragment [7], Z(OMe)–Ala–Cys(Ad)–Asn–Thr–Ala–$NHNH_2$, was prepared in a stepwise manner also starting from H–Thr–Ala–OMe.[6] The Np ester was employed for condensation of the Asn residue, then the mixed anhydride (MA) procedure[16] and the Su ester for the next two residues, Cys(Ad) and Ala, respectively. The resulting pentapeptide ester was converted to [7] by the usual hydrazine treatment as described above.

Protected β-hCGRP was prepared by successive azide condensations[17] of seven peptide fragments obtained above. The amount of the acyl component was increased from 2 to 5 eq as the chain elongation progressed. Each product was purified by precipitation from DMSO or a mixture of DMF and HMPA with MeOH. Throughout this synthesis, Phe was used as the diagnostic amino acid in acid hydrolysis (Table I). By comparison of the recovery of Phe with those of newly added amino acids after each condensation, satisfactory incorporation of each fragment was ascertained.

TABLE I. Amino Acid Ratios in 6 N HCl Hydrolysates of Synthetic β-hCGRP and Its Intermediates

	Protected peptides							Synthetic β-hCGRP
	25—37	21—37	17—37	14—37	10—37	6—37	1—37	
Asp	2.13	2.38	2.23	2.36	2.21	2.24	3.61	3.29 (3)
Thr	0.94	1.07	0.86	1.08	0.99	2.66	3.85	3.67 (4)
Ser	1.91	2.08	3.55	3.78	3.85	4.05	4.02	3.88 (4)
Pro	0.95	1.02	1.00	1.07	1.05	0.95	1.10	1.11 (1)
Gly	1.02	2.26	3.27	4.10	4.26	4.54	4.81	4.46 (4)
Ala	1.01	1.16	1.12	1.14	1.88	2.23	4.32	3.84 (4)
Cys								0.82 (1)
Val	1.93	2.99	2.99	2.91	3.08	3.94	4.16	3.94 (4)
Met[a)]		1.11	0.74	0.80	0.73	0.94	0.87	0.91 (1)
Leu				1.95	2.99	3.17	3.44	3.07 (3)
Phe[b)]	2.00	2.00	2.00	2.00	2.00	2.00	2.00	2.00 (2)
Lys	0.96	1.88	1.97	1.87	1.93	2.04	2.12	2.00 (2)
His					0.87	0.95	1.00	1.08 (1)
Arg			1.12	0.96	2.00	2.13	2.33	2.22 (2)
Recov. (%)	61	74	71	93	94	97	78	91

a) Met + Met(O). *b*) Diagnostic amino acid.

The protected form of β-hCGRP thus obtained was treated with $(CF_3COO)_3Tl$ (1.2 eq) in the presence of anisole in TFA in an ice-bath for 60 min to establish the disulfide bond between two Cys(Ad) residues. The product was next treated with 1 M TMSOTf/TFA in the presence of PhSPh and *m*-cresol in an ice-bath for 180 min to remove all protecting groups, and after addition of NH_4I and MeSMe, for an additional 30 min to reduce Met(O) to Met without affecting the disulfide bond. The deprotected product thus obtained was briefly treated with diluted ammonia to reverse the possible N→O shift and at the same time, to ensure the complete hydrolysis of the trimethylsilyl moieties attached. The treated product was next purified by gel-filtration on Sephadex G-15, followed by ion-exchange chromatography on a CM-Trisacryl column. The product was finally purified by high-performance liquid chromatography (HPLC) on a Nucleosil 5C18 column with gradient elution [MeCN (25—40%) in 0.1% TFA] to obtain a homogeneous compound (yield 12% from protected β-hCGRP), possessing a retention time on HPLC identical with that of the standard sample of β-hCGRP prepared by the usual air-oxidation procedure. The molecular weight of the synthetic peptide was ascertained by FAB-mass spectrometry.

In order to obtain the standard sample of β-hCGRP, protected β-hCGRP was treated with 1 M TMSOTf–thioanisole/TFA in an ice-bath for 180 min to remove all protecting groups, including the two S–Ad groups and then after addition of NH_4I and MeSMe, for 30 min to reduce Met(O). The product was incubated with 2-mercaptoethanol in 6 M guanidine–HCl in 0.1 M Tris–HCl buffer for 18 h, then gel-filtered on Sephadex G-25 and submitted to air-oxidation in a highly diluted solution as usual. The progress of the reaction was monitored by means of the Ellman test[18)] and the product was purified as stated above by gel-filtration, ion-exchange chromatography and finally HPLC (yield 7.4%).

Thus, we were able to synthesize β-hCGRP containing the disulfide bond and the Met residue in a somewhat better yield than that of the time-consuming air-oxidation procedure, by first establishing the disulfide bond, followed by reduction of Met(O), together with complete removal of other protecting groups.

Synthetic β-hCGRP lowered the serum Ca and Pi levels in rats and its potency was

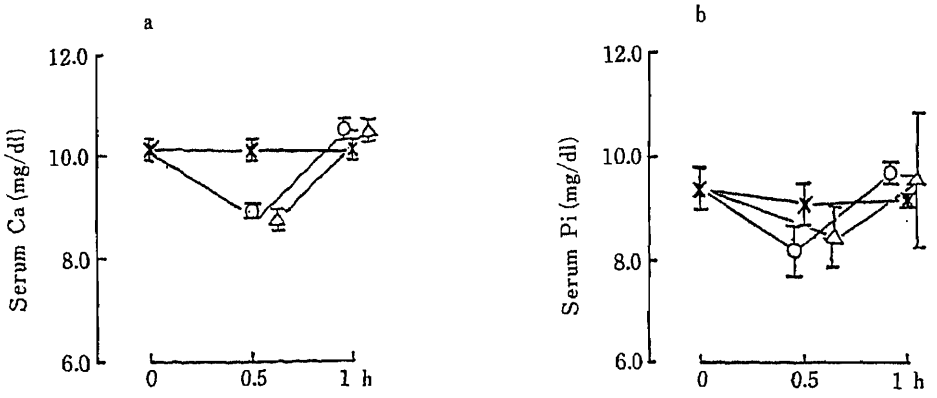

Fig. 2. Effect of Synthetic β-hCGRP on Serum Ca and Pi in Rats (Dose 80 μg/kg, i.v.)

a, Effect on Ca in serum; b, effect on Pi in serum.
—△—, synthetic β-hCGRP; —○—, synthetic α-hCGRP; —×—, vehicle.

judged to be equivalent to that of α-hCGRP, as shown in Fig. 2. In the *in vitro* assay using ^{45}Ca-labeled newborn mouse calvaria,[19] synthetic β-hCGRP inhibited PTH-stimulated bone-resorption dose-dependently and no difference in the inhibitory potencies was found between α- and β-hCGRPs.

Experimental

General experimental methods employed in this investigation are essentially the same as described in our previous synthesis of α-hCGRP.[6]

HPLC was conducted with a Waters 204 compact model. FAB-MS spectra were obtained on a ZAB SE instrument (VG Analytical Co., England) mass spectrometer equipped with a FAB ion source. Leucine aminopeptidase (LAP, Lot. No. L-6007) was purchased from Sigma. TLC was performed on silica gel (Kiesel-gel G, Merck) and *Rf* values refer to the following solvent systems: Rf_1 $CHCl_3$–MeOH–H_2O (8:3:1), Rf_2 $CHCl_3$–MeOH–AcOH (9:1:0.5), Rf_3 *n*-BuOH–pyridine–AcOH–H_2O (4:1:1:2), Rf_4 *n*-BuOH–AcOH–pyridine–H_2O (30:20:6:24).

Unless otherwise stated, protected peptides were purified as follows, after the reaction mixture had become negative to ninhydrin, the solvent was removed by evaporation *in vacuo* and the residue was treated with 5% citric acid and ether. The resulting powder was washed with 5% citric acid, 5% $NaHCO_3$, and H_2O (named procedure A) and then precipitated from appropriate solvents.

Z(OMe)–Ser(Bzl)–Asn–Phe–Val–Pro–Thr–Asn–Val–Gly–Ser(Bzl)–Lys(Z)–Ala–Phe–NH_2 [1] (Positions 25—37)——A mixture of Z(OMe)–Ser(Bzl)–OSu (7.85 g, 16.3 mmol), Et_3N (2.7 ml, 19.4 mmol), and HOBt (0.11 g, 0.81 mmol) in DMF (10 ml) was added to a solution of a TFA-treated sample of Z(OMe)–Asn–Phe–Val–Pro–Thr–Asn–Val–Gly–Ser(Bzl)–Lys(Z)–Ala–Phe–NH_2 (6.80 g, 4.08 mmol) in DMSO–DMF–HMPA (2:1:1, 100 ml) containing Et_3N (0.57 ml, 4.08 mmol) and the solution was stirred for 12 h. The product was purified by procedure A, followed by precipitation from DMSO with MeOH; yield 7.10 g (94%), mp 278—281 °C, $[\alpha]_D^{15}$ −34.7° (*c*=0.8, DMSO), Rf_2 0.79. Amino acid ratios in a 6 N HCl hydrolysate: Asp 2.13, Thr 0.94, Ser 1.91, Pro 0.95, Gly 1.02, Ala 1.01, Val 1.93, Phe 2.00, Lys 0.96 (recovery of Phe, 61%). *Anal.* Calcd for $C_{93}H_{121}N_{17}O_{23}\cdot 4H_2O$: C, 58.26; H, 6.78; N, 12.42. Found: C, 58.23; H, 6.43; N, 12.54.

Z(OMe)–Met(O)–Val–Lys(Z)–OMe——A mixture of Z(OMe)–Met(O)–OTcp (2.80 g, 5.50 mmol), Et_3N (1.41 ml, 10.1 mmol) and a TFA-treated sample of Z(OMe)–Val–Lys(Z)–OMe (2.56 g, 4.59 mmol) in DMF (20 ml) was stirred for 14 h. The product was purified by procedure A, followed by recrystallization from MeOH and ether; yield 2.77 g (86%), mp 168—172 °C, $[\alpha]_D^{15}$ −27.2° (*c*=0.8, MeOH), Rf_1 0.77. *Anal.* Calcd for $C_{34}H_{48}N_{14}O_{10}S\cdot H_2O$: C, 56.49; H, 6.97; N, 7.75. Found: C, 56.70; H, 6.68; N, 7.68.

Z(OMe)–Gly–Met(O)–Val–Lys(Z)–OMe——A mixture of Z(OMe)–Gly–OSu (1.93 g, 5.75 mmol), HOBt (0.10 g, 0.77 mmol), Et_3N (1.34 ml, 9.61 mmol) and a TFA-treated sample of the above tripeptide ester (2.70 g, 3.83 mmol) in DMF (30 ml) was stirred for 14 h. The product was purified by procedure A, followed by recrystallization from MeOH and ether; yield 2.21 g (76%), mp 147—150 °C, $[\alpha]_D^{15}$ −31.1° (*c*=0.6, MeOH), Rf_1 0.62. *Anal.* Calcd for $C_{36}H_{51}N_5O_{11}S$: C, 56.75; H, 6.75; N, 9.19. Found: C, 56.68; H, 6.80; N, 8.90.

Z(OMe)–Gly–Met(O)–Val–Lys(Z)–$NHNH_2$ [2] (Positions 21—24)——The above tetrapeptide ester (2.20 g, 2.89 mmol) in MeOH (10 ml) was treated with 80% hydrazine hydrate (0.90 ml, 5 eq) for 24 h, then the solvent was

removed by evaporation and the residue was treated with H_2O. The resulting powder was recrystallized from MeOH and EtOH; yield 2.0 g (91%), mp 192—196 °C, $[\alpha]_D^{15}$ −28.8° (c=0.5, MeOH), Rf_1 0.57. Amino acid ratios in a 6 N HCl hydrolysate: Gly 1.03, Met N.D., Val 0.95, Lys 1.00 (recovery of Lys, 97%). *Anal.* Calcd for $C_{35}H_{51}N_7O_{10}S$: C, 55.18; H, 6.75; N, 12.86. Found: C, 55.44; H, 6.86; N, 12.66.

Z(OMe)–Asn–Thr–Ala–OMe——A mixture of Z(OMe)–Asn–ONp (6.50 g, 15.6 mmol), HOBt (0.21 g, 1.56 mmol), Et_3N (2.18 ml, 15.6 mmol) and a TFA-treated sample of Z(OMe)–Thr–Ala–OMe (2.88 g, 7.82 mmol) in DMF (15 ml) was stirred for 14 h. The product was purified by procedure A, followed by precipitation from DMF with MeOH; yield 3.0 g (79%), mp 222—225 °C, $[\alpha]_D^{15}$ −11.4° (c=0.5, DMF), Rf_1 0.63. *Anal.* Calcd for $C_{21}H_{30}N_4O_9$: C, 52.27; H, 6.27; N, 11.61. Found: C, 52.17; H, 6.36; N, 11.85.

Z(OMe)–Cys(Ad)–Asn–Thr–Ala–OMe——The MA [prepared from 5.25 g (8.74 mmol) of the Z(OMe)–Cys(Ad)–OH DCHA salt] in THF (20 ml) was added to an ice-chilled solution of a TFA-treated sample of Z(OMe)–Asn–Thr–Ala–OMe (2.81 g, 5.82 mmol) in DMF (20 ml) containing Et_3N (0.82 ml, 5.82 mmol) and the mixture was stirred for 5 h. The product was purified by procedure A, followed by precipitation from DMF with AcOEt; yield 2.30 g (55%), mp 172—175 °C, $[\alpha]_D^{15}$ −19.5° (c=0.9, DMF), Rf_1 0.73. *Anal.* Calcd for $C_{34}H_{49}N_5O_{10}S \cdot 2H_2O$: C, 54.02; H, 7.07; N, 9.27. Found: C, 53.95; H, 6.77; N, 9.40.

Z(OMe)–Ala–Cys(Ad)–Asn–Thr–Ala–OMe——A mixture of Z(OMe)–Ala–OSu (1.25 g, 3.57 mmol), Et_3N (0.92 ml, 6.60 mmol) and a TFA-treated sample of Z(OMe)–Cys(Ad)–Asn–Thr–Ala–OMe (2.14 g, 2.97 mmol) in DMF (50 ml) was stirred for 14 h. The product was purified by procedure A, followed by precipitation from DMF with MeOH; yield 1.46 g (62%), mp 227—232 °C, $[\alpha]_D^{15}$ −19.9° (c=0.5, DMF), Rf_1 0.70. *Anal.* Calcd for $C_{37}H_{54}N_6O_{11}S$: C, 56.19; H, 6.88; N, 10.63. Found: C, 55.93; H, 6.81; N, 10.34.

Z(OMe)–Ala–Cys(Ad)–Asn–Thr–Ala–NHNH$_2$ [7] (Positions 1—5)——The above pentapeptide ester (1.40 g, 1.77 mmol) in DMF (10 ml) was treated with 80% hydrazine hydrate (0.55 ml, 5 eq) at room temperature for 24 h, then the solvent was removed by evaporation. Treatment of the residue with H_2O afforded a powder, which was precipitated from DMF with MeOH; yield 1.30 g (93%), mp 264—267 °C, $[\alpha]_D^{15}$ −15.5° (c=0.5, DMF), Rf_1 0.67. Amino acid ratios in a 6 N HCl hydrolysate: Ala 2.00, Asp 1.07, Thr 0.97 (recovery of Ala 83%). *Anal.* Calcd for $C_{36}H_{54}N_8O_{10}S \cdot 2H_2O$: C, 52.28; H, 7.07; N, 13.55. Found: C, 52.52; H, 6.79; N, 13.45.

Z(OMe)–Gly–Met(O)–Val–Lys(Z)–Ser(Bzl)–Asn–Phe–Val–Pro–Thr–Asn–Val–Gly–Ser(Bzl)–Lys(Z)–Ala–Phe–NH$_2$, Z(OMe)–(β-hCGRP 21—37)–NH$_2$——The azide prepared from fragment [2] (1.65 g, 2.17 mmol) in DMF (5 ml) and Et_3N (0.36 ml, 2.60 mmol) were added to an ice-chilled solution of a TFA-treated sample of fragment [1] (2.00 g, 1.08 mmol) in DMF–DMSO–HMPA (1 : 3 : 1, 10 ml) containing Et_3N (0.15 ml, 1.08 mmol) and the mixture was stirred for 14 h. The product was purified by procedure A, followed by precipitation from DMSO with MeOH; yield 2.10 g (81%), mp 275—280 °C $[\alpha]_D^{15}$ −20.2° (c=1.4, DMSO), Rf_1 0.70. *Anal.* Calcd for $C_{119}H_{160}N_{22}O_{30}S \cdot 9H_2O$: C, 55.55; H, 6.97; N, 11.98. Found: C, 55.31; H, 6.71; N, 11.95.

Z(OMe)–Ser(Bzl)–Arg(Mts)–Ser(Bzl)–Gly–Gly–Met(O)–Val–Lys(Z)–Ser(Bzl)–Asn–Phe–Val–Pro–Thr–Asn–Val–Gly–Ser(Bzl)–Lys(Z)–Ala–Phe–NH$_2$, Z(OMe)–(β-hCGRP 17—37)–NH$_2$——The azide prepared from fragment [3] (1.50 g, 1.58 mmol) in DMF (2 ml) and Et_3N (0.26 ml, 1.90 mmol) were added to an ice-chilled solution of a TFA-treated sample of Z(OMe)–(β-hCGRP 21—37)–NH$_2$ (1.90 g, 0.79 mmol) in DMF–DMSO–HMPA (1 : 3 : 1, 15 ml) containing Et_3N (0.11 ml, 0.79 mmol) and the mixture was stirred for 14 h. The product was purified by procedure A, followed by precipitation from DMSO with MeOH; yield 2.06 g (83%), mp 272—276 °C, $[\alpha]_D^{15}$ −25.3° (c=0.7, DMSO), Rf_1 0.62. *Anal.* Calcd for $C_{156}H_{207}N_{29}O_{38}S_2 \cdot 6H_2O$: C, 57.31; H, 6.75; N, 12.43. Found: C, 56.98; H, 6.56; N, 12.83.

Z(OMe)–Gly–Leu–Leu–Ser(Bzl)–Arg(Mts)–Ser(Bzl)–Gly–Gly–Met(O)–Val–Lys(Z)–Ser(Bzl)–Asn–Phe–Val–Pro–Thr–Asn–Val–Gly–Ser(Bzl)–Lys(Z)–Ala–Phe–NH$_2$, Z(OMe)–(β-hCGRP 14—37)–NH$_2$——The azide prepared from fragment [4] (0.76 g, 1.58 mmol) in DMF (2 ml) and Et_3N (0.26 ml, 1.90 mmol) were added to an ice-chilled solution of a TFA-treated sample of Z(OMe)–(β-hCGRP 17—37)–NH$_2$ (2.00 g, 0.63 mmol) in DMF–DMSO–HMPA (1 : 3 : 1, 5 ml) containing Et_3N (0.88 ml, 0.63 mmol) and the mixture was stirred for 14 h. The product was purified by procedure A, followed by precipitation from DMSO with MeOH; yield 2.00 g (92%), mp 273—277 °C, $[\alpha]_D^{15}$ −7.4° (c=1.0, DMSO), Rf_1 0.57. *Anal.* Calcd for $C_{170}H_{232}N_{32}O_{40}S_2 \cdot 8H_2O$: C, 56.90; H, 6.97; N, 12.49. Found: C, 56.44; H, 6.72; N, 12.84.

Z(OMe)–His–Arg(Mts)–Leu–Ala–Gly–Leu–Leu–Ser(Bzl)–Arg(Mts)–Ser(Bzl)–Gly–Gly–Met(O)–Val–Lys(Z)–Ser(Bzl)–Asn–Phe–Val–Pro–Thr–Asn–Val–Gly–Ser(Bzl)–Lys(Z)–Ala–Phe–NH$_2$, Z(OMe)–(β-hCGRP 10—37)–NH$_2$——The azide prepared from fragment [5] (0.75 g, 0.87 mmol) in DMF (10 ml) and Et_3N (0.15 ml, 1.08 mmol) were added to an ice-chilled solution of a TFA-treated sample of Z(OMe)–(β-hCGRP 14—37)–NH$_2$ (1.0 g, 0.29 mmol) in DMF–DMSO (1 : 3, 20 ml) containing Et_3N (0.04 ml, 0.29 mmol) and the mixture was stirred for 14 h. The product was purified by procedure A, followed by precipitation from DMSO with MeOH; yield 1.00 g (84%), mp 276—279 °C, $[\alpha]_D^{15}$ −12.7° (c=1.0, DMSO), Rf_1 0.57. *Anal.* Calcd for $C_{200}H_{277}N_{41}O_{47}S_3$: C, 58.53; H, 6.80; N, 13.99. Found: C, 58.26; H, 6.99; N, 13.96.

Z(OMe)–Thr–Cys(Ad)–Val–Thr–His–Arg(Mts)–Leu–Ala–Gly–Leu–Leu–Ser(Bzl)–Arg(Mts)–Ser(Bzl)–Gly–Gly–Met(O)–Val–Lys(Z)–Ser(Bzl)–Asn–Phe–Val–Pro–Thr–Asn–Val–Gly–Ser(Bzl)–Lys(Z)–Ala–Phe–NH$_2$, Z-(OMe)–(β-hCGRP 6—37)–NH$_2$——The azide prepared from fragment [6] (0.72 g, 0.98 mmol) in DMF (1 ml) and

Et_3N (0.16 ml, 1.17 mmol) were added to an ice-chilled solution of a TFA-treated sample of Z(OMe)-(β-hCGRP 6—37)-NH_2 (0.50 g, 0.12 mmol) in DMF–HMPA (1 : 1, 5 ml) containing Et_3N (0.02 ml, 0.14 mmol) and the mixture was stirred at −15 °C for 72 h and then at 4 °C for 24 h. The product was purified by procedure A, followed by precipitation from a mixture of DMF and HMPA with MeOH; yield 0.45 g (79%), mp 263 °C dec., $[\alpha]_D^{15}$ −24.5° (c = 0.2, DMSO), Rf_1 0.60. *Anal.* Calcd for $C_{226}H_{319}N_{45}O_{53}S_4 \cdot 13H_2O$: C, 55.57; H, 7.13; N, 12.93. Found: C, 55.32; H, 6.93; N, 13.15.

Z(OMe)-Ala-Cys(Ad)-Asn-Thr-Ala-Thr-Cys(Ad)-Val-Thr-His-Arg(Mts)-Leu-Ala-Gly-Leu-Leu-Ser(Bzl)-Arg(Mts)-Ser(Bzl)-Gly-Gly-Met(O)-Val-Lys(Z)-Ser(Bzl)-Asn-Phe-Val-Pro-Thr-Asn-Val-Gly-Ser(Bzl)-Lys(Z)-Ala-Phe-NH_2, protected β-hCGRP——The azide prepared from the above protected pentapeptide hydrazide [7] (0.19 g, 0.24 mmol) in DMF (1 ml) and Et_3N (40 μl, 0.28 mmol) were added to an ice-chilled solution of a TFA treated sample of Z(OMe)-(β-hCGRP 6—37)-NH_2 (0.22 g, 47 μmol) in DMF–HMPA (1 : 1, 2 ml) containing Et_3N (6.6 μl, 47 μmol) and the mixture was stirred for 24 h. The product was purified by procedure A, followed by precipitation from DMF–HMPA (1 : 1) with MeOH; yield 0.22 g (81%), mp 263 °C dec., $[\alpha]_D^{15}$ −36.1° (c = 0.5, DMSO), Rf_1 0.71. *Anal.* Calcd for $C_{253}H_{361}N_{51}O_{60}S_5 \cdot 19H_2O$: C, 54.46; H, 7.21; N, 12.80. Found: C, 54.22; H, 7.08; N, 12.54.

Synthetic β-hCGRP, [H-(β-hCGRP 1—37)-NH_2]——(a) By the $(CF_3COO)_3Tl$-Oxidation Procedure: Protected β-hCGRP (50 mg) in TFA (5.0 ml) was treated with $(CF_3COO)_3Tl$ (6.23 mg, 1.2 eq) in the presence of anisole (50 μl) in an ice-bath for 60 min, then TFA was removed by evaporation and dry ether was added. The resulting powder was treated with 1 M TMSOTf/TFA (4.6 ml) in the presence of PhSPh (at a concentration of 0.5 M) and *m*-cresol (234 μl) in an ice-bath for 180 min. Then NH_4I (27 mg, 20 eq) and MeSMe (14 μl, 20 eq) were added and treatment was continued for an additional 30 min. After addition of dry ether, the resulting powder was collected by centrifugation and dissolved in ice-chilled MeOH–H_2O (1 : 1, 5 ml). The pH of the solution was adjusted to 7,5 with 5% NH_4OH, then after 10 min, to 3.0 with AcOH. The solution was applied to a column of Sephadex G-15 (1.8 × 136 cm), which was eluted with 1 N AcOH. The fractions corresponding to the front main peak [6.7 ml each, tube Nos. 16—21, determined by ultraviolet (UV) absorption measurement at 227 nm] were combined and the solvent was removed by lyophilization to give a powder; yield 31.1 mg (86%).

The crude deprotected peptide thus obtained was dissolved in 0.01 M $AcONH_4$ buffer (pH 6.5) and the solution was applied to a column of CM-Trisacryl (2 × 7 cm), which was eluted with the same buffer (104 ml) and then with a linear gradient formed from the same buffer containing 0.2 M NaCl (100 ml) through a mixing flask containing the starting buffer (250 ml). The fractions corresponding to the main peak (5.2 ml each, tube Nos. 83—103, monitored by UV absorption measurement at 227 nm) were combined and the solvent was removed by lyophilization. For desalting, the residue was submitted to gel-filtration on a Sephadex G-15 column (1.8 × 136 cm), which was eluted with 1 N AcOH. Lyophilization of the desired fractions (monitored by the Folin–Lowry test)[20] gave a fluffy powder; yield 7.5 mg (24.1%).

Subsequent purification was performed by reversed phase HPLC on a Nucleosil 5C18 column (4.6 × 150 mm), which was eluted with a gradient of MeCN (25% to 40% in 30 min) in 0.1% TFA at a flow rate of 1.0 ml/min. The eluate corresponding to the main peak (Fig. 3a, retention time 18 min, detected by UV absorption measurement at 233 nm) was collected and the solvent was removed by lyophilization. The residue, dissolved in 0.5 N AcOH, was applied to a column of Sephadex G-15 as described above. Lyophilization of the desired eluates gave a white fluffy powder; yield 4.4 mg (12.2% from protected hCGRP), $[\alpha]_D^{23}$ −78.8° (c = 0.1, 0.5 N AcOH), FAB-MS m/z: 3794 $(M+H)^+$ (Fig. 4).

The synthetic peptide exhibited a single band in disk isoelectrofocusing (Fig. 4) on 7.5% polyacrylamide gel (0.5 × 7.0 cm) containing Pharmalyte (pH 9—11): mobility, 6.3 cm from the origin toward the cathodic end of the gel, after running at 200 V for 5 h. The purified product exhibited a retention time (20 min) in HPLC identical with that of the sample obtained in (b), when a YMC AM-302 ODS column (4.6 × 150 mm) was eluted with a linear gradient of MeCN (25—40% in 30 min) in 0.1% TFA at a flow rate of 1.0 ml/min (Fig. 3b). Amino acid ratios in a 6 N HCl hydrolysate are listed in Table I. Amino acid ratios in a LAP digest (numbers in parentheses are theoretical values): Thr 3.48 (4), Ser + Asn 4.53 (4+3), Pro 1.16 (1), Gly 4.38 (4), Ala 3.94 (4), Cys 0.78 (1), Val 3.46 (4), Met 0.93 (1), Leu 3.04 (3), Phe 2.00 (2), Lys 2.12 (2), His 0.86 (1), Arg 1.98 (2), recovery of Phe 82%.

(b) By the Air-Oxidation Procedure: Protected β-hCGRP (53.7 mg, 10.2 μmol) was treated with 1 M TMSOTf–thioanisole/TFA (5.0 ml) in an ice-bath for 180 min, then for an additional 30 min after addition of NH_4I (30 mg, 20 eq) and MeSMe (15 μl, 20 eq). Dry ether was added. The resulting powder was dissolved in MeOH (3 ml), then 2-mercaptoethanol (72 μl, 100 eq) and 6 M guanidine–HCl in 0.1 M Tris–HCl buffer (5 ml) were added and the solution (pH 8.0), after being kept at 4 °C for 18 h, was applied to a column of Sephadex G-25 (1.8 × 136 cm), which was eluted with 1 N AcOH. The fractions corresponding to the front main peak (4 ml each, tube Nos. 38—50, monitored by UV absorption measurement at 227 nm) were combined and diluted with H_2O (500 ml). The solution, after being adjusted to pH 8.0 with 5% NH_4OH, was kept at 4 °C for 3 d, during which time the Ellman test value (412 nm) dropped from 0.059 to a constant value of 0.002. After lyophilization, the product was purified as stated above, first by gel-filtration of Sephadex G-15 (yield, 20.7 mg, 53.5%), then by ion-exchange chromatography on CM-Trisacryl (yield 4.4 mg, 11.3%) and finally by HPLC on a Cosmosil 5C18 column (yield 2.9 mg, 7.4% from protected β-hCGRP); $[\alpha]_D^{23}$ −75.9°

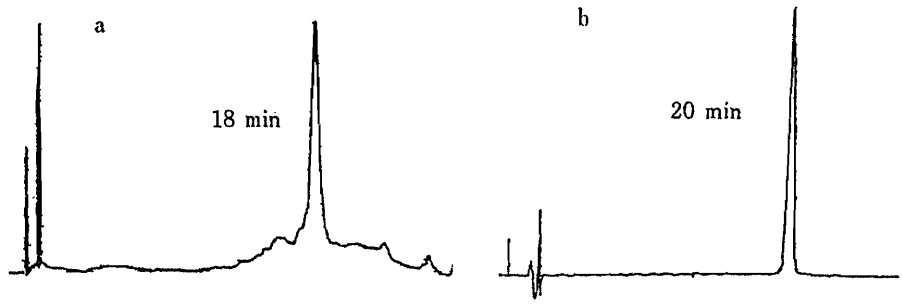

Fig. 3. HPLC of Synthetic β-hCGRP

a, CM-purified sample on a Nucleosil column; b, mixture of the HPLC-purified samples obtained by the new method and the air-oxidation method, on a YMC AM-302 ODS column.

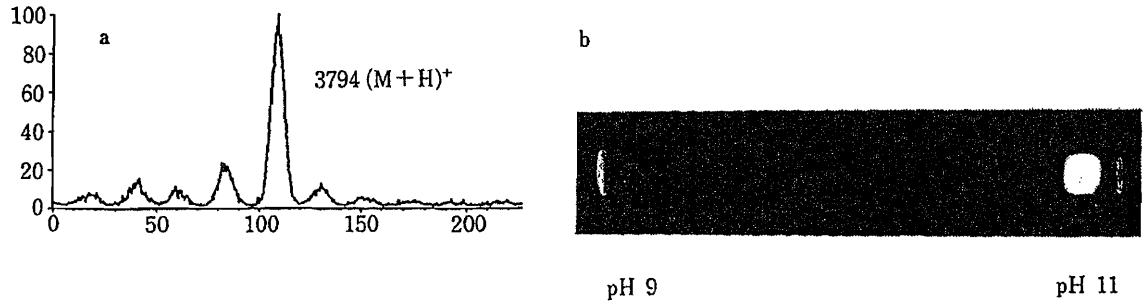

Fig. 4. FAB-MS and Disk Isoelectrofocusing of Synthetic β-hCGRP

a, FAB-MS; b, disk isoelectrofocusing.

(c=0.1, 0.5N AcOH), Rf_3 0.45, Rf_4 0.82. FAB-MS m/z: 3794 $(M+H)^+$. A single peak (retention time, 18 min; monitored by UV absorption measurement at 233 nm) on an HPLC analytical Nucleosil 5C18 column (4.6 × 150 mm) was obtained by gradient elution with MeCN (25—45%, 30 min) in 0.1% TFA at a flow rate of 1.0 ml/min. Amino acid ratios in a 6N HCl hydrolysate and a LAP digest (numbers in parentheses): Asp 3.49, Asn (N.D.), Thr 3.60 (3.68), Ser 3.70 (4.19), Pro 0.95 (0.98), Gly 4.06 (3.95), Ala 3.92 (3.94), Cys 0.82 (0.90), Val 3.39 (3.65), Met 0.89 (1.02), Leu 2.82 (2.85), Phe 2.00 (2.00), Lys 1.82 (1.99), His 0.99 (0.80), Arg 2.07 (1.75), recovery of Phe 95% (95%).

Acknowledgement The authors are grateful to Drs. Nobuharu Shigematsu and Hirokazu Tanaka, Tsukuba Research Laboratory, Fujisawa Pharmaceutical Co., Ltd., for measurement of FAB mass spectra.

References and Notes

1) Part CLV: N. Fujii, A. Otaka, N. Sugiyama, M. Hatano, and H. Yajima, *Chem. Pharm. Bull.*, **35**, 3880 (1987).
2) Amino acids used in this investigation are of the L-configuration. The following abbreviations are used: Z=benzyloxycarbonyl, Z(OMe)=*p*-methoxybenzyloxycarbonyl, Boc=*tert*-butoxycarbonyl, Ad=1-adamantyl, MBzl=*p*-methoxybenzyl, Mts=mesitylenesulfonyl, Bzl=benzyl, HOBt=*N*-hydroxybenzotriazole, Tcp=2,4,5-trichlorophenyl, Su=*N*-hydroxysuccinimidyl, DMF=dimethylformamide, DMSO=dimethylsulfoxide, HMPA=hexamethylphosphoramide, TMSOTf=trimethylsilyl trifluoromethanesulfonate, TFA=trifluoroacetic acid, MeSMe=dimethylsulfide, PhSPh=diphenyl sulfide, cDNA=complementary deoxyribonucleic acid, mRNA=messenger ribonucleic acid, FAB-MS=fast atom bombardment mass spectrometry, PTH=parathyroid hormone, DCHA=dicyclohexylamine.
3) M. G. Rosenfeld, J. J. Mermod, S. G. Amara, L. W. Swanson, P. E. Sawchenko, J. Rivier, W. W. Vale, and R. M. Evans, *Nature* (London), **304**, 129 (1983).
4) H. R. Morris, M. Panico, T. Etienne, J. Tippins, S. I. Girgis, and I. MacIntyre, *Nature* (London), **308**, 746 (1984).
5) P. H. Steenbergh, J. W. M. Hoppener, J. Zandberg, C. J. M. Lips, and H. S. Jansz, *FEBS Lett.*, **183**, 403 (1985); P. H. Steenbergh, J. W. M. Hoppener, J. Zandberg, A. Visser, C. J. M. Lips, and H. S. Jansz, *ibid.*, **209**, 97 (1986).
6) N. Fujii, H. Yajima, A. Otaka, S. Funakoshi, M. Nomizu, K. Akaji, I. Yamamoto, K. Torizuka, K. Kitagawa,

T. Akita, K. Ando, T. Kawamoto, Y. Shimonishi, and T. Takao, *J. Chem. Soc., Chem. Commun.*, **1985**, 602; *idem*, *Chem. Pharm. Bull.*, **34**, 613 (1986).
7) N. Fujii, A. Otaka, S. Funakoshi, K. Bessho, and H. Yajima, *J. Chem. Soc., Chem. Commun.*, **1987**, 163.
8) B. Iselin, *Helv. Chim. Acta*, **44**, 61 (1961); N. Fujii, T. Sasaki, S. Funakoshi, H. Irie, and H. Yajima, *Chem. Pharm. Bull.*, **26**, 650 (1978).
9) D. Landini, G. Modena, F. Montanari, and G. Scorrano, *J. Am. Chem. Soc.*, **92**, 7168 (1970); E. Izeboud and H. C. Beyerman, *Recl. Trav. Chim. Pays-Bas*, **97**, 1 (1978).
10) N. Fujii, A. Otaka, S. Funakoshi, H. Yajima, O. Nishimura, and M. Fujino, *Chem. Pharm. Bull.*, **34**, 869 (1986).
11) H. Yajima, M. Takeyama, J. Kanaki, and K. Mitani, *J. Chem. Soc., Chem. Commun.*, **1978**, 482.
12) N. Fujii, A. Otaka, O. Ikemura, K. Akaji, S. Funakoshi, Y. Hayashi, Y. Kuroda, and H. Yajima, *J. Chem. Soc., Chem. Commun.*, **1987**, 274; N. Fujii, A. Otaka, O. Ikemura, M. Hatano, A. Okamachi, S. Funakoshi, M. Sakurai, T. Shioiri, and H. Yajima, *Chem. Pharm. Bull.*, **35**, 3447 (1987).
13) N. Fujii, A. Otaka, S. Funakoshi, K. Bessho, T. Watanabe, K. Akaji, and H. Yajima, *Chem. Pharm. Bull.*, **35**, 2339 (1987).
14) G. W. Anderson, J. E. Zimmermann, and F. M. Callahan, *J. Am. Chem. Soc.*, **85**, 3039 (1963).
15) J. Pless and R. A. Boissonnas, *Helv. Chim. Acta*, **46**, 1609 (1963).
16) J. R. Vaughan Jr., *J. Am. Chem. Soc.*, **73**, 3547 (1951); T. Wieland, W. Kern, and R. Sehring, *Justus Liebigs Ann. Chem.*, **569**, 117 (1950); R. A. Boissonnas, *Helv. Chim. Acta*, **34**, 874 (1951).
17) J. Honzl and J. Rudinger, *Collect. Czech. Chem. Commun.*, **26**, 2333 (1961).
18) G. L. Ellman, *Arch. Biochem. Biophys.*, **82**, 70 (1959).
19) I. Yamamoto, N. Kitamura, J. Aoki, C. Shigeno, M. Hino, K. Asonuma, K. Torizuka, N. Fujii, A. Otaka, and H. Yajima, *Calcif. Tissue Int.*, **38**, 339 (1986).
20) O. H. Lowry, N. J. Rosebrough, A. L. Farr, and R. J. Randall, *J. Biol. Chem.*, **193**, 265 (1951).

[Chem. Pharm. Bull. 35(12)4777—4788(1987)]

Application of Cyanophosphates in Organic Synthesis. Reactivity of α-Cyano-α-diethylphosphonooxy Anions

TAKUSHI KURIHARA,* KAZUNORI SANTO, SHINYA HARUSAWA, and RYUJI YONEDA

Osaka University of Pharmaceutical Sciences, 2-10-65, Kawai, Matsubara, Osaka 580, Japan

(Received May 27, 1987)

The utility of the cyanohydrin diethylphosphates derived from aldehydes (arylaldehydes, crotonaldehyde, and cinnamaldehyde) as an acyl anion equivalent was examined. Deprotonation of cyanophosphates with *n*-butyllithium in the presence of tetramethylethylenediamine in tetrahydrofuran at −78 °C followed by reactions with alkyl(acyl) halides, carbonyl compounds, and α,β-unsaturated nitriles or esters, as well as cyanophosphates themselves, afforded alkylated (acylated) products, mixed benzoin and acyloin phosphates, polysubstituted cyclopropanes, and diarylfumaronitriles in moderate yields, respectively.

Keywords——cyanophosphate; diethyl phosphorocyanidate; lithium cyanide; acyl anion equivalent; carbon–carbon bond formation; benzoin phosphate; cyclopropane; diarylfumaronitrile; *n*-butyllithium

A variety of ketone cyanohydrin *O*-diethylphosphates (cyanophosphates), which were easily prepared by reaction of ketones with diethyl phosphorocyanidate (DEPC) in the presence of lithium cyanide (LiCN), have been widely utilized as versatile intermediates for the synthesis of α,β-unsaturated nitriles,[1] arylacetonitriles,[2] 4-hydroxy-3-phenylbenzonitriles,[3] γ-oxy-α,β-unsaturated nitriles,[4] 4-arylangelonitriles,[5] 2-alkenenitriles,[6] and so on.[7] Our systematic investigations in this area have led to a new nucleophilic acyl synthon, obtained by deprotonation of the aldehyde-cyanophosphates. Recently, masked reagents with C=O, umpolung, such as anions of cyanohydrins, protected cyanonhydrins, α-dialkylaminonitriles, and α-alkyl or α-aryl-*N*-acylaminonitriles have proved to be powerful tools for carbon–carbon bond formation in many synthetic transformations.[8] Extensive studies on trimethylsilyl (TMS)-cyanohydrins by Hünig and his collaborators are especially well known.[9] However, the reactivity of an acyl anion equivalent derived from cyanophosphate has hitherto been unreported. We describe here the reactions of the anion of aldehyde (arylaldehydes, crotonaldehyde and cinnamaldehyde) cyanophosphates with alkyl and acyl halides, and carbonyl compounds, as well as activated olefins. Self-condensation of arylaldehyde cyanophosphates to give diarylfumaronitriles is also described.

Alkylation and Acylation

The cyanophosphates (**2**) used in this paper were prepared by reaction of aldehydes (**1**) with DEPC (3 eq) and LiCN (3 eq) in tetrahydrofuran (THF) at room temperature in good yields (Chart 1 and Table V). Deprotonation of **2a** with bases, such as lithium diisopropylamide (LDA) and *n*-butyllithium (BuLi) in the presence or absence of tetramethylethylenediamine (TMEDA) or hexamethylphosphoramide (HMPA) was carried out, followed by treatment with ethyl iodide at −78 °C in THF. The best result was obtained with *n*-BuLi (1.2 eq) and TMEDA (1.2 eq) (Chart 2). In this manner, several kinds of alkylated products (**3**—**7**) were obtained in 48—93% yields starting from **2a** (see Table I). These products may be

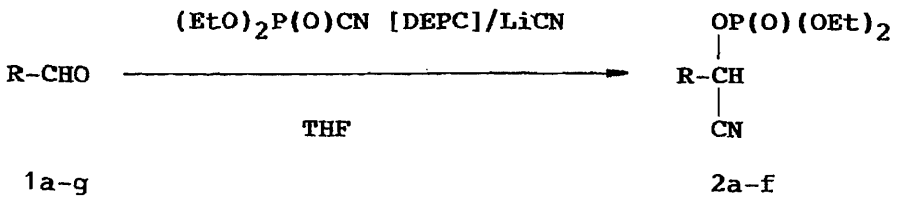

a: R=C_6H_5, b: R=*p*-ClC_6H_4, c: R=*p*-MeC_6H_4, d: R=*p*-$C_6H_5C_6H_4$
e: R=*trans*-MeCH=CH, f: R=*trans*-C_6H_5CH=CH, g: R=*p*-$MeOC_6H_4$

Chart 1

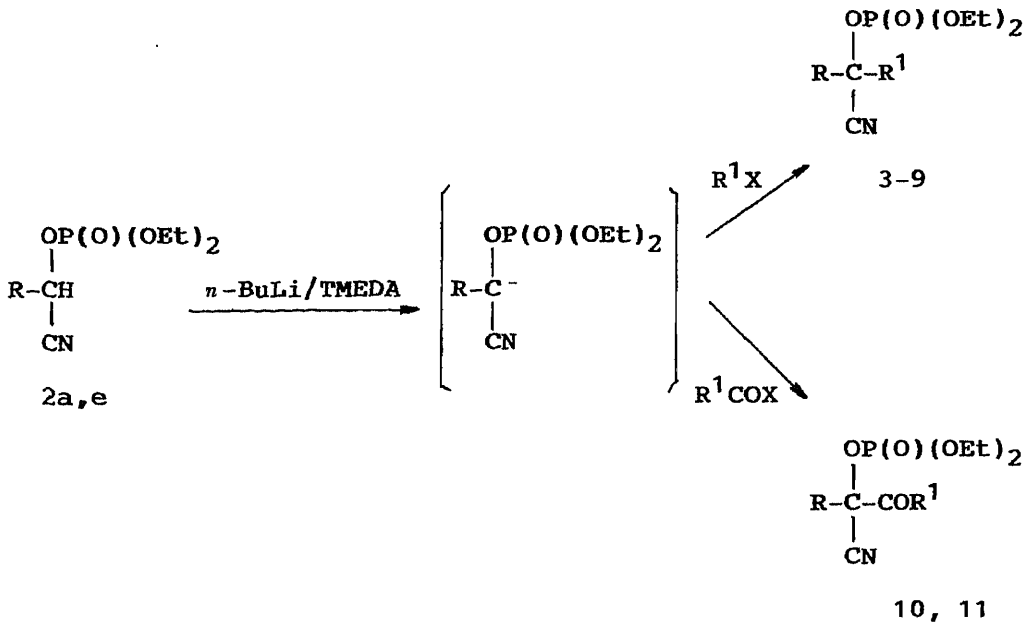

Chart 2

TABLE I. Yields of Alkylated and Acylated Cyanophosphates

Starting compd.	R^1X or R^1COX	Product (%)	R	R^1
2a	EtI	**3** (93)	C_6H_5	Et
2a	MeI	**4** (87)	C_6H_5	Me
2a	$C_6H_5CH_2Br$	**5** (86)	C_6H_5	$C_6H_5CH_2$
2a	CH_2=$CHCH_2Br$	**6** (88)	C_6H_5	CH_2=$CHCH_2$
2a	*n*-C_4H_9Br	**7** (48)	C_6H_5	*n*-C_4H_9
2e	EtI	**8** (90)	MeCH=CH	Et
2e	$C_6H_5CH_2Br$	**9** (76)	MeCH=CH	$C_6H_5CH_2$
2a	C_6H_5COCl	**10** (90)	C_6H_5	C_6H_5
2a	EtOCOCl	**11** (59)	C_6H_5	EtO

applicable to the preparation of α,β-unsaturated nitriles.[1] The anion of **2a** also reacted with benzoyl chloride and ethyl chloroformate to give the acylated products (**10** and **11**) in 90% and 59% yields, respectively. Regiospecific alkylation of **2e** with ethyl iodide and benzyl bromide gave **8** (90%) and **9** (76%), which were found to be a mixture of (*E*)/(*Z*)=95/5 and (*E*)/(*Z*)=93/7, respectively, as judged from proton nuclear magnetic resonance (^{1}H-NMR)

spectra. The alkylated products derived from **2e** may be good precursors for the preparation of γ-oxy-α,β-unsaturated nitriles *via* allylic rearrangement[4] and of 2-alkenenitriles by reaction with organocopper reagents.[6] Alkylation of **2f**, however, did not give satisfactory results because of contamination with the allylic rearrangement product. The cyanohydrin phosphate of an aliphatic aldehyde such as cyclohexylaldehyde failed to give an alkylated or acylated product with *n*-BuLi and TMEDA, and only the starting material was recovered.

Mixed Benzoins and Acyloins

Condensations of the protected cyanohydrins with ketones and aldehydes in the presence of LDA[10] or a phase-transfer catalyst[11] to give benzoins and acyloins are well known. From this point of view, deprotonation of **2a** followed by the addition of 4-chlorobenzaldehyde (**1b**) afforded a mixture of *O*-diethylphosphonobenzoin (**12a**, 24%) and benzoin (**13a**, 58%), which were separated by column chromatography on silica gel (SiO_2), after quenching by the addition of water (condition A). Hydrolysis of **12a** with 0.5 N NaOH in THF gave **13a** in 84% yield. It is interesting that when the reaction mixture was quenched by the addition of acetic acid, instead of water, followed by neutralization with sodium bicarbonate solution (condition B), only benzoin cyanohydrin phosphate (**14a**) was isolated in 89% yield (Chart 3). Structural assignment of **14a** was readily performed by alkaline hydrolysis (0.5 N NaOH) to give **13a** as well as by spectroscopic means [OH band at 3330 cm^{-1} in the infrared (IR) spectrum, CN-carbon signal at δ 111 in the carbon-13 nuclear magnetic resonance (^{13}C-NMR) spectrum and especially the mass spectrum (MS), which exhibited a parent peak at *m/z* 382 ($M^+ - HCN$) and showed the same fragment ions as **12a**]. Similarly, 4-methyl-, 4-phenyl-, and 4-methoxybenzaldehydes (**1c**, **1d**, and **1g**) gave the corresponding benzoin phosphates (**12b—d**)[12] and benzoins (**13b—d**) under condition A, and **14b—d** under condition B; the yields are summarized in Table II.

All the unsymmetrical benzoins (**12a—d** and **13a—d**) thus obtained are products in which the carbonyl group is adjacent to a phenyl ring bearing no substituent. Further isomeric benzoins (**12e—g** and **13e—g**), in which the carbonyl group is adjacent to a phenyl ring having

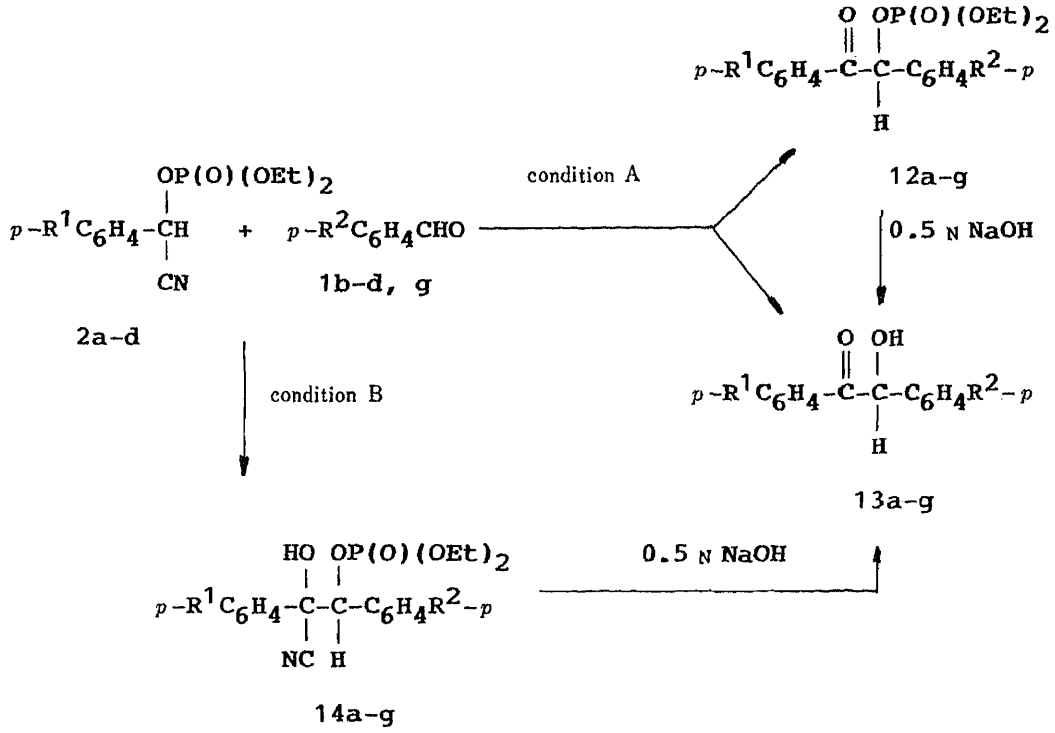

Chart 3

TABLE II. Yields of Benzoin Derivatives (12—14)

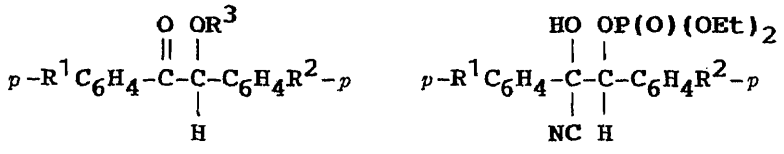

12: $R^3=P(O)(OEt)_2$
13: $R^3=H$

14

	R^1	R^2	Condition A Yield (%) of 12/13	Condition B Yield (%) of 14
a	H	Cl	24/58	89
b	H	Me	42/52	83
c	H	OMe	62/30	96
d	H	C_6H_5	61/34	89
e	Cl	H	21/70	78
f	Me	H	30/56	96
g	C_6H_5	H	24/58	89

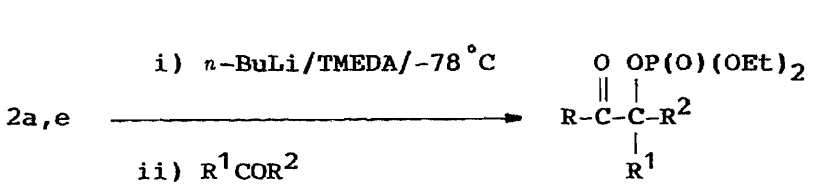

15a: $R^1=R^2=-(CH_2)_5-$
16a: $R^1=R^2=-(CH_2)_4-$
15b: $R^1=R^2=-(CH_2)_5-$
16b: $R^1=R^2=Me$
17b: $R^1=C_6H_5$, $R^2=Me$
18b: $R^1=R^2=C_6H_5$
a: $R=C_6H_5$
b: $R=trans$-MeCH=CH

Chart 4

a substituent at C-4, were also prepared from the substituted cyanophosphates (**2b—d**). However, the thermodynamically stable 4-methoxybenzoin derivatives could not be prepared because of the instability of *p*-anisaldehyde cyanophosphate. The same procedure (condition A) as described for benzoin condensation is applicable to prepare a variety of mixed acyloin phosphates (**15a**, **16a** and **15b—18b**) as shown in Chart 4.

Cyclopropanes

Polysubstituted cyclopropanes have been prepared by reactions of active methylene compounds with ethyl phosphoenolpyruvate,[13] with α-halo esters in the presence of a strong base,[14] and with the betaines derived from 1,2-dicarbonyl compounds and HMPA.[15] These reactions proceed *via* Michael addition followed by 1,3-elimination of the leaving groups. Treatment of **2a** with an α,β-unsaturated ketone such as 3-buten-2-one under condition A gave the acyloin (**19**, 36%)[16] and its phosphate (**20**, 21%), which were probably formed *via* 1,2-addition of an anion to the enone, along with the 1,4-addition product **21** in 9.4% yield. On the other hand, the anion of **2a** reacted with ethyl acrylate within 5 min to yield ethyl 2-cyano-2-phenylcyclopropanecarboxylate in 40% yield.[17] In a similar manner, **2a**, **b**, **e**, and **f** were converted to 1,2-tri- or tetra-substituted cyclopropanes (**22**) by reactions with ethyl acrylate, ethyl methacrylate, acrylonitrile, and methacrylonitrile, yielding a mixture of (*Z*)- and (*E*)-isomers or a single isomer (see Table III). The mechanism of the cyclopropane formation involves the initial Michael addition of the anion to an activated double bond followed by cyclization with liberation of the diethylphosphonooxy function. ^{1}H-NMR spectroscopy was very useful for the assignments of (*Z*)- and (*E*)-stereochemistries of

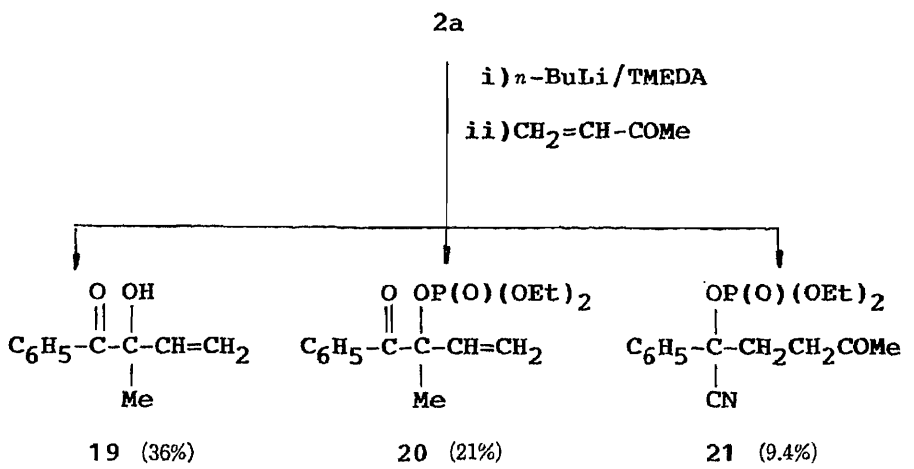

Chart 5

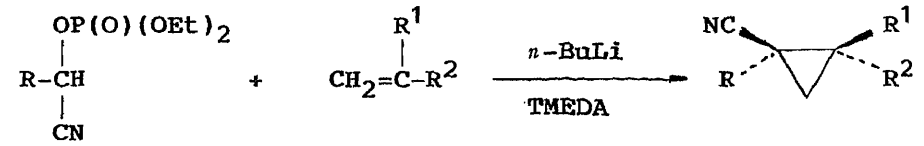

2a,b,e,f

R^1=H or Me
R^2=CO_2Et or CN

22a-h

Chart 6

TABLE III. Yields of Substituted Cyclopropanes (22)

Compd.	R	R^1	R^2	Yield (%) (Ratio of isomers)
22a	C_6H_5	CO_2Et	H	40
22b	C_6H_5	CO_2Et	Me	51
22c	C_6H_5	Me	CN	60
22d	*p*-ClC_6H_4	CO_2Et	Me	85
22e	Me-CH=CH	CO_2Et	Me	48
22f	Me-CH=CH	CN	Me	49
22f'	Me-CH=CH	Me	CN	(**22f**:**22f'** (40:60))
22g	C_6H_5-CH=CH	CO_2Et	H	57
22g'	C_6H_5-CH=CH	H	CO_2Et	(**22g**:**22g'** (58:42))
22h	C_6H_5-CH=CH	CN	Me	28
22h'	C_6H_5-CH=CH	Me	CN	(**22h**:**22h'** (36:64))

cyclopropanes. Namely, the ^{1}H-NMR spectrum of **22g** showed relatively large downfield shifts (at δ 2.24 and 2.16) of the H-1 signal and one of the C-3 methylene proton signals, respectively; the latter can be explained by the deshielding effects of the nitrile and ethoxycarbonyl groups, both of which are located in close proximity. Upon irradiation of the α-proton of the styryl group, a nuclear Overhauser effect (NOE) enhancement of the proton at δ 2.24 was observed. Thus, the signals at δ 2.24 [doublet of doublets (dd), J=8.0 and 6.7 Hz]

TABLE IV. Selected ^{1}H-NMR Data for Cyclopropanes (**22**)

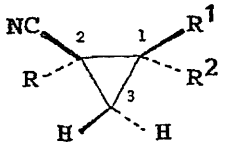

Compd.	^{1}H-NMR ($CDCl_3$) (300 MHz) J (Hz)			
	R^1	R^2		
	1β-H (1β-CH_3)	1α-H (1α-CH_3)	3β-H	3α-H
22a		2.37 dd $J_{cis}=8.5$ $J_{trans}=6.8$	2.24 dd $J_{gem}=5.4$ $J_{trans}=6.8$	1.85 dd $J_{gem}=5.4$ $J_{cis}=8.5$
22b		(1.0 s)	2.41 d $J=5.5$	1.67 d $J=5.5$
22c	(1.86 s)		2.28 d $J=6.0$	1.80 d $J=6.0$
22d		(1.0 s)	2.42 d $J=5.4$	1.63 d $J=5.4$
22e		(1.34 s)	2.25 d $J=5.5$	1.18 d $J=5.5$
22f		(1.43 s)	2.04 d $J=6.3$	1.34 d $J=6.3$
22f'	(1.70 s)		1.71 and/or 1.58 d, $J=6.7$	
22g		2.24 dd $J_{cis}=8.0$ $J_{trans}=6.7$	2.16 dd $J_{gem}=5.1$ $J_{trans}=6.7$	1.60 dd $J_{gem}=5.1$ $J_{cis}=8.0$
22g'	2.65 dd $J_{cis}=8.4$ $J_{trans}=7.8$		1.94 dd $J_{gem}=5.6$ $J_{cis}=8.4$	1.87 dd $J_{gem}=5.6$ $J_{trans}=7.8$
22h		(1.52 s)	2.20 d $J=6.2$	1.52 d $J=6.2$
22h'	(1.78 s)		1.77 and/or 1.99 d, $J=6.2$	

and δ 2.16 (dd, $J=6.7$ and 5.1 Hz) were assigned as 1α-H and 3β-H respectively, and the 3α-H signal was observed at δ 1.60 (dd, $J=8.0$ and 5.1 Hz). In contrast, the C-3 methylene protons of **22g'** appeared as a doublet of doublets at δ 1.94 ($J=8.4$ and 5.6 Hz) and δ 1.87 ($J=7.8$ and 5.6 Hz), which are deshielded to the same extent by the nitrile or the ethoxycarbonyl group, respectively. These results clearly indicate that **22g** is the (*Z*)-isomer and **22g'** is the (*E*)-isomer. Generally speaking, in a cyclopropane ring, the coupling between *trans* vicinal protons is greatest and that of geminal protons is minimum.[18] This can be of great value in stereochemical assignments of the products, 1,2,2-trisubstituted cyclopropanes (**22a**, **22g** and **22g'**). The stereochemical assignments of 1,1,2,2-tetrasubstituted cyclopropanes are rather easy because a large downfield shift in one of the C-3 methylene protons is observed in the (*Z*)-isomer (see Table IV).

Diarylfumaronitriles

A number of methods for the preparation of α,α'-dicyanostilbene, which can be used as a substrate for photocyclization,[19] have been reported.[20] Among them, we were interested in the reaction of α-cyanobenzyl benzenesulfonate[20c] with potassium cyanide to give an α,α'-dicyanostilbene. However, this procedure suffered from the serious disadvantages of being time-consuming and giving only a low yield. When **2a** was treated with **2a** under condition A

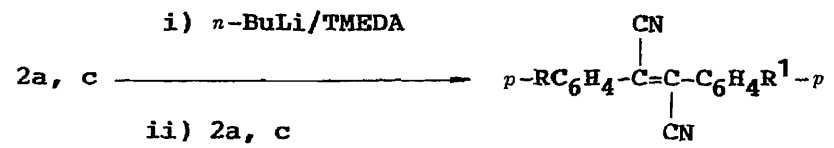

23a: R=R¹=H
23b: R=R¹=Me
23c: R=H, R¹=Me

Chart 7

as described for the preparation of benzoins, diphenylfumaronitrile (**23a**), mp 161—163 °C (lit. mp 161 °C),[20c] was obtained in 76% yield. The structure of **23a** was confirmed by its melting point and ultraviolet (UV) spectroscopic evidence[20d] (see Experimental). The 4,4′-dimethyl and 4-methyl derivatives (**23b** and **23c**) were analogously prepared in 77% and 80% yields, respectively.

In summary, in view of the ease of the preparation of aldehyde cyanophosphates, the reactions mentioned above provide a simple and versatile method for carbon–carbon bond formation and synthesis of mixed benzoin and acyloin phosphates, polysubstituted cyclopropanes and diarylfumaronitriles. Although the reactions were limited to aryl- or allylaldehyde cyanophosphates, we believe that these results extend the usefulness of cyanophosphates in organic synthesis.

Experimental

All melting points and boiling points are uncorrected. IR and UV spectra were recorded with Shimadzu IR-435 and JASCO UVIDEC-505 spectrophotometers. ^{1}H- and ^{13}C-NMR spectra were taken with a Varian XL-300 spectrometer and chemical shifts are given in parts per million (ppm) with tetramethylsilane as an internal standard. MS were recorded with a Hitachi M-80 spectrometer. For column chromatography, SiO_2 (Merck Art 7734) was used.

General Procedure for the Preparation of Cyanophosphates (2a—2d)——A solution of an aldehyde (**1**) (10 mmol), DEPC (30 mmol) and LiCN (30 mmol) in THF (30 ml) was stirred at room temperature for 5 min. After removal of the THF by evaporation, the residue was dissolved in water (10 ml) and benzene–EtOAc (1 : 1, 50 ml). The organic layer was separated, washed with brine, dried (Na_2SO_4), and concentrated. The residual oil was purified by column chromatography using benzene–EtOAc (4 : 1) as an eluent to give the corresponding α-diethylphosphonooxyarylacetonitriles (**2**) as an oil. The boiling points are as follows: **2a**, bp 149 °C (3 mmHg); **2b**, bp 138 °C (0.06 mmHg); **2c**, bp 160 °C (0.03 mmHg) (Kugelrohr). **2d** was analyzed by means of high-resolution MS because of its thermal instability. The cyanophosphates usually exhibited strong absorption bands at 1240—1290 and 970—1100 cm^{-1} in the IR spectra. The ^{1}H-NMR spectra of **2** showed multiplets at δ 1.30—1.42 (6H, 2×OCH$_2$C$\underline{\text{H}}_3$) and δ 4.05—4.20 (4H, m, 2×OC$\underline{\text{H}}_2$CH$_3$). The physicochemical data are summarized in Table V.

General Procedure for Alkylation and Acylation of 2a and 2e——A solution of **2a** (**2e**) (5 mmol) in THF (15 ml) was added to a solution of *n*-BuLi (15% hexane solution, 3.84 ml, 6 mmol) and TMEDA (697 mg, 6 mmol) in THF (10 ml) at −78 °C under N_2. After stirring for 20 min, a solution of an alkyl or acyl halide (R^{1}X or R^{1}COX) (10 mmol) in THF (15 ml) was added dropwise at −78 °C. The reaction flask was then removed from the cooling bath and the mixture was stirred for 30 min. The reaction mixture was concentrated *in vacuo* and the residue was dissolved in water (10 ml) and benzene–EtOAc (1 : 1). The organic layer was separated, washed with brine, dried (Na_2SO_4), and concentrated. The residual oil was purified by column chromatography using benzene–EtOAc (4 : 1) as an eluent to give the corresponding product (**3**—**11**) as an oil. The boiling point of **4a** is bp 177 °C (5 mmHg). The other products were analyzed by high-resolution MS because of their thermal instability. The phosphates usually exhibited strong absorption bands at 1280 and 960—1060 cm^{-1} in the IR spectra and multiplets at δ 1.20—1.40 (6H, m, 2×OCH$_2$C$\underline{\text{H}}_3$) and 3.90—4.25 (4H, m, 2×OC$\underline{\text{H}}_2$CH$_3$) in the ^{1}H-NMR spectra.

2-Diethylphosphonooxy-2-phenylbutanenitrile (**3**): ^{1}H-NMR ($CDCl_3$) δ: 1.0 (3H, t, J=7 Hz, CH$_2$C$\underline{\text{H}}_3$), 2.31 (2H, m, C$\underline{\text{H}}_2$CH$_3$), 7.3—7.7 (5H, m, Ph). MS *m/z*: 317 (M$^+$). High-resolution MS Calcd for $C_{14}H_{20}NO_4P$: 297.1128. Found: 297.1128.

2-Diethylphosphonooxy-2-phenylpropanenitrile (**4**): ^{1}H-NMR ($CDCl_3$) δ: 2.13 (3H, s, CH_3), 7.27—7.75 (5H, m, Ph). MS *m/z*: 283 (M$^+$). *Anal.* Calcd for $C_{13}H_{18}NO_4P$: C, 55.12; H, 6.40; N, 4.95. Found: C, 55.02; H, 6.36; N, 4.84.

2-Diethylphosphonooxy-2,3-diphenylpropanenitrile (**5**): ^{1}H-NMR ($CDCl_3$) δ: 3.34 and 3.62 (1H, ABq, J=

TABLE V. Physicochemical Data for Cyanophosphates (2)[a]

Compd.	Yield (%)	^{1}H-NMR ($CDCl_3$) δ J (Hz) CHOP(O)=	Formula	Analysis (%) Calcd (Found)		
				C	H	N
2a	82	6.05 d, J=9	$C_{12}H_{16}NO_4P$	53.53 (53.21	5.99 5.75	5.20 5.15)
2b	94	6.03 d, J=6	$C_{12}H_{15}ClNO_4P$	47.46 (47.40	4.98 5.05	4.61 4.76)
2c	100	6.01 d, J=8.9	$C_{13}H_{18}NO_4P$	55.12 (55.27	6.40 6.53	4.95 5.02)
2d	85	6.10 d, J=6	$C_{18}H_{20}NO_4P$		[b]	

a) Compounds **2e** and **2f**: see ref. 21. *b*) High-resolution MS Calcd for $C_{18}H_{20}NO_4P$: 345.1128. Found: 345.1127.

14 Hz, CH_2Ph), 7.09—7.53 (10H, m, Ph). MS *m/z*: 359 (M^+). High-resolution MS Calcd for $C_{19}H_{22}NO_4P$: 359.1285. Found: 359.1296.

2-Diethylphosphonooxy-2-phenyl-4-pentenenitrile (**6**): ^{1}H-NMR ($CDCl_3$) δ: 2.96 and 3.14 (each 1H, dd, J=14, 7 Hz, CH_2), 5.23 (2H, m, CH_2=), 5.65 (1H, ddt, J=17, 10, 7 Hz, =CH), 7.26—7.62 (5H, m, Ph). MS *m/z*: 309 (M^+). High-resolution MS Calcd for $C_{15}H_{20}NO_4P$: 309.1131. Found: 309.1130.

2-Diethylphosphonooxy-2-phenylhexanenitrile (**7**): ^{1}H-NMR ($CDCl_3$) δ: 0.88 (3H, t, J=7 Hz, CH_3), 1.38 (4H, m, $CH_2\underline{CH_2}\underline{CH_2}CH_3$), 2.37 (2H, m, $C\underline{H_2}CH_2CH_2CH_3$), 7.40—7.62 (5H, m, Ph). MS *m/z*: 325 (M^+). High-resolution MS Calcd for $C_{16}H_{24}NO_4P$: 325.1441. Found: 325.1440.

α-Benzoyl-α-diethylphosphonooxyphenylacetonitrile (**10**): IR (neat) cm^{-1}: 1700 (CO). ^{1}H-NMR ($CDCl_3$) δ: 7.32—7.85 (10H, m, Ph). MS *m/z*: 373 (M^+). High-resolution MS Calcd for $C_{19}H_{20}NO_5P$: 373.1077. Found: 373.1062.

α-Diethylphosphonooxy-α-ethoxycarbonylphenylacetonitrile (**11**): IR (neat) cm^{-1}: 1750 (CO). ^{1}H-NMR ($CDCl_3$) δ: 1.35 (3H, m, $CO_2CH_2C\underline{H_3}$), 4.30 (2H, m, $CO_2C\underline{H_2}CH_3$), 7.26—7.71 (5H, m, Ph). MS *m/z*: 342 (M^+). High-resolution MS Calcd for $C_{15}H_{20}NO_6P$: 341.1026. Found: 341.1010.

2-Diethylphosphonooxy-2-ethyl-3-butenecarbonitrile (**8**): This was a mixture of (*E*)- and (*Z*)-isomers in the ratio of 95:5 as judged from the ^{1}H-NMR spectrum. The ^{1}H-NMR spectral data for the (*E*)- and (*Z*)-isomers were obtained from the spectrum of the mixture. ^{1}H-NMR ($CDCl_3$) of (*E*)-**10** δ: 1.08 (3H, t, J=7 Hz, $CH_2C\underline{H_3}$), 1.83 (3H, dd, J=6.6, 1.5 Hz, $C\underline{H_3}$–CH=), 2.08 (2H, m, CH_2CH_3), 5.63 (1H, dd, J=15, 1.5 Hz, CH_3–CH=C$\underline{H}$–), 6.26 (1H, dq, J=15, 6.5 Hz, CH_3–C$\underline{H}$=). ^{1}H-NMR ($CDCl_3$) of (*Z*)-**10** δ: 5.55 (1H, br d, J=11 Hz, CH_3–CH=C$\underline{H}$–); other signals are ambiguous due to overlapping with those of (*E*)-**10**. MS *m/z*: 261 (M^+). High-resolution MS Calcd for $C_{11}H_{20}NO_4P$: 261.1128. Found: 261.1107.

2-Benzyl-2-diethylphosphonooxy-3-butenecarbonitrile (**9**): This was a mixture of (*E*)- and (*Z*)-isomers in the ratio of 93:7 as judged from ^{1}H-NMR spectrum. The ^{1}H-NMR spectral data for the (*E*)- and (*Z*)-isomers were obtained from the spectrum of the two mixture. ^{1}H-NMR ($CDCl_3$) of (*E*)-**11** δ: 1.78 (3H, dd, J=6.5, 1.7 Hz, CH_3CH=), 3.21 and 3.36 (1H, ABq, J=14 Hz, CH_2Ph), 5.70 (1H, dd, J=15, 1.7 Hz, CH_3–CH=C$\underline{H}$), 6.16 (1H, dq, J=15, 6.5 Hz, $C\underline{H_3}$–CH=), 7.31—7.33 (5H, m, Ph). ^{1}H-NMR ($CDCl_3$) of (*Z*)-**11** δ: 5.59 (1H, dd, J=11, 2 Hz, CH_3–CH=C$\underline{H}$), 5.88 (1H, dq, J=11, 7 Hz, CH_3–C$\underline{H}$=); other signals are ambiguous due to overlapping with those of (*E*)-**11**. MS *m/z*: 323 (M^+). High-resolution MS Calcd for $C_{16}H_{22}NO_4P$: 323.1286. Found: 323.1299.

General Procedure for Reaction of Cyanophosphates (2) with Arylaldehydes (1)——Condition A: A solution of a cyanophosphate (**2**) (3 mmol) in THF (5 ml) was added to a solution of *n*-BuLi (15% hexane solution, 2.3 ml, 3.6 mmol) and TMEDA (418 mg, 3.6 mmol) in THF (10 ml) at −78 °C under N_2. After stirring of the above mixture for 30 min, a solution of an arylaldehyde (**1**) (3.6 mmol) in THF (5 ml) was added dropwise at −78 °C, and the whole was stirred for 5 min at this temperature, then quenched by the addition of water (10 ml). A mixture of benzene–hexane (100 ml) (1:1) was added and the organic layer was separated, washed with water and dried (Na_2SO_4). Removal of the solvent by evaporation gave an oil, which was subjected to column chromatography. The first fraction of the benzene eluate gave the coresponding benzoin (**13**) [4′-chlorobenzoin (**13a**), mp 114—116 °C (lit.[22] mp 116 °C); 4′-methylbenzoin (**13b**), mp 116—117 °C (lit.[22] mp 116 °C); 4′-methoxybenzoin (**13c**), mp 87—89 °C (lit.[23] mp 87—89 °C); 4-chlorobenzoin (**13e**), mp 89—90 °C (lit.[24] mp 90—91 °C); 4-methylbenzoin (**13f**), mp 109—110 °C (lit.[24] mp 110 °C); 4′-phenylbenzoin (**13d**): mp 144—146 °C (propanol). IR (KBr) cm^{-1}: 3400 (OH), 1680 (CO). ^{1}H-NMR ($CDCl_3$) δ: 4.59 (1H, br s, OH), 5.99 (1H, d, J=7 Hz, C$\underline{H}$OH), 7.28—8.01 (14H, m, Ph). MS *m/z*: 288 (M^+).

Anal. Calcd for $C_{20}H_{16}O_2 \cdot 1/2H_2O$: C, 80.78; H, 5.76. Found: C, 81.00; H, 5.37. 4-Phenylbenzoin (**13g**), mp 148—150 °C (propanol). IR (KBr) cm^{-1}: 3500 (OH), 1680 (CO). ^{1}H-NMR ($CDCl_3$) δ: 4.58 (1H, br s, OH), 5.97 (1H, br s, CHOH), 7.36 (14H, m, Ph). MS *m/z*: 288 (M^+). *Anal.* Calcd for $C_{20}H_{16}O_2$: C, 83.31; H, 5.59. Found: C, 83.26; H, 5.70]. The second fraction of the benzene–EtOAc (4 : 1) eluate gave the corresponding *O*-diethylphosphonobenzoin (**12**) as a viscous oil, which showed a single spot on TLC (SiO_2, benzene–EtOAc, 4 : 1). The oily *O*-diethylphosphonobenzoins (**12a—g**) were analyzed by means of high-resolution MS because of their thermal instability. The *O*-phosphates usually exhibited strong absorption bands at 1260 and 960—1060 cm^{-1} in the IR spectra and multiplets at δ 1.10—1.40 (6H, m, $2 \times OCH_2CH_3$) and 3.80—4.20 (4H, m, $2 \times OCH_2CH_3$) in the ^{1}H-NMR spectra.

4′-Chloro-*O*-diethylphosphonobenzoin (**12a**): IR (neat) cm^{-1}: 1690 (CO). ^{1}H-NMR ($CDCl_3$) δ: 6.59 (1H, d, J = 8.4 Hz, CH), 7.31—7.93 (9H, m, Ph). MS *m/z*: 382 (M^+). High-resolution MS Calcd for $C_{18}H_{20}ClO_5P$: 382.0738. Found: 382.0736.

4′-Methyl-*O*-diethylphosphonobenzoin (**12b**): IR (neat) cm^{-1}: 1690 (CO). ^{1}H-NMR ($CDCl_3$) δ: 2.31 (3H, s, CH_3), 6.61 (1H, d, J = 7.9 Hz, CH), 7.14—7.93 (9H, m, Ph). MS *m/z*: 362 (M^+). High-resolution MS Calcd for $C_{19}H_{23}O_5P$: 362.1281. Found: 362.1288.

4′-Methoxy-*O*-diethylphosphonobenzoin (**12c**): IR (neat) cm^{-1}: 1690 (CO). ^{1}H-NMR ($CDCl_3$) δ: 3.75 (3H, s, OCH_3), 6.63 (1H, d, J = 8.0 Hz, CH), 6.84—7.92 (9H, m, Ph). MS *m/z*: 378 (M^+). High-resolution MS Calcd for $C_{19}H_{23}O_6P$: 378.1232. Found: 378.1230.

4′-Phenyl-*O*-diethylphosphonobenzoin (**12d**): IR (neat) cm^{-1}: 1700 (CO). ^{1}H-NMR ($CDCl_3$) δ: 6.68 (1H, d, J = 7.8 Hz, CH), 7.34—7.98 (14H, m, Ph). MS *m/z*: 425 (M^+). High-resolution MS Calcd for $C_{24}H_{25}O_5P$: 424.1440. Found: 424.1438.

4-Chloro-*O*-diethylphosphonobenzoin (**12e**): IR (neat) cm^{-1}: 1690 (CO). ^{1}H-NMR ($CDCl_3$) δ: 6.55 (1H, d, J = 8.3 Hz, CH), 7.33—7.89 (9H, m, Ph). MS *m/z*: 382 (M^+). High-resolution MS Calcd for $C_{18}H_{20}ClO_5P$: 382.0738. Found: 382.0735.

4-Methyl-*O*-diethylphosphonobenzoin (**12f**): IR (neat) cm^{-1}: 1690 (CO). ^{1}H-NMR ($CDCl_3$) δ: 2.35 (3H, s, CH_3), 6.62 (1H, d, J = 8.3 Hz, CH), 7.17—7.84 (9H, m, Ph). MS *m/z*: 362 (M^+). High-resolution MS Calcd for $C_{19}H_{23}O_5P$: 362.1281. Found: 362.1285.

4-Phenyl-*O*-diethylphosphonobenzoin (**12g**): IR (neat) cm^{-1}: 1690 (CO). ^{1}H-NMR ($CDCl_3$) δ: 6.66 (1H, d, J = 7.9 Hz, CH), 7.35—8.02 (14H, m, Ph). MS *m/z*: 424 (M^+). High-resolution MS Calcd for $C_{24}H_{25}O_5P$: 424.1440. Found: 424.1438.

Condition B: After the reaction of an anion of **2** with **1** had reached completion, the mixture was quenched by the addition of glacial acetic acid followed by neutralization with saturated $NaHCO_3$ solution. The whole was extracted with a mixture of benzene–hexane (1 : 1, 100 ml) and the extract was washed with brine and dried (Na_2SO_4). Removal of the solvent by evaporation gave a viscous oil, which was purified by column chromatography using benzene–EtOAc (4 : 1) as an eluent to give the corresponding 2,3-diaryl-3-diethylphosphonooxy-2-hydroxypropionitrile (**14**), which was recrystallized from benzene–ligroin. The compounds **14** showed no absorption band due to the CN group, and usually exhibited strong absorption bands at 1260 and 960—1060 cm^{-1} in the IR spectra and multiplets at δ 1.10—1.38 (6H, m, $2 \times OCH_2CH_3$) and 3.60—4.0 (4H, m, $2 \times OCH_2CH_3$) in the ^{1}H-NMR spectra due to the *O*-phosphate group. The physicochemical data are summarized in Table VI.

Hydrolysis of 12a and 14a——A solution of **12a** (**14a**) (1 mmol) and 0.5 N NaOH (1 ml) in THF (5 ml) was stirred vigorously at room temperature for 2 h. The reaction mixture was diluted with water (50 ml) and extracted with benzene. The extract was washed with brine and dried (Na_2SO_4). Removal of the solvent by evaporation gave a solid, which was recrystallized from isopropanol to give **13a** in 83% (85%) yield.

General Procedure for the Preparation of Acyloin Phosphates (15a, 16a, and 15b—18b)——A mixture of a cyanophosphate (**2a** or **2e**) (3 mmol) and a ketone (3.6 mmol) was treated under condition A as described for the reaction of **2** with arylaldehyde to give an oil. This was purified by column chromatography using benzene–EtOAc (4 : 1) to give the corresponding acyloin phosphate (**15a**, **16a**, or **15e—18e**) as an oil, which showed a single spot on TLC (SiO_2, benzene–EtOAc, 4 : 1). The products were analyzed by means of high-resolution MS because of their thermal instability. The phosphates usually exhibited strong absorption bands at 1260—1270 and 1060—960 cm^{-1} in the IR spectra. The ^{1}H-NMR spectra of the phosphates showed multiplets at δ 1.20—1.42 (6H, $OCH_2CH_3 \times 2$) and 4.05—4.20 (4H, $OCH_2CH_3 \times 2$).

α-Diethylphosphonooxycyclohexyl Phenyl Ketone (**15a**): This was prepared from **2a** and cyclohexanone in 54% yield. IR (neat) cm^{-1}: 1680 (CO). ^{1}H-NMR ($CDCl_3$) δ: 1.59—2.38 (10H, m, $5 \times CH_2$), 7.39—8.12 (5H, m, Ph). MS *m/z*: 341 (M^+). High-resolution MS Calcd for $C_{17}H_{25}O_5P$: 340.1440. Found: 340.1438.

α-Diethylphosphonooxycyclopentyl Phenyl Ketone (**16a**): This was prepared from **2a** and cyclopentanone in 64% yield. IR (neat) cm^{-1}: 1680 (CO). ^{1}H-NMR ($CDCl_3$) δ: 1.70—1.96 (4H, m, $2 \times CH_2$), 2.32—2.50 (4H, m, $2 \times CH_2$), 7.41—8.05 (5H, m, Ph). MS *m/z*: 327 (M^+). High-resolution MS Calcd for $C_{16}H_{23}O_5P$: 326.1282. Found: 326.1285.

α-Diethylphosphonooxycyclohexyl 1-Propenyl Ketone (**15b**): This was prepared from **2e** and cyclohexanone in 73% yield. IR (neat) cm^{-1}: 1700 (CO). ^{1}H-NMR ($CDCl_3$) δ: 1.58—2.09 (10H, m, $5 \times CH_2$), 1.92 (3H, dd, J = 6.9,

TABLE VI. Physicochemical Data for Compound **14**

Compd.	mp (°C)	IR ν (KBr) cm^{-1} (OH)	Formula	Analysis (%) Calcd (Found)		
				C	H	N
14a[a]	142—144	3200	$C_{19}H_{21}ClNO_5P$	55.68	5.17	3.42
				(55.60	4.95	3.47)
14b	157—159	3200	$C_{20}H_{24}NO_5P$	61.68	6.21	3.59
				(61.88	6.17	3.62)
14c	130—132	3200	$C_{20}H_{24}NO_6P$	59.24	5.96	3.45
				(59.62	6.01	3.57)
14d	146—148	3200	$C_{25}H_{26}NO_5P$	66.50	5.80	3.10
				(66.76	5.58	3.27)
14e	136—138	3200	$C_{19}H_{21}ClNO_5P$	55.68	5.16	3.41
				(55.78	5.00	3.48)
14f	160—162	3200	$C_{20}H_{24}NO_5P$	61.68	6.21	3.59
				(61.65	6.18	3.65)
14g	165—167	3200	$C_{25}H_{26}NO_5P$	66.50	5.80	3.10
				(66.47	5.80	3.10)

a) The ^{13}C-NMR spectrum showed a signal due to a nitrile carbon at δ_{111}.

1.8 Hz, $=CH-C\underline{H}_3$), 6.64 (1H, dd, $J=14$, 1.8 Hz, $CH_3-CH=C\underline{H}$), 7.04 (1H, dq, $J=14$ Hz, 6.9 $CH_3-C\underline{H}=$). MS *m/z*: 305 (M^+). High-resolution MS Calcd for $C_{14}H_{25}O_5P$: 304.1440. Found: 304.1450.

2-Diethylphosphonooxy-2-methyl-4-hexen-3-one (**16b**): This was prepared from **2e** and acetone in 70% yield. IR (neat) cm^{-1}: 1700 (CO). ^1H-NMR ($CDCl_3$) δ: 1.60 (6H, s, $2\times CH_3$), 1.93 (3H, dd, $J=6.8$, 1.8 Hz, $=CH-C\underline{H}_3$), 6.70 (1H, dd, $J=15$, 1.8 Hz, $CH_3-CH=C\underline{H}$), 7.07 (1H, dq, $J=15$, 6.8 Hz, $CH_3-C\underline{H}=$). MS *m/z*: 265 (M^+). High-resolution MS Calcd for $C_{11}H_{22}O_5P$: 265.1205. Found: 265.1203.

2-Diethylphosphonooxy-2-phenyl-4-hexen-3-one (**17b**): This was prepared from **2e** and acetophenone in 73% yield. IR (neat) cm^{-1}: 1700 (CO). ^1H-NMR ($CDCl_3$) δ: 1.82 (3H, dd, $J=6.9$, 1.6 Hz, $=CH-C\underline{H}_3$), 1.98 (3H, s, CH_3), 6.41 (1H, dd, $J=15$, 1.6 Hz, $CH_3-CH=C\underline{H}$), 7.02 (1H, dq, $J=15$, 6.9 Hz, $CH_3-C\underline{H}=$), 7.30—7.44 (5H, m, Ph). MS *m/z*: 326 (M^+). High-resolution MS Calcd for $C_{16}H_{23}O_5P$: 326.1284. Found: 326.1282.

1-Diethylphosphonooxy-1,1-diphenyl-3-penten-2-one (**18b**): This was prepared from **2e** and benzophenone in 51% yield. IR (neat) cm^{-1}: 1700 (CO). ^1H-NMR ($CDCl_3$) δ: (3H, dd, $J=6.9$, 1.7 Hz, $=CH-C\underline{H}_3$), 6.63 (1H, dd, $J=15$, 1.7 Hz, $CH_3-CH=C\underline{H}$), 7.07 (1H, dq, $J=15$, 6.9 Hz, $CH_3-C\underline{H}=$), 7.03—7.40 (10H, m, Ph). MS *m/z*: 388 (M^+). High-resolution MS Calcd for $C_{21}H_{25}O_5P$: 388.1438. Found: 388.1435.

Reaction of 2a with 3-Buten-2-one——A mixture of **2a** (807 mg, 3 mmol) and 3-buten-2-one (252 mg, 3.6 mmol) in THF (10 ml) was treated under condition A as described for the preparation of benzoins to give a crude oil, which was subjected to column chromatography. The first fraction of the benzene eluate gave 2-hydroxy-2-methyl-1-phenyl-3-buten-1-one (**19**)[16] (190 mg, 36%) as an oil. IR (neat) cm^{-1}: 3500 (OH), 1680 (CO). ^1H-NMR ($CDCl_3$) δ: 1.67 (3H, s, CH_3), 4.44 (1H, s, OH), 5.34 (1H, dd, $J=10.5$, 1.1 Hz, 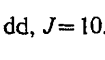), 5.54 (1H, dd, $J=16.8$, 1.1 Hz,), 6.22 (1H, dd, $J=16.8$, 10.5 Hz, $=CH$), 7.41—8.04 (5H, m, Ph). MS *m/z*: 176 (M^+). The following benzene–EtOAc (4:1) eluate gave 2-diethylphosphonooxy-2-methyl-1-phenyl-3-buten-1-one (**20**) (200 mg, 21%) and 5-cyano-5-diethylphosphonooxy-5-phenylpentan-2-one (**21**) (96 mg, 9.4%), each as an oil. **20**: IR (neat) cm^{-1}: 1690 (CO), 1290 (P=O), 1060—960 (P–O–C). ^1H-NMR ($CDCl_3$) δ: 1.14—1.27 (6H, m, $2\times OCH_2C\underline{H}_3$), 1.88 (3H, s, CH_3), 3.75—4.02 (4H, m, $2\times OC\underline{H}_2CH_3$), 5.32 (1H, d, $J=10.7$ Hz,), 5.46 (1H, d, $J=17.5$ Hz,), 6.27 (1H, dd, $J=$ 17.5, 10.7 Hz, $-CH=$), 7.36—8.03 (5H, m, Ph). MS *m/z*: 313 ($M^+ + 1$). High-resolution MS Calcd for $C_{15}H_{22}O_5P$: 313.1202. Found: 313.1187. **21**: IR (neat) cm^{-1}: 1710 (CO), 1260 (P=O), 1060—960 (P–O–C). ^1H-NMR ($CDCl_3$) δ: 1.21—1.30 (6H, m, $2\times OCH_2C\underline{H}_3$), 2.14 (3H, s, CH_3), 2.41—2.79 (4H, m, CH_2CH_2), 3.89—4.12 (4H, m, $2\times OC\underline{H}_2CH_3$), 7.41—7.63 (5H, m, Ph). MS *m/z*: 339 (M^+). High-resolution MS Calcd for $C_{16}H_{22}NO_5P$: 339.1235. Found: 339.1286.

General Procedure for the Preparation of Cyclopropanes (22a—22h)——A mixture of a cyanophosphate (**2**) (3 mmol) and an α,β-unsaturated ester or nitrile (6 mmol) in THF was treated under condition A as described for the preparation of benzoin to give a crude oil, which was purified by column chromatography (benzene). The ^1H-NMR spectral data for cyclopropane ring protons as well as 1-methyl protons are summarized in Table IV.

(*Z*)-Ethyl 2-Cyano-2-phenylcyclopropanecarboxylate (22a)——This was prepared from **2a** and ethyl acrylate as a single isomer (oil), bp 143 °C (3 mmHg). IR (neat) cm^{-1}: 2200 (CN), 1720 (CO). ^{1}H-NMR ($CDCl_3$) δ: 1.33 (3H, t, J= 7.3 Hz, $CO_2CH_2C\underline{H}_3$), 4.30 (2H, q, J=7.3 Hz, $CO_2C\underline{H}_2CH_3$), 7.35 (5H, br s, Ph). MS *m/z*: 215 (M^+). *Anal.* Calcd for $C_{13}H_{13}NO_2$: C, 72.53; H, 6.08; N, 6.08. Found: C, 72.51; H, 6.25; N, 6.22.

(*Z*)-Ethyl 2-Cyano-1-methyl-2-phenylcyclopropanecarboxylate (22b)——This was prepared from **2a** and ethyl methacrylate as a single isomer (oil), bp 138 °C (3 mmHg). IR (neat) cm^{-1}: 2200 (CN), 1720 (CO). ^{1}H-NMR ($CDCl_3$) δ: 1.36 (3H, t, J=7.3 Hz, $CO_2CH_2C\underline{H}_3$), 4.31 (2H, q, J=7.3 Hz, $CO_2C\underline{H}_2CH_3$), 7.32—7.40 (5H, m, Ph). MS *m/z*: 229 (M^+). *Anal.* Calcd for $C_{14}H_{15}NO_2$: C, 73.34; H, 6.59; N, 6.11. Found: C, 73.18; H, 6.63; N, 5.90.

(*E*)-1-Methyl-2-phenylcyclopropane-1,2-dicarbonitrile (22c)——This was prepared from **2a** and methacrylonitrile as a single isomer, mp 89—91 °C (benzene–ligroin). IR (KBr) cm^{-1}: 2200 (CN). ^{1}H-NMR ($CDCl_3$) δ: 7.43 (5H, br s, Ph). MS *m/z*: 182 (M^+). *Anal.* Calcd for $C_{12}H_{10}N_2$: C, 79.09; H, 5.53; N, 15.38. Found: C, 79.07; H, 5.54; N, 15.30.

(*Z*)-Ethyl 2-Cyano-1-methyl-2-*p*-chlorophenylcyclopropanecarboxylate (22d)——This was prepared from **2b** and ethyl methacrylate as a single isomer (oil), bp 142 °C (0.004 mmHg). IR (neat) cm^{-1}: 2200 (CN), 1720 (CO). ^{1}H-NMR ($CDCl_3$) δ: 1.35 (3H, t, J=6.8 Hz, $CO_2CH_2C\underline{H}_3$), 4.30 (2H, q, J=6.8 Hz, $CO_2C\underline{H}_2CH_3$), 7.28 and 7.38 (each 2H, each d, J=8.5 Hz, Ph). MS *m/z*: 264 (M^+). *Anal.* Calcd for $C_{14}H_{14}ClNO_2$: C, 63.75; H, 5.35; N, 5.31. Found: C, 63.71; H, 5.41; N, 5.10.

(*Z*)-Ethyl 2-Cyano-1-methyl-2-(1-propenyl)cyclopropanecarboxylate (22e)——This was prepared from **2e** and ethyl methacrylate as a single isomer (oil), bp 100 °C (3 mmHg). IR (neat) cm^{-1}: 2200 (CN), 1720 (CO). ^{1}H-NMR ($CDCl_3$) δ: 1.31 (3H, t, J=7.3 Hz, $CO_2CH_2C\underline{H}_3$), 1.78 (3H, dd, J=6.6, 1.6 Hz, $=CH-C\underline{H}_3$), 4.23 (2H, q, J=7.3 Hz, $CO_2C\underline{H}_2CH_3$), 5.17 (1H, dd, J=15, 1.6 Hz, $CH_3-CH=C\underline{H}$), 6.05 (1H, dq, J=15, 6.6 Hz, $CH_3-C\underline{H}=$). MS *m/z*: 193 (M^+). *Anal.* Calcd for $C_{11}H_{15}NO_2$: C, 68.37; H, 7.82; N, 7.25. Found: C, 68.36; H, 7.82; N, 7.23.

(*Z*)- and (*E*)-1-Methyl-2-(1-propenyl)cyclopropane-1,2-dicarbonitriles (22f and 22f')——These were prepared from **2e** and methacrylonitrile as a mixture of (*Z*)- and (*E*)-isomers, which were separated by column chromatography (benzene). (*Z*)-Isomer (**22f**): bp 150 °C (2 mmHg) (Kugelrohr). IR (KBr) cm^{-1}: 2200 (CN). ^{1}N-NMR ($CDCl_3$) δ: 1.81 (3H, dd, J=6.6, 1.7 Hz, $=CH-C\underline{H}_3$), 5.13 (1H, dd, J=15, 1.7 Hz, $CH_3-CH=C\underline{H}$), 6.12 (1H, dq, J=15, 6.6 Hz, $CH_3-CH=$). MS *m/z*: 146 (M^+). *Anal.* Calcd for $C_9H_{10}N_2$: C, 73.94; H, 6.90; N, 19.16. Found: C, 74.05; H, 7.06; N, 18.81. (*E*)-Isomer (**22f'**): IR (KBr) cm^{-1}: 2200 (CN). ^{1}H-NMR ($CDCl_3$) δ: 1.82 (3H, dd, J=6.6, 1.6 Hz, $=CH=C\underline{H}_3$), 5.26 (1H, dd, J=14, 1.6 Hz, $CH_3-CH=C\underline{H}$), 6.15 (1H, dq, J=14, 6.6 Hz, $CH_3-CH=$). MS *m/z*: 146 (M^+). High-resolution MS Calcd for $C_9H_{10}N_2$: 146.0844. Found: 146.0857.

(*Z*)- and (*E*)-Ethyl 2-Cyano-2-styrylcyclopropanecarboxylates (22g and 22g')——These were prepared from **2f** and ethyl acrylate as a mixture of (*Z*)- and (*E*)-isomers, which were separated by column chromatography (benzene). (*Z*)-Isomer (**22g**): Oil, bp 162 °C (3 mmHg). IR (neat) cm^{-1}: 2200 (CN), 1720 (CO). ^{1}H-NMR ($CDCl_3$) δ: 1.33 (3H, t, J=7.3 Hz, $CO_2CH_2C\underline{H}_3$), 4.28 (2H, q, J=7.3 Hz, $CO_2C\underline{H}_2CH_3$), 5.57 (1H, d, J=15.8 Hz, Ph–CH=C<u>H</u>), 6.97 (1H, d, J=15.8 Hz, Ph–CH=), 7.27—7.34 (5H, m, Ph). MS *m/z*: 241 (M^+). *Anal.* Calcd for $C_{15}H_{15}NO_2$: C, 74.66; H, 6.27; N, 5.81. Found: C, 74.45; H, 6.30; N, 5.64. (*E*)-Isomer (**22g'**): Oil, bp 162 °C (3 mmHg). IR (neat) cm^{-1}: 2200 (CN), 1720 (CO). ^{1}H-NMR ($CDCl_3$) δ: 1.27 (3H, t, J=7.3 Hz, $CO_2CH_2C\underline{H}_3$), 4.20 (2H, q, J=7.3 Hz, $CO_2C\underline{H}_2CH_3$), 6.05 (1H, d, J=16.2 Hz, Ph–CH=C<u>H</u>), 6.97 (1H, d, J=16.2 Hz, Ph–CH=), 7.26—7.37 (5H, m, Ph). MS *m/z*: 241 (M^+). *Anal.* Calcd for $C_{15}H_{15}NO_2$: C, 74.66; H, 6.27; N, 5.81. Found: C, 74.72; H, 6.33; N, 5.70.

(*Z*)- and (*E*)-1-Methyl-2-styrylcyclopropanecarboxylates (22h and 22h')——These were prepared from **2f** and methacrylonitrile as a mixture of (*Z*)- and (*E*)-isomers, which were separated by column chromatography (benzene). (*Z*)-Isomer (**22h**): mp 126—128 °C (benzene–ligroin). IR (KBr) cm^{-1}: 2200 (CN). ^{1}H-NMR ($CDCl_3$) δ: 5.74 (1H, d, J=15.8 Hz, Ph–CH=C<u>H</u>), 6.98 (1H, d, J=15.8 Hz, Ph–CH=), 7.34—7.38 (5H, m, Ph). MS *m/z*: 208 (M^+). *Anal.* Calcd for $C_{14}H_{12}N_2$: C, 80.74; H, 5.81; N, 13.45. Found: C, 81.09; H, 5.78; N, 13.25. (*E*)-Isomer (**22h'**): mp 119—121 °C (benzene–ligroin). IR (KBr) cm^{-1}: 2200 (CN). ^{1}H-NMR ($CDCl_3$) δ: 5.85 (1H, d, J=15.8 Hz, Ph–C<u>H</u>=CH), 7.03 (1H, d, J=15.8 Hz, Ph–CH=), 7.30—7.42 (5H, m, Ph). MS *m/z*: 208 (M^+). *Anal.* Calcd for $C_{14}H_{12}N_2$: C, 80.74; H, 5.81; N, 13.45. Found: C, 81.09; H, 5.76; N, 13.31.

General Procedure for the Preparation of Diarylfumaronitriles (23a—c)——After the anion formation of a cyanophosphate (**2a** or **2c**) (5 mmol) under the ordinary conditions had been completed, a solution of **2a** (**2c**) (6 mmol) in THF (5 ml) was added dropwise at −78 °C, and stirring was continued for 10 min at room temperature. Work-up gave an oily residue, which was purified by column chromatography using benzene as an eluent to give **23**.

α,α'-Diphenylfumaronitrile (23a)——Yield: 76%. mp 162—163 °C (EtOH) (lit.[19c] 161 °C). UV_{max}^{EtOH} nm (log ε): 235 (4.1), 325 (3.9) [lit.[19d] $UV_{max}^{50\%\ EtOH}$ nm log ε): 238 (4.0), 331 (3.91)]. MS *m/z*: 230 (M^+).

α,α'-Di-*p*-tolylfumaronitrile (23b)——Yield: 73%. mp 196—197 °C (EtOH) (lit.[19e] mp 197 °C). UV_{max}^{EtOH} nm (log ε): 215 (4.1), 235 (3.9), 343 (4.2). MS *m/z*: 258 (M^+).

α-Phenyl-α'-*p*-tolylfumaronitrile (23c)——Yield: 80%. mp 138—140 °C (EtOH). UV_{max}^{EtOH} nm (log ε): 218 (4.1), 235 (3.9), 338 (4.2). MS *m/z*: 244 (M^+). *Anal.* Calcd for $C_{17}H_{12}N_2$: C, 83.58; H, 4.95; N, 11.47. Found: C, 83.55; H, 5.07; N, 11.09.

Acknowledgment We thank Miss M. Nabae and Miss M. Danjo for the measurements of NMR spectra and MS, and Mrs. Y. Tsukamoto for microanalysis.

References and Notes

1) S. Harusawa, R. Yoneda, T. Kurihara, Y. Hamada, and T. Shioiri, *Tetrahedron Lett.*, **25**, 427 (1984).
2) S. Harusawa, S. Nakamura, S. Yagi, T. Kurihara, Y. Hamada, and T. Shioiri, *Synth. Commun.*, **14**, 1365 (1984).
3) S. Harusawa, M. Miki, J. Hirai, and T. Kurihara, *Chem. Pharm. Bull.*, **33**, 899 (1985); T. Kurihara, S. Harusawa, J. Hirai, and R. Yoneda, *J. Chem. Soc., Perkin Trans. 1*, **1987**, 1771.
4) S. Harusawa, M. Miki, R. Yoneda, and T. Kurihara, *Chem. Pharm. Bull.*, **33**, 2164 (1985); T. Kurihara, M. Miki, R. Yoneda, and S. Harusawa, *ibid.*, **34**, 2747 (1986).
5) M. Miki, T. Wakita, S. Harusawa, and T. Kurihara, *Chem. Pharm. Bull.*, **33**, 3558 (1986).
6) R. Yoneda, S. Harusawa, and T. Kurihara, *Chem. Pharm. Bull.*, **35**, 913 (1987).
7) T. Kurihara, M. Hanakawa, S. Harusawa, and R. Yoneda, *Chem. Pharm. Bull.*, **34**, 4545 (1986).
8) J. D. Albricht, *Tetrahedron*, **39**, 3207 (1983), and references cited therein.
9) S. Hünig and H. Reichelt, *Chem. Ber.*, **119**, 1772 (1986), and references cited therein.
10) S. Hünig and G. Wehner, *Synthesis*, **1975**, 391.
11) M. D. Rozwadowska, *Tetrahedron*, **41**, 3135 (1985).
12) Benzoin phosphates are useful for the preparation of substituted phenylchalcone oxides (unpublished results).
13) von U. Schmidt, R. Schroer, and A. Hochrainer, *Justus Liebigs Ann. Chem.*, **733**, 180 (1970).
14) L. L. MaCoy, *J. Am. Chem. Soc.*, **84**, 2246 (1962).
15) H. Faudeut and R. Burgada, *Synthesis*, **1980**, 642.
16) B. Mauze, A. Doucoure, and L. Miginiac, *J. Organomet. Chem.*, **215**, 1 (1981).
17) A part of this study has been reported as a brief communication: R. Yoneda, K. Santo, S. Harusawa, and T. Kurihara, *Synth. Commun.*, **17**, 921 (1987).
18) K. B. Wiberg and B. J. Nist, *J. Am. Chem. Soc.*, **85**, 2788 (1963).
19) *a*) M. V. Sargent and C. J. Timmons, *J. Chem. Soc.*, **1964**, 5544; *b*) K. Ichimura and S. Watanabe, *Bull. Chem. Soc. Jpn.*, **49**, 2220 (1976); *c*) *Idem, ibid.*, **49**, 2224 (1976).
20) *a*) L. Chalanay and E. Knoevenagel, *Chem. Ber.*, **25**, 285 (1892); *b*) J. T. Thurston and R. L. Shriner, *J. Org. Chem.*, **2**, 183 (1937); *c*) R. M. Dodson and H. W. Turner, *J. Am. Chem. Soc.*, **73**, 4517 (1951); *d*) D. G. Coe, M. M. Gale, R. P. Linstead, and C. J. Timmons, *J. Chem. Soc.*, **1957**, 123; *e*) T. Mukaiyama, I. Kuwajima, and K. Ohno, *Bull. Soc. Chem. Jpn.*, **38**, 1954 (1965).
21) T. Kurihara, M. Miki, K. Santo, S. Harusawa, and R. Yoneda, *Chem. Pharm. Bull.*, **34**, 4620 (1986).
22) R. J. Arnold and R. C. Fuson, *J. Am. Chem. Soc.*, **58**, 1295 (1936).
23) L. Krepski, S. M. Heilmann, and J. K. Rasmussen, *Tetrahedron Lett.*, **24**, 4075 (1983).
24) W. S. Ide and J. S. Buck, *Org. React.*, **4**, 269 (1948).

[Chem. Pharm. Bull. 35(12)4789—4792(1987)]

Studies on the Constituents of Umbelliferae Plants. XVII.[1] Structures of Three New Ligustilide Derivatives from *Ligusticum wallichii*

MASARU KOBAYASHI* and HIROSHI MITSUHASHI

Faculty of Pharmaceutical Sciences, Hokkaido University, Kita-ku, Sapporo 060, Japan

(Received June 1, 1987)

The Chinese Umbelliferae plant *Ligusticum wallichii* was found to contain all the new components previously found in *Cnidium officinale*, which is closely related with *L. wallichii* and is used as the source plant of the crude drug "senkyu" in Japan. Three ligustilide derivatives, senkyunolide K (**2**), senkyunolide L (**3**), and senkyunolide M (**4**) were isolated simultaneously and their structures were elucidated as 4β-hydroxylsenkyunolide A (**2**), 6-hydroxy-7-chloro-6,7-dihydroligustilide (**3**) and 6-butyryl-7-hydroxy-6,7-dihydroligustilide (**4**) on the basis of the spectral properties. Treatment of ligustilide 6,7-epoxide with hydrochloric acid readily gave **3** and thus **3** was considered to have been formed during the extraction of the plant.

Keywords——senkyunolide; phthalide; *Ligusticum wallichii*; Umbelliferae

Volatile alkylphthalide derivatives are the common and unique constituents of the two Umbelliferae crude drugs "senkyu," the dried rhizomes of *Cnidium officinale* (syn. *Ligusticum officinale*), and "toki," the dried roots of *Angelica acutiloba*, though the content in the latter is less than one-tenth of that in the former. The predominant compound is ligustilide (**1**) in both plants. In the previous reports we showed that they both contain a variety of oxygenated derivatives of **1**.[1,2] Two novel ligustilide dimers were also found to occur as minor components of *A. acutiloba* extract.[1] *C. officinale* is closely related with the important Chinese Umbelliferae plant *Ligusticum wallichii* (syn. *L. sinense*) which is used frequently as an ingredient in the prescriptions of traditional Chinese medicines. In the present study, we analyzed the lipids of *L. wallichii* and confirmed that it contains all the new components found in *C. officinale*, namely, pregnenolone (**5**), coniferyl ferulate (**6**), falcarindiol (**7**), and nine hydroxyphthalide derivatives (senkyunolide B to senkyunolide J, **8**—**16**).[1] Three phthalide derivatives, senkyunolide K, senkyunolide L (which is probably an artifact), and senkyunolide M, were isolated simultaneously and their structures were shown to be **2**, **3**, and **4** respectively.

The crude lipid of *L. wallichii* rhizome, commercially obtained in Chengdu, Sichuan, China, was separated by solvent extraction and partition and subjected to chromatography as described in the previous report.[2] It gave compounds **5** to **16** in a pure state or as a mixture (senkyunolide H to senkyunolide J, **14**—**16**). They were identified by comparison with authentic samples previously isolated from *C. officinale* (Experimental). We could not find marked differences between *C. officinale* and *L. wallichii*, either in the nature or relative compositions of the components. As far as the chemical components are concerned, their differences are no more than those ordinarily seen in strain variations of the same plant, grown in fairly different localities. The main exception was that *L. wallichii* produces a significant amount of ligustilide dimer levistolide *A* (**17**)[3] which we were unable to detect in *C. officinale*. Also, the amounts of polar and non-polar extracts from *L. wallichii* were significantly higher than in the case of *C. officinale*. As described in the preceding work,[1] the

oxygenated phthalide derivatives are composite products formed from those originally present in the plant, and those derived by autoxidation of major non-polar phthalides. Prolonged storage after the preparation of the crude drug would greatly affect the content of oxygenated phthalides, and hence the nature of the crude drug itself.

Senkyunolide K (**2**), $[\alpha]_D$ −6°, $C_{12}H_{16}O_3$ was a monohydroxy phthalide derivative. It was suggested to be a derivative of the major component senkyunolide A (**18**),[4] as indicated by the similar infrared (IR, 3400, 1760, 1735, 1610 cm^{-1}), proton nuclear magnetic resonance [^{1}H-NMR, δ 0.91 (3H, t, J=7.0 Hz, 13-H), 4.70 (1H, t, J=7.5 Hz, hydroxy mithine), 5.24 (1H, dd, J=7.5, 3.5 Hz, 3-H), 6.04 (1H, dt, J=10.0, 4.5 Hz, 6-H), 6.30 (1H, br d, J=10.0 Hz)], ultraviolet [UV, 273 nm (ε, 2600)] and mass (MS, m/z 208 (M^+), 190 (M^+-H_2O), 133 (M^+-H_2O, C_4H_9)] spectra. The signal of the C-3 proton (δ 5.24) was strongly deshielded, compared with that of senkyunolide A (δ 4.9, dd, J=8.0, 4.0 Hz).[4] It is a result of the deshielding effect of the nearly parallel C-4 hydroxyl group, and limited the stereochemistry to 3*S*,4*R* or 3*R*,4*S*. A decoupling experiment showed that the hydroxymethine proton at δ 4.7 was coupled with the methylene protons at δ 2.71 (m), which in turn were coupled with C-6 olefinic proton at δ 6.04. Horeau determination[5] of the configuration at C-4 showed it to be *R*, and hence that of C-3 is *S*. Senkyunolide L was thus shown to be 4β-hydroxysenkyunolide A (**2**).

Senkyunolide L (**3**), $[\alpha]_D$ 0°, $C_{12}H_{15}ClO_3$ is a chlorohydrin derivative of **1**. It showed the signals due to the 3(10)-*Z* butylidene side chain in the ^{1}H-NMR spectrum [δ 0.96 (3H, t, J=7.3 Hz), 1.51 (2H, sext, J=7.3 Hz), 2.38 (2H, dt, J=7.8, 7.3 Hz), 5.36 (1H, t, J=7.8 Hz). The UV spectrum of **3** [272 nm (ε, 18400) was similar to that of 6,7-dihydroligustilide [272 nm (ε, 17800).[6] It has a chlorohydrin group in the cyclohexene ring and the methine signals appeared at δ 4.35 (ddd, J=5.0, 3.0, 3.0 Hz) and at 4.63 (d, J=3.0 Hz). Its MS showed peaks at m/z 244 and 242 as the characteristic molecular ions and at m/z 207 (M^+-Cl), 200 ($M^+-C_3H_6$), and 198 ($M^+-C_2H_4O$). The ion at m/z 198 is due to the retro-Deals–Alder-type cleavage with loss of a C_2H_4O fragment and indicated that the location of the hydroxyl group is at C-6. The C-10 olefinic proton (δ 5.36) was not influenced by nearby substituents. Epoxidation of **1** followed by brief treatment with hydrochloric acid in tetrahydrofuran readily gave **3** in 80% overall yield. The structure of senkyunolide L was thus shown to be **3**, the chlorohydrin derivative of **1**. The coupling constant of the C-6 and C-7 protons (3.0 Hz) was similar to that (4.0 Hz) of the 6,7-*Z* dihydroxyligustilide derivative senkyunolide H (**14**) and different from that of the 6,7-*E*-diol senkyunolide I (**15**, 6.5 Hz), both of which were obtained by acid hydrolysis of the 6,7-epoxyligustilide.[2] Although the opening of epoxide rings generally affords *E*-isomers, the substitution reaction with chlorine at C-7, which is conjugated with the diene, apparently involves a different pathway and compound **3** was regarded as the *Z*-isomer. Chlorinated natural products are not unusual (for example, many marine natural products), but compound **3** was supposed to be a secondary product derived from the reaction of ligustilide 6,7-epoxide with residual hydrogen chloride in the chloroform which was used for the extraction. Ligustilide 6,7-epoxide is known to occur in *L. wallichii*.[7]

Senkyunolide M (**4**), $[\alpha]_D$ 0°, $C_{16}H_{22}O_4$, is also a derivative of 6,7-dihydroligustilide as indicated by the UV [272 nm (ε, 17000)] and ^{1}H-NMR [δ 0.95 (3H, t, J=7.3 Hz), 1.50 (2H, sext, J=7.3 Hz), 2.36 (2H, dt, J=7.8, 7.3 Hz), 5.26 (1H, t, J=7.8 Hz)] spectra. Other signals were those of a butyryl group [δ 0.95 (3H, t, J=7.5 Hz), 1.64 (2H, sext, J=7.5 Hz), 2.59 (2H, t, J=7.5 Hz)], and a secondary hydroxyl group at δ 4.92 (d, J=8.0 Hz). The methine proton adjacent to the butyryl group appeared at δ 2.80 (1H, ddd, J=11.2, 8.0, 3.5 Hz) and it was shown by a decoupling experiment to be coupled with a hydroxy methine at δ 4.92. Its MS showed the ions derived from cleavage of the butyryl side chain (m/z 71 and 207), and an ion due to the retro-Deals–Alder cleavage at m/z 180 which indicates the hydroxyl group to be at C-4 or C-7. The C-10 olefinic proton (δ 5.26) appeared at a similar position to that in **1** (δ 5.22)

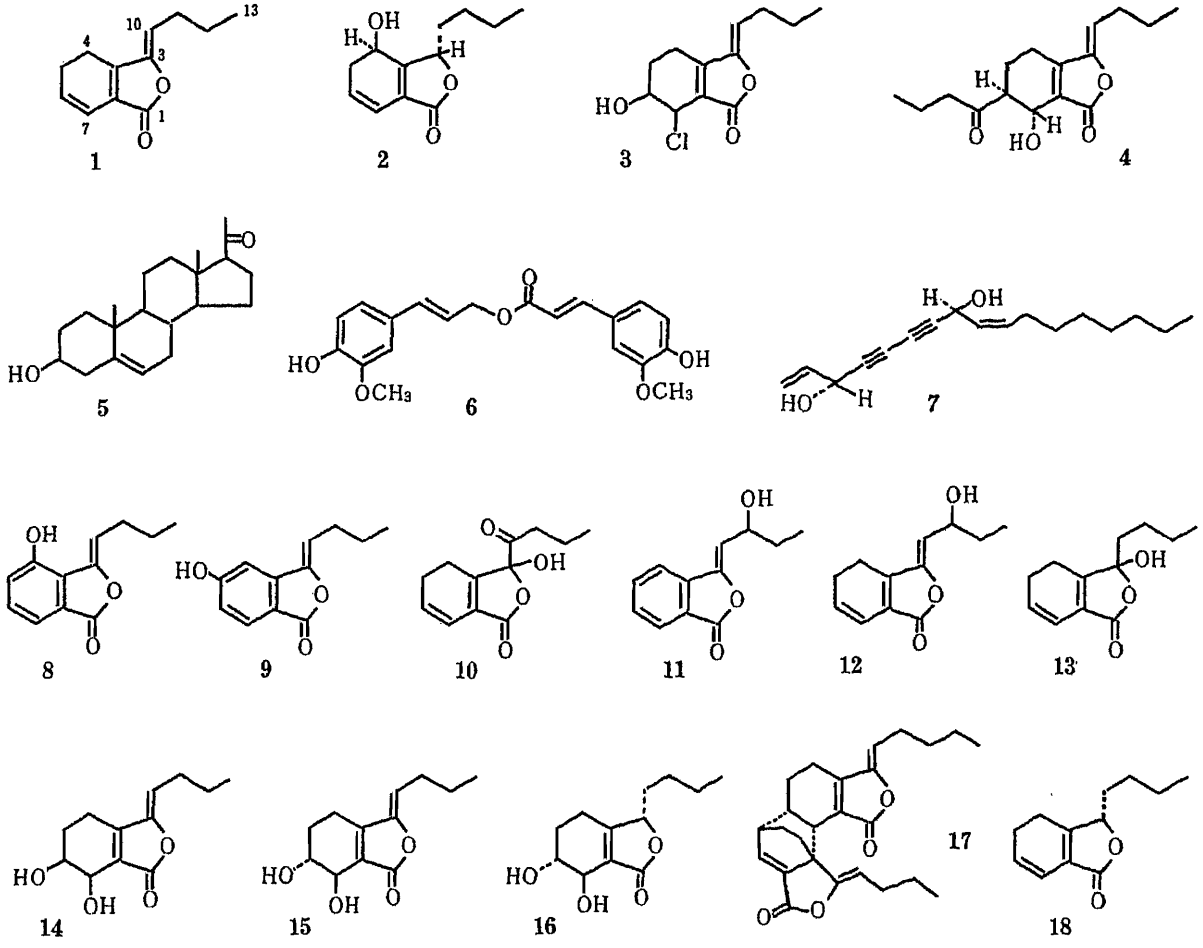

Chart 1

and there was no nuclear Overhauser effect (NOE) between this proton and the hydroxymethine proton. These results indicate compound **4** to be 6-butyryl 7-hydroxy 6,7-dihydroligustilide. The coupling constant (8.0 Hz) between the C-6 and C-7 protons suggests the relative configuration of the substituents at C-6 and C-7 to be *E*-diequatorial. This is the first reported alkylphthalide derivative having a side chain on the cyclohexane ring. Alkylphthalides are known to be biosynthesized from polyketide precursors.[8] Compound **4** is a new type of phthalide possibly derived by the combination of an ordinary phthalide unit and butyryl coenzyme A.

Experimental

Optical rotations were determined on a JASCO DIP-4 digital polarimeter. ^{1}H- and ^{13}C-NMR spectra were determined on a JEOL FX-200 spectrometer at 200 MHz (^{1}H) and 50 MHz (^{13}C) in $CDCl_3$ solution with tetramethylsilane as an internal standard. Electron impact (EI)-MS were determined on a JEOL JMS D-300 spectrometer. IR spectra were determined on a JASCO A-102 spectrometer. Chromatography was carried out on a column of silica gel by the flash chromatography method.[9]

Fractionation of *L. wallichii* Extract——Commercial rhizomes of *L. wallichii*, cultivated in Sichuan Province, China, were used. The dried and pulverized material (3.1 kg) was extracted thoroughly with hexane and Et_2O, then with MeOH. The MeOH extract was partitioned with a mixture of $CHCl_3$–MeOH–H_2O (8 : 4 : 3) and separated into a lipid fraction (lower layer, 110 g) and MeOH–H_2O-soluble fraction (upper layer, 220 g). The lipid fraction was combined with the hexane–Et_2O extract (215 g) and partitioned with a mixture of hexane–MeOH–H_2O (20 : 10 : 2) twice, yielding an upper layer (190 g) which consisted of mainly triglycerides, and a lower layer (97 g) which contained more polar lipids. A portion of the lower extract (54 g) was charged on a column of silica gel (1 kg) and eluted with

ethyl acetate–hexane (13:87, 15 l), ethyl acetate–hexane (3:7, 5 l), MeOH–$CHCl_3$ (6:94, 6 l) and MeOH–$CHCl_3$ (3:7, 5 l). The eluates (1 l each) were collected, monitored by thin-layer chromatography (TLC), and combined as follows: fr. 1, 2 (a, 1.2 g), 3 (b, 2.9 g), 4, 5 (c, 8.7 g), 6, 7 (d, 3.9 g), 8—15 (e, 4.8 g), 16, 17 (f, 6 g), 18—20 (g, 4.5 g), 21 (h, 4.5 g), 22 (i, 3.6 g), 23—26 (j, 2.9 g), 27—31 (k, 5.3 g). Fr. a contained mostly ligustilide and a smaller amount of butylidenephthalide. Frs. b and c were mixtures of volatile alkylphthalide derivatives. Fr. d was a mixture of senkyunolide A (**18**) and fatty acids. Frs. f and g were mixtures of coniferyl ferulate (**6**) and ferulic acid. Frs. h, i, and j were mixtures containing polar phthalides (**14**, **15**, **16**).

Fr. e was separated by column chromatography with ethyl acetate–hexane (4:6) to give subfractions A (4 g) and B (0.73 g). Chromatography of subfraction B with MeOH–$CHCl_3$ (1:99) gave coniferyl ferulate (**6**, 80 mg), senkyunolide F (**12**, 300 mg) and a mixture (180 mg) which contained senkyunolide K (**2**). It was purified by column chromatography with Et_2O–$CHCl_3$ (1:9) to give **2** (22.3 mg). Column chromatography of subfraction A with MeOH–$CHCl_3$ (1:99) gave senkyunolide B (**8**, 30 mg), pregnenolone (**5**, 80 mg) and senkyunolide E (**11**, 30 mg). The complex mixtures which eluted before and after these three compounds were combined again and separated by column chromatography. Elution with $CHCl_3$ gave 1.35 g of levistolide A (**17**). Its ^{1}H-NMR and MS data were identical with those recorded in ref. 3. Elution with Et_2O–$CHCl_3$ (1:19) gave first a mixture containing senkyunolide B (**8**), senkyunolide D (**10**), and senkyunolide C (**9**), and then a mixture containing senkyunolide G (**13**), senkyunolide L (**3**) and senkyunolide M (**4**). Further elution with Et_2O–$CHCl_3$ (1:19) gave falcarindiol (**7**, 150 mg). The mixture containing **8**, **9**, and **10** was purified by column chromatography with Et_2O–$CHCl_3$ (1:19) to give **8** (30 mg), **10** (40 mg) and **9** (85 mg) in that order. The mixture containing **13**, **3**, and **4** was separated by elution with MeOH–$CHCl_3$ (1:19) to give a mixture (500 mg) containing **13** and **3**, and pure **4** (13.2 mg). Compounds **13** (180 mg) and **3** (67 mg) were obtained by purification of the mixture by column chromatography with ethyl acetate–hexane (4:6). Identification of compounds **1**—**16** and **18** was carried out by thin-layer chromatographic (TLC) comparison with authentic samples using several solvent systems as described in the preceding report.[1]

Senkyunolide K (2)——Oil, $[\alpha]_D$ −6° (c=1.27, $CHCl_3$). ^{1}H-NMR, see the text. UV λ_{max}^{EtOH} nm (ε): 273 (2600). IR ν_{max}^{neat} cm^{-1}: 3400, 1760 (shoulder), 1730, 1610. MS m/z: 208 (M^+), 190 (M^+-H_2O), 133 (M^+-H_2O, C_4H_9), 105 (M^+-H_2O, C_4H_9, CO). High-resolution MS m/z: Found 208.10840. Calcd for $C_{12}H_{16}O_3$ (M^+) 208.10990.

Horeau Determination of Senkyunolide K (2)——Compound **2** (3.3 mg, 16 μmol) was treated with α-phenylbutyric anhydride (10 mg, 32 μmol) and worked up in the usual way.[5] The rotation of the acid in benzene solution (1 ml) was +0.18°. The acid excess was dextrorotatory and the molecule has 4*R* configuration. The blank solution obtained in the same way from α-phenylbutyric anhydride alone showed 0±0.005°.

Senkyunolide L (3)——Oil, $[\alpha]_D$ 0° (c=1.24, $CHCl_3$). ^{1}H-NMR: see the text. UV λ_{max}^{EtOH} nm (ε): 272 (18400). IR ν_{max}^{neat} cm^{-1}: 3400, 1745, 1640. MS m/z: 242 and 244 (M^+), 213 ($M^+-C_2H_5$), 207 (M^+-Cl), 200 ($M^+-C_3H_6$), 198 ($M^+-C_2H_4O$), 169 ($213-C_2H_4O$). High-resolution MS m/z: Found 242.07076. Calcd for $C_{12}H_{15}ClO_3$ (M^+) 242.07096.

Conversion of Ligustilide (1) to Senkyunolide L (3)——A solution of **1** (100 mg) in CH_2Cl_2 (2 ml) was treated with *m*-chloroperbenzoic acid (100 mg) and warmed at 60 °C for 1 h. The solution was washed with saturated $NaHCO_3$ solution, H_2O, and saturated NaCl solution, and the solvent was evaporated off. The residue was dissolved in 1.5 ml of tetrahydrofuran. Addition of 0.15 ml of concentrated HCl solution resulted in immediate chlorination. The mixture was diluted with Et_2O and washed with H_2O and saturated NaCl solution, and the solvent was evaporated off. The residue was purified with Et_2O–$CHCl_3$ (12:88) to give **3** (81.3 mg). The identity with natural **3** was confirmed by ^{1}H-NMR spectral comparison and TLC on a silica gel plate with Et_2O–$CHCl_3$ (15:85).

Senkyunolide M (4)——Oil, $[\alpha]_D$ 0° (c=0.72, $CHCl_3$). ^{1}H-NMR: see the text. ^{13}C-NMR δ: C-1 (168.5), C-3 (151.5 or 148.0), C-4 (23.6), C-5 (22.3), C-6 (53.3), C-7 (64.2), C-8 (127.4), C-9 (148.0 or 151.5), C-10 (114.1), C-11 (28.1), C-12 (20.8), C-13 (13.7 or 13.8), C-14 (211.3), C-15 (45.1), C-16 (16.9), C-17 (13.8 or 13.7). UV λ_{max}^{EtOH} nm (ε): 272 (17000). IR ν_{max}^{neat} cm^{-1}: 3400, 1760, 1700, 1675, 1640. MS m/z: 278 (M^+), 235 ($M^+-C_3H_7$), 207 ($M^+-C_4H_7O$), 190 ($M^+-C_4H_7O$, OH), 180, 175, 165, 161, 71. High-resolution MS: Found 278.15068. Calcd for $C_{16}H_{22}O_4$ (M^+) 278.15178.

References

1) Part XVI: T. Tsuchida, M. Kobayashi, K. Kaneko, and H. Mitsuhashi, *Chem. Pharm. Bull.*, **35**, 4460 (1987).
2) M. Kobayashi, M. Fujita, and H. Mitsuhashi, *Chem. Pharm. Bull.*, **35**, 1427 (1987); *idem*, *ibid.*, **32**, 3770 (1984).
3) *a*) M. Kaouadji, H. Reutenauer, A. J. Chulia, and A. Marsura, *Tetrahedron Lett.*, **24**, 4677 (1983); *b*) M. Cichy, V. Wray, and G. Hofle, *Justus Liebigs Ann. Chem.*, **1984**, 397.
4) T. Yamagishi and H. Kaneshima, *Yakugaku Zasshi*, **97**, 237 (1977).
5) A. Horeau and A. Nouaille, *Tetrahedron Lett.*, **1971**, 1939.
6) H. Mitsuhashi and U. Nagai, *Tetrahedron*, **19**, 1277 (1963).
7) M. Kaouadji, F. De Pachtere, C. Pouget, A. J. Chulia, and S. Lavaitte, *J. Nat. Prod.*, **49**, 872 (1986).
8) H. Mitsuhashi and M. Nomura, *Chem. Pharm. Bull.*, **14**, 777 (1966).
9) W. C. Still, M. Kahn, and A. Mitra, *J. Org. Chem.*, **43**, 2923 (1978).

[Chem. Pharm. Bull. 35(12)4793—4802(1987)]

Synthetic Studies of (±)-Lysergic Acid and Related Compounds[1)]

TAKUSHI KURIHARA,* TATSUYA TERADA, SHINYA HARUSAWA, and RYUJI YONEDA

Osaka University of Pharmaceutical Sciences, 2-10-65, Kawai, Matsubara, Osaka 580, Japan

(Received June 8, 1987)

A new and simple method for a formal synthesis of (±)-lysergic acid (**1**), *via* a four-step sequence starting from the aldehyde (**13**), is described. A very high yield of the product was obtained after purification by column chromatography at the end of the process, without isolation of intermediates.

Keywords——(±)-lysergic acid; Uhle's ketone; benz[*cd*]indole-5-carbaldehyde; ethyl 3-aminopropionate; lithium diisopropylamide; indolo[3,4,5-*gh*]isoquinoline; 1,8-diazabicyclo[5.4.0]-7-undecene; mesyl chloride; 2D-NMR; NOE

While a number of syntheses of lysergic acid (**1**), which has been regarded as a central target molecule among Ergot alkaloids, have been reported,[2)] no methodology suitable for practical use has hitherto been presented. Thus, establishment of a simple method to produce large quantities of lysergic acid (**1**) continues to attract the interest of synthetic chemists. We report here a simple and facile synthetic route to (±)-lysergic acid (**1**) according to the methodology developed for tetrahydroindeno[2,1-*b*]pyridine (**3**) as a model compound starting from indene-3-carbonyl chloride (**2**).[3)] The advantage of this methodology is that the

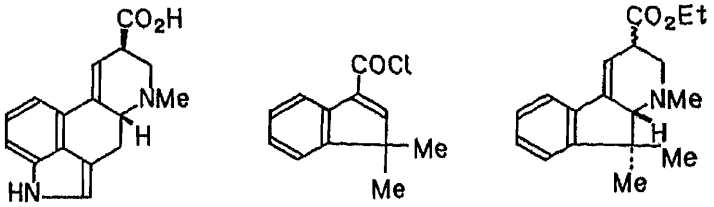

1 2 3

Chart 1

final product is obtained after purification by column chromatography at the end of the process, without purification of intermediates. Application of this methodology for the total synthesis of lysergic acid (**1**) requires the preparation of the 1-benzoyl-1,2,2a,3-tetrahydrobenz[*cd*]indole-5-carbonyl chloride (**11**), which has a masked indolic system, in order to avoid the possible introduction of aromaticity of the C-ring.[2a)] Thus, the carbonyl chloride (**11**) was prepared as follows. Cyanophosphorylation of Uhle's ketone (**4**),[2a)] which has been utilized as a starting material for the total synthesis of **1**, with diethyl phosphorocyanidate (DEPC) and lithium cyanide (LiCN)[4)] gave the cyanophosphate (**5**), which was then treated with boron trifluoride etherate ($BF_3 \cdot OEt_2$) to afford the α,β-unsaturated nitrile (**6**).[2a)] Hydrolysis of the cyanide function of **6** was successfully achieved *via* a stepwise route, which involves the initial isolation of an amide (**7**) by heating of **6** with 77% sulfuric acid (H_2SO_4), then refluxing of **7** in concentrated hydrochloric acid (HCl)–acetic acid (AcOH) (1 : 1) solution

to give an amino acid (**8**) isolated as a hydrochloride salt. Schotten–Baumann reaction of **8** with benzoyl chloride gave a benzoate (**9**) in 72% overall yield from **4**. This was then chlorinated with thionyl chloride ($SOCl_2$) to give 1-benzoyl-1,2,2a,3-tetrahydrobenz[*cd*]-indole-5-carbonyl chloride (**11**) quantitatively. Numerous attempts to hydrolyze the CN function in **6** directly to **8** were unsuccessful under both acidic and basic conditions. The

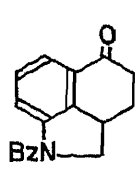

4

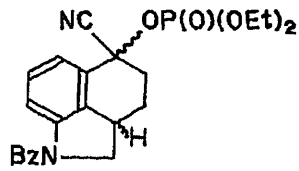

5

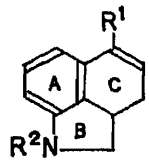

Boc R
MeNCH$_2$CHCO$_2$Et
14: R=H
33: R=Me

6: R^1=CN, R^2=Bz
7: R^1=CONH$_2$, R^2=Bz
8: R^1=CO$_2$H, R^2=H
9: R^1=CO$_2$H, R^2=Bz
10: R^1=CO$_2$H, R^2=CO$_2$Et
11: R^1=COCl, R^2=Bz
12: R^1=COCl, R^2=CO$_2$Et
13: R^1=CHO, R^2=Bz

Bz=benzoyl
Boc=*tert*-butoxycarbonyl

Chart 2

carbonyl chloride (**11**) thus obtained, however, was only slightly soluble in tetrahydrofuran (THF) and the condensation of **11** with ethyl 3-(*N*-*tert*-butoxycarbonyl-*N*-methyl-amino)propionate (**14**) in the presence of lithium diisopropylamide (LDA) in THF at −78 °C gave a complex mixture, from which the product (**15**) could not be obtained. In order to overcome the problem of the solubility in THF, the protective group of **11** was changed to an ethoxycarbonyl group. The corresponding carbonyl chloride (**12**) was analogously prepared from **8** *via* Schotten–Baumann reaction (with ethyl chloroformate) followed by chlorination in 84% overall yield. Although the solubility in THF was not greatly improved, reaction of **12** with **14** proceeded smoothly to yield a viscous oil, whose mass spectrum (MS) showed a parent peak at *m/z* 718 ($M^+ + 1$). However, the proton nuclear magnetic resonance (^{1}H-NMR) spectrum of this product was not sufficiently well resolved for the assignment of the protons (300 MHz, $CDCl_3$). Thus, without further investigation, this was submitted to the

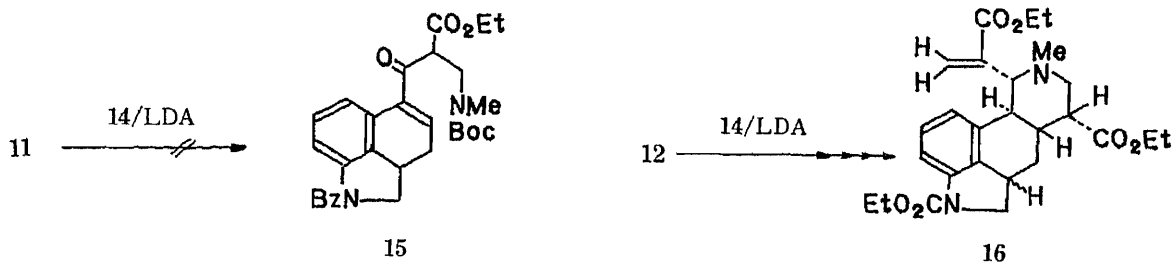

15 **16**

Chart 3

following reaction sequences developed for the model compound, namely i) sodium borohydride ($NaBH_4$) reduction ii) mesylation with methanesulfonyl chloride (MsCl) and pyridine iii) de-*tert*-butoxycarbonylation sequence [2.3 N HCl in ethyl acetate (EtOAc)] iv) treatment with 1,8-diazabicyclo[5.4.0]-7-undecene (DBU) in dimethyl sulfoxide (DMSO), without purification of the resulting intermediates.[3] The crude oil finally obtained was purified by silica gel (SiO_2) column chromatography to give a crystalline product (**16**) [mp 140—141 °C, MS *m/z*: 470 (M^+), high-resolution MS Calcd for $C_{26}H_{34}N_2O_6$: 470.2418. Found: 470.2415] in 18% overall yield from **12**. The infrared (IR) spectrum of **16** showed strong carbonyl absorptions at

TABLE I. Selected ^{13}C- and ^{1}H-NMR Data for Compound **16** δ in $CDCl_3$

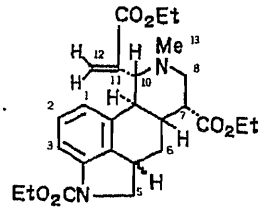

Number	Carbon	Proton J (Hz)	Number	Carbon	Proton J (Hz)
1	113.73 d	6.56 (d, J=8)	8	60.34 t	2.45 (dd, J=12, 3, -H)
2	128.20 d	7.04 (br t, J=8)			3.30 dd, J=12, 3, -H)
3	119.43 d	7.56 (br)	10	65.22 d	3.44 (d, J=11)
5	57.19 t		10a	43.22 d	3.50 (t, J=11)
5a	34.45 d		11[b]	134.97 s	
6	34.48 t	1.58,[a] 2.22 (m)	12[b]	128.73 t	6.04 (s), 6.44 (s)
6a	40.51 d	1.58 (m)	13[b]	43.51 q	2.17 (s)
7	46.49 d	2.79 (q, J=3)			

a) Overlapped with 6a-H. *b*) Numberings 11, 12, and 13 were used for convenience.

1720 and 1710 cm^{-1}. The ^{1}H-NMR spectrum showed the presence of three $CO_2CH_2CH_3$ groups, N-CH_3 protons at δ 2.18, and terminal methylene protons at δ 6.04 and 6.44 as well as the protons of the 1,2,2a,3,4,5-hexahydrobenz[*cd*]indole skeleton. Selected ^{1}H-NMR and carbon-13 nuclear magnetic resonance (^{13}C-NMR) spectral data are summarized in Table I. On the basis of these results, the structure of **16** was supposed to be ethyl 2-(4,7-diethoxycarbonyl-9-methyl-4,5,5a,6,6a,7,8,9,10,10a-decahydroindolo-[3,4,5-*gh*]isoquinolin-10-yl)propenoate. From the two-dimensional (2D) ^{1}H–^{13}C chemical shift correlation spectrum (H–C COSY) of **16**, it was found that signal due to 10a-H appears as a triplet at δ 3.50 with J= 11 Hz. This signal was collapsed to a sharp doublet (J= 11 Hz) by irradiation of the signal at δ 1.58 (6-H_{ax} and 6a-H). This clearly indicates that 10a-H also couples with 10-H with J= 11 Hz. Thus, the C/D-*trans* fusion, as well as the *trans* relative configuration between 10- and 10a-H, was deduced. This is consistent with the structure of the Ergot alkaloid, paspaclavine.[5] Furthermore, the α-configuration of the ethoxycarbonyl group at C-7 was deduced from the signal of 7-H, which appeared as a sharp quartet with J=3 Hz.[6]

Chart 4 shows how **12** could give rise to the final product **16** *via* the reaction sequences mentioned above: namely condensation of the carbonyl chloride (**12**) with **14** in the presence of LDA followed by Michael addition of **14** to the resulting β-keto ester (**17**) gives **18**. Reduction of **18** with $NaBH_4$ gives the alcohol (**19**), which was then mesylated to **20**. De-*tert*-butoxycarbonylation of **20** and heating of **21** with DBU in DMSO gives the cyclized product (**16**) with liberations of methanesulfonic acid and methylamine.

Attempts to synthesize the β-keto esters such as **15** or **17** through the carbonyl chlorides (**11** and **12**) were unsuccessful. Thus, our effort was directed at the reaction of the aldehyde (**13**) with **14**. The aldehyde (**13**) had been prepared by Woodward *et al.*,[2a] and afterward Ramage *et al.*[2c] optimized the procedure to allow satisfactory production of **13** as a key intermediate for the synthesis of lysergic acid (**1**). However, since the nitrile (**6**) is readily available in a large quantity and high yield (100%) from Uhle's ketone (**4**), in our case, **13** was alternatively prepared by reduction of **6** with diisobutylaluminum hydride (DIBAL) in 47% yield. Reaction of the aldehyde (**13**) with **14** in the presence of LDA in THF at −78 °C gave the alcohol (**22**) [MS m/z: 520 (M^+)] as an oily mixture of diastereoisomers in quantitatives yield, after purification by column chromatography on SiO_2. The IR spectrum of **22** showed

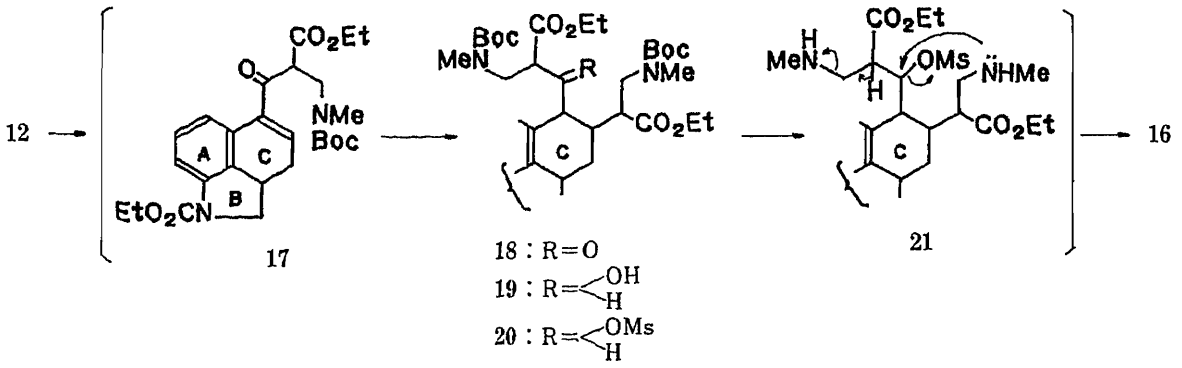

Chart 4

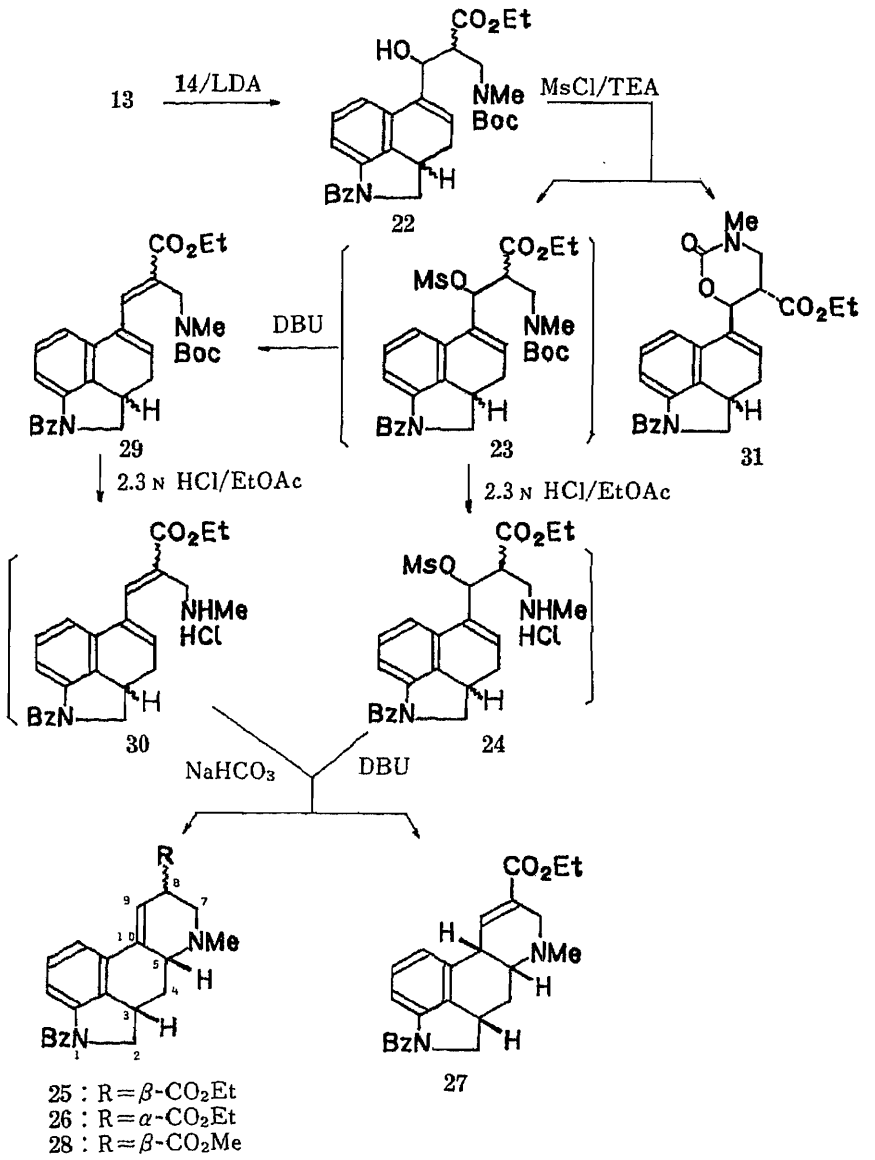

Chart 5

three carbonyl absorptions at 1720, 1680, and 1640 cm^{-1}, as well as a hydroxy absorption at 3400 cm^{-1}. This product was treated with MsCl and triethylamine (TEA) in dichloromethane (CH_2Cl_2) at room temperature to give the mesylate (**23**), which was, without purification,

TABLE II. ^{1}H-NMR, IR, UV, and Mass Spectral Data for Compounds **25** (**26**), and **27**

Compd.	**25**	**26**[a]	**27**
^{1}H-NMR ($CDCl_3$)			
δ J (Hz)			
Protons			
3-H	3.41 (m)		3.44—3.70 (m)
4-H_{eq}	2.55 (m)		2.53 (br)
4-H_{ax}	1.39 (q, J=11.5)	1.42 (q, J=11.5)	1.54 (td, J=13, 3)
5-H	3.04 (br d, J=11.5)	2.89 (br d, J=11.5)	2.82 (q, J=3.6)
7-H_{eq}	3.26 (dd, J=11.5, 6.1)	3.44 (d, J=11.5)	3.44—3.70 (m)
7-H_{ax}	2.67 (t, J=11.5)	2.57 (dd, J=11.5, 5)	2.98 (dt, J=16.2, 3)
8-H	3.62 (m)		
9-H	6.55 (br s)		7.33 (t, J=3)
N-CH_3	2.50 (s)	2.47 (s)	2.46 (s)
IR (KBr) ν			
cm^{-1} (C=O)	1730, 1640		1710, 1645
UV (EtOH)			
nm (log ε)	254 (4.51), 307 (3.80)		267 (4.09), 293 (3.95)
MS m/z	402 (M^+)		402 (M^+)

a) The ^{1}H-NMR spectral data for **26** were obtained from the spectrum of a mixture of the two isomers (**25** and **26**).

submitted to the usual cleavage of the *tert*-butoxycarbonyl (*tert*-Boc) group by 2.3 N HCl–EtOAc. Cyclization of the resulting hydrochloride (**24**) was performed by treatment with DBU in DMSO at room temperature to afford the desired ethyl *N*-benzoyl-2,3-dihydrolysergates (**25** and **26**) in 54% combined yield from **22** as an isomeric mixture in the ratio of 2 : 1 (by ^{1}H-NMR spectroscopy), along with the isomer (**27**), mp 178—180 °C, in 8% overall yield from **22**. Recrystallization of the above mixture from EtOAc afforded the homogeneous 8β-isomer (**25**), mp 147—148 °C, whose spectroscopic data were very similar to those of the corresponding methyl ester (**28**).[2e] Hydrolysis of **25** with concentrated HCl in methanol (MeOH) and ordinary esterification (dry HCl and MeOH) of the carboxylic acid followed by mild benzoylation[2f] afforded **28**, mp 165—168 °C, the IR and ^{1}H-NMR spectra of which were identical with those of the authentic **28**, provided by Ninomiya. Since **28** has already been converted to lysergic acid,[2a,c,e] the present work amounts to a formal synthesis of (±)-lysergic acid (**1**).

Table II shows the IR, ultraviolet (UV), MS, and selected ^{1}H-NMR spectral data of compounds **25** (**26**), and **27**. The IR and UV spectra clearly indicate the presence of an α,β-unsaturated ester moiety in the structure **27**. The C/D-*cis* ring junction of **27** was determined from the signal pattern of 5-H which appeared as a quartet with J=3.6 Hz at δ2.82 and collapsed to a broad singlet on irradiation of 4-H_α or 4-H_β.

Another approach to the tetracyclic compounds was investigated. When the crude product obtained by mesylation of **22** was first treated with DBU in DMSO, the diene ester (**29**) was obtained as an unstable oil, but the yield was very poor (18%). Usual cleavage of the *tert*-Boc group of **29** followed by treatment with saturated $NaHCO_3$ afforded a mixture of unsaturated esters (**25**/**26**) and the conjugate ester (**27**) in 44% combined yield and 12% yield from **29**, respectively. Therefore, the former approach is superior to the latter. Even on a 9 g scale, the four-step sequence starting from the aldehyde (**13**) can be run without isolation of intermediates to produce **25** (**26**) and **27** in 62% (7.95 g) overall yield. Hence, we have developed a new and simple method for the synthesis of **25** (**26**).

The main disadvantage during the synthetic route described above is that in the mesylation of **22** a side reaction occurs with the formation of a polar compound (**31**). Thus,

the isolation of the side product was attempted. After usual mesylation of **22**, the crude product was purified by SiO_2 column chromatography [benzene–EtOAc (2:1)] to yield a crystalline product (**31**) in 30% yield.[7] The molecular formula was determined by high-resolution MS, indicating $C_{26}H_{26}N_2O_5$ for **31**. The ^{1}H-NMR spectrum exhibited no *tert*-butyl group, although three carbonyl absorptions (1720, 1710, and 1640 cm^{-1}) are observed in the IR spectrum. Consequently, the structure of **31** was determined as ethyl 3-methyl-6-(1-benzoyl-1,2,2a,3-tetrahydrobenz[*cd*]indol-5-yl)-2-oxo-3,4,5,6-tetrahydro-1,3-oxazine-5-carboxylate. The *trans* stereochemistry between 5-H and 6-H was deduced from the signal pattern of 6-H_{ax} which appeared as a doublet with $J=9$ Hz. Although the mechanistic details of this side reaction have not been established,[8] it was suggested that the methanesulfonyloxy group may participate in the formation of **31**, because no reaction took place on heating of **22** with TEA in the absence of MsCl in CH_2Cl_2. Thus, **22** was chlorinated with *N*-chlorosuccinimide (NCS) and triphenylphosphine (Ph_3P)[9] to give the chloride (**32**), which was then submitted to the de-*tert*-Boc sequence followed by treatment with DBU in DMSO to give a mixture of unsaturated esters (**25** and **26**) (43% from **22**) and **27** (6% from **22**), the yields of which could not be improved.

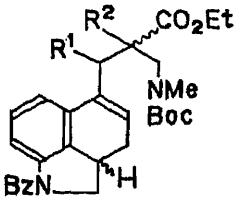

32: R^1=Cl, R^2=H
34: R^1=OH, R^2=Me
35: R^1=Cl, R^2=Me

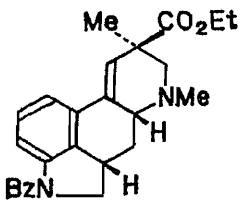

36

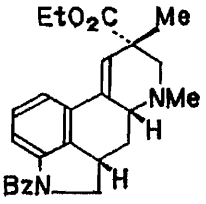

37

Chart 6

Next, synthesis of (±)-lysergine, along with development of the methodology of the synthesis of (±)-lysergic acid (**1**), was attempted. The condensation of the aldehyde (**13**) with **33** under the same conditions as described for the preparation of **22** gave the alcohol (**34**) as diastereomixtures in 95% yield. The alcohol (**34**) did not afford the mesylate on treatment with MsCl in the presence of TEA, pyridine, or even *n*-butyllithium. Therefore, **34** was chlorinated with $SOCl_2$ (method A) or NCS-Ph_3P[9] (method B) to give the chloride (**35**) as an oil (mixture of diastereoisomers) in 23% and 36% yields, respectively. Cleavage of the *tert*-Boc group of **35** (obtained *via* methods A and B) followed by treatment with DBU in DMSO at 60 °C gave a mixture of the desired unsaturated esters [**36**/**37**: 30%/26% from **35** (method A) and **36**/**37**: 65%/6.5% from **35** (method B)]. The ^{1}H-NMR spectrum of **36** was very similar to that of **37**, except for the chemical shifts of 8-CH_3 (δ 1.48 in **36** and δ 1.28 in **37**) and 7-H_2 [**36**: δ 2.68 (d, $J=11.5$ Hz, 7-H_{ax}), 2.89 (dd, $J=11.5$, 1.4 Hz, 7-H_{eq}) and **37**: δ 2.15 (d, $J=11.5$ Hz, 7-H_{ax}), 3.49 (d, $J=11.5$ Hz, 7-H_{eq})]. The two compounds (**36** and **37**) are therefore epimeric at C-8. Upon irradiation of 8-CH_3, a nuclear Overhauser effect (NOE) enhancement was observed at 7-H_{ax} and 5-H, and irradiation of 5-H gave NOE enhancement at 3-H and 7-H_{ax} in compound **37**. Thus, the relative configuration between 8-CH_3 and 3-H, 5-H, and 7-H_{ax} was deduced as being all-*cis* in compound **37**. It is considered that the distinct difference of the products (**36**/**37**) ratios is responsible for the result that the respective chlorides obtained *via* methods A and B have different ratios of diastereoisomers.

Finally, hydrolysis of **36** (**37**) and subsequent decarboxylation aiming at the preparation of *N*-benzoyl-2,3-dihydrolysergine was attempted, but so far without success.

Experimental

Melting points were determined on a Yanagimoto micro melting point apparatus and are uncorrected. IR and UV spectra were recorded on a Shimadzu IR-435 and a JASCO UVIDEC-505 spectrophotometers. MS were taken on a Hitachi M-80 spectrometer. ^{1}H- and ^{13}C-NMR spectra were taken with tetramethylsilane as an internal standard on a Varian XL-300 spectrometer, in $CDCl_3$ unless otherwise noted. The solvent for extraction was a mixture of benzene–EtOAc (1 : 1) unless otherwise noted, and was dried over anhydrous Na_2SO_4. For column chromatography, SiO_2 (Merck 7734 and 9385) was used.

1-Benzoyl-1,2,2a,3-tetrahydrobenz[*cd*]indole-5-carbonitrile (6)——A solution of a mixture of DEPC (19.07 g, 117 mmol) and Uhle's ketone (**4**) (10.86 g, 39 mmol) in THF (75 ml) was added to LiCN (3.86 g, 117 mmol) suspended in THF (100 ml) with ice cooling, and the mixture was stirred for 30 min at room temperature. The mixture was concentrated *in vacuo*, water (20 ml) was added to the residue and the aqueous mixture was extracted. The extract was washed with H_2O, and brine, and dried. Removal of the solvent gave an oil (**5**), which was dissolved in dry benzene (30 ml). $BF_3 \cdot OEt_2$ (16.59 g, 117 mmol) was added to the benzene solution and the mixture was stirred for 1.5 h at room temperature. Water was added with ice cooling under vigorous stirring and the aqueous mixture was extracted. The extract was washed with H_2O, and brine, then dried, and evaporated. The resulting solid was recrystallized from benzene–petroleum ether to give **6** (10.05 g, 90%) as colorless crystals, mp 149—150 °C (lit.[2a] 142—144 °C). IR ν_{max}^{Nujol} cm^{-1}: 2200 (CN), 1630 (CO). ^{1}H-NMR δ: 2.34 (1H, ddd, J=18, 15.5, 2.6 Hz, 3-H), 2.84 (1H, m, 3-H), 3.62 (1H, m, 2a-H), 3.83 (1H, t, J=11 Hz, 2-H), 4.50 (1H, br, 2-H), 6.83 (1H, dd, J=6.3, 2.6 Hz, 4-H), 7.1—7.7 (8H, m, Ph).

1-Benzoyl-1,2,2a,3-tetrahydrobenz[*cd*]indole-5-carboxamide (7)——Compound **6** (8.59 g, 30 mmol) was added to a 77% H_2SO_4 solution (90 ml) in limited amounts at room temperature and the mixture was heated at 90 °C for 2.2 h. The solution was poured into ice-water under stirring, and the resulting white precipitate was collected by filtration, washed with H_2O, and dried to give **7** (9.13 g, 100%). Recrystallization from dimethylformamide (DMF)–H_2O gave colorless crystals, mp 270—273 °C. IR ν_{max}^{Nujol} cm^{-1}: 3400—3100 (NH_2), 1670 ($CONH_2$), 1620 (CO). ^{1}H-NMR (DMSO-d_6) δ: 2.18 (1H, t, J=16 Hz, 3-H), 2.66 (1H, m, 3-H), 3.48 (1H, m, 2a-H), 3.89 (1H, br s, 2-H), 4.20 (1H, br, 2-H), 6.55 (1H, d, J=5.9 Hz, 4-H), 7.0—8.0 (10H, m, Ph and $CONH_2$). *Anal.* Calcd for $C_{19}H_{16}N_2O_2$: C, 74.98; H, 5.30; N, 9.21. Found: C, 74.68; H, 5.59; N, 9.48.

1,2,2a,3-Tetrahydrobenz[*cd*]indole-5-carboxylic Acid Hydrochloride (8)——A solution of **7** (9.13 g, 3 mmol) in concentrated HCl–AcOH (1 : 1) (200 ml) was refluxed for 15 h. After removal of the solvents by evaporation *in vacuo*, the residue was dissolved in H_2O (400 ml). The aqueous solution was extracted with EtOAc in order to remove the soluble material. The aqueous portion was concentrated to dryness to give the hydrochloride of **8** (7.12 g, 100%). Recrystallization from MeOH–ether gave colorless crystals, mp 216—217 °C. IR ν_{max}^{Nujol} cm^{-1}: 1690 (CO). ^{1}H-NMR (DMSO-d_6) δ: 2.32 (1H, td, J=17, 2.6 Hz, 3-H), 2.84 (1H, dt, J=17, 7 Hz, 3-H), 3.42 (1H, t, J=10 Hz, 2-H), 3.50 (1H, m, 2a-H), 4.08 (1H, dd, J=10, 7 Hz, 2-H), 7.21 (1H, dd, J=7, 2.6 Hz, 4-H), 7.25—7.83 (3H, m, Ph). *Anal.* Calcd for $C_{12}H_{12}ClNO_2$: C, 60.63; H, 5.09; N, 5.89. Found: C, 60.74; H, 5.09; N, 5.87.

Schotten–Baumann Reaction of Amino Acid (8) with Benzoyl Chloride (or Ethyl Chloroformate)——General Procedure: Benzoyl chloride (843 mg, 6 mmol) [ethyl chloroformate (651 mg, 6 mmol)] was added to a solution of **8** (1.19 g, 5 mmol) in 0.2 N NaOH solution (30 ml) with ice cooling. The mixture was stirred for 1 h at room temperature and acidified by the addition of 10% HCl with cooling. The resulting precipitate was collected by filtration, washed with H_2O, and dried. Recrystallization from DMF–H_2O gave a grayish powder.

1-Benzoyl-1,2,2a,3-tetrahydrobenz[*cd*]indole-5-carboxylic Acid (9)——Yield, 80%. mp 237—240 °C. IR ν_{max}^{Nujol} cm^{-1}: 1710 (CO). ^{1}H-NMR (DMSO-d_6) δ: 2.24 (1H, td, J=15, 2.3 Hz, 3-H), 2.70 (1H, m, 3-H), 3.48 (1H, m, 2a-H), 3.88 (1H, br s, 2-H), 4.20 (1H, br, 2-H), 7.08—8.0 (9H, m, Ph and 4-H), 12.70 (1H, br, CO_2H). *Anal.* Calcd for $C_{19}H_{15}NO_3$: C, 74.74; H, 4.95; N, 4.59. Found: C, 74.73; H, 4.98; N, 4.71.

1-Ethoxycarbonyl-1,2,2a,3-tetrahydrobenz[*cd*]indole-5-carboxylic Acid (10)——Yield, 84%. mp 255—256 °C. IR ν_{max}^{Nujol} cm^{-1}: 1700, 1670 (CO). ^{1}H-NMR (DMSO-d_6) δ: 1.28 (3H, t, J=7 Hz, $CO_2CH_2C\underline{H}_3$), 2.24 (1H, t, J=17 Hz, 3-H), 2.75 (1H, dt, J=17, 7.1 Hz, 3-H), 3.43 (1H, m, 2a-H), 3.60 (1H, t, J=10.5 Hz, 2-H), 4.20 (2H, br, $CO_2C\underline{H}_2CH_3$), 4.32 (1H, t, J=10.5 Hz, 2-H), 7.06—7.60 (4H, m, Ph and 4-H), 12.70 (1H, s, CO_2H). *Anal.* Calcd for $C_{15}H_{15}NO_4$: C, 65.92; H, 5.53; N, 5.13. Found: C, 65.97; H, 5.43; N, 4.99.

Without purification of the intermediates, the ketone (**4**) (30.34 g, 109 mmol) was successfully converted to **9** (72% overall yield from **4**) under the same conditions as described above.

Chlorination of the Carboxylic Acids (9 and 10)——General Procedure: $SOCl_2$ (2.6 ml, 35 mmol) was added to a solution of a carboxylic acid (8.8 mmol) in dry benzene (50 ml), and the mixture was heated at 95 °C for 2.5 h with stirring. After the mixture had been concentrated *in vacuo*, the residue was recrystallized from dry benzene with the aid of Norite to give the corresponding carbonyl chloride.

1-Benzoyl-1,2,2a,3-tetrahydrobenz[*cd*]indole-5-carbonyl Chloride (11)——Yield, 100%. mp 180—181 °C. IR ν_{max}^{Nujol} cm^{-1}: 1750, 1630 (CO). ^{1}H-NMR δ: 2.38 (1H, t, J=16 Hz, 3-H), 2.90 (1H, m, 3-H), 3.58 (1H, br s, 2a-H), 3.82 (1H, t, J=10.2 Hz, 2-H), 4.45 (1H, br, 2-H), 6.80—7.80 (9H, m, Ph and 4-H). *Anal.* Calcd for $C_{15}H_{14}ClNO_3$: C, 70.48; H, 4.36; N, 4.33. Found: C, 70.53; H, 4.27; N, 4.22.

1-Ethoxycarbonyl-1,2,2a,3-tetrahydrobenz[*cd*]indole-5-carbonyl Chloride (12)——Yield, 100%. mp 128—130 °C. IR ν_{max}^{Nujol} cm^{-1}: 1750, 1690 (CO). ^{1}H-NMR δ: 1.37 (3H, t, J=7 Hz, $CO_2CH_2\underline{CH_3}$), 2.39 (1H, ddd, J=17.7, 15.2, 2.5 Hz, 3-H), 2.95 (1H, dt, J=17.7, 6.6 Hz, 3-H), 3.52 (1H, m, 2a-H), 3.63 (1H, t, J=10.3 Hz, 2-H), 4.32 (2H, m, $CO_2\underline{CH_2}CH_3$), 4.45 (1H, br, 2-H), 7.20—7.80 (4H, m, Ph and 4-H). *Anal.* Calcd for $C_{15}H_{14}ClNO_3$: C, 61.75; H, 4.84; N, 4.80. Found: C, 61.76; H, 4.78; N, 4.68.

1-Benzoyl-1,2,2a,3-tetrahydrobenz[*cd*]indole-5-carbaldehyde (13)——DIBAL (1.5 M toluene solution, 3.3 ml, 5 mmol) was added to a solution of **6** (573 mg, 2 mmol) in dry benzene (30 ml) with ice cooling, and the mixture was stirred for 2 h at 65 °C, then cooled to room temperature. Benzoyl chloride (1.4 g, 10 mmol) and TEA (1.01 g, 10 mmol) were added, and the mixture was stirred for 1 h at room temperature. The reaction was quenched by the addition of H_2O (5 ml) and saturated NH_4Cl solution (8 ml), and then the mixture was neutralized by the addition of 10% H_2SO_4 (3.3 ml). The whole was extracted with EtOAc and the extract was washed with brine, dried, and evaporated. The residue was purified by column chromatography [benzene–EtOAc (5 : 1)] to give **13** (268 mg, 47%), which was recrystallized from EtOH as colorless crystals, mp 175—176 °C (lit.[2a] mp 179.5—180.5 °C).[10] IR ν_{max}^{KBr} cm^{-1}: 1680, 1620 (CO). ^{1}H-NMR δ: 2.41 (1H, ddd, J=17.6, 15.1, 2.6 Hz, 3-H), 2.92 (1H, br s, 3-H), 3.59 (1H, m, 2a-H), 3.83 (1H, t, J=10.9 Hz, 2-H), 4.45 (1H, br, 2-H), 6.95 (1H, br d, J=6.1 Hz, 4-H), 7.0—7.90 (8H, m, Ph), 9.73 (1H, s, CHO).

Ethyl 2-(4,7-Diethoxycarbonyl-9-methyl-4,5,5a,6,6a,7,8,9,10,10a-decahydroindolo[3,4,5-*gh*]isoquinolin-10-yl)-propenoate (16)——The preparation of LDA was carried out as follows: *n*-butyllithium (1.6 M hexane solution, 6.9 ml, 10.8 mmol) was added to a solution of diisopropylamine (1.09 g, 10.8 mmol) in THF (10 ml) at −78 °C under N_2, and the mixture was stirred for 20 min. A solution of ethyl 3-(*N*-*tert*-butoxycarbonyl-*N*-methylamino)propionate (**14**) (2.5 g, 10.8 mmol) in THF (5 ml) was then added to the solution at −78 °C, and the mixture was stirred for 20 min. A solution of **12** (1.04 g, 3.6 mmol) in THF (25 ml) was added dropwise, and the whole was stirred for another 20 min at this temperature. The reaction was quenched by the addition of H_2O, and THF was removed by evaporation. The residue was extracted, and the extract was washed with brine, dried, and concentrated. The residue was dissolved in EtOH (75 ml), and the $NaBH_4$ (680 mg, 18 mmol) was added. After the mixture had been stirred for 4 h, acetic acid was added to decompose excess $NaBH_4$, and EtOH was removed by evaporation. The residue was extracted, and the extract was washed with H_2O and brine, dried, and concentrated. To a solution of this residue in dry pyridine (28 ml) was added MsCl (3.3 g, 29 mmol), and the mixture was stirred for 4 h at room temperature. The reaction mixture was made alkaline by the addition of 10% NH_4OH, diluted with H_2O (100 ml), and extracted with $CHCl_3$. The extract was washed with H_2O, dried, and evaporated. The residue was dissolved in 2.3 N HCl in EtOAc (16 ml) and the mixture was stirred for 1.5 h at room temperature. After removal of the solvent by evaporation, the residue was dissolved in DMSO (3 ml) containing DBU (2.18 g, 18 mmol). The mixture was allowed to stand for 3 h, diluted with cold H_2O (10 ml), then extracted. The extract was washed with H_2O and brine, dried, and evaporated. The residue was purified by column chromatography [benzene–EtOAc (1 : 1)] to give **16** (300 mg, 18% overall yield from **12**). Recrystallization from EtOH gave colorless crystals, mp 141—142 °C. IR ν_{max}^{KBr} cm^{-1}: 1720, 1710 (CO). ^{1}H-NMR δ: 1.28—1.38 (9H, m, 3 × $CO_2CH_2\underline{CH_3}$), 1.58 (2H, m, 6-H, 6a-H), 2.17 (3H, s, NCH_3), 2.22 (1H, m, 6-H), 2.45 (1H, dd, J=12, 3 Hz, 8-H), 2.79 (1H, q, J=3 Hz, 7-H), 3.30 (1H, dd, J=12, 3 Hz, 8-H), 3.44 (1H, d, J=11 Hz, 10-H), 3.50 (1H, t, J=11 Hz, 10a-H), 4.20—4.44 (7H, m, 3 × $CO_2\underline{CH_2}CH_3$, 5-H), 6.04 and 6.44 (each 1H, each s, $=CH_2$), 6.56 (1H, d, J=8 Hz, 1-H), 7.04 (1H, br t, J=8 Hz, 2-H), 7.56 (1H, br, 3-H). MS *m/z*: 470 (M^+). High-resolution MS (HRMS) Calcd for $C_{26}H_{34}N_2O_6$: 470.2418. Found: 470.2415. *Anal.* Calcd for $C_{26}H_{34}N_2O_6$: C, 66.36; H, 7.28; N, 5.95. Found: C, 66.43; H, 7.29; N, 5.84.

Ethyl 2-(*N*-*tert*-Butoxycarbonyl-*N*-methylamino)methyl-3-hydroxy-3-(1-benzoyl-1,2,2a,3-tetrahydrobenz[*cd*]indol-5-yl)propionate (22)——A solution of **14** (1.46 g, 6.3 mmol) in THF (5 ml) was added to a solution of LDA [prepared from diisopropylamine (640 mg, 6.3 mmol)] in THF (5 ml) at −78 °C under N_2, and the mixture was stirred for 20 min. A solution of **13** (1.24 g, 4.2 mmol) in THF (25 ml) was added dropwise at −78 °C, and the whole was stirred for 30 min. The reaction was quenched by the addition of H_2O, and THF was removed by evaporation. The residue was extracted, and the extract was washed with H_2O and brine, dried, and evaporated. The residue was purified by column chromatography [benzene–EtOAc (3 : 1)] to give **22** (2.18 g, 99%) as an oil. IR ν_{max}^{neat} cm^{-1}: 3400 (OH), 1720, 1680 (CO). The ^{1}H-NMR spectrum was not sufficiently well resolved for assignment of the signals. MS *m/z*: 520 (M^+). HRMS Calcd for $C_{30}H_{36}N_2O_6$: 520.2575. Found: 520.2571.

Ethyl 1-Benzoyl-2,3-dihydrolysergates (25 and 26) and 1-Benzoyl-8-ethoxycarbonyl-2,3-dihydro-6-methyl-$\Delta^{8,9}$-ergoline (27)——Method A: MsCl (504 mg, 4.4 mmol) was added to a solution of **22** (1.77 g, 3.4 mmol) and TEA (516 mg, 5.1 mmol) in CH_2Cl_2 (40 ml), and the mixture was stirred for 15 min at room temperature. Work-up as described for the preparation of **16** gave a mesylate (**23**), which was then dissolved in 2.3 N HCl–EtOAc (16 ml). After being stirred for 1.5 h, the mixture was concentrated, and the residue was dissolved in DMSO (2 ml) and DBU (1.04 g, 6.8 mmol). Work-up gave an oil, which was subjected to column chromatography. The first eluate with EtOAc gave **27** (6.8% from **22**) as colorless crystals and a mixture of **25** and **26** (578 mg, 42% from **22**) as an oil. Crystallization from EtOAc gave homogeneous **25** as colorless crystals.

25: mp 147—148 °C (from EtOAc). IR ν_{max}^{KBr} cm^{-1}: 1730, 1640 (CO). ^{1}H-NMR δ: 1.31 (3H, t, J=7.3 Hz, $CO_2CH_2\underline{CH_3}$), 1.39 (1H, q, J=11.5 Hz, 4-H_{ax}), 2.50 (3H, s, NCH_3), 2.67 (1H, t, J=11.5 Hz, 7-H_{ax}), 3.04 (1H, br d,

J=11.5 Hz, 5-H), 3.26 (1H, dd, J=11.5, 6.1 Hz, 7-H_{eq}), 3.62 (1H, m, 8-H), 3.70 (1H, t, J=11 Hz, 2-H_{α}), 4.22 (2H, q, J=7.3 Hz, $CO_2C\underline{H}_2CH_3$), 4.30 (1H, br, 2-H), 6.55 (1H, br s, 9-H), 7.26—7.60 (8H, m, Ph). UV λ_{max}^{EtOH} nm (log ε): 254 (4.51), 307 (3.80). *Anal.* Calcd for $C_{25}H_{26}N_2O_3$: C, 74.60; H, 6.51; N, 6.96. Found: C, 74.33; H, 6.48; N, 6.86.

26: (The ^{1}H-NMR spectral data for **26** were obtained from the spectrum of a mixture of two isomers.) ^{1}H-NMR δ: 1.27 (3H, t, J=7.3 Hz, $CO_2CH_2C\underline{H}_3$), 1.42 (1H, q, J=11.5 Hz, 4-H_{ax}), 2.47 (3H, s, NCH_3), 2.57 (1H, dd, J=11.5, 5 Hz, 7-H_{ax}), 2.89 (1H, br d, J=11.3 Hz, 5-H), 3.44 (1H, d, J=11.5 Hz, 7-H_{eq}), 3.16 (1H, br, 8-H), 4.22 (2H, q, J=7.3 Hz, $CO_2C\underline{H}_2CH_3$).

27: mp 178—180 °C (from EtOAc). IR ν_{max}^{KBr} cm^{-1}: 1710, 1645 (CO). ^{1}H-NMR δ: 1.30 (3H, t, J=7.3 Hz, $CO_2CH_2C\underline{H}_3$), 1.54 (1H, td, J=13, 3 Hz, 4-H_{ax}), 2.46 (3H, s, NCH_3), 2.82 (1H, q, J=3.6 Hz, 5-H), 2.98 (1H, dt, J=16.2, 3 Hz, 7-H_{ax}), 4.22 (3H, m, $CO_2C\underline{H}_2CH_3$, 2-H_{α}), 4.50 (1H, br s, 2-H_{β}), 7.33 (1H, d, J=3 Hz, 9-H), 6.80—7.60 (8H, m, Ph). UV λ_{max}^{EtOH} nm (log ε): 267 (4.09), 293 (3.95). *Anal.* Calcd for $C_{25}H_{26}N_2O_3$: C, 74.60; H, 6.51; N, 6.96. Found: C, 74.60; H, 6.55; N, 6.88.

Even on a 9.0 g (32 mmol) scale, the four-step sequence starting from the aldehyde (**13**) as described above can be run without isolation of intermediates to produce **27** (1.01 g, 8%) and a mixture of **25** (**26**) (6.94 g, 54%).

Method B: A solution of **29** (90 mg) in 2.3 N HCl–EtOAc (2.5 ml) was allowed to stand for 1.5 h. Work-up gave an oil, which was purified by column chromatography (EtOAc) to give **27** (8 mg, 12%) and a mixture of **25** and **26** (30 mg, 44%), the spectra (IR, ^{1}H-NMR) of which were identical with those of the samples prepared in Method A.

Method C: A solution of Ph_3P (435 mg, 1.5 mmol) in THF (5 ml) was added to a solution of NCS (221 mg, 1.5 mmol) in THF (15 ml), and the mixture was stirred for 25 min at room temperature. A solution of **22** (520 mg, 1 mmol) in THF (7 ml) was added to the resulting pasty solution, and the whole was stirred for 1 h. The reaction mixture was diluted with benzene–EtOAc (60 ml) and the whole was washed with H_2O, brine, dried, and evaporated. The residue, including the chloride (**32**), which was unstable during purification by column chromatography (EtOAc), was submitted to de-*tert*-butoxycarbonylation [2.3 N HCl–EtOAc (9 ml)] and cyclization with DBU (456 mg, 3 mmol) in DMSO (2 ml) as usual. The resulting crude oil was purified by column chromatography to give a mixture of **25** and **26** (172 mg, 43%), and **27** (23 mg, 6%). These products were identical with the samples prepared by method A, based on comparison of their IR and ^{1}H-NMR spectra.

Methyl 1-Benzoyl-2,3-dihydrolysergate (28)——A solution of a mixture of **25** and **26** (201 mg, 0.5 mmol) and concentrated HCl (1 ml) in MeOH (20 ml) was refluxed for 6 h. After removal of the solvent by evaporation, the residue was dried *in vacuo* over P_2O_5 for 14 h, then dissolved in dry MeOH (5 ml) and 2 N HCl in MeOH (1 ml). The mixture was stirred for 24 h at room temperature under N_2. The solvent was removed *in vacuo*, and the residue was neutralized with 10% K_2CO_3 and extracted with CH_2Cl_2. The extract was washed with brine, dried and evaporated. The residue was again dissolved in dry MeOH (20 ml) containing benzoyl chloride (0.5 ml) and pyridine (0.5 ml), and the mixture was stirred for 5 min at room temperature. The reaction mixture was concentrated *in vacuo*, and the residue was extracted with CH_2Cl_2. The extract was washed with H_2O and brine, dried, and concentrated. The residue was purified by column chromatography (EtOAc) to give an oil (116 mg, 60%), which is an epimeric mixture of **28**. Crystallization of the oil from EtOAc gave a solid, which was recrystallized from EtOAc to give **28**, mp 165—168 °C (lit.[2e] mp 165—168 °C). The IR and ^{1}H-NMR spectra were identical with those of an authentic sample.

Ethyl 2-(*N*-*tert*-Butoxycarbonyl-*N*-methylamino)methyl-3-(1-benzoyl-1,2,2a,3-tetrahydrobenz[*cd*]indol-5-yl)-propenoate (29)——The crude mesylate (**23**) obtained from **22** (520 mg, 1 mmol) was dissolved in DMSO (1.5 ml) and DBU (304 mg, 2 mmol) and the mixture was stirred for 5 min at room temperature. Water was added, and the aqueous solution was extracted. The extract was washed with H_2O and brine, dried, and evaporated. The residue was purified by column chromatography [benzene–EtOAc (5 : 1)] to give **29** (90 mg, 18%) as a colorless oil. IR ν_{max}^{neat} cm^{-1}: 1710, 1690, 1640 (CO). The ^{1}H-NMR spectrum was not sufficiently well resolved for assignment of the signals. MS *m/z*: 502 (M^+). HRMS Calcd for $C_{30}H_{34}N_2O_5$: 502.2469. Found: 502.2465.

Ethyl 3-Methyl-6-(1-benzoyl-1,2,2a,3-tetrahydrobenz[*cd*]indol-5-yl)-2-oxo-3,4,5,6-tetrahydro-1,3-oxazine-5-carboxylate (31)——The crude product obtained by mesylation of **22** (1.92 g, 3.7 mmol) as described above was subjected to column chromatography. The benzene–EtOAc eluate gave **31** (490 mg, 30%) as a solid, which was recrystallized from EtOAc to give colorless crystals, mp 161—163 °C. IR ν_{max}^{KBr} cm^{-1}: 1720, 1710, 1640 (CO). ^{1}H-NMR δ: 1.17 (3H, t, J=7 Hz, $CO_2CH_2C\underline{H}_3$), 2.18 (1H, br t, J=16 Hz, 3-H_{ax}), 2.60 (1H, br, 3-H_{eq}), 3.08 (3H, s, NCH_3), 3.73 (1H, dd, J=12, 9 Hz, 4-H), 3.78 (1H, t, J=11.5 Hz, 2-H), 4.11 (2H, q, J=7 Hz, $CO_2C\underline{H}_2CH_3$), 5.29 (1H, d, J=9 Hz, 6-H), 6.10 (1H, br m, 4-H), 7.0—7.60 (8H, m, Ph). *Anal.* Calcd for $C_{26}H_{26}N_2O_5$: C, 69.94; H, 5.87; N, 6.27. Found: C, 69.81; H, 5.93; N, 6.20.

Ethyl 2-(*N*-*tert*-Butoxycarbonyl-*N*-methylamino)methyl-3-hydroxy-2-methyl-3-(1-benzoyl-1,2,2a,3-tetrahydrobenz[*cd*]indol-5-yl)propionate (34)——A solution of **33** (368 mg, 1.5 mmol) in THF (5 ml) was added dropwise to a solution of LDA [prepared from diisopropylamine (152 mg, 1.5 mmol)] in THF (5 ml) at −78 °C, and the mixture was stirred for 20 min at −78 °C. A solution of **13** (289 mg, 1 mmol) in THF (10 ml) was added dropwise to this solution, and the whole was stirred for another 20 min. Work-up as described for the preparation of **22** gave an oil, which was purified by column chromatography [benzene–EtOAc (4 : 1)] to give **32** (494 mg, 95%) as a colorless oil. IR ν_{max}^{neat} cm^{-1}: 3400 (OH), 1720, 1690, 1640 (CO). The ^{1}H-NMR spectrum was not sufficiently well resolved for assignment of the signals. MS *m/z*: 534 (M^+). HRMS Calcd for $C_{31}H_{38}N_2O_6$: 534.2731. Found: 534.2726.

Ethyl 2-(*N*-*tert*-Butoxycarbonyl-*N*-methylamino)methyl-3-chloro-2-methyl-3-(1-benzoyl-1,2,2a,3-tetrahydrobenz-[*cd*]indol-5-yl)propionate (35)——Method A: $SOCl_2$ (2 ml) was added to a solution of **34** (534 mg, 1 mmol) in dry benzene (10 ml), and the mixture was allowed to stand for 30 min at room temperature, then refluxed for 1 h. The mixture was concentrated *in vacuo*, then the residue was made alkaline by the addition of saturated $NaHCO_3$ with cooling, and extracted with $CHCl_3$. The extract was washed with H_2O, dried, and concentrated. The residue was purified by column chromatography [benzene–AcOEt (4 : 1)] to give **35** (153 mg, 23%) as a pale yellow oil. IR ν_{max}^{neat} cm^{-1}: 1720, 1690, 1645 (CO). The ^{1}H-NMR spectrum was not sufficiently well resolved for assignment of the signals. MS *m/z*: 552 (M^+), 554 (M^++2). HRMS Calcd for $C_{31}H_{37}ClN_2O_5$: 552.2393. Found: 552.2388.

Method B: A solution of Ph_3P (263 mg) in THF (5 ml) was added to a solution of NCS (134 mg, 1 mmol) in THF (10 ml) at room temperature. Then a solution of **34** (267 mg, 0.5 mmol) in THF (5 ml) was added to the resulting pasty solution. Work-up as described for the preparation of **32** gave a crude oil, which was purified by column chromatography [benzene–EtOAc (4 : 1)] to give **35** (101 mg, 36%) as a pale yellow oil, which was identical with a sample prepared by method A, based on comparison of their IR spectra.

Ethyl 1-Benzoyl-8-methyl-2,3-dihydrolysergate (36) and Ethyl 1-Benzoyl-8-methyl-2,3-dihydroisolysergate (37)——Route A: The chloride (**35**) (153 mg, 0.23 mmol) obtained *via* method A was submitted to de-*tert*-butoxycarbonylation [2.3 N HCl–EtOAc (2 ml)], followed by treatment with DBU (105 mg, 0.69 mmol) in DMSO (1 ml) at 60 °C for 3 h. Work-up gave an oil, which was purified by column chromatography (EtOAc) to give **36** (30 mg, 30%) from the earlier fraction and **37** (25 mg, 26%) from the later fraction, each as an oil.

36: IR ν_{max}^{neat} cm^{-1}: 1720, 1640 (CO). ^{1}H-NMR δ: 1.30 (3H, t, J=7 Hz, $CO_2CH_2C\underline{H}_3$), 1.36 (1H, q, J=11 Hz, 4-H_{ax}), 1.48 (3H, s, CH_3), 2.49 (3H, s, NCH_3), 2.60 (1H, br, 4-H_{eq}), 2.68 (1H, d, J=11.5 Hz, 7-H_{ax}), 2.82 (1H, br d, J=11.5 Hz, 5-H), 2.89 (1H, dd, J=11.5, 1.4 Hz, 7-H_{eq}), 3.40 (1H, m, 3-H), 3.69 (1H, t, J=11 Hz, 2-H_α), 4.20 (2H, q, J=7 Hz, $CO_2C\underline{H}_2CH_3$), 4.24 (1H, br, 2-H_β), 6.54 (1H, br s, 9-H), 7.10—7.64 (8H, m, Ph). UV λ_{max}^{EtOH} nm (log ε): 255 (4.45), 305 (3.76). MS *m/z*: 416 (M^+). HRMS Calcd for $C_{26}H_{28}N_2O_3$: 416.2101. Found: 416.2099.

37: IR ν_{max}^{neat} cm^{-1}: 1720, 1640 (CO). ^{1}H-NMR δ: 1.23 (3H, t, J=7.3 Hz, $CO_2CH_2C\underline{H}_3$), 1.28 (3H, s, CH_3), 1.37 (1H, q, J=11.9 Hz, 4-H_{ax}), 2.15 (1H, d, J=11.5 Hz, 7-H_{ax}), 2.45 (3H, s, NCH_3), 2.54 (1H, br s, 4-H_{eq}), 2.81 (1H, br d, J=11.5 Hz, 5-H), 3.40 (1H, br m, 3-H), 3.49 (1H, d, J=11.5 Hz, 7-H_{eq}), 3.68 (1H, t, J=11 Hz, 2-H_α), 4.0—4.30 (3H, m, $CO_2C\underline{H}_2CH_3$, 2-H_β)), 6.40 (1H, s, 9-H), 7.0—7.66 (8H, m, Ph). UV λ_{max}^{EtOH} nm (log ε): 254 (4.33), 306 (3.63). MS *m/z*: 416 (M^+). HRMS Calcd for $C_{26}H_{28}N_2O_3$: 416.2101. Found: 416.2099.

Route B: The chloride (**35**) (170 mg, 0.3 mmol) obtained *via* method B was treated as described in route A to give **36** (84 mg, 65%) and **37** (8 mg, 6.5%). These products were identical with the samples obtained by route A, based on comparison of their IR and ^{1}H-NMR spectra.

Acknowledgement The authors are very grateful to Professor I. Ninomiya, Kobe Women's College of Pharmacy, for his continuing interest and kind encouragement throughout this work, and for providing ^{1}H-NMR spectrum of an authentic sample. We also thank Miss M. Nabae and Miss M. Danjo for the measurements of NMR spectra and MS, and Mrs. Y. Tsukamo for microanalyses.

References and Notes

1) Preliminary communication: T. Kurihara, T. Terada, and R. Yoneda, *Chem. Pharm. Bull.*, **34**, 442 (1986).
2) *a*) E. C. Kornfeld, E. J. Fornefeld, G. B. Kline, M. J. Mann, D. E. Morrison, R. G. Jones, and R. B. Woodward, *J. Am. Chem. Soc.*, **78**, 3087 (1956); *b*) M. Julia, F. Le Goffic, J. Igolen, and M. Baillarge, *Tetrahedron Lett.*, **1969**, 1569; *c*) R. Ramage, V. W. Armstrong, and S. Coulton, *Tetrahedron*, **37**, supplement 1, 157 (1981); *d*) W. Oppolzer, E. Frabcotte, and K. Battig, *Helv. Chim. Acta*, **64**, 478 (1981); *e*) I. Ninomiya, C. Hashimoto, T. Kiguchi, and T. Naito, *J. Chem. Soc., Perkin Trans. 1*, **1985**, 941; *f*) J. Rebek, Jr., D. F. Tai, and Y. K. Shue, *J. Am. Chem. Soc.*, **106**, 1813 (1984).
3) T. Kurihara, T. Terada, S. Satoda, and R. Yoneda, *Chem. Pharm. Bull.*, **34**, 2786 (1986).
4) S. Harusawa, R. Yoneda, T. Kurihara, Y. Hamada, and T. Shioiri, *Tetrahedron Lett.*, **25**, 427 (1984).
5) H. Tscherter and H. Hauth, *Helv. Chim. Acta*, **57**, 113 (1974).
6) The stereochemistry of 5a-H is ambiguous due to overlapping of the signal of this proton with other signals in the ^{1}H-NMR spectrum.
7) Purification of the mesylate (**23**) by column chromatography (SiO_2) was unsuccessful.
8) T. Kurihara, T. Terada, Y. Matsubara, and R. Yoneda, *Heterocycles*, **26**, 641 (1987).
9) A. J. Bose and B. Lai, *Tetrahedron Lett.*, **1973**, 3937.
10) As mentioned in a preliminary communication,[1] the aldehyde (**13**) was also prepared by the following method. A stream of H_2 was slowly bubbled through a solution of **11** (1.05 g, 4.6 mmol) in a mixture of EtOAc–xylene (3 : 1) (200 ml) containing *N*,*N*-dimethylaniline (669 mg, 5.5 mmol) and 10% Pd–$BaSO_4$ (1 g) for 2 h at 90—100 °C. During this period additional 10% Pd–$BaSO_4$ (0.2 g) was added every 30 min. The catalyst was removed by filtration, and the filtrate was concentrated *in vacuo*. The residue was purified by column chromatography [benzene–AcOEt (5 : 1)] to give **13** (719 mg, 54%).

[Chem. Pharm. Bull. 35(12)4803—4812(1987)]

Studies on Pyrazolo[3,4-*d*]pyrimidine Derivatives. XVI.[1] Preparation of Reissert Compounds from Condensed Pyrimidine Systems Catalyzed by Lewis Acids

TAKEO HIGASHINO,*,[a] SUSUMU SATO,[b] AKIRA MIYASHITA,[a] and TATSUHIKO KATORI[b]

School of Pharmaceutical Sciences, University of Shizuoka,[a] 2-2-1 Oshika, Shizuoka 422, Japan and Central Research Laboratories, S S Pharmaceutical Co., Ltd.,[b] 1143 Nanpeidai, Narita 286, Japan

(Received June 15, 1987)

Among various Lewis acids, aluminium chloride ($AlCl_3$) was the most effective catalyst for the formation of the Reissert compound ($\mathbf{2}_{1a}$, 5-benzoyl-4,5-dihydro-1-phenyl-1*H*-pyrazolo[3,4-*d*]-pyrimidine-4-carbonitrile) of 1-phenyl-1*H*-pyrazolo[3,4-*d*]pyrimidine ($\mathbf{1}_1$) by using benzoyl chloride and trimethylsilyl cyanide (TMSCN) in anhydrous methylene chloride (CH_2Cl_2).

Application of this method to derivatives of the following condensed pyrimidines, 1*H*-pyrazolo[3,4-*d*]pyrimidine (**1**), 9*H*-purine (**3**), 3*H*-1,2,3-triazolo[4,5-*d*]pyrimidine (**5**), and quinazoline (**7**), gave the corresponding new series of Reissert compounds (**2**, **4**, **6**, **8**, and **9**), which could not be prepared by the standard method using potassium cyanide and acid chloride in aqueous media.

Keywords——catalyst; aluminium chloride; Reissert compound; condensed pyrimidine; trimethylsilyl cyanide; acid chloride

It would appear that Reissert compounds[1,2a] derived from condensed pyrimidine systems are potentially useful as synthetic intermediates. In the pyrazolo[3,4-*d*]pyrimidine area, it was also reported that when attempts were made to form 5-benzoyl-4,5-dihydro-1-phenyl-1*H*-pyrazolo[3,4-*d*]pyrimidine-4-carbonitrile ($\mathbf{2}_{1a}$), one of the Reissert compounds of the pyrazolo[3,4-*d*]pyrimidine system, by the standard method[3] using benzoyl chloride and potassium cyanide in a chloroform–water solvent system, 1-phenyl-1*H*-pyrazolo[3,4-*d*]-pyrimidine ($\mathbf{1}_1$)[2b] underwent ring fission, resulting in the formation of 5-amino-1-phenyl-1*H*-pyrazole-4-carbaldehyde (**10**) and *N*-formylbenzamide (**11**).[2c] In 1977, Ruchirawat *et al.* obtained the Reissert compound of isoquinoline (2-benzoyl-1,2-dihydro-1-isoquinoline-carbonitrile) in anhydrous media using benzoyl chloride, trimethylsilyl cyanide (TMSCN), and a catalytic amount of aluminium chloride, which was an effective catalyst, in methylene chloride.[13] Recently, we reported that application of this method to $\mathbf{1}_1$ yielded the anticipated Reissert compound $\mathbf{2}_{1a}$.[2d]

Firstly, in order to select the most effective catalyst, the effects of various Lewis acids on the Reissert formation of $\mathbf{1}_1$ in anhydrous media was examined, and the results were compared with that in the absence of Lewis acid. Thus, $\mathbf{1}_1$ in methylene chloride was stirred under the reaction conditions shown in Table I with equimolar amounts of TMSCN and benzoyl chloride, and a catalytic amount of a Lewis acid (1/5—1/10 mol). Lewis acids used in the reaction were as follows: aluminium chloride, zinc chloride, titanium(IV) chloride, and boron trifluoride etherate. As shown in Table I, the presence of each Lewis acid increased the yield of the Reissert compound $\mathbf{2}_{1a}$ and reduced the reaction time as compared with those in the absence of Lewis acid. Moreover, it became clear that, among the Lewis acids used, aluminium chloride was the most effective catalyst with regard to the yield of the Reissert

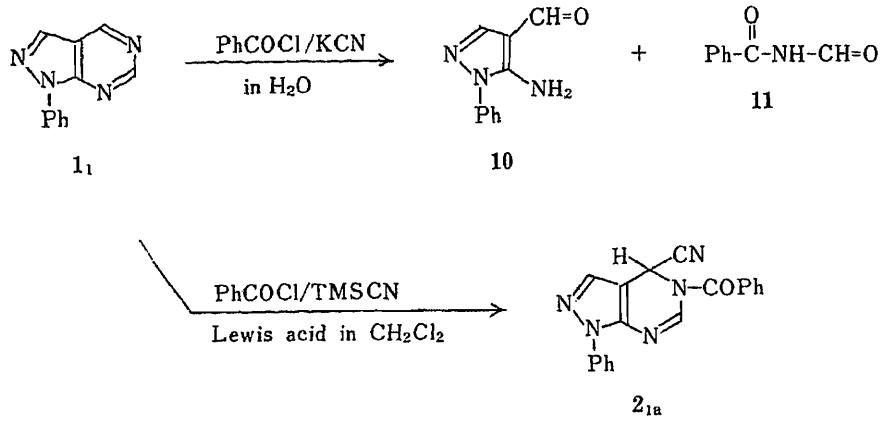

Chart 1

TABLE I. Reissert Compound Formation of $\mathbf{1}_1$ using PhCOCl and TMSCN in the Presence of Lewis Acids in CH_2Cl_2 to $\mathbf{2}_{1a}$

Lewis acid	Mol. ratio (PhCOCl/Lewis acid)	Reaction time (h)	Yield of $\mathbf{2}_{1a}$ (%)
—	—	96	12
$AlCl_3$	10/1	13	95
$ZnCl_2$	10/1	22	66
$TiCl_4$	10/1	22	78
$BF_3 \cdot Et_2O$	5/1	72	52

compound $\mathbf{2}_{1a}$ and reaction time. Therefore, this method using aluminium chloride as a catalyst in anhydrous media was applied to the Reissert compound formation of derivatives of the following condensed pyrimidine rings; 1*H*-pyrazolo[3,4-*d*]pyrimidine (**1**), 9*H*-purine (**3**), 3*H*-1,2,3-triazolo[4,5-*d*]pyrimidine (**5**), and quinazoline (**7**).

In the pyrazolo[3,4-*d*]pyrimidine area, application of Reissert compound formation in the presence of aluminum chloride to 1-phenyl- ($\mathbf{1}_1$),[2b] 6-methyl-1-phenyl- ($\mathbf{1}_2$), and 1-methyl-1*H*-pyrazolo[3,4-*d*]pyrimidines ($\mathbf{1}_3$)[2c] gave the corresponding Reissert compounds ($\mathbf{2}_{1a}$, $\mathbf{2}_{2a}$, and $\mathbf{2}_{3a}$) in satisfactory yields. In addition to benzoyl chloride, use of ethyl chloroformate, acetyl chloride, benzenesulfonyl chloride, and *p*-substituted benzoyl chlorides provided the corresponding Reissert compounds ($\mathbf{2}_{1b}$—$\mathbf{2}_{1g}$, $\mathbf{2}_{2e}$, and $\mathbf{2}_{3b}$) in good yields, as shown in Chart 2.

The experimental results shown in Chart 2 demonstrate that, in the pyrazolo[3,4-*d*]pyrimidine system, selective mono-Reissert formation across the 4,5-double bond rather than the 6,7-double bond proceeds, indicating that phenyl and methyl groups at the 1-position prevent the formation of Reissert compounds across the 6,7-double bond. In fact, even when a blocking group was present at the 4-position, the Reissert compound formation of 4-methyl- ($\mathbf{1}_4$)[2b] and 4-ethoxy-1-phenyl-1*H*-pyrazolo[3,4-*d*]pyrimidines ($\mathbf{1}_5$)[4a] with benzoyl chloride and TMSCN in the presence of aluminium chloride did not proceed, giving none of the corresponding Reissert compounds across the 6,7-double bond.

In the 9*H*-purine area, no work on Reissert compound formation has been reported in the literature. When Reissert compound formation of 9-phenyl-9*H*-purine ($\mathbf{3}_1$)[5a] was attempted by the standard method[3] using benzoyl chloride and potassium cyanide in a chloroform–water solvent system, $\mathbf{3}_1$ underwent ring fission of the imidazole ring, giving 4-benzamido-5-(*N*-phenylformamido)pyrimidine (**12**) in 23% yield, which was easily converted

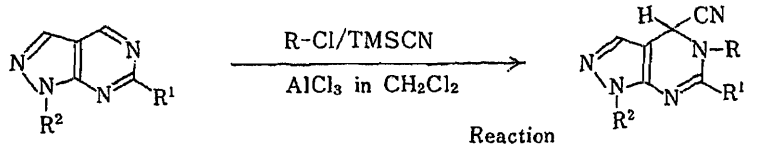

1	R^1	R^2	R	Reaction time (h)	2	Yield (%)
1_1	H	Ph	PhCO	13	2_{1a}	95
1_1	H	Ph	EtOCO	25	2_{1b}	88
1_1	H	Ph	Ac	36	2_{1c}	63
1_1	H	Ph	$PhSO_2$	336	2_{1d}	41
1_1	H	Ph	p-MeC_6H_4CO	8	2_{1e}	84
1_1	H	Ph	p-$MeOC_6H_4CO$	18	2_{1f}	73
1_1	H	Ph	p-$NO_2C_6H_4CO$	18	2_{1g}	65
1_2	Me	Ph	PhCO	17	2_{2a}	76
1_2	Me	Ph	p-MeC_6H_4CO	21	2_{2e}	41
1_3	H	Me	PhCO	51	2_{3a}	73
1_3	H	Me	EtOCO	31	2_{3b}	83

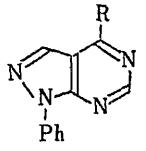

1	R
1_4	Me
1_5	EtO

Chart 2

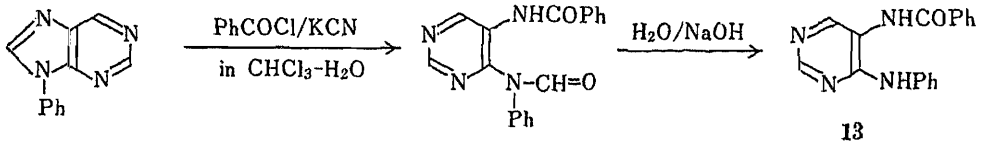

3_1 12 13

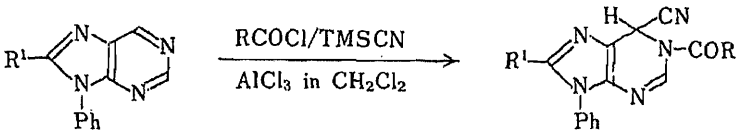

3	R^1	R	Reaction time (h)	4	Yield (%)
3_1	H	Ph	16	4_{1a}	48
3_1	H	EtO	72	4_{1b}	51
3_2	Me	Ph	8	4_{2a}	50
3_2	Me	EtO	20	4_{2b}	46

Chart 3

into 4-anilino-5-benzamidopyrimidine (**13**) by alkaline hydrolysis for structure determination.

The treatment of 3_1 and 8-methyl-9-phenyl-9*H*-purine (3_2)[5b] with equimolar quantities of benzoyl chloride and TMSCN, and a catalytic amount of aluminium chloride in methylene

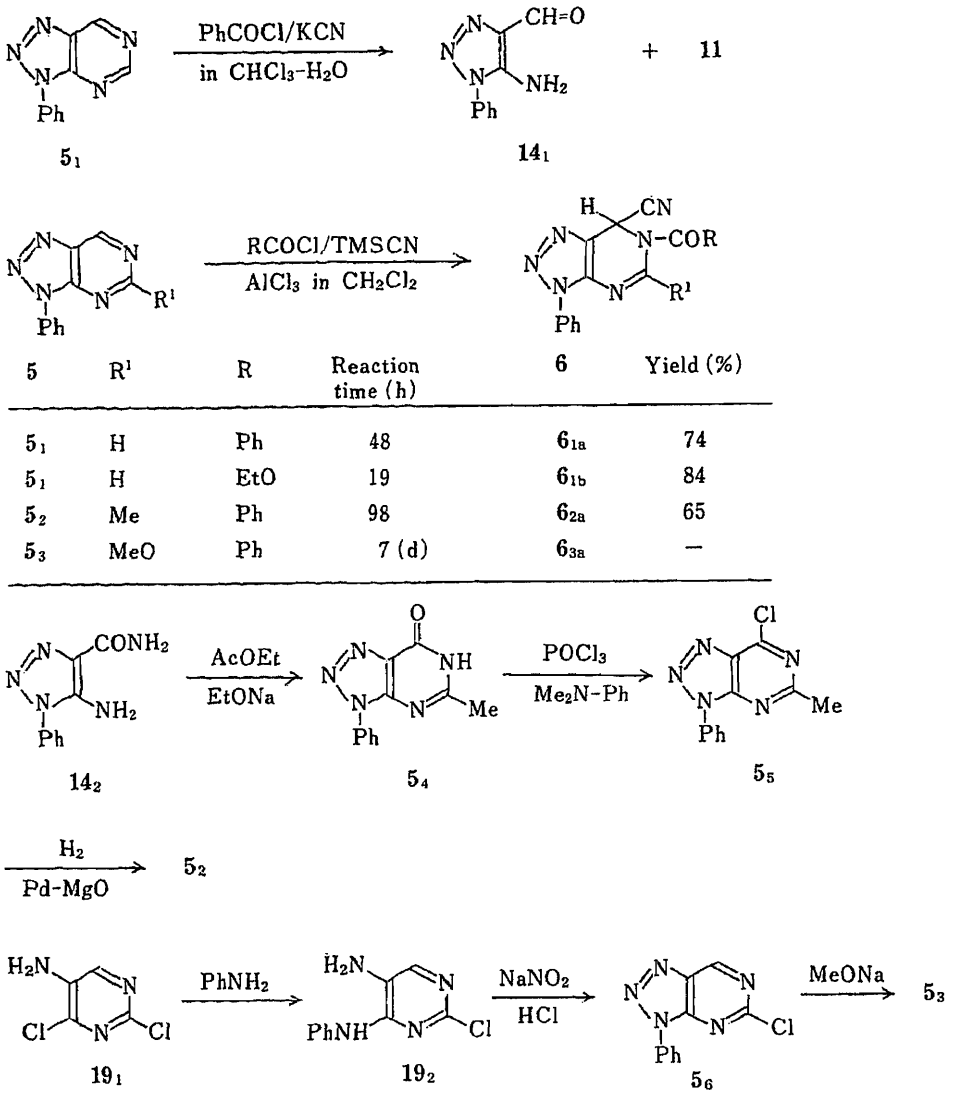

5	R¹	R	Reaction time (h)	6	Yield (%)
5_1	H	Ph	48	6_{1a}	74
5_1	H	EtO	19	6_{1b}	84
5_2	Me	Ph	98	6_{2a}	65
5_3	MeO	Ph	7 (d)	6_{3a}	—

Chart 4

chloride, gave the corresponding Reissert compounds 1-benzoyl-1,6-dihydro-9-phenyl-9*H*-purine-6-carbonitrile (4_{1a}) and the 8-methyl derivative of 4_{1a} (4_{2a}), respectively. Use of ethyl chloroformate in the cases of 3_1 and 3_2 provided the Reissert compounds 4_{1b} and 4_{2b}, respectively. The results are summarized in Chart 3.

In the 3*H*-1,2,3-triazolo[4,5-*d*]pyrimidine area, it was reported that when attempts were made to form 6-benzoyl-6,7-dihydro-3-phenyl-3*H*-1,2,3-triazolo[4,5-*d*]pyrimidine-7-carbonitrile (6_{1a}), one of the Reissert compounds of the 3*H*-1,2,3-triazolo[4,5-*d*]pyrimidine, by the standard method[3] using benzoyl chloride and aqueous potassium cyanide, 3-phenyl-3*H*-1,2,3-triazolo[4,5-*d*]pyrimidine (5_1)[2f] underwent ring fission, resulting in the formation of 5-amino-1-phenyl-1*H*-1,2,3-triazole-4-carboxaldehyde (14_1) and **11**.[2c] However, in the same Reissert formation as described for **2** and **4**, use of benzoyl chloride and ethyl chloroformate in the case of 5_1 resulted in the formation of the corresponding selective mono-Reissert compounds across the 6,7-double bond, such as 6-benzoyl- (6_{1a}) and 6-ethoxycarbonyl-6,7-dihydro-3-phenyl-3*H*-1,2,3-triazolo[4,5-*d*]pyrimidine-7-carbonitriles (6_{1b}). Similarly, use of benzoyl chloride in the case of 5-methyl-3-phenyl-3*H*-1,2,3-triazolo[4,5-*d*]pyrimidine (5_2) gave 6-benzoyl-6,7-dihydro-5-methyl-3-phenyl-3*H*-1,2,3-triazolo[4,5-*d*]pyrimidine-7-carbo-

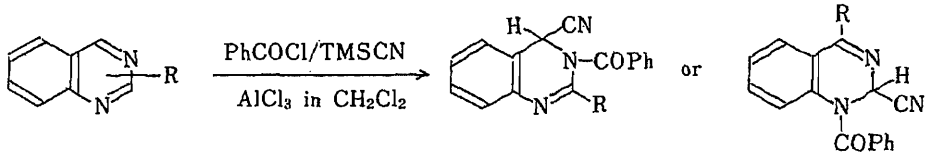

7	R	Reaction time (h)	8	Yield (%)	9	Yield (%)
7_1[9]	H	48	8_{1a}	67		
7_2	2-Me	3	8_{2a}	80		
7_3	4-OEt	3			9_{3a}	95
7_4[9]	4-Me	48			9_{4a}	73

Chart 5

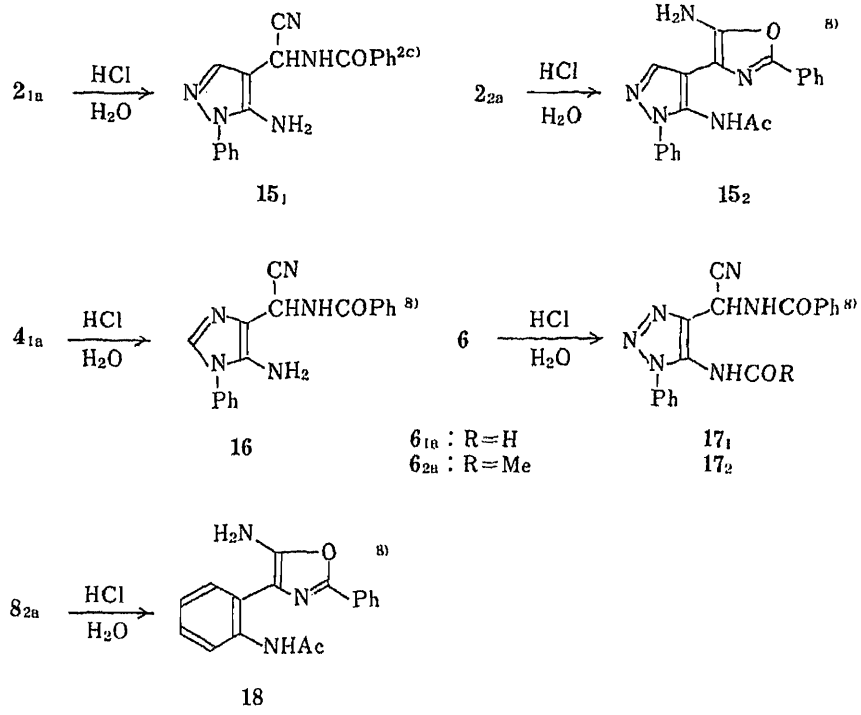

Chart 6

nitrile ($\mathbf{6}_{2a}$). The results are summarized in Chart 4.

Application of this Reissert compound formation to 5-methoxy-1-phenyl-1*H*-1,2,3-triazolo[4,5-*d*]pyrimidine ($\mathbf{5}_3$) did not give the anticipated Reissert compound ($\mathbf{6}_{3a}$) and the starting material was recovered. This indicates that steric hindrance caused by an alkoxy group at the 5-position prevents the formation of the mono-Reissert compound across the 6,7-double bond.

Compound $\mathbf{5}_2$ was prepared starting from 5-amino-1-phenyl-1*H*-1,2,3-triazole-4-carboxamide ($\mathbf{14}_2$).[6] The process in Chart 4, involving successive condensation of $\mathbf{14}_2$ with ethyl acetate, chlorination, and finally dechlorination with catalytic reduction over Pd–MgO, gave $\mathbf{5}_2$ with an overall yield of almost 40% based on the starting $\mathbf{14}_2$. Compound $\mathbf{5}_3$ was also prepared from 5-amino-2,4-dichloropyrimidine ($\mathbf{19}_1$)[7] by way of $\mathbf{19}_2$ and the chloro compound ($\mathbf{5}_6$) as shown in Chart 4.[8]

In the quinazoline area, it was reported by Popp and coworkers[9] that the Reissert

TABLE II. Melting Points, Elemental Analytical, and MS Data for **2**, **4**, **6**, **8**, and **9**

Compd.	mp (°C)	Formula	Analysis (%) Calcd (Found)			MS *m/z* M^+
			C	H	N	
$\mathbf{2}_{1a}$ [2d]	175—176[a,f]	$C_{19}H_{13}N_5O$	69.71	4.00	21.40	
$\mathbf{2}_{1b}$	115—116[a,g]	$C_{15}H_{13}N_5O_2$	61.01	4.44	23.72	295
			(60.68	4.52	23.28)	
$\mathbf{2}_{1c}$	184—185[a,g]	$C_{14}H_{11}N_5O$	63.38	4.18	26.40	265
			(63.31	4.20	26.40)	
$\mathbf{2}_{1d}$	109—110[a,h]	$C_{18}H_{13}N_5O_2S$	59.49	3.61	19.27	363
			(59.26	3.61	19.02)	
$\mathbf{2}_{1e}$	197—198[a,g]	$C_{20}H_{15}N_5O$	70.37	4.43	20.52	341
			(70.37	4.46	20.32)	
$\mathbf{2}_{1f}$	188—189[a,g]	$C_{20}H_{15}N_5O_2$	67.22	4.23	19.60	357
			(67.13	4.26	19.46)	
$\mathbf{2}_{1g}$	202—203[b,g]	$C_{19}H_{12}N_6O_3$	61.29	3.25	22.57	372
			(61.34	3.24	22.51)	
$\mathbf{2}_{2a}$	155—156[b,g]	$C_{20}H_{15}N_5O$	70.37	4.43	20.52	341
			(70.18	4.48	20.25)	
$\mathbf{2}_{2c}$	194—195[b,g]	$C_{21}H_{17}N_5O$	70.96	4.82	19.71	355
			(70.86	4.87	19.50)	
$\mathbf{2}_{3a}$	107—108[c,g]	$C_{14}H_{11}N_5O$	63.38	4.18	26.40	265
			(63.55	4.20	26.42)	
$\mathbf{2}_{3b}$	123—124[c,g]	$C_{10}H_{11}N_5O_2$	51.49	4.75	30.03	233
			(51.55	4.76	29.51)	
$\mathbf{4}_{1a}$	192—193[b,g]	$C_{19}H_{13}N_5O$	69.71	4.00	21.40	327
			(69.55	4.02	21.51)	
$\mathbf{4}_{1b}$	119—120[a,g]	$C_{15}H_{13}N_5O_2$	61.01	4.44	23.72	295
			(60.97	4.43	23.76)	
$\mathbf{4}_{2a}$	166—167[a,g]	$C_{20}H_{15}N_5O$	70.37	4.43	20.52	341
			(70.37	4.42	20.61)	
$\mathbf{4}_{2b}$	141—142[d,g]	$C_{16}H_{15}N_5O_2$	62.12	4.89	22.64	309
			(62.16	4.88	22.49)	
$\mathbf{6}_{1a}$	160—161[a,f]	$C_{18}H_{12}N_6O$	65.84	3.68	25.59	328
			(65.58	3.72	25.37)	
$\mathbf{6}_{1b}$	131—132[d,i]	$C_{14}H_{12}N_6O_2$	56.75	4.08	28.37	296
			(56.76	4.08	28.35)	
$\mathbf{6}_{2a}$	164—166[c,g]	$C_{19}H_{14}N_6O$	66.65	4.12	24.55	342
			(66.60	4.15	24.67)	
$\mathbf{8}_{1a}$ [2g]	171—172[a,h]	$C_{16}H_{11}N_3O$	73.55	4.24	16.08	
$\mathbf{8}_{2a}$	121[e,h]	$C_{17}H_{13}N_3O$	74.16	4.76	15.26	
			(73.85	4.71	15.19)	
$\mathbf{9}_{3a}$	88[a,h]	$C_{18}H_{15}N_3O_2$	70.80	4.95	13.76	305
			(70.80	4.89	13.75)	

a) Colorless needles. *b*) Colorless prisms. *c*) Colorless plates. *d*) Pale yellow needles. *e*) Orange needles. *f*) Recrystallized from benzene. *g*) Recrystallized from AcOEt. *h*) Recrystallized from benzene–petroleum ether. *i*) Recrystallized from MeOH.

compound formation of quinazoline ($\mathbf{7}_1$) using Ruchirawat's method selectively gave the mono-Reissert compound ($\mathbf{8}_{1a}$, 3-benzoyl-3,4-dihydro-4-quinazolinecarbonitrile) in 67% yield. They also reported[9] that application of this Reissert compound formation to 4-methylquinazoline ($\mathbf{7}_4$) provided the mono-Reissert compound ($\mathbf{9}_{4a}$, 1-benzoyl-1,2-dihydro-4-methyl-2-quinazolinecarbonitrile) and selectively functionalized the 1,2-double bond.

TABLE III. IR and ^{1}H-NMR Spectral Data for **2**, **4**, **6**, **8**, and **9**

Compd.	IR ν_{max}^{KBr} cm^{-1} [12]	^{1}H-NMR ($CDCl_3$) ppm
2_{1b}	1740 (CO)	8.00—7.70 (2H, m, Ph-H), 7.89 (1H, s, C^6-H), 7.60—7.20 (3H, m, Ph-H), 7.50 (1H, s, C^3-H), 6.18 (1H, s, C^4-H), 4.40 (2H, q, J=6.5 Hz, $O\underline{CH_2}CH_3$), 1.38 (3H, t, J=6.5 Hz, $CH_2\underline{CH_3}$)
2_{1c}	1694 (CO)	8.00—7.70 (2H, m, Ph-H), 7.73 (1H, s, C^6-H), 7.60—7.05 (3H, m, Ph-H), 7.57 (1H, s, C^3-H), 6.30 (1H, s, C^4-H), 2.47 (3H, s, $COCH_3$)
2_{1d}	1370, 1170 (SO_2)	8.15—7.10 (12H, m, Ph-H, C^6-H, and C^3-H), 6.22 (1H, s, C^4-H)
2_{1e}	1680 (CO)	8.00—7.00 (11H, m, Ph-H, C^6-H, and C^3-H), 6.30 (1H, s, C^4-H), 2.40 (3H, s, CH_3)
2_{1f}	1680 (CO)	8.00—7.00 (9H, m, Ph-H, C^6-H, and C^3-H), 6.92 (2H, d, J=9.0 Hz, Ph-H), 6.25 (1H, s, C^4-H), 3.80 (3H, s, OCH_3)
2_{1g} [a]	1310, 1520 (NO_2), 1700	8.36 (2H, d, J=8.0 Hz, Ph-H), 8.75—7.20 (7H, m, Ph-H, C^6-H, and C^3-H), 7.95 (2H, d, J=8.0 Hz, Ph-H), 6.70 (1H, s, C^4-H)
2_{2a}	1672 (CO)	8.10—7.80 (2H, m, Ph-H), 7.70—7.10 (9H, m, Ph-H and C^3-H), 6.20 (1H, s, C^4-H), 2.05 (3H, s, CH_3)
2_{2e}	1662 (CO)	8.10—7.80 (2H, m, Ph-H), 7.70—7.10 (8H, m, Ph-H and C^3-H), 6.20 (1H, s, C^4-H), 2.43 (3H, s, CH_3), 2.08 (3H, s, CH_3)
2_{3a}	1680 (CO)	7.80—7.10 (7H, m, Ph-H, C^6-H, and C^3-H), 6.23 (1H, s, C^4-H), 3.80 (3H, s, CH_3)
2_{3b}	1740 (CO)	7.88 (1H, s, C^6-H), 7.40 (1H, s, C^3-H), 6.20 (1H, s, C^4-H), 4.40 (2H, q, J=6.5 Hz, $O\underline{CH_2}CH_3$), 3.80 (3H, s, CH_3), 1.41 (3H, t, J=6.5 Hz, $CH_2\underline{CH_3}$)
4_{1a} [b]	1690 (CO)	7.88 (1H, s, C^2-H), 7.80—7.20 (11H, m, Ph-H and C^8-H), 6.47 (1H, s, C^6-H)
4_{1b}	1740 (CO)	7.77 (1H, s, C^2-H), 7.70—7.20 (5H, m, Ph-H), 7.54 (1H, s, C^8-H), 6.22 (1H, s, C^6-H), 4.40 (2H, q, J=6.5 Hz, $O\underline{CH_2}CH_3$), 1.37 (3H, t, J=6.5 Hz, $CH_2\underline{CH_3}$)
4_{2a}	1680 (CO)	7.80—7.15 (11H, m, Ph-H and C^2-H), 6.39 (1H, s, C^6-H), 2.37 (3H, s, CH_3)
4_{2b}	1730 (CO)	7.83 (1H, s, C^2-H), 7.80—7.10 (5H, m, Ph-H), 6.30 (1H, s, C^6-H), 4.40 (2H, q, J=6.5 Hz, $O\underline{CH_2}CH_3$), 2.31 (3H, s, CH_3), 1.39 (3H, t, J=6.5 Hz, $CH_2\underline{CH_3}$)
6_{1a}	1690 (CO)	8.05—7.25 (11H, m, Ph-H and C^5-H), 6.51 (1H, s, C^7-H)
6_{1b}	1765 (CO)	8.07 (1H, s, C^5-H), 8.00—7.80 (2H, m, Ph-H), 7.63—7.30 (3H, m, Ph-H), 6.44 (1H, s, C^7-H), 4.48 (2H, q, J=6.5 Hz, $O\underline{CH_2}CH_3$), 1.44 (3H, t, J=6.5 Hz, $CH_2\underline{CH_3}$)
6_{2a}	1680 (CO)	8.35—7.80 (4H, m, Ph-H), 7.70—7.30 (6H, m, Ph-H), 6.41 (1H, s, C^7-H), 2.12 (3H, s, CH_3)
8_{2a}	1680 (CO)	7.80—7.18 (9H, m, Ph-H and aromatic H), 6.17 (1H, s, C^4-H), 2.04 (3H, s, CH_3)
9_{3a}	1660 (CO)	7.90—6.60 (9H, m, Ph-H and aromatic H), 6.80 (1H, s, C^2-H), 4.32 (2H, q, J=7.0 Hz, $O\underline{CH_2}CH_3$), 1.42 (3H, t, J=7.0 Hz, $CH_2\underline{CH_3}$)

a) ^{1}H-NMR in $(CD_3)_2SO$. *b*) ^{1}H-NMR in a mixture of $CDCl_3$ and $(CD_3)_2SO$.

The same selective mono-Reissert compound formation was found to occur with 2-methyl- (7_2)[10] and 4-ethoxyquinazolines (7_3).[11] Thus, application of the Reissert compound formation as described for **2** to 7_2 resulted in the formation of the anticipated mono-Reissert compound (8_{2a}, 3-benzoyl-3,4-dihydro-2-methyl-4-quinazolinecarbonitrile). The reaction of 7_3 yielded the mono-Reissert compound (9_{3a}, 1-benzoyl-1,2-dihydro-4-ethoxy-2-quinazolinecarbonitrile) across the 1,2-double bond.

Structural determination of the new series of Reissert compounds was accomplished on the basis of analytical and spectral data (Tables II, III, and IV) and the results obtained from the following experiments (shown in Chart 6). Thus, 2_{1a}, 2_{2a}, 4_{1a}, 6_{1a}, 6_{2a}, 8_{2a} in an acid medium underwent ring fission, resulting in the formation of the α-benzamido-1*H*-pyrazole-4-acetonitrile (15_1),[2d] 4-(4-pyrazolyl)oxazole (15_2),[8] α-benzamido-1*H*-imidazole-4-acetonitrile (**16**),[8] α-benzamido-1*H*-1,2,3-triazole-4-acetonitriles (17_1 and 17_2),[8] 4-aryl-2-phenyloxazole (**18**),[8] respectively, confirming the positions bonded with cyano and benzoyl groups in the new series of Reissert compounds.

The above observations provide a useful synthetic method for the Reissert compounds from condensed pyrimidines. Studies on the reactivity of the new series of Reissert

TABLE IV. ^{13}C-NMR Spectral Data for **2**, **4**, **6**, **8** and **9**

Compd.	^{13}C-NMR ($CDCl_3$) ppm
$\mathbf{2_{1b}}$	14.1 (q, CH_3), 42.9 (d, C^4), 65.1 (t, CH_2), 96.7 (s), 115.8 (s, CN), 122.5 (d), 127.3 (d), 129.0 (d), 135.1 (d), 138.3 (s), 140.7 (s), 142.1 (d), 151.4 (s, CO)
$\mathbf{2_{1c}}$	22.0 (q, CH_3), 41.0 (d, C^4), 97.8 (s), 116.8 (s, CN), 122.0 (d), 127.1 (d), 129.0 (d), 136.2 (d), 138.2 (s), 140.7 (s), 145.1 (d), 170.3 (s, CO)
$\mathbf{2_{1d}}$	43.2 (d, C^4), 96.3 (s), 114.9 (s, CN), 122.6 (d), 127.5 (d), 127.9 (d), 129.0 (d), 130.0 (d), 134.8 (d), 135.3 (d), 136.3 (s), 138.0 (s), 140.1 (s), 141.3 (d)
$\mathbf{2_{1e}}$ [a]	21.1 (q, CH_3), 41.6 (d, C^4), 98.5 (s), 116.8 (s, CN), 122.0 (d), 127.1 (s), 128.8 (d), 129.0 (d), 129.4 (d), 129.7 (d), 136.0 (d), 138.1 (s), 141.0 (s), 143.3 (s), 145.5 (d), 169.6 (s, CO)
$\mathbf{2_{1f}}$ [a]	41.6 (d, C^4), 55.5 (q, CH_3), 98.6 (s), 114.2 (d), 116.9 (s, CN), 122.0 (d), 123.5 (s), 127.1 (d), 129.0 (d), 132.1 (d), 135.9 (d), 138.2 (s), 141.1 (s), 145.7 (d), 162.9 (s), 169.1 (s, CO)
$\mathbf{2_{1g}}$ [a]	41.7 (d, C^4), 98.3 (s), 116.5 (s, CN), 122.1 (d), 123.9 (d), 127.2 (d), 129.1 (d), 130.9 (d), 136.2 (d), 137.6 (s), 138.1 (s), 140.7 (s), 144.9 (d), 149.5 (s), 168.4 (s, CO)
$\mathbf{2_{2a}}$ [a]	26.2 (q, CH_3), 42.2 (d, C^4), 99.9 (s), 117.0 (s, CN), 121.7 (d), 126.9 (d), 129.0 (d), 133.2 (d), 134.3 (s), 135.1 (d), 138.3 (s), 142.0 (s), 153.4 (s), 170.8 (s, CO)
$\mathbf{2_{2c}}$ [a]	21.1 (q, CH_3), 26.2 (q, CH_3), 42.2 (d, C^4), 99.9 (s), 117.1 (s, CN), 121.7 (d), 126.9 (d), 129.1 (d), 129.6 (d), 131.4 (s), 135.1 (d), 138.3 (s), 142.1 (s), 144.0 (s), 153.6 (s), 170.7 (s, CO)
$\mathbf{2_{3a}}$	34.4 (q, CH_3), 42.0 (d, C^4), 95.8 (s), 115.9 (s, CN), 129.1 (d), 129.2 (d), 131.4 (s), 132.9 (d), 133.9 (d), 140.9 (s), 143.2 (d), 169.6 (s, CO)
$\mathbf{2_{3b}}$ [a]	14.0 (q, CH_3), 34.0 (q, CH_3), 43.0 (d, C^4), 64.6 (t, CH_2), 95.4 (s), 117.1 (s, CN), 134.1 (d), 140.4 (s), 142.5 (d), 151.7 (s, CO)
$\mathbf{4_{1a}}$ [a]	44.4 (d, C^6), 115.9 (s, CN),[b] 116.9 (s),[b] 123.6 (d), 127.9 (d), 128.8 (d), 129.3 (d), 129.4 (d), 131.7 (s), 131.9 (d), 132.5 (s), 134.4 (s), 136.3 (d), 142.1 (d), 169.8 (s, CO)
$\mathbf{4_{1b}}$	14.1 (q, CH_3), 45.9 (d, C^6), 65.0 (t, CH_2), 115.4 (s, CN),[b] 116.2 (s),[b] 123.7 (d), 128.2 (d), 129.5 (d), 132.2 (s), 134.4 (s), 135.8 (d), 139.9 (d), 151.8 (s, CO)
$\mathbf{4_{2a}}$ [a]	13.7 (q, CH_3), 44.3 (d, C^6), 114.4 (s),[b] 115.9 (s, CN),[b] 127.0 (d), 128.2 (d), 128.8 (d), 129.2 (d), 132.0 (s), 132.4 (d), 133.8 (s), 140.9 (d), 144.3 (s), 169.8 (s, CO)
$\mathbf{4_{2b}}$ [a]	13.7 (q, CH_3), 13.9 (q, CH_3), 45.7 (d, C^6), 64.4 (t, CH_2), 113.6 (s),[b] 116.2 (s, CN),[b] 127.1 (d), 128.7 (d), 129.3 (d), 132.3 (s), 133.9 (s), 139.1 (d), 144.3 (s), 151.8 (s, CO)
$\mathbf{6_{1a}}$	43.2 (d, C^7), 114.6 (s, CN), 122.5 (d), 124.3 (s), 129.6 (d), 129.7 (d), 129.8 (d), 131.1 (s), 133.7 (d), 135.7 (s), 137.1 (s), 146.2 (d), 169.6 (s, CO)
$\mathbf{6_{1b}}$	14.1 (q, CH_3), 44.1 (d, C^7), 65.8 (t, CH_2), 114.6 (s, CN), 122.2 (d), 123.2 (s), 129.1 (d), 129.4 (d), 135.4 (s), 136.9 (s), 144.4 (d), 151.1 (s, CO)
$\mathbf{6_{2a}}$	26.2 (q, CH_3), 42.9 (d, C^7), 114.6 (s, CN), 121.6 (d), 125.1 (s), 128.0 (d), 128.7 (d), 129.1 (d), 129.2 (d), 133.5 (d), 135.3 (s), 137.4 (s), 155.6 (s), 170.4 (s, CO)
$\mathbf{8_{2a}}$	25.8 (q, CH_3), 43.9 (d, C^4), 115.7 (s, CN), 119.7 (s), 125.3 (d), 125.6 (d), 127.7 (d), 128.7 (d), 129.0 (d), 130.8 (d), 133.1 (d), 134.1 (s), 140.2 (s), 151.3 (s), 169.5 (s, CO)
$\mathbf{9_{3a}}$	13.9 (q, CH_3), 60.1 (d, C^2), 62.9 (t, CH_2), 115.7 (s, CN),[b] 117.8 (s),[b] 123.6 (d), 125.5 (d), 128.6 (d), 128.7 (d), 131.7 (d), 132.2 (d), 133.4 (s), 137.7 (s), 162.6 (s), 168.5 (s, CO)

a) ^{13}C-NMR in $(CD_3)_2SO$. *b*) Assignments may be interchanged.

compounds are now in progress and will shortly be reported in a separate paper.

Experimental

All melting points are uncorrected. Infrared absorption (IR) spectra were recorded on a Jasco A-102 diffraction grating IR spectrometer. Proton nuclear magnetic resonance (^{1}H-NMR) spectra were measured at 60 MHz on a Hitachi R-24B high-resolution NMR spectrometer, and ^{13}C-NMR spectra were taken at 90 MHz on a JEOL JNM-FX90Q FTNMR spectrometer. Chemical shifts are quoted in parts per million (ppm) with tetramethylsilane as an internal standard, and coupling constants (J) are given in Hz. The following abbreviations are used: s = singlet, d = doublet, t = triplet, q = quartet, m = multiplet, and br s = broad singlet. Mass spectra (MS) were recorded on a JEOL JMS D-100 mass spectrometer. Samples were vaporized in a direct inlet system. Column chromatography was carried out on SiO_2, Wakogel C-200 (200 mesh). Thin-layer chromatography (TLC) was performed on precoated Kieselgel 60 F_{254} plates (Merck) with $CHCl_3$.

Reissert Compound Formation of Condensed Pyrimidines (1, 3, 5 and 7) Catalyzed by Lewis Acids——The procedure for the Reissert compound 5-carbethoxy-4,5-dihydro-1-phenyl-1*H*-pyrazolo[3,4-*d*]pyrimidine-4-carbonitrile ($\mathbf{2}_{1b}$) is described as a typical example. Ethyl chloroformate (570 mg, 5.2 mmol) was added to a well stirred solution of 1-phenyl-1*H*-pyrazolo[3,4-*d*]pyrimidine ($\mathbf{1}_1$, 980 mg, 5.0 mmol) in freshly distilled CH_2Cl_2 (25 ml), then TMSCN (532 mg, 5.2 mmol) was added. After 5 min, $AlCl_3$ (66.7 mg, 0.5 mmol) was added at once, and the whole was stirred at room temperature until the starting material $\mathbf{1}_1$ had disappeared (25 h), as monitored by TLC. The solution was washed with H_2O, 5% HCl, H_2O, 5% NaOH, and H_2O. The CH_2Cl_2 solution was dried over Na_2SO_4 and concentrated. The residue was passed through a column of SiO_2 with $CHCl_3$ to remove impurities. Recrystallization from AcOEt gave $\mathbf{2}_{1b}$ as colorless needles, mp 115—116 °C, in 88% yield (1300 mg).

Yields, melting points, analytical and spectral data for the new Reissert compounds (**2**, **4**, **6**, **8**, and **9**) are listed in Charts 2—5 and Tables II—IV.

6-Methyl-1-phenyl-1*H*-pyrazolo[3,4-*d*]pyrimidine ($\mathbf{1}_2$)——A solution of 4-chloro-6-methyl-1-phenyl-1*H*-pyrazolo[3,4-*d*]pyrimidine[4b] (33.5 g, 136.8 mmol) in a mixture of benzene (280 ml) and MeOH (140 ml) was added to a catalyst prepared from 1% $PdCl_2$ (100 ml) and MgO (2.7 g), and the mixture was shaken in an H_2 stream. The reaction was stopped when 136 mmol of H_2 had been absorbed. The catalyst was filtered off and the filtrate was concentrated under reduced pressure. The residue was decomposed with diluted aqueous NH_3 and extracted with $CHCl_3$. The extract was washed with H_2O, dried over Na_2SO_4, and concentrated to dryness under reduced pressure. The residue was recrystallized from petroleum benzin to give $\mathbf{1}_2$ as colorless needles, mp 99—100 °C, in 90% yield (25.8 g). *Anal.* Calcd for $C_{12}H_{10}N_4$: C, 68.55; H, 4.79; N, 26.65. Found: C, 68.65; H, 4.87; N, 26.93. MS *m/z*: 210 (M^+). ^{1}H-NMR ($CDCl_3$): 9.08 (1H, s, C^4-H), 8.13 (1H, s, C^3-H), 8.40—8.10 (2H, m, Ph-H), 7.70—7.10 (3H, m, Ph-H), 2.85 (3H, s, CH_3). ^{13}C-NMR ($CDCl_3$): 26.4 (q), 113.6 (s), 120.9 (d), 126.3 (d), 129.0 (d), 133.6 (d), 138.8 (s), 152.0 (d), 153.0 (s), 165.7 (s).

Reaction of 9-Phenyl-9*H*-purine ($\mathbf{3}_1$) with Benzoyl Chloride in the Presence of KCN——A solution of KCN (260 mg, 4 mmol) in H_2O (1 ml) was added dropwise to a stirred solution of $\mathbf{3}_1$ (392 mg, 2 mmol) and benzoyl chloride (281 mg, 2 mmol) in $CHCl_3$ (4 ml), and the mixture was stirred for 1 h. The reaction mixture was poured into a large amount of H_2O and extracted with $CHCl_3$. The extract was washed with H_2O, dried over Na_2SO_4, and concentrated under reduced pressure. The residue was chromatographed on a column of SiO_2 with $CHCl_3$. The first fraction gave 5-benzamido-4-(*N*-phenylformamido)pyrimidine (**12**) as colorless needles from benzene, mp 144—145 °C, in 23% yield (146 mg). The second fraction gave the starting $\mathbf{3}_1$ in 24% yield (94 mg).

12: *Anal.* Calcd for $C_{18}H_{14}N_4O_2$: C, 67.91; H, 4.43; N, 17.60. Found: C, 67.65; H, 4.44; N, 17.65. MS *m/z*: 318 (M^+). IR ν_{max}^{KBr} cm^{-1}: 3250 (NH), 1720, 1650 (C=O). ^{1}H-NMR ($CDCl_3$): 9.40 (1H, s, CH=O), 8.85 (1H, s, pyrimidine H), 8.78 (1H, s, pyrimidine H), 8.50—7.00 (11H, m, Ph-H and NH). ^{13}C-NMR ($(CD_3)_2SO$): 125.3 (d), 126.4 (s), 126.9 (d), 127.5 (d), 128.1 (d), 128.9 (d), 131.9 (d), 133.0 (s), 137.1 (s), 153.9 (s), 155.0 (d), 156.6 (d), 165.1 (s).

Alkaline Hydrolysis of 12——A mixture of **12** (50 mg) and 2 N NaOH (1 ml) was heated for 5 min on a steam bath. The reaction mixture was poured into a large amount of H_2O and extracted with $CHCl_3$. The extract was dried over Na_2SO_4, and concentrated under reduced pressure, and the residue was chromatographed on a column of SiO_2 with $CHCl_3$. The first fraction gave 4-anilino-5-benzamidopyrimidine (**13**) as colorless needles from MeOH, mp 193.5—194.5 °C, in 57% yield (26 mg). MS *m/z* Calcd for $C_{17}H_{14}N_4O$: 290.1167 (M^+). Observed: 290.1182. IR ν_{max}^{KBr} cm^{-1}: 3250 (NH), 1658 (C=O). ^{1}H-NMR ($CDCl_3$–($(CD_3)_2SO$): 9.70 (1H, br s, exchangeable with D_2O, NH), 8.52 (1H, s, pyrimidine H), 8.49 (1H, s, pyrimidine H), 8.40 (1H, br s, exchangeable with D_2O, NH), 8.20—7.00 (10H, m, Ph-H).

Benzoylation of 5-Amino-4-anilinopyrimidine[5a]——Benzoyl chloride (140 mg, 1 mmol) was added to a solution of 5-amino-4-anilinopyrimidine (186 mg, 1 mmol) in pyridine (1 ml) and the mixture was stirred overnight at room temperature. The separated crystals were collected by suction, washed with H_2O, and recrystallized from MeOH–benzene to give **13** as colorless needles in 80% yield (232 mg).

3,6-Dihydro-5-methyl-3-phenyl-7*H*-1,2,3-triazolo[4,5-*d*]pyrimidin-7-one ($\mathbf{5}_4$)——A mixture of 5-amino-1-phenyl-1*H*-1,2,3-triazole-4-carboxamide ($\mathbf{14}_2$, 40.6 g, 0.2 mol) and AcOEt (40 ml) in EtONa solution prepared by dissolving Na (9.2 g, 0.4 mol) in an EtOH (400 ml) was refluxed under stirring for 20 h. The EtOH was removed under reduced pressure, and H_2O (1 : 1) was added to the residue. After the insoluble crystals had been filtered off, the filtrate was neutralized with AcOH and the separated crystals were recrystallized from MeOH to give $\mathbf{5}_4$ as slightly yellow needles, mp 267—268 °C (dec.), in 78% yield (35.5 g). *Anal.* Calcd for $C_{11}H_9N_5O$: C, 58.14; H, 3.99; N, 30.82. Found: C, 58.20; H, 4.04; N, 31.08. IR ν_{max}^{KBr} cm^{-1}: 1695 (C=O). ^{1}H-NMR ($CDCl_3$): 8.2—6.9 (5H, m, Ph-H), 6.2—4.7 (1H, br, NH), 2.4 (3H, s, CH_3).

7-Chloro-5-methyl-3-phenyl-3*H*-1,2,3-triazolo[4,5-*d*]pyrimidine ($\mathbf{5}_5$)——*N*,*N*-Dimethylaniline (3.5 g) was added dropwise to a stirred mixture of $\mathbf{5}_4$ (5.0 g) and $POCl_3$ (40 ml), and the mixture was refluxed for 30 min in an oil bath. The $POCl_3$ was removed under reduced pressure and a large amount of H_2O was added to the residue. The reaction mixture was stirred for 5 min, and extracted with benzene. The extract was dried over Na_2SO_4, concentrated, and chromatographed on a column of SiO_2 with benzene. The first fraction gave $\mathbf{5}_5$ as yellow needles from benzene, mp 114—116 °C, in 76% yield (4.1 g). *Anal.* Calcd for $C_{11}H_8ClN_5$: C, 53.78; H, 3.28; N, 28.51. Found: C, 53.76; H, 3.26; N, 28.54. ^{1}H-NMR ($CDCl_3$): 8.40—7.45 (5H, m, Ph-H), 2.89 (3H, s, CH_3).

5-Methyl-3-phenyl-3*H*-1,2,3-triazolo[4,5-*d*]pyrimidine (5_2)——A solution of 5_5 (3.6 g, 14 mmol) in benzene (50 ml) was added to a catalyst prepared from 1% $PdCl_2$ (10 ml) and MgO (2.7 g) in H_2O (10 ml), and the mixture was shaken in an H_2 stream. The reaction was stopped when 313 ml (14 mmol) of H_2 had been absorbed. The same work-up as described for 1_2 gave 5_2 as colorless plates from benzene, mp 158—159 °C, in 72% yield (2.2 g). *Anal.* Calcd for $C_{11}H_9N_5$: C, 62.55; H, 4.30; N, 33.16. Found: C, 62.69; H, 4.36; N, 33.11. ^{1}H-NMR ($CDCl_3$): 9.50 (1H, s, C^7-H), 8.50—7.40 (5H, m, Ph-H), 2.93 (3H, s, CH_3).

Acknowledgement The authors are greatly indebted to the staff of the central analysis room of the University of Shizuoka for elemental analysis and mass spectral measurement.

References and Notes

1) Part XV: T. Higashino, S. Sato, A. Miyashita, and T. Katori, *Chem. Pharm. Bull.*, **35**, 4078 (1987).
2) *a*) T. Higashino, H. Kokubo, and E. Hayashi, *Chem. Pharm. Bull.*, **33**, 950 (1985); *b*) T. Higashino, Y. Iwai, and E. Hayashi, *Yakugaku Zasshi*, **94**, 666 (1974); *c*) T. Higashino, H. Kokubo, A. Goto, M. Takemoto, and E. Hayashi, *Chem. Pharm. Bull.*, **32**, 3690 (1984); *d*) T. Higashino, S. Sato, A. Miyashita, and T. Katori, *ibid.*, **34**, 4569 (1986); *e*) T. Higashino, Y. Iwai, and E. Hayashi, *ibid.*, **24**, 3120 (1976); *f*) T. Higashino, T. Katori, and E. Hayashi, *ibid.*, **27**, 2431 (1979); *g*) T. Higashino, H. Kokubo, and E. Hayashi, *ibid.*, **32**, 3900 (1984).
3) *a*) W. E. McEwen and R. L. Cobb, *Chem. Rev.*, **55**, 511 (1955); *b*) F. D. Popp, "Advances in Heterocyclic Chemistry," Vol. 9, ed. by A. R. Katoritzky and A. J. Boulton, Academic Press, Inc., New York, 1968, p. 1; *c*) *Idem*, *ibid.*, Vol. 24, 1979, p. 187.
4) *a*) C. C. Cheng and R. K. Robins, *J. Org. Chem.*, **21**, 1240 (1956); *b*) *Idem*, *ibid.*, **23**, 191 (1958).
5) *a*) E. Hayashi, N. Shimada, and Y. Matsuoka, *Yakugaku Zasshi*, **99**, 114 (1979); *b*) E. Hayashi, N. Shimada, Y. Matsuoka, and Y. Miwa, *ibid.*, **99**, 207 (1979).
6) A. Dornow and J. Helberg, *Chem. Ber.*, **93**, 2001 (1960).
7) N. Whittaker, *J. Chem. Soc.*, **1951**, 1565.
8) Unpublished data. The results obtained from acid hydrolysis will be reported in detail in a separate paper.
9) J. Kant, F. D. Popp, B. L. Joshi, and B. C. Uff, *Chem. Ind.* (London), **1984**, 415.
10) A. Bischler, *Ber.*, **24**, 506 (1891).
11) M. T. Bogert and C. E. May, *J. Am. Chem. Soc.*, **31**, 509 (1909).
12) No absorption due to the cyano group was seen in the IR spectra. This is compatible with the reported absence of the cyano group absorption of 2_{1a} and 8_{1a}.[3d,g]
13) S. Ruchirawat, N. Phadungkul, M. Chuankamnerdkarn, and C. Thebtaranonth, *Heterocycles*, **6**, 43 (1977).

[Chem. Pharm. Bull. 35(12)4813—4818(1987)]

Studies on *Cerbera*. IV.[1] Polar Cardenolide Glycosides from the Leaves of *Cerbera odollam* and *Cerbera manghas*

TATSUO YAMAUCHI,*,[a] FUMIKO ABE,[a] and ALFRED S. C. WAN[b]

Faculty of Pharmaceutical Sciences, Fukuoka University,[a] 8-19-1 Nanakuma, Jonan-ku, Fukuoka 814-01, Japan and Department of Pharmacy, Faculty of Science, National University of Singapore,[b] 10 Kent Ridge Crescent, Singapore 0511

(Received June 19, 1987)

Glucos-3-ulosyl-thevetosides of 17α-digitoxigenin and 17α-tanghinigenin were obtained from air-dried leaves of *Cerbera manghas* and *C. odollam*. From fresh leaves, oleagenin glucosyl-thevetoside and digitoxigenin gentiotriosyl-thevetoside were isolated besides known glycosides, glucosyl-thevetosides of digitoxigenin and tanghinigenin. The difference between the cardenolide glycosides of the air-dried leaves and of the fresh leaves, and the glycosides patterns in the two species are discussed.

Keywords——*Cerbera odollam*; *Cerbera manghas*; Apocynaceae; cardenolide; 17α-cardenolide glucos-3-ulosyl-thevetoside; cerleaside B; oleagenin glucosyl-thevetoside; digitoxigenin gentiotriosyl-thevetoside

In the preceding paper of this series, we described the cardenolide monoglycosides from the air-dried leaves of *Cerbera odollam* GAERTN. and *C. manghas* L., and showed the presence of oleagenin α-L-thevetoside (cerleaside A), 8β-hydroxy-17β- and 17α-digitoxigenin α-L-thevetosides (17β- and 17α-cerdollaside), and 17β- and 17α-digitoxigenin α-L-acofriosides (17β- and 17α-solanoside), together with the four major monosides, 17β- and 17α-neriifolin and 17β- and 17α-deacetyltanghinin.[1] Since the ratio of 17α-cardenolide monosides to the corresponding 17β-isomers was larger in the air-dried leaves, we investigated the presence of the 17α-isomers in the polar glycoside fractions of the air-dried leaves and the fresh leaves. This paper deals with the isolation from the leaves and the structure determinations of new polar glycosides, tentatively designated as compounds **1**—**4**, as well as known biosides,[2] the β-D-glucosyl-(1→4)-α-L-thevetosides of 17β- and 17α-digitoxigenin (**5** and **6**, respectively) and of 17β- and 17α-tanghinigenin (**7** and **8**, respectively), and the known triosides,[2] gentiobiosyl-(1→4)-α-L-thevetosides of digitoxigenin (**9**) and tanghinigenin (**10**).

The extraction and isolation of the polar glycosides from the air-dried leaves and stems were carried out as described previously.[1] The benzene and $CHCl_3$ extractives from the MeOH percolate mainly contained the monosides. The biosides and triosides in the BuOH extractives were fractionated by chromatography on columns of one or more of MCI-gel, octadecyl silica and silica gel. The MeOH homogenate from the fresh leaves was eluted with MeOH repeatedly and the MeOH eluate was treated as described for the air-dried leaves. Yields of the biosides and triosides are presented in Table I.

Compounds **1** and **2** were isolated from the air-dried leaves. Compound **1** afforded an $M^+ + Na$ peak at *m/z* 717.347, two mass units smaller than those of **5** and **6**, in the fast atom bombardment (FAB)-mass spectrum (MS), and the molecular formula was determined to be $C_{36}H_{54}O_{13}$. The carbon-13 nuclear magnetic resonance (^{13}C-NMR) spectrum showed 36 carbon signals, of which 30 signals coincided with those of the 17α-digitoxigenin α-L-thevetoside moiety of **6**. Of the remaining 6 signals, one carbonyl carbon signal at δ 207.7, one

TABLE I. Yields of Polar Cardenolide Glycosides from the Air-Dried Leaves and Fresh Leaves (mg)

Plant materials Date of harvest, place, weight	Biosides							Triosides		Tetraoside
	1	2	3	5	6	7	8	9	10	4
Air-dried leaves[a]										
Cerbera odollam July, 1986, Singapore, 0.4 kg	35	4	t[b]	t	t	t				
Cerbera manghas March, 1986, Taiwan, 2.7 kg	120	20	3	10	370	13	28	24	25	
Fresh leaves										
Cerbera odollam Jan., 1986, Singapore, 1.2 kg			27	38		11				
Cerbera manghas Feb., 1986, Okinawa, 0.75 kg				26		180		t		
Cerbera manghas Aug., 1986, Fukuoka, 1.8 kg				300				260		5

a) Yields of monosides were presented in the preceding paper.[1] b) "t" means a trace amount.

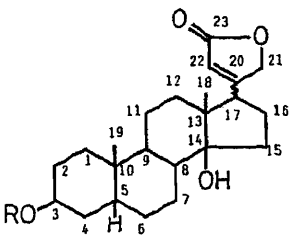

1 : 17α, R=a
4 : 17β, R=c
5 : 17β, R=b
6 : 17α, R=b
9 : 17β, R=d

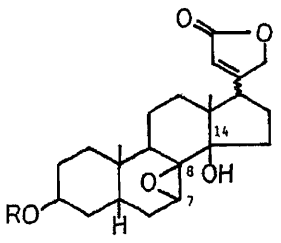

2 : 17α, R=a
7 : 17β, R=b
8 : 17α, R=b
10 : 17β, R=d

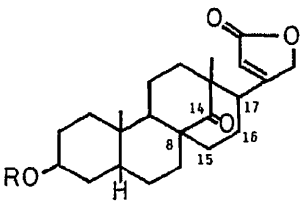

3 : R=b

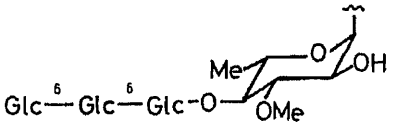

c

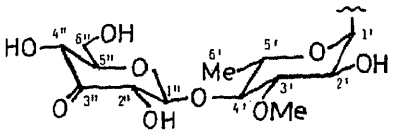

a

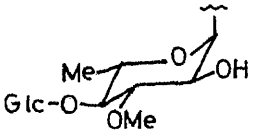

b

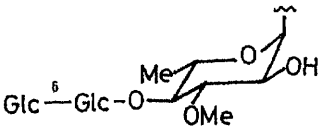

d

Chart 1

primary carbinol carbon signal at δ 62.4 and an anomeric carbon signal at δ 105.9 suggested the presence of a hexosulosyl moiety. A doublet at δ 5.45 in the proton nuclear magnetic resonance (^{1}H-NMR) spectrum was ascribable to an anomeric proton (H-1″). All the protons due to the hexosulose were assigned by means of ^{1}H–^{1}H COSY experiments. The coupling constants between H-1″ and H-2″, and H-4″ and H-5″ were 8 and 10 Hz, respectively, suggesting the relation of H-1″/H-2″ and H-4″/H-5″ to be diaxial in both cases. The terminal sugar was therefore considered to be β-D-glucos-3-ulose which is linked to the 4-hydroxyl of L-thevetose, based on the downfield shift of the C-4 signal of L-thevetose in the ^{13}C-NMR spectrum in comparison with that of 17α-digitoxigenin α-L-thevetoside.[1]

TABLE II. ^{1}H Chemical Shifts of **1**, **2**, **3** and **4**, δ (ppm) from Tetramethylsilane in Pyridine-d_5 (J/Hz in Parentheses)

	1	2	3	4
H-18,19	0.85, 1.19	0.99, 1.21	0.72, 0.90	0.82, 1.03
H-21	4.82, 4.98 (dd, 18, 1)	4.78, 4.93 (dd, 18, 2)	4.73, 4.83 (dd, 18, 2)	5.03, 5.31 (d, 18)
H-22	6.12 (d, 1)	6.10 (d, 2)	5.89 (d, 2)	6.14 (brs)
H-3α	4.16 (brs)	4.06 (brs)	4.09 (brs)	4.11 (brs)
H-17	3.42 (t, 9)	3.26 (t, 9)	2.98 (brd, 7)	2.81 (dd, 5, 9)
H-1′	5.19 (d, 4)	5.17 (d, 4)	5.16 (d, 4)	5.12 (d, 4)
H-2′	4.00 (dd, 9, 4)	3.99 (dd, 9, 4)	4.00 (dd, 9, 4)	
H-3′	4.10 (t, 9)	4.09 (t, 9)	4.06 (t, 9)	
H-4′	3.92 (t, 9)	3.91 (t, 9)	3.90 (t, 9)	
H-6′	1.70 (d, 6)	1.69 (d, 6)	1.67 (d, 6)	1.74 (d, 6)
3′-OMe	3.89	3.88	3.94	3.98
H-1″	5.45 (d, 8)	5.48 (d, 8)	5.35 (d, 8)	5.31 (d, 8)
Others	4.75 (H-2″, dd, 8, 1) 4.96 (H-4″, dd, 10, 1) 3.86 (H-5″, brd, 10) 4.43 (H-6″a, dd, 12, 4) 4.52 (H-6″b, dd, 12, 2)	4.74 (H-2″, dd, 8, 1) 4.97 (H-4″, dd, 9, 3) 4.43 (H-6″a, dd, 12, 4) 4.52 (H-6″b, dd, 12, 1) 3.39 (H-7α, d, 5)	2.68 (H-9, m) 4.37 (H-6″a, dd, 12, 5) 4.54 (H-6″b, dd, 12, 2)	5.07, 5.08 (H-1″, H-1‴, d, 8)

Reduction of **1** with $NaBH_4$ afforded two products, of which one product (**1**-1) was identical with **6**. The other product (**1**-2) was characterized as the β-D-allopyranosyl-α-L-thevetoside of 17α-digitoxigenin by a comparison of the ^{13}C-NMR signals with those of the known allopyranoside,[3] and all the proton signals of the sugar moieties were confirmed by ^{1}H–^{1}H COSY experiments.

Compound **2** was isolated in a small amount. The FAB-MS showed the M^++Na peak at m/z 731.325, suggesting **2** to be a dehydro derivative of **7** or **8**. The structure was assigned as 17α-tanghinigenin β-D-glucos-3-ulosyl-(1→4)-α-L-thevetoside on the basis of ^{1}H- and ^{13}C-NMR comparisons with **1**, **8**, and 17α-tanghinigenin α-L-thevetoside.

Compound **3** was isolated from the MeOH homogenate of the fresh leaves of *C. odollam* as one of the major biosides. The characteristic staining of oleagenin with diluted H_2SO_4 reagent was obtained on a thin layer chromatography (TLC) plate. By ^{1}H- and ^{13}C-NMR analysis, the aglycone and sugar moieties were identified as oleagenin and β-D-glucosyl-(1→4)-α-L-thevetose. On enzymic hydrolysis, **3** afforded cerleaside A (oleagenin α-L-thevetoside) and glucose. Compound **3** is therefore oleagenin β-D-glucosyl-(1→4)-α-L-thevetoside and was named cerleaside B.

Compound **4** was obtained from fresh leaves of *C. manghas* as the most polar glycoside.

TABLE III. ^{13}C Chemical Shifts of the Polar Cardenolide Glycosides, δ (ppm) from Tetramethylsilane in Pyridine-d_5

	6	1	2	3	9	4
C-1	30.3	30.3	32.0[a]	29.1[a]	30.2	30.2
C-2	26.8[a]	26.8[a]	27.3	26.8[b]	26.8[a]	26.8[a]
C-3	73.7	73.8	72.9	73.4	73.6	73.7
C-4	31.0	31.0	32.2[a]	30.2[a]	31.0	31.0
C-5	36.8	36.8	34.1	37.1	36.8	36.8
C-6	27.1[a]	27.1[a]	28.2	26.9[b]	27.1[a]	27.1[a]
C-7	21.6	21.6	50.9	24.4	21.5[b]	21.5[b]
C-8	41.7	41.7	64.4	47.4[c]	41.9	41.9
C-9	36.0	36.0	32.2	45.9	35.8	35.9
C-10	35.4	35.4	33.9	37.5	35.5	35.5
C-11	20.6	20.6	20.0	21.3	22.0[b]	21.9[b]
C-12	31.7	31.7	33.6	43.9	39.9	39.9
C-13	49.4	49.4	51.7	48.8[c]	50.1	50.1
C-14	85.2	85.2	82.1	221.2	84.6	84.6
C-15	31.0	31.0	32.8[a]	42.5	33.2	33.2
C-16	24.9	25.0	26.3	32.2	27.3[a]	27.3[a]
C-17	48.9	48.9	49.0	52.8	51.5	51.5
C-18	18.6	18.5[b]	19.5	23.3	16.2	16.2
C-19	23.9	23.4	24.3	26.2	23.9	23.9
C-20	172.8	172.8	171.7	171.8	175.9	175.9
C-21	74.1	74.1	74.0	73.3	73.7	73.6
C-22	116.6	116.6	116.9	116.2	117.6	117.6
C-23	174.1	174.1	174.0	173.7	174.4	174.4
C-1′	98.5	98.5	98.5	98.5	98.5	98.5
C-2′	73.7	73.8	73.8[b]	73.7	73.6	73.7
C-3′	85.3	85.3	85.2	85.2	85.4	85.4
C-4′	81.8	81.9	81.9	81.8	81.4	81.5
C-5′	67.4	67.2	67.2	67.4	67.5	67.6
C-6′	18.6	18.4[b]	18.6	18.6	18.7	18.7
3′-OMe	61.0	61.1	61.1	61.0	61.0	60.9
C-1″ (1‴,1⁗)	105.1	105.9	105.9	105.1	104.8, 105.6	104.8, 105.5 (×2)
C-2″ (2‴,2⁗)	75.8	78.7	78.7	75.7	75.2, 75.5	75.1, 75.2, 75.5
C-3″ (3‴,3⁗)	78.3[b]	207.7	207.7	78.3	78.4 (×2)[c]	78.3 (×3)[c]
C-4″ (4‴,4⁗)	72.1	73.8	73.7[b]	72.1	71.7, 72.1	71.5, 71.6, 72.1
C-5″ (5‴,5⁗)	78.2[b]	78.4	78.4	78.2	77.1, 78.3[c]	77.0 (×2), 78.2[c]
C-6″ (6‴,6⁗)	63.1	62.4	62.4	63.1	70.8, 62.8	70.1, 70.7, 62.8

a—*c*) Signal assignments marked *a*), *b*) or *c*) in each column may be reversed.

The molecular formula was considered to be $C_{48}H_{76}O_{23}$, based on the $M^+ + Na$ peak at *m/z* 1043, suggesting **4** to be a tetraoside. The presence of three hexoses was shown by the fragment peaks at *m/z* 857, 695, and 533 together with the $(M-1)^-$ peak at *m/z* 1019 in the negative FAB-MS. In the ^1H-NMR spectrum, four anomeric proton signals were observed at δ 5.07 (d, $J=8$ Hz), 5.08 (d, $J=8$ Hz), 5.12 (d, $J=4$ Hz), and 5.31 (d, $J=8$ Hz). The signal at δ 5.12 was assigned to L-thevetose. The ^{13}C-NMR spectrum also showed the presence of a gentiobiosyl-neriifolin (thevetin B) moiety. Since the carbon signals due to the terminal glucose unit were also observed and the carbon signals at δ 70.7 and 70.1 were both assignable to the glucosylated C-6 of glucose, the linkages between the three glucose units were determined to be $1\rightarrow6\beta$. Finally, **4** was subjected to enzymic partial hydrolysis to yield **5** and **9**, and the structure was thus confirmed.

While monosides and biosides of 17α-cardenolides were present as the major glycosides

in air-dried leaves,[1] no biosides or triosides of 17α-cardenolides were isolated from fresh leaves, indicating that isomerization at C-17 and deglucosylation had occurred during the air-drying procedure.

It should be noted that glycosides having the hexos-3-ulosyl moiety were seen only as 17α-digitoxigenin and 17α-tanghinigenin glycosides in the air-dried leaves. The oxidation of the 3-hydroxyl group of the terminal glucose in the biosides is thought to occur during the air-drying procedure and appears to prevent further enzymic transformation into monosides.

Whilst cerleaside A occurs in the air-dried leaves of *Cerbera odollam*, cerleaside B was obtained as one of the major biosides from the fresh leaves, confirming that oleagenin is one of the natural cardenolides in *Cerbera*. This is the first report of the isolation of a cardenolide tetraoside having a gentiotriosyl moiety. The amount of tanghinigenin glycosides in *C. manghas* varied from sample to sample. No glucosyl-cerdollaside was obtained from the fresh leaves, probably because of its low content.

Experimental

Melting points, optical rotations, ^{1}H-NMR, ^{13}C-NMR and MS data were obtained as described in the preceding paper.[1] Column chromatography and TLC were conducted with the following solvent systems: solv. 1, $CHCl_3$–MeOH–H_2O (bottom layer); solv. 2, EtOAc–MeOH–H_2O (top layer). Spots on the TLC plate were detected by spraying with diluted H_2SO_4 and heating the plate. High-performance liquid chromatography (HPLC) was run on a Waters ALC 200 equipped with a Radial Pack C_{18} column.

Extraction and Isolation of 1 and 2 from the Air-Dried Leaves——Isolation of the monosides from the air-dried leaves of *C. odollam* (collected in Singapore, July, 1986) (400 g) and *C. manghas* (collected in Taiwan, March, 1986) (2.7 kg) has been described in the preceding paper.[1] After extraction of the monosides with benzene and $CHCl_3$, the H_2O layer was concentrated *in vacuo* to half its original volume and extracted with BuOH. The BuOH extractives were passed through an MCI-gel (Mitsubishi CHP 20P) column and the column was eluted with H_2O–MeOH, gradually increasing the MeOH concentration to 100%. The eluates from 60% to 80% MeOH were combined and the solvent was evaporated off *in vacuo*. The residue was chromatographed on a silica gel column with solv. 1 (7:2:1—7:3:1) to isolate biosides (**1**—**8** from *C. manghas*, **1**—**7** from *C. odollam*) and triosides (**9** and **10** from *C. manghas*) (Table I).

17α-Digitoxigenin β-D-Glucos-3-ulosyl-(1→4)-α-L-thevetoside (1) and $NaBH_4$ Reduction of 1——A solid, $[\alpha]_D^{27}$ −93.5° (*c*=0.40, MeOH). FAB-MS *m/z*: 717.347 (Calcd for $C_{36}H_{54}O_{13}$+Na, 717.346). A solution of **1** (25 mg) in EtOH (2 ml) was stirred at room temperature, and $NaBH_4$ (10 mg) was added portionwise. After being stirred for 20 min, the mixture was diluted with H_2O and extracted with BuOH. The BuOH extract was chromatographed on a silica gel column with solv. 1 (7:2:1) to isolate two products as solids, (**1**-1, 6 mg; **1**-2, 6 mg). In a comparison of the ^{1}H-NMR spectra, all signals of **1**-1 and of **6** were identical. Compound **1**-2: $[\alpha]_D^{24}$ −88.3° (*c*=0.30, MeOH). ^{1}H-NMR δ (ppm): 0.86, 1.19 (3H, each s, H-18, H-19), 3.42 (1H, t, *J*=9 Hz, H-17), 4.14 (1H, br s, H-3α), 4.82, 4.97 (1H each, dd, *J*=18, 1 Hz, H-21a, b), 6.12 (1H, d, *J*=1 Hz, H-22), 5.17 (1H, d, *J*=4 Hz, H-1′), 3.99 (1H, dd, *J*=9, 4 Hz, H-2′), 4.08 (1H, t, *J*=9 Hz, H-3′), 3.88 (1H, t, *J*=9 Hz, H-4′), 4.27 (1H, m, H-5′), 1.69 (3H, d, *J*=6 Hz, H-6′), 3.90 (3H, s, 3′-OMe), 5.73 (1H, d, *J*=8 Hz, H-1″), 3.96 (1H, dd, *J*=8, 3 Hz, H-2″), 4.73 (1H, t, *J*=3 Hz, H-3″), 4.21 (1H, dd, *J*=3, 9 Hz, H-4″), 4.44 (1H, m, H-5″), 4.36 (1H, dd, *J*=5, 11 Hz, H-6″a), 4.49 (1H, dd, *J*=1, 11 Hz, H-6″b).

17α-Tanghinigenin β-D-Glucos-3-ulosyl-(1→4)-α-L-thevetoside (2)——A solid, $[\alpha]_D^{27}$ −69.5° (*c*=0.20, MeOH). FAB-MS *m/z*: 731.325 (Calcd for $C_{36}H_{52}O_{14}$+Na, 731.325).

Isolation of 3 from the Fresh Leaves of *C. odollam*——Fresh leaves (collected in Singapore, Jan., 1986) (1.2 kg) were homogenized with MeOH. The homogenate was packed in a column and was exhaustively eluted with MeOH. The total MeOH extract was concentrated *in vacuo* to 2 l and the deposit was filtered off. The filtrate was diluted with H_2O and extracted with BuOH. The BuOH extract was passed through an MCI gel column and the column was eluted with H_2O–MeOH with increasing MeOH concentration. The fractions containing biosides and triosides were combined and subjected to silica gel column chromatography with solv. 1 (7:2:1—7:3:2) and solv. 2 (6:1:5—4:1:3) to isolate **3**, **5** and **7** (Table I).

Oleagenin β-D-Glucosyl-(1→4)-α-L-thevetoside (Cerleaside B) (3) and Enzymic Hydrolysis of 3——Prisms from MeOH, mp 250—253 °C, $[\alpha]_D^{24}$ −30.5° (*c*=0.32, MeOH). FAB-MS *m/z*: 717.346 (Calcd for $C_{36}H_{54}O_{13}$+Na: 717.346). Compound **3** (5 mg) was dissolved in 25% EtOH (2 ml) and shaken with snail digestive juice (acetone-dried powder) (3 mg) for 5 h at 38 °C. The mixture was then diluted with H_2O and extracted with BuOH. The BuOH extract showed a spot and peak corresponding to cerleaside A on TLC (solv. 1 (7:2:1), *Rf* 0.80) and HPLC (solv. 30% CH_3CN–H_2O, 1 ml/min, t_R 14.2), respectively. Glucose was detected from the H_2O layer by TLC.

Isolation of 4 from the Fresh Leaves of *C. manghas*——Fresh leaves of *C. manghas*, cultivated in the greenhouse

of Fukuoka University, were harvested in Aug., 1986 (1.8 kg), and were homogenized with MeOH. The MeOH homogenate was filtered and the filtrate was treated in the same manner as described above. Compound **4** (5 mg) was isolated along with **5** and **9** (Table I).

Fresh leaves of *C. manghas* collected in Okinawa in Feb., 1986 (0.75 kg) were homogenized in the same manner as described above. Compounds **5**, **7**, and **9** were isolated (Table I).

Digitoxigenin β-D-Gentiotriosyl-(1→4)-α-L-thevetoside (4) and Enzymic Hydrolysis of 4——A solid, $[\alpha]_D^{27}$ −25.7° (c=0.11, MeOH). FAB-MS m/z: 1043 ($C_{48}H_{76}O_{23}$+Na), negative FAB-MS m/z: 1019 (M−1)$^-$, 857 (M−Glc−1)$^-$, 695 (857−Glc)$^-$, 533 (695−Glc)$^-$. Compound **4** (2 mg) was dissolved in 20% EtOH (1 ml) and shaken with cellulase (Sigma Chem. Co., Ltd.) (1 mg) for 5 h at 38 °C. The mixture was diluted with H_2O and extracted with BuOH. The BuOH extract showed two spots identical with **5** and **9** on TLC (solv. 1 (7:3:1) *Rf* **5**; 0.66, **9**; 0.23) and HPLC (solv. 30% CH_3CN–H_2O, 1 ml/min, t_R **5**; 12.2, **9**; 6.3).

Acknowledgements We thank Prof. S. Yaga of Ryukyu University and Mr. R. Chen of Taipei City for supplying the leaves of *Cerbera manghas*. Our thanks are also due to Misses Y. Iwase and S. Hachiyama of Fukuoka University, for NMR and MS measurements. This work was supported by the JSPS-NUS Scientific Cooperation Programme.

References

1) Part III: T. Yamauchi, F. Abe, and A. S. C. Wan, *Chem. Pharm. Bull.*, **35**, 2744 (1987).
2) F. Abe and T. Yamauchi, *Chem. Pharm. Bull.*, **25**, 2744 (1977).
3) H. Okabe, Y. Miyahara, and T. Yamauchi, *Chem. Pharm. Bull.*, **30**, 3977 (1982).

[Chem. Pharm. Bull. 35(12)4819—4828(1987)]

Syntheses and Antihypertensive Activities of 1,4-Dihydropyridine-5-phosphonate Derivatives. III[1)]

IWAO MORITA,* YUKO HARUTA, TOSHIO TOMITA, MASAMI TSUDA, KAZUHISA KANDORI, MASAHIRO KISE, and KIYOSHI KIMURA

Research Laboratories, Nippon Shinyaku Co., Ltd., Nishiohji-hachijo, Minami-ku, Kyoto 601, Japan

(Received May 28, 1987)

Various 1- and 2-substituted and 1,2-fused 1,4-dihydropyridine-5-phosphonate derivatives were designed and synthesized as analogues of 1,4-dihydropyridine-3,5-dicarboxylate, and their antihypertensive activities were examined. Several compounds proved to be equal or superior to nifedipine in lowering blood pressure in normotensive and spontaneously hypertensive rats. Among these compounds, 1-substituted 1,4-dihydropyridine derivatives showed potent antihypertensive activities. The structure–activity relationships are discussed.

Keywords——1,4-dihydropyridine derivative; phosphonate derivative; 1,2-fused 1,4-dihydropyridine; calcium antagonist; antihypertensive activity; nifedipine; structure–activity relationship

In the previous paper,[2)] the authors reported the synthesis of 1,4-dihydropyridine-5-phosphonates (I) and the antihypertensive activities of these compounds, which were expected to have more prolonged calcium antagonistic activity and better bioavailability than nifedipine. Among them, methyl 2,6-dimethyl-4-(2-nitrophenyl)-5-(2-oxo-1,3,2-dioxaphosphorinan-2-yl)-1,4-dihydropyridine-3-carboxylate (DHP-218), which is approximately 7 times more active than nifedipine and has long-lasting antihypertensive activity,[3)] was chosen for clinical evaluation.

Recently, various new 1- and 2-substituted 1,4-dihydropyridines have been reported. Flordipine[4)] is a first development dihydropyridine compound with a substituent on the nitrogen atom (1-position). It exhibits antihypertensive activity in rats and dogs when given by the oral route. FR-7534[5)] and nilvadipine[5a,6)] are dihydropyridine-related compounds which are substituted in the 2-position with a hydroxymethyl and a cyano group, respectively, in place of the methyl group of nifedipine. Among them, nilvadipine, which shows long-lasting antihypertensive activity, has been reported to be clinically effective. 2-Amino[7)] and 1,2-fused derivatives[8)] have also been synthesized and their antihypertensive activity examined. The former was active, but the latter was not.

In this paper, the synthesis and the antihypertensive activities of 1- and 2-substituted and 1,2-fused 1,4-dihydropyridine-5-phosphonate derivatives (II—IV) are described, and the structure–activity relationships of these compounds are discussed.

Chemistry

1-Substituted-1,4-dihydropyridine-5-phosphonates (II)——The 1-substituted-1,4-dihydropyridines (II) listed in Table I were synthesized by the two routes shown in Chart 2. As described in the previous paper,[2)] the 1-arylideneacetonylphosphonates **4**[2)] were allowed to react with the appropriate *N*-substituted 3-aminocrotonates **3** in 2-propanol under reflux to afford II in 13—59% yields, except for compound **9** (R^1: NMe_2, 3%; method A). In this case, the reaction of **4** with *N*-isopropyl (**3d**) and *N*-methoxy 3-aminocrotonates (**3q**) did not afford

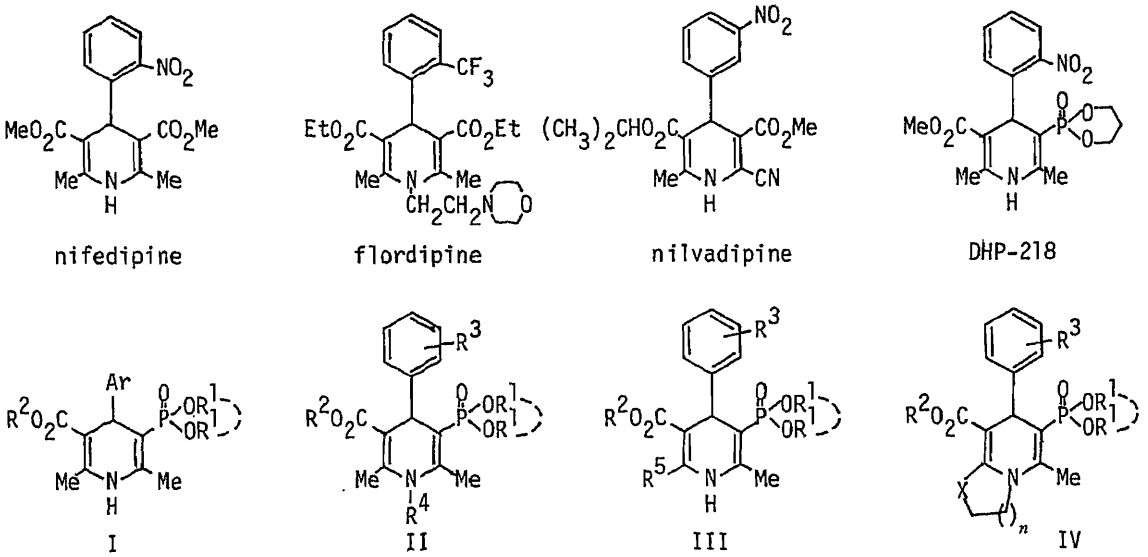

Chart 1

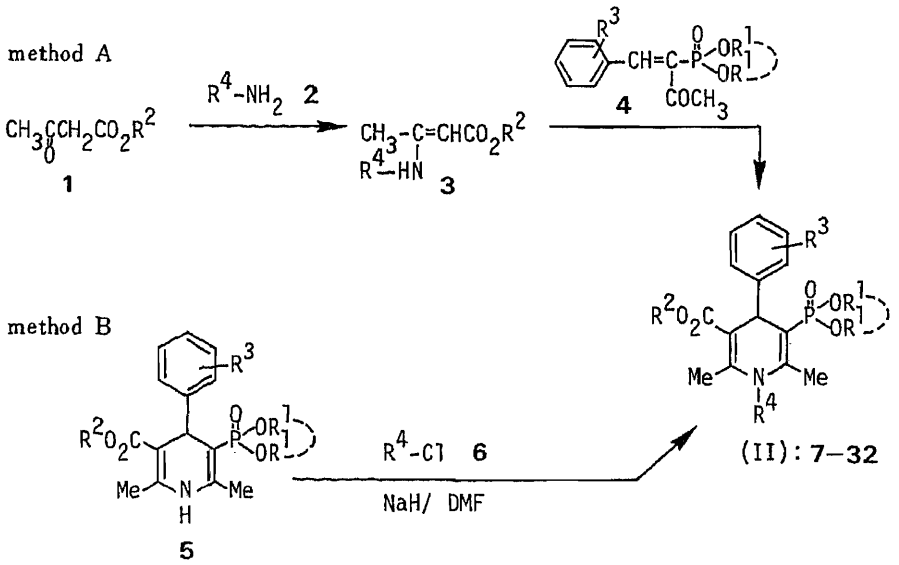

Chart 2

II (R^4: iso-Pr, OMe) because of steric hindrance and the absence of the enamine form, respectively. The *N*-substituted 3-aminocrotonates **3** were prepared from acetoacetates **1** with appropriate primary amines **2**, by the reported procedure[9] (Table II).

Compound II were also prepared by the alkylation of 1,4-dihydropyridines (**5**)[1,2] in the presence of sodium hydride in 13—56% yields (method B).

2-Substituted-1,4-dihydropyridines III——The 2-substituted-1,4-dihydropyridines (**35**—**37**, **39**) (R^5: CH_2OH or CN) listed in Table III were synthesized through the routes shown in Chart 3.

The reaction of **4** with methyl 3-amino-4,4-dimethoxylcrotonate (**34**) in ethanol under reflux gave 2-dimethylacetal compounds (**35a**—**c**) in moderate yields. The deprotection of the 2-dimethylacetal group in the presence of 6 N HCl in acetone at 0—10 °C afforded 2-formyl compounds (**36a**—**c**) in moderate yields. The reduction of the 2-formyl group with sodium borohydride in methanol at 0 °C gave the 2-hydroxymethyl compounds (**37a**—**c**) in good

TABLE I. Physical and Biological Properties of 1,4-Dihydropyridine-5-phosphonates (II)

Compd. No.	R^1	R^2	R^3	R^4	Method[a]	Yield (%)	mp (°C)	Crystn.[b] solvent	Formula[c]	Antihypertensive potency[d]
7	$CH_2CH_2CH_2$	Me	2-NO_2	Me	A	43	192—193	a	$C_{19}H_{23}N_2O_7P$	5—6
8	$CH_2CH_2CH_2$	Me	2-NO_2	Et	A	23	190—191	b	$C_{20}H_{25}N_2O_7P$	6
9	$CH_2CH_2CH_2$	Me	2-NO_2	Pr	A	25	125—126	b	$C_{21}H_{27}N_2O_7P$	5
10	$CH_2CH_2CH_2$	Me	2-NO_2	$CH_2CH=CH_2$	A	39	182—183	b	$C_{21}H_{25}N_2O_7P$	5
11	$CH_2CH_2CH_2$	Me	2-NO_2	$CH_2C_6H_5$	A	39	186—187	b	$C_{25}H_{27}N_2O_7P$	4
12	$CH_2CH_2CH_2$	Me	2-NO_2	CH_2CH_2OMe	A	23	151—152	b	$C_{21}H_{27}N_2O_8P$	4—5
13	$CH_2CH_2CH_2$	Me	2-NO_2	CH_2OMe	B	56	177—178	a	$C_{20}H_{25}N_2O_8P$	6
14	$CH_2CH_2CH_2$	Me	2-NO_2	CH_2OEt	B	39	129—131	b	$C_{21}H_{27}N_2O_8P$	4
15	$CH_2CH_2CH_2$	Me	3-NO_2	NMe_2	A	3	194—195	c	$C_{20}H_{26}N_3O_7P$	2
16	$CH_2CH_2CH_2$	Me	2-CF_3	CH_2CH_2N	B	13	174—176	d	$C_{25}H_{32}F_3N_2O_6P$	3
17	$CH_2CH_2CH_2$	iso-Bu	2-NO_2	Et	A	18	190—191	b	$C_{23}H_{31}N_2O_7P$	3
18	$CH_2CH_2CH_2$	$CH_2CH=CH_2$	2-NO_2	Et	A	30	178—180	d	$C_{22}H_{27}N_2O_7P$	3
19	$CH_2CH_2CH_2$	CH_2	2-NO_2	Et	A	35	182—183	d	$C_{23}H_{29}N_2O_7P$	3
20	$CH_2CH_2CH_2$	$CH_2CH_2OCH_2C_6H_5$	2-NO_2	Et	A	59	Oil	—	$C_{28}H_{33}N_2O_8P$[e]	3
21	$CH_2CH_2CH_2$	CH_2CH_2OMe	2-NO_2	Et	A	26	138—142	b	$C_{22}H_{29}N_2O_8P$	3
22	$CH_2CH_2CH_2$	$CH_2CH_2\underset{\displaystyle Me}{\underset{\vert}{N}}CH_2C_6H_5$	2-NO_2	Me	A	43	114—115	b	$C_{28}H_{34}N_3O_7P$	3
23	$CH_2CH_2CH_2$	Me	2-CF_3	Me	A	33	195—196.5	d	$C_{20}H_{23}F_3NO_5P$	4—5
24	$CH_2CH_2CH_2$	Me	2-$OCHF_2$	Me	A	21	186—192	b	$C_{20}H_{24}F_2NO_6P$	3
25	$CH_2CH_2CH_2$	Me	2-CF_3	Et	A	34	190—191	d	$C_{21}H_{25}F_3NO_5P$	5
26	$CH_2CH_2CH_2$	Me	2-$OCHF_2$	Et	A	20	105—108	d	$C_{21}H_{26}F_2NO_6P$	4
27	$CH_2CH_2CH_2$	Me	3-NO_2	Et	A	51	Oil	—	$C_{20}H_{25}N_2O_7P$[f]	4
28	$CH_2CH_2CH_2$	Me	2,3-Cl_2	Et	A	47	135—136	b	$C_{20}H_{24}Cl_2NO_5P$	3
29	$CH_2\underset{\displaystyle Me}{\underset{\vert}{CH}}=CH_2$	Me	2-NO_2	Et	A	46	Oil	—	$C_{23}H_{29}N_2O_7P$[g]	2
30	$CH_2\underset{\displaystyle Me}{\underset{\vert}{C}}CH_2$	Me	2-NO_2	Et	A	35	141—142	b	$C_{22}H_{29}N_2O_7P$	4
31	$CH_2\underset{\displaystyle Me}{\underset{\vert}{CH}}=CH_2$	Me	3-NO_2	Et	A	24	Oil	—	$C_{23}H_{29}N_2O_7P$[h]	3—4
32	$CH_2\underset{\displaystyle Me}{\underset{\vert}{C}}CH_2$	Me	3-NO_2	Et	A	33	153—154	b	$C_{22}H_{29}N_2O_7P$	4—5
33	CO_2Me[i]	Me	2-NO_2	Me	A	8	186—187	b	$C_{18}H_{20}N_2O_6$	3

a) See Experimental. *b*) Solvent for recrystallization: a, AcOEt; b, AcOEt–ether; c, ether; d, AcOEt–hexane; e, AcOEt–ethanol. *c*) All compounds were analyzed for C, H and N; the analytical results were within ±0.4% of the calculated values. *d*) Numbers in the column indicate the following: 1, little or no effect at 30 mg/kg; 2, effective at 30 mg/kg; 3, effective at 10 mg/kg; 4, effective at 3 mg/kg; 5, effective at 1 mg/kg; 6, effective at 0.3 mg/kg (nifedipine: 6). The effective dose causes 25% lowering of the blood pressure. *e*) $5/2\,H_2O$. *f*) $2H_2O$. *g*) $1/2\,H_2O$. *h*) $1/4\,H_2O$. *i*) Corresponding 3, 5-dicarboxylate derivatives: dimethyl 1,2,6-trimethyl-4-(2-nitrophenyl)-1,4-dihydropyridine-3,5-dicarboxylate.

TABLE II. 3-(*N*-Substituted)aminocrotonates (3)

Compd. No.	R^2	R^4	bp (°C, mmHg) or mp (°C)	Yield (%)	Lit. bp (°C, mmHg) or mp (°C) (Yield)
3a	Me	Me	63—66	69	65—67 (52%)[a]
3b	Me	Et	93—96 (10)	62	108 (18) (57%)[a]
3c	Me	Pr	102—107 (8)	79	120—121 (20) (73%)[a]
3d	Me	iso-Pr	95—96 (9)	38	
3e	Me	$CH_2CH=CH_2$	103—106 (8)	84	
3f	Me	$CH_2C_6H_5$	146—156 (2)	85	
3g	Me	CH_2CH_2OMe	100—102 (1)	80	
3h	Me	NMe_2	80 (10)	77	75—78 (12) (—%)[b]
3i	iso-Bu	Et	103—107 (2)	70	
3j	$CH_2CH=CH_2$	Et	100—102 (5)	76	
3k	CH_2-cyclopropyl	Et	107—108 (7)	85	
3m	$CH_2CH_2OCH_2C_6H_5$	Et	169—171 (0.6)	75	
3n	CH_2CH_2OMe	Et	112—115 (2)	59	
3p	$CH_2CH_2NCH_2C_6H_5$ (Me)	Et	166—168 (0.6)	48	
3q	Me	OMe	77—79 (20)	76	

a, *b*) See ref. 9*a* and 9*b*, respectively.

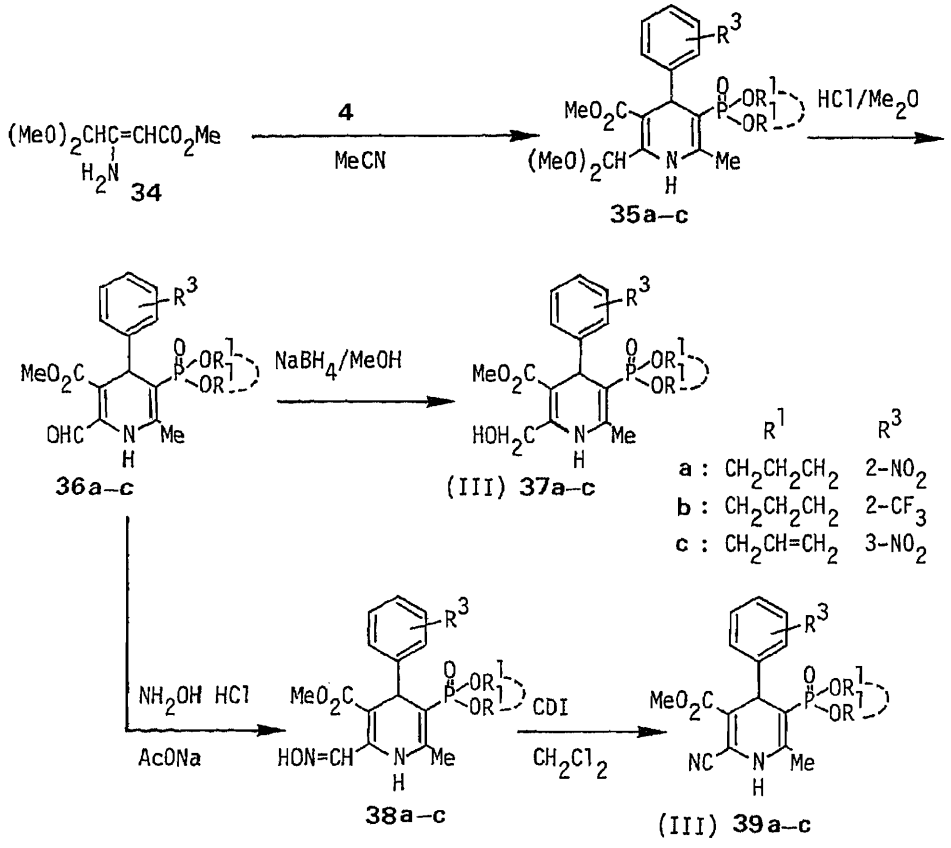

Chart 3

yields, but for **37a** a temperature of −10 °C was employed.

Next, the 2-cyano compounds (**39a—c**) were obtained by the dehydration of 2-aldoxime compounds (**38a—c**), which were obtained from the 2-formyl compounds (**36a—c**) by

TABLE III. Physical and Biological Properties of 1,4-Dihydropyridine-5-phosphonates (III)

Compd. No.	R^1	R^2	R^3	R^5	Yield (%)	mp (°C)	Crystn.[a] solvent	Formula[b]	Antihypertensive potency[c]
35a	$CH_2CH_2CH_2$	Me	2-NO_2	$CH(OMe)_2$	31	118—123	a	$C_{20}H_{25}N_2O_9P$[d]	—
35b	$CH_2CH_2CH_2$	Me	2-CF_3	$CH(OMe)_2$	45	Oil	—	$C_{21}H_{25}F_3NO_6P$[e]	—
35c	$CH_2CH=CH_2$	Me	3-NO_2	$CH(OMe)_2$	63	Oil	—	g)	—
36a	$CH_2CH_2CH_2$	Me	2-NO_2	CHO	23	135—136	a	$C_{18}H_{19}N_2O_8P$	—
36b	$CH_2CH_2CH_2$	Me	2-CF_3	CHO	82	Oil	—	g)	—
36c	$CH_2CH=CH_2$	Me	3-NO_2	CHO	53	Oil	—	g)	—
37a	$CH_2CH_2CH_2$	Me	2-NO_2	CH_2OH	72	170—171	b	$C_{18}H_{21}N_2O_8P$	3
37b	$CH_2CH_2CH_2$	Me	2-CF_3	CH_2OH	60	f)	—	$C_{19}H_{21}F_3NO_6P$	3
37c	$CH_2CH=CH_2$	Me	3-NO_2	CH_2OH	90	Oil	—	$C_{21}H_{25}N_2O_8P$	3
39a	$CH_2CH_2CH_2$	Me	2-NO_2	CN	53	228—229	c	$C_{18}H_{18}N_3O_7P$	5
39b	$CH_2CH_2CH_2$	Me	2-CF_3	CN	69	188—189	d	$C_{19}H_{18}F_3N_2O_5P$	5
39c	$CH_2CH=CH_2$	Me	3-NO_2	CN	93	f)	—	$C_{21}H_{22}N_3O_7P$	2
41a	$CH_2CH_2CH_2$	Et	2-NO_2	NH_2	44	240—241 (dec.)	e	$C_{18}H_{22}N_3O_7P$	2
41b	$CH_2CH_2CH_2$	Et	2-CF_3	NH_2	33	246—247	a	$C_{19}H_{22}F_3N_2O_5P$	4
41c	$CH_2CH=CH_2$	Et	3-NO_2	NH_2	40	129—130 (dec.)	a	$C_{21}H_{26}N_3O_7P$ ·HCl	3
41d	$CH_2CH=CH_2$	Et	2-CF_3	NH_2	35	126—127 (dec.)	a	$C_{22}H_{26}F_3N_2O_5P$[d] ·HCl	2

a—*c*) See footnotes *b* to *d* in Table I. *d*) $1/2H_2O$. *e*) H_2O. *f*) Noncrystalline powder. *g*) These compounds were not analyzed because each was an unstable oil.

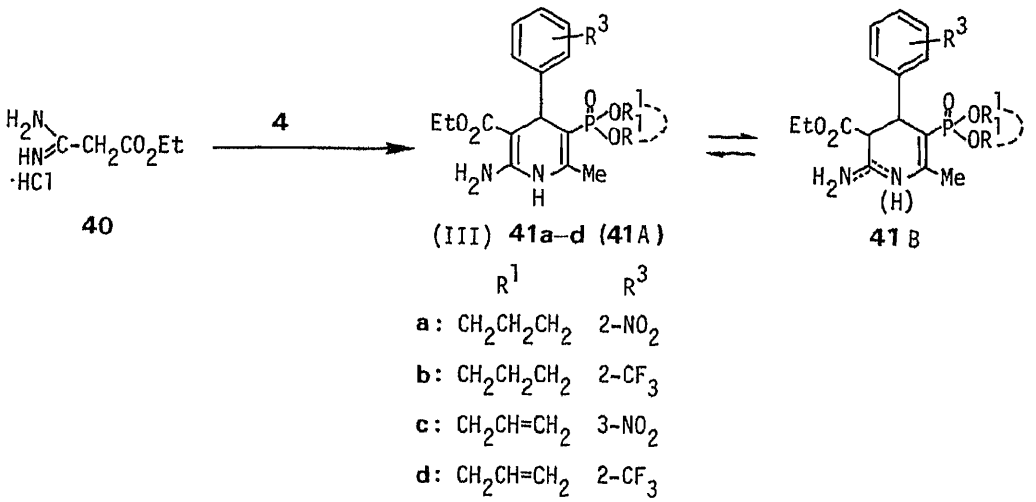

Chart 4

treatment with hydroxylamine hydrochloride in the presence of sodium acetate in quantitative yields; the dehydration of **38a**—**c** proceeded in good yields.

The 2-amino-1,4-dihydropyridines (**41a**—**d**) (R^5: NH_2) were synthesized through the route shown in Chart 4. The condensation of **4** with ethyl amidinoacetate hydrochloride (**40**) in ethanol under reflux gave the 2-amino compounds (**41a**—**d**) in 33—44% yields. The 2-amino compounds are presumed to exist as a tautomers (**41A**, B) from their proton nuclear magnetic resonance (^{1}H-NMR) spectra, like the corresponding 3,5-dicarboxylate derivatives[7] (Chart 4), and were slightly unstable.

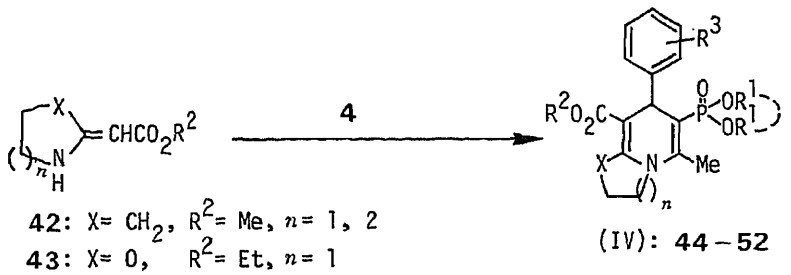

Chart 5

TABLE IV. Physical and Biological Properties of 1,4-Dihydropyridine-5-phosphonates (IV)

Compd. No.	R^1	R^2	R^3	X	n	Yield (%)	mp (°C)	Crystn.[a] solvent	Formula[b]	Antihypertensive potency[c]
44	$CH_2CH_2CH_2$	Me	2-NO_2	CH_2	1	66	220—223	b	$C_{20}H_{23}N_2O_7P$	I
45	Me	Me	3-NO_2	CH_2	1	51	156—157	b	$C_{19}H_{23}N_2O_7P$	I
46	$CH_2CH=CH_2$	Me	3-NO_2	CH_2	1	80	Oil	—	$C_{23}H_{27}N_2O_7P$	I
47	$CH_2CH_2CH_2$	Me	2-NO_2	CH_2	2	21	206—209	a	$C_{21}H_{25}N_2O_7P$	I
48	Me	Me	3-NO_2	CH_2	2	44	97—99	c	$C_{20}H_{25}N_2O_7P$	I
49	$CH_2CH=CH_2$	Me	3-NO_2	CH_2	2	53	71—74	c	$C_{24}H_{29}N_2O_7P$	I
50	$CH_2CH_2CH_2$	Me	2-CF_3	CH_2	1	45	190—192	b	$C_{21}H_{23}F_3NO_5P$	I
51	$CH_2CH_2CH_2$	Me	2-CF_3	CH_2	2	45	230—231	b	$C_{22}H_{25}F_3NO_5P$	I
52	$CH_2CH_2CH_2$	Et	2-NO_2	O	1	38	250—252	a	$C_{20}H_{23}N_2O_8P$	I

a—*c*) See footnotes *b* to *d* in Table I.

1,2-Fused 1,4-Dihydropyridines (IV)——The 1,2-fused 1,4-dihydropyridines (IV) listed in Table IV were synthesized through the route shown in Chart 5. The condensation of **4** with cyclic enaminoesters (**42**, **43**) in MeCN under reflux gave the 1,2-fused 1,4-dihydropyridines (**44**—**52**) in 21—80% yields.

Pharmacology

The compounds listed in Tables I, III and IV were examined for antihypertensive activity. Blood pressure was measured in unanesthetized rats with normal blood pressure (normotensive rats) and spontaneously hypertensive rats (SHR). Male normotensive Wistar rats weighing 310—450 g (18 weeks or older) were placed in a supine position under ether anesthesia and a polyethylene catheter filled with heparinized saline was inserted into the femoral artery and connected with a pressure transducer (Nihon Kohden MPU-0.5). Blood pressure measurements were started under restraint after the rats had recovered from anesthesia, and blood pressure levels were recorded continuously on a potentiometric recorder (Toa EPR-10A or EPR) *via* a preamplifier (Nihon Kohden AP-621G). After the blood pressure had become stable, the test compounds (prepared as suspensions in 0.5% methylcellulose (MC) solution) were administered orally at various doses (0.3, 1, 3, 10, or 30 mg/kg).

Some of the compounds with potent antihypertensive activity in normotensive rats were tested for antihypertensive activity in SHR. Male SHR weighing 280—300 g were purchased at the age of 15 weeks and housed in our laboratory. Systolic blood pressure was measured by the tail cuff plethysmographic method under mild restraint with a programmable sphygmomanometer (PS-802; Riken Kaihatsu). Before blood pressure measurements, rats were placed in a warm box at 35—37 °C for 10 min. The test compounds were administered orally as

described above. The dose (in mg/kg) which produced a 30% drop in blood pressure was calculated from the regression line as the ED_{30} value (Table VI).

Results and Discussion

The antihypertensive activities of the new 1,4-dihydropyridines (II—IV) are shown in Tables I, III and IV.

It is generally known that in 1,4-dihydropyridine-3,5-dicarboxylate derivatives, a substituent at the 1-position causes a decrease of the activity,[10] though flordipine is a potent antihypertensive agent. However, compounds II in our present study showed antihypertensive activity comparable to that of nifedipine.[11] Thus, we suspected that the size of the 1-substituent influences the antihypertensive activity, and the activities are assumed to decrease in the following order: (R^4); ethyl, methoxymethyl, methyl, propyl, allyl, 2-methoxyethyl, ethoxymethyl, benzyl, 2-morpholinoethyl, dimethylamino. Compound **16** with a 2-morpholinoethyl group as a phosphonate analogue of flordipine showed disappointingly low activity. The 1-methyl compound (**7**) exhibited activity about 20 times that of the corresponding 3, 5-dicarboxylate compound (**33**).

As regards the 2-substituted-1,4-dihydropyridines (III), compounds **39a** and **39b** with a 2-CN substituent were the most active. Those with 2-CH_2OH and 2-NH_2 substituents were moderately active. The 5-diallyl phosphonate compounds (**39c**, **41d**) were less active than the 5-cyclic phosphonates (**39a**, **39b**, **41a**).

The 1,2-fused 1,4-dihydropyridines (IV), which were cyclized at the 1 and 2 positions of strongly active II (**8**, **9**), were expected to be as active as the 1- and 2-substituted-1,4-dihydropyridines (II), but, contrary to expectation, they were all (**44**—**52**) inactive.

Next, the active 1,4-dihydropyridines (II and III) listed in Tables I and III were examined for antihypertensive activity in unanesthetized SHR. Among them, the seven compounds listed in Table V showed activities equal or superior to that of nifedipine. The antihypertensive activities of the most active compound (**7**) was approximately four times that of nifedipine

TABLE V. Antihypertensive Activity of the Active Compounds (II, III), DHP-218, and Nifedipine in SHR

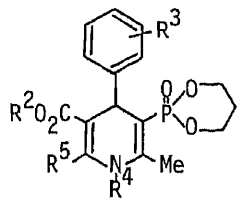

Compd. No.	R^2	R^3	R^4	R^5	ED_{30}[a] (mg/kg)	Rel. potency[b]
7	Me	2-NO_2	Me	Me	0.4	3.8
8	Me	2-NO_2	Et	Me	0.6	2.5
13	Me	2-NO_2	CH_2OMe	Me	1.0	1.5
37a	Me	2-NO_2	H	CH_2OH	2.3	0.7
39a	Me	2-NO_2	H	CN	1.1	1.4
39b	Me	2-CF_3	H	CN	1.6	0.9
41a	Et	2-NO_2	H	NH_2	0.9	1.7
DHP-218	Me	2-NO_2	H	Me	0.2	7.5
Nifedipine					1.5	1.0

a) See Pharmacology in the text. *b*) Potency relative to that of nifedipine.

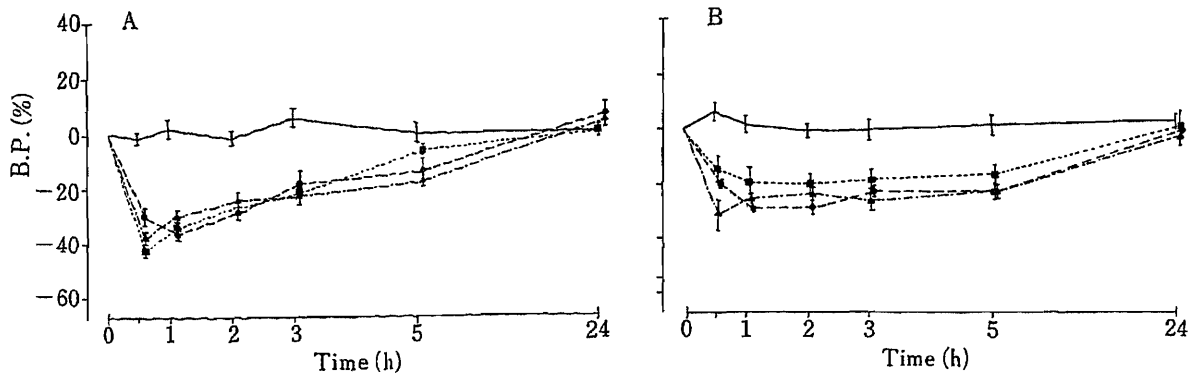

Fig. 1. Antihypertensive Activities of **7**, **8**, **13**, **37a**, **39a**, and **41a** in SHR (1 mg/kg, *p.o.*)

A: ——, control; --■--, **7**; --●--, **8**; —▲—, **13**.
B: ——, control; --■--, **37a**; --●--, **39a**; —▲—, **41a**.

and one-half that of DHP-218.

In general, the 1-substituted compounds had a strong and long-lasting antihypertensive activity, but the 2-substituted compounds showed a milder and longer-lasting activity than that of II (Fig. 1). However, none of them was more active than DHP-218.

Experimental

Melting points were determined with a Büchi melting point apparatus and are uncorrected. Infrared (IR) spectra were measured on a Hitachi IR-215 spectrophotometer. ^{1}H-NMR spectra were recorded on a Varian YX-200 spectrometer in deuterochloroform solution. Chemical shifts are given in δ (ppm) with tetramethylsilane as an internal standard. The following abbreviations are used: s=singlet, d=doublet, t=triplet, q=quartet, m=multiplet, br=broad. Mass spectra (MS) were measured on a Hitachi RMU-6M instrument. Column chromatography was performed on Wako-gel C-200.

General Procedure for *N*-Substituted-3-aminocrotonates (3)——The appropriate primary amine (**2**) (0.6 mol) was added dropwise to a stirred solution of an acetoacetate (**1**, 0.5 mol) in water (40 ml) (or benzene, 80 ml) at 0—5 °C. After 18 h at room temperature with stirring, the reaction mixture was extracted with AcOEt (2×200 ml) and dried ($MgSO_4$), and the solvent was removed *in vacuo*. The residue was distilled to give the corresponding **3** in good yield (Table II).

General Procedure for 1-Substituted-1,4-dihydropyridines (II)——Method A: A solution of **3** (7.7 mmol) and **4**[2] (7 mmol) in dry MeCN (20 ml) was refluxed for 10—24 h with continuous removal of water by a Soxhlet extractor with a dehydrating agent (activated $CaSO_4$). The MeCN solution was concentrated to dryness and the residue obtained was subjected to chromatography on silica gel with hexane–AcOEt as an eluent to give II in 3—59% yield as an oil or crystals. The crystals were recrystallized from appropriate solvents.

Typical examples are given below.

Method A: Methyl 1-Ethyl-2,6-dimethyl-4-(2-nitrophenyl)-5-(2-oxo-1,3,2-dioxaphosphorinan-2-yl)-1,4-dihydropyridine-3-carboxylate (8)——Treatment of methyl 3-ethylaminocrotonate (**3b**, 0.87 g, 7.7 mmol) and **4** (R^1=$CH_2CH_2CH_2$, R^3=2-NO_2, 2.18 g, 7.7 mmol) according to the general method gave **8** (0.85 g, 23%) as yellow crystals, mp 190—191 °C (from ether–AcOEt). *Anal.* Calcd for $C_{20}H_{25}N_2O_7P$: C, 54.80; H, 5.89; N, 6.48. Found: C, 55.05; H, 5.77; N, 6.42. MS *m/z* (%): 436 (M^+, 13.1), 419 (100). IR (KBr): 1700, 1640, 1530, 1245 cm^{-1}. ^{1}H-NMR: 1.26 (3H, t, J=8 Hz, CH_2CH_3), 1.62—1.80 (1H, m, >CH), 2.32—2.55 (1H, m, >CH), 2.37 (3H, s, 2-CH_3), 2.64 (3H, d, J_{P-H}=4 Hz, 6-CH_3), 3.65 (3H, s, CO_2CH_3), 3.77 (2H, q, J=8 Hz, CH_2CH_3), 3.93—4.68 (4H, m, 2×OCH_2), 5.55 (1H, d, J_{P-H}=12 Hz, C_4-H), 7.20—7.32 (1H, m, ArH), 7.36—7.46 (2H, m, ArH), 7.66 (1H, d, J=8 Hz, ArH).

Method B: Methyl 1-Methoxymethyl-2,6-dimethyl-4-(2-nitrophenyl)-5-(2-oxo-1,3,2-dioxaphosphorinan-2-yl)-1,4-dihydropyridine-3-carboxylate (13)——A solution of methyl 2,6-dimethyl-4-(2-nitrophenyl)-5-(2-oxo-1,3,2-dioxaphosphorinan-2-yl)-1,4-dihydropyridine-3-carboxylate[2] (2.45 g, 6 mmol) in dry *N*,*N*-dimethylformamide (DMF, 15 ml) was added to a stirred solution of sodium hydride (0.317 mg, 50% dispersion in oil, 6.6 mmol) in dry tetrahydrofuran (THF, 15 ml) at room temperature. After 1 h, methoxymethyl chloride (0.531 g, 6.6 mmol) was added to the reaction mixture at −15 °C, and then the reaction mixture was stirred for 16 h. After removal of the solvent, the residue was chromatographed on silica gel with AcOEt–hexane as an eluent to afford **13** (1.50 g, 56%) as yellow

crystals, mp 177—178 °C (from AcOEt). *Anal.* Calcd for $C_{20}H_{25}N_2O_8P$: C, 53.10; H, 5.57; N, 6.19. Found: C, 53.34; H, 5.73; N, 6.24. MS *m/z* (%): 452 (M^+, 17.5), 435 (100). IR (KBr): 1695, 1530, 1350 cm^{-1}. ^{1}H-NMR: 1.60—1.82 (1H, m, >CH), 2.28—2.54 (1H, m, >CH), 2.39 (3H, s, 2-CH_3), 2.65 (3H, d, J_{P-H}=2.5 Hz, 6-CH_3), 3.36 (3H, s, OCH_3), 3.65 (3H, s, CO_2CH_3), 3.90—4.66 (4H, m, 2×OCH_2), 4.82 (2H, s, 1-CH_2O), 5.52 (1H, d, J_{P-H}=12 Hz, C_4-H), 7.20—7.30 (1H, m, ArH), 7.34—7.48 (2H, m, ArH), 7.66 (1H, d, *J*=8 Hz, ArH).

Compounds (**14** and **16**) were also prepared by method B.

Methyl 3-Amino-4,4-dimethoxy-2-butenoate (34)——NH_3 gas was bubbled through an ice-cooled methanolic (15 ml) solution of methyl 4,4-dimethoxy-3-oxobutanoate (8.74 g, 0.05 mol), which was prepared by the method of Royals and Robinson,[12] in an ice-bath. After 20 h, the reaction mixture was concentrated *in vacuo* and the residue was distilled to afford **34** (7.43 g, 85%), bp 95—96 °C (5 mmHg). IR (film): 3430, 3320, 1670, 1625, 1560, 1275 cm^{-1}. ^{1}H-NMR: 3.35 (6H, s, 2×OCH_3), 3.66 (3H, s, CO_2CH_3), 4.79 (2H, s, >CH- and =CH-), 5.70—7.50 (2H, br, NH_2).

Methyl 2-Dimethoxymethyl-6-methyl-4-(2-nitrophenyl)-5-(2-oxo-1,3,2-dioxaphosphorinan-2-yl)-1,4-dihydropyridine-3-carboxylate (35a)——A solution of **4** (R^1=$CH_2CH_2CH_2$, R^3=2-NO_2, 9.3 g, 0.03 mol) and **34** (5.3 g, 0.03 mol) in MeCN (45 ml) was refluxed with stirring for 36 h. After removal of the solvent, the residue was chromatographed on silica gel with AcOEt–hexane as an eluent to afford **35a** (5.78 g, 41%), which was recrystallized from ether–AcOEt (4.90 g, 35%), mp 174—175.5 °C. *Anal.* Calcd for $C_{20}H_{25}N_2O_9P$: C, 51.29; H, 5.38; N, 5.98. Found: C, 51.14; H, 5.33; N, 5.93. MS *m/z* (%): 468 (M^+, 20.5), 419 (100). IR (KBr): 3350, 3220, 3100, 1695, 1650, 1530, 1360 cm^{-1}. ^{1}H-NMR: 1.60—1.77 (1H, m, >CH), 2.37—2.62 (1H, m, >CH), 2.50 (3H, d, J_{P-H}=2 Hz, 6-CH_3), 3.33 (3H, s, OCH_3), 3.46 (3H, s, OCH_3), 3.62 (3H, s, CO_2CH_3), 3.83—4.05 (1H, m), 4.22—4.70 (3H, m, 2×OCH_2), 5.65 (1H, d, J_{P-H}=10 Hz, C_4-H), 5.95 (1H, s, 2-CH<), 6.90 (1H, d, J_{P-H}=5 Hz, NH), 7.22—7.34 (1H, m, ArH), 7.42—7.60 (2H, m, ArH), 7.72 (1H, dd, *J*=1, 8 Hz, ArH).

The other dimethoxyacetal compounds **35b** (R^1: -$(CH_2)_3$-, R^3: 2-CF_3), and **35c** (R^1: CH_2CH=CH_2, R^3: 3-NO_2) were prepared in the same way. Because compound **35c** was obtained as an unstable oil, it was not analyzed.

Methyl 2-Formyl-6-methyl-4-(2-nitrophenyl)-5-(2-oxo-1,3,2-dioxaphosphorinan-2-yl)-1,4-dihydropyridine-3-carboxylate (36a)——A solution of **35a** (3.04 g, 6.5 mmol) and 6 N HCl (2 ml) in acetone (30 ml) was kept in a refrigerator for 4 d. The reaction mixture was neutralized with $NaHCO_3$ and concentrated at room temperature *in vacuo*. The residue was poured into ice-water and extracted with $CHCl_3$ (3×20 ml), then the extract was washed with water, dried ($MgSO_4$) and concentrated to dryness. The residue obtained was chromatographed on silica gel with AcOEt–hexane as an eluent to give **38** (1.40 g, 51%) as yellow crystals, mp 135—136 °C (from ether–AcOEt). *Anal.* Calcd for $C_{18}H_{19}N_2O_8P$: C, 51.19; H, 4.53; N, 6.63. Found: C, 51.32; H, 4.50; N, 6.68. MS *m/z* (%): 422 (M^+, 15), 268 (100). IR (KBr): 3360, 3080, 1695, 1640, 1530, 1370 cm^{-1}. ^{1}H-NMR: 1.70—1.78 (1H, m, >CH), 2.36—2.60 (1H, m, >CH), 2.55 (3H, d, J_{P-H}=2 Hz, 6-CH_3), 3.73 (3H, s, CO_2CH_3), 3.85—4.08 (1H, m), 4.20—4.70 (3H, m, 2×OCH_2), 5.75 (1H, d, J_{P-H}=10 Hz, C_4-H), 7.09 (1H, d, J_{P-H}=5 Hz, NH), 7.26—7.56 (3H, m, ArH), 7.79 (1H, d, *J*=8 Hz, ArH), 10.34 (1H, s, CHO). The other formyl compounds **36b** (R^1: -$(CH_2)_3$-, R^3: 2-CF_3) and **36c** (R^1: CH_2CH=CH_2, R^3: 3-NO_2) were prepared in the same way, but each compound was obtained as an unstable oil which was not analyzed.

Methyl 2-Hydroxymethyl-6-methyl-4-(2-nitrophenyl)-5-(2-oxo-1,3,2-dioxaphosphorinan-2-yl)-1,4-dihydropyridine-3-carboxylate (37a)——$NaBH_4$ (38 mg, 0.996 mmol) was added to a stirred solution of the formyl compound **36a** (350 mg, 0.83 mmol) in methanol (6 ml) at −10 °C. After being stirred for 1 h at 10 °C, the mixture was neutralized with aqueous HCl and concentrated at 30 °C *in vacuo*. The residue was extracted with $CHCl_3$ (2×15 ml). The $CHCl_3$ layer was washed with water and dried ($MgSO_4$). The solvent was removed and the residue was chromatographed on silica gel with AcOEt–hexane as an eluent to give **37a** (305 mg, 86.6%) as yellow crystals, which were recrystallized from AcOEt to gave **37a** (253 mg, 71.9%), mp 170—171 °C. *Anal.* Calcd for $C_{18}H_{21}N_2O_8P$: C, 50.95; H, 4.99; N, 6.60. Found: C, 50.80; H, 4.97; N, 6.51. MS *m/z* (%): 424 (M^+, 3.5), 31 (100). IR (KBr): 3350, 3200, 1700, 1635, 1530 cm^{-1}. ^{1}H-NMR: 1.58—1.91 (1H, m, >CH), 2.32—2.58 (1H, m, >CH), 2.42 (3H, d, J_{P-H}=2.5 Hz, 6-CH_3), 3.57 (3H, s, CO_2CH_3), 3.83—4.66 (4H, m, 2×OCH_2), 4.56 and 4.84 (2H, each d, *J*=16 Hz, 2-CH_2OH), 5.62 (1H, d, J_{P-H}=10 Hz, C_4-H), 7.22—7.33 (1H, m, ArH), 7.42—7.65 (3H, m, ArH+NH), 7.71 (1H, d, *J*=8 Hz, ArH).

Methyl 2-(Hydroxyimino)methyl-6-methyl-4-(2-nitrophenyl)-5-(2-oxo-1,3,2-dioxaphosphorinan-2-yl)-1,4-dihydropyridine-3-carboxylate (38a)——Hydroxylamine hydrochloride (177 mg, 1.2 eq) was added to a stirred solution of **36a** (0.90 g) in methanol (5 ml) at room temperature, followed by addition of AcONa (221 mg) in water (1 ml). After being stirred for 2 h, the mixture was concentrated at 30 °C *in vacuo*. The residue was extracted with $CHCl_3$. The $CHCl_3$ layer was washed with aqueous $NaHCO_3$, and water, and dried ($MgSO_4$). The solvent was removed to give the crude oil **38a** (0.92 g, a quantitative yield). ^{1}H-NMR: 1.67—1.98 (1H, m, >CH), 2.21—2.70 (1H, m, >CH), 2.43 (3H, d, J_{P-H}=2 Hz, 6-CH_3), 3.60 (3H, s, CO_2CH_3), 4.07—4.72 (4H, m, 2×OCH_2), 5.65 (1H, d, J_{P-H}=10 Hz, C_4-H), 7.02—7.80 (5H, m, ArH+NH), 8.69 (1H, s, 2-CH=), 10.4—10.8 (1H, br, NOH).

Methyl 2-Cyano-6-methyl-4-(2-nitrophenyl)-5-(2-oxo-1,3,2-dioxaphosphorinan-2-yl)-1,4-dihydropyridine-3-carboxylate (39a)——A solution of the above **38a** (0.90 g) and CDI (1.0 g, 3 eq) in CH_2Cl_2 (15 ml) was refluxed with stirring for 2 d. When the reaction mixture was washed with aqueous HCl, the product crystallized out of the solution. The precipitated crystals were collected by filtration and washed with water to give **39a** (0.557 g, 64.7%), which was recrystallized from AcOEt–methanol to yield **39a** as yellow crystals (0.460 g, 53.3%), mp 228—229 °C. *Anal.* Calcd for $C_{18}H_{18}N_3O_7P$: C, 51.56; H, 4.33; N, 10.02. Found: C, 51.18; H, 4.55; N, 10.03. MS *m/z* (%): 419 (M^+, 1.3), 265 (100).

IR (KBr): 3250, 3180, 3080, 2230, 1715, 1635, 1530 cm^{-1}. ^{1}H-NMR (CD_3OD): 1.74—1.95 (1H, m, >CH), 2.13—2.32 (1H, m, >CH), 2.37 (3H, d, J_{P-H}=2.5 Hz, 6-CH_3), 3.65 (3H, s, CO_2CH_3), 3.93—4.59 (4H, m, 2×OCH_2), 5.67 (1H, d, J_{P-H}=10 Hz, C_4-H), 7.36—7.47 (1H, m, ArH), 7.50—7.68 (2H, m, ArH), 7.79 (1H, dd, J=1, 8 Hz, ArH).

Ethyl 2-Amino-6-methyl-4-(2-nitrophenyl)-5-(2-oxo-1,3,2-dioxaphosphorinan-2-yl)-1,4-dihydropyridine-3-carboxylate (41a)——A solution of **4** (R^1=$CH_2CH_2CH_2$, R^3=2-NO_2, 1.55 g, 5 mmol) and ethyl amidinoacetate hydrochloride[12] (0.833 g, 5 mmol) in absolute ethanol (15 ml) was added to a solution of sodium ethoxide (10 mmol) in absolute ethanol (6 ml). The mixture was refluxed with stirring for 6 h. After removal of the solvent, the residue was subjected to chromatography on silica gel with AcOEt–methanol (1 : 20) as an eluent to give **41a** (0.921 g, 44%) as yellow crystals, mp 240—241 °C (AcOEt–ethanol). *Anal.* Calcd for $C_{18}H_{22}N_3O_7P$: C, 51.07; H, 5.24; N, 9.93. Found: C, 51.05; H, 5.35; N, 10.02. IR (KBr): 3450, 3220, 1675, 1650, 1530 cm^{-1}. ^{1}H-NMR: **41A** [1.16 (3H, t, J=8 Hz, $CH_2\underline{CH_3}$), 1.40—2.00 (2H, m, >CH_2), 2.25 (3H, d, J_{P-H}=2.5 Hz, 6-CH_3), 3.80—4.64 (6H, m, 2×OCH_2+$\underline{CH_2}CH_3$), 5.58 (1H, d, J_{P-H}=10 Hz, C_4-H), 6.58 (2H, br s, NH_2), 7.12—7.29 (1H, m, ArH), 7.40—7.55 (2H, m, ArH), 7.71 (1H, d, J=8 Hz, ArH), 8.34 (1H, br, NH)] and **41B** [1.28 (3H, t, J=8 Hz, $CH_2\underline{CH_3}$), 2.55 (3H, d, J_{P-H}=2.5 Hz, 6-CH_3), 5.05 (1H, br d, J_{P-H}=10 Hz, C_4-H), 7.55—7.66 (2H, m, ArH), 7.91 (1H, d, J=8 Hz, ArH)]. The ^{1}H-NMR spectrum of this compound in $CDCl_3$ indicated that the ratio of **41A** : **41B** was 3 : 1, but when D_2O was added, the ^{1}H-NMR spectrum showed only **41A** (D_2O). Compound **41b** also showed the same ^{1}H-NMR spectrum. However, the ^{1}H-NMR spectra of **41** hydrochlorides (**41c, d**) indicated the presence of the **41B** form. These results suggest that compound **41** exists as tautomers (**41A** and **41B**), as shown in Chart 4.

Methyl 5-Methyl-7-(2-nitrophenyl)-6-(2-oxo-1,3,2-dioxaphosphorinan-2-yl)-1,2,3,7-tetrahydroindolizine-8-carboxylate (44)——A solution of **4** (R^1=$CH_2CH_2CH_2$, R^3=2-NO_2, 2.0 g, 6.43 mmol) and methyl α-(tetrahydro-2-pyrrolidinylidene)acetate[13] (1.0 g, 7.07 mmol) in MeCN (15 ml) was refluxed with stirring for 10 h. The precipitate was collected by filtration, and the crystals (2.04 g) obtained were recrystallized from iso-Pr_2O–AcOEt to give **44** (1.85 g, 66%) as yellow crystals, mp 220—223 °C. *Anal.* Calcd for $C_{20}H_{23}N_2O_7P$: C, 55.30; H, 5.34; N, 6.45. Found: C, 55.30; H, 5.29; N, 6.48. MS *m/z* (%): 434 (M^+, 12.4), 417 (100). IR (KBr): 1695, 1620, 1570, 1360 cm^{-1}. ^{1}H-NMR: 1.60—1.74 (1H, m, >CH), 1.84—2.20 (2H, m, C_2-H_2), 2.40—2.60 (1H, m, >CH), 2.62 (3H, d, J_{P-H}=2 Hz, 5-CH_3), 2.79—2.98 and 3.14—3.30 (2H, m, C_1-H_2), 3.58 (3H, s, CO_2CH_3), 3.58—3.70 and 3.80—3.92 (2H, m, C_3-H_2), 3.94—4.70 (4H, m, 2×OCH_2), 5.66 (1H, d, J_{P-H}=10 Hz, C_7-H), 7.20—7.30 (1H, m, ArH), 7.40—7.50 (2H, m, ArH), 7.68—7.72 (1H, m, ArH).

References and Notes

1) This work was presented at the 36th Meeting of the Kinki Branch, Pharmaceutical Society of Japan, Osaka, 1986.
2) Part I: I. Morita, S. Tada, K. Kunimoto, M. Tsuda, M. Kise, and K. Kimura, *Chem. Pharm. Bull.*, **35**, 3898 (1987); Part II: I. Morita, K. Kunimoto, M. Tsuda, S. Tada, M. Kise, and K. Kimura, *Chem. Pharm. Bull.*, **35**, 4144 (1987).
3) Y. Kimura, H. Fukui, M. Tanaka, M. Okamoto, A. Morino, A. Miura, K. Kimura, and H. Enomoto, *Arzneim.-Forsch.*, **36**, 1329 (1986).
4) B. Loev and J. R. Shroff, U. S. Patent 4258042 (1981) [*Chem. Abstr.*, **95**, 42928*a* (1981)]; W. S. Mann, P. S. Wolf, R. D. Smith, and B. Loev, *Pharmacologist*, **24**, 137 (1982); S. M. Ringel, A. Darragh, J. Rosenthal, F. S. Caruso, and R. A. Vukovich, *J. Clin. Pharmacol.*, **33**, 231P (1983).
5) *a*) Y. Sato, Ger. Offen. 2756226 (1978) [*Chem. Abstr.*, **89**, 109132*h* (1978)]; *b*) S. R. Jolly, L. A. Menahan, and G. J. Gross, *Life Sci.*, **27**, 2339 (1980); G. J. Gross, M. J. Diemer, D. C. Warltier, and H. F. Hardmann, *Gen. Pharmacol.*, **12**, 199 (1981).
6) D. C. Warltier, M. G. Zyvoloski, H. L. Brooks, and G. J. Gross, *Eur. J. Pharmacol.*, **80**, 149 (1982); *Drugs of the Future*, **8**, 776 (1983).
7) H. Meyer, F. Bossert, and H. Horstmann, *Justus Liebigs Ann. Chem.*, **1977**, 1895; H. Meyer, E. Wehinger, F. Bossert, K. Stoepel, and W. Vater, *Arzneim.-Forsch.*, **31**, 1173 (1981).
8) H. Meyer, F. Bossert, and H. Horstmann, *Justus Liebigs Ann. Chem.*, **1977**, 1888.
9) *a*) P. C. Anderson and B. Staskun, *J. Org. Chem.*, **30**, 3033 (1965); *b*) H. Ahlbrecht and H. Henk, *Chem. Ber.*, **108**, 1659 (1975).
10) R. A. Janis and D. J. Triggle, *J. Med. Chem.*, **26**, 775 (1983).
11) W. Vater, G. Kroneberg, F. Foffmeister, H. Kaller, A. Oberdolf, W. Puls, K. Schlossmann, and K. Stoepel, *Arzneim.-Forsch.*, **22**, 1 (1972).
12) E. E. Royals and A. G. Robinson, III, *J. Am. Chem. Soc.*, **78**, 4161 (1956).
13) D. J. Collins, *J. Chem. Soc.*, **1963**, 1337.
14) J.-P. Célérier, E. Deloisy, G. Lhommet, and P. Maitte, *J. Org. Chem.*, **44**, 3089 (1979).

[Chem. Pharm. Bull. 35(12)4829—4838(1987)]

Synthetic Nucleosides and Nucleotides. XXVII.[1] Selective Inhibition of Deoxyribonucleic Acid Polymerase α by 1-β-D-Arabinofuranosyl-5-styryluracil 5′-Triphosphates and Related Nucleotides: Influence of Hydrophobic and Steric Factors on the Inhibitory Action

SHUNJI IZUTA and MINEO SANEYOSHI*

Faculty of Pharmaceutical Sciences, Hokkaido University, Kita-12, Nishi-6, Kita-ku, Sapporo 060, Japan

(Received June 1, 1987)

Eight kinds of 5-substituted 1-β-D-arabinofuranosyluracil 5′-triphosphates ((*E*)-(3-nitrostyryl) (**6**), (*E*)-(3-aminostyryl) (**9**), (*E*)-(4-nitrostyryl) (**7**), (*E*)-(4-aminostyryl) (**10**), (*E*)-styryl (**8**), phenethyl (**11**), (*RS*)-(3-azido-2-hydroxypropyl) (**17**), and (*RS*)-(3-amino-2-hydroxypropyl) (**18**) derivatives) were synthesized. Among these analogs, araUTPs bearing strongly hydrophobic styryl groups at the 5-position (**6**—**10**) were shown to have selective and strong inhibitory action on deoxyribonucleic acid (DNA) polymerase α purified from cherry salmon (*Oncorhynchus masou*) testes. The 5-azidopropyl derivative (**17**) also inhibited this polymerase. The compounds with a nitro and an amino group on the 5-styryl substituent showed essentially the same activity, but the 5-phenethyl derivative (**11**) and the 5-aminopropyl derivative (**18**) showed greatly reduced inhibitory action. On the other hand, in the case of DNA polymerase β, all the analogs showed similar inhibitory effects. The influence of hydrophobic and steric effects of substituents at the 5-position of araUTP on DNA polymerases α and β are discussed.

Keywords——5-(*E*)-styryl araUTP; DNA polymerase α; DNA polymerase β; hydrophobic effect; cherry salmon testes

At least three species of deoxyribonucleic acid (DNA)-dependent DNA polymerase, termed α, β, and γ,[2] exist in eukaryotic tissues or cells. These polymerases, as well as viral DNA polymerases, have been purified from several sources, and their properties have been examined. To obtain information about the precise roles of these polymerases *in vivo*, species-specific inhibitors would be useful tools. For example, aphidicolin (which specifically inhibits DNA polymerase α) and 2′,3′-dideoxythymidine 5′-triphosphate (which shows preferential inhibitory action on DNA polymerase β and γ) are available.[3-5] However, their specificity *in vivo* is not satisfactory. Thus, we have been searching for new classes of nucleotide analogs which act more efficiently and more selectively on various DNA polymerases. These compounds might also be potential antitumor or antiviral agents.

Arabinofuranosyl nucleotides (*e.g.*, araTTP) inhibit DNA polymerase α more than β.[6,7] Recently we reported that 2′-azido-2′-deoxy araATP showed a more selective inhibitory effect than araATP, but its amino counterparts inhibited both polymerases to similar extent.[8] We also previously found that a hydrophobic group at the 5-position of araUTP could increase the affinity of the analog for DNA polymerase α, based on experiments using several araUTPs modified at the 5-position with alkyl chains.[9] Concerning hydrophobic effects in the purine series, 2-(*p*-*n*-butylanilino)-6-substituted purine nucleotides were found to have strong affinities for DNA polymerase α.[10]

On the other hand, DeClercq *et al.* reported that 2′-deoxyUMPs modified with strongly hydrophobic styryl groups at the 5-position showed remarkable inhibitory effects on

eukaryotic thymidylate synthase.[11] Thus, we have synthesized several 5-(substituted)styryl araUTPs and related compounds, and examined their inhibitory effects on DNA polymerases α and β purified from developing cherry salmon (*Oncorhynchus masou*) testes.

Synthesis

Many procedures for the introduction of substituents at the 5-position of a uracil ring have been reported. The method with palladium as a catalyst is very convenient,[12] and Bigge *et al.* used it to synthesize various 5-styryl-2′-deoxyuridines and 5′-monophosphate derivatives.[13] We applied this method for the present synthetic study (Chart 1).

1-β-D-Arabinofuranosyluracil[14] (**1**) was lead to the 5-chloromercuri derivative (**2**) by treatment with mercuric acetate and sodium chloride,[15] and then 3-nitrostyrene, 4-nitrostyrene, or styrene itself was reacted in the presence of palladium as a catalyst in methanol. 1-β-D-Arabinofuranosyl-5-(*E*)-(3-nitrostyryl)uracil (**3**), 1-β-D-arabinofuranosyl-5-(*E*)-(4-nitrostyryl)uracil (**4**), and 1-β-D-arabinofuranosyl-5-(*E*)-styryluracil (**5**) were obtained in yields of 22%, 19%, and 49%, respectively. The proton nuclear magnetic resonance (^{1}H-NMR) spectra of these nucleosides showed that the coupling constants (*J*) of the vinyl moieties of all styryl groups at the 5-position were in the range of 16.1—16.6 Hz, indicating that the all styryl substituents were "*trans*," as reported by Bigge *et al.*[13] All the synthesized nucleosides were converted to the corresponding 5′-monophosphates by phosphorylation with phosphoryl chloride in triethyl phosphate.[16] Further phosphorylation to the 5′-triphosphate derivatives was performed by the phosphoroimidazolidate method[17] with some modifications.[18] In all cases, total yields of phosphorylation from nucleoside were about 50%. The nitro groups of 5-(*E*)-(3-nitrostyryl) araUTP (**6**) and 5-(*E*)-(4-nitrostyryl) araUTP (**7**) were reduced with hydrazine hydrate in the presence of a catalytic amount of Raney Ni (W-2),[13] giving 5-(*E*)-(3-aminostyryl) araUTP (**9**) and 5-(*E*)-(4-aminostyryl) araUTP (**10**) in 78% and 83% yields, respectively. The vinyl group of 5-(*E*)-styryl araUTP (**8**) was reduced under 1 atm pressure of hydrogen in the presence of palladium–carbon,[13] and 5-phenethyl araUTP (**11**) was obtained in a yield of 50%.

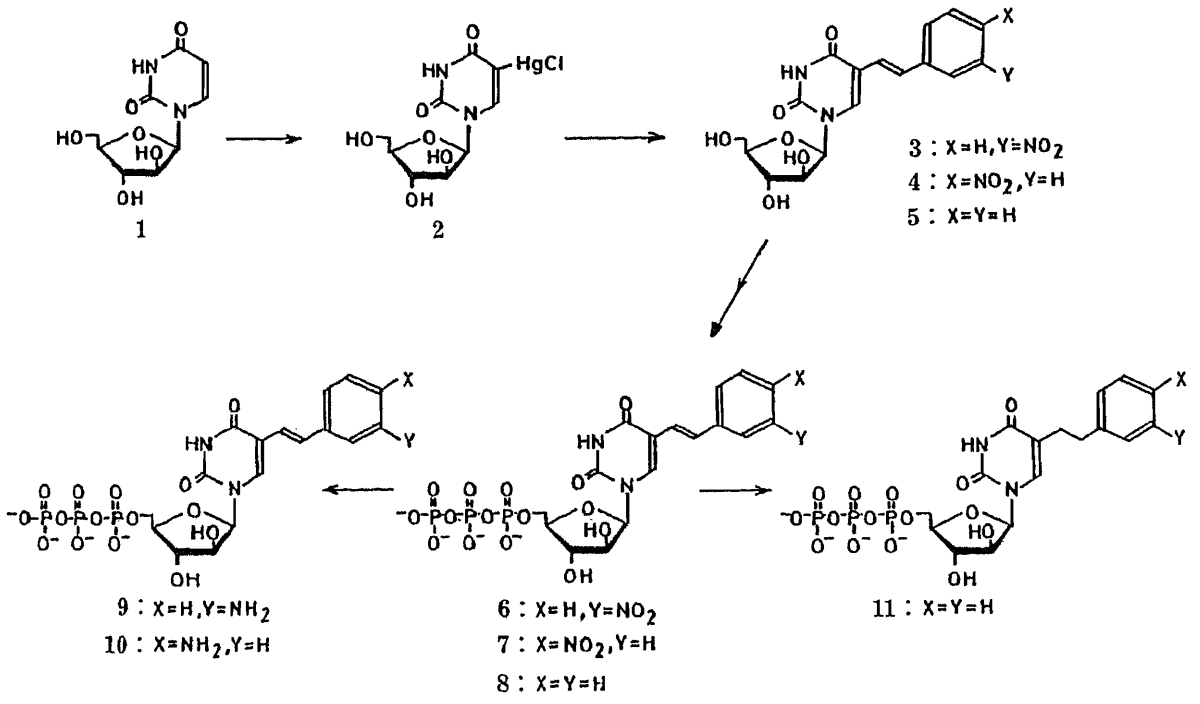

Chart 1

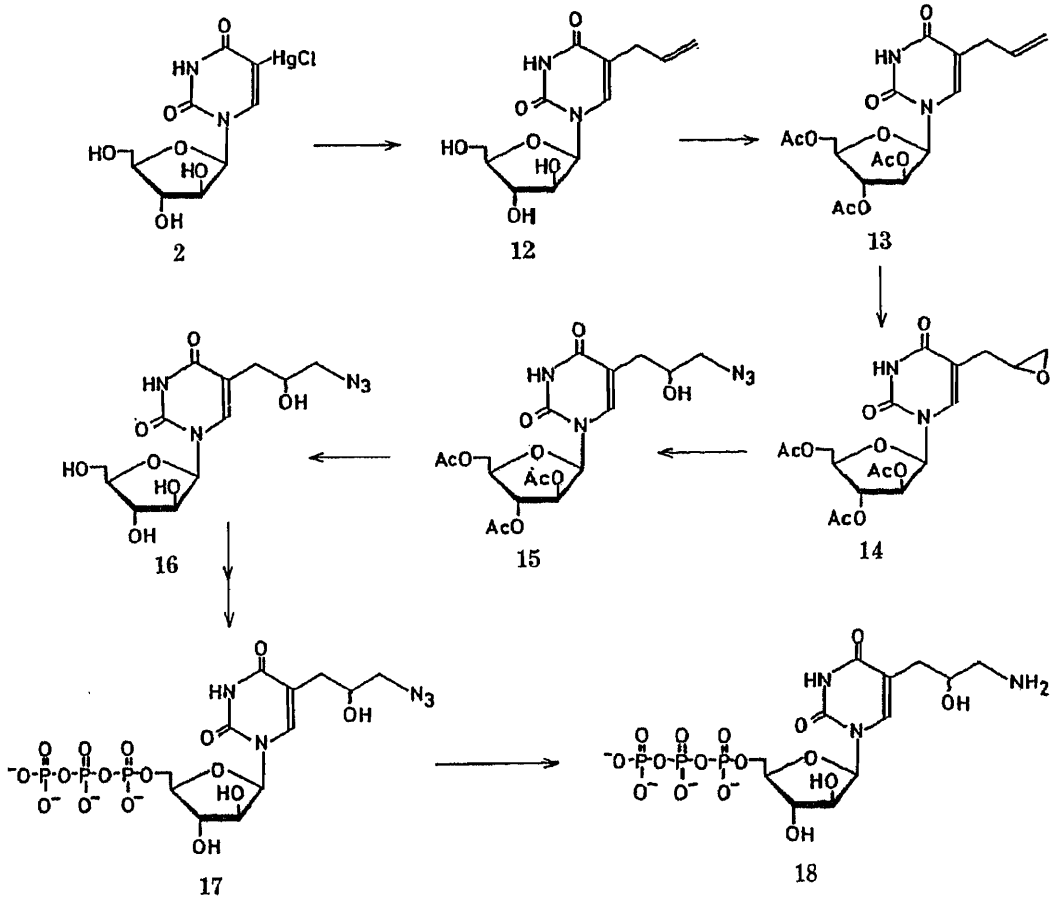

Chart 2

On the other hand, for comparison of the effect of hydrophobicity of substituents at the 5-position of araUTP, we also synthesized 5-alkyl derivatives (Chart 2). 5-Allyl-1-β-D-arabinofuranosyluracil (**12**) was synthesized from **2** with allyl chloride in the presence of palladium as a catalyst.[19] The hydroxy groups at the 2′-, 3′-, and 5′-positions of **12** were acetylated, and the allyl group was oxidized with *m*-chloroperbenzoic acid,[20] followed by cleavage of the resulting epoxy ring with lithium azide. ^{1}H-NMR spectra showed that compound **14** or **15** was a mixture of (*R*)- and (*S*)-products in the ratio of about 1 : 1. However, we used these compounds as such, since the isomers were difficult to separate. Compound **15** was treated with methanolic ammonia to give the free nucleoside (**16**). Then **16** was converted to its 5′-triphosphate in the same manner as described above. 5-(*RS*)-(3-Azido-2-hydroxypropyl) araUTP (**17**) was converted to the 3-amino counterpart (**18**) by reduction with hydrogen sulfide in 50% aqueous pyridine.[21]

All chemically synthesized nucleotide analogs were purified by paper chromatography and paper electrophoresis.

Biological Evaluation

Inhibitory Effects of Various AraUTP Analogs on DNA Polymerases α and β——The inhibitory effects of eight newly synthesized araUTP analogs on DNA-dependent DNA polymerases α and β purified from developing cherry salmon (*Oncorhynchus masou*) testes[8] were examined with activated salmon sperm DNA as a template-primer. The activity without analogs was taken as 100%, and the remaining activity (%) at various concentrations of analogs was measured. The resulting inhibition curves are shown in Fig. 1-A (DNA

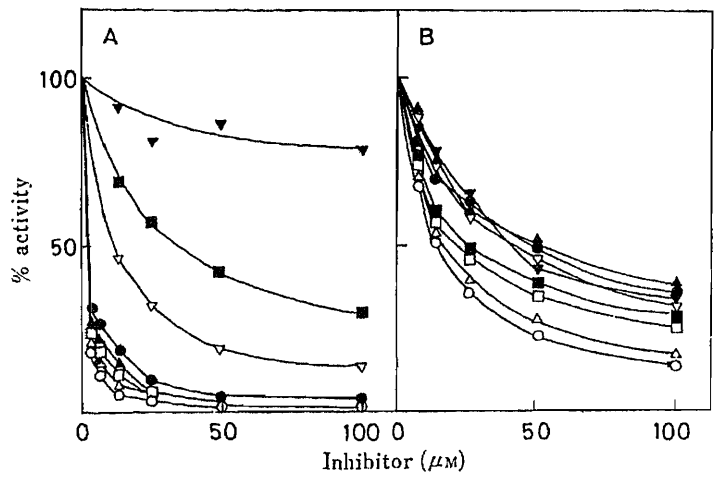

Fig. 1. Inhibitory Effects of Various 5-(Substituted)styryl araUTPs and Related Compounds on DNA Polymerases α (A) and β (B)

○—○, 5-(*E*)-(3-nitrostyryl) araUTP (**6**); ●—●, 5-(*E*)-(3-aminostyryl) araUTP (**9**); △—△, 5-(*E*)-(4-nitrostyryl) araUTP (**7**); ▲—▲, 5-(*E*)-(4-aminostyryl) araUTP (**10**); □—□, 5-(*E*)-styryl araUTP (**8**); ■—■, 5-phenethyl araUTP (**11**); ▽—▽, 5-(*RS*)-(3-azido-2-hydroxypropyl) araUTP (**17**); ▼—▼, 5-(*RS*)-(3-amino-2-hydroxypropyl) araUTP (**18**).

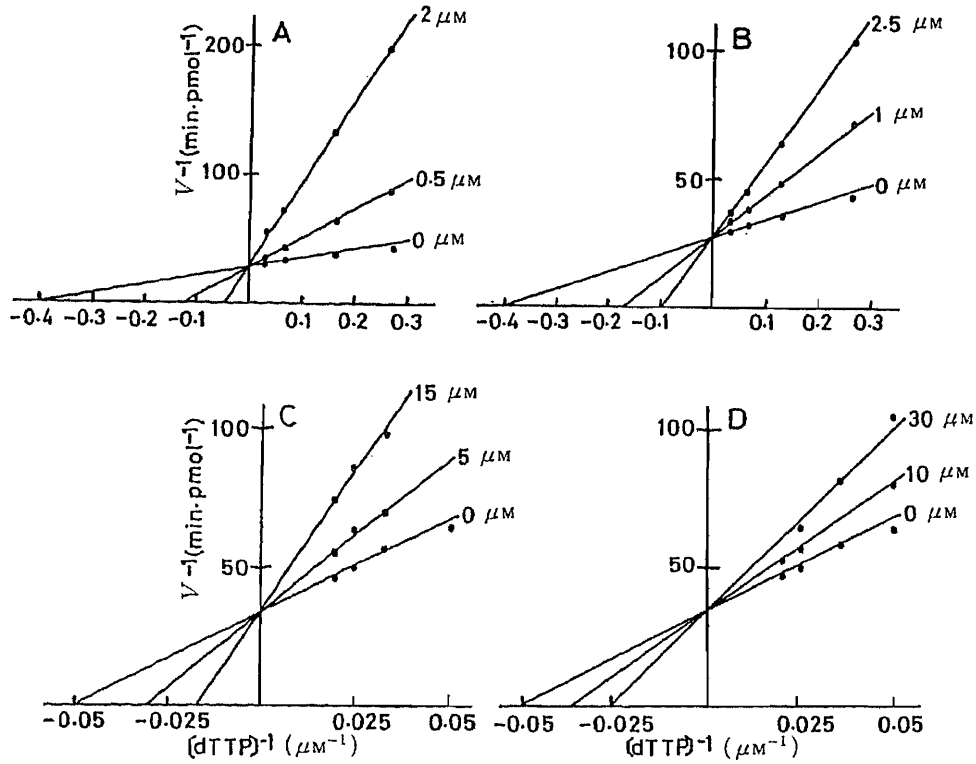

Fig. 2. Lineweaver–Burk Plots for the Inhibition of DNA Polymerases α (A, B) and β (C, D) by 5-(*E*)-(3-Nitrostyryl) araUTP (**6**) (A, C) and 5-(*E*)-(3-Aminostyryl) araUTP (**9**) (B, D)

polymerase α) and Fig. 1-B (DNA polymerase β). As can be seen in Fig. 1-A, all araUTP analogs (**6**—**10**) having styryl groups at the 5-position inhibited DNA polymerase α very strongly. A strong inhibitory effect was also found in the case of the 5-azidopropyl derivative

TABLE I. Kinetic Parameters of Various araUTPs

Compound	DNA polymerase α		DNA polymerase β		K_i/K_m for pol. α / K_i/K_m for pol. β
	K_i (μM)	K_i/K_m	K_i (μM)	K_i/K_m	
dTTP	2.5 (K_m)		20 (K_m)		
5-(*E*)-(3-Nitrostyryl) araUTP (**6**)	0.25	0.10	8.5	0.43	0.24
5-(*E*)-(3-Aminostyryl) araUTP (**9**)	0.80	0.32	33	1.65	0.19
5-(*E*)-(4-Nitrostyryl) araUTP (**7**)	0.45	0.18	8.5	0.43	0.42
5-(*E*)-(4-Aminostyryl) araUTP (**10**)	0.60	0.24	30	1.50	0.16
5-(*E*)-Styryl araUTP (**8**)	0.50	0.20	10	0.50	0.40
5-Phenethyl araUTP (**11**)	4.9	1.96	16	0.80	2.45
5-(*RS*)-(3-Azido-2-hydroxypropyl) araUTP (**17**)	2.0	0.80	22	1.10	0.73
5-(*RS*)-(3-Amino-2-hydroxypropyl) araUTP (**18**)	61	24.4	23	1.15	21

(**17**), but the corresponding amino derivative (**18**) showed a greatly reduced inhibitory effect on this polymerase. In contrast, there was no marked difference of inhibitory effects between the compounds with a nitro group and an amino group on the 5-styryl moiety. However, the inhibitory effect of 5-phenethyl araUTP (**11**) was less than that of 5-styryl araUTP (**8**).

On the other hand, in the case of DNA polymerase β (Fig. 1-B), all the analogs showed similar inhibitory effects, and the kind of substituent at the 5-position had no influence on the activity.

Analyses of Inhibition Mode and Determination of Kinetic Constants (K_i Values)——We next examined the mode of inhibition of DNA polymerases α and β by these araUTP analogs using Lineweaver–Burk plots. In this analysis, activated DNA was used as a template-primer. As a typical example, plots of data for the inhibition of DNA polymerases α and β by 5-(*E*)-(3-nitrostyryl) araUTP (**6**) and 5-(*E*)-(3-aminostyryl) araUTP (**9**) are shown in Fig. 2. All the araUTP analogs were essentially competitive with natural substrate dTTP for both DNA polymerases α and β.

Based on these analyses, the kinetic constants (K_i values) were determined by replots of apparent K_m value *versus* the concentration of the analog, and the results are summarized in Table I. For DNA polymerase α, the K_i values of all analogs except for 5-phenethyl araUTP (**11**) and 5-(*RS*)-(3-amino-2-hydroxypropyl) araUTP (**18**) were much smaller than the K_m value of the natural substrate dTTP. For DNA polymerase β, the K_i values of all analogs were very similar to the K_m value of dTTP.

Discussion

Recently we have reported that the inhibitory effect of 5-ethyl araUTP on eukaryotic DNA polymerase α was less than that of araUTP or araTTP owing to the steric hindrance of the substituent at the 5-position of the uracil ring, but longer alkyl chain-modified derivatives, 5-*n*-propyl and 5-*n*-butyl araUTP, recovered inhibitory action as a result of their hydrophobic effect.[9] In order to examine the hydrophobic effect of the substituent at the 5-position of araUTP in more detail, we have synthesized several araUTPs modified at the 5-position with strongly hydrophobic styryl groups, and examined their inhibitory effects on DNA polymerases α and β purified from cherry salmon (*Oncorhynchus masou*) testes.[22]

As can be seen in Fig. 1, all 5-styryl derivatives of araUTP (**6**—**10**) showed very strong inhibitory effects on DNA polymerase α. The K_i values of these analogs were much smaller than the K_m value of the natural substrate dTTP; 5-(*E*)-(3-nitrostyryl) araUTP (**6**) showed the smallest K_i value of 0.25 and its K_i/K_m value was 0.10. Although the K_i values of 5-aminostyryl derivatives (**9**, **10**) were somewhat higher than those of 5-nitrostyryl derivatives (**6**, **7**), the

K_i/K_m values were about 0.3 suggesting that these analogs still have strong affinity for DNA polymerase α. In contrast, among the 5-alkyl derivatives of araUTP, the K_i value of the 5-aminopropyl derivative (**18**) was remarkably larger than that of the 5-azidopropyl derivative (**17**). This indicates that the hydrophobic effect of the substituent at the 5-position of araUTP has a greater effect on the affinity for DNA polymerase α than does the kind of substituent. However, 5-phenethyl araUTP (**11**) which is thought to have similar hydrophobicity at the 5-position to the 5-styryl derivative showed a K_i/K_m value of 1.96 and was found to show lower affinity for DNA polymerase α. This finding indicates that not only hydrophobicity but also steric hindrance of the 5-substituent on the uracil ring affects the affinity of the analog for DNA polymerase α. Therefore, as reported in the case of 5-(*E*)-(2-bromovinyl)-2′-deoxyuridine,[23] intramolecular hydrogen bonding between the vinyl group at the 5-position of 5-(*E*)-(substituted)styryl araUTP and O^4 of the uracil ring could be important for the affinity to this polymerase.

In the case of DNA polymerase β, all analogs showed weak inhibitory effects, and K_i values of all analogs including 5-alkyl derivatives were essentially similar. Thus, neither hydrophobicity nor steric hindrance at the 5-position of araUTP affects the affinity of the analogs for DNA polymerase β. Knowledge of these differencies between DNA polymerases α and β will be useful for the design of species-specific inhibitors.

A smaller value of the ratio of (K_i/K_m value for DNA polymerase α)/(K_i/K_m value for DNA polymerase β), indicates selectivity for DNA polymerase α, although the K_i values of the 5-aminostyryl derivatives (**9**, **10**) for DNA polymerase α were larger than these of the 5-nitrostyryl derivatives (**6**, **7**), these two 5-aminostyryl derivatives of araUTP were found to be more selective inhibitors for DNA polymerase α than the styryl derivatives.

We are attempting to prepare a new affinity adsorbent for specific purification of DNA polymerase α, by using a strong and selective inhibitor for this enzyme as a ligand. 5-(*E*)-(3-Aminostyryl) araUTP (**9**) and 5-(*E*)-(4-aminostyryl) araUTP (**10**) are potential candidates for this affinity ligand. Affinity chromatography on resin carrying these compounds as ligands is being examined.

Experimental

General Methods——Melting points were determined with Yanaco MP-3 apparatus and are uncorrected. Ultraviolet (UV) spectra were recorded on a Shimadzu UV-240 recording spectrophotometer. ^{1}H-NMR spectra were obtained on a JEOL JNM-FX 200 NMR spectrometer with tetramethylsilane as an internal standard. Chemical shifts are reported in ppm (δ), and signals are described as s (singlet), d (doublet), and m (multiplet). Mass spectra (MS) were measured on a JEOL JMS-D-300 mass spectrometer. Infrared (IR) spectra were obtained on a JASCO IRA-2 spectrometer. Thin layer chromatography was performed with pre-coated Silica gel 60 F254 plates (Merck) and silica gel Column chromatography was carried out on Wako-gel C-200. Radioactivity was measured with a Packard TRI-CARB C-480 liquid scintillation counter with toluene scintillator.

1-β-D-Arabinofuranosyl-5-chloromercuriuracil (2)——1-β-D-Arabinofuranosyluracil (**1**) (3.0 g, 12.4 mmol) was dissolved in 17 ml of water, then 4.1 g (12.9 mmol) of mercuric acetate in 24 ml of water was added, and the mixture was stirred for 24 h at 50 °C. The mixture was cooled to room temperature, and the white precipitate was collected by filtration, and washed with 100 ml of 0.16 M aqueous sodium chloride and 5 ml of ethanol. The white solid was ground and dried. 5.8 g (97%). mp 173—174 °C (dec.). *Anal.* Calcd for $C_9H_{11}N_2O_6 \cdot HgCl \cdot H_2O$: C, 21.70; H, 2.63; N, 5.62. Found: C, 21.69; H, 2.63; N, 5.47.

1-β-D-Arabinofuranosyl-5-(*E*)-(3-nitrostyryl)uracil (3)——A mixture of a suspension of 2.0 g (4.19 mmol) of **2** in 10 ml of methanol, 1.89 g (12.6 mmol) of 3-nitrostyrene and 35 ml (3.5 mmol) of methanolic solution of 0.1 M lithium tetrachloropalladate was refluxed for 24 h. The solution was filtered, and hydrogen sulfide gas was bubbled through the filtrate for 90 s. The precipitate of mercuric sulfide was filtered off through celite, and the filtrate was evaporated under reduced pressure. The residue was purified by silica gel (100 g) column chromatography. Elution was performed with 8—12% methanol in chloroform. The fractions containing **3** were combined and evaporated to dryness. The residue was crystallized from methanol to give **3** as yellow crystals. 360 mg (22%). mp 249.5—250.5 °C. UV $\lambda_{max}^{H_2O}$ nm (ε): 298 (19800), $\lambda_{min}^{H_2O}$ nm: 232, $\lambda_{max}^{0.1N\,HCl}$ nm: 298, $\lambda_{min}^{0.1N\,HCl}$ nm: 232, $\lambda_{max}^{0.1N\,NaOH}$ nm: 306, $\lambda_{min}^{0.1N\,NaOH}$ nm: 242.

^{1}H-NMR (DMSO-d_6+D_2O): 8.28 (s, 1H, H-6), 8.1—7.6 (m, 4H, aromatic), 7.54 (d, 1H, vinylic, J=16.1 Hz), 7.12 (d, 1H, vinylic, J=16.1 Hz), 6.15 (d, 1H, H-1′, J=4.9 Hz), 4.10 (m, 1H, H-2′), 3.98 (m, 1H, H-3′). MS *m/z*: 259 (heterocyclic base), 188, 142, 115. *Anal.* Calcd for $C_{17}H_{17}N_3O_8$: C, 52.18; H, 4.38; N, 10.74. Found: C, 52.08; H, 4.36; N, 10.57.

1-β-D-Arabinofuranosyl-5-(*E*)-(4-nitrostyryl)uracil (4)——A mixture of a suspension of 1.26 g (2.6 mmol) of **2** in 10 ml of methanol, 1.0 g (6.77 mmol) of 4-nitrostyrene and 26 ml (2.6 mmol) of methanolic solution of 0.1 M lithium tetrachloropalladate was refluxed for 24 h. The mixture was filtered, and hydrogen sulfide gas was bubbled through the filtrate for 90 s, followed by filtration through celite. The filtrate was evaporated, and the residue was purified by silica gel (130 g) column chromatography. Elution was performed with 10% methanol in chloroform. The fractions containing **4** were combined and evaporated to dryness. The residue was crystallized from methanol to afford **4** as orange-yellow crystals. 196 mg (19%). mp 243—244 °C. UV $\lambda_{max}^{H_2O}$ nm (ε): 366 (15900), $\lambda_{min}^{H_2O}$ nm: 284, $\lambda_{max}^{0.1NHCl}$ nm: 366, $\lambda_{min}^{0.1NHCl}$ nm: 284, $\lambda_{max}^{0.1NNaOH}$ nm: 315, $\lambda_{min}^{0.1NNaOH}$ nm: 282. ^{1}H-NMR (DMSO-d_6+D_2O): 8.17 (s, 1H, H-6), 7.74 (d, 2H, aromatic, J=8.8 Hz), 7.62 (d, 2H, aromatic, J=8.8 Hz), 7.57 (d, 1H, vinylic, J=16.1 Hz), 7.34 (d, 1H, vinylic, J=16.1 Hz), 6.05 (d, 1H, H-1′, J=4.9 Hz). MS *m/z*: 259 (heterocyclic base), 188, 142, 115. *Anal.* Calcd for $C_{17}H_{17}N_3O_8$: C, 52.18; H, 4.38; N, 10.74. Found: C, 52.00; H, 4.33; N, 10.54.

1-β-D-Arabinofranosyl-5-(*E*)-styryluracil (5)——A mixture of a suspension of 1.5 g (3.1 mmol) of **2** in 15 ml of methanol, 1.0 g (9.6 mmol) of styrene and 30 ml (3.0 mmol) of methanolic solution of 0.1 M lithium tetrachloropalladate was refluxed for 24 h. The mixture was filtered, and hydrogen sulfide gas was bubbled through the filtrate for 90 s, followed by filtration through celite. The filtrate was evaporated and the residue was purified by silica gel (100 g) column chromatography. Elution was performed with 8—10% methanol in chloroform. The fractions containing **5** were combined and evaporated to dryness. The residue was crystallized from methanol–water to give **5** as colorless crystals. 530 mg (49%). mp 237—238 °C. UV $\lambda_{max}^{H_2O}$ nm (ε): 308 (18000), $\lambda_{min}^{H_2O}$ nm: 238, $\lambda_{max}^{0.1NHCl}$ nm: 308, $\lambda_{min}^{0.1NHCl}$ nm: 238, $\lambda_{max}^{0.1NNaOH}$ nm: 308, $\lambda_{min}^{0.1NNaOH}$ nm: 244. ^{1}H-NMR (DMSO-d_6+D_2O): 8.06 (s, 1H, H-6), 7.8—7.3 (m, 5H, aromatic), 7.28 (d, 1H, vinylic, J=16.6 Hz), 6.90 (d, 1H, vinylic, J=16.1 Hz), 6.05 (d, 1H, H-1′, J=4.9 Hz), 4.10 (m, 1H, H-2′), 3.98 (m, 1H, H-3′). MS *m/z*: 346 (molecular ion), 214 (heterocyclic base), 143, 115. *Anal.* Calcd for $C_{17}H_{18}N_2O_6$: C, 58.96; H, 5.24; N, 8.09. Found: C, 58.97; H, 5.14; N, 8.03.

5-Allyl-1-β-D-arabinofuranosyluracil (12)——A mixture of a suspension of 3.0 g (6.3 mmol) of **2** in 50 ml of methanol, 5.2 ml (63.7 mmol) of allyl chloride and 16 ml (1.6 mmol) of 0.1 M methanolic solution of lithium tetrachloropalladate was stirred for 24 h at room temperature. The solution was filtered, and hydrogen sulfide gas was bubbled through the filtrate for 40 s, followed by filtration through celite. The filtrate was neutralized with Dowex 1×2 (bicarbonate form), and the resin was removed by filtration and washed with methanol. The combined filtrate and washing were evaporated, and the residue was purified by silica gel (50 g) column chromatography. Elution was performed with 8—10% methanol in chloroform. The fractions containing **12** were combined and evaporated. The residue was crystallized from acetonitrile to give **12** as colorless crystals. 1.15 g (64%). mp 161.5—163 °C. UV $\lambda_{max}^{H_2O}$ nm (ε): 267 (9000), $\lambda_{min}^{H_2O}$ nm: 235, $\lambda_{max}^{0.1NHCl}$ nm: 267, $\lambda_{min}^{0.1NHCl}$ nm: 235, $\lambda_{max}^{0.1NNaOH}$ nm: 267, $\lambda_{min}^{0.1NNaOH}$ nm: 243. ^{1}H-NMR (DMSO-d_6+D_2O); 7.51 (s, 1H, H-6), 6.00 (d, 1H, H-1′, J=4.9 Hz), 5.9—5.7 (m, 1H, 5-CH_2C$\underline{H}$=CH_2), 5.1—5.0 (m, 2H, 5-CH_2CH=C$\underline{H}_2$), 4.03 (m, 1H, H-2′), 3.91 (m, 1H, H-3′), 3.7—3.5 (m, 3H, H-4′ and H-5′), 2.95 (d, 2H, 5-C$\underline{H}_2$CH=CH_2, J=6.1 Hz). MS *m/z*: 284 (molecular ion), 181, 152. *Anal.* Calcd for $C_{12}H_{16}N_2O_6$: C, 50.70; H, 5.67; N, 9.86. Found: C, 50.84; H, 5.73; N, 10.05.

5-Allyl-1-β-D-(2,3,5-tri-*O*-acetylarabinofuranosyl)uracil (13)——A mixture of a solution of 1.70 g (5.98 mmol) of **12** in 30 ml of pyridine and 2.5 ml (26.5 mmol) of acetic anhydride was stirred for 24 h at room temperature. The mixture was cooled in an ice-water bath, then 3 ml of methanol was added and the whole was stirred for 20 min. The solvent was evaporated off, and removed completely by co-evaporation with ethanol. Crystallization of the residue from ethanol gave **13** as colorless crystals. 2.3 g (94%). mp 138.5—139.5 °C. MS *m/z*: 419 (molecular ion), 259, 139, 97, 43. *Anal.* Calcd for $C_{18}H_{22}N_2O_9$: C, 52.68; H, 5.40; N, 6.83. Found: C, 52.55; H, 5.50; N, 6.96.

5-(*RS*)-(2,3-Epoxypropyl)-1-β-D-(2,3,5-tri-*O*-acetylarabinofuranosyl)uracil (14)——Compound **13** (2.0 g, 4.87 mmol) was dissolved in 50 ml of methylene chloride, and 2.6 g (15.1 mmol) of *m*-chloroperbenzoic acid was added. The mixture was stirred for 24 h at room temperature. After being washed with saturated $NaHCO_3$ aqueous solution and water, the organic layer was filtered through Whatman 1PS filter paper, and the solvent was evaporated off. The residue was purified by silica gel (100 g) column chromatography. Elution was performed with 3—4% methanol in chloroform. The fractions containing **14** were combined and evaporated to dryness. The residue was crystallized from ethanol to give **14** as colorless crystals. 0.86 g (41%). mp 136.5—137 °C. UV λ_{max}^{MeOH} nm (ε): 267 (9000), λ_{min}^{MeOH} nm: 235, $\lambda_{max}^{0.1NHCl}$ nm: 267, $\lambda_{min}^{0.1NHCl}$ nm: 235, $\lambda_{max}^{0.1NMeONa}$ nm: 267, $\lambda_{min}^{0.1NMeONa}$ nm: 243. ^{1}H-NMR ($CDCl_3$+D_2O): 7.48 and 7.45 (s, 1H, total H-6), 6.3 (m, 1H, H-1′), 5.4 (m, 1H, H-2′), 5.1 (m, 1H, H-3′), 4.4—4.2 (m, 3H, H-4′ and H-5′), 3.0 (m, 1H, 5-CH_2C$\underline{H}$(O)CH_2), 2.8 (m, 2H, 5-CH_2CH(O)C$\underline{H}_2$), 2.5 (m, 2H, 5-C$\underline{H}_2$CH(O)CH_2). MS *m/z*: 426 (molecular ion), 307, 259, 139, 97, 43. *Anal.* Calcd for $C_{18}H_{22}N_2O_{10}$: C, 50.71; H, 5.20; N, 6.57. Found: C, 50.46; H, 5.23; N, 6.53.

5-(*RS*)-(3-Azido-2-hydroxypropyl)-1-β-D-(2,3,5-tri-*O*-acetylarabinofuranosyl)uracil (15)——A solution of 700 mg (1.64 mmol) of **14** in 20 ml of dimethylformamide (DMF) was treated with 240 mg (4.90 mmol) of lithium azide. The mixture was stirred for 24 h at 65 °C, then the solvent was evaporated off. The residue was dissolved in

30 ml of chloroform, and washed with water three times. The organic layer was filtered through Whatman 1PS filter paper, and the filtrate was evaporated. The residue was purified by silica gel (70 g) column chromatography. Elution was performed with 4—5% methanol in chloroform. The fractions containing **15** were combined and evaporated to dryness, giving a foam. 380 mg (49%). UV λ_{max}^{MeOH} nm (ε): 267 (9000), λ_{min}^{MeOH} nm: 235, $\lambda_{max}^{0.1NHCl}$ nm: 267, $\lambda_{min}^{0.1NHCl}$ nm: 235, $\lambda_{max}^{0.1NMeONa}$ nm: 267, $\lambda_{min}^{0.1NMeONa}$ nm: 243. ^{1}H-NMR ($CDCl_3+D_2O$): 7.54 and 7.49 (s, 1H, total H-6), 6.3 (m, 1H, H-1′), 5.4 (m, 1H, H-2′), 5.1 (m, 1H, H-3′), 4.6—4.5 (m, 3H, H-4′ and H-5′), 4.3 (m, 1H, 5-CH_2C<u>H</u>(OH)CH_2N_3), 3.3 (m, 2H, 5-CH_2CH(OH)C<u>H</u>$_2N_3$), 2.6 (m, 2H, 5-C<u>H</u>$_2$CH(OH)CH_2N_3). IR (Nujol): 2080 cm^{-1} ($-N_3$).

1-β-D-Arabinofuranosyl-5-(*RS*)-(3-azido-2-hydroxypropyl)uracil (16)——Compound **15** (310 mg, 0.66 mmol) was dissolved in 0.5 ml of methanol, and 3.8 ml (0.99 mmol) of 0.26 N methanolic sodium methoxide was added. The mixture was stirred for 5 h at room temperature, neutralized with Dowex 50 × 8 (proton form) and filtered. The resin was washed with methanol, and the combined filtrate and washings were evaporated to dryness to give a form. 200 mg (90%). This compound was used for the next reaction immediately.

General Method for Phosphorylation——Phosphoryl chloride (1.5 mmol) was added to 0.5 mmol of synthetic nucleoside (**3**, **4**, **5**, or **16**) in 5 ml of triethyl phosphate under cooling below 0 °C. The mixture was stirred for 24 h at 0 °C. The solution was poured into 30 ml of saturated $NaHCO_3$ aqueous solution and extracted with chloroform (30 ml) three times. The combined organic layers were re-extracted with water (15 ml). The aqueous layers were combined and diluted with water to give a final volume of 300 ml, and applied to a column of diethylaminoethyl (DEAE)-cellulose (2.9 × 25 cm, bicarbonate form). The column was washed with 500 ml of water, and eluted with a linear gradient from water (1 l) to 0.2 M triethylammonium bicarbonate (1 l). Fractions containing desired nucleotide were combined and evaporated to dryness, and co-evaporation with 50% aqueous ethanol was carried out to remove residual triethylamine. The obtained 5′-monophosphate derivative was converted to the 5′-triphosphate by the following method. The 5′-monophosphate derivative (0.2 mmol) was dissolved in 1 ml of DMF and evaporated to dryness. This process was repeated twice, then 1 mmol of *N*,*N*′-carbonyldiimidazole was added to the residue in 2 ml of DMF, and the mixture was stirred for 3.5 h at room temperature. After confirmation of the complete conversion to the 5′-phosphoroimidazolidate derivative by paper electrophoresis (in 50 mM triethylammonium bicarbonate, 700 V, 30 min), 0.8 ml of methanol was added to decompose excess reagent, and the mixture was stirred for 30 min at room temperature. Then 2 ml (2 mmol) of 1 M tributylammonium pyrophosphate in DMF was added, and the mixture was stirred for 24 h at room temperature. Water (10 ml) was added and the nucleotide was adsorbed on 1 g of charcoal. The mixture was filtered through celite. After washing with 100 ml of water, elution was carried out with 200 ml of 50% aqueous ethanol–3% NH_4OH. The eluate was evaporated, and the residue was dissolved in 100 ml of water and applied to a column of DEAE-cellulose (2.9 × 25 cm, bicarbonate form). The column was washed with 500 ml of water, and then eluted with a linear gradient from water (1 l) to 0.5 M triethylammonium bicarbonate (1 l). The combined fractions containing the 5′-triphosphate derivative were evaporated and co-evaporated with 50% aqueous ethanol to dryness. Through the above procedure, 5-(*E*)-(3-nitrostyryl) araUTP (**6**), 5-(*E*)-(4-nitrostyryl) araUTP (**7**), 5-(*E*)-styryl araUTP (**8**), and 5-(*RS*)-(2-hydroxy-3-azidopropyl) araUTP (**17**) were synthesized from the corresponding nucleosides in yields of about 50%.

5-(*E*)-(3-Aminostyryl) araUTP (9)——A mixture of **6** (2000 OD_{298} units, 0.10 mmol) in 5 ml of water, 100 μl of hydrazine hydrate and a catalytic amount of Raney Ni (W-2) was stirred for 4 h at room temperature. The solution was filtered through celite, and the filter was washed with 200 ml of 50% aqueous ethanol–3% NH_4OH. The combined filtrate and washings were evaporated to dryness. The residue was dissolved in 250 ml of water and applied to a column of DEAE-cellulose (2.9 × 25 cm, bicarbonate form). The column was washed with 500 ml of water, and eluted with a linear gradient from water (1 l) to 0.5 M triethylammonium bicarbonate (1 l). The combined fractions containing **9** were evaporated and co-evaporated with 50% aqueous ethanol to dryness. 1370 OD_{300} units (78%). UV $\lambda_{max}^{H_2O}$ nm (ε): 300 (15000), $\lambda_{max}^{H_2O}$ nm: 253, $\lambda_{max}^{0.1NHCl}$ nm: 291, $\lambda_{min}^{0.1NHCl}$ nm: 253, $\lambda_{max}^{0.1NNaOH}$ nm: 308, $\lambda_{min}^{0.1NNaOH}$ nm: 262. Ninhydrin possitive (violet).

5-(*E*)-(4-Aminostyryl) araUTP (10)——A mixture of a solution of 1240 OD_{366} units (80 μmol) of **7** in 5 ml of water, 100 μl of hydrazine hydrate and a catalytic amount of Raney Ni (W-2) was stirred for 4 h at room temperature. The mixture was filtered through celite, and the filter was washed with 200 ml of 50% aqueous ethanol–3% NH_4OH. The combined filtrates and washings were evaporated to dryness. The residue was dissolved in 250 ml of water, and applied to a column of DEAE-cellulose (2.9 × 25 cm, bicarbonate form). After washing of the column with 500 ml of water, elution was performed with a linear gradient from water (1 l) to 0.5 M triethylammonium bicarbonate (1 l). The combined fraction containing **10** were evaporated and co-evaporated with 50% aqueous ethanol to dryness. 970 OD_{325} units (83%). UV $\lambda_{max}^{H_2O}$ nm (ε): 325 (15000), $\lambda_{min}^{H_2O}$ nm: 247, $\lambda_{max}^{0.1NHCl}$ nm: 310, $\lambda_{min}^{0.1NHCl}$ nm: 240, $\lambda_{max}^{0.1NNaOH}$ nm: 325, $\lambda_{min}^{0.1NNaOH}$ nm: 252. Ninhydrin positive (violet).

5-Phenethyl araUTP (11)——A mixture of 1800 OD_{308} units (0.10 mmol) of **8** in 1 ml of water and 0.1 g of palladium–carbon was stirred under 1 atm pressure of hydrogen for 24 h at room temperature. The solution was filtered through celite, and the filter was washed with 200 ml of 50% aqueous ethanol–3% NH_4OH. The combined filtrate and washings were evaporated to dryness. The residue was dissolved in 200 ml of water, and applied to a column of DEAE-cellulose (2.9 × 25 cm, bicarbonate form). After washing of the column with 500 ml of water, elution was performed with a linear gradient from water (1 l) to 0.5 M triethylammonium bicarbonate (1 l). The

TABLE II. Analytical Results and Constants of Synthetic Nucleotides

Compound	UV, $\lambda_{max}^{H_2O}$ nm (ε)	ε (P) Found	Paper chromatography[a] ($Rf \times 100$)	Paper electrophoresis[b] (Rf dTTP[c])
6	298 (19800)	6600	28	0.9
9	300 (15000)	4900	23	0.8
7	366 (15900)	5100	22	0.9
10	325 (15000)	4800	15	0.8
8	308 (18000)	5900	37	0.9
11	267 (9000)	2800	38	1.0
17	267 (9000)	2900	42	1.0
18	267 (9000)	2900	36	0.9

a) Solvent system, ethanol: 0.5 M sodium acetate (pH 7.5, 1 : 1, v/v). *b*) In 0.5 M citrate buffer (pH 3.3, 700 V, 30 min). *c*) Relative value with respect to dTTP.

combined fractions containing **11** were evaporated and co-evaporated with 50% aqueous ethanol to dryness. 1800 OD_{267} units (50%). UV $\lambda_{max}^{H_2O}$ nm (ε): 267 (9000), $\lambda_{min}^{H_2O}$ nm: 236, $\lambda_{max}^{0.1NHCl}$ nm: 267, $\lambda_{min}^{0.1NHCl}$ nm: 236, $\lambda_{max}^{0.1NNaOH}$ nm: 267, $\lambda_{min}^{0.1NNaOH}$ nm: 245.

5-(*RS*)-(3-Amino-2-hydroxypropyl) araUTP (18)——Hydrogen sulfide gas was gently bubbled into a solution of 1000 OD_{267} units (0.11 mmol) of **17** in 1 ml of 50% aqueous pyridine for 6 h at room temperature. The solvent was evaporated off, and the residue was dissolved in 100 ml of water and applied to a column of DEAE-cellulose (2.9 × 25 cm, bicarbonate form). After washing of the column with 500 ml of water, elution was performed with a linear gradient from water (1 l) to 0.5 M triethylammonium bicarbonate (1 l). The combined fractions containing **18** were evaporated and co-evaporated with 50% aqueous ethanol to dryness. 640 OD_{267} units (64%). UV $\lambda_{max}^{H_2O}$ nm (ε): 267 (9000), $\lambda_{min}^{H_2O}$ nm: 235, $\lambda_{max}^{0.1NHCl}$ nm: 267, $\lambda_{min}^{0.1NHCl}$ nm: 235, $\lambda_{max}^{0.1NNaOH}$ nm: 267, $\lambda_{min}^{0.1NNaOH}$ nm: 243. Ninhydrin positive (violet).

Analytical Results and Constants of Synthetic Nucleotide Analogs——All chemically synthesized nucleotide analogs (**6**—**11**, **17**, and **18**) were purified by paper electrophoresis and paper chromatography. Phosphorus analysis data and *Rf* values of products on paper electrophoresis (in 50 mM citrate buffer, pH 3.3) and on paper chromatography (in ethanol–0.5 M sodium acetate 1 : 1, v/v) are summarized in Table II.

DNA Polymerases α and β——DNA polymerases α_1 (without primase activity) and β were purified from cherry salmon (*Oncorhynchus masou*) testes as described previously.[8]

All operations were carried out at 0—4 °C. Cherry salmon testes were homogenized in 50 mM Tris–HCl buffer (pH 7.5, containing 10 mM β-mercaptoethanol, 1 mM ethylenediaminetetraacetic acid (EDTA), 20% glycerol, 0.5 mM phenylmethylsulfonyl fluoride, and 0.5 mM benzamidine) with a Teflon pestle homogenizer (600 rev/min, 4 strokes). The homogenate was stirred for 40 min, and then centrifuged at 13000 × *g* for 40 min. DNA polymerase α_1 was extracted in the supernatant fraction. After the first phosphocellulose column chromatography, this enzyme was precipitated by the addition of 60% saturated ammonium sulfate and collected by centrifugation.

The extraction of DNA polymerase β was performed by rehomogenization of the pellet obtained from the first step in 50 mM Tris–HCl buffer containing 0.5 M KCl using a Waring blender (1 min × 4). The homogenate was stirred for 40 min, and centrifuged at 13000 × *g* for 40 min; the supernatant was collected. After the first phosphocellulose column chromatography, the enzyme was precipitated by the addition of 50—80% saturated ammonium sulfate and collected by centrifugation.

Each of the polymerases was further purified by means of sequential column chromatographies on DEAE-cellulose, phosphocellulose (second), hydroxyapatite, blue-agarose, and single-stranded DNA-cellulose. The final sample showed a specific activity of 100000 units/mg for DNA polymerase α_1 with activated DNA as a template-primer, and 170000 units/mg for DNA polymerase β with poly(rA)–oligo$(dT)_{12-18}$ as a template-primer.

Assay Condition for DNA Polymerases α_1 and β——The standard assay mixture (25 μl) for DNA polymerase α_1 was contained 100 μg/ml activated salmon sperm DNA, 50 mM Tris–HCl (pH 8.0), 4 mM $MgCl_2$, 15% glycerol, 1 mM dithiothreitol, 400 μg/ml bovine serum albumin, 100 μM dATP, 100 μM dGTP, 100 μM dCTP, 25 μM [^{3}H]dTTP (5 cpm/pmol), 0—100 μM synthetic nucleotide analog, and 0.5 unit of enzyme. In the DNA polymerase β assay system, the same mixture except for 50 mM glycine–KOH (pH 9.5) instead of Tris–HCl, and addition of 80 mM KCl, was used. The enzyme reaction was carried out for 30 min at 37 °C.

When kinetic analysis was performed, the concentrations of [^{3}H]dTTP and inhibitors were varied.

References and Notes

1) Part XXVI: S. Suzuki, S. Izuta, C. Nakayama and M. Saneyoshi, *J. Biochem.* (Tokyo), **102**, 853 (1987).

2) M. Fry, "Enzymes of Nucleic Acid Synthesis and Modification," Vol. 1, ed. by S. T. Jacob, CRC Press, Boca Raton, FL, 1982.
3) S. Ikegami, T. Taguchi, M. Ohashi, H. Nagano and Y. Mano, *Nature* (London), **275**, 458 (1978).
4) R. A. Dicioccio, K. Chadha and B. I. S. Srivastava, *Biochim. Biophys. Acta*, **609**, 224 (1980).
5) M. A. Waquar, H. T. Evans and J. A. Huberman, *Nucleic Acids Res.*, **5**, 1933 (1978).
6) A. Matsukage, K. Ono, A. Ohashi, T. Takahashi, C. Nakayama and M. Saneyoshi, *Cancer Res.*, **38**, 3079 (1978).
7) K. Ono, A. Ohashi, A. Yamamoto, A. Matsukage, T. Takahashi, M. Saneyoshi and T. Ueda, *Cancer Res.*, **39**, 4673 (1979).
8) T. Yamaguchi and M. Saneyoshi, *Nucleic Acids Res. Symposium Series*, **11**, 153 (1982).
9) K. Ono, A. Ohashi, M. Ogasawara, A. Matsukage, T. Takahashi, C. Nakayama and M. Saneyoshi, *Biochemistry*, **20**, 5088 (1981).
10) N. N. Khan, G. E. Wright, L. W. Dudycz and N. C. Brown, *Nucleic Acids Res.*, **12**, 3695 (1984).
11) E. DeClercq, J. Balzarini, C. F. Bigge, T. C. Kalaritis and M. P. Mertes, *Biochem. Pharmacol.*, **30**, 495 (1981).
12) D. E. Bergstrom, *Nucleosides & Nucleotides*, **1**, 1 (1982).
13) C. F. Bigge, P. Kalaritis, J. R. Deck and M. P. Mertes, *J. Am. Chem. Soc.*, **102**, 2033 (1980).
14) A. Hampton and A. W. Nichol, *Biochemistry*, **5**, 2076 (1966).
15) D. E. Bergstrom and J. L. Ruth, *J. Carbohydr. Nucleosides and Nucleotides*, **4**, 257 (1977).
16) K. Yoshikawa, T. Kato and T. Takenishi, *Bull. Chem. Soc. Jpn.*, **42**, 3505 (1969).
17) M. Maeda, A. D. Petal and A. Hampton, *Nucleic Acids Res.*, **4**, 2843 (1977).
18) T. Yamaguchi and M. Saneyoshi, *Chem. Pharm. Bull.*, **32**, 1441 (1984).
19) J. L. Ruth and D. E. Bergstrom, *J. Org. Chem.*, **43**, 2870 (1978).
20) A. Kampf, C. J. Pillar, W. J. Woodford and M. P. Mertes, *J. Med. Chem.*, **19**, 909 (1976).
21) T. Adachi, Y. Yamada, I. Inoue and M. Saneyoshi, *Synthesis*, **45** (1977).
22) S. Izuta and M. Saneyoshi, *Nucleic Acids Res. Symposium Series*, **15**, 73 (1984).
23) L. Párkányi, A. Kálman, T. Kovács, A. Szabolcs and L. Otvös, *Nucleic Acids Res.*, **11**, 7999 (1983).

[Chem. Pharm. Bull. 35(12)4839—4845(1987)]

Indonesian Medicinal Plants. I. New Furanoditerpenes from *Arcangelisia flava* MERR. (2). Stereostructure of Furanoditerpenes Determined by Nuclear Magnetic Resonance Analysis

YOSHIYUKI KAWAKAMI,* YASUSHI NAGAI, YUKUO NEZU, TADASHI SATO, TOSHINOBU KUNII, and KENGO KAGEI

Tsukuba Research Laboratories, Eisai Co., Ltd., 1-3, Tokodai 5-chome, Toyosato-machi, Tsukuba-gun, Ibaraki 300-26, Japan

(Received February 4, 1987)

The stereostructures of four furanoditerpenes which were isolated from *Arcangelisia flava* MERR., 6-hydroxyarcangelisin, 2-dehydroarcangelisinol, tinophyllol, and 6-hydroxyfibleucin, were elucidated by a differential nuclear Overhauser effect (NOE) method and two-dimensional nuclear magnetic resonance (2D NMR). The stereostructures of two franoditerpenes, fibraurin and 6-hydroxyfibraurin, which had not been completely determined, were also elucidated.

Keywords——*Arcangelisia flava*; Menispermaceae; furanoditerpene; stereochemistry; NOE difference NMR spectroscopy; two-dimensional NMR

The stem of *Arcangelisia flava* MERR. (Menispermaceae) is an important component of folk medicine in Indonesia (Indonesian name: Jamu). In the previous paper,[1] we reported the isolation of four new [6-hydroxyarcangelisin (**1**), 2-dehydroarcangelisinol (**2**), tinophyllol (**3**), and 6-hydroxyfibleucin (**4**)] and three known furanoditerpenes [fibraurin (**5**),[2] 6-hydroxyfibraurin (**6**),[2] and fibleucin[3]] from *A. flava* and the elucidation of their plane structures.

Numerous furanoditerpenes, including fibraurin,[2] 6-hydroxyfibraurin,[2] fibleucin,[3] chasmanthin,[4-6] palmarin,[5,7,8] columbin,[5,7-10] jateorin,[5] isojateorin,[5,7] and tinophyllon,[11,12] have been isolated from Menispermaceae plants. The plane structural relationships of these compounds have been reported.[2,5] However, the stereochemical features of fibraurin and its hydrogenated derivative, palmarin, were not established. Hori *et al.*[2] determined the α-epoxide configuration of fibraurin by an optical rotatory dispersion (ORD) technique. On the other hand, Islam *et al.*[13,14] reported that the 2,3-epoxide of palmarin has the β-configuration based on X-ray analysis.

This paper deals with stereostructural studies on six furanoditerpenes, **1**, **2**, **3**, **4**, **5**, and **6** (Chart 1), by nuclear Overhauser effect (NOE) difference nuclear magnetic resonance (NMR) spectroscopy and two-dimensional NMR (2D NMR) spectroscopy.

6-Hydroxyarcangelisin (1)

Detailed 400 MHz ^{1}H-NMR decoupling experiments disclosed that **1** has the same structure of rings A and C as **5**[2]: two epoxide protons at δ 3.88 and δ 3.67 were coupled (J= 4.4 Hz) to each other, and the signal at δ 3.88 (H-2) was coupled to a signal at δ 5.00 (H-1) (J= 2.5 Hz). The signal at δ 5.46 (J= 12.1 Hz) due to H-12 was coupled to C_{11} methylene proton signals at δ 2.31 and δ 1.88, and the coupling constant of H-12 (J= 12.1 Hz) indicated the axial orientation. These ^{1}H-NMR data showed that the furan ring exists in equatorial orientation at C_{12} as in **5** and **6**.[2] The 2D NMR spectrum was measured in order to confirm the configuration. Figure 1 shows a spectrum of **1** obtained by 2D correlated spectroscopy (COSY).

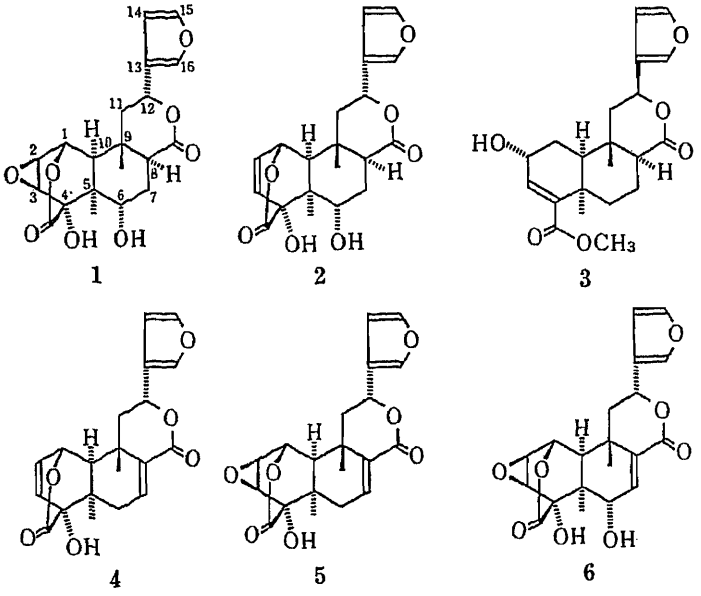

Chart 1

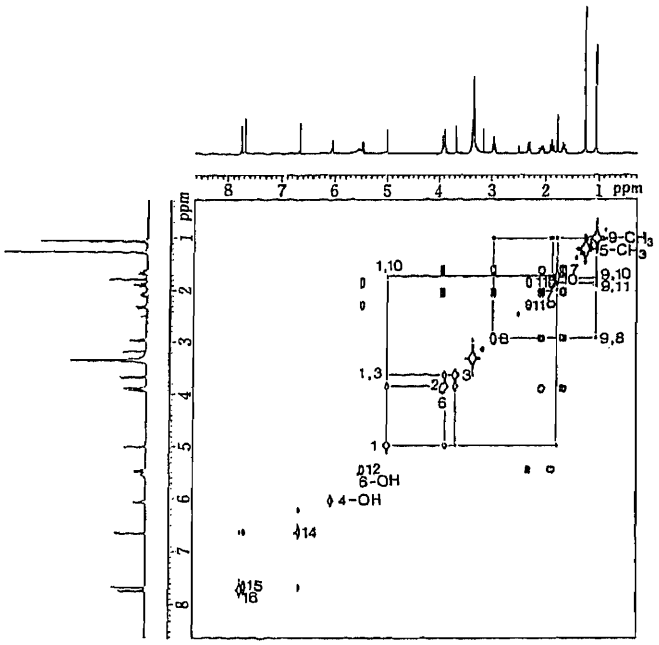

Fig. 1. COSY Spectrum of **1** (in DMSO-d_6)

A very small coupling constant ($J=0.3$ Hz) due to an almost 90° angle was observed between the H-1 and H-10 protons. Also, long-range couplings between 9-CH_3 and H-8, 9-CH_3 and H-10, and 9-CH_3 and H-11α were observed, whereas no long-range coupling was observed for the 5-CH_3 protons. These W-configuration couplings between 9-CH_3, H-8, H-10, and H-11α indicated that 9-CH_3, H-8, H-10 and H-11α were axially oriented. In order to confirm the spatial relationships of other protons in **1**, the 2D NOE correlated NMR spectrum (NOESY) was measured (Fig. 2).

No cross-peaks between the 5-CH_3 and the 9-CH_3 were observed in the NOESY spectrum. This result indicated that 5-CH_3 and 9-CH_3 were on opposite sides of the plane defined by ring B. Thus, it can be presumed that 5-CH_3 and 9-CH_3 have α-configuration (axial) and β-configuration (axial), respectively, assuming that the lactone on the ring A

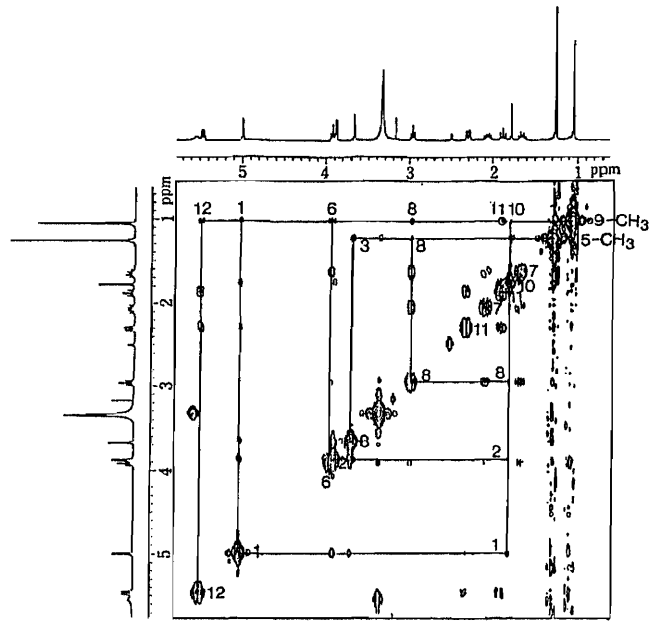

Fig. 2. NOESY Spectrum of **1** (in DMSO-d_6)

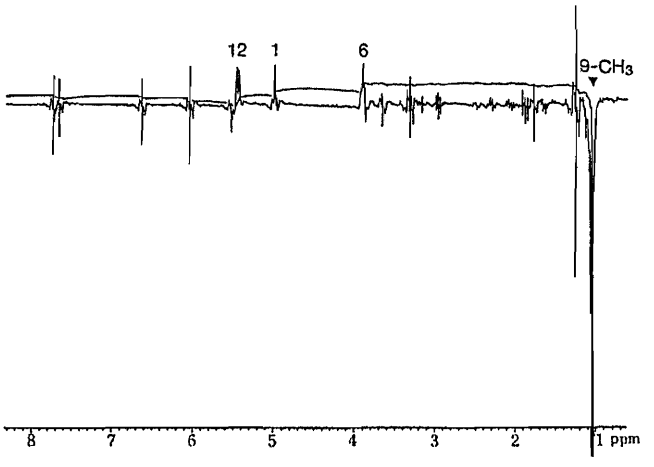

Fig. 3. NOE Measurement of **1** Irradiated at δ 1.03 (9-CH_3)

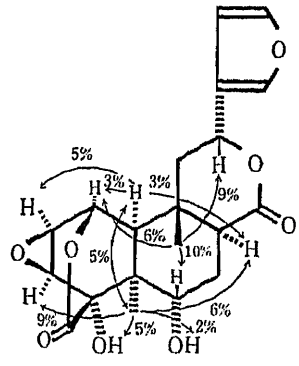

Fig. 4. NOE Results for **1**
Values are percent increase of signal area.

retains β-configuration.[5] Reliable NOE cross-peaks were observed between 5-CH_3 and H-8, 5-CH_3 and H-10, and 5-CH_3 and H-3. Further NOE cross-peaks were observed between 9-CH_3 and H-6, and 9-CH_3 and H-12. These results indicated that the hydroxyl group at C-6 has α-configuration, the furan ring at C-12 has α-configuration, and the 2,3-epoxide has β-configuration. Moreover, cross-peaks were observed between 9-CH_3 and H-8, 9-CH_3 and H-10, and 9-CH_3 and H-11α, reflecting W-configurations of the protons.

Next, we carried out NOE difference spectroscopy experiments. The results are presented in Figs. 3 and 4.

Figure 3 shows an NOE difference spectrum of **1** with irradiation of the 9-CH_3 protons (δ 1.03). Clear NOE enhancements were observed at H-1, H-6, and H-12, but not at H-8, H-10, and H-11α. Thus the cross-peaks on 9-CH_3 between H-1, H-6, and H-12 were real NOE cross-peaks in the NOESY spectrum (Fig. 2). A large NOE (10%) was observed at the H-6 proton when the 9-CH_3 protons (δ 1.03) were irradiated and a 6% NOE was observed at H-8 when the 5-CH_3 protons (δ 1.26) were irradiated. The infrared (IR) spectrum implies the presence of intramolecular hydrogen-bonding between 4-OH and 6-OH (3300 cm^{-1}). Furthermore, the coupling constant between H-6 and H-7 (J=8.8 Hz), and also that between

H-7 and H-8 (J=9.9 Hz) indicated a conformational distortion of ring B. On the basis of these results, it seemed reasonable to assume that ring B exists in a twist boat conformation. Ring C exists in a chair conformation based on the large NOE (9%) between 9-CH_3 and H-12 and the spin coupling (W-configuration long-range coupling) between 9-CH_3 and H-11α.

From the above results, the stereostructure of 6-hydroxyarcangelisin is represented by formula **1** (Chart 1).

2-Dehydroarcangelisinol (2)

The ^{1}H-NMR spectra of **2** and **1** showed almost identical in chemical shifts and coupling values of the H-6, H-7α, H-7β, H-8, H-11α, H-11β, H-12, and 9-CH_3 protons. The only difference was the presence of an olefin group (δ 6.53, dd, J=8.0, 5.0 Hz, H-2; 6.14, dd, J=8.0, 1.8 Hz, H-3) in the former. From all the above data, it is clear that **2** has the partial structure with the 6α-equatorial hydroxyl group and the 12α-equatorial furan ring as shown in Chart 1. This conclusion was firmly supported by NOE experiments. Irradiation of the 9-CH_3 protons (δ 1.03) afforded a 10% NOE enhancement of the H-6 signal and a 9% NOE enhancement of the H-12 signal (Fig. 5). Furthermore, irradiation of the 5-CH_3 protons (δ 1.06) caused an NOE enhancement in the H-8 (8%) signal, which is in agreement with all the above conclusions.

The stereostructure of 2-dehydroarcangelisinol (**2**) is thus as depicted in Chart 1.

Tinophyllol (3)

A large NOE (14%) was observed at the H-2 proton when the 9-CH_3 protons (δ 0.84) were irradiated (Fig. 6). This result indicated that the hydroxyl group at C-2 has the α-configuration. The furan ring at C-12 was determined to take the β-equatorial configuration because an NOE enhancement (17%) was observed at the H-12 proton when the H-8 proton was irradiated, whereas no NOE enhancement was observed between the 9-CH_3 and H-12 protons. The substitution pattern of the furan ring was supported by the fact that ring C of tinophyllon[11,12] retains a boat conformation with the furan ring at C-12 in the β-equatorial configuration. Furthermore, the coupling constant between H-1 and H-2 (J=8.0 Hz) indicated that ring A exists in a diplanar conformation (10β sofa form). Finally, the conformation of ring B was determined to be chair because of the NOE between 9-CH_3 and H-7β and the NOE between H-6α and H-8 (1,3-diaxial interaction).

The stereostructure of tinophyllol (**3**) was thus determined to be as depicted in Chart 1.

6-Hydroxyfibleucin (4)

A large NOE enhancement (20%) between the 9-CH_3 and H-6 protons indicated that the hydroxyl group at C-6 has α-configuration and ring B existed in a boat conformation. Also,

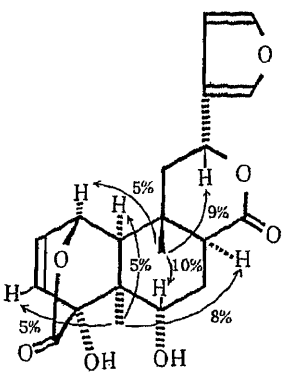

Fig. 5. NOE Results for **2**
Values are percent increase of signal area.

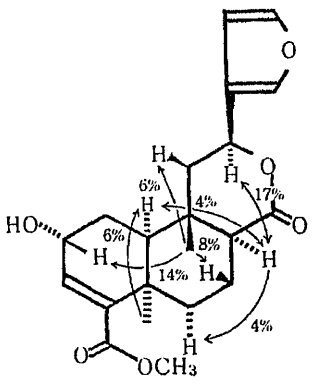

Fig. 6. NOE Results for **3**
Values are percent increase of signal area.

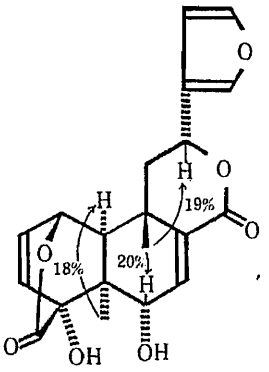

Fig. 7. NOE Results for **4**
Values are percent increase of signal area.

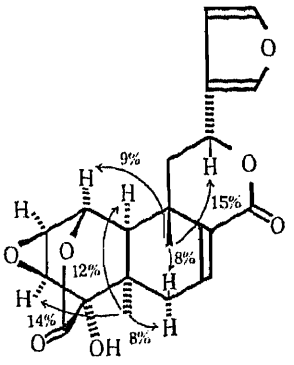

Fig. 8. NOE Results for **5**
Values are percent increase of signal area.

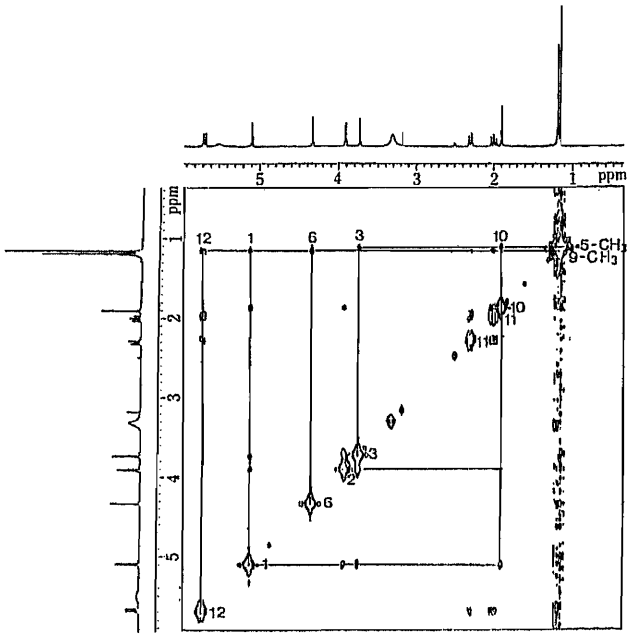

Fig. 9. NOESY Spectrum of **6** (in DMSO-d_6)

the furan ring at C-12 was determined to take α-configuration because a large NOE (19%) was observed between the 9-CH_3 and H-12 protons (Fig. 7). The stereostructure of 6-hydroxyfibleucin (**4**) was determined to be as depicted in Chart 1.

Fibraurin (5)

It was reported by Hori *et al.*[2] that the 2,3-epoxy group of fibraurin takes the α-configuration on the basis of ORD experiments. However, Islam *et al.*[13,14] proposed the β-configuration for a palmarin derivative based on X-ray analysis. The 2,3-epoxy groups of fibraurin and palmarin must have the same configuration. In our experiments (Fig. 8), 14% NOE was observed at H-3 when the 5-CH_3 protons were irradiated. Thus, it was concluded that the 2,3-epoxy group takes the β-configuration as in the structure of **1**, in agreement with the X-ray analysis of palmarin.

Consequently, the stereostructure of fibraurin should be revised at the 2,3-epoxide group as presented in Chart 1.

6-Hydroxyfibraurin (6)

The structure of 6-hydroxyfibraurin had been determined by Hori *et al.*[2] except for the configuration of the hydroxyl group at C-6. The NOESY experiment showed reliable NOE

cross-peaks between the 9-CH_3 and the H-6 protons (Fig. 9). The configuration of the hydroxyl group at C-6 was thus confirmed to be α-equatorial. Consequently, the stereostructure of 6-hydroxyfibraurin (**6**) should be revised as in the case of **5** (Chart 1).

Further work on the structural elucidation of other new furanoditerpenes from *A. flava* is in progress, and will be reported elsewhere.

Experimental

^{1}H-NMR spectra were obtained in dimethyl sulfoxide-d_6 at 35 °C on a JEOL GX400 spectrometer operating at 400 MHz. The 2D correlated spectra (COSYP) were measured by the use of a 2D correlation sequence with a 90° mixing pulse, and P-type peak selection. Data processing was carried out with the standard JEOL software. An f_2 spectral width of 3333.3 Hz over 1024 data points gave a digital resolution of 6.51 Hz. A total of 512 spectra, each of 16 transients, gave, with appropriate incrementing of the evolution delay, an f_1 width of 3333.3 Hz and a digital resolution of 6.51 Hz (with zero filling). The 2D NOE spectra were obtained with the usual pulse sequence. The spectral widths were 3333.3 Hz in f_2 and f_1, giving a digital resolution of 6.51 Hz with a 1024 × 512 data point matrix. The mixing time was 500 ms.

6-Hydroxyarcangelicin (1)——mp 274 °C (dec.), colorless prisms from MeOH, $[\alpha]_D^{20}$ +55.27 (pyridine, c=0.54). *Anal.* Calcd for $C_{20}H_{22}O_8$: C, 61.53; H, 5.68. Found: C, 61.40; H, 5.71. UV λ_{max}^{EtOH} nm; 213. FD-MS (*m/z*): 390 (M^+), EI-MS (*m/z*): 391 (M^++1). IR ν^{Nujol} cm^{-1}: 3330, 1780, 1705, 1602, 1508, 875, 812. ^{1}H-NMR (400 MHz, DMSO-d_6) δ: 7.75 (1H, d, J=1.6 Hz, H-16), 7.68 (1H, dd, J=1.8, 1.6 Hz, H-15), 6.65 (1H, d, J=1.8 Hz, H-14), 6.06 (1H, s, 4-OH), 5.54 (1H, d, J=3.3 Hz, 6-OH), 5.46 (1H, dd, J=12.1, 4.0 Hz, H-12), 5.00 (1H, d, J=2.5 Hz, H-1), 3.92 (1H, td, J=8.8, 3.3 Hz, H-6), 3.88 (1H, dd, J=4.4, 2.5 Hz, H-2), 3.67 (1H, d, J=4.4 Hz, H-3), 2.97 (1H, t, J=9.9 Hz, H-8), 2.31 (1H, dd, J=13.5, 4.0 Hz, H-11β), 2.07 (1H, m, H-7α), 1.88 (1H, dd, J=13.5, 12.1 Hz, H-11α), 1.78 (1H, s, H-10), 1.65 (1H, m, H-7β), 1.26 (3H, s, 5-CH_3), 1.05 (3H, s, 9-CH_3).

2-Dehydroarcangelisinol (2)——mp 208—212 °C (dec.), colorless prisms from MeOH, $[\alpha]_D^{20}$ +98.8 (pyridine, c=0.25). *Anal.* Calcd for $C_{20}H_{22}O_7$: C, 64.16; H, 5.92. Found: C, 64.18; H, 5.98. UV λ_{max}^{EtOH} nm: 214. FD-MS (*m/z*): 375 (M^++1), EI-MS (*m/z*): 375 (M^++1), 374 (M^+). IR ν^{Nujol} cm^{-1}: 3370, 3285, 1772, 1708, 1510, 875, 808. ^{1}H-NMR (400 MHz, DMSO-d_6) δ: 7.72 (1H, d, J=1.6 Hz, H-16), 7.63 (1H, dd, J=1.8, 1.6 Hz, H-15), 6.63 (1H, d, J=1.8 Hz, H-14), 6.53 (1H, dd, J=8.0, 5.0 Hz, H-2), 6.14 (1H, dd, J=8.0, 1.8 Hz, H-3), 5.84 (1H, s, 4-OH), 5.59 (1H, d, J=4.0 Hz, 6-OH), 5.47 (1H, dd, J=12.0, 4.0 Hz, H-12), 5.26 (1H, dd, J=5.0, 1.8 Hz, H-1), 4.00 (1H, ddd, J=9.0, 8.0, 4.0 Hz, H-6), 2.90 (1H, t, J=9.0 Hz, H-8), 2.34 (1H, dd, J=13.5, 4.0 Hz, H-11β), 2.10 (1H, m, H-7α), 1.88 (1H, dd, J=13.5, 12.0 Hz, H-11α), 1.66 (1H, m, H-7β), 1.59 (1H, s, H-10), 1.06 (3H, s, 5-CH_3), 1.03 (3H, s, 9-CH_3).

Tinophyllol (3)——mp 229—231 °C (dec.), colorless prisms from MeOH, $[\alpha]_D^{20}$ −19.3 (pyridine, c=0.5). *Anal.* Calcd for $C_{21}H_{26}O_6$: C, 67.36; H, 7.00. Found: C, 67.37; H, 7.15. UV λ_{max}^{EtOH} nm: 216. EI-MS (*m/z*): 374 (M^+). IR ν^{Nujol} cm^{-1}: 3470, 3130, 1730, 1718, 1495, 878, 815. ^{1}H-NMR (400 MHz, DMSO-d_6) δ: 7.73 (1H, d, J=1.6 Hz, H-16), 7.68 (1H, dd, J=1.8, 1.6 Hz, H-15), 6.55 (1H, d, J=1.8 Hz, H-14), 6.25 (1H, d, J=4.0 Hz, H-3), 5.49 (1H, dd, J=12.0, 6.0 Hz, H-12), 4.96 (1H, br s, 2-OH), 4.34 (1H, ddd, J=8.0, 8.0, 4.0 Hz, H-2), 3.68 (3H, s, 4-OCH_3), 2.79 (1H, dd, J=10.0, 3.0 Hz, H-8), 2.43 (1H, dd, J=11.0, 3.0 Hz, H-6β), 2.14 (1H, dd, J=14.0, 8.0 Hz, H-1β), 2.06 (1H, dd, J=14.0, 6.0 Hz, H-11α), 1.93 (1H, ddd, J=14.0, 8.0, 6.0 Hz, H-1α), 1.87 (1H, dd, J=14.0, 12.0 Hz, H-11β), 1.80 (1H, d, J=6.0 Hz, H-10), 1.61 (1H, m, H-7α), 1.32 (3H, s, 5-CH_3), 1.18 (2H, m, H-6α and H-7β), 0.84 (3H, s, 9-CH_3).

6-Hydroxyfibleucin (4)——mp 195—204 °C (dec.), colorless plates from MeOH, $[\alpha]_D^{20}$ −59.1 (pyridine, c=0.49). *Anal.* Calcd for $C_{20}H_{20}O_7$: C, 64.51; H, 5.41. Found: C, 64.53; H, 5.36. UV λ_{max}^{EtOH} nm: 211, 231. FD-MS (*m/z*): 373 (M^++1), 372 (M^+), EI-MS (*m/z*): 373 (M^++1). IR ν^{Nujol} cm^{-1}: 3300, 1770, 1703, 1637, 1601, 1508, 873, 812. ^{1}H-NMR (400 MHz, DMSO-d_6) δ: 7.74 (1H, d, J=1.6 Hz, H-16), 7.62 (1H, dd, J=1.8, 1.6 Hz, H-15), 6.89 (1H, d, J=2.0 Hz, H-7), 6.62 (1H, d, J=1.8 Hz, H-14), 6.57 (1H, dd, J=8.0, 5.0 Hz, H-2), 6.21 (1H, dd, J=8.0, 1.8 Hz, H-3), 6.00 (1H, s, 4-OH), 5.68 (1H, dd, J=12.0, 2.5 Hz, H-12), 5.65 (1H, d, J=3.0 Hz, 6-OH), 5.35 (1H, dd, J=5.0, 1.8 Hz, H-1), 4.47 (1H, dd, J=3.0, 2.0 Hz, H-6), 2.32 (1H, dd, J=13.0, 2.5 Hz, H-11β), 2.00 (1H, dd, J=13.0, 12.0 Hz, H-11α), 1.79 (1H, s, H-10), 1.18 (3H, s, 9-CH_3), 0.99 (3H, s, 5-CH_3).

Fibraurin (5)——mp 285 °C (dec.), colorless prisms from dioxane–MeOH, $[\alpha]_D^{20}$ −29.3 (pyridine, c=1.0). *Anal.* Calcd for $C_{20}H_{20}O_7$: C, 64.51; H, 5.41. Found: C, 64.38; H, 5.23. UV λ_{max}^{EtOH} nm: 217, 230. EI-MS (*m/z*): 372 (M^+). IR ν^{Nujol} cm^{-1}: 3450, 3125, 1768, 1692, 1632, 1502, 875, 815. ^{1}H-NMR (400 MHz, DMSO-d_6) δ: 7.76 (1H, d, J=1.6 Hz, H-16), 7.67 (1H, dd, J=1.8, 1.6 Hz, H-15), 7.25 (1H, dd, J=8.0, 2.8 Hz, H-7), 6.64 (1H, d, J=1.8 Hz, H-14), 6.50 (1H, s, 4-OH), 5.67 (1H, dd, J=12.0, 2.5 Hz, H-12), 5.09 (1H, d, J=2.9 Hz, H-1), 3.87 (1H, dd, J=4.2, 2.9 Hz, H-2), 3.67 (1H, d, J=4.2 Hz, H-3), 2.34 (1H, dd, J=17.0, 8.0 Hz, H-6α), 2.32 (1H, dd, J=14.0, 2.5 Hz, H-11β), 1.95 (1H, dd, J=14.0, 12.0 Hz, H-11α), 1.79 (1H, s, H-10), 1.71 (1H, dd, J=17.0, 2.8 Hz, H-6β), 1.17 (3H, s, 9-CH_3), 1.08 (3H, s, 5-CH_3).

6-Hydroxyfibraurin (6)——mp 295—304 °C (dec.), colorless plates from MeOH $[\alpha]_D^{20}$ +26.3 (pyridine, c=0.5). *Anal.* Calcd for $C_{20}H_{20}O_8$: C, 61.85; H, 5.19. Found: C, 61.87; H, 5.24. UV λ_{max}^{EtOH} nm: 212, 230. FD-MS (*m/z*): 388

(M^+), EI-MS (*m/z*): 389 ($M^+ + 1$). IR ν^{Nujol} cm^{-1}: 3300, 1782, 1698, 1639, 1507, 873, 810. ^{1}H-NMR (400 MHz, DMSO-d_6) δ: 7.76 (1H, d, J=1.6 Hz, H-16), 7.69 (1H, dd, J=1.8, 1.6 Hz, H-15), 6.86 (1H, d, J=2.8 Hz, H-7), 6.64 (1H, d, J=1.8 Hz, H-14), 6.34 (1H, s, 4-OH), 5.68 (1H, dd, J=12.0, 2.0 Hz, H-12), 5.51 (1H, br s, 6-OH), 5.10 (1H, d, J=2.9 Hz, H-1), 4.33 (1H, d, J=2.8 Hz, H-6), 3.91 (1H, dd, J=4.2, 2.9 Hz, H-2), 3.74 (1H, d, J=4.2 Hz, H-3), 2.29 (1H, dd, J=14.0, 2.0 Hz, H-11β), 2.04 (1H, dd, J=14.0, 12.0 Hz, H-11α), 1.90 (1H, s, H-10), 1.18 (3H, s, 9-CH_3), 1.16 (3H, s, 5-CH_3).

Acknowledgement The authors thank Drs. Y. Miyake and M. Kuwada of Eisai Co., Ltd. for their valuable suggestion and discussion.

References

1) T. Kunii, K. Kagei, Y. Kawakami, Y. Nagai, Y. Nezu, and T. Sato, *Chem. Pharm. Bull.*, **33**, 479 (1985).
2) T. Hori, A. King, K. Nakanishi, S. Sasaki, and M. Woods, *Tetrahedron*, **23**, 2649 (1967).
3) K. Ito and H. Furukawa, *J. Chem. Soc., Chem. Commun.*, **1969**, 654.
4) G. Ferguson and K. M. S. Islam, *J. Chem. Soc., B*, **1969**, 620.
5) K. H. Overton, N. G. Weir, and A. Wylie, *J. Chem. Soc., C*, **1966**, 1482.
6) D. H. R. Barton and D. Elad, *J. Chem. Soc., C*, **1956**, 2085.
7) D. H. R. Barton, K. H. Overton, and A. Wylie, *J. Chem. Soc., C*, **1962**, 4809.
8) D. H. R. Barton and L. M. Jackson, *J. Chem. Soc., C*, **1962**, 4816.
9) M. P. Cave and E. J. Soboczenski, *J. Am. Chem. Soc.*, **78**, 5317 (1956).
10) K. H. Overton, N. G. Weir, and A. Wylie, *Proc. Chem. Soc., London*, **1961**, 211.
11) G. Aguilar-Santos, *Chem. Ind.* (London), **1965**, 1074.
12) L. Brehm, O. J. R. Hodder, and T. G. Halsall, *J. Chem. Soc.*, **1971**, 2529.
13) K. M. S. Islam, G. Ferguson, K. H. Overton, and D. W. Melville, *Chem. Commun.*, **1967**, 167.
14) G. Ferguson and K. M. S. Islam, *J. Chem. Soc., B*, **1969**, 162.
15) A. Bax, "Two-Dimensional Nuclear Magnetic Resonance in Liquids," ed. by D. Reidel, Dordrecht, 1982.

[Chem. Pharm. Bull. 35(12)4846—4850(1987)]

Studies on the Constituents of *Pueraria lobata*. III.[1] Isoflavonoids and Related Compounds in the Roots and the Voluble Stems

JUN-EI KINJO,[a] JUN-ICHI FURUSAWA,[a] JUNKO BABA,[a] TAKASHI TAKESHITA,[a] MASAKI YAMASAKI,[b] and TOSHIHIRO NOHARA*,[a]

Faculty of Pharmaceutical Sciences,[a] Kumamoto University, 5–1 Oe-honmachi, Kumamoto 862, Japan and Department of Biochemistry, Medical School,[b] Kumamoto University, Honjo, Kumamoto 860, Japan

(Received May 18, 1987)

Two new isoflavone glycosides, the 8-*C*-apiosyl(1→6) glucosides of daidzein and genistein, were isolated from the roots and the voluble stems of *Pueraria lobata* (WILLD.) OHWI. Thirteen known isoflavonoids and related compounds were also found.

Keywords——*Pueraria lobata*; Leguminosae; isoflavonoid; isoflavone apiosyl-glucoside; ^{13}C-NMR spectrum

Puerariae Radix, the root of *Pueraria lobata* (WILLD.) OHWI (Leguminosae), is a very important Chinese traditional medicine. It has been used as an antipyretic and spasmolytic agent. Studies on the chemical constituents of this plant have been carried out by many investigators, and various isoflavonoids have been found.[2] Recently, we reported the occurrence of triterpenoidal saponins from this plant and elucidated the structures of seven sapogenols from the hydrolysate of the crude saponin fraction.[3] Furthermore, we isolated two novel aromatic glycosides, puerosides A and B.[4] In the course of these studies, we have also isolated many isoflavonoids and related compounds including new glycosides from both the aerial and underground parts of *P. lobata*. This paper deals with the structural elucidation of these compounds by spectroscopic means.

The methanolic extract of the fresh roots of the title plant was partitioned between *n*-BuOH and water. A combination of silica gel, Sephadex LH-20 and MCI gel CHP 20P column chromatographies of the organic phase with various solvent systems, resulted in the isolation of compounds **1**—**11**. Similarly, the methanolic extract of the fresh voluble stems of this plant gave twelve compounds **1**, **3**—**6**, **8**—**10**, **12**—**15**. They were identified as daidzein (**3**),[2a] formononetin (**4**),[5] genistein (**5**),[6] daidzin (**6**),[2a] daidzein 4′,7-diglucoside (**7**),[2d] puerarin (**8**),[2c] PG-1 (**9**), PG-3 (**10**),[2d] puerarin xyloside (**11**),[2c] genistin (**12**),[7] genistein 8-*C*-glucoside (**13**),[8] coumestrol (**14**)[9] and isoliquiritigenin (**15**),[10] by comparison of their carbon-13 nuclear magnetic resonance (^{13}C-NMR) spectral data (Table I) and other physical and spectral data (see Experimental). Among these compounds, this is the first report of the isolation of **12**—**15** from this plant.

Compound **1**, colorless needles, mp 188—190 °C was positive to the ferric chloride reagent. The proton nuclear magnetic resonance (^{1}H-NMR) spectrum of **1** showed a characteristic signal at δ 8.27 ascribable to H-2 of the isoflavone. Moreover, signals due to an aromatic A_2X_2 system (2H, d, J=8 Hz, δ 7.39; 2H, d, J=8 Hz, δ 7.98), an AX coupling pattern (1H, d, J=8 Hz, δ 7.01; 1H, d, J=8 Hz, δ 7.98) and a glycosidic moiety were observed. Methanolysis of **1** in 1 N HCl–MeOH gave puerarin (**8**) and methyl apioside. Based on these observations, **1** was presumed to be 8-*C*-apiosyl-glucosyl-daidzein. The ^{13}C-NMR spectrum

TABLE I. ^{13}C-NMR Spectral Data for Compounds **1**—**13** (67 MHz, in DMSO-d_6, δ Values)

	1	**2**	**3**	**4**	**5**	**6**	**7**	**8**	**9**	**10**	**11**	**12**	**13**
Aglycone													
C-2	152.7	153.7	152.6	153.0	153.8	153.3	153.6	152.7	152.7	153.0	152.4	154.3	153.6
C-3	123.1[a)]	122.0[a)]	123.5[a)]	124.2[a)]	122.2[a)]	123.7[a)]	123.3[a)]	123.1[a)]	123.2[a)]	123.1[a)]	122.9[a)]	122.6[a)]	122.0[a)]
C-4	175.3	180.5	174.6	174.6	180.1	175.0	174.6	175.3	175.2	175.4	174.8	180.4	180.4
C-5	126.4	161.0	127.2	127.2	162.0	127.0	126.9	126.4	126.4	126.5	126.0	161.1	160.7
C-6	115.0	98.8	115.0	115.1	98.9	115.6	115.6	115.0	115.0	115.2	115.1	99.6	98.7
C-7	160.8	163.0	162.4	162.6	164.3	161.3	161.4	160.9	160.8	160.9	160.9	162.7	162.9
C-8	112.1	103.9	102.0	102.1	93.6	103.3	103.4	112.3	112.2	112.2	112.3	94.7	103.9
C-8a	156.0	156.2	157.4	157.4	157.5	156.9	157.1	156.1	156.0	156.0	155.9	157.0	156.2
C-4a	116.7	104.5	116.6	116.6	104.4	118.4	118.4	116.7	116.7	116.8	116.6	106.1	104.5
C-1′	122.5[a)]	121.1[a)]	122.5[a)]	123.2[a)]	121.1[a)]	122.3[a)]	125.2[a)]	122.5[a)]	122.9[a)]	123.0[a)]	122.4[a)]	121.2[a)]	121.2[a)]
C-2′	130.0	130.0	130.0	130.0	130.0	130.0	129.9	130.0	115.3	112.9	129.8	130.2	130.1
C-3′	115.0	115.0	114.9	113.5	115.0	114.9	115.9	115.0	144.5	147.1	114.8	115.2	115.1
C-4′	156.8	157.3	157.1	158.9	157.4	157.0	156.9	156.8	144.9	146.1	157.0	157.2	157.0
C-5′									116.3	115.2			
C-6′									120.0	121.4			
Glucose													
C-1	73.3	73.1				99.9	100.0, 100.3	73.3	73.3	73.4	73.2	99.7	73.1
C-2	70.6	70.5				72.9	73.0, 73.2	70.7	70.7	70.8	70.5	72.8	70.5
C-3	78.2	78.5				76.0	76.4, 76.5	78.4	78.3	78.3	78.4	75.8	78.4
C-4	70.1	70.5				69.4	69.6, 69.7	70.1	70.1	70.1	70.2	69.4	70.2
C-5	79.8	79.8				76.9	76.9, 77.1	81.3	81.3	81.3	80.0	76.7	81.3
C-6	68.1	68.2				60.5	60.7, 60.7	61.1	61.1	61.1	69.1	60.5	61.2
Apiose										Xylose			
C-1	108.8	108.9								55.6 C-1	103.7		
C-2	75.6	75.6								(OMe) 2	72.9		
C-3	78.6	78.7								3	76.4		
C-4	73.1	73.1								4	69.4		
C-5	62.8	63.0								5	65.4		

a) The values may be interchangeable in each column.

(Table I) of **1** also supported the presence of the terminal apiosyl moiety, based on a comparison with the ^{13}C-NMR spectral data for that of apiin.[11] Furthermore, glycosylation shifts at C-5 and C-6 of the *C*-glucosyl residue were observed. Therefore, **1** could be represented as daidzein 8-*C*-apiosyl(1→6)glucoside.

Compound **2**, was isolated as a white amorphous powder. Ordinary methanolysis of **2** furnished genistein 8-*C*-glucoside (**13**) and methyl apioside. Comparison of the ^{13}C-NMR spectral data of **2** and **1** showed that the signals of the sugar moiety were in agreement with each other. Based on these data, **2** could be identified as genistein 8-*C*-apiosyl(1→6)glucoside.

Compounds **1** and **2** seem to be the first examples of naturally occurring isoflavonoids having the apiosyl residue as a sugar moiety.

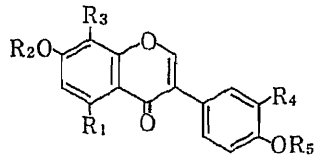

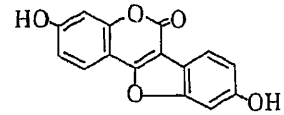

14

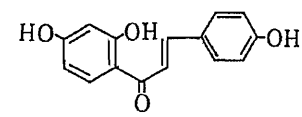

15

	R_1	R_2	R_3	R_4	R_5
1	H	H	-glc-(6)-api	H	H
2	OH	H	-glc-(6)-api	H	H
3	H	H	H	H	H
4	H	H	H	H	Me
5	OH	H	H	H	H
6	H	glc	H	H	H
7	H	glc	H	H	glc
8	H	H	glc	H	H
9	H	H	glc	OH	H
10	H	H	glc	OMe	H
11	H	H	-glc-(6)-xyl	H	H
12	OH	glc	H	H	H
13	OH	H	glc	H	H

Experimental

Melting points were determined on a Yanagimoto micromelting point apparatus and are uncorrected. The ^{1}H- and ^{13}C-NMR spectra were measured at 60 and 67.5 MHz, respectively, using tetramethylsilane (TMS) as an internal standard, and chemical shifts are given in the δ scale. Column chromatography was carried out with Sephadex LH-20, MCI gel CHP 20P and Kieselgel 60, thin layer chromatography (TLC) was conducted on precoated Kieselgel 60 F_{254} plates and spots were visualized by ultraviolet (UV) illumination (254 nm) and by spraying $FeCl_3$ or 10% sulfuric acid reagent.

Extraction and Isolation——The fresh roots of *Pueraria lobata* (3 kg), collected in Kumamoto, were extracted with MeOH under reflux. The extract was concentrated and partitioned between *n*-BuOH and water. Evaporation of the organic layer gave a residue (63 g), which was chromatographed on Sephadex LH-20 with MeOH to yield a triterpenoid saponin fraction and a flavonoid fraction (47 g). The flavonoid fraction was subjected to a combination of silica gel ($CHCl_3$–MeOH = 9 : 1→7 : 3), Sephadex LH-20 (H_2O–MeOH = 1 : 0→0 : 1) and MCI gel CHP 20P (H_2O–MeOH = 1 : 0→1 : 1) chromatographies to afford **1** (0.01%), **2** (0.001%), **3** (0.01%), **4** (0.0003%), **5** (0.001%), **6** (0.1%), **7** (0.02%), **8** (0.1%), **9** (0.03%), **10** (0.003%) and **11** (0.002%). The fresh voluble stems of *P. lobata* (4.1 kg) were extracted with MeOH. Removal of MeOH from the extract under reduced pressure gave the crude extract (500 g), which was partitioned between EtOAc and water, and then the water phase was partitioned into *n*-BuOH. The EtOAc phase was evaporated, and the residue was chromatographed on silica gel ($CHCl_3$–MeOH = 1 : 0→4 : 1), and Sephadex LH-20 (H_2O–MeOH = 1 : 1) columns to furnish **3** (0.002%), **4** (0.0002%), **5** (0.0009%), **14** (0.002%), **15** (0.0007%). In a similar manner, **1** (0.003%), **6** (0.003%), **8** (0.009%), **9** (0.002%), **10** (0.002%), **12** (0.002%) and **13** (0.002%) were obtained from the *n*-BuOH phase.

Daidzein 8-*C*-Apiosyl(1→6)glucoside (1)——Colorless needles, mp 188—190 °C, $[\alpha]_D^{32}$ −24.1° (c = 0.5, dimethylsulfoxide (DMSO)). UV λ_{max}^{MeOH} nm (log ε): 308 (3.90), 270 (4.10), 247 (4.18) (sh), 241 (4.23). ^{1}H-NMR (DMSO-d_6 + D_2O) δ: 6.83 (2H, d, J = 8 Hz, H-3′), 7.01 (1H, d, J = 8 Hz, H-6), 7.39 (2H, d, J = 8 Hz, H-2′), 7.98 (1H, d, J = 8 Hz, H-5), 8.27 (1H, s, H-2). ^{13}C-NMR: Table I.

Methanolysis of 1——A solution of **1** (50 mg) in 1 N HCl–MeOH (10 ml) was heated under reflux for 2 h. The product was neutralized with 1 N NaOH–MeOH and the inorganic precipitate was removed by filtration. The filtrate was subjected to silica gel column chromatography ($CHCl_3$–MeOH–H_2O = 7 : 3 : 0.5) to give puerarin (**8**, 30 mg), which was shown to be identical with an authentic sample by ^{13}C-NMR comparison (152.4, 123.0, 174.9, 126.1, 114.9, 161.0, 112.5, 156.0, 116.7, 122.4, 129.9, 114.9, 157.1, 73.3, 70.7, 78.6, 70.3, 81.6, 61.3, C-2-8,8a,4a,1′-4′,glc-1-6). Methyl apioside was identified as the suger moiety by TLC analysis (*Rf*, 0.35; solv., $CHCl_3$–MeOH = 9 : 1) in comparison with an authentic sample obtained from apiin.

Genistein 8-*C*-Apiosyl(1→6)glucoside (2)——A white amorphous powder, $[\alpha]_D^{31}$ −27.4° (*c* = 0.5, DMSO). UV λ_{max}^{MeOH} nm (log ε): 270 (4.15), 264 (4.10) (sh). ^{1}H-NMR (DMSO-d_6 + D_2O) δ: 6.30 (1H, s, H-6), 6.83 (2H, d, *J* = 8 Hz, H-3′), 7.40 (2H, d, *J* = 8 Hz, H-2′), 8.33 (1H, s, H-2). ^{13}C-NMR: Table I.

Methanolysis of 2——A solution of **2** (50 mg) in 1 N HCl–MeOH (10 ml) was heated under reflux for 2 h. The reaction mixture was worked up as described in the case of **1**. The filtrate was shown to contain genistein 8-*C*-glucoside (**13**) and methyl apioside from the ^{13}C-NMR spectrum (153.8, 121.7, 180.0, 160.5, 98.7, 162.7, 104.1, 156.1, 104.5, 121.2, 130.4, 115.0, 157.0, 73.1, 71.0, 78.4, 70.5, 81.3, 61.0, C-2-8,8a,4a,1′-4′,glc-1-6) and by TLC analysis (*Rf*, 0.35; solv., $CHCl_3$–MeOH = 9 : 1), respectively.

Daidzein (3)——Colorless needles, mp 300 °C [ref. 12*a*, 315—323 °C]. UV λ_{max}^{MeOH} nm (log ε): 303 (4.00) (sh), 259 (4.38) (sh), 249 (4.40), 238 (4.38) (sh). EI-MS *m/z*: 254 (M^+), 137, 118, 105. ^{1}H-NMR (DMSO-d_6 + D_2O) δ: 6.83 (2H, d, *J* = 8 Hz, H-3′), 6.88 (1H, d, *J* = 2 Hz, H-8), 6.97 (1H, dd, *J* = 9, 2 Hz, H-6), 7.43 (2H, d, *J* = 8 Hz, H-2′), 7.96 (1H, d, *J* = 9 Hz, H-5), 8.27 (1H, s, H-2). ^{13}C-NMR: Table I.

Formononetin (4)——Colorless needles, mp 252—254 °C [ref. 12*b*, 259 °C]. UV λ_{max}^{MeOH} nm (log ε): 311 (4.04), 259 (4.45), (sh), 248 (4.49), 240 (4.41) (sh). ^{1}H-NMR (DMSO-d_6 + D_2O) δ: 3.80 (3H, s, 4′-OMe), 6.87 (1H, d, *J* = 2 Hz, H-8), 6.93 (1H, d, *J* = 8 Hz, 6-H), 6.97 (2H, d, *J* = 9 Hz, H-3′), 7.51 (2H, d, *J* = 9 Hz, H-2′), 7.98 (1H, d, *J* = 8 Hz, 5-H), 8.21 (1H, s, H-2). ^{13}C-NMR: Table I.

Genistein (5)——Colorless plates, mp 297—298 °C [ref. 12*c*, 297—298 °C]. UV λ_{max}^{MeOH} nm (log ε): 264 (4.45). EI-MS *m/z*: 270 (M^+), 153. ^{1}H-NMR (DMSO-d_6 + D_2O) δ: 6.22 (1H, d, *J* = 2 Hz, H-8), 6.38 (1H, d, *J* = 2 Hz, H-6), 6.81 (2H, d, *J* = 8 Hz, H-3′), 7.37 (2H, d, *J* = 8 Hz, H-2′), 8.31 (1H, s, H-2). ^{13}C-NMR: Table I.

Daidzin (6)——Colorless needles, mp 235—237 °C [ref. 12*a*, 234—236 °C]. $[\alpha]_D^{30}$ −33.6° (*c* = 0.5, DMSO) [ref. 12*a*, −36.4° (0.02 N NaOH)]. UV λ_{max}^{MeOH} nm (log ε): 306 (3.70) (sh), 270 (4.23), 248 (4.40). ^{1}H-NMR (DMSO-d_6 + D_2O) δ: 6.83 (2H, d, *J* = 8 Hz, H-3′), 7.15 (1H, dd, *J* = 8, 2 Hz, H-6), 7.23 (1H, d, *J* = 2 Hz, H-8), 7.43 (2H, d, *J* = 8 Hz, H-2′), 8.06 (1H, d, *J* = 8 Hz, H-5), 8.34 (1H, s, H-2). ^{13}C-NMR: Table I.

Daidzein 4′,7-Diglucoside (7)——Colorless needles, mp 245—247 °C, $[\alpha]_D^{33}$ −44.2° (*c* = 0.5, DMSO). UV λ_{max}^{MeOH} nm (log ε): 298 (4.06), 248 (4.23). ^{1}H-NMR (DMSO-d_6 + D_2O) δ: 7.15 (1H, dd, *J* = 8, 2 Hz, H-6), 7.17 (2H, d, *J* = 8 Hz, H-3′), 7.22 (1H, d, *J* = 2 Hz, H-8), 7.55 (2H, d, *J* = 8 Hz, H-2′), 8.07 (1H, d, *J* = 8 Hz, H-5), 8.38 (1H, d, *J* = 8 Hz, H-5). ^{13}C-NMR: Table I.

Puerarin (8)——A white amorphous powder, $[\alpha]_D^{30}$ +9.2° (*c* = 0.5, DMSO). UV λ_{max}^{MeOH} nm (log ε): 308 (3.85), 271 (4.11), 250 (4.20) (sh), 242 (4.23). ^{1}H-NMR (DMSO-d_6 + D_2O) δ: 4.90 (1H, d, *J* = 9 Hz, glc H-1), 6.83 (2H, d, *J* = 8 Hz, H-3′), 7.02 (1H, d, *J* = 9 Hz, H-6), 7.40 (2H, d, *J* = 8 Hz, H-2′), 7.98 (1H, d, *J* = 8 Hz, H-5), 8.28 (1H, s, H-2). ^{13}C-NMR: Table I.

PG-1 (9)——Colorless needles, mp 248—250 °C, $[\alpha]_D^{32}$ +15.6° (*c* = 0.5, DMSO). UV λ_{max}^{MeOH} nm (log ε): 309 (3.94) (sh), 295 (4.06), 272 (4.09), 238 (4.23), 224 (4.22). ^{1}H-NMR (DMSO-d_6 + D_2O) δ: 4.88 (1H, d, *J* = 9 Hz, glc H-1), 6.7—7.1 (3H in total, m, B ring-H), 7.01 (1H, d, *J* = 8 Hz, H-6), 7.97 (1H, d, *J* = 8 Hz, H-5), 8.24 (1H, s, H-2). ^{13}C-NMR: Table I.

PG-3 (10)——Colorless needles, mp 214—216 °C $[\alpha]_D^{31}$ +16.5° (*c* = 0.2, DMSO). UV λ_{max}^{MeOH} nm (log ε): 311 (3.78) (sh), 289 (3.98), 239 (4.15) (sh), 224 (4.20). ^{1}H-NMR (DMSO-d_6 + D_2O) δ: 3.85 (3H, s, 3′-OMe), 4.97 (1H, d, *J* = 9 Hz, glc H-1), 6.7—7.4 (4H in total, m, H-2′, 5′, 6′, 6), 8.03 (1H, d, *J* = 8 Hz, H-5), 8.34 (1H, s, H-2). ^{13}C-NMR: Table I.

Puerarin Xyloside (11)——A white amorphous powder, $[\alpha]_D^{31}$ −8.4° (*c* = 0.5, DMSO). UV λ_{max}^{MeOH} nm (log ε): 252 (4.10), 232 (3.96). ^{1}H-NMR (DMSO-d_6 + D_2O) δ: 4.88 (1H, d, *J* = 9 Hz, glc H-1), 6.85 (2H, d, *J* = 8 Hz, H-3′), 7.03 (1H, d, *J* = 8 Hz, H-6), 7.42 (2H, d, *J* = 8 Hz, H-2′), 7.97 (1H, d, *J* = 8 Hz, H-5), 8.30 (1H, s, H-2). ^{13}C-NMR: Table I.

Genistin (12)——Colorless needles, mp 258—260 °C [ref. 12*c*, 256 °C], $[\alpha]_D^{33}$ −30.4° (*c* = 0.5, DMSO) [ref. 12*c*, −28° (0.02 N NaOH)]. UV λ_{max}^{MeOH} nm (log ε): 326 (3.70), 261 (4.40). ^{1}H-NMR (DMSO-d_6 + D_2O) δ: 6.43 (1H, d, *J* = 2 Hz, H-6), 6.67 (1H, d, *J* = 2 Hz, H-8), 6.80 (2H, d, *J* = 8 Hz, H-3′), 7.37 (2H, d, *J* = 8 Hz, H-2′), 8.34 (1H, s, H-2). ^{13}C-NMR: Table I.

Genistein 8-*C*-Glucoside (13)——Colorless needles, mp 221—223 °C, $[\alpha]_D^{30}$ +13.0° (*c* = 0.5, DMSO). UV λ_{max}^{MeOH} nm (log ε): 265 (4.46). ^{1}H-NMR (DMSO-d_6 + D_2O) δ: 4.75 (1H, d, *J* = 9 Hz, glc H-1), 6.36 (1H, s, H-6), 6.87 (2H, d, *J* = 8 Hz, H-3′), 7.42 (2H, d, *J* = 8 Hz, H-2′), 8.33 (1H, s, H-2). ^{13}C-NMR: Table I.

Coumestrol (14)——A white amorphous powder. UV λ_{max}^{MeOH} nm (log ε): 350 (4.18), 304 (3.85), 244 (4.11), 220 (4.04). EI-MS *m/z* 268 (M^+), 240, 149. ^{1}H-NMR (DMSO-d_6 + D_2O) δ: 6.92 (2H, d, *J* = 2 Hz, H-5′, 8), 7.10 (2H, dd, *J* = 8, 2 Hz, H-3′, 6), 7.63 (1H, d, *J* = 8 Hz, H-2′), 7.86 (1H, d, *J* = 8 Hz, H-5). ^{13}C-NMR (DMSO-d_6) δ: 98.6 (d), 102.0 (d), 102.9 (d), 104.1 (d), 113.6 (s), 113.9 (s), 114.5 (s), 120.5 (d), 122.6 (d), 154.6 (s), 155.9 (s), 156.9 (s), 157.5 (s), 159.4

(s), 161.1 (s).

Isoliquiritigenin (15)——A white amorphous powder. UV λ_{max}^{MeOH} nm (log ε): 367 (4.29). EI-MS m/z: 256 (M^+), 137, 120. ^{1}H-NMR (DMSO-d_6+D_2O) δ: 6.32 (1H, d, J=2 Hz, H-3′), 6.44 (1H, dd, J=8, 2 Hz, H-5′), 6.87 (2H, d, J=8 Hz, H-3, 5), 7.76 (2H, d, J=8 Hz, H-2, 6), 7.77 (2H, br s, α, β-H), 8.37 (1H, d, J=9 Hz, 6′-H). ^{13}C-NMR (DMSO-d_6) δ: 125.7, 131.1, 115.8, 160.2 (C-1-4), 114.9, 165.0, 102.6, 165.8, 108.0, 132.7 (C-1′-6′), 144.1, 117.3, 191.4 (C-α, β, >C=O).

Acknowledgement We are grateful to Assistant Prof. Y. Ida of Showa University, School of Pharmaceutical Sciences, for valuable advice concerning the identification of apiin and apiose. This work was supported in part by a grant from the Ministry of Education, Science and Culture, Japan.

References and Notes

1) Part III in the series "Studies on the Constituents of *Pueraria lobata*." References 3 and 4 below form Parts I and II, respectively, in this series.
2) *a*) S. Shibata, T. Murakami, and Y. Nishikawa, *Yakugaku Zasshi*, **79**, 757 (1959); *b*) S. Shibata, M. Harada, and T. Murakami, *ibid.*, **79**, 863 (1959); *c*) Y. Nishikawa and T. Ando, *Chem. Pharm. Bull.*, **8**, 688 (1960); *d*) T. Kinoshita, *Gendai Toyo Igaku*, **3**, 58 (1982).
3) J. Kinjo, I. Miyamoto, K. Murakami, K. Kida, T. Tomimatsu, M. Yamasaki, and T. Nohara, *Chem. Pharm. Bull.*, **33**, 1293 (1985).
4) J. Kinjo, J. Furusawa, and T. Nohara, *Tetrahedron Lett.*, **26**, 6101 (1985).
5) W. Baker and R. Robinson, and N. M. Simpson, *J. Chem. Soc.*, **1933**, 274.
6) A. T. Hudson and R. Bentley, *J. Chem. Soc., Chem. Commun.*, **1969**, 830.
7) M. Hasegawa, *J. Am. Chem. Soc.*, **79**, 1738 (1957).
8) G. G. Zapesochnaya and N. A. Laman, *Khim. Prir. Soedin*, **1977**, 862.
9) E. M. Bickoff, R. L. Lyman, A. L. Livingston, and A. N. Booth, *J. Am. Chem. Soc.*, **80**, 3969 (1958).
10) E. C. Bate-Smith and T. Swain, *J. Chem. Soc.*, **1953**, 2185.
11) Y. Ida, Y. Sato, M. Otsuka, and J. Shoji, Abstracts of Papers, The 32nd Annual Meeting of the Pharmacognosical Society of Japan, Okayama, Oct. 1985, p. 28; ^{13}C-NMR signals of terminal apiosyl residue, 108.9, 75.7, 78.6, 73.1, 63.1 (C-1-6).
12) *a*) M. Windholz, S. Budavari, R. F. Blumetti, and E. S. Otterbein (eds.), "The Merck Index," 10th ed., Merck & Co., Inc., Rahway, N. J., U.S.A., 1983, p. 2795; *b*) *Idem*, *ibid.*, p. 4127; *c*) *Idem*, *ibid.*, p. 4244.

[Chem. Pharm. Bull. 35(12)4851—4855(1987)]

Effects of Phytosterols on Anti-complementary Activity

HARUKI YAMADA,*[,a] MASAMI YOSHINO,[a] TSUKASA MATSUMOTO,[a] TAKAYUKI NAGAI,[a] HIROAKI KIYOHARA,[a] JONG-CHOL CYONG,[a] AKIRA NAKAGAWA,[b] HARUO TANAKA[b] and SATOSHI ŌMURA[b,c]

Oriental Medicine Research Center[a] and Department of Microbial Chemistry,[c] The Kitasato Institute and School of Pharmaceutical Science,[b] Kitasato University, Shirokane, Minato-ku, Tokyo 108, Japan

(Received May 26, 1987)

Several phytosterols, stigmasterol, campesterol and β-sitosterol, were shown to have potent anti-complementary activities. Stigmasterol was the most potent. A marked consumption of C4 was observed to have occurred when serum was incubated with these phytosterols, and β-sitosterol and stigmasterol showed higher C4 consumption than campesterol. After the incubation of serum with these phytosterols in the absence of Ca^{2+} ions, cleavage of C3 in the serum was detected by immunoelectrophoresis. Stigmasterol caused greater C3 cleavage than the other two compounds. Stigmasterol also showed higher consumption of complement than campesterol and β-sitosterol when rabbit erythrocytes were used in the assay system in the absence of Ca^{2+} ions. These results indicate that these phytosterols activate complement *via* both the alternative and classical pathways.

Keywords——stigmasterol; β-sitosterol; campesterol; anti-complementary activity; complement activation

The complement system plays an important role in host defence, inflammation or allergic reactions, and activation of the complement system occurs *via* both the classical and alternative pathways.[1] The classical pathway is activated by immune complexes containing immunoglobulin M (IgM) and immunoglobulin G (IgG) antibodies, acute-phase proteins such as C-reactive protein, and ribonucleic acid (RNA) tumor viruses. The alternative pathway is directly activated by polysaccharides, certain immunoglobulins, viruses, fungi, bacteria, certain animal cells and parasites. Some anti-complementary polysaccharides, for example, lipopolysaccharides,[2] β(1→3)glucan,[3] 6-branched β(1→3)glucan,[3] and inulin[4] have already been isolated from bacteria, fungi and plants. Recently, potent anti-complementary activity has also been observed in the extracts of several Chinese herbs,[5] and these active principles were characterized as complex arabinogalactans.[5b-e,i-l] However, not many low-molecular weight organic substances having anti-complementary activity have been reported. During screening for anti-complementary substances, we have found potent anti-complementary activity of several phytosterols, β-sitosterol, stigmasterol and campesterol, isolated from soybean meal.

In the present paper, we describe the anti-complementary activity of these three phytosterols and their modes of action.

Materials and Methods

Materials——Normal human serum (NHS) was obtained from a healthy adult. β-Sitosterol, stigmasterol and campesterol were purchased from Sigma Co. The chemical structures of these compounds are shown in Fig. 1. The purity of these phytosterols was checked by high performance liquid chromatography (HPLC). Commercial β-sitosterol was a mixture of β-sitosterol and campesterol, and therefore it was purified by HPLC using a YMC-Pak A-

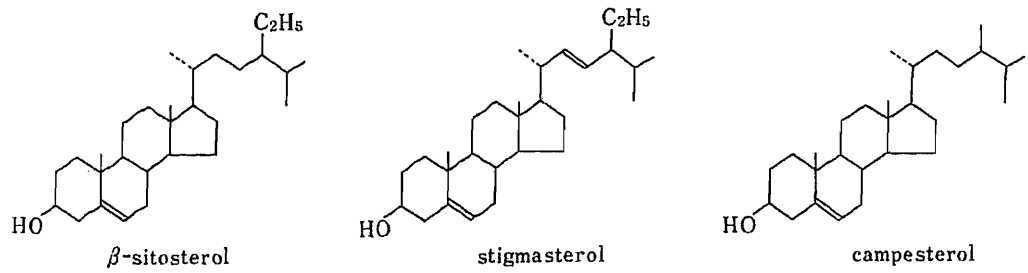

Fig. 1. Structures of Phytosterols

312 ODS column (6 × 150 mm) with 100% MeOH. The apparatus used for HPLC was a Waters model ALC/GPC 244 equipped with a model 441 UV detector (Waters Assoc., Milford, MA) set at 214 nm and a model R 410 differential refractometer (Waters Assoc., Milford, MA).

Anti-complementary Activity——Each of the phytosterols was dissolved in isopropanol then diluted with water to a final concentration of 5% isopropanol, and these solutions were used for assay. The anti-complementary activity was measured as described previously.[5a,b] Gelatin–veronal-buffered saline (pH 7.4) containing 500 μM Mg^{2+} and 150 μM Ca^{2+} (GVB^{2+}) was prepared as described previously.[5b] Various dilutions of sample in 5% isopropanol (50 μl) were incubated with 50 μl of NHS and 50 μl of GVB^{2+}. The mixtures were incubated at 37 °C for 30 min and the residual total hemolytic complement (TCH_{50}) was determined by a method using IgM–hemolysin-sensitized sheep erythrocytes (EA) at 1×10^8 cells/ml. NHS was incubated with 5% isopropanol and GVB^{2+} to provide a control. The anti-complementary activity of the phytosterol was expressed as the percentage inhibition with respect to TCH_{50} of the control.

Determination of Complement Hemolysis through the Alternative Complement Pathway (ACH_{50})——ACH_{50} was determined[5b] in 10 mM ethylene glycol-bis(β-aminoethyl ether)*N,N,N′,N′*-tetracetic acid (EGTA) containing 2 mM $MgCl_2$ in GVB^{2-} (Mg^{2+}–EGTA–GVB^{2-}). A sample was incubated with Mg^{2+}–EGTA–GVB^{2-} and NHS at 37 °C for 30 min, and the residual complement of the mixtures was measured in terms of the hemolysis of rabbit erythrocytes (5×10^7 cells/ml) incubated with Mg^{2+}–EGTA–GVB^{2-}.

Crossed Immunoelectrophoresis——NHS was incubated with an equal volume of the solution of the phytosterol with Mg^{2+}–EGTA–GVB^{2-} for 30 min at 37 °C. The serum was then subjected to crossed immunoelectrophoresis to locate the C3 cleavage products.[5b] Shortly after the first run (barbital buffer pH 8.6, ionic strength 0.025, with 1% agarose), the second run was carried out on a gel plate (1.5-mm layer) containing 0.5% rabbit anti-human C3 serum at a potential gradient of 1 mA/cm for 10 h. After the electrophoresis, the plate was fixed and stained with Ponceau 3R.

Determination of C4——Titration of C4 was performed[5b] using intermediate cells $EAC1^{gp}$ for C4. $EAC1^{gp}$ cells were prepared from EA (1×10^9 cells/ml) incubated with C1 solution (1×10^{12} SFU/ml) in the ratio of 28 : 1 at 4 °C for 1 h.

Results

The anti-complementary activities of the phytosterols are shown in Fig. 2. Stigmasterol, campesterol and β-sitosterol all had potent activities, and stigmasterol was the most potent. Under the same conditions, anti-complementary arabinogalactan mixture (1000 μg/ml) showed about 80% of the anti-complementary activity (data not shown). The activation of the classical pathway is initiated by C1 which exists in NHS as a Ca^{2+} dependent complex of three subunits. Activated C1 then activates C4 and C2. Therefore we measured the C4 content in NHS after the incubation with phytosterols to determine their involvement in the activation of the classical pathway. NHS was incubated with stigmasterol, campesterol and β-sitosterol in GVB^{2+} at 37 °C for 30 min, and the residual activity of C4 was estimated by hemolytic assay (Fig. 3). The three phytosterols decreased the C4 content of NHS dose dependently. When NHS incubated with 100 μg/ml of stigmasterol or β-sitosterol was used for C4 titration, 90% of the hemolytic titer of C4 was consumed. Campesterol also decreased the C4 content of NHS significantly. These results showed that the classical pathway was activated by these phytosterols. Because Ca^{2+} is required for the activation of complement *via* the classical pathway but not the alternative pathway, the activation through the alternative pathway was

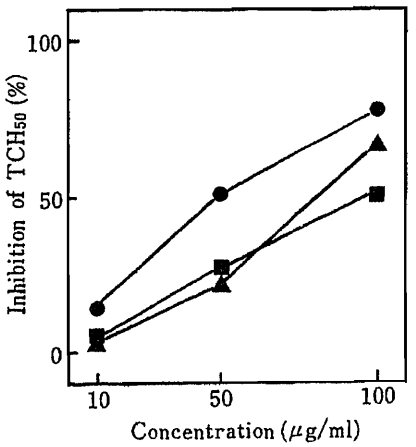

Fig. 2. Anti-complementary Activity of Phytosterols

Stigmasterol (●), campesterol (▲), β-sitosterol (■).

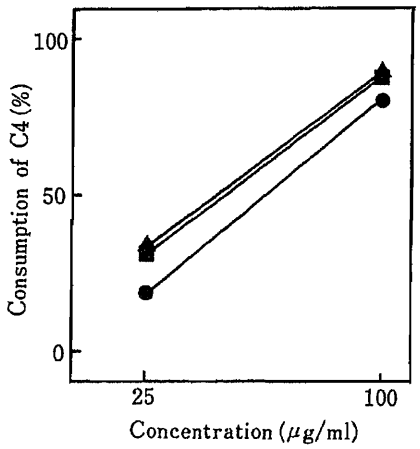

Fig. 3. Consumption of C4 by Phytosterols

Stigmasterol (■), campesterol (●), β-sitosterol (▲).

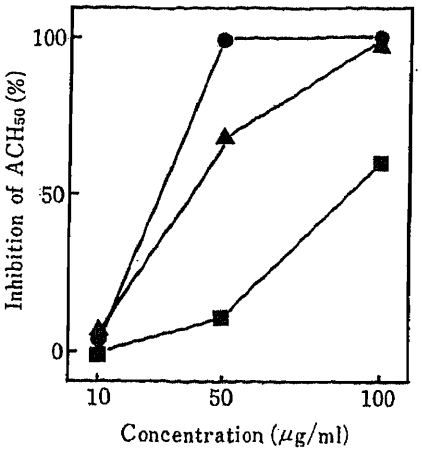

Fig. 4. ACP Activity of Phytosterols

Stigmasterol (●), campesterol (▲), β-sitosterol (■).

measured by the use of Ca^{2+} depleted NHS in the presence of EGTA. When these phytosterols were incubated with NHS in Mg^{2+}–EGTA–GVB^{2-} at 37 °C for 30 min and a hemolytic assay (ACH_{50}) was carried out using rabbit erythrocytes, stigmasterol, campesterol and β-sitosterol showed dose-dependent anti-complementary activities on ACH_{50} (ACP activity) (Fig. 4). In the case of stigmasterol, 100% ACP activity was observed when a concentration of 50 μg/ml was used for the assay. The order of ACP activities of these phytosterols was stigmasterol > campesterol > β-sitosterol. The activation of the alternative pathway causes C3 cleavage due to the activation of C3 but does not require the activation of C1, C4 or C2, or the presence of Ca^{2+}. Therefore, crossed immunoelectrophoresis was carried out after the incubation of NHS with these phytosterols in Mg^{2+}–EGTA–GVB^{2-} to determine whether C3 activation had occurred. When crossed immunoelectrophoresis was carried out after the incubation of NHS with 5% isopropanol as the solvent in Mg^{2+}–EGTA–GVB^{2-}, a slight cleavage of C3 was apparent, but more significant cleavage of C3 was obtained in the serum treated with these phytosterols (Fig. 5). Potent ACP-active stigmasterol caused the greatest C3 cleavage. These results indicated that the alternative pathway was also activated by these phytosterols. It should be noted that 5% isopropanol showed about 20% ACP activity when water was used as the control.

Discussion

The present investigation demonstrated that the phytosterols β-sitosterol, stigmasterol

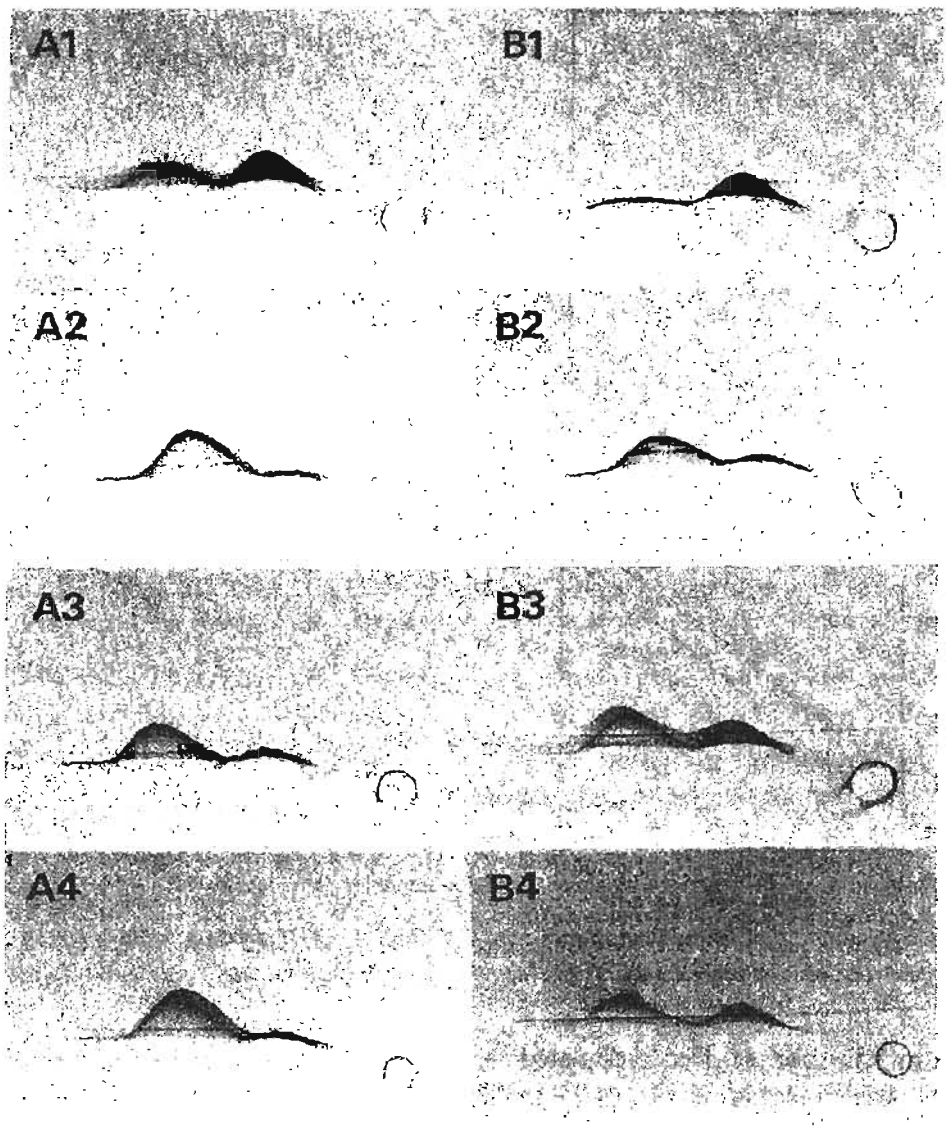

Fig. 5. C3 Activation by Phytosterols

NHS was incubated with an equal volume of (1) 5% isopropanol, (2) stigmasterol, (3) campesterol, or (4) β-sitosterol (0.1 mg/ml) with GVB^{2+} (A) or Mg^{2+}–EGTA–GVB^{2-} (B) at 37 °C for 30 min. The sera were then subjected to crossed immunoelectrophoresis, to locate C3 cleavage products. The anode is to the left.

and campesterol showed potent anti-complementary activities. During this study, Ebihara *et al.* reported that 3β-hydroxystigmast-5-ene-7-one obtained from the root of *Dichroa febrifuga* LOUR also has potent anti-complementary activity, as did several other sterols,[6] but they did not report the mode of action of this activity. Phytosterols used in this study were not soluble in water, so several organic solvents (5% in water) were tested for ability to solubilize the phytosterols and for effect on the anti-complementary activity. Isopropanol was shown to have rather lower activity than others such as dimethylsulfoxide, tetrahydrofuran, ethanol and methanol (unpublished results). In the present experiment, stigmasterol was shown to have the most potent anti-complementary activity among the phytosterols tested. However, it is not known whether these activities depend on the specific structure of these phytosterols, because stigmasterol showed the highest solubility in 5% isopropanol, whereas some insoluble precipitates appeared in the case of the other two phytosterols after the addition of water to

make 5% isopropanol solution.

We found this activity in soybean meal extract, which contains stigmasterol and campesterol as the major constituents. It is known that these phytosterols are contained widely in many plants, including several Chinese herbs. These phytosterols activated the complement system *via* not only the classical but also the alternative pathway. The alternative pathway does not require antibodies and is directly activated by bacteria, viruses, fungi, helminth and protozoan parasites, and lymphoblastoid cells.[1] Thus, in general, the alternative pathway constitutes the natural defence mechanism of the non-immune host. Therefore these phytosterols are suggested to have potent non-specific immunopotentiating activities.

It has been reported that some Chinese herbs and their prescriptions (Kampo hozai) have various immunomodulating activities such as interferon-producing activity,[5a,7] mitogenic activity,[5a,8] anti-complementary activity,[5] adjuvant activity,[9] host-mediated anti-tumor activity,[10,11a] reticuloendothelial system activation[11] *etc*. These activities have been generally observed in the high-molecular weight fractions of Chinese herbal extract,[5] but few low-molecular weight substances having these activities have been reported. We have not yet examined whether these phytosterols have other immunomodulating activities, but the present results suggested that these phytosterols may be responsible, at least in part (together with high-molecular-weight substances such as polysaccharide), for the immunomodulating activities of Chinese herbal extract.

Acknowledgement The authors wish to thank Miss S. Miura for her technical assistance in a part of this work.

References

1) T. G. Egwang and A. D. Befus, *Immunology*, **51**, 207 (1984).
2) *a*) L. H. Muschel, K. Schmoker and P. M. Webb, *Proc. Soc. Exp. Biol. Med.*, **117**, 639 (1964); *b*) H. Gewurz, H. S. Shin and S. E. Mergenhagen, *J. Exp. Med.*, **128**, 1049 (1968); *c*) R. L. Marcus, H. S. Shin and M. M. Mayer, *Proc. Natl. Acad. Sci. U.S.A.*, **68**, 1351 (1971).
3) *a*) T. Okuda, Y. Yoshioka, T. Ikekawa, G. Chihara and K. Nishioka, *Nature* (London), *New Biol.*, **238**, 59 (1972); *b*) J. Hamuro, U. Hadding and D. Bitter-Suermann, *Immunology*, **34**, 695 (1978).
4) O. Götze and H. J. Müller-Eberhard, *J. Exp. Med.*, **134**, 90s (1971).
5) *a*) H. Yamada, H. Kiyohara, J.-C. Cyong, Y. Kojima, Y. Kumazawa and Y. Otsuka, *Planta Med.*, **50**, 163 (1984); *b*) H. Yamada, H. Kiyohara, J.-C. Cyong and Y. Otsuka, *Molecular Immunology*, **22**, 295 (1985); *c*) H. Kiyohara, H. Yamada, J.-C. Cyong and Y. Otsuka, *J. Pharmacobio-Dyn.*, **9**, 339 (1986); *d*) H. Yamada, K. Ohtani, H. Kiyohara, J.-C. Cyong, Y. Otsuka, Y. Ueno and S. Ōmura, *Planta Med.*, **1985**, 121; *e*) H. Yamada, Y. Otsuka and S. Ōmura, *ibid.*, **1986**, 311; *f*) H. Yamada, J.-C. Cyong and Y. Otsuka, *Int. J. Immunopharmacol.*, **8**, 71 (1986); *g*) H. Yamada, T. Naga., J.-C. Cyong, Y. Otsuka, M. Tomoda, N. Shimizu and K. Shimada, *Carbohydr. Res.*, **144**, 101 (1985); *h*) H. Yamada, T. Nagai, J.-C. Cyong, Y. Otsuka, M. Tomoda, N. Shimizu and R. Gonda, *ibid.*, **156**, 137 (1986); *i*) H. Yamada, H. Kiyohara, J.-C. Cyong and Y. Otsuka, *ibid.*, **159**, 275 (1987); *j*) H. Kiyohara, H. Yamada and Y. Otsuka, *ibid.*, **167**, 221 (1987); *k*) H. Yamada, S. Yanahira, H. Kiyohara, J.-C. Cyong and Y. Otsuka, *Phytochemistry*, in press; *l*) H. Yamada, H. Kiyohara and Y. Otsuka, *Carbohydr. Res.*, in press.
6) T. Ebihara, T. Kawai, M. Kuroyanagi, T. Miyase, T. Noro, A. Ueno and S. Fukushima, Abstracts of Papers, 106th Annual Meeting of the Pharmaceutical Society of Japan, Chiba, April 1986, p. 514.
7) Y. Kojima, Y. Kumazawa, N. Shibukawa, K. Otsuka and K. Mizunoe, *Proceedings Symposium WAKAN-YAKU*, **13**, 101 (1980).
8) Y. Kumazawa, K. Mizunoe and Y. Otsuka, *Immunology*, **47**, 75 (1982).
9) Y. Kumazawa, Y. Nakatsuru, H. Fujisawa, C. Nishimura, K. Mizunoe, Y. Otsuka and K. Nomoto, *J. Pharmacobio-Dyn.*, **8**, 417 (1985).
10) T. Miyazaki, *Gendai Toyoigaku*, **4**, 61 (1983).
11) *a*) G. Chihara, *Proceedings Symposium WAKAN-YAKU*, **16**, 44 (1983); *b*) K. Mizutani, K. Ohtani, R. Sumino, T. Shiota, R. Kasai, O. Tanaka, S. Hatono, M. Ushijima and T. Fuwa, *J. Pharmacobio-Dyn.*, **8**, s-66 (1985).

[Chem. Pharm. Bull. 35(12)4856—4861(1987)]

Enzyme Labeling of Steroids by the *N*-Succinimidyl Ester Method. Preparation of Glucose Oxidase-Labeled Antigen for Use in Enzyme Immunoassay[1)]

HIROSHI HOSODA, REIKO TSUKAMOTO, MAKIKO SHISHIDO, WATARU TAKASAKI and TOSHIO NAMBARA*

Pharmaceutical Institute, Tohoku University, Aobayama, Sendai 980, Japan

(Received June 27, 1987)

Enzyme labeling of a steroid with glucose oxidase by the *N*-succinimidyl ester method was investigated. The activated ester of a testosterone derivative was treated with glucose oxidase to give a labeled antigen. Various molar ratios of steroid to enzyme, ranging from 2 to 100, were employed; the degrees of hapten substitution were found to be 0.7—13. Satisfactory immunoreactivities with an anti-testosterone antiserum in the enzyme immunoassay procedure were obtained with the labeled antigens prepared at molar ratios higher than 4. The effect of steroid/enzyme molar ratio in the labeling on the sensitivity of the testosterone assay was then examined. It was found that the sensitivity of the assay is significantly influenced by the molar ratio, and a higher ratio results in a decrease in assay sensitivity. A dose–response curve with a high sensitivity could be obtained by the use of the labeled antigen prepared at a molar ratio of 6. The active ester method proved to be useful for the preparation of glucose oxidase-labeled antigens as well as for alkaline phosphatase, β-galactosidase and horseradish peroxidase labelings, because of its simplicity and excellent reproducibility.

Keywords——enzyme immunoassay; steroid enzyme labeling; *N*-succinimidyl ester method; testosterone; glucose oxidase; anti-testosterone antiserum; immunoreactivity; immunoassay sensitivity

Enzyme-labeled antigens for use in the heterogeneous enzyme immunoassay of steroid hormones have usually been prepared by condensation of the carboxyl groups of a steroid with the amino groups of lysine residues in an enzyme. The mixed anhydride and carbodiimide methods have mainly been used for the enzyme labeling. The sensitivity and reproducibility of enzyme immunoassays are influenced by the coupling method. We have previously shown that the *N*-succinimidyl ester method is useful for alkaline phosphatase (AP),[2)] β-galactosidase (β-GAL)[3)] and horseradish peroxidase (HRP)[4)] labelings. Further, the three enzymes have been compared with regard to the effects of steroid/enzyme molar ratio in the labeling on the immunoreactivity of the labeled antigen with an anti-steroid antiserum and on the assay sensitivity.[2,4)]

Glucose oxidase (GOD) is also frequently used as an enzyme label, but little work has been done on labeling of steroids or other haptens with the enzyme by the *N*-succinimidyl ester method. This paper deals with the preparation of GOD-testosterone conjugates by the active ester method, and with the immunological properties of the antigens in an enzyme immunoassay system.

Materials and Methods

Materials——GOD (EC 1.1.3.4) from *Aspergillus niger* (grade I, 281 U/mg) was obtained from Boehringer–Mannheim Yamanouchi Co. (Tokyo); HRP (EC 1.11.1.7) (grade I-C, 261 units/mg) was from Toyobo Co., Ltd. (Osaka). The *N*-succinimidyl ester of 4-hydroxytestosterone 4-hemiglutarate (I) was prepared by the method

previously established in these laboratories.[5] Anti-testosterone antiserum used was that reported in the previous paper.[6] Goat anti-rabbit immunoglobulin G (IgG) antiserum and normal rabbit serum were purchased from Daiichi Radioisotope Labs., Ltd. (Tokyo).

Buffer Solution——A 0.05 M phosphate buffer (PB), pH 7.3, was used in the labeling. In the enzyme immunoassay procedure, PB containing 0.1% gelatin and 0.9% NaCl (buffer A) was used. The measurement of GOD activity was carried out in a 0.05 M acetate buffer, pH 5.0 (buffer B).

Preparation of Testosterone–GOD Conjugates——Dioxane solutions (0.15 ml) containing calculated amounts of the testosterone *N*-succinimidyl ester (II) corresponding to steroid/GOD molar ratios of 2, 4, 6, 10, 20, 30, 50 and 100 (M.W. of GOD, 160000)[7] were each added to a solution of GOD (1.5 mg) in PB (0.3 ml) at 0°C, and the mixture was gently stirred at 4°C for 4 h. After addition of PB (1.1 ml), the resulting solution was dialyzed against cold PB (3 l) for 2 d. A 0.5 ml aliquot of the dialyzed conjugate solution was transferred to a test tube; the solutions were stored at 4°C at a concentration of 500 μg/ml, adjusted with buffer A. The remaining conjugate solution was used for determination of the number of steroid molecules incorporated per enzyme molecule. Simultaneously, in order to test the efficiency of the dialysis, a calculated amount of I corresponding to a steroid/enzyme molar ratio of 170 was added before dialysis to another steroid–enzyme conjugate solution prepared at a molar ratio of 30. The recovery of enzymic activity in the coupling procedure was also tested using the native enzyme in PB as a control. The labeled antigens were stable for several months as regards enzymic activity and immunoreactivity under these storage conditions. For the immunoassay procedure, the solution was diluted with buffer A containing 0.5% normal rabbit serum.

Determination of the Number of Testosterone Molecules Incorporated per GOD Molecule——Spectrometric analysis was carried out by comparing the absorbances at 253 and 280 nm of the conjugate with those of GOD and I as controls in PB. The constants used were as follows: M.W. of GOD, 160000; ε values for GOD were 80000 (253 nm) and 170000 (280 nm),[7] and for steroid, 13000 (253 nm) and 1400 (280 nm).

Immunoreactivity and Antibody Dilution Curve——The enzyme immunoassay procedures were carried out in duplicate or triplicate in a glass test tube (10 ml) as follows: GOD-labeled testosterone (5 ng) in the buffer (0.1 ml) containing normal rabbit serum and buffer A (0.1 ml) were added to anti-testosterone antiserum (0.1 ml) diluted 1 : 500 or more in buffer A, and the mixture was incubated at 4°C for 4 h. Goat anti-rabbit IgG antiserum (0.1 ml) diluted 1 : 30 with buffer A containing 0.3% ethylenediaminetetraacetic acid was added to the incubation mixture, and the solution was vortex-mixed, then allowed to stand at 4°C for 16 h. After addition of buffer A (1.5 ml) the resulting solution was centrifuged at 3000 rpm for 10 min, and the supernatant was removed by aspiration. The immune precipitate was washed once with buffer A (1.5 ml) and used for measurement of the enzymic activity. At the same time, the procedure without addition of the first antibody was carried out to provide a blank value. An experiment using only the enzyme-labeled steroid was also carried out to obtain 100% enzymic activity.

Inhibition of the Binding of Enzyme-Labeled Antigen to Antibody by Addition of Testosterone——A solution of testosterone (50 pg) in buffer A (0.1 ml) and GOD-labeled testosterone (1—5 ng) in the buffer (0.1 ml) were added to diluted antiserum (0.1 ml), and the mixture was incubated at 4°C for 4 h. Separation of free and bound enzyme-labeled antigens was carried out as described above. Simultaneously, the procedure without addition of testosterone or the first antibody was carried out to provide B_0 and non-specific binding (background) values.

Measurement of Enzymic Activity——The immune precipitate was diluted with buffer B (1.2 ml) containing 3-(*p*-hydroxyphenyl)propionic acid (HPPA) (0.08%), glucose (9%), and HRP (0.0001%), vortex-mixed, and incubated at 25°C for 1 h. The reaction was terminated by addition of 3% NaN_3–0.5 M NaOH (1 : 1, 2 ml). The fluorescence intensity was then measured at 405 nm with excitation at 320 nm. The background was estimated as a percentage of the intensity for B_0; the zero reference used consisted of these solutions.

In the case of the recovery test for enzymic activity or the use of only enzyme-labeled testosterone as described above, these procedures were applied to the enzyme solution.

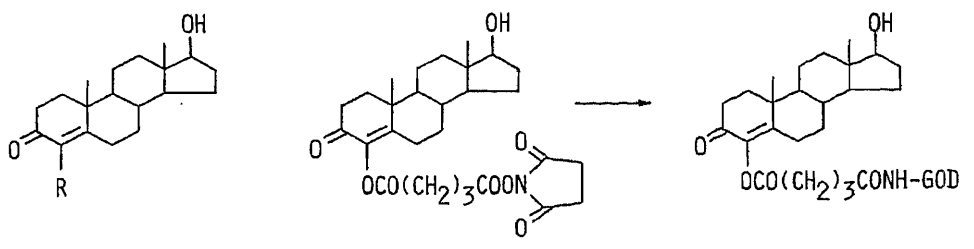

testosterone: R = H
I: R = $OCO(CH_2)_3COOH$

II

III

Chart 1

Results and Discussion

The purpose of this work was to examine the immunoreactivity of the testosterone–GOD conjugate prepared by the *N*-succinimidyl ester method with the anti-testosterone antiserum in the enzyme immunoassay procedure, and the sensitivity of the testosterone assay using the labeled antigen. The *N*-succinimidyl ester (II) prepared from I by condensation with *N*-hydroxysuccinimide in the presence of a water-soluble carbodiimide was reacted with GOD to give enzyme-labeled antigen (III). The enzyme labeling was carried out by mixing II with the enzyme in phosphate buffer (pH 7.3)–dioxane. The activated ester should react readily with free amino groups of the enzyme. Various molar ratios of the steroid to enzyme, ranging from 2 to 100, were used. The reaction mixtures were dialyzed against the buffer to remove the unreacted steroid. The loss of enzymic activity was less than 20% under the coupling conditions used. Spectrometric analysis showed that the average number of steroid molecules incorporated per GOD molecule (degree of hapten substitution) ranged from 0.7 to 13 (Fig. 1).

The anti-testosterone antiserum used in the enzyme immunoassay was that elicited in a rabbit by immunization with the conjugate of I with bovine serum albumin, that is, a homologous assay system.[8] This antiserum has an affinity constant of $2 \times 10^{10}\,\mathrm{M}^{-1}$ for testosterone, in the radioimmunoassay procedure.[6] The bound and free enzyme-labeled antigens were separated by a double antibody method. The enzymic activity of the immune precipitate was determined by a fluorimetric method using an HRP–HPPA system, *i.e.* measurement of hydrogen peroxide produced by the catalytic action of GOD in the presence of glucose.

Immunoreactivities of the enzyme-labeled antigens obtained with various steroid/enzyme molar ratios were investigated at 1 : 500 dilution of the anti-testosterone antiserum. The amount (5 ng) of the antigen fixed corresponds to *ca.* 9 pg of testosterone, if the degree of hapten substitution is 1. The results are shown in Fig. 1. The binding ability increased with increasing molar ratio, and reached a plateau at a ratio of 50; satisfactory reactivities were obtained with the labeled antigens prepared at molar ratios higher than 4. It should be noted that the unreacted steroid in the enzyme labeling was effectively removed by the dialysis: this conclusion was based on the fact that the labels prepared at a molar ratio of 30 with and without addition of I as a tracer showed similar degrees of hapten substitution.

The effect of the steroid/enzyme molar ratio on the sensitivity of the testosterone assay

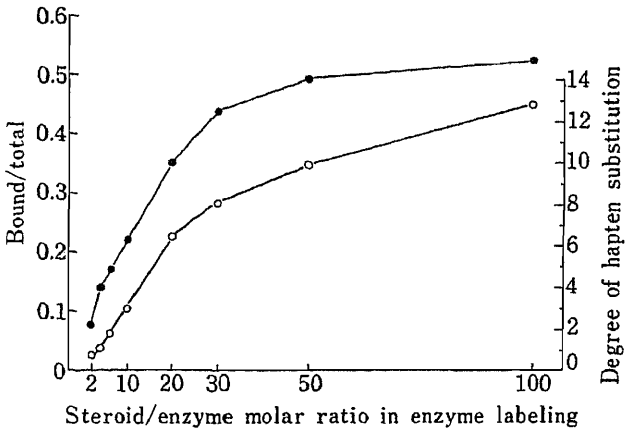

Fig. 1. Immunoreactivities of GOD-Labeled Antigens (●) with the Anti-testosterone Antiserum and Degrees of Hapten Substitution in the GOD-Labels (○)

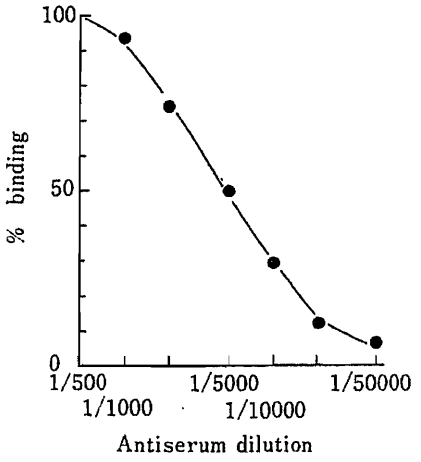

Fig. 2. An Antibody Dilution Curve with the GOD-Labeled Antigen Prepared at a Molar Ratio of 10

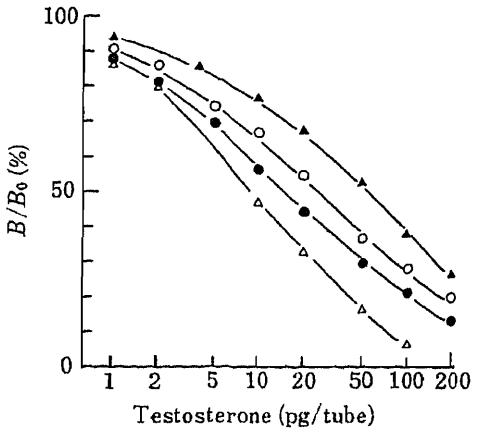

Fig. 3. Dose-Response Curves for Fluorimetric Testosterone Enzyme Immunoassays Using GOD (●)-, HRP (△)-, AP (○)- and β-GAL (▲)-Labeled Antigens

was then examined. For this purpose, an appropriate dilution of anti-testosterone antiserum for use in enzyme immunoassay was determined by construction of antibody dilution curves. The result obtained with the GOD-labeled antigen (5 ng) prepared at a molar ratio of 10 is shown in Fig. 2. The binding ability was expressed for convenience as a percentage of that obtained with 1 : 500 dilution. The dilution showing 50% binding can be defined as a titer. Therefore, the use of the antiserum diluted approximately 1 : 5000 may be suitable for obtaining a dose–response curve. In practice, however, various dilutions were employed in the comparative study of sensitivity. Similar antibody dilution curves were obtained in the cases of other labeled antigens. Sensitivities obtainable with the assay systems were tested by examining the inhibition of enzymic activity caused by the addition of 50 pg of testosterone per tube, *i.e.* the extent of inhibition at the point of 50 pg of the steroid in the dose–response curve, as shown in Fig. 3. Various amounts (1—5 ng) of the GOD label were used. The assays were assessed in terms of the fluorescence intensity for B_0 and non-specific binding (background). The criterion that the background obtained should be less than 10% was employed in this work. The results are listed in Table I. The data showed that the sensitivity was significantly influenced by the molar ratio and a higher ratio resulted in a decrease in assay sensitivity. The assays using the GOD-labeled antigens (5 or 2 ng) prepared at molar ratios of 2—30 were sensitive with over 50% inhibition. On the other hand, the labels prepared at molar ratios of 50 and 100 gave comparatively low sensitivities and the use of a smaller amount (1 ng) of the label was not very effective in terms of sensitivity.

A typical dose–response curve for the testosterone enzyme immunoassay using the GOD label (5 ng) prepared at a molar ratio of 6, together with those reported for the fluorimetric assays using AP,[2] β-GAL and HRP[4] as labels, where the same anti-steroid antiserum and haptenic derivative (I) were used, is shown in Fig. 3; the substrates used were 4-methylumbelliferyl phosphate for AP, 4-methylumbelliferyl β-D-galactopyranoside for β-GAL, and HPPA for HRP. These were the "best" standard curves obtained with each assay system. In the case of GOD label, the amount of testosterone needed to displace 50% of the bound label was 14 pg. With the label prepared at a molar ratio of 100, it was estimated to be over 150 pg. It can be seen that the sensitivity of the present assay is low when compared with that of the assay using HRP, but higher than those with AP and β-GAL. The minimal detectable amount of testosterone, that is, twice the standard deviation of the zero determination (B_0, $n=10$) was 1 pg. Based on a balance between sensitivity and precision, we recommend steroid/GOD

TABLE I. Inhibition of Bound Enzymic Activity of GOD-Labeled Antigens by 50 pg of Testosterone

Molar ratio	Amount of label (ng)	Antiserum dilution	Inhibition (%)	NSB[a] (%)
2	5	1:10000	58	11
		1:20000	74	17
4	5	1:10000	58	7
		1:20000	77	10
6	5	1:10000	61	4
		1:20000	70	7[b]
10	5	1:20000	53	3
		1:40000	46	4
	2	1:10000	65	2
		1:20000	67	4
20	5	1:40000	34	2
		1:80000	43	3
	2	1:20000	69	2
		1:60000	58	6
30	5	1:60000	25	6
		1:80000	33	7
	2	1:40000	51	5
		1:60000	52	8
50	5	1:60000	23	8
		1:80000	27	10
	2	1:40000	49	2
		1:60000	47	3
100	5	1:60000	23	1
		1:80000	21	1
	2	1:60000	30	1
		1:80000	33	1

a) Non-specific binding (background). *b*) The dose-response curve shown in Fig. 3 was obtained with this system.

molar ratios ranging from 4 to 8 (10—20 in the assay using 2 ng of the label). In general, however, it is desirable to estimate the degree of hapten substitution, since the labeling rate is influenced by various factors, such as pH, solvent volume, and reactivity of steroid derivatives. It should be mentioned that GOD itself can be more sensitively assayed with respect to the minimal detectable amount by using *p*-hydroxyphenylacetic acid instead of HPPA,[9] but the former agent gave a rather low sensitivity when applied to the present immunoassay system.

The present work showed that the *N*-succinimidyl ester method is useful in the preparation of GOD-labeled antigen as well as for AP, β-GAL and HRP labels. Enzyme labeling of steroids or other haptens with GOD has been carried out by the mixed anhydride[10] and carbodiimide[11] methods, which are not always satisfactory with respect to reproducibility. The immunoreactivity of the GOD-labeled antigen prepared by the present method, in which a high enzymic activity was recovered, was found to increase reasonably with increasing steroid/enzyme molar ratio. In view of the availability of 30 lysine residues[7] for labeling, the effect of the molar ratio in the labeling on the assay sensitivity was not unexpected. It seems likely that a 1:1 steroid–enzyme conjugate is suitable for obtaining a high sensitivity, since the immunoreaction between this antigen and the antibody molecule is efficiently responsive to a minimum amount of the antigen to be measured; a higher degree of hapten substitution results in a decrease in assay sensitivity. In fact, the use of the label

prepared at a molar ratio of 4, in which the degree of steroid substitution was 1, resulted in the highest sensitivity. It should be noted, however, that the GOD labels having substitution degrees up to 6 gave satisfactory sensitivities under appropriate conditions. We are interested in the result on the order of assay sensitivity, shown in Fig. 3. This problem is under investigation.

The findings obtained here should be useful in the development of hapten enzyme immunoassays. A colorimetric GOD detection system using 3,3′,5,5′-tetramethylbenzidine as a chromogen will be reported elsewhere. Application of the active ester method to other enzymes which are currently employed in enzyme immunoassays is in progress.

Acknowledgement This work was supported by a grant from the Ministry of Education, Science and Culture of Japan.

References and Notes

1) Part CCXXXIV of "Studies on Steroids" by T. Nambara; Part CCXXXIII: J. Goto, Y. Sano, K. Tsuchiya (née Sato) and T. Nambara, *J. Chromatogr.*, in press.
2) H. Hosoda, W. Takasaki, S. Aihara and T. Nambara, *Chem. Pharm. Bull.*, **33**, 5393 (1985).
3) H. Hosoda, Y. Sakai, H. Yoshida and T. Nambara, *Chem. Pharm. Bull.*, **27**, 2147 (1979).
4) H. Hosoda, T. Karube, N. Kobayashi and T. Nambara, *Chem. Pharm. Bull.*, **33**, 249 (1985).
5) H. Hosoda, Y. Sakai, H. Yoshida, S. Miyairi, K. Ishii and T. Nambara, *Chem. Pharm. Bull.*, **27**, 742 (1979).
6) H. Hosoda, K. Tadano, S. Miyairi and T. Nambara, *J. Steroid Biochem.*, **10**, 513 (1979).
7) H. Tsuge, O. Natsuaki and K. Ohashi, *J. Biochem.* (Tokyo), **78**, 835 (1975).
8) B. K. Van Weemen and A. H. W. M. Schuurs, *Immunochemistry*, **12**, 667 (1975).
9) E. Ishikawa, M. Imagawa, S. Hashida, S. Yoshitake, Y. Hamaguchi and T. Ueno, *J. Immunoassay*, **4**, 209 (1983).
10) G. Holder, "Enzyme Labelled Immunoassay of Hormones and Drugs," ed. by S. B. Pal, Walter de Gruyter, Berlin, 1978, p. 221; H. Arakawa, M. Maeda and A. Tsuji, *Chem. Pharm. Bull.*, **30**, 3036 (1982).
11) H. Arakawa, M. Maeda and A. Tsuji, *Clin. Chem.*, **31**, 430 (1985).

[Chem. Pharm. Bull. 35(12)4862—4867(1987)]

Antifungal Properties of Solanum Alkaloids

GENJIRO KUSANO, AKIRA TAKAHASHI, KAZUHIRO SUGIYAMA and SHIGEO NOZOE*

Pharmaceutical Institute, Tohoku University, Aobayama, Sendai 980, Japan

(Received March 30, 1987)

The antifungal activities of several solanum alkaloids and their derivatives were examined against a variety of fungal strains such as *Candida albicans* and *Trichophyton* spp. Solacongestidine (I) showed the strongest activity (minimum inhibitory concentration) against *C. albicans* (0.8 μg/ml), *T. rubrum* (0.4 μg/ml) and *Cryptococcus albidus* (0.78 μg/ml), and also showed lesser activities against a wide range of fungi. Solafloridine (II) and verazine (VII) showed activities against *C. albicans* (3.1 and 6.2 μg/ml, respectively) and *T. rubrum* (25 and 3.1 μg/ml, respectively), while other alkaloids such as solasodine (III), tomatidine (IV), tomatillidine (V) and solanocapsine (VI) and related compounds (VIII—XIX) showed much lower activities. Solacongestidine also prolonged the survival time of mice infected with *C. albicans*.

Keywords——antifungal activity; solanum alkaloid; solacongestidine; solafloridine; verazine; *Candida albicans*; *Trichophyton rubrum*; *Trichophyton mentagrophytes*; *Cryptococcus albidus*

A number of azasteroids and steroidal alkaloids with substantial antimicrobial activity have been reported,[1-11] although no useful drugs have yet been found among these compounds. In the course of our research on antifungal compounds obtained from higher plants and mushrooms, we found that some solanum alkaloids such as solacongestidine (I) and solafloridine (II) showed strong activity against *Candida albicans*, *Trichophyton rubrum*, *Cryptococcus neoformans* and so on. Because the antifungal activities of these compounds showed no depression when tested in the presence of 10% serum, these alkaloids were chosen as targets of further research aimed at the development of antifungal agents for treatment of some systemic mycoses. Furthermore, solacongestidine (I) showed potent inhibition of cholesterol biosynthesis from 24,25-dihydrolanosterol. The experimental results suggested that one of the sites of its action is the step of 14α-demethylation of dihydrolanosterol. Because the step of 14α-demethylation is common to the biosyntheses of cholesterol and ergosterol from lanosterol, solacongestidine (I) was expected to inhibit ergosterol biosynthesis from lanosterol, resulting in disturbances of fungal growth.[12] Therefore, some stock solanum alkaloids and related compounds were examined for antifungal activity. In this article we wish to report the results and to discuss their significance.

Experimental

Solacongestidine (I),[13] solafloridine (II),[13] solasodine (III),[14] tomatidine (IV),[14] tomatillidine (V),[15a,b] and solanocapsine (VI)[16] were obtained as a result of research on solanum alkaloids in the Steroids Section of the National Institute of Arthritis, Metabolic Diseases and Digestive Diseases (NIAMDD) of the National Institutes of Health (NIH), U.S.A. Verazine (VII) was given by Prof. K. Kaneko in the Faculty of Pharmaceutical Sciences of Hokkaido University (Sapporo, Japan). Dihydrosolasodine (VIII) was prepared by reduction of solasodine (III) with $NaBH_4$ in methanol.[17] The *N*-methyl derivative (IX) of VIII was prepared by treatment of VIII with methyl iodide in *N*,*N*-dimethylformamide. 3,16-*O*-Diacetylpseudosolasodine (X) was prepared by treatment of solasodine (III) with

acetic anhydride containing zine chloride.[18] 16-*O*-Acetylpseudosolasodine (XI) was obtained by stirring X in 1% methanolic Na_2CO_3 solution at room temperature, followed by recrystallization from methanol after SiO_2 chromatography. 3,16-*O*-Diacetylpseudotomatidine (XII) and 16-*O*-acetylpseudotomatidine (XIII) were obtained from tomatidine (IV) by similar treatment. A mixture (XIV) of glycosides of solacongestidine and solafloridine was obtained from the alkaloids fraction of the fruits of *Solanum congestiflorum*. The mixture provided solacongestidine and solafloridine on incubation with Taka-diastase.[19] Dehydrosolacongestidine (XV) was prepared by oxidation of solacongestidine (I) with the Jones reagent.[13] Dihydrosolacongestidine (XVI) was obtained by hydrogenation in the presence of platinum dioxide.[13] The quaternary salt (XVII) of solacongestidine was prepared by treatment of solacongestidine with methyl iodide in acetone containing anhydrous Na_2CO_3.[13] These compounds (VIII—XVII) have been described in the cited references (synthetic methods and physical properties). 27-Norsolacongestidine (XIX) was synthesized with reference to the method which Schreiber and Adam applied to synthesize solacongestidine,[20] as follows. An *n*-hexane solution of *n*-butyl lithium (15%) (0.64 ml, 1 mmol) was added to an anhydrous ether solution (4 ml) containing 2-bromopyridine 95 μl (1 mmol), and the mixture was stirred at -40 °C for 30 min. An anhydrous ether solution (10 ml) containing pregnenolone acetate (350 mg, 0.978 mmol) was added to the above solution over 30 min. Stirring was continued for another hour, the reaction temperature was allowed to rise to -20 °C, and the mixture was stirred for a further 30 min. Then, the temperature was allowed to rise to 0 °C and ether (20 ml) containing water (1 ml) was added. The ether layer was separated and the aqueous layer was extracted with ether twice. The combined ether solution was shaken with 3% HCl three times. The acidic solution was alkalized with ammonia water to give a precipitate. After SiO_2 chromatography of the products, 3β-acetoxy-20-(pyridyl-2)-pregn-5-en-20-ol (26.5 mg, 6.2%) and 20-(pyridyl-2)-pregn-5-ene-3,20-diol (XVIII) (105.8 mg, 27.4%) were obtained. NMR ($CDCl_3$) ppm of the acetate: 0.75 (3H, s, C_{18}-3H), 1.04 (3H, s, C_{19}-3H), 1.59 (3H, s, C_{21}-3H), 2.02 (3H, s, $OCOCH_3$), 4.34 (1H, m, $C_{3\alpha}$-H), 5.34 (1H, m, C_6-H), 7.00—7.04 (2H, m, 3′-H and 5′-H on the pyridyl ring), 7.66 (1H, m, 4′-H), 8.43 (1H, m, 6′-H). NMR ($CDCl_3$) ppm of diol: 0.94 (3H, s, C_{18}-3H), 1.02 (3H, s, C_{19}-3H), 1.59 (3H, s, C_{21}-3H), 3.35 (1H, m, $C_{3\alpha}$-H), 5.30 (1H, m, C_6-H), 7.00—7.40 (2H, m, 3′-H and 5′-H on the pyridyl ring), 7.64 (1H, m, 4′-H), 8.42 (1H, m, 6′-H). After confirmation of the structure by nuclear magnetic resonance (NMR) spectroscopy, phosphorus oxychloride (0.5 ml) was added to pyridine (3.5 ml) containing the acetate (108.7 mg), with cooling on ice. The reaction temperature was increased to the reflux point for 2 h and then the solvent was evaporated off under reduced pressure. After alkalization of the residue with ammonia water, extraction with ether was carried out. The ether layer was washed with water and dried over Na_2SO_4. The products were subjected to SiO_2 chromatography and the expected dehydrate (43.5 mg, 41.7%) was eluted with *n*-hexane–$CHCl_3$ (2 : 1). Mass spectrum (MS) *m/z*: 420 ($M^+ + 1$), 405. IR ($CHCl_3$) cm^{-1}: 1720 ($OCOCH_3$), 1584, 1560, 1465, 1430 (pyridyl ring), 905 (>C=CH_2). NMR ($CDCl_3$) ppm: 0.59 (3H, s, C_{18}-3H), 0.96 (3H, s, C_{19}-3H), 2.00 (3H, s, $OCOCH_3$), 4.35 (1H, m, $C_{3\alpha}$-H), 5.2—5.6 (3H, m, C_6-H, C_{21}-2H), 7.0—7.5 (2H, m, 3′-H and 5′-H on the pyridyl ring), 7.66 (1H, m, 4′-H), 8.63 (1H, m, 6′-H). Next, the dehydrate (104.4 mg, 0.25 mmol) was dissolved in glacial acetic acid (7 ml) and hydrogenated in the presence of PtO_2 (20 mg) by stirring overnight. After alkalization of the reaction solution with ammonia water, it was extracted with ether. The ether layer was washed with saturated saline solution and dried over Na_2SO_4, followed by chromatography on SiO_2. Elution with $CHCl_3$–MeOH (10 : 1) provided 3β-acetoxy-22,26-imino-27-nor-cholestane (53.4 mg, 50%). MS *m/z*: 429 (M^+), 414, 84 (base peak). IR ($CHCl_3$) cm^{-1}: 1720 ($OCOCH_3$). NMR ($CDCl_3$) ppm: 0.64 (3H, s, C_{18}-3H), 0.81 (3H, s, C_{19}-3H), 0.91 (3H, d, J=5.6 Hz, C_{21}-3H), 2.00 (3H, s, $OCOCH_3$), 2.55 (2H, m, C_{26}-2H), 3.06 (1H, m, C_{22}-H), 4.62 (1H, m, $C_{3\alpha}$-H).

Iminonorcholestanyl acetate (52.0 mg) was hydrolyzed by stirring with 2% methanolic KOH at room temperature for 2 h. After usual treatment, 22,26-imino-27-norcholestan-3β-ol (48.9 mg) was obtained. MS *m/z*: 387 (M^+), 84 (base peak). IR ($CHCl_3$) cm^{-1}: 3600 (OH). NMR ($CDCl_3$) ppm: 0.64 (3H, s, C_{18}-3H), 0.79 (3H, s, C_{19}-3H), 0.92 (3H, d, J=5.7 Hz, C_{21}-3H), 2.56 (2H, m, C_{26}-2H), 3.10 (1H, m, C_{22}-H), 3.54 (1H, m, $C_{3\alpha}$-H). The *N*-chloride (47.2 mg) of the above imino alcohol was prepared by treatment of the alcohol (45.0 mg) with *N*-chlorosuccinimide in CH_2Cl_2 (6 ml) at -10 °C. 27-Norsolacongestidine (XIX, 21.1 mg) was obtained by refluxing the chloride (42.2 mg) in 5% methanolic KOH for 2 h. MS *m/z*: 385 (M^+), 370, 356, 111 (base peak). IR ($CHCl_3$) cm^{-1}: 3625 (OH), 1650 (C=N). NMR ($CDCl_3$) cm^{-1}: 0.68 (3H, s, C_{18}-3H), 0.80 (3H, s, C_{19}-3H), 1.06 (3H, d, J=6.7 Hz, C_{21}-3H), 3.40 (1H, m, $C_{3\alpha}$-H).

The *in vitro* antifungal activities of these compounds (I—XIX) were assayed by the serial two-fold dilution method on Sabouraud glucose agar (1st screening test). The results were expressed as the values of minimum inhibitory concentration (MIC: μg/ml). The following fungi were used for the assay: *Candida albicans* (50157), (55463), *C. pseudotropicalis* (56363), *C. famata* (50866), *C. kefyr* (59763), *Cryptococcus albidus* (C-3), *C. neoformans* (58063), *Rhodotorula glutinis* (59663), *Trichosporon cutaneum* (51271), *Geotrichum candidum* (30266), *Aspergillus fumigatus* (22167), *A. candidus* (21967), *Fonsecaea pedrosoi* (11758), *Microsporum gypseum* (11668), *Phialophora verrucosa* (24172), *Sporothrix schenckii* (30166), *Trichophyton rubrum* sc., and *T. mentagrophytes* sc.

The mother fungi were inoculated on a Sabouraud agar slant and incubated at 27 °C for 2 d (yeast fungi) or for 7—14 d (thread fungi). Emulsion having 10^6 cells/ml of yeast fungi was prepared by adjusting the volume with saline solution containing 0.1% (w/v) Tween-80. Emulsion having 10^6 spores/ml was prepared as follows. The above saline solution (4 ml) was added to an incubated slant and the surface of the slant was scraped with a platinum loop. The

solution containing the spores was filtered through two sheets of gauze and used to prepare the above emulsion. The emulsion (0.01 ml) was added to each well of a NUNCRON R 24-well plate (NUNC K.K.) containing 0.1 ml of two-fold dilutions of the test alkaloids and 0.9 ml of Sabouraud glucose agar. Incubation was carried out at 27 °C for 2 d (*C. albicans* and *Cryptococcus neoformans*), for 5 d (*Aspergillus fumigatus* and *Microsporum gypseum*) or for 7 d (other fungi).

In the 2nd screening test to examine the effect of serum addition, MICs were assessed by using Sabouraud glucose agar containing 10% horse serum.

The therapeutic effect of solacongestidine (I) was assayed in mice infected intravenously with *C. albicans* sc. (mice-SPF-ddY type, 4 weeks old, male). The toxicity of I was determined on oral and intraperitoneal administration to mice.

Results

The antifungal activities of several solanum alkaloids against *C. albicans* and *Trichophyton* spp. are shown in Table I. Solacongestidine (I) showed the strongest inhibition of *C. albicans* and *T. rubrum*, followed by verazine (VII) and solafloridine (II). The MICs of solasodine (III), tomatidine (IV), tomatillidine (V) and dihydrosolasodine (VII) were more than 100 μg/ml against four tested fungi. The inhibitory activities of solacongestidine and solafloridine were the same as in the 1st screening test in spite of the presence of 10% serum. Because many toxic compounds with substantial antifungal activity show marked loss of activity in the presence of serum, the results of the 2nd screening test with solacongestidine and solafloridine are of considerable interest.

The spectrum of antifungal activities of solacongestidine against more than a dozen fungi is shown in Table II. It is interesting that solacongestidine inhibited *Cryptococcus albidus*, *C. neoformans*, *C. famata* and *Trichosporon cutaneum*, while it showed MIC values of more than 100 μg/ml against *C. tropicalis*, *C. collielosa*, *Geotrichum candidum*, *Aspergillus fumigatus*, *A. candidus*, and so on.

The results of the bioassay *in vivo* with solacongestidine are shown in Fig. 1. For

Table I. The Antifungal Activities (MIC, μg/ml) of Some Solanum Alkaloids against *Candida albicans*, *Trichophyton rubrum*, and *T. mentagrophytes*

Compound	*C. albicans*	*T. rubrum*	*T. mentagrophytes*
Solacongestidine (I)	0.8	0.4	1.5
Solafloridine (II)	6.2	25	>100
Solasodine (III)	>100	>100	>100
Tomatidine (IV)	>100	>100	>100
Tomatillidine (V)	>100	>100	>100
Solanocapsine (VI)	>100	>100	>100
Verazine (VII)	3.1	3.1	12.5

Table II. The Antifungal Activities of Solacongestidine against Various Fungi

Fungi	MIC (μg/ml)	Fungi	MIC (μg/ml)
Candida tropicalis	>100	*Trichosporon cutaneum*	3.13
C. kefyr	6.25	*Geotrichum candidum*	>100
C. famata	3.13	*Aspergillus fumigatus*	>100
C. collielosa	>100	*A. candidus*	>100
Cryptococcus albidus	0.78	*Fonsecaea pedrosoi*	>100
C. neoformans	1.56	*Microsporum gypseum*	3.13
Phodotorula glutinis	6.25	*Phialophora verrucosa*	>100
		Sporothrix schenckii	6.25

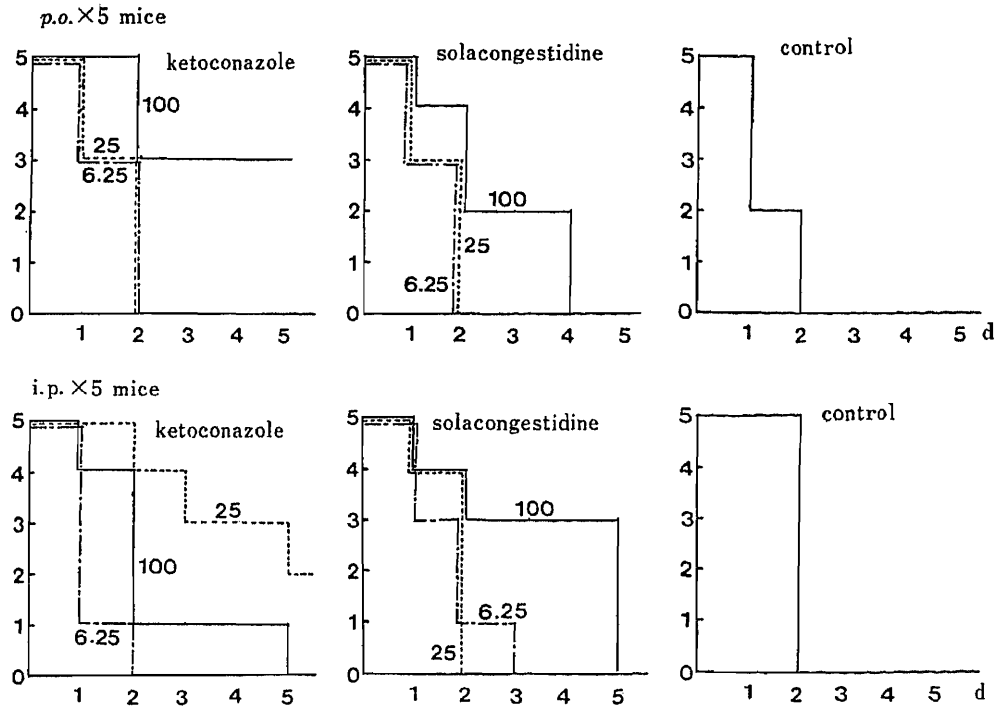

Fig. 1. The Therapeutic Efficacy of Solacongestidine in Mice Infected with *Candida albicans*, as Compared with Ketoconazole

Values are given in mg per kg body weight of mouse.

TABLE III. The Antifungal Activities (MIC, μg/ml) of Some Derivatives of Solanum Alkaloids against *Candida albicans* (*C.a*), *Trichophyton rubrum* (*T.r*), and *T. mentagrophytes* (*T.m*)

Compound	*C.a*	*T.r*	*T.m*
Dihydrosolasodine (VIII)	>100	>100	>100
N-Methyldihydrosolasodine (IX)	25	25	25
3,16-*O*-Diacetylpseudosolasodine (X)	>100	>100	>100
16-*O*-Acetylpseudosolasodine (XI)	>100	>100	>100
3,16-*O*-Diacetylpseudotomatidine (XII)	>100	>100	>100
16-*O*-Acetylpseudotomatidine (XIII)	>100	>100	>100
A mixture (XIV) of glycosides of solacongestidine and solafloridine	>100	>100	>100
Dehydrosolacongestidine (XV)	25	6.2	25
Dihydrosolacongestidine (XVI)	>100	>100	>100
The quaterary salt (XVII) of solacongestidine	25	>100	>100
20(Pyridyl-2)-pregn-5-ene-3,20-diol (XVIII)	>100	>100	>100
27-Norsolacongestidine (XIX)	>100	>100	>100

comparison, ketoconazole was also examined. It was concluded that solacongestidine prolonged the survival time of mice infected with *C. albicans*, compared to the untreated mice. The toxicity of solacongestidine to mice was as follows: three mice out of 3 died when 300 mg/kg of solacongestidine was given orally, but all of three mice tested survived when given 300 mg/kg by i.p. administration.

Dihydrosolasodine (VIII), its *N*-methyl derivative (IX), 3,16-*O*-diacetylpseudosolasodine (X), 16-*O*-acetylpseudosolasodine (XI), 3,16-*O*-diacetylpseudotomatidine (XII), 16-*O*-acetyl-

pseudotomatidine (XIII), a mixture (XIV) of glycosides of solacongestidine and solafloridine, dehydrosolacongestidine (XV), dihydrosolacongestidine (XVI), its quaternary salt (XVII), 20-(pyridyl-2)-pregn-5-ene-3β,20-diol (XVIII) and 27-norsolacongestidine (XIX) were examined for growth inhibition of *C. albicans*, *Trichophyton mentagrophytes*, and *T. rubrum*. *N*-Methyldihydrosolasodine (VIII) showed on MIC of 25 μg/ml but the other compounds had MIC values of more than 100 μg/ml. It is interesting that 27-norsolacongestidine did not show substantial antifungal activity.

Discussion

Solacongestidine (I), a steroidal alkaloid obtained from *Solanum congestiflorum*, showed strong inhibition of the growth of *C. albicans*, *T. rubrum* and *C. albidus*. The MICs were 0.4—1 μg/ml, and the activity was not decreased in the presence of serum. Because the intraperitoneal administration of 300 mg/kg of solacongestidine (I) did not kill any of three mice, the toxicity of I was thought not to be so high. Thus, solacongestidine was chosen as a target of research aimed at the development of antifungal drugs.

As a next step, various solanum alkaloids and related compounds were examined to look for more prospective compounds, although no compound more active than solacongestidine (I) has been found so far.

A number of azasteroids and steroidal alkaloids with substantial antimicrobial activity have been reported. The following compounds have been reported to show MIC values of 1—50 μg/ml: 2-methyl-2-aza-5α-cholestane,[1] 3-methyl-3-aza-5α-cholestane,[1] 1′,4′,5′,6′-tetrahydropyridino[*a*-4,3]-4-aza-5-cholestene,[2] 2′,3′-dihydropyrimidazolino[*a*-4,3]-4-aza-5-cholestene,[2] hexahydropyrimido[*a*-4,3]-4-aza-5-cholestene,[2] tetrahydroimidazolino[*a*-4,3]-4-aza-5-cholestene,[2] androstane-17-oxime *O*-dimethylaminoethyl derivatives,[3] 16β-amino-17-hydroxy-20-ketopregnene derivatives,[4] 17β-amino-3,5-androstadiene,[5] 17β-amino-5-androstene,[5] 4-aza-22-oxa-5α-cholestane,[6] 4-methyl-4-aza-22-oxa-5α-cholestane,[6] 17β-isopentyloxy-4-aza-5α-androstane,[7] 17β-isopentyloxy-4-methyl-4-aza-5α-androstane,[7] 4,17α-dimethyl-4-aza-5α-androstan-17β-ol acetate,[8] and tomatidine[9] (22 μg/ml gave 100% inhibition against *Polyporus versicolor*, and 45—50% inhibition against *Pyricularia oryzae* and *Rhizoctonia solani*) It is noteworthy that 15-aza-24-methylene-D-homocholesta-8,14-dien-3β-ol almost completely inhibited the growth of *Ustilago maydis* at 0.25 μg/ml.[10]

Although useful antifungal drugs have not been established in the categories of azasteroids and steroidal alkaloids, our results and the reported data seem to suggest that effective compounds may be discovered or created. It is interesting that a minor change in the side chain moiety can decrease the activity. For example, solacongestidine (a C_{25R} methyl group) showed strong inhibition, while verazine (a C_{25S} methyl group) showed lower activity and 27-norsolacongestidine showed much lower activity (> 100 μg/ml). It seems important that solacongestidine showed strong inhibition against *C. albicans*, *T. rubrum* and *C. albidus*, while it showed lower inhibition against *C. pseudotropicalis* (MIC 6.25 μg/ml), *T. mentagrophytes* (1.5), *C. neoformans* (1.56), *C. famata* (3.13), and *T. cutaneum* (3.13). The MICs against several other fungi such as *A. fumigatus* and *C. tropicalis* were more than 100 μg/ml. It appears that the antifungal activity of solacongestidine (I) may be specific to certain genera of fungi. Our research will be continued with the aim of finding prospective compounds among azasteroids and steroidal alkaloids that show specific inhibition against *C. albicans*, taking account of the results of the report that steroidal alkaloids bearing a basic nitrogen atom in ring F, shared or unshared with ring E, with bonding capabilities α to the steroid plane may be teratogenic.[11]

Acknowledgement Our thanks are due to Sankyo Co. for the biological assays.

References and Notes

1) N. J. Doorenbos, S. S. Vaidya and R. E. Havranek, *Chem. Ind.*, **1967**, 704.
2) N. J. Doorenbos and M. T. Wu, *J. Pharm. Sci.*, **54**, 1290 (1965).
3) W. Nagata, T. Sugawara, M. Narisada, T. Okada, K. Sasakura, M. Murakami and Y. Hayase, *Chem. Pharm. Bull.*, **14**, 174 (1966).
4) C. G. Bergstrom, *J. Med. Chem.*, **11**, 875 (1968).
5) W. E. Solomons and N. J. Doorenbos, *J. Pharm. Sci.*, **63**, 19 (1974).
6) N. J. Doorenbos and P. C. Boosle, *Chem. Ind.*, **1970**, 1660.
7) N. J. Doorenbos and W. E. Solomons, *J. Pharm. Sci.*, **62**, 638 (1973).
8) N. J. Doorenbos and S. J. M. Brown, *J. Pharm. Sci.*, **60**, 1234 (1971).
9) B. Wolters, *Arch. Pharm.*, **297**, 748 (1964).
10) S. P. Woloshuk, H. D. Sisler and S. R. Dutky, *Antimicrob. Agents Chemother.*, **16**, 81 (1979).
11) W. Gaffield and R. F. Keeler, *Adv. Exp. Med. Biol.*, **177**, 241 (1984).
12) G. Kusano, A. Takahashi, S. Nozoe, Y. Sonoda and Y. Sato, *Chem. Pharm. Bull.*, **35**, 4321 (1987).
13) Y. Sato, Y. Sato, H. Kaneko, E. Bianchi and H. Kataoka, *J. Org. Chem.*, **34**, 1577 (1969).
14) Commercially available (Aldrich).
15) *a*) E. Bianchi, C. D. Djerassi, H. Budzikiewicz and Y. Sato, *J. Org. Chem.*, **30**, 754 (1965); *b*) G. Kusano, T. Takemoto, Y. Sato and D. Johnson, *Chem. Pharm. Bull.*, **24**, 661 (1976).
16) M. Nagai and Y. Sato, *Tetrahedron Lett.*, **1970**, 2911.
17) G. Kusano, N. Aimi and Y. Sato, *J. Org. Chem.*, **35**, 2624 (1970).
18) Y. Sato, H. G. Latham, Jr. and E. Mosettig, *J. Org. Chem.*, **22**, 1496 (1957).
19) Obtained from Sankyo Co., Ltd. (Tokyo).
20) K. Schreiber and G. Adam, *Tetrahedron*, **20**, 1707 (1964).

[Chem. Pharm. Bull. 35(12)4868—4871(1987)]

Detection of Elution Profile of Protein in the Presence of Phenyl-Based Detergent during High-Performance Liquid Chromatography of Cytochrome P-450

SUSUMU IMAOKA* and YOSHIHIKO FUNAE

Laboratory of Chemistry, Osaka City University Medical School, Asahimachi, Abeno-ku, Osaka 545, Japan

(Received May 25, 1987)

Cytochrome P-450 (P-450) isozymes are well separated by high-performance liquid chromatography with an ion-exchange column using buffer containing 0.4% Emulgen 911 (polyphenyl ether) as a detergent. However, it is impossible to monitor the elution profile of protein at 280 nm in the presence of Emulgen. Thus, we have developed a technique for determining the elution profile of protein in the presence of Emulgen. The absorption maximum and minimum of Emulgen 911 were at 276 and 244 nm, respectively. At 244 nm, the elution profile of 0.5 nmol (35 μg) of P-450 was detected as a peak in the presence of 0.4% Emulgen 911. The peak area increased linearly with increasing amount of P-450 up to 5 nmol (350 μg). Identification and estimation of the purity of the eluted P-450 are possible by dual monitoring at 244 and 417 nm, the wavelength for the detection of hemoprotein.

Keywords——HPLC; cytochrome P-450; ion-exchange chromatography; phenyl-based detergent

Introduction

Cytochrome P-450 (P-450) in rat liver microsomes has many isozymes.[1-4] We have separated and purified these hemoproteins by high-performance liquid chromatography (HPLC) using an ion-exchange column.[5-7] Such chromatography is usually done using a buffer containing Emulgen, which is a phenyl-based detergent that absorbs light at 280 nm. Hemoprotein is monitored at 405 or 417 nm and protein at 280 nm. Guengerich and Martin used Lubrol (alkyl ether detergent) instead of Emulgen to detect proteins at 280 nm during the chromatography of P-450, and they found that the separation with Lubrol was not different from those with other phenyl-based detergents in diethylaminoethyl (DEAE)-cellulose chromatography.[8,9] However, only Emulgen 911 gave good resolution of P-450 isozymes on HPLC using a DEAE-5PW column; Lubrol did not.[10]

It is advantageous to monitor at multiple wavelengths for the identification and characterization of proteins. In the chromatography of the hemoprotein P-450, simultaneous detection of the heme and the protein moiety is important for identification of the eluted protein. We have now developed a way to detect P-450 and its protein moiety continuously in the presence of Emulgen during chromatography.

Experimental

Chemicals and Animals——Male Sprague-Dawley rats weighing 250—300 g were obtained from Nippon Clea (Tokyo, Japan). Sodium phenobarbital (PB, 80 mg/kg, dissolved in saline) was given intraperitoneally daily for 4 d. Rat liver microsomes were prepared as described elsewhere.[7] Bovine serum albumin (BSA) was obtained from Sigma Chemical Co. (St. Louis, MO) and other reagents from Wako Pure Chemical Industries (Osaka, Japan). Emulgen 911 and 913 were gifts from Kao Corporation (Tokyo, Japan).

Assays——The amount of protein in the eluate containing Emulgen was measured by the method of Dulley and Grieve[11] with some modifications, and the amount of P-450 was estimated spectrally by the method of Omura and Sato.[12] The absorption spectrum of Emulgen and the optical density of BSA solution were measured in cells of 10 mm path-length using a 220A spectrophotometer (Hitachi, Tokyo, Japan).

Apparatus——An Altex model 100 gradient HPLC apparatus (Berkeley, CA) and a DEAE-5PW anion-exchange column (7.5 i.d. × 75 mm, Toyo Soda Mfg. Co., Tokyo, Japan) were used for the chromatography. Protein and hemoprotein were monitored with a variable-wavelength spectrophotometer (UV-8, Toyo Soda). The peak area was calculated on a data processor (C-R1A, Shimadzu Industrial Co., Kyoto, Japan). Two spectrophotometers were connected in tandem at the outlet of the column, and detection was done in the ultraviolet and visible regions. Each monitor was linked to a data processor and the peak areas detected in the ultraviolet and visible regions were calculated independently.

Chromatography——One milliliter of rat liver microsomes treated with PB (50 mg protein/ml, 1.44 nmol P-450/mg protein) was solubilized by adding 0.125 ml of 10% sodium cholate (pH 7.5) and 0.125 ml of 10% Emulgen 913. Solubilized microsomes (400 μl) or purified P-450 (P-450PB-4, 14.4 nmol P-450/mg protein, major PB-inducible form[7]) was injected into the HPLC column. Ion-exchange chromatography using DEAE-5PW was done at a flow rate of 1.0 ml/min taking 30 min with a linear gradient of sodium acetate from 0 to 0.2 M in 0.02 M Tris–acetate buffer (pH 7.5) containing 0.4% Emulgen 911 and 20% glycerol.

Results and Discussion

HPLC using an ion-exchange column and a buffer containing Emulgen provides good resolution of P-450.[5-7] Continuous monitoring is possible during HPLC. However, Emulgen disturbs the detection of protein at 280 nm because it is a phenyl-based detergent with an absorption maximum at 276 nm (shown in Fig. 1). P-450 is a hemoprotein, so it can be detected at 417 nm. If chromatographic profiles at 417 nm and in the ultraviolet region are obtained, they will provide information about the elution peaks.

The absorption minimum of Emulgen 911 was at 244 nm (Fig. 1). Using BSA, we ascertained whether protein could be detected at 244 nm. BSA was dissolved in 0.02 M Tris buffer containing 0.4% Emulgen 911 and 20% glycerol (the first buffer of the ion-exchange HPLC of P-450) and the optical density was measured at 244 nm using a photometer. The absorbance at 244 nm of BSA at concentrations from 50 to 1000 μg/ml is plotted in Fig. 2. The plot was linear. The intercept of this curve on the y-axis was the same as the optical density of the buffer without BSA. Therefore, at this wavelength, protein can be detected linearly in spite

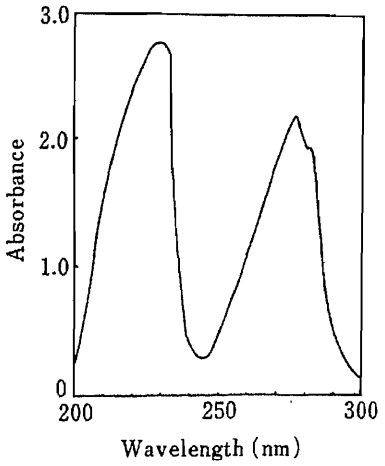

Fig. 1. Absorption Spectrum of 0.1% Aqueous Solution of Emulgen 911

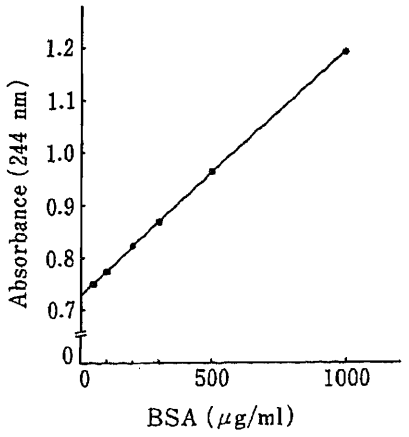

Fig. 2. Correlation between Concentration of BSA and Optical Density at 244 nm

BSA in the concentration range from 50 to 1000 μg/ml was dissolved in 0.02 M Tris-acetate buffer, pH 7.5, containing 0.4% Emulgen 911 and 20% glycerol, and the optical density was measured in cells of 10 mm path-length using a photometer.

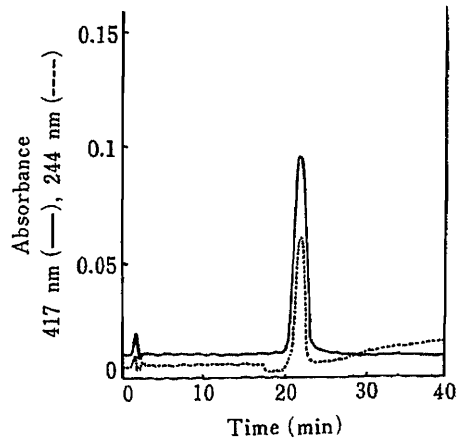

Fig. 3. Chromatographic Profile of Purified P-450PB-4

The solid and dashed lines show the absorbances at 417 and 244 nm, respectively. Two nanomoles of P-450 was injected into the HPLC column. Chromatography on DEAE-5PW was done at a flow rate of 1 ml/min taking 30 min with a linear gradient of sodium acetate from 0 to 0.2 M in 0.02 M Tris-acetate buffer, pH 7.5, containing 0.4% Emulgen 911 and 20% glycerol.

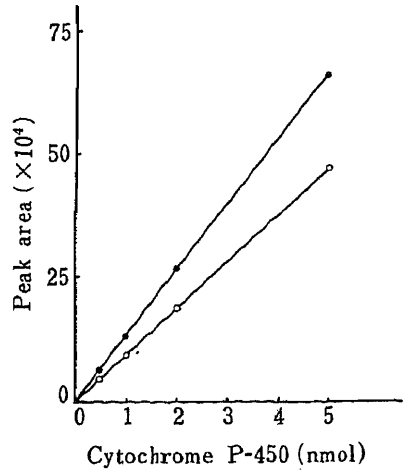

Fig. 4. Correlation between Peak Area and Amount of Purified P-450PB-4 Injected into the HPLC Column

The closed and open circles indicate the peak areas at 417 and 244 nm, respectively. Here, 0.5 to 5 nmol of P-450 was chromatographed under the same conditions as in Fig. 3.

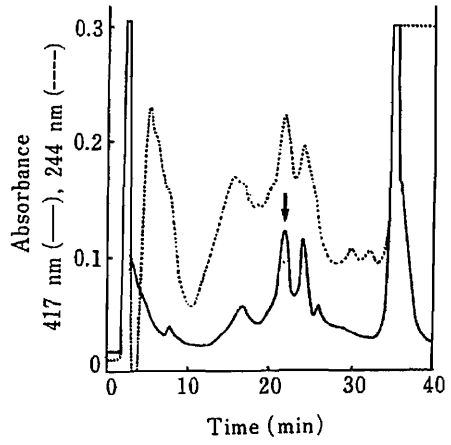

Fig. 5. Chromatographic Profile of Solubilized Rat Hepatic Microsomes Induced with PB

The solid and dashed lines show the absorbances at 417 and 244 nm, respectively. The peak indicated by the arrow is the P-450PB-4 fraction. Ion-exchange chromatography was done under the same conditions as in Fig. 3.

of the presence of 0.4% Emulgen 911.

Next, purified P-450PB-4[7] was chromatographed with dual monitoring at 244 and 417 nm. The chromatographic profile with dual monitoring is shown in Fig. 3. The peak areas monitored at 244 and 417 nm were calculated by a data processor. The area over the base-line was taken as that of the peak, and the peak area calculated at 244 nm was not affected by the existence of Emulgen. Therefore, the correlation curve (shown in Fig. 4) between the amounts of P-450 injected and the peak areas measured at 244 nm passes through the origin. At least 0.5 nmol (35 μg) of P-450 was detectable in this way. Both peak areas increased linearly over 5 nmol. The ratio of the peak area at 417 nm divided by that at 244 nm was constant (1.41) for all amounts of P-450 injected. Therefore, the optical density at 244 nm reflected the amount of protein.

Figure 5 shows a typical chromatogram of solubilized microsomes treated with PB. The peak at the retention time of 22 min is the P-450PB-4 fraction. When purified P-450PB-4 was injected into the HPLC column, the absorbance at 244 nm was lower than that at 417 nm (Fig. 3). However, the absorbance of the P-450PB-4 fraction of solubilized microsomes at 244 nm

was much higher than that at 417 nm (Fig. 5). This result implies that the P-450PB-4 fraction in Fig. 5 contains impurities. In fact, the specific content of this fraction was 4.98 nmol/mg, one-third of that of our purified P-450PB-4 (14.4 nmol/mg). At the retention times of 5 and 15 min in Fig. 5, much protein or other species absorbing at 244 nm was seen, but this had little absorbance at 417 nm and was not hemoprotein. Identification and judgement of the purity of eluted P-450 was possible by comparing the chromatographic profiles monitored at 244 and 417 nm.

HPLC allows continuous monitoring and multiple detection, giving much information about eluted substances. This detection system should also be useful to analyze other membrane proteins in the presence of non-ionic detergents such as Emulgen or Triton.

References

1) F. P. Guengerich, G. A. Dannan, S. T. Wright, M. V. Martin and L S. Kaminsky, *Biochemistry*, **21**, 6019 (1982).
2) D. J. Waxman and C. Walsh, *Biochemistry*, **22**, 4846 (1983).
3) T. Kamataki, K. Maeda, Y. Yamazoe, T. Nagai and R. Kato, *Arch. Biochem. Biophys.*, **225**, 758 (1983).
4) D. E. Ryan, S. Iida, A. W. Wood, P. E. Thomas, C. S. Liever and W. Levin, *J. Biol. Chem.*, **259**, 1239 (1984).
5) A. N. Kotake and Y. Funae, *Proc. Natl. Acad. Sci. U.S.A.*, **77**, 6473 (1980).
6) S. K. Bansal, J. H. Love and H. L. Gurtoo, *J. Chromatogr.*, **297**, 119 (1984).
7) Y. Funae and S. Imaoka, *Biochim. Biophys. Acta*, **842**, 119 (1985).
8) F. P. Guengerich and M. V. Martin, *Arch. Biochem. Biophys.*, **205**, 365 (1980).
9) F. P. Guengerich, *Pharmacol. Ther.*, **A6**, 99 (1979).
10) S. Imaoka and Y. Funae, *J. Chromatogr.*, **375**, 83 (1986).
11) J. R. Dulley and P. A. Grieve, *Anal. Biochem.*, **64**, 136 (1975).
12) T. Omura and R. Sato, *J. Biol. Chem.*, **239**, 2379 (1964).

[Chem. Pharm. Bull. 35(12)4872—4877(1987)]

Effect of Serial Administration of Ginsenoside-Rb_2 in Diabetic Rats: In Terms of Carbohydrate and Lipid Metabolites

TAKAKO YOKOZAWA,*,[a] HIKOKICHI OURA,[a] and YUJI KAWASHIMA[b]

Department of Applied Biochemistry, Research Institute for Wakan-Yaku, Toyama Medical and Pharmaceutical University,[a] Sugitani, Toyama 930-01, Japan and Central Research Laboratories, Yamanouchi Pharmaceutical Co., Ltd.,[b] 1-8 Azusawa-1-chome, Itabashi-ku, Tokyo 174, Japan

(Received June 2, 1987)

In order to study the mechanism of hypoglycemic action of ginsenoside-Rb_2 in diabetic rats, experiments were performed to determine carbohydrate metabolites and the levels of lipid constituents. The rats treated with ginsenoside-Rb_2 showed a significant decrease of glucose in the hepatic tissue. The level of hepatic glycogen was slightly increased after ginsenoside-Rb_2 administration. The glucose-6-phosphate level tended to increase, the pyruvate level was unchanged, and the lactate level tended to decrease. There was, however, no accumulation of total lipid in hepatic tissue. In rats given ginsenoside-Rb_2, the levels of triglyceride, non-esterified fatty acid, 3-hydroxybutyrate, and acetoacetate were markedly decreased, showing a trend toward restoration of the normal state and inducing an increase in lipids in the adipose tissue. The hypoglycemic action of ginsenoside-Rb_2 is discussed on the basis of the present results.

Keywords——ginsenoside-Rb_2; streptozotocin-induced diabetic rat; carbohydrate metabolite; lipid constituent

An ability of ginseng to enhance the general metabolic status has been suggested, and various studies on this crude drug have been carried out. In our laboratory, the effects of ginseng have so far been studied from the viewpoint of biosynthesis of deoxyribonucleic acid (DNA), ribonucleic acid (RNA) and protein, and metabolism of carbohydrate and lipid.[1-6] Recent experiments using various isolated saponins demonstrated that ginsenoside-Rb_2, whose structure was identified by Sanada *et al.*,[7] has a potent physiological action on carbohydrate and lipid metabolism in normal rats.[8,9] In another experiment using diabetic rats, in which the major abnormality is carbohydrate dysbolism, 6 d of ginsenoside-Rb_2 administration resulted in a significant decrease in blood glucose level.[10,11] The ginsenoside-Rb_2-treated group showed a significant rise of glucokinase activity in the liver, while there was a significant decrease in the activity of glucose-6-phosphatase.[10] These experiments prompted us to study the mechanism of hypoglycemic action of ginsenoside-Rb_2 in diabetic rats. In the present study, as a part of our research on the mechanism of the action to decrease blood glucose level, the effects of ginsenoside-Rb_2 on carbohydrate metabolites and lipid constituents in the liver, adipose tissue, and serum were investigated.

Materials and Methods

Animals——Male rats of the Wistar strain, weighing 150—160 g, were employed in this experiment. The rats were divided into 3 groups of six rats each. Two groups were made diabetic by intraperitoneal injection of streptozotocin (65 mg/kg body weight, dissolved in 10 mM citrate buffer adjusted to pH 4.5).[12] Several days after the injection, the blood glucose level was determined and rats with a glucose level of 315—550 mg/dl were used as diabetic rats. These streptozotocin-induced diabetic rats exhibited a marked elevation in blood glucose level compared to non-diabetic rats (445.2 ± 34.0 *vs.* 117.6 ± 4.0 mg/dl). When ginsenoside-Rb_2 was successively given at the dose of 10 mg

once a day, the blood glucose level fell to 267.4±39.6 mg/dl after 6 d of administration (significantly decreased by 40% of the control value), as reported previously.[10,11] Animals were housed in an air-conditioned room with lighting from 6 a.m. to 6 p.m. The room temperature (about 22°C) and humidity (about 60%) were controlled automatically. They were fed on laboratory pellet chow (obtained from CLEA Japan Inc., Tokyo; protein 24.0%, lipid 3.5%, carbohydrate 60.5%) and tap water freely, but the pellet diet was removed from the rat cage at 7 a.m. on the experimental day. The body weight of the rats used in this experiment was 237.8±7.4 g in the case of non-diabetic rats, while it was slightly lower in diabetic rats. The ginsenoside-Rb_2 administered group showed an increment of about 4% in comparison with the control group (231.1±4.2 *vs.* 221.8±5.7 g). However, there were no statistically significant differences between the control and ginsenoside-Rb_2-treated groups.

Saponin——Ginsenoside-Rb_2 was isolated and purified from the extract of roots of *Panax ginseng* C.A. MEYER according to the procedure of Sanada *et al.*[7] This preparation was found to be pure by various chemical and physicochemical analyses.

Treatment with Ginsenoside-Rb_2——Ginsenoside-Rb_2 (10 mg/rat/d) dissolved in saline was administered intraperitoneally to rats for 6 d, while control rats were treated with an equal volume of saline. At 8 h after the last treatment, rats were sacrificed by means of a blow on the head, and exsanguinated. Rats were killed between 3 and 4 p.m. to avoid the effect of circadian variation. The blood was collected in a conical centrifuge tube. The serum was separated by centrifugation immediately after collection of the blood. The liver and epididymal adipose tissue were removed quickly. The liver was placed in liquid nitrogen, while the adipose tissue was cooled on ice.

Determination of Glycogen in the Liver——A portion of the liver was digested with 3 ml of 1 N NaOH in a boiling water bath for 60 min, and glycogen was precipitated by the addition of 2 ml of EtOH and purified according to the method of Roe and Dailey.[13] Liver glycogen was determined by the anthrone–H_2SO_4 method, with glucose as the standard.[14]

Determination of Glucose in the Liver——Liver was homogenized with 9 volumes of cold 0.9% NaCl. A portion of the homogenate was deproteinized with equimolar amounts of $ZnSO_4$ and $Ba(OH)_2$,[15] and precipitates were removed by centrifugation. Glucose in the supernatant was determined using a commercial reagent (Glucose B-Test Wako obtained from Wako Pure Chemical Industries, Ltd., Osaka, Japan) based on the glucose-oxidase method.[16]

Determination of Glucose-6-phosphate in the Liver[17]——Frozen liver was powdered in a porcelain mortar continuously chilled with liquid N_2. Aliquots of the powder were transferred to a chilled glass homogenizer. Five volumes of 0.6 N perchloric acid (PCA) were added and the mixture was homogenized. Precipitated proteins were removed by centrifugation at 3000×*g* for 10 min. Aliquots of the supernatant were neutralized to pH 3.5 with K_2CO_3. The solution was allowed to stand in an ice bath for about 15 min and then the supernatant was pipetted off. A portion of the supernatant was used for the assay. The supernatant fluid (1 ml), triethanolamine buffer (0.4 M; pH 7.6), nicotinamide adenine dinucleotide phosphate (NADP) (20 mM), $MgCl_2$ (0.5 M), and glucose-6-phosphate dehydrogenase (0.25 mg protein/ml) were placed in a cuvette, and the increase of optical density at 340 nm was determined with a Hitachi 200-20 spectrophotometer.

Determination of Pyruvate in the Liver[18]——Liver was homogenized with 4 volumes of 5% trichloroacetic acid (TCA) and then centrifuged at 3000×*g* for 10 min. The supernatant fluid obtained was used for the estimation of pyruvate by the 2,4-dinitrophenylhydrazone method.

Determination of Lactate in the Liver[19]——A portion of the liver was homogenized with 5 volumes of 1 N PCA and precipitates were removed by centrifugation at 3000×*g* for 10 min. Aliquots of the supernatant were neutralized to pH 3.5 with K_2CO_3. The solution was allowed to stand in an ice bath for about 10 min and then precipitated $KClO_4$ was filtered off. Lactate in the supernatant was determined by a spectrophotometric method, based on measurement of the increase of optical density at 340 nm.

Determination of Total Lipid, Triglyceride, Total Cholesterol, Phospholipid, and Non-esterified Fatty Acid in the Liver, and Adipose Tissue——Liver was homogenized with 3 volumes of ice-cold 0.9% NaCl solution. The homogenate was filtered through 4 layers of gauze and 1 ml of the filtrate was mixed with 20 ml of $CHCl_3$–MeOH (2:1, v/v). Epididymal adipose tissue was placed immediately in 20 ml of $CHCl_3$–MeOH mixture (2:1, v/v). Total lipid was extracted from both tissues by shaking. The residual tissues were then removed, and the $CHCl_3$–MeOH solution was partitioned and washed by the method of Folch *et al.*[20] The organic solution was evaporated and the residue was dried over P_2O_5 overnight. The concentration of total lipid was determined by gravimetry. A portion of the $CHCl_3$–MeOH solution extracted from both tissues was used for the estimation of triglyceride, total cholesterol, phospholipid, and non-esterified fatty acid. Determinations were performed by using commercial reagents (TG-Five Kainos obtained from Kainos Laboratories, Inc., Tokyo, Japan; Cholesterol B-Test Wako obtained from Wako Pure Chemical Industries, Ltd.; Phospholipids-Test Wako obtained from Wako Pure Chemical Industries, Ltd.; NEFA Kainos obtained from Kainos Laboratories, Inc.).

Determination of Triglyceride, Non-esterified Fatty Acid, Total Cholesterol, 3-Hydroxybutyrate, and Acetoacetate in the Serum——Triglyceride, non-esterified fatty acid, and total cholesterol were determined by using commercial reagents as described above. 3-Hydroxybutyrate was determined spectrophotometrically by measuring the increase of optical density at 340 nm resulting from the oxidation of 3-hydroxybutyrate by 3-hydroxybutyrate dehydrogenase and nicotinamide adenine dinucleotide (NAD).[21] The determination of acetoacetate was based on the decrease in

extinction at 340 nm due to the oxidation of reduced nicotinamide adenine dinucleotide (NADH).[22]

Statistics——The significance of differences between the non-diabetic and diabetic rats (control or ginsenoside-Rb_2-treated group) was tested by means of Student's *t*-test.

Results

Effect of Ginsenoside-Rb_2 on Carbohydrate Metabolites in the Liver

Compared to non-diabetic rats, streptozotocin-induced diabetic rats exhibited a significant elevation of hepatic glucose, and a tendency toward an increase of pyruvate and lactate. The contents of glycogen and glucose-6-phosphate behaved differently from those of the other carbohydrate metabolites, decreasing by approximately 20% and 12%, respectively (Table I). When ginsenoside-Rb_2 was successively given at the dose of 10 mg once a day, the hepatic glucose content fell to 9.42 mg/tissue after 6 d of administration (significantly decreased by 27% of the control value). In contrast, administration of ginsenoside-Rb_2 to rats slightly increased the amounts of glycogen and glucose-6-phosphate. These changes are in reciprocal relation to that of hepatic glucose content. However, pyruvate and lactate contents showed no appreciable changes when ginsenoside-Rb_2 was administered.

Effect of Ginsenoside-Rb_2 on the Lipid Constituents in the Liver

Table II shows the hepatic lipid constituent contents. A slight increase of the total lipid content was seen in streptozotocin-induced diabetic rats as compared with the non-diabetic

Table I. Effect of Ginsenoside-Rb_2 on Carbohydrate Metabolites in the Liver

	Glycogen (mg/tissue)	Glucose (mg/tissue)	Glucose-6-phosphate (mg/tissue)	Pyruvate (mg/tissue)	Lactate (mg/tissue)
Non-diabetic rat	168.9±17.8	8.89±0.51	0.41±0.06	0.19±0.04	11.58±0.96
	(100)	(100)	(100)	(100)	(100)
Diabetic rat					
Control	134.5±14.9	12.97±1.00	0.36±0.02	0.25±0.03	13.63±1.61
	(80)	(146)[a]	(88)	(132)	(118)
	[100]	[100]	[100]	[100]	[100]
Rb_2	152.1± 7.7	9.42±0.52	0.44±0.04	0.25±0.01	11.20±1.14
	(90)	(106)	(107)	(132)	(97)
	[113]	[73]*	[122]	[100]	[82]

Figures in parentheses are percentages of the non-diabetic or diabetic control value. *a*) *, significantly different from the non-diabetic or diabetic control value, $p<0.01$.

Table II. Effect of Ginsenoside-Rb_2 on the Lipid Constituents in the Liver

	Total lipid (mg/tissue)	Triglyceride (mg/tissue)	T. cholesterol (mg/tissue)	Phospholipid (mg/tissue)
Non-diabetic rat	188.4±4.9	26.0±2.0	8.9±0.5	91.3±1.2
	(100)	(100)	(100)	(100)
Diabetic rat				
Control	201.3±5.1	36.6±2.5	8.8±0.6	82.5±1.3
	(107)	(141)[a]	(99)	(90)[b]
	[100]	[100]	[100]	[100]
Rb_2	192.3±6.3	27.8±3.6	9.2±0.2	98.5±1.6
	(102)	(107)	(103)	(108)[a]
	[96]	[76]*	[105]	[119]**

Figures in parentheses are percentages of the non-diabetic or diabetic control value. *, significantly different from the non-diabetic or diabetic control value, $p<0.05$, *a*) $p<0.01$, *b*) **, $p<0.001$.

TABLE III. Effect of Ginsenoside-Rb_2 on the Lipid Constituents in the Adipose Tissue

	Total lipid (mg/tissue)	Triglyceride (mg/tissue)	Phospholipid (mg/tissue)	Non-esterified fatty acid (mg/tissue)
Non-diabetic rat	218.4±15.0	167.3±12.1	16.0±1.4	2.47±0.21
	(100)	(100)	(100)	(100)
Diabetic rat				
Control	131.0± 9.8	105.4± 7.0	11.8±0.9	2.15±0.11
	(60)[b]	(63)[b]	(74)[a]	(87)
	[100]	[100]	[100]	[100]
Rb_2	183.7±10.1	152.6±11.2	14.6±1.0	2.13±0.10
	(84)	(91)	(91)	(86)
	[140]**	[145]**	[124]*	[99]

Figures in parentheses are percentages of the non-diabetic or diabetic control value. *, significantly different from the non-diabetic or diabetic control value, $p<0.05$, *a*) $p<0.01$, *b*) **, $p<0.001$.

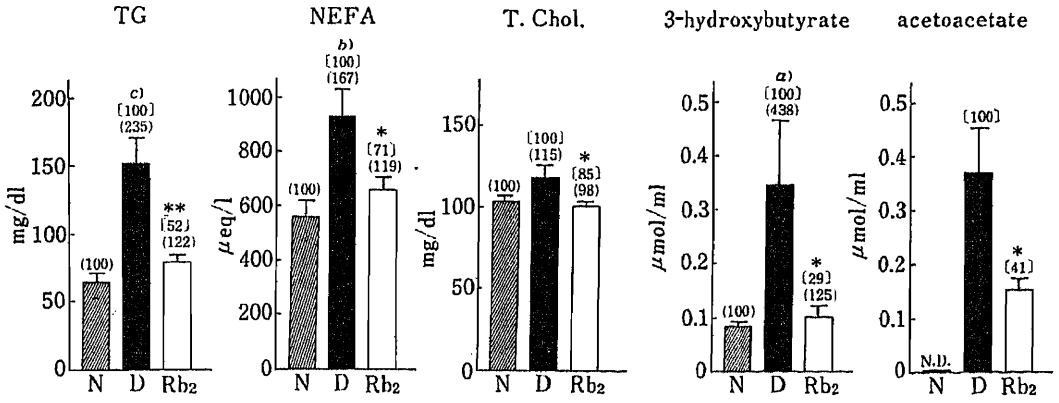

Fig. 1. Effect of Ginsenoside-Rb_2 on the Lipid Constituents in the Serum

N, non-diabetic rat; D, diabetic rat (control group); Rb_2, diabetic rat (ginsenoside-Rb_2-treated group). Figures in parentheses are percentages of the non-diabetic or diabetic control value. *a*) *, Significantly different from the non-diabetic or diabetic control value, $p<0.05$, *b*) **, $p<0.01$, *c*) $p<0.001$. Abbreviations: TG, triglyceride; NEFA, non-esterified fatty acid; T. Chol., total cholesterol.

rats. This change was reflected in the triglyceride content; as shown in Table II, the triglyceride content in the liver was increased to 36.6 mg/tissue compared with 26.0 mg/tissue in normal rats. The data in Table II further indicate that the amount of phospholipid was decreased significantly as compared with non-diabetic rats, while it was remarkably high in the ginsenoside-Rb_2-administered group. On the other hand, hepatic triglyceride was extremely low, at a near-normal level, in the ginsenoside-Rb_2-administered group. Administration of ginsenoside-Rb_2 to rats caused no appreciable changes of the total lipid and total cholesterol contents of the liver.

Effect of Ginsenoside-Rb_2 on the Lipid Constituents in the Adipose Tissue

As shown in Table III, the contents of lipid constituents were significantly decreased in streptozotocin-induced diabetic rats as compared with the non-diabetic rats, as follows: total lipid (40%), triglyceride (37%), and phospholipid (26%). A striking increase in total lipid and triglyceride contents was observed after 6 administrations of ginsenoside-Rb_2. The phospholipid content also increased by 24% when ginsenoside-Rb_2 was administered. However, non-esterified fatty acid showed no appreciable change.

Effect of Ginsenoside-Rb_2 on the Lipid Constituents in the Serum

Figure 1 shows the effect of ginsenoside-Rb_2 on the lipid constituents in the serum. The levels of triglyceride, non-esterified fatty acid, 3-hydroxybutyrate, and acetoacetate were significantly increased in diabetic rats as compared with the non-diabetic rats. The rats treated with ginsenoside-Rb_2 showed a significant decrease in triglyceride level; as shown in Fig. 1, the triglyceride level was about 48% less at the 6th day in the ginsenoside-Rb_2-treated group as compared with the control group. Similarly, administration of ginsenoside-Rb_2 to rats resulted in a significant decrease in the non-esterified fatty acid from 928 to 659 μeq/l. Furthermore, a conspicuous decrease was observed in the levels of 3-hydroxybutyrate and acetoacetate. The 3-hydroxybutyrate level, which was 0.35 μmol/ml, decreased to 0.10 μmol/ml in rats treated with ginsenoside-Rb_2. The level of acetoacetate decreased to 0.15 μmol/ml on average. The level of total cholesterol was also about 15% lower after 6 administrations.

Discussion

As reported previously,[8,9] in normal rats, intraperitoneal administration of ginsenoside-Rb_2 caused a decrease in hepatic glycogen content followed by an increase in the content of glucose-6-phosphate and in the activities of glucose-6-phosphate dehydrogenase, phosphofructokinase, malic enzyme and acetyl-CoA carboxylase in the hepatic tissue. In the adipose tissue, increased lipoprotein lipase activity, decreased hormone-sensitive lipase activity, and increased triglyceride content were found. A series of effects of ginsenoside-Rb_2 to facilitate carbohydrate and lipid metabolism were observed. Namely, in normal rats, increased metabolism in the glycolytic system, starting from the decomposition of hepatic glycogen, led to an increase in the triglyceride content in the adipose tissue through the very-low-density lipoprotein in the blood.

On the other hand, whereas no decrease in blood glucose level was found in normal rats, a single administration of ginsenoside-Rb_2 caused a slight decrease of blood glucose in diabetic rats, as reported previously.[23] In addition, when ginsenoside-Rb_2 at a dose of 10 mg/d was administered for 6 consecutive days, the blood glucose level was significantly decreased.[10]

In the present study, the blood glucose-decreasing effect was investigated in terms of carbohydrate metabolites and the levels of lipid constituents. A significant decrease in glucose of the hepatic tissue in proportion to the decrease in blood glucose was found. The contents of hepatic glucose-6-phosphate and glycogen, which had been decreased because of the diabetic condition, were slightly increased after the intraperitoneal administration of ginsenoside-Rb_2. Glucose-6-phosphate is an important compound, being at the junction of several metabolic pathways (glycolysis, gluconeogenesis, the hexose monophosphate shunt, glycogenesis, and glycogenolysis). In glycolysis it is converted to pyruvate and lactate through the Embden–Meyerhof pathway. However, the rats of the ginsenoside-Rb_2-treated group showed a lesser effect on the contents of pyruvate and lactate in the liver. There was also no accumulation of total lipid in hepatic tissue, indicating that the decreased glucose was not accumulated as lipids.

Dysbolism of lipids occurs in cases of diabetes and the dysbolism is reflected in various parameters in the blood.[24–27] In rats with streptozotocin-induced diabetes examined in the present study, the levels of triglyceride, non-esterified fatty acid, 3-hydroxybutyrate, and acetoacetate were markedly higher than those under normal conditions. However, in rats given ginsenoside-Rb_2, such levels were significantly decreased, showing a trend toward restoration to the normal state and inducing an increase in lipids in the adipose tissue.

On the basis of these findings, it is speculated that, in diabetic rats, ginsenoside-Rb_2 first

facilitates the use of blood glucose in the liver and consequently leads to an increase in triglyceride in the adipose tissue, as in normal rats. Its action to promote glycogen synthesis in the liver was also suggested. The above findings and previously reported effects[10,11] of ginsenoside-Rb_2, *i.e.*, a marked decrease in blood glucose level and improvement in diabetic symptoms such as glycosuria, polyphagia, over-drinking, and polyuria, suggest that ginsenoside-Rb_2 may be useful to treat diabetes.

References

1) H. Oura and T. Yokozawa, "Yakuyo Ninjin," ed. by H. Oura, A. Kumagai, S. Shibata, and K. Takagi, Kyoritsu Shuppan, Tokyo, 1981, p. 90.
2) T. Yokozawa, H. Seno, and H. Oura, *Chem. Pharm. Bull.*, **23**, 3095 (1975).
3) T. Yokozawa and H. Oura, *Chem. Pharm. Bull.*, **24**, 987 (1976).
4) T. Yokozawa, K. Kanai, M. Takefuji, and H. Oura, *Chem. Pharm. Bull.*, **24**, 3202 (1976).
5) T. Yokozawa, N. Kitahara, S. Okuda, and H. Oura, *Chem. Pharm. Bull.*, **27**, 419 (1979).
6) T. Yokozawa and H. Oura, *Chem. Pharm. Bull.*, **27**, 2497 (1979).
7) S. Sanada, N. Kondo, J. Shoji, O. Tanaka, and S. Shibata, *Chem. Pharm. Bull.*, **22**, 421 (1974).
8) T. Yokozawa, T. Kobayashi, H. Oura, and Y. Kawashima, *Chem. Pharm. Bull.*, **32**, 2766 (1984).
9) T. Yokozawa, T. Kobayashi, A. Kawai, H. Oura, and Y. Kawashima, *Chem. Pharm. Bull.*, **32**, 4490 (1984).
10) T. Yokozawa, T. Kobayashi, H. Oura, and Y. Kawashima, *Chem. Pharm. Bull.*, **33**, 869 (1985).
11) T. Yokozawa, M. Kiso, H. Oura, S. Yano, and Y. Kawashima, *J. Med. Pharm. Soc. WAKAN-YAKU*, **2**, 372 (1985).
12) A. Junod, A. E. Lambert, L. Orci, R. Pictet, A. E. Gonet, and A. E. Renold, *Proc. Soc. Exp. Biol. Med.*, **126**, 201 (1967).
13) J. H. Roe and R. E. Dailey, *Anal. Biochem.*, **15**, 245 (1966).
14) N. V. Carroll, R. W. Longley, and J. H. Roe, *J. Biol. Chem.*, **220**, 583 (1956).
15) T. Momose, Y. Yano, and K. Ohashi, *Chem. Pharm. Bull.*, **11**, 968 (1963).
16) Y. Kameno, "Rinsyo Kagaku Bunseki," Vol. III, ed. by M. Niwa, M. Kitamura, and M. Saito, Tokyo Kagaku Dojin, Tokyo, 1981, p. 1.
17) G. Lang and G. Michal, "Methods of Enzymatic Analysis," Vol. 3, ed. by H. U. Bergmeyer, Academic Press, New York and London, 1974, p. 1238.
18) T. E. Friedmann and G. E. Hangen, *J. Biol. Chem.*, **147**, 415 (1943).
19) I. Gutmann and A. W. Wahlefeld, "Methods of Enzymatic Analysis," Vol. 3, ed. by H. U. Bergmeyer, Academic Press, New York and London, 1974, p. 1464.
20) J. Folch, M. Lees, and G. H. Sloane Stanley, *J. Biol. Chem.*, **226**, 497 (1957).
21) D. H. Williamson and J. Mellanby, "Methods of Enzymatic Analysis," Vol. 4, ed. by H. U. Bergmeyer, Academic Press, New York and London, 1974, p. 1836.
22) J. Mellanby and D. H. Williamson, "Methods of Enzymatic Analysis," Vol. 4, ed. by H. U. Bergmeyer, Academic Press, New York and London, 1974, p. 1840.
23) T. Yokozawa, T. Kobayashi, H. Oura, and Y. Kawashima, *J. Med. Pharm. Soc. WAKAN-YAKU*, **1**, 22 (1984).
24) W. B. Kannel, T. Gordon, and W. P. Castelli, *Am. J. Clin. Nutr.*, **32**, 1238 (1979).
25) E. L. Bierman, A. P. Amaral, and B. H. Belknap, *Diabetes*, **15**, 675 (1966).
26) M. Greenfield, O. Kolterman, J. Olefsky, and G. Reaven, *Diabetologia*, **18**, 441 (1980).
27) D. Weiland, C. E. Monden, and G. M. Reaven, *Diabetologia*, **18**, 335 (1980).

[Chem. Pharm. Bull. 35(12)4878—4882(1987)]

Overproduction of Cellular and Activated Ha-*ras* Proteins by Mutating a Synthetic Gene

KAZUNOBU MIURA,[a] HIROYUKI KAMIYA,[a] MINEKO TOMINAGA,[a] YASUHIKO INOUE,[a] MORIO IKEHARA,[b] SHIGERU NOGUCHI,[c] SUSUMU NISHIMURA[c] and EIKO OHTSUKA*,[a]

Faculty of Pharmaceutical Sciences, Hokkaido University,[a] Kita-12, Nishi-6, Kita-ku, Sapporo 060, Japan, Faculty of Pharmaceutical Sciences, Osaka University,[b] 1-6, Yamada-oka, Suita, Osaka 565, Japan and National Cancer Center Research Institute,[c] 5-1-1 Tsukiji, Chuo-ku, Tokyo 104, Japan

(Received June 15, 1987)

A synthetic gene for c-Ha-*ras* (Val-12) has been modified by cassette mutagenesis using restriction sites, *Cla*I-*Bss*HII, to encode c-Ha-*ras* Gly-12. Genes for c-Ha-*ras* (Leu-61 and Arg-61) have been synthesized by joining newly synthesized oligodeoxyribonucleotides containing appropriate codons, together with previously obtained synthetic fragments. These genes have been expressed in *E. coli* and the products (p21) isolated. The guanosine diphosphate binding properties and guanosine triphosphatase activities of these p21 derivatives were studied.

Keywords——synthetic oligodeoxyribonucleotide; phosphoramidite method; restriction enzyme; cassette mutagenesis; DNA ligase; GTPase activity; GDP binding

The *ras* gene family, designated as Ha-*ras*, Ki-*ras*, and N-*ras*, codes for an evolutionally conserved group of proteins in eukaryotes,[1] and their activated products have been found to be responsible for neoplastic transformation in human cancer.[2] The cellular (c) *ras* family genes code a protein called p21, whose molecular weight is 21000. Activation of c-*ras* family genes occurs upon amino acid substitution at either the 12th or 61st codon, resulting from a single base substitution. The human c-Ha-*ras* gene in bladder carcinoma was activated by the replacement of glycine with valine at position 12, resulting from a single base change of G to T.[1b]

We have previously synthesized a gene encoding c-Ha-*ras* protein (Val-12) and the gene was expressed efficiently in *E. coli* under the control of the *E. coli* tryptophan promoter to give p21 (Val-12).[3] In order to compare the biochemical properties of activated p21 and the normal p21 (Gly-12), isolation of a large quantities of these proteins would be necessary. In this paper we describe the use of cassette mutagenesis to obtain a gene for the normal p21 (Gly-12) and the re-assembly method to construct genes encoding other forms of activated p21 (Leu-61, Arg-61) using chemically synthesized gene fragments. The isolation and biochemical properties of these overproduced gene products are also described.

Materials and Methods

Materials——Enzymes and materials were essentially the same as described.[4] A plasmid pRV12 which contained the synthetic gene for p21 (Val-12) and previously designated as pHR-L9 was obtained as described.[3] *Bcl*I and *Bss*HII were purchased from Boehringer Mannheim Co. and New England Biolabs Co., respectively.

Oligonucleotides were prepared by the phosphoramidite method using an Applied Biosystems model 380A DNA synthesizer and purified as described.[3]

Construction of Plasmids and Transformation of *E. coli*——Kination and ligation of oligodeoxyribonucleotides

were performed as described.[3] pRG12 was constructed using a duplex with 52 base pairs (bp) obtained by ligation of 6 oligonucleotides. pRL61 and pRR61 were prepared by ligation of newly synthesized oligonucleotides as well as previously synthesized fragments. Five sub-fragments consisting of about *ca.* 100 bp were first prepared for obtaining the genes, which were joined to the *Cla*I-*Sal*I site of pGH-L9[4] using essentially the same conditions as described.[3]

The base sequence was confirmed by the Maxam–Gilbert method[5] or the termination method.[6]

Isolation of p21 and Mutants

c-Ha-*ras* p21 proteins were isolated from *E. coli* harboring pRG12, pRL61 or pRR61 by the procedure reported previously.[7] The yield of p21 (Arg-61) was 30 mg from 21 of culture medium. p21 (Gly-12) and p21 (Leu-61) were also obtained in yields of 10—30 mg from the same medium.

Results

Cassette Mutation for p21 (Gly-12) Gene

To obtain p21 (Gly-12), a plasmid pRG12 was constructed by cassette mutagenesis. Sites for two restriction enzymes in a synthetic gene for p21 (Val-12)[3] were used for this purpose. The *Cla*I-*Bss*HII fragment in pRV12[3] was replaced by a duplex with 52 bp which contained the glycine codon, GGT, as shown in Fig. 1. The duplex was prepared by joining of oligodeoxyribonucleotides using T4 DNA ligase followed by treatment with *Bss*HII. pRG12 thus obtained was used to transform *E. coli* HB101 and the protein p21 (Gly-12) was produced by induction with indolylacrylic acid. The base sequence of the plasmid was determined to confirm that the mutation had occurred at the 12 position.

Construction of Plasmids Containing Genes for p21 (Leu-61) and p21 (Arg-61)

For substitution of Gln-61 with leucine, two oligodeoxyribonucleotides were prepared to alter CAA to CTG and ligated with the rest of the fragments. The gene was joined to the

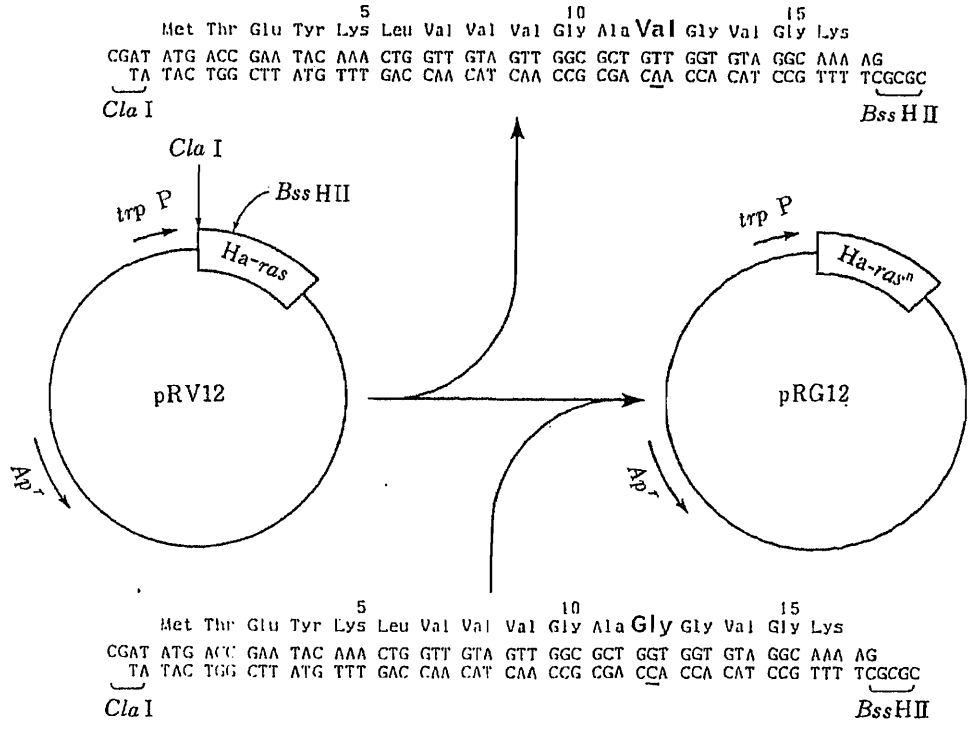

Fig. 1. Mutation at the 12th Position by Cassette Mutagenesis

The vector carrying c-Ha-*ras* (Val-12) gene was cleaved with *Cla*I and *Bss*HII. Then the duplex DNA cassette was ligated with the gapped plasmid. Ha-*ras*^{n} indicates the normal Ha-*ras* gene.

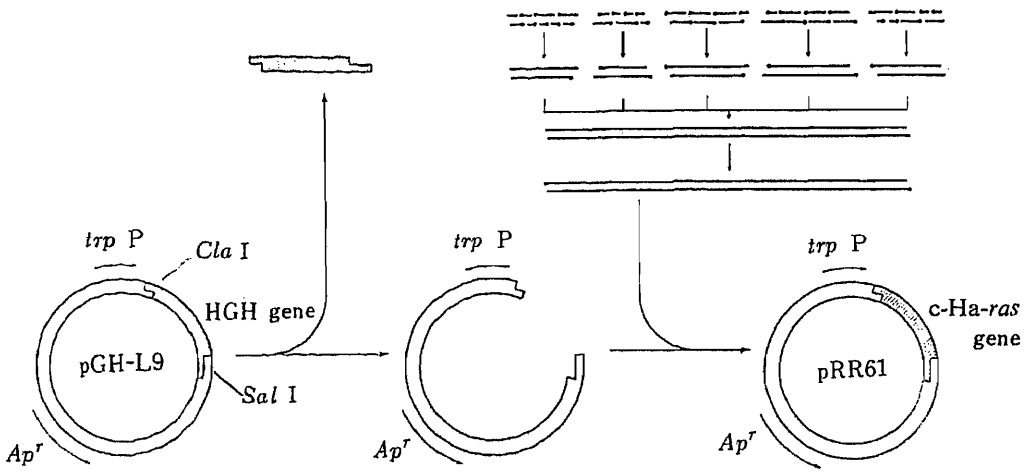

Fig. 2. Reconstruction of Mutated Genes and Their Insertion into the Expression Vector

The phosphorylated oligonucleotides were annealed and ligated. Five subfragments were further ligated to yield the whole gene. pGH-L9 that carries *E. coli trp* promoter was cleaved with *Cla*I and *Sal*I. The synthetic c-Ha-*ras* gene was inserted into the vector by ligation. A dot (•) indicates terminal phosphate.

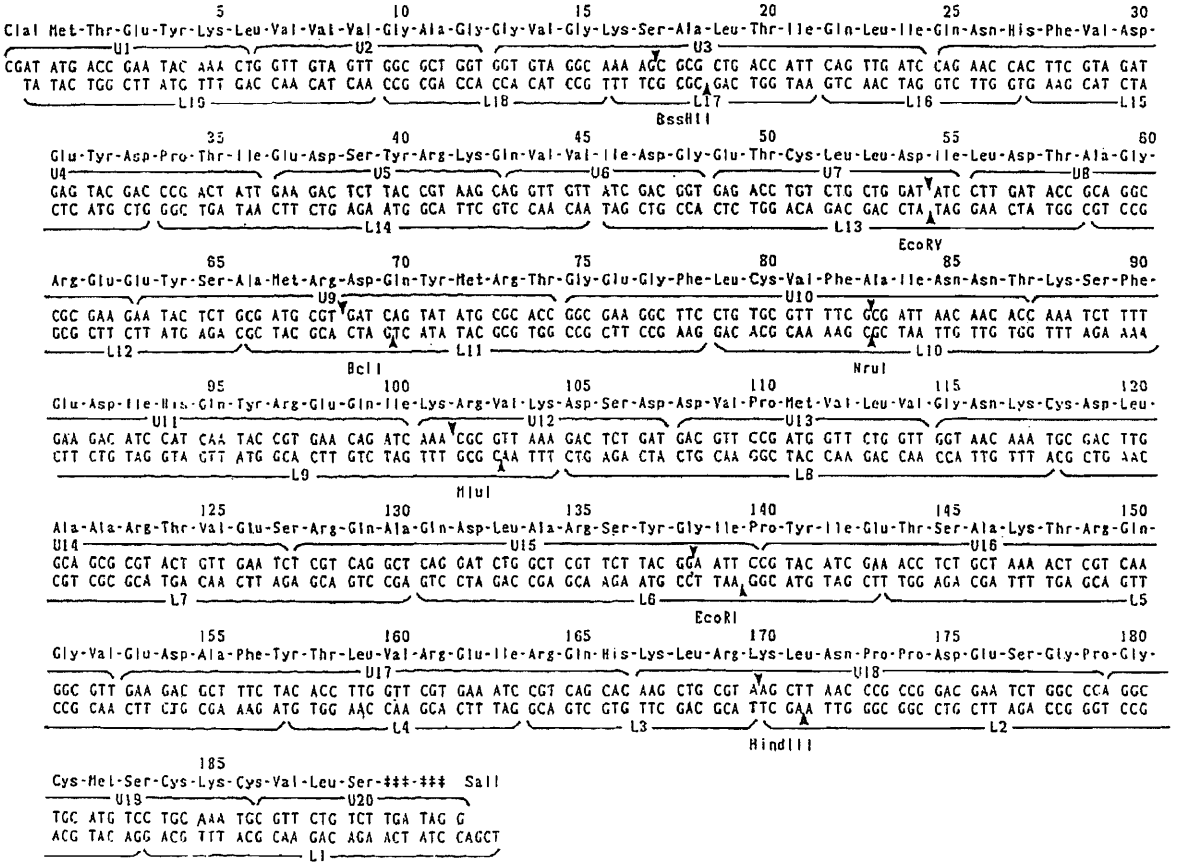

Fig. 3. The Amino Acid Sequence of p21 (Arg-61) and Its Synthetic Gene Having 7 Restriction Sites

Lines indicate oligonucleotide fragments for synthesis of the gene. ▲ indicates a cleavage site.

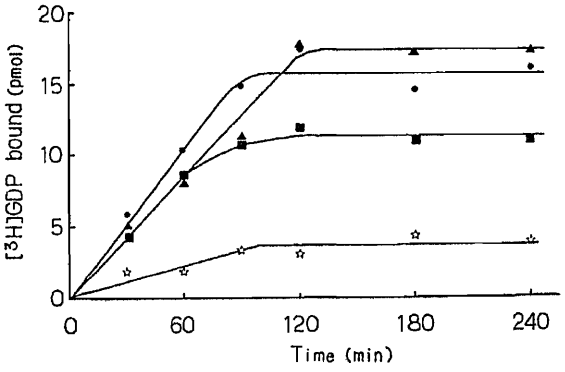

Fig. 4. [^{3}H]GDP Binding Activity was Measured Using 40 pmol of Each Purified p21

p21 was incubated with 4 μM [^{3}H]GDP in 50 mM Hepes-NaOH (pH 7.5)/0.5 mM $MgSO_4$/100 mM NaCl/1 mM dithiothreitol (total volume 50 μl) at 37 °C. The reaction was stopped at 0 °C with 1 ml of ice-cold 50 mM Hepes-NaCl (pH 8.0)/0.25 mM $MgSO_4$. The radioactivity retained on a nitrocellulose filter was counted.

●—●, Gly-12; ▲—▲, Val-12; ■—■, Leu-61; ☆—☆, Arg-61.

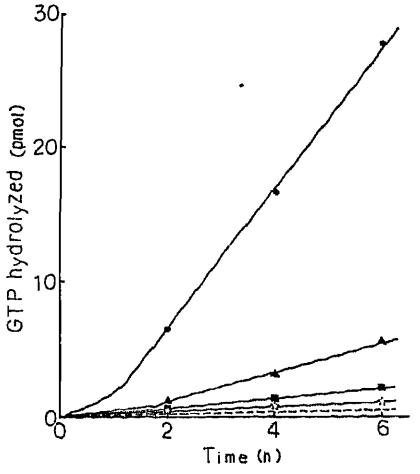

Fig. 5. GTPase Activity was Measured Using 40 pmol of Each p21

p21 was incubated with 4 μM [γ-^{32}P]GTP at 37 °C. The reaction was stopped at 0 °C by addition of 1 M $HClO_4$/1 mM KH_2PO_4, then 20 mM ammonium molybdate and isopropyl acetate were added. After vigorous stirring and centrifugation, the radioactivity in the organic phase was counted.

●—●, Gly-12; ▲—▲, Val-12; ■—■, Leu-61; ☆—☆, Arg-61; ---- represents the control.

larger fragment of the *Cla*I-*Sal*I digest of pGH-L9 to yield pRL61.

For construction of pRR 61 containing the codon for Arg at the 61 position, oligodeoxyribonucleotides having CGC or the complementary sequence were used. Six other oligonucleotides were also used to incorporate three restriction sites, *Nru*I, *Mlu*I and *Eco*RV, in pRR61 (Fig. 2). The base sequence of the newly synthesized gene was confirmed by the Maxam-Gilbert method. The structure is shown in Fig. 3.

Properties of Normal p21 (Gly-12) and Mutants (Val-12, Leu-61 and Arg-61)

The guanosine diphosphate (GDP)-binding activities of p21 (Leu-61 and Arg-61) were measured together with those of the normal p21 and p21 (Val-12) using [^{3}H]GDP.[7a] The results are shown in Fig. 4. All p21 proteins bound GDP with different velocities and reached equilibrium after 2 h. Inhibition was observed on addition of a 20-fold excess of GDP, guanosine triphosphate (GTP) and dGTP. However, other nucleoside triphosphates (adenosine triphosphate (ATP), cytidine triphosphate (CTP) and uridine triphosphate (UTP)) did not have any effect (data not shown). It may be concluded that activation of p21 dose not affect the base specificity in binding.

The GTPase activities of these[8] p21 proteins were compared, as shown in Fig. 5. Mutations at positions 12 and 61 caused marked decreases of the activity.

Discussion

Mutations of a synthetic gene were performed by two different approaches in the present work. The gene was originally designed for cassette mutagenesis of the 12th position. The mutated gene was expressed with high efficiency in *E. coli*, and p21 (Gly-12) was obtained in quantity, which allowed crystallization of the protein. The 61st position was mutated by reconstruction of the gene using appropriate synthetic oligonucleotides. This method was

found to be feasible in this size of gene, since synthetic oligomers previously obtained could mostly be used and ligation of properly designed gene fragments would give higher yields of mutants than mutageneses involving cleavage reactions with restriction enzymes.

Several site-directed mutageneses of c-Ha-*ras* genes yield p21 proteins mutated at the 12th and 61st codons.[9] The present result on the GTPase activity is consistent with that reported earlier.[9c]

The mutated genes described here can be further used to alter the structure of p21 in large areas. Studies along this line will be reported elsewhere.

Acknowledgements This work was supported in part by a Grant-in-Aid from the Ministry of Health and Welfare for a Comprehensive 10-Year Strategy for Cancer Control, Japan.

References

1) *a*) E. H. Chang, M. A. Gonda, R. W. Ellis, E. M. Scolnick and D. W. Lowrg, *Proc. Natl. Acad. Sci. U.S.A.*, **79**, 4848 (1982); *b*) E. Taparowsky, K. Shimizu, M. Goldfarb and M. Wigler, *Proc. Natl. Acad. Sci. U.S.A.*, **80**, 2112 (1983).
2) H. Land, I. F. Parada and R. A. Weinberg, *Science*, **222**, 771 (1983).
3) K. Miura, Y. Inoue, H. Nakamori, S. Iwai, E. Ohtsuka, M. Ikehara, S. Noguchi and S. Nishimura, *Jpn. J. Cancer Res.*, **77**, 45 (1986).
4) M. Ikehara, E. Ohtsuka, T. Tokunaga, Y. Taniyama, S. Iwai, K. Kitano, S. Miyamoto, T. Ohgi, Y. Sakuragawa, K. Fujiyama, T. Ikari, M. Kobayashi, T. Miyake, S. Shibahara, A. Ono, T. Ueda, T. Tanaka, H. Baba, T. Miki, A. Sakurai, T. Oishi, O. Chisaka and K. Matsubara, *Proc. Natl. Acad. Sci. U.S.A.*, **81**, 5956 (1984).
5) A. M. Maxam and W. Gilbert, *Proc. Natl. Acad. Sci. U.S.A.*, **74**, 560 (1977).
6) F. Sanger, S. Nicklen and A. R. Coulson, *Proc. Natl. Acad. Sci. U.S.A.*, **74**, 5463 (1977).
7) *a*) J. B. Gibbs, I. S. Sigal, M. Poe and E. M. Scolnick, *Proc. Natl. Acad. Sci. U.S.A.*, **81**, 5704 (1984); *b*) R. B. Stein, P. S. Robinson and E. M. Scolnick, *J. Virol*, **50**, 343 (1984).
8) E. De Vendittis, M. Masullo and V. Bocchini, *J. Biol. Chem.*, **261**, 4445 (1986).
9) *a*) P. H. Seeburg, W. W. Colby, D. J. Capon, D. V. Goeddel and A. D. Levinson, *Nature* (London), **312**, 71 (1984); *b*) C. J. Der, T. Finkel and G. M. Cooper, *Cell*, **44**, 167 (1986); *c*) R. W. Sweet, S. Yokoyama, T. Kamata, J. R. Feramisco, M. Rosenberg and M. Gross, *Nature* (London), **311**, 273 (1984).

[Chem. Pharm. Bull. 35(12)4883—4890(1987)]

Effect of Skin Surface Temperature on Transdermal Absorption of Flurbiprofen from a Cataplasm

HITOSHI SASAKI,*[,a] JUNZO NAKAMURA,[a] JUICHIRO SHIBASAKI,[a] YOSHIO ISHINO,[b] KAZUHIRO MIYASATO,[b] and TOSHIYUKI ASHIZAWA[b]

Faculty of Pharmaceutical Sciences, Nagasaki University,[a] Bunkyo-machi 1–14, Nagasaki 852, Japan and Research Laboratories, Sansho Pharmaceutical Co., Ltd.,[b] Nishitomita 262–1, Honjo, Saitama 367, Japan

(Received April 23, 1987)

Transdermal absorption of flurbiprofen (FP) from a cataplasm (CFP) and its anti-inflammatory effect were investigated in the rat under various skin temperature conditions. As the skin temperature was raised, the plasma concentration of FP after application of the cataplasm increased significantly. It was demonstrated by a release and *in vitro* penetration experiment that skin penetration is the rate-determining step for absorption, and both release and penetration increased with a rise of temperature. Moreover, the *in vivo* transdermal absorption behavior was estimated by a deconvolution method from the plasma concentration data after intravenous administration and topical application of FP.

The Arrhenius plot of the *in vitro* penetration data at various temperature gave a nearly straight line and the activation energy calculated from the slope was 16.7 kcal/mol. The skin accumulation of FP decreased with a rise of temperature in the *in vivo* experiment while no significant change was seen in the *in vitro* experiment, suggesting participation of the increase of blood flow in the former experiment.

Though the anti-inflammatory effect was demonstrated at the normal skin temperature and under cooling, the effect was not found under warming. In addition, a considerable effect was observed with a control CFP which is free from FP when used under cooling.

From these results, it is suggested that the transdermal absorption of FP from CFP increased with a rise of skin surface temperature, and both factors, the concentration of FP absorbed and topical cooling, contribute to the anti-inflammatory effect.

Keywords——flurbiprofen; cataplasm; percutaneous absorption; plasma level; skin temperature; deconvolution; release rate; Arrhenius plot; skin accumulation; anti-inflammatory effect

Recently, local chemotherapy by percutaneous drug delivery has attracted renewed interest from the standpoint of optimization of drug delivery.[1] Topical application should concentrate the drug in the tissues to which it is applied and diminish the drug concentration in other tissues and blood. It could also minimize the side effect of gastrointestinal damage and the first-pass effect observed in the case of oral administration.[2]

Flurbiprofen (FP) is an orally active, nonsteroidal anti-inflammatory drug found to be effective in the treatment of rheumatoid arthritis, but its side effect of gastrointestinal damage has limited its utilization.[3] Therefore, topical application of FP warrants investigation as an alternative to oral treatment. However, it is well-known that most drugs can not penetrate the skin readily, and many factors may influence the skin penetration.[4] In this context, we have reported that a rise of skin surface temperature could increase the transdermal absorption of methyl salicylate from a cataplasm.[5]

In the present study, transdermal absorption characteristics of FP from a cataplasm at various skin temperatures were investigated with both *in vitro* and *in vivo* techniques. In addition, the anti-inflammatory effects at various skin temperatures were evaluated.

Experimental

Materials——FP was obtained commercially (Nippon Zanbon Co., Ltd., Tokyo, Japan) and used without further purification. Styrene isoprene block copolymer was also obtained commercially (Kimura Industry Co., Ltd., Tokyo, Japan). All other chemicals were of reagent grade.

Preparation of a Cataplasm of FP——A cataplasm (CFP) containing FP was prepared by Sansho Pharmaceutical Co., Ltd. (Saitama, Japan). The formulation contains FP (2 mg), olive oil (115 mg), styrene isoprene block copolymer (78 mg) and other minor constituents (19 mg) in 14 cm^2. The CFP has a water-absorbent resin sheet on the drug reservoir phase to cool the skin surface. The structure of the cataplasm is shown in Fig. 1. CFP containing no FP was prepared to evaluate the net effect of cooling on inflammation.

Control of Skin Surface Temperature——In the *in vivo* absorption and the anti-inflammatory experiments, the skin surface temperature after CFP application was controlled by the following treatments. Condition A: A polyvinyl bag containing ice-water was put on the CFP. Condition B: Water was added to a water-absorbent resin sheet of the CFP. Condition C: No treatment was carried out. Condition D: A chemical warmer (Hakugen Co., Ltd., Tokyo, Japan) was put on the CFP. In the anti-inflammatory experiment, condition D′ was used instead of condition D; in this case, the rat foot on which the CFP was applied was wrapped with a polyvinyl bag and placed in a water bath at 41°C.

By manual monitoring during each treatment, the skin temperature could be maintained within a narrow range, as shown in Table I. The skin surface temperature was measured with a thermometer having a platinum resistance sensor (model EH200-06, Chino Works. Ltd., Tokyo, Japan) during experiments.

***In Vivo* Transdermal Absorption Experiment**——Male Wistar albino rats weighing 250—300 g, whose abdominal hair was removed with animal clippers and a shaver at 24 h before the experiment, were used under anesthesia with pentobarbital, given intraperitoneally. CFP (available area; 14 cm^2) covered with a protective peel liner was applied on the abdominal skin, and treatment A, B, C or D was employed for controlling the skin temperature. After the temperature had reached a constant level, the liner was removed from the CFP to start the absorption experiment. Blood samples were collected from the jugular vein at fixed intervals. A mixture of 0.2 ml of plasma and 0.2 ml of MeOH was shaken and centrifuged, and FP in the supernatant was determined by HPLC.

Intravenous Administration Experiment——A polyethylene glycol solution of FP (2.5 mg/ml) was injected into the femoral vein of three rats weighing 250—300 g (dose; 500 μg/head), and the plasma concentration of FP was determined by high performance liquid chromatography (HPLC) at fixed intervals. The mean plasma levels of FP (C_p) *versus* time obeyed biexponential kinetics as represented by Eq. 1.

$$C_p = 9.18e^{-2.15t} + 8.77e^{-0.16t} \quad (1)$$

Release and *in Vitro* Penetration Experiments——A diffusion cell similar to that reported by Loftsson and Bodor,[6] was used for the release and *in vitro* penetration experiments. It has a 6.8 cm^2 donor area and a 49 ml receptor volume. Cellulose membranes (pore size 24 Å, Visking Co., Ltd., U.S.A) were used as diffusion membranes for the release experiment. The full-thickness abdominal skin excised from a rat weighing 250—300 g, whose hair had been removed as in the *in vivo* experiment, was used for the *in vitro* penetration experiment. The diffusion cell and receptor medium, isotonic sodium phosphate-buffered saline (pH 7.4) containing kanamycin sulfate (100 ppm), were placed in a thermostated chamber at least 10 h before the experiment, in which the temperature was regulated at the mean of each *in vivo* experiment. Just before the experiment, the excised skin or cellulose membrane was mounted in the diffusion cell, the receptor phase was filled with the medium, and finally the CFP was applied on the skin or membrane surface of the donor side. The receptor phase was stirred with a magnetic stirrer covered with an adiabator

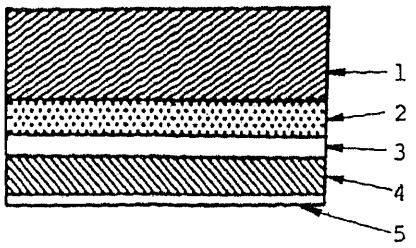

Fig. 1. Structure of CFP (Section Diagram)

1, Rayon-polyester coverstrip; 2, water-absorbent resin sheet; 3, polyester-unwoven textile, the upper side of which is laminated with polyethylene; 4, drug reservoir; 5, protective peel liner.

TABLE I. Skin Surface Temperature of Abdomen and Foot in Rats under Various Conditions

Temperature condition[a]	Temperature (°C)			
	Abdomen		Foot	
	Mean	Range	Mean	Range
A	24.7	23.4—25.8	7.0	6.5— 7.3
B	34.2	33.6—34.7	14.9	13.4—16.4
C	36.5	35.0—37.2	21.0	20.2—21.7
D and D′	41.7	41.0—42.5	40.0	38.6—40.2

a) See the text.

which serves to prevent heat flow. At appropriate intervals, an aliquot (0.5 ml) of the receptor fluid was withdrawn and mixed with 0.5 ml of MeOH. After shaking followed by centrifuging, the supernatant was used for HPLC assay.

Skin Accumulation——At the end of the experiments, the skin removed from the cell in the *in vitro* experiment and that excised from the rat abdomen in the *in vivo* experiment were placed in a test tube containing a mixture of phosphate buffer solution (pH 7.4, 25 ml) and MeOH (25 ml). After homogenization followed by filtration, FP in the filtrate was determined by HPLC.

Determination of Remaining FP in CFP——At the end of the *in vitro* and *in vivo* experiments, the CFP was removed and placed in a test tube containing 20 ml of chloroform. The tube was shaken for 20 min, then 30 ml of MeOH was added and the tube was shaken again for 5 min. After centrifugation, the supernatant was subjected to HPLC assay.

Anti-inflammatory Test——The anti-inflammatory effect was evaluated in terms of the suppressive effect on the swelling edema according to the method of Riesterer and Jaques[7] with minor modifications. The edema was induced by dropping a 100 g iron weight from 1 m height onto the right hind paw of the rats (150—200 g). A CFP or CFP containing no FP was immediately applied to the edema area and foot skin temperature was controlled as described above. The CFP was removed hourly and the volume of the right hind paw was measured by using a plethysmometer (model KN-357, Natsume Works Co., Ltd., Tokyo, Japan). After the measurement, the foot was again covered with the CFP. The swelling (percent) was calculated as $100 \times (b/a - 1)$ (a, paw volume before producing the edema; b, paw volume measured hourly after producing the edema) in order to evaluate the effect.

Analytical Method——FP was determined by the use of an HPLC system according to the method of Albert *et al.*[8] with minor modifications. The HPLC apparatus (LC-6A pump, Shimadzu Co., Ltd., Kyoto, Japan; model 7125 injector, Rheodyne Inc., California, U.S.A.) was equipped with a fluorescence spectromonitor (RF-530, Shimadzu Co., Ltd.). The column was a bonded octadecylsilane-silica gel (Fine SIL C_{18}, Japan Spectroscopic Co., Ltd., Tokyo, Japan) of 10 μm particle size (250 × 4.6 mm i.d.) and was used at room temperature. A mixture of MeOH–0.01 M citrate buffer solution (75:25, v/v) was used as the mobile phase at a flow rate of 1.0 ml/min after being passed through a 0.45 μm pore size membrane filter (Toyo Roshi Co., Ltd., Tokyo, Japan). The peak was detected fluorometrically at 250 and 315 nm (excitation and emission, respectively). Standard solutions were chromatographed and calibration lines were constructed on the basis of peak-area measurements.

Estimation of *in Vivo* Percutaneous Absorption Behavior of FP in CFP by Deconvolution——For calculation, plasma FP concentrations after intravenous injection and percutaneous application of CFP were assigned as weight and output functions, respectively. Practically, the theoretical values obtained from Eq. 1 were used as the data for the weight function instead of experimental data. This served to prevent the divergence of solutions and to generate any desired datum corresponding to the other function. Mean plasma concentrations obtained in the *in vivo* transdermal absorption experiment (Fig. 2) were used as the data for the output function. In addition, the solutions were obtained after normalization of the data with respect to dose: 500 μg in intravenous injection and 2000 μg in percutaneous application.

Analysis of Data with a Microcomputer——The results of the intravenous administration experiment were analyzed on the basis of biexponential kinetics. The *in vivo* absorption behavior of FP estimated by deconvolution and the experimental data obtained in the release and *in vitro* penetration experiments were analyzed on the basis of single exponential kinetics. These analyses were performed by means of a microcomputer.

Results

In Vivo Transdermal Absorption Experiment

Figure 2 shows the plasma concentration of FP after application of the CFP on the rat abdomen under conditions A, B, C and D. As the skin temperature was raised, the plasma concentration of FP increased significantly. Under all conditions except for D, the plasma levels increased initially and thereafter a nearly constant level was maintained.

Release and *in Vitro* Penetration Experiments

The release of FP from CFP is illustrated in Fig. 3. The release was very fast under all conditions and the recoveries in 3 h were higher than 70% of the initial content. Figure 4 represents the penetration of FP through an excised rat skin. The penetration of FP was relatively slow and the recoveries were somewhat low in comparison with release from the CFP. The release and penetration were both greatly enhanced by a rise of skin temperature.

Absorption Behavior Estimated by Deconvolution

Since it is difficult to measure the transdermal absorption behavior of FP experimentally,

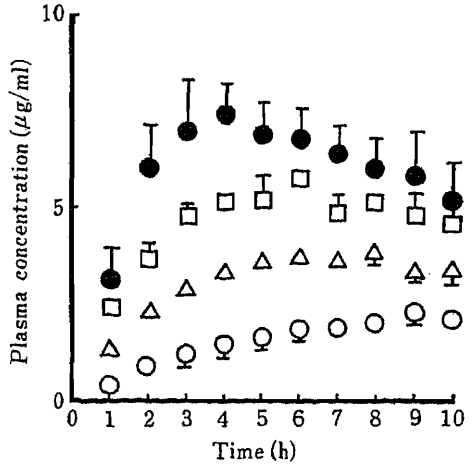

Fig. 2. Plasma Concentration of FP after Application of CFP under Various Temperature Conditions

○, condition A; △, condition B; □, condition C; ●, condition D. Each point represents the mean ± S.E. from at least 3 rats.

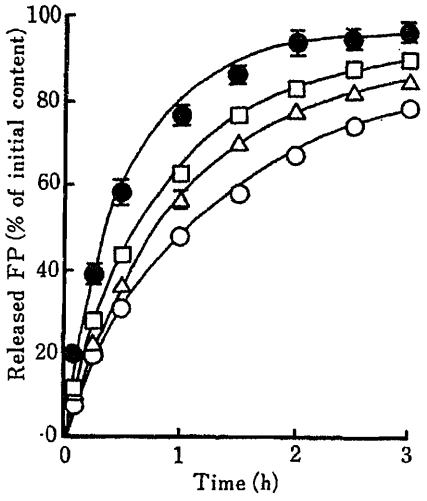

Fig. 3. Release of FP from CFP across a Cellulose Membrane at Various Temperatures

○, 24.7°C; △, 34.2°C; □, 36.5°C; ●, 41.7°C. Each point represents the mean ± S.E. from 3 experiments. The solid lines are calculated values based on first-order kinetics.

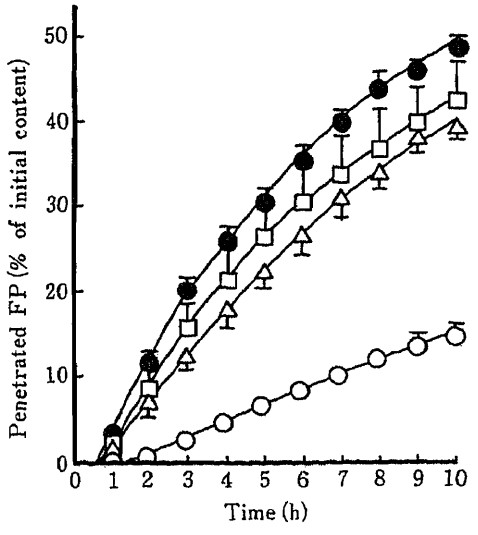

Fig. 4. Penetration of FP in CFP through Excised Rat Skin at Various Temperatures

○, 24.7°C; △, 34.2°C; □, 36.5°C; ●, 41.7°C. Each point represents the mean ± S.E. from at least 3 experiments. The solid lines are calculated values based on first-order kinetics.

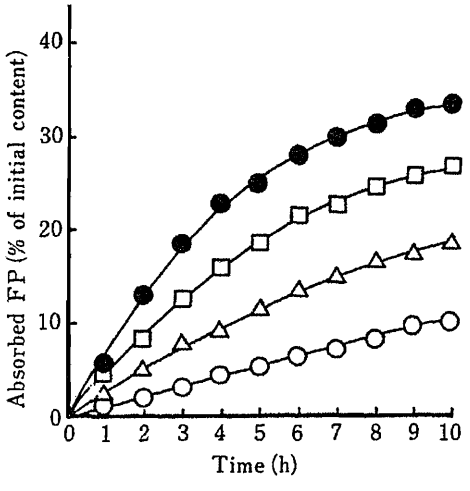

Fig. 5. Absorption Behavior of FP from CFP Calculated by a Deconvolution Method from the Data Obtained in Intravenous and Transdermal Experiments

○, condition A; △, condition B; □, condition C; ●, condition D. Details are given in the experimental section.

it was estimated by a deconvolution method as described in the experimental section. The time course of absorbed FP thus obtained (% of initial content) is shown in Fig. 5.

The absorption of FP was greatly enhanced by a rise of temperature and it was found that the flux under condition D was about 4 times higher than that under condition A.

Skin Accumulation

Figure 6 shows the skin accumulation of FP at 10 h in the *in vivo* and *in vitro* experiments.

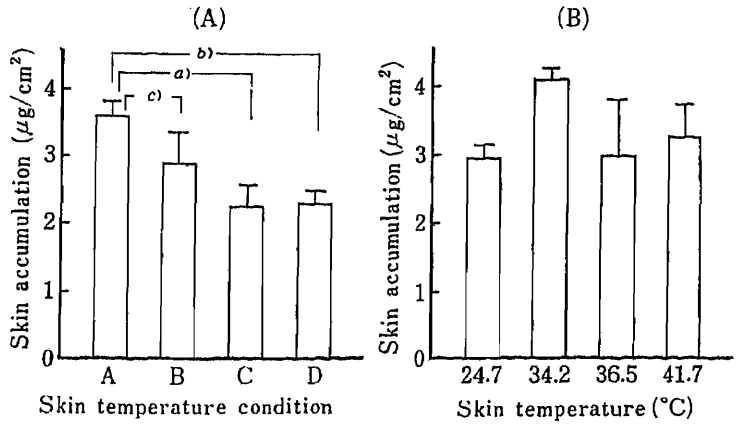

Fig. 6. Skin Accumulation of FP at 10 h after Application of CFP in the *in Vivo* (A) and *in Vitro* (B) Experiments

Results are expressed as the mean ± S.E. at least 3 experiments. Statistical evaluations were performed by using Student's *t*-test (*a*), $p<0.05$; *b*), $p<0.01$; *c*), not significantly different).

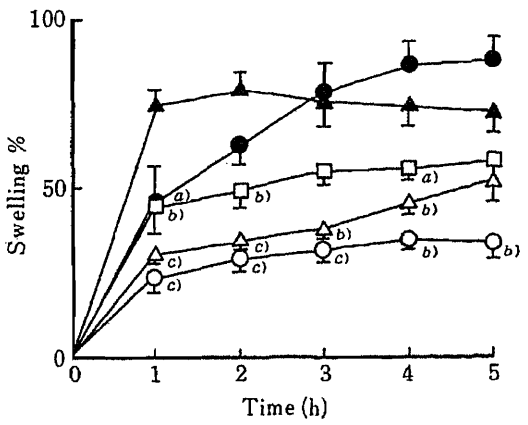

Fig. 7. Effect of CFP under Various Temperature Conditions on the Swelling Edema in Hind Paw of Rats Produced by a Strong Blow

▲, control; ○, condition A; △, condition B; □, condition C; ●, condition D'. The rats in the control group were given no treatment after edema induction. Each point represents the mean ± S.E. from at least 4 rats. Statistical evaluations were performed by using Student's *t*-test. Significantly different from control (*a*) $p<0.05$; *b*) $p<0.01$; *c*) $p<0.001$). Significant differences from the corresponding data in Fig. 8 were found at 2 and 3 h in condition B, and at 4 h in condition C ($p<0.05$); at 1 and 4 h in condition B, and at 3 and 5 h in condition C ($p<0.02$).

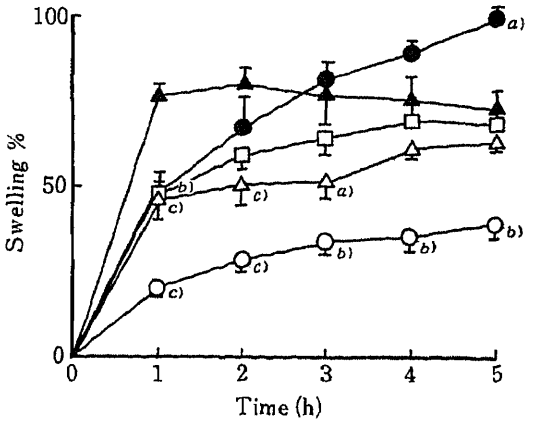

Fig. 8. Effect of CFP without FP under Various Temperature Conditions on the Swelling Edema Produced by a Strong Blow in Hind Paw of Rats

For details, see the legend to Fig. 7.

A tendency for skin accumulation of FP to decrease with a rise of skin temperature was observed in the *in vivo* experiment, but not in the *in vitro* experiment.

Anti-inflammatory Effect

Anti-inflammatory effects of CFP at various skin temperatures are shown in Fig. 7. The effect was evaluated in terms of the suppressive effect on the swelling edema in the foot of rats produced by a strong blow. The edema was suppressed significantly under condition C and especially under cooling conditions A and B, but no effect was found under warming

condition D′.

Figure 8 shows the anti-inflammatory effect of temperature when CFP containing no FP was applied. The application under cooling conditions (A and B) suppressed the swelling significantly.

Discussion

In the present investigation, the *in vivo* and *in vitro* transdermal absorption and pharmacological effect of FP in the CFP were examined under various temperature conditions. A rise of skin temperature resulted in an increase of the FP plasma concentration (Fig. 2), as in the case of salicylic acid,[9] carbinoxamine[9] and methyl salicylate.[5] Moreover, the release (Fig. 3) and skin penetration (Fig. 4) of FP were also enhanced with a rise of temperature.

Release data (Fig. 3) were analyzed by the use of Eq. 2:

$$A=FA_0(1-e^{-k_r t}) \tag{2}$$

where A is the amount of FP appearing in the receptor phase, F is the available fraction of the applied dose (A_0) and k_r is a release rate constant. On the other hand, penetration data were analyzed by the use of Eq. 3 in which a lag time was taken into consideration, based on the experimental data in Fig. 4:

$$A=FA_0[1-e^{-k_p(t-\tau)}] \tag{3}$$

where k_p is a penetration rate constant and τ is a lag time. Furthermore, the deconvolution data were analyzed by the use of Eq. 2 using k_a (absorption rate constant) instead of k_r, where A is the absorbed amount of FP, since the lag times were practically not recognized in Fig. 5. The values of parameters involved in the equations are presented in Table II. Our findings from Table II may be summarized as follows. (1) With a rise of temperature, all the rate

Table II. Parameters of the Absorption Behavior of FP from CFP

Data of	Parameter	Temperature (°C)			
		A (24.7)	B (34.2)	C (36.5)	D (41.7)
Release experiment[a]	k_r (h^{-1})	0.94	1.09	1.32	1.99
	F	0.81	0.87	0.89	0.94
In vitro penetration experiment[b]	k_p (h^{-1})	0.04	0.10	0.13	0.15
	F	0.57	0.69	0.60	0.65
	Lag time (h)	1.42	0.79	0.73	0.60
Deconvolution[a]	k_a (h^{-1})	0.03[c]	0.07	0.14	0.20
	F	0.36	0.36	0.36	0.39

a) Analyzed on the basis of single exponential kinetics with an available fraction (F). *b*) Analyzed on the basis of single exponential kinetics with an available fraction (F) and a lag time. *c*) This value was obtained by analysis at a fixed F value of 0.36, the value for conditions B and C; good convergence was usually not obtainable without such fixing.

Table III. Remaining FP in CFP 24 h after the Start of the Experiment under Temperature Condition C

Experiment	Remaining FP (% of applied dose)	Experiment	Remaining FP (% of applied dose)
In vitro penetration	13, 19	*In vivo* absorption	53, 57

constants (k_r, k_p and k_a) increased. (2) The value of k_r was considerably larger than that of k_p under all conditions, indicating that skin penetration is the rate-determining step for absorption. (3) The value of k_a is close to that of k_p under all conditions, reflecting a good agreement of the *in vivo* and *in vitro* experiments. (4) Lag times recognized in the *in vitro* experiments become shorter with a rise of temperature, which might be further evidence for increasing ease of transfer of the drug across the skin with increasing temperature. Disappearance of the lag times in the *in vivo* data (Fig. 5) is probably due to the blood flow in the skin. (5) The available fraction of FP(F) in release experiments was in the range of 0.81 to 0.94 and showed a tendency to increase with a rise of temperature. On the other hand, the values of F from the *in vitro* penetration experiment and deconvolution data were in the ranges of 0.57 to 0.69 and 0.36 to 0.39, respectively, and showed no dependence on temperature. The difference of F between these two cases was confirmed by measurement of the remaining FP in CFP at 24 h after the start of the experiments under condition C (Table III). It is considered that the release of FP from CFP might be limited depending on the experimental method employed.

Blank *et al.*[10] studied the rate of percutaneous absorption of the alcohols from MeOH through octanol over a temperature range 5—50°C *in vitro* and demonstrated that their flux was an exponential function of the temperature. Further, they calculated the activation energies of the alcohols from an Arrhenius plot. In the present investigation, an Arrhenius plot was prepared of the data from the *in vitro* penetration experiment (Table II), to which one more point at 29°C ($k_p=0.05\,h^{-1}$) was added by performing another series of experiments at that temperature. An approximately straight line was obtained and the apparent activation energy calculated from its slope was 16.7 kcal/mol. Blank *et al.* reported that the mean values of activation energies of polar and non-polar alcohols were 16.5 and 10.0 kcal/mol, respectively. The activation energy of FP was nearly equal to that of polar alcohols in spite of its possible lipophilicity. FP, with its complex molecular structure, might interact more strongly with the skin, resulting in a larger activation energy.

The skin accumulation of FP was not clearly related with skin temperature in the *in vitro* experiment (Fig. 6B). A tendency for decreasing accumulation with increasing temperature was, however, recognized in the *in vivo* experiment (Fig. 6A), and this might be due to enhancement of drug clearance resulting from an increase of blood flow.

A suppressive effect of CFP on the swelling edema in the foot of rats was observed at normal temperature (condition C) and especially on cooling (conditions A and B). However, the effect was not apparent under condition D (Fig. 7) where the plasma levels of FP were the highest. Thus, the skin temperature has a greater influence than the absorbed amount of FP. It is well-known that cooling itself has an anti-inflammatory effect. In fact, CFP containing no FP showed an appreciable effect simply due to the cooling action (Fig. 8), but CFP was more effective when it contained FP, as seen in conditions B and C (compare the corresponding data in Figs. 7 and 8).

In conclusion, it is suggested that the transdermal absorption of FP from CFP increased with a rise of skin surface temperature, and both the concentration of FP absorbed and topical cooling are important factors in the use of CFP for topical inflammation. On the other hand, the increase of the drug absorption that occurs on warming might be advantageous when a systemic effect of FP is required after topical application.

Acknowledgement We with to thank Kyoko Ideguchi and Kazuyoshi Kanai for skilled technical assistance. This work was supported in part by a Grant-in-Aid for Scientific Research from the Ministry of Education, Science and Culture, Japan.

References

1) R. Brandau and B. H. Lippold, "Dermal and Transdermal Absorption," Wissenschaftliche Verlagsgesellschaft

mbH, Stuttgart, 1982; F. Theeuwes, *Pharmacol. Ther.*, **13**, 149 (1981).
2) Y. W. Chien, *Drug Dev. Ind. Pharm.*, **9**, 497 (1983).
3) E. M. Glenn, N. Rohloff, B. J. Bowman, and S. C. Lyster, *Agents and Actions*, **3**, 210 (1973); S. S. Adams, *Drugs Exptl. Clin. Res.*, **2**, 27 (1977).
4) R. J. Scheuplein and I. H. Blank, *Physiological Reviews*, **51**, 702 (1971); A. M. Kligman, *Drug Dev. Ind. Pharm.*, **9**, 521 (1983); C. R. Behl, G. L. Flynn, E. E. Linn, and W. M. Smith, *J. Pharm. Sci.*, **73**, 1287 (1984); P. H. Dugard and R. C. Scott, *Int. J. Pharmaceut.*, **28**, 219 (1986).
5) H. Sasaki, Y. Kubota, T. Tomita, J. Nakamura, J. Shibasaki, I. Ohya, T. Ashizawa, and K. Miyasato, *Yakuzaigaku*, **46**, 259 (1986).
6) T. Loftsson and N. Bodor, *J. Pharm. Sci.*, **70**, 756 (1981).
7) L. Riesterer and R. Jaques, *Pharmacology*, **3**, 243 (1970).
8) K. S. Albert, W. R. Gillespie, A. Raabe, and M. Garry, *J. Pharm. Sci.*, **73**, 1823 (1984).
9) T. Arita, R. Hori, T. Anmo, M. Washitake, M. Akatsu, and T. Yajima, *Chem. Pharm. Bull.*, **18**, 1045 (1970).
10) I. H. Blank, R. J. Scheuplein, and D. J. MacFarlane, *J. Invest. Dermatol.*, **49**, 582 (1967).

[Chem. Pharm. Bull. 35(12)4891—4897(1987)]

Binding of Human Epidermal Growth Factor to Tissue Homogenates of the Rat

SHIGEO YANAI,[a] YUICHI SUGIYAMA,[a] DONG CHOOL KIM,[a] HIROAKI SATO,[a] TOHRU FUWA,[b] TATSUJI IGA*,[a] and MANABU HANANO[a]

Faculty of Pharmaceutical Sciences, University of Tokyo,[a] Hongo, Bunkyo-ku, Tokyo 113, Japan, and The Central Research Laboratories, Wakunaga Pharmaceutical Co., Ltd.,[b] Shimokotachi, Koda-cho, Takata-gun, Hiroshima 729-64, Japan

(Received May 13, 1987)

A study on binding of human epidermal growth factor (hEGF) to various rat tissue homogenates showed the existence of specific binding in the liver, kidney, small intestines (duodenum, jejunum and ileum), stomach, lung and heart. The extent of the specific binding in the liver was at least ten times as large as those in other tissues. However, no specific binding was observed in the spleen, muscle or brain. Binding kinetic analyses using tissue homogenates of the liver, kidney and small intestines showed that the binding capacities (n) differed remarkably among the tissues, whereas the tissue differences in the dissociation constants (K_d) were minimal (1—6 nM). In our previous report on the contributions of various tissues to hEGF removal from the systemic circulation in rats after i.v. administration, the uptakes of hEGF by the liver, kidney, small intestines, stomach and spleen showed remarkable saturation, which may represent the operation of a receptor-dependent uptake mechanism. In the present *in vitro* experiment, specific bindings in these tissues except the spleen were indeed identified, suggesting that specific binding plays an important role in the tissue distribution of hEGF. Some other mechanism may be involved in the hEGF distribution to the spleen, because specific binding to this tissue was not detected *in vitro*. Comparing hEGF binding kinetic data (at 4°C) for isolated rat hepatocytes with those for the homogenate, the binding parameters showed little difference between the two preparations, indicating that, at least under normal conditions, EGF receptors are not down-regulated and most of them exist on the cell surface.

Keywords——human epidermal growth factor; EGF receptor; specific binding; rat tissue homogenate; isolated rat hepatocyte; receptor-dependent uptake

Introduction

Epidermal growth factor (EGF), which has been isolated from the submandibular gland of the mouse and from human urine,[1-3] is a polypeptide which shows various biological actions on living animals as well as on isolated organs and cells. It is known that EGF promotes the proliferation and the cornification of the epithelial tissues and the synthesis of certain proteins, as well as RNA and DNA.[1,4,5] These proliferation-promoting effects of EGF may be applicable to a practical treatment for arteriosclerosis or ulcer.

The mechanism of EGF uptake by the hepatocytes was elucidated to be receptor-mediated endocytosis,[6-8] that is, the complex of EGF receptors existing on the cell surface and EGF forms vesicles at a specific domain on the cell membrane, and then undergoes endocytosis into the cell. Kinetic analyses of the receptor-dependent hepatic uptake have been reported.[8,9] However, little has been reported on EGF uptake mechanism by other tissues.

Previously, in our laboratory, kinetic analysis of the tissue distribution of human EGF (hEGF) in rats was performed *in vivo*.[10] It was found that the distributions of ^{125}I-hEGF to the liver, kidney, small intestines, stomach and spleen were much greater than could be accounted for by distribution to the extracellular space of each tissue, and that the hEGF

uptake by these tissues showed remarkable saturation.[10] These results suggested the existence of specific binding of hEGF in these tissues. Therefore, the present study was designed to elucidate whether specific binding of hEGF occurs in various tissues by using their homogenates, with the aim of accounting for the saturable tissue distributions *in vivo*. Furthermore, to investigate the number of receptors existing on the cell surface and inside the cell, we also attempted to compare the hEGF binding to isolated rat hepatocytes with that to the homogenate.

Experimental

Animals——Adult male Wistar rats (Nihon Seibutsu Zairyo, Tokyo, Japan) weighing 200—250 g were used throughout the experiments. The animals were housed under conditions of controlled temperature and lighting with access to food and water *ad libitum*.

Materials——Sodium iodide-125 (100 mCi/ml) was purchased from the Radiochemical Center (Amersham Corp., Arlington Heights, IL), bovine serum albumin (BSA) (fraction V) from Sigma Chemical Co., (St. Louis, MO), Sephadex G-25 from Pharmacia Fine Chemicals (Uppsala, Sweden), trichloroacetic acid (TCA) from Wako Pure Chemical Industries, Ltd. (Osaka, Japan), and silicone oil ($d=1.05$) from Aldrich Chemical Co. (Milwaukee, WI). All other reagents were commercial products of analytical grade.

Biosynthetic hEGF obtained from *Escherichia coli via* the synthesized coding sequence described previously[11,12] was used in all the experiments. The hEGF was radiolabeled with ^{125}I-Na by the chloramine-T method.[13] Unreacted ^{125}I-Na was removed on a Sephadex G-25 column, and the ^{125}I-hEGF was eluted in the void volume. The ^{125}I-hEGF had a specific activity of 0.5—1.0 mCi/nmol; it was more than 95% precipitable in 15% TCA, and more than 98% of ^{125}I-hEGF binding to a specific antiserum was displaced by an excess amount of unlabeled hEGF (6 nmol).

Experimental Procedure——The tissues were excised from rats and 4% (w/v) homogenate of each tissue was prepared by using a Teflon homogenizer. The buffer used in the preparation of homogenates and the binding assay contained 0.25 M sucrose, 0.2 mM $CaCl_2$, 10 mM $MgCl_2$, 100 mM NaCl, 10 mM Hepes–Tris (pH 7.4) and 0.1% (w/v) BSA.

Binding of ^{125}I-hEGF was measured by a rapid filtration technique.[8] The binding reaction was initiated by addition of 800 μl of the 4% tissue homogenate to 200 μl of the buffer containing 0.03 μCi of ^{125}I-hEGF and various concentrations of unlabeled hEGF (0.6—100 nM). After incubation for 60 min at 4 °C, 200 μl of the reaction mixture was immediately filtered through a glass microfiber filter (Whatman GF/F; Whatman Ltd., Maidstone, England), which was quickly washed once with 5 ml of ice-cold buffer to separate the tissue-associated ligands from free ligands. Radioactivity on the filter was determined in a gamma-counter (model ARC-300, Aloka Co. Ltd., Tokyo, Japan). The binding was corrected for nonspecific adsorption on the filter. The nonspecific adsorption was 1—1.5% of the total count.

Hepatocytes were prepared by the procedure of Baur *et al.*[14] The cell viability was determined by means of the trypan blue exclusion test; cells with more than 90% viability were used for the binding experiments. Isolated hepatocytes were suspended in the buffer and a part of this suspension was homogenized. The isolated cells and the homogenates were made up to a reaction volume of 600 μl with the buffer containing 0.02 μCi of ^{125}I-hEGF and various concentrations of unlabeled hEGF. The protein concentration in the reaction mixture was approximately 10 mg protein/ml. After incubation for 60 min at 4 °C, the ^{125}I-hEGF bound to the cell homogenate was measured by the method described above. The binding of ^{125}I-hEGF to the cells was measured as follows. To separate the cells and the cell-associated ligands from the incubation medium rapidly, the centrifugal filtration method was used.[14] A centrifuge tube contained a layer of 100 μl of silicone oil on the top of 50 μl of 3 M KOH. The incubation mixture (200 μl) was placed on top of the silicone layer. On centrifugation in a Beckmann microfuge, the cells together with binding ligands passed through the silicone oil and entered the bottom fluid. After separation, the amounts of the bound and unbound ligand were determined by the methods described above. The binding was corrected for the amount of adherent fluid, 0.62 μl/mg of cellular protein.[15] In these experiments, the increase in the TCA-soluble radioactivity was always less than 5% of the total radioactivity during the incubation period, indicating insignificant degradation of labeled hEGF under the incubation conditions used (data not shown).

Data Analysis——The data on EGF binding to various tissue homogenates were analyzed on the assumption of a single class of binding sites and nonspecific binding by using the equation

$$C_b=\frac{n\cdot Pt\cdot C_f}{K_d+C_f}+\alpha\cdot C_f \qquad (1)$$

were C_b and C_f are the bound and unbound concentrations of hEGF, respectively, Pt is the concentration of tissue

proteins, n and K_d denote the binding capacity (per mg protein) and the dissociation constant, respectively, and α is the proportional constant related to the nonspecific binding. The binding parameters were obtained by an iterative non-linear least-squares method[16] based on Eq. 1. The initial estimates of the binding parameters were obtained from Scatchard plots.

Results

Figure 1 shows the time courses of ^{125}I-hEGF binding to the homogenates of the liver, kidney and jejunum in the absence and presence of an excess amount of unlabeled hEGF. Binding equilibrium was attained within 60 min at 4 °C in each case.

In Fig. 2, the extents of the specific and nonspecific bindings of hEGF to various tissue homogenates are shown. The total and the nonspecific bindings were determined as the percent bindings of ^{125}I-hEGF in the absence and presence of an excess amount of unlabeled hEGF (100 nM), respectively. The specific binding was then obtained by subtracting the nonspecific binding from the total binding. Specific binding was detected in the liver, kidney, duodenum, jejunum, ileum, lung, heart and stomach. The extent of the specific binding was greatest in the liver and those in other tissues were less than one-tenth of that in the liver. On the other hand, specific binding was not detected in the spleen, muscle or brain.

The equilibrium bindings of ^{125}I-hEGF to 3.2% tissue homogenates were determined in the presence of various amounts of unlabeled hEGF, and typical results are shown in Fig. 3 as Scatchard plots. For all the tissues tested, both a single class of specific binding sites and a nonspecific binding were detected. The binding parameters listed in Table I showed that the values of n differed remarkably among the tissues, while the tissue differences in the values of K_d were minimal.

The bindings of hEGF to the intact hepatocytes and the homogenes prepared from the same hepatocytes were compared (Fig. 4). The amounts of the bound hEGF were normalized with respect to the protein concentration. Both the intact hepatocytes and the homogenates gave comparable results; the values of K_d for the cells and the homogenate were approximately 3.3 and 3.8 nM and the binding capacities were approximately 0.10 and 0.12 pmol/mg protein, respectively.

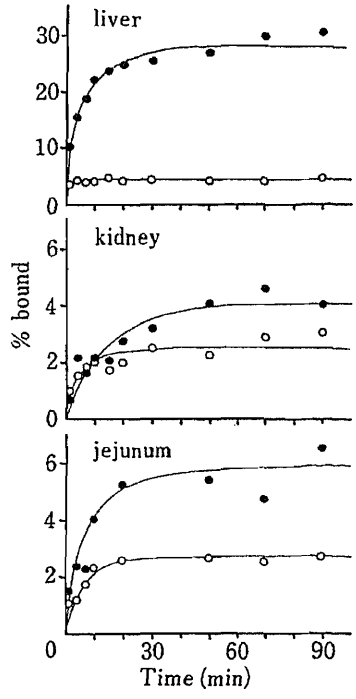

Fig. 1. Time Course of ^{125}I-hEGF Binding to Rat Tissue Homogenates

Homogenates (3.2%) were incubated at 4 °C in the absence (●) and presence (○) of unlabeled hEGF (50 nM). Samples were filtered as described in Experimental. The solid lines are visual fits.

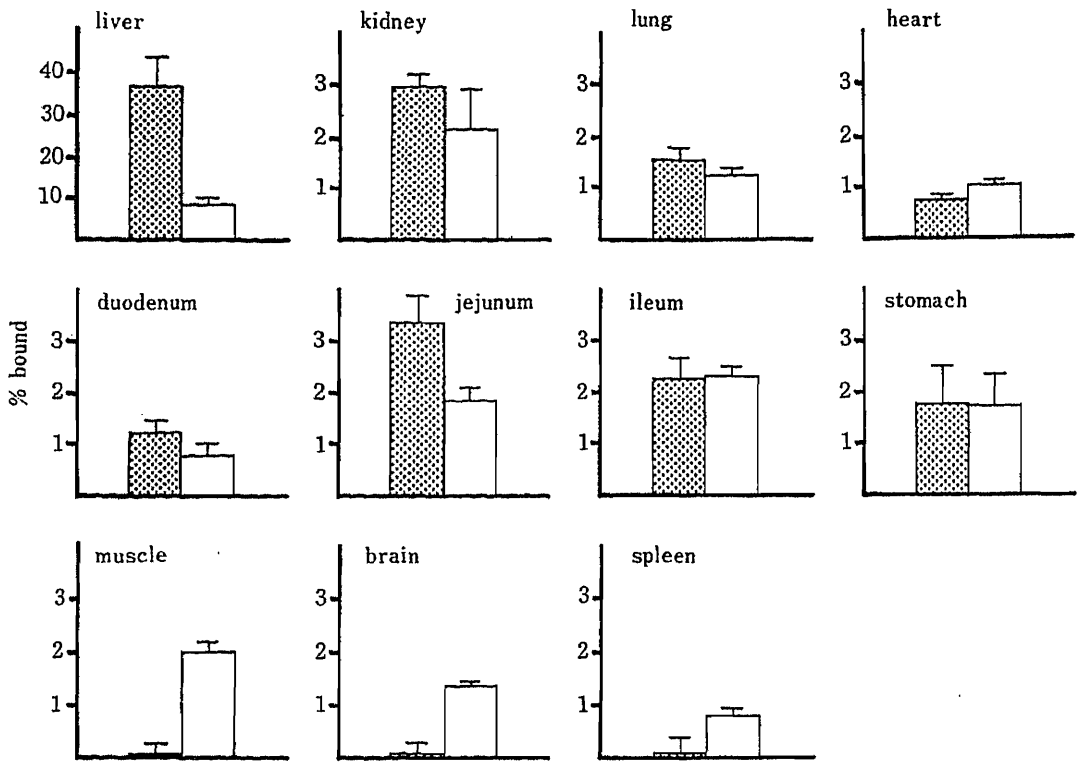

Fig. 2. Specific and Nonspecific Bindings of ^{125}I-hEGF to Homogenates (3.2%) Prepared from Various Rat Tissues

The shadowed bars represent specific binding and the white bars, nonspecific binding. They were determined as the percent bindings of ^{125}I-hEGF in the absence and presence of an excess amount of unlabeled hEGF (100 nM), and the specific binding was obtained by subtracting the nonspecific binding from the total binding. Results are mean ± S.E. of 4—8 experiments.

Discussion

In the present study, the existence of specific binding sites for hEGF in the rat kidney, duodenum, jejunum, ileum, lung, heart and stomach as well as in the liver were demonstrated. The extent of the specific binding was by far the greatest in the liver (Fig. 2). We previously reported that the liver is the main organ responsible for the clearance of hEGF from the body.[10] In addition, it has been suggested that the specific binding of hEGF to cell-surface receptors may govern the hepatic clearance of hEGF.[7,8] Our present result is thus consistent with previous findings by us and others. This large binding capacity of the liver for hEGF may be important in regulating the distribution and disposition of the peptide in the body. On the other hand, the specific binding capacities of other tissues are minor compared to that of the liver, though the high affinities ($K_d = 1$—6 nM) may suggest some physiological function, as discussed below. With regard to the small intestines, the specific binding for hEGF seems to exist relatively evenly over the intestines (Table I). Previously, the presence of high-affinity binding sites for hEGF were shown by Forgue-Lafitte *et al.*[17] using isolated rat intestinal epithelial cells. In that report, the values of K_d and n were approximately 1 nM and 0.02 pmol/mg protein respectively, which are comparable with those obtained in the present study using intestinal homogenates (Table I). In our previous *in vivo* experiment,[10] it was suggested that hEGF binds to the intestinal cells from the basolateral side. We recently obtained preliminary results (data not shown) showing that hEGF added to the luminal side of the rat intestines decreased the microclimate-pH of the jejunum, probably by acting on the

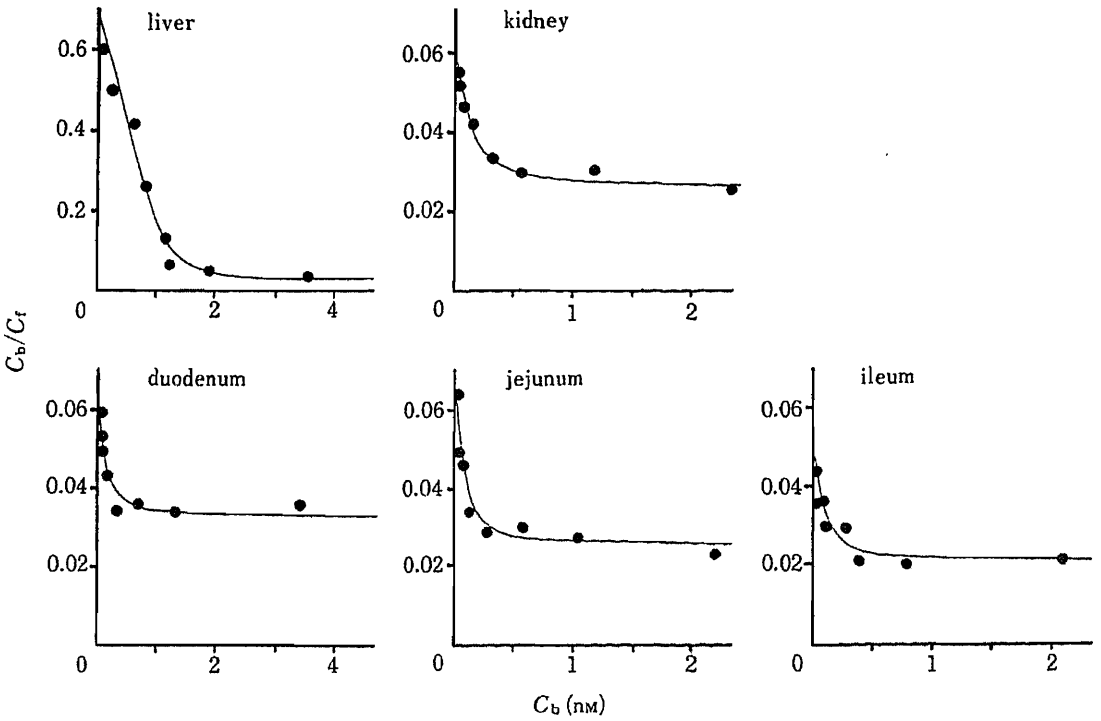

Fig. 3. Typical Scatchard Plots of hEGF Binding to Rat Tissue Homogenates

Tissue homogenates (3.2%) were incubated for 60 min at 4 °C with 0.03 μCi of ^{125}I-hEGF and various concentrations of unlabeled hEGF (0.6—100 nM). The solid lines were calculated by a non-linear iterative least-squares method, and the binding parameters obtained for these preparations are; $K_d = 1.7$ nM, $n = 0.2$ pmol/mg protein (liver); $K_d = 4.8$ nM, $n = 0.04$ pmol/mg protein (kidney); $K_d = 1.7$ nM, $n = 0.03$ pmol/mg protein (duodenum); $K_d = 1.5$ nM, $n = 0.03$ pmol/mg protein (jejunum); $K_d = 3.8$ nM, $n = 0.04$ pmol/mg protein (ileum).

TABLE I. Binding Parameters of hEGF to Various Rat Tissue Homogenates[a]

Tissues	Number of preparation	K_d (nM)	n^{b} (pmol/g tissue)	n (pmol/mg protein)	α^{c} (ml/g tissue)
Liver	6	1.09±0.36	24.9±3.20	0.15±0.02	3.37±0.69
Kidney	3	5.63±1.60	6.02±1.60	0.05±0.01	0.65±0.21
Duodenum[d]	2	1.49	1.24	0.03	0.54
Jejunum	4	1.00±0.42	0.83±0.39	0.01±0.01	0.47±0.20
Ileum[d]	2	2.39	1.72	0.02	0.60

a) Binding data was fitted to Eq. 1, and the binding parameters represent the mean±S.E. except for the duodenum and ileum. *b*) Corrected for the dilution of tissue homogenates. *c*) A proportional constant related to the nonspecific binding. *d*) Average from two preparations.

brush-border membrane. These findings suggest that hEGF may bind to both sides of the cell membrane (basolateral and brush-border membranes). To confirm this, it will be necessary to identify the hEGF bindings by using isolated membrane vesicles.

In general there are relatively small differences in the values of K_d among tissues, but the values of n exhibit great tissue differences, and that for the liver is the greatest, as shown in Table I. It has been reported that both high-affinity and low-affinity EGF receptors exist in many cell types.[18-20] The number of high-affinity receptors is much smaller than that of low-affinity receptors. The difference of physiological function between the two types of receptors is not clear, but it was suggested that high-affinity receptors may affect the mitogenic signal.[18]

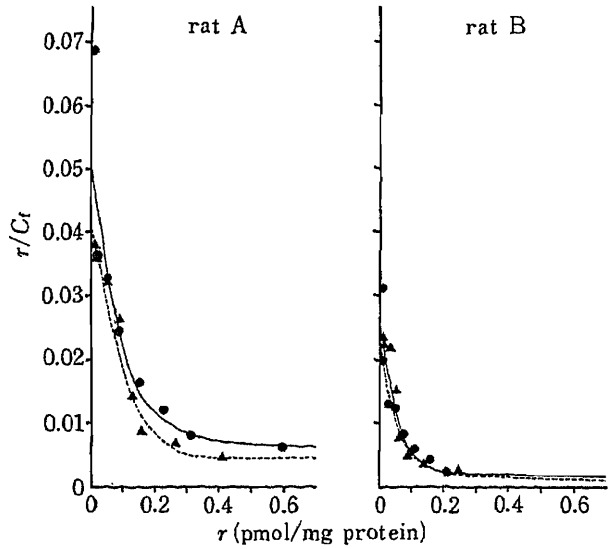

Fig. 4. Comparison of the Scatchard Plots of hEGF Binding between Isolated Rat Hepatocytes (●) and Cell Homogenates (▲)

The cell suspension and its homogenate were prepared from the same rat. The amount of the binding ligand is normalized per mg of protein. The solid (cell) and broken (homogenate) lines were calculated by a non-linear iterative least-squares method, and the binding parameters for these preparations are; rat A, $K_d = 2.7$ nM, $n = 0.13$ pmol/mg protein (cell), $K_d = 4.1$ nM, $n = 0.16$ pmol/mg protein (homogenate); rat B, $K_d = 3.8$ nM, $n = 0.08$ pmol/mg protein (cell), $K_d = 3.4$ nM, $n = 0.08$ pmol/mg protein (homogenate).

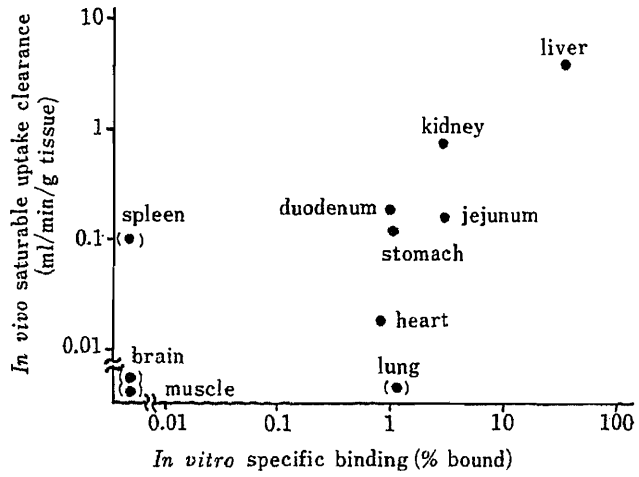

Fig. 5. Correlation between *in Vitro* Specific Binding Activity and *in Vivo* Receptor-Dependent Uptake Clearance among Various Tissues

The *in vitro* specific binding activities for tissues were obtained from the data shown in Fig. 1. The *in vivo* receptor-dependent uptake clearances (V_{max}/K_m) were obtained previously[10] in our laboratory. Parentheses mean that *in vitro* specific binding activity and/or *in vivo* saturable uptake clearance were not detected; that is, for the lung, *in vivo* saturable uptake was not observed, but *in vitro* specific binding was detected (1.5%), while for the spleen, *in vitro* specific binding was not observed, although *in vivo* saturable uptake clearance was clear (0.1 ml/min/g tissue). For the brain and muscle, neither was detected.

Previous kinetic analysis of the tissue distribution of hEGF in rats *in vivo* clarified the contribution of each tissue to the uptake of hEGF from the systemic circulation. The amount of ^{125}I-hEGF taken up by each tissue was determined after coadministration of various amounts of unlabeled hEGF.

The results showed that among the tissues examined, the distributions of ^{125}I-hEGF to the liver, kidney, small intestines, stomach and spleen were much greater than could be accounted for by the extracellular space of each tissue and that the uptake of hEGF by these tissues showed remarkable saturation, which may represent the operation of a receptor-dependent uptake mechanism.[10] When the saturable uptake clearance in each tissue obtained from this *in vivo* experiment was plotted against the specific binding activity of each tissue *in vitro* obtained from the present study, a good correlation between them was observed (Fig. 5).

In particular, saturable uptakes by the liver, kidney and small intestines, in which specific binding was detected *in vitro*, were also observed *in vivo*. However, in the lung and spleen, the opposite results were obtained; that is, *in vivo* saturable uptake clearance was not detected in the lung, whereas specific binding *in vitro* was not detected in the spleen. The reason for this discrepancy is not yet known.

It seemed of interest to compare the EGF binding activities between liver cell homogenate and isolated liver cells (intact cells). Such a comparison may allow us to determine the intracellular distribution of EGF receptors. As shown in Fig. 4, both preparations gave comparable hEGF binding activities in either rat liver examined. The values of K_d and n in the cell system were 3.3 nM and 0.10 pmol/mg protein, while those in the homogenate system were 3.8 nM and 0.12 pmol/mg protein, respectively (all the values are the averages of two independent experiments). This result suggests that the EGF receptors may exist mostly on the cell surface. In other words, the EGF receptors may not be down-regulated under physiologically normal conditions.

Previously in our laboratory, the binding of hEGF to rat liver sinusoidal membrane vesicle (SMV) was kinetically analyzed. The values of K_d and n obtained from that experiment were 1.8 nM and 5.4 pmol/mg protein, respectively.[21] The increase in the value of n *versus* the homogenate is approximately 50-fold and that of Na^+,K^+-adenosine triphosphatase (ATPase) specific activity, which is a marker enzyme of SMV, is approximately 40-fold. Thus, the comparable enrichments of the binding and the enzymatic activities confirmed that most of the EGF receptors are present on the sinusoidal membrane of the liver cell.

In conclusion, we have elucidated the existence of specific bining sites for EGF in several rat tissues, in which the saturable uptake was observed in our previous *in vivo* experiments. These results can account for the tissue differences in the distribution of hEGF. However, the physiological role of the specific binding in each tissue remains to be determined.

Acknowledgements This study was supported in part by a Grant-in-Aid for Scientific Research provided by the Ministry of Education, Science and Culture of Japan.

References

1) G. Carpenter and S. Cohen, *Annu. Rev. Biochem.*, **48**, 193 (1979).
2) D. Gospodarowicz, G. Greenburg, H. Bialecki and B. R. Zetter, *In Vitro*, **14**, 85 (1978).
3) J. Schlessinger, A. B. Schreiber, A. Levi, I. Lax, T. Livermann and Y. Yarden, *CRC Crt. Rev, Biochem.*, **14**, 93 (1983).
4) N. Shimizu, *Receptors and Recognition*, **B-16**, 109 (1984).
5) S. Cohen, *J. Biol. Chem.*, **237**, 1555 (1962).
6) D. M. Moriarity and Jr. Savage, *Arch. Biochem. Biophys.*, **203**, 506 (1980).
7) R. J. St. Hilaire and A. L. Jones, *Hepatology*, **2**, 601 (1982).
8) W. A. Dunn and A. L. Hubbard, *J. Cell Biol.*, **98**, 2148 (1984).
9) H. S. Wiley and D. D. Cunningham, *Cell*, **25**, 433 (1981).
10) D. C. Kim, Y. Sugiyama, H. Sato, T. Fuwa, T. Iga and M. Hanano, *J. Pharm. Sci.*, in press.
11) S. Sumi, A. Hasegawa, S. Yagi, K. Miyoshi, A. Kanazawa, S. Nakagawa and M. Suzuki, *J. Biotechnol.*, **2**, 59 (1985).
12) S. Nakagawa, S. Yoshida, Y. Hirao, S. Kasuga and T. Fuwa, *Differentiation*, **29**, 284 (1985).
13) I. Vlodavsky, K. D. Brown and D. Gospodarowicz, *J. Biol. Chem.*, **253**, 3744 (1978).
14) H. Baur, S. Kasperek and E. Pfaff, *Hoppe-Seyler's Z. Physiol. Chem.*, **356**, 827 (1975).
15) W. J. Brock and M. Vore, *J. Pharmacol. Exp. Ther.*, **229**, 175 (1984).
16) K. Yamaoka, Y. Tanigawara, T. Nakagawa and T. Uno, *J. Pharmacobio-Dyn.*, **4**, 879 (1981).
17) M. E. Forgue-Lafitte, M. Laburthe, M. C. Chamblier, A. J. Moody and G. Rosselin, *FEBS Lett.*, **114**, 243 (1980).
18) A. C. King and P. Cuatrecasas, *J. Biol. Chem.*, **257**, 3053 (1982).
19) J. A. Fernandez-Pol, *J. Biol. Chem.*, **260**, 5003 (1985).
20) I. P. Gradhaug and T. Christoffersen, *Eur. J. Biochem.*, **164**, 267 (1987).
21) K. Yachi, Y. Sugiyama, H. Sato, D. C. Kim, T. Fuwa, T. Iga and M. Hanano, *J. Biochem.* (Tokyo), submitted.

[Chem. Pharm. Bull. 35(12)4898—4906(1987)]

Disposition Characteristics of Lipophilic Mitomycin C Prodrug in an Intra-arterial Muscle Infusion System

TOSHIYUKI KAKUTANI, YUMI SUEMATSU, WING YIN CHEAH, ETSUKO SUMIMOTO, and MITSURU HASHIDA*

Faculty of Pharmaceutical Sciences, Kyoto University, Yoshida Shimoadachi-cho, Sakyo-ku, Kyoto 606, Japan

(Received May 15, 1987)

A new experimental system was applied to obtain information about the local disposition of lipophilic mitomycin C (MMC) prodrugs after intra-arterial injection. Rabbit hind leg was perfused *in situ* using a single-pass technique and the outflow concentration–time curves of drugs following pulse injection were evaluated by using statistical moment analysis. Moment parameters (moments) were transformed to disposition parameters which express local disposition characteristics together with respect to elimination, distribution, and dispersion. Six lipophilic derivatives of MMC were tested together with the parent drug. Dimethylsulfoxide (DMSO) was used as a model injection vehicle that can be mixed with blood. Using this system, the following results were obtained. 1) Local disposition of the drug is decided by the balance of its affinities for intravascular and extravascular components. 2) Disposition can be modified by derivation of the drug to a more lipophilic prodrug. 3) Higher lipophilicity of a drug results in a larger organ clearance in the absence of albumin, but a smaller clearance in albumin-containing perfusate. 4) In the case of DMSO injection, intermediate clearance values are obtained regardless of the lipophilicity of drugs, and it was suggested that DMSO decreases both partitioning from the injection vehicle to the tissue and plasma protein binding.

Keywords——single-pass perfusion system; drug disposition; rabbit muscle tissue; mitomycin C; lipophilic prodrug; statistical moment analysis; intra-arterial injection; plasma protein binding; dimethylsulfoxide

Intra-arterial injection and local perfusion methods have been used in cancer chemotherapy since the 1950s.[1] An improvement in drug effectiveness and ultimate therapeutic success have been reported for these medical techniques.[2] Intra-arterial infusion is expected to offer a distinct advantage in comparison with common systemic administration; that is, it increases drug delivery to the area supplied by the cannulated artery and reduces systemic drug exposure. Although the theoretical justification for the advantage of intra-arterial infusion has been discussed,[3] exact information useful for pharmaceutical dosage design has not been obtained.

In the systemic administration mode, many attempts have been made to deliver cytotoxic drugs to the tumor site by means of drug delivery systems,[4] *i.e.*, the utilization of physical devices, the chemical transformation of drug to prodrugs,[5,6] and combinations of the two.[7] Recently, combined systems of physical devices and intra-arterial infusion have been developed as a chemo-embolization method, in which microcapsules,[8] starch,[9] and oily X-ray contrast medium (Lipiodol)[10] are used as controlled release devices. However, application of the prodrug approach to local infusion has not been tried, although the low-molecular-weight prodrug approach seems to be free from some of the disadvantages of colloid-size carriers.

In order to achieve precise chemotherapy through prodrug-based intra-arterial infusion, the effects of the physicochemical properties of drugs and the mode of injection should

be clarified. We have established an experimental system in which rabbit hind leg is perfused *in situ* using a single-pass technique and data are analyzed based on statistical moment theory.[11] In previous papers, the effect of plasma protein binding on local drug disposition[12] and the regeneration characteristics of a prodrug[13] were investigated. In the present study, this system was used to elucidate the local disposition characteristics of lipophilic derivatives of mitomycin C (MMC) and the effects of the physicochemical properties of the drug and the injection vehicle were clarified.

Experimental

Materials——MMC was supplied by Kyowa Hakko Kogyo, Japan. Lipophilic MMC derivatives, propyloxycarbonyl MMC (propyl-MMC), benzyl MMC, benzyloxycarbonyl MMC (z-MMC), pentyloxycarbonyl MMC (pentyl-MMC), nonyloxycarbonyl MMC (nonyl-MMC), and cholesteryloxycarbonyl MMC (chol-MMC) were prepared as reported previously.[6] The structures, physicochemical properties, and protein binding characteristics of these compounds are summarized in Table I. All other chemicals were of reagent grade and were obtained commercially (Nakarai Chemicals, Japan).

***In Situ* Perfusion of Rabbit Hind Leg**——Figure 1 illustrates the whole animal experimental system. Details of the procedures were reported previously.[11] Male domestic rabbits weighing 1.99±0.13 (mean±S.D.) kg were anesthetized with urethane, and the right legs were essentially isolated from the body by arterio-venous perfusion. The right iliolumbar vessels, common iliac vessels, and saphenous vein of the right hip were each ligated. The right femoral artery and vein were cannulated with vinyl tubing (i.d. 0.8 mm, o.d. 1.2 mm, Dural Plastics, Australia) and the inflow (arterial side) and outflow (venous side) cannula were kept at the level of the thigh during the experiment. In this preparation, there was almost complete recovery of the perfusate in venous outflow (95.6±5.0%), and mixing of blood from the body was suppressed to 4.4±2.6%. The weight of the perfused muscle was 50.9±8.0 g.

Tyrode's solution (137 mM NaCl, 2.68 mM KCl, 1.80 mM $CaCl_2$, 11.9 mM $NaHCO_3$, 0.362 mM NaH_2PO_4, 0.492 mM $MgCl_2$, and 5.55 mM D-glucose) with (system I) or without (system II) bovine serum albumin (Fraction V, Armour Pharmaceutical Co., U.K.) at a concentration of 4.7% (w/v) was used as the perfusate. The perfusate (37°C, gassed with 95%O_2–5%CO_2, pH 7.4) was pumped into the cannulated artery with the aid of a peristaltic roller pump at a rate of 1.66 ml/min. Test compounds were dissolved in the perfusate or dimethylsulfoxide (DMSO) and injected into the line of perfusion flow *via* a six-position rotary valve injector (type 50 Teflon rotary valves, Rheodyne, CA). Test samples (0.1 ml) were put into the flow as a pulse function by this procedure. When DMSO was used as an

TABLE I. Structures, Physicochemical Properties and Protein Binding Characteristics of MMC and Lipophilic MMC Derivatives

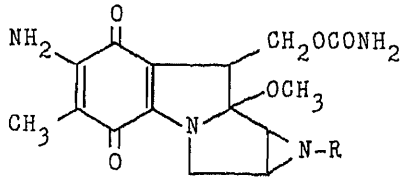

Compound	R	mp (°C)	PC_{oct}[a]	Solubility (mM)[b]			Free fraction[c] in system I (+albumin)
				Water	Sesame oil	Hexane ($\times 10^3$)	
MMC	H	>270	0.414	2.73	0.0180	0.234	0.907±0.0113
Propyl-MMC	$COOC_3H_7$	203—207	32.7	0.333	0.104	<0.02	0.691±0.0170
Benzyl MMC	$CH_2C_6H_5$	119—121	38.6	1.49	4.17	0.726	0.693±0.00732
Z-MMC	$COOCH_2C_6H_5$	102—104	113	0.523	3.29	0.415	0.214±0.0162
Pentyl-MMC	$COOC_5H_{11}$	89—93	279	0.590	3.48	2.02	0.160±0.00320
Nonyl-MMC	$COOC_9H_{19}$	139—141	3670	0.00025	15.2	0.304	0[d]
Chol-MMC	$COOC_{27}H_{45}$	140—142	7610	0.00025	12.1	6.61	0

a) Partition coefficient between *n*-octanol and water. *b*) Determined at 25°C. *c*) Each value is the mean±S.D. of five experiments; details of determination methods were reported in ref. 12. *d*) Compounds can not be detected in the free form.

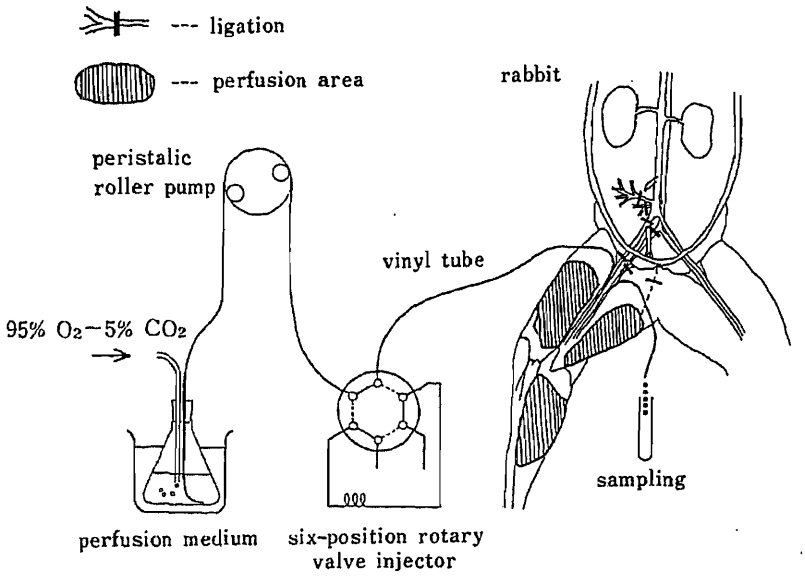

Fig. 1. *In Situ* Perfusion System of Rabbit Hind Leg

injection vehicle, Tyrode's solution containing albumin was used as the perfusate (system III).

Sampling and Assay——The details of the sampling and assay procedures were also described in the previous report.[11] The outflow perfusate was collected in weighed test tubes at appropriate time intervals (at first 1—2 s, subsequently 10 s—2 min). In the case of Evans blue and MMC, the concentration in the surpernate was measured after centrifugation for 15 min at 1500 rpm. The optical density of Evans blue was determined at 620 nm. MMC was determined by measuring antimicrobial activity against *Escherichia coli* B using a disc-plate method.[6,11] Lipophilic derivatives were determined by high performance liquid chromatography (HPLC) in a reverse-phase mode after extraction with ethyl acetate. The stationary phase used was a Cosmosil $5C_{18}$ packed column (4.6 × 150 mm, Nakarai Chemicals, Japan) and mixtures of methanol and distilled water were used as the mobile phase.

Moment Analysis——The present perfusion system is considered as a "black box" with linear disposition, and is denoted by the subscript *i*. The disposition function of this system is reflected in the output response to a unit pulse input, and is obtained by way of the concentration–time course in the outflow. The transit time of each drug molecule through the organ is statistically distributed according to the stochastic disposition process and the obtained outflow curve can be evaluated by moment analysis. The statistical concept of moments was introduced into pharmacokinetics by Yamaoka *et al.*[14] and Cutler,[15] and it has many applications in pharmacokinetic analysis as a model-independent method. The first three (zero-th to second) statistical moment parameters (moments) are defined as follows;

$$auc_i = \int_0^\infty C_i\,dt \tag{1}$$

$$\bar{t}_i = \int_0^\infty t \cdot C_i\,dt/auc_i \tag{2}$$

$$\sigma_i^2 = \int_0^\infty (t-\bar{t}_i)^2 \cdot C_i\,dt/auc_i \tag{3}$$

where t is time and C_i is the concentration of the substance normalized by expressing it as a fraction of the total injected amount in unit volume of outflow fluid (with dimensions of "% of dose/ml"). auc_i, $\bar{t}_i$, and σ_i^2 are the area under the outflow concenration–time curve, the mean transit time of the drug through the tissue, and the variance of the transit time, respectively.

The moments were calculated by numerical integration using the linear trapezoidal formula and extrapolation to infinite time based on a mono-exponential equation (infinite calculation method).[11] The risk of error in moment calculation increases with the magnitude of the extrapolation required[14,16] and the approximate (finite) values of moments were also calculated for data points with concentrations higher than 0.3% of dose/ml by using the linear trapezoidal rule (finite calculation method).[11] Vascular reference substance (VRS) is assumed neither to distribute to extravascular tissue nor to be eliminated, and a mixture of Evans blue and albumin was employed as the VRS.

Calculation of Disposition Parameters from Moments——The calculation methods from moments, auc_i, $\bar{t}_i$, and

TABLE II. Derivation of the Disposition Parameters from Moments

Disposition	intrinsic clearance:	$CL_{int,i}=V_i/\bar{t}_{el,i}$	
(a)	Distribution		
(i)	Extent	distribution volume:	$V_i=Q_i\cdot\bar{t}_i/F_i$
		tissue distribution ratio:	$k_i=(\bar{t}_i/F_i)/\bar{t}_B-1$
		corrected mean transit time:	$\bar{t}_{cor,i}=\bar{t}_i/F_i$
(b)	Elimination		
(i)	Extent	recovery ratio:	$F_i=auc_i/auc_{VRS}$
		extraction ratio:	$E_i=1-F_i$
(ii)	Rate	mean elimination time:	$\bar{t}_{el,i}=\bar{t}_i/E_i$
		first-order elimination rate constant:	$k_{el,i}=1/\bar{t}_{el,i}$
Dispersion	dispersion ratio:		$d_i=(\sigma_i^2)^{1/2}/\bar{t}_i$

Q_i, flow rate of perfusion; $\bar{t}_B$, mean transit time of VRS; auc_{VRS}, area under the curve of VRS.

σ_i^2, to disposition parameters which express the local disposition characteristics of the drug are summarized in Table II, and the detailed theoretical background was reported in the previous paper.[11] The partition concept between mobile-stationary phases[17] and the plate theory[18] of chromatographic systems were introduced into the organ perfusion system. Derivation of disposition parameters from model-independent moments was carried out based on either of the following physiological models.

1) The well-stirred model[19,20] (one-compartment perfusion model[21,22]).
2) A multiphase mamillary compartment model in which only the central compartment possesses the elimination process (as represented by the two-compartment perfusion model[3,22]).

$CL_{int,i}$ is the intrinsic clearance.[19,20] k_i (tissue distribution ratio) is the ratio of mass of drug in tissue to that in perfusate under steady-state conditions and corresponds to the capacity factor in a chromatographic system.[17] $\bar{t}_{cor,i}$ (corrected mean transit time) is the true value of mean transit time of drug molecules and corresponds to the retention time.[17] F_i (recovery ratio) and E_i (extraction ratio) represent the ratios of outflowed and extracted drug amounts to input dose, respectively. $\bar{t}_{el,i}$ (mean elimination time) is mean time value of drug elimination and corresponds to mean residence time (MRT) in a whole-body recirculation system.[14,16] The dispersion ratio, d_i, gives information for selecting the preferred model. When model 1 or 2 is valid, the dispersion ratio takes a value of 1 or more than 1, respectively. In the case of insufficient mixing, the value of d_i becomes less than 1. In particular, when d_i equals zero, it represents a condition of plug flow in which mixing in the system can be neglected (the parallel tube model[20]).

Results

Outflow Patterns and Moments

Figure 2 illustrates typical concentration–time curves of pentyl-MMC. In Fig. 2A, the results in the initial 3 min are plotted on a normal scale; Fig. 2B shows the whole concentration–time curves over 30 min plotted on a semilogarithmic scale. The concentration of pentyl-MMC rose rapidly to a peak, then fell off in a manner described by a sum of exponentials. As compared with system I (+albumin), system II (−albumin) showed a diminution in outflow concentrations, but the slopes in the terminal phase were essentially similar. The outflow pattern of system III (DMSO) was rather closer to that of system II than to that of system I in the first 3 min, but showed the fastest decline in the terminal phase among them.

The outflow patterns of other compounds in the case of system II also showed diminutions in peak concentration relative to those of system I, and system III usually gave intermediate patterns between systems I and II. The differences between systems I and II were attributable to the free fractions in system I.

The outflow patterns of test compounds in each system were evaluated by moment analysis. Table III lists the moments of all compounds for system III with the moments of the VRS. Although a derivative with higher lipophilicity passed more slowly in system II and more quickly in system I,[12] the lipophilicity had no special influence in the case of DMSO injection. Because the moments are complex parameters reflecting all the disposition character-

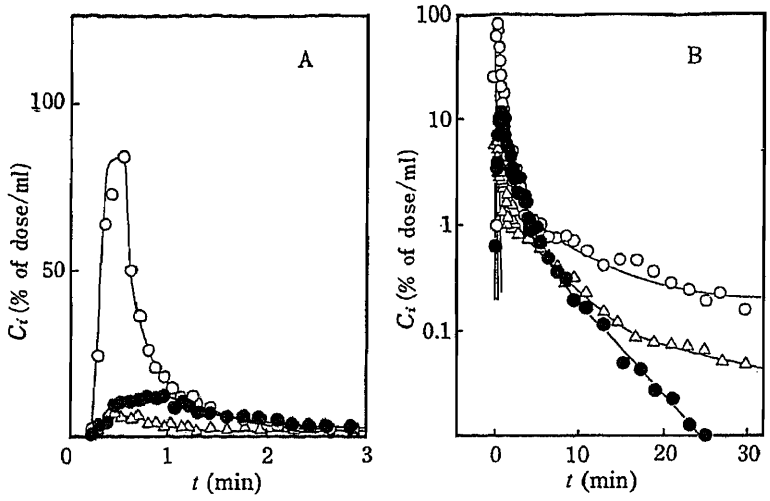

Fig. 2. Typical Outflow Concentration–Time Curve of Pentyl-MMC

○, system I (+albumin); △, system II (−albumin); ●, system III (DMSO).
A, initial 3 min; B, whole period.

TABLE III. Moment Parameters (Moments) for VRS and MMC Derivatives in System III (DMSO)

Compound	Moments	auc_i (% of dose·min/ml)	$\bar{t}_i$ (min)	σ_i^2 (min^2)
VRS (6)	Infinite	53.9±4.20	1.11±0.114	1.60±0.619
	Finite	53.3±3.75	1.02±0.157	0.946±0.363
MMC (5)	Infinite	26.9±5.83	4.05±0.186	40.2±9.28
	Finite	24.2±5.39	2.32±0.193	6.35±1.13
Propyl-MMC (5)	Infinite	16.5±1.67	3.12±0.274	50.6±61.6
	Finite	15.3±1.60	1.91±0.210	2.66±0.769
Benzyl MMC (5)	Infinite	19.0±1.66	3.04±0.225	19.2±3.63
	Finite	17.4±1.57	1.98±0.247	3.77±0.989
Z-MMC (5)	Infinite	19.8±3.30	2.84±0.127	22.7±8.64
	Finite	17.6±3.10	1.57±0.198	1.79±0.466
Pentyl-MMC (5)	Infinite	21.3±2.29	3.20±0.152	37.6±19.7
	Finite	19.6±2.34	1.98±0.180	2.83±0.642
Nonyl-MMC (5)	Infinite	16.6±1.96	11.5±1.18	388±177
	Finite	12.0±1.78	2.98±0.321	5.66±1.00
Chol-MMC (5)	Infinite	3.85±1.84	5.75±1.14	78.9±71.6
	Finite	2.28±1.51	1.14±0.407	0.831±0.809

Each value is the mean±S.D., with the number of experiments in parenthesis.

istics, it seemed difficult to analyze the lipophilicity–disposition relationship only in terms of the first three moments.

Relationships between Disposition Characteristics and Lipophilicity of Drugs

The disposition parameters were derived independently from moments by using the equations in Table II, and they allowed the detailed evaluation of tissue disposition characteristics. Figures 3—5 show the relationships of calculated extraction ratio (E_i), tissue distribution ratio (k_i), and mean elimination time ($\bar{t}_{el,i}$) to the PC_{oct} values of the tested compounds. These values were obtained from the mean values of infinite moments and the results from finite moments were essentially similar to them.

Concerning E_i values, the following conclusions may be drawn (Fig. 3). Higher

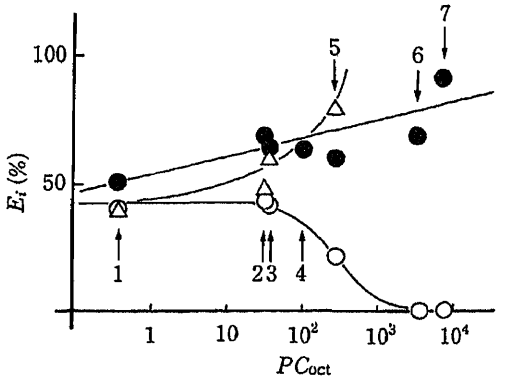

Fig. 3. Relationships between Extraction Ratio, E_i, and Partition Coefficient (*n*-Octanol/Water), PC_{oct}

○, system I (+albumin); △, system II (−albumin); ●, system III (DMSO).
1, MMC; 2, propyl-MMC; 3, benzyl MMC; 4, Z-MMC; 5, pentyl-MMC; 6, nonyl-MMC; 7, chol-MMC.

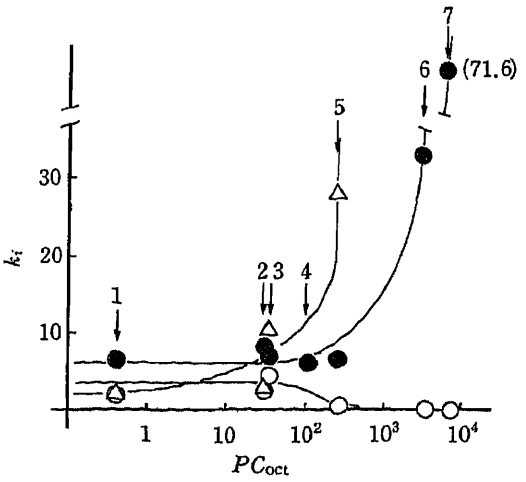

Fig. 4. Relationships between Tissue Distribution Ratio, k_i, and Partition Coefficient (*n*-Octanol/Water), PC_{oct}

○, system I (+albumin); △, system II (−albumin); ●, system III (DMSO).
1, MMC; 2, propyl-MMC; 3, benzyl MMC; 4, Z-MMC; 5, pentyl-MMC; 6, nonyl-MMC; 7, chol-MMC.

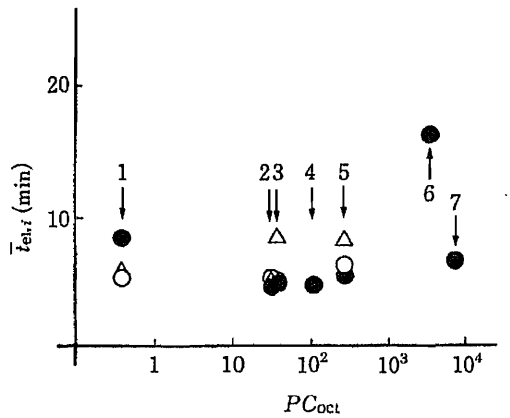

Fig. 5. Relationships between Mean Elimination Time, $\bar{t}_{el,i}$, and Partition Coefficient (*n*-Octanol/Water), PC_{oct}

○, system I (+albumin); △, system II (−albumin); ●, system III (DMSO).
1, MMC; 2, propyl-MMC; 3, benzyl MMC; 4, Z-MMC; 5, pentyl-MMC; 6, nonyl-MMC; 7, chol-MMC.

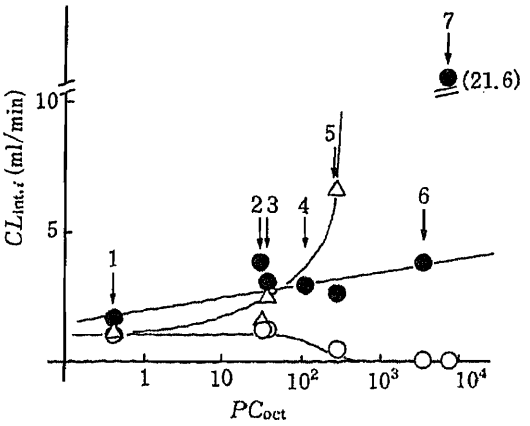

Fig. 6. Relationships between Intrinsic Clearance, $CL_{int,i}$, and Partition Coefficient (*n*-Octanol/Water), PC_{oct}

○, system I (+albumin); △, system II (−albumin); ●, system III (DMSO).
1, MMC; 2, propyl-MMC; 3, benzyl MMC; 4, Z-MMC; 5, pentyl-MMC; 6, nonyl-MMC; 7, chol-MMC.

lipophilicity resulted in larger elimination in the absence of albumin in the intravascular space. Plasma protein binding decreased the organ extraction, and in the presence of albumin, higher lipophilicity resulted in lower elimination. It is possible that the decrease of the colloidal osmotic pressure enlarged the distribution volume in system II. However, the difference in organ extraction between the cases with and without albumin was mainly determined by the free fraction of drug in each system. In the case of DMSO injection, the organ extraction was not influenced so much by lipophilicity, and it was suggested that the effects of lipophilicity on the distribution to the extravascular space and on the binding to intravascular albumin

canceled each other out. In addition, DMSO enhanced the organ uptake of relatively weakly lipophilic compounds such as MMC and propyl-MMC (against systems I and II; $p<0.05$ by Student's t-test).

The value of k_i showed the same dependency on PC_{oct} as E_i in each system (Fig. 4). Highly lipophilic derivatives, nonyl-MMC and chol-MMC, showed high tissue distribution even in DMSO solution, suggesting that albumin binding was restricted by their water-insolubility. Although the extent of elimination was dependent on lipophilicity, the elimination rates ($\bar{t}_{el,i}$) were constant in all cases (Fig. 5).

Figure 6 illustrates the relationships between PC_{oct} and intrinsic clearance. Because the elimination rates were independent of lipophilicity (Fig. 5), this parameter seemed to be mainly determined by the distribution extent (intrinsic clearance is expressed as $V_i/\bar{t}_{el,i}$). Dispersion ratios greater than 1 were obtained for all cases, indicating that the necessary condition for calculation in Table II was attained.

Discussion

In this paper, we have examined the local disposition characteristics of MMC prodrugs, focusing on their quantity. The muscle was used as the model tissue since it has a continuous capillary endothelium and occupies a large part of the body. DMSO was used as the model vehicle for elucidating the effect of vehicle properties; although DMSO is not practically used, it can dissolve even highly lipophilic drugs and mix with perfusate. The present results suggested that drug molecules should be transformed to more lipophilic forms with the smallest possible affinity for intravascular albumin, in order to achieve effective local perfusion therapy. The possibility for controlling tissue distribution by the selection of an injection vehicle with appropriate physicochemical properties was also demonstrated. Concerning the regeneration process of MMC from the prodrug, which is crucial for the therapeutic efficacy of the present modality, the results of pharmacokinetic analysis will be reported together with a new theoretical approach.[13]

Miyauchi *et al.* expressed the "apparent" intrinsic clearance in terms of the intrinsic clearances for the influx, efflux, and sequestration processes as follows.[23]

$$CL_{int,i} \approx \frac{CL_{int,seq} \times CL_{int,inf}}{CL_{int,seq} + CL_{int,eff}} \tag{4}$$

If $CL_{int,seq} \ll CL_{int,eff}$ is not attained, the contribution of $CL_{int,inf}$ to $CL_{int,i}$ can not be neglected. That is, the influx rate into the extravascular space is largely reflected in the elimination rate from the perfusate, in the case of a relatively slow efflux rate. For propyl-MMC, it was confirmed that the *in vitro* sequestration rate was smaller than the elimination rate from the perfusate compartment.[13] Whereas the lipophilic derivatives show a wide variation in *in vitro* stability,[6] their mean elimination times from the perfusate were approximately constant (Fig. 5). These facts suggest that the derivatives are eluted slowly from the extravascular space of the muscle tissue. A large part of the extraction ratio corresponds to the ratio of drug which is diffused into the extravascular space in a short time and will be recovered in outflow fluids according to an irreversible (non-linear) process.

The most distinctive feature of this experimental system is the application of statistical moment analysis to a local perfusion single-pass system. In the field of physiology, numerous analytical models have been proposed for a local perfusion system. However, such models are sometimes more sophisticated than is warranted by the experimental data.[11,24] In this investigation, a simple model is used only for the derivation of the physiologically meaningful parameters from moments. Each process occurring in this system is evaluated with statistical concepts of sum, mean, and variance, and the obtained parameters are free from restrictions

arising from complex modeling. Thus, the moment analysis enabled us to evaluate the disposition characteristics of drugs in a local perfusion system, and the effects of the physicochemical properties of drugs on their disposition were elucidated.

In moment analysis, the terminal slope extrapolation produces calculation errors. It is not easy to choose a starting point for the terminal phase or to discriminate between the terminal phase and the subsequent apparent plateau phase. The finite calculation method is free from such errors. The lipophilicity–disposition relationships derived from the finite moments were essentially similar to those from the infinite moments, though there was some underestimation of moments (Table III).[11,16] Consequently, the values of V_i, k_i, $\bar{t}_{cor,i}$, F_i, $\bar{t}_{el,i}$, and d_i, were underestimated and the values of $CL_{int,i}$, E_i, and $k_{el,i}$ were overestimated. The finite moment calculation is useful for relative evaluation. However, the infinite moments are necessary for quantitative evaluation, and a suitable criterion for accurate determination of the terminal slope is required.

Concerning the impulse response of a single-pass system observed as a log-convex disposition curve, Weiss has recently proved that it has the mono-exponential terminal phase; this supports the validity of the moment calculation.[25] Wide applicability of statistical moment analysis to single-pass dilution systems has already been suggested by Yamaoka and Nakagawa.[26] Because the moments are defined by transfer functions using Laplace transformation, network theory can also be applied to this analytical system.[27] Based on network theory, we have elucidated the effect of plasma protein binding on tissue distribution based on the results for systems I and II, and the general assumption that only the unbound form is available for organ uptake was confirmed.[12] In addition, Homer and Weathersby had calculated the moment values for complicated models constructed with various assumptions such as well-stirred, plug flow, radial diffusion, and axial diffusion.[28] They indicated that the moment analysis of experimental crude data would give fundamental information for model selection. Based on these considerations, statistical moment analysis can be concluded to be a useful tool for analyzing drug disposition at the organ level and for devising systematic strategies for the development of a new dosage modality.

Acknowledgements The authors thank Professor Hitoshi Sezaki, Faculty of Pharmaceutical Sciences, Kyoto University, Kyoto, Japan for his valuable suggestions and constructive discussions during this work. A part of this work was supported by a Grant-in-Aid for Scientific Research from the Ministry of Education, Science, and Culture, Japan.

References and Notes

1) C. T. Klopp, T. C. Alford, J. Bateman, G. N. Berry, and T. Winship, *Ann. Surg.*, **132**, 811 (1950); O. Creech, Jr., E. T. Krementz, R. F. Ryan, and J. N. Winblad, *ibid.*, **148**, 616 (1958).
2) D. Jinnai, H. Mogami, H. Higashi, T. Hayakawa, N. Kanari, and R. Yamada, *Brain Nerve*, **19**, 333 (1967); Y. Inuyama, "Mitomycin C: Current Status and New Developments," ed. by S. K. Carter and S. T. Crooke, Academic Press, New York, 1979, p. 173.
3) W. W. Eckman, C. S. Patlak, and J. D. Fenstermacher, *J. Pharmacokinet. Biopharm.*, **2**, 257 (1974).
4) R. L. Juliano, "Drug Delivery Systems," ed. by R. L. Juliano, Oxford University Press, New York, 1980, p. 3; G. Gregoriadis, *Nature* (London), **265**, 407 (1977).
5) Y. Takakura, S. Matsumoto, M. Hashida, and H. Sezaki, *Cancer Res.*, **44**, 2505 (1984).
6) H. Sasaki, E. Mukai, M. Hashida, T. Kimura, and H. Sezaki, *Int. J. Pharmaceut.*, **15**, 49 (1983); H. Sasaki, M. Fukumoto, M. Hashida, T. Kimura, and H. Sezaki, *Chem. Pharm. Bull.*, **31**, 4083 (1983).
7) M. Hashida and H. Sezaki, "Microspheres and Drug Therapy. Pharmaceutical, Immunological and Medical Aspects," ed. by S. S. Davis, L. Illum, J. G. McVie, and E. Tomlinson, Elsevier Biomedical Press, New York, 1984, p. 281; H. Sasaki, T. Kakutani, M. Hashida, and H. Sezaki, *J. Pharm. Pharmacol.*, **37**, 461 (1985); H. Sasaki, T. Kakutani, M. Hashida, T. Kimura, and H. Sezaki, *Chem. Pharm. Bull.*, **33**, 2968 (1985).
8) R. Nemoto and T. Kato, "Microspheres and Drug Therapy. Pharmaceutical, Immunological and Medical Aspects," ed. by S. S. Davis, L. Illum, J. G. McVie, and E. Tomlinson, Elsevier Biomedical Press, New York,

1984, p. 229.
9) W. D. Ensminger, J. W. Gyves, P. Stetson, and S. W. Andrews, *Cancer Res.*, **45**, 4464 (1985).
10) K. Iwai, H. Maeda, and T. Konno, *Cancer Res.*, **44**, 2115 (1984).
11) T. Kakutani, K. Yamaoka, M. Hashida, and H. Sezaki, *J. Pharmacokinet. Biopharm.*, **13**, 609 (1985).
12) T. Kakutani, E. Sumimoto, and M. Hashida, *J. Pharmacokinet. Biopharm.*, in press.
13) T. Kakutani, R. Atsumi, E. Sumimoto, and M. Hashida, *Chem. Pharm. Bull.*, **35**, 4907 (1987).
14) K. Yamaoka, T. Nakagawa, and T. Uno, *J. Pharmacokinet. Biopharm.*, **6**, 547 (1978).
15) D. J. Cutler, *J. Pharm. Pharmacol.*, **30**, 476 (1978).
16) S. Riegelman and P. S. Collier, *J. Pharmacokinet. Biopharm.*, **8**, 509 (1980).
17) L. R. Snyder and J. J. Kirkland, "Introduction to Modern Liquid Chromatography," 2nd ed., John Wiley and Sons, Inc., New York, 1979, p. 15.
18) A. B. Littlewood, "Gas Chromatography. Principles, Techniques, and Application," 2nd ed., Academic Press, New York, 1970, p. 144.
19) M. Rowland, L. Z. Benet, and G. G. Graham, *J. Pharmacokinet. Biopharm.*, **1**, 123 (1973).
20) K. S. Pang and M. Rowland, *J. Pharmacokinet. Biopharm.*, **5**, 625 (1977).
21) M. Weiss and W. Förster, *Eur. J. Clin. Pharmacol.*, **16**, 287 (1979).
22) M. Weiss, *J. Math. Biol.*, **15**, 305 (1982).
23) S. Miyauchi, Y. Sugiyama, Y. Sawada, K. Morita, T. Iga, and M. Hanano, *J. Pharmacokinet. Biopharm.*, **15**, 25 (1987).
24) M. Silverman and C. Trainor, *Fed. Proc., Fed. Am. Soc. Exp. Biol.*, **41**, 3054 (1982); J. B. Bassingthwaighte, *ibid.*, **41**, 3040 (1982).
25) M. Weiss, *J. Theor. Biol.*, **116**, 355 (1985); M. Weiss, *J. Pharmacokinet. Biopharm.*, **14**, 635 (1986).
26) K. Yamaoka and T. Nakagawa, *J. Chromatogr.*, **93**, 1 (1974); *idem*, *ibid.*, **117**, 1 (1976).
27) R. L. Schoenfeld, *Ann. N. Y. Acad. Sci.*, **108**, 69 (1963); A. Rescigno and G. Segre, "Drug and Tracer Kinetics," Blaisdell, Massachusetts, 1966, p. 75.
28) L. D. Homer and P. K. Weathersby, *J. Theor. Biol.*, **87**, 349 (1980).

[Chem. Pharm. Bull. 35(12)4907—4914(1987)]

Deconvolution Analysis of the Regeneration Process of Mitomycin C from Prodrug in a Muscle Perfusion System Based on Statistical Moment Theory

TOSHIYUKI KAKUTANI, RYO ATSUMI, ETSUKO SUMIMOTO, and MITSURU HASHIDA*

Faculty of Pharmaceutical Sciences, Kyoto University, Yoshida Shimoadachi-cho, Sakyo-ku, Kyoto 606, Japan

(Received May 15, 1987)

A new experimental system was developed to elucidate the local characteristics of regeneration of drugs from prodrugs and was applied to propyloxycarbonyl mitomycin C (propyl-MMC), a lipophilic prodrug of mitomycin C (MMC). Rabbit hind leg was perfused with a single-pass technique and outflow concentration–time curves of propyl-MMC and regenerated MMC after pulse injection of propyl-MMC were evaluated by using statistical moment analysis. The outflow concentration–time profile after injection of MMC was also analyzed. Through Laplace transformation of the convolution function for the regeneration process, the first three moment parameters (moments) were led to secondary parameters which express the regeneration and sequestration characteristics of the prodrug such as the regeneration and sequestration ratios of the prodrug, mean regeneration time, and variance of the regeneration time. The pharmacokinetic behavior of propyl-MMC and MMC was thus expressed from the viewpoints of distribution, sequestration, regeneration, and dispersion, as well as extent and rate. It was confirmed that lipophilic derivation produced a larger tissue distribution and that rapid regeneration of the drug from the prodrug resulted in large local bioavailability of the parent drug.

Keywords——single-pass perfusion system; rabbit muscle tissue; mitomycin C; lipophilic prodrug; statistical moment analysis; regeneration process; deconvolution

Cancer chemotherapy with cytotoxic drugs is often complicated by their indiscriminate action on both tumor and normal cells. Hence, an approach by which the cytotoxicity is directed specifically to cancer cells would be of great value. Based on biopharmaceutical considerations, many attempts have been made to deliver cytotoxic drugs to the tumor site by means of drug delivery systems.[1] Cancer drug delivery systems have been developed based on chemical transformation of drug molecules to macromolecular[2] or lipophilic prodrugs,[3] and the use of integrated formulations combining physical and chemical approaches.[4]

Intra-arterial drug administration to the tumor site is another promising way of achieving selective chemotherapy. Although the application of the above delivery systems to this therapeutic modality is expected to be advantageous, little is known about the disposition behavior of the pharmaceutically modified drug in local tissue after administration through the artery. Therefore, development of an experimental methodology for analyzing drug disposition in the target organ not only from a phenomenal point but also from a pharmacokinetical one is required.

To acquire detailed information in a local infusion system, we developed an experimental system in which rabbit hind leg was perfused *in situ* by using a single-pass technique and data were analyzed based on the statistical moment theory.[5] In previous studies, this system was applied to elucidate the local disposition characteristics of intra-arterially injected mitomycin C (MMC) and six lipophilic derivatives from the viewpoints of distribution, elimination, and dispersion, and the effects of the physicochemical properties of the drug[5,6] and protein

binding[7] on the disposition were examined. The present study was undertaken to clarify the characteristics of one of these derivatives, propyloxycarbonyl MMC (propyl-MMC) with respect to regeneration of the parent drug. Deconvolution was newly applied to data analysis and a scheme representing the disposition and regeneration processes of propyl-MMC is proposed.

Experimental

Materials——MMC was supplied by Kyowa Hakko Kogyo, Japan. Propyl-MMC was prepared as reported previously.[3] Their structures and physicochemical properties are shown in Table I. All other chemicals were of reagent grade and were obtained commercially (Nakarai Chemicals, Japan).

***In Situ* Perfusion of Rabbit Hind Leg**——The details of the experimental procedures were reported previously.[5] Male domestic rabbits weighing 1.96±0.07 (mean±S.D.) kg were anesthetized with urethane, and the right leg was essentially isolated from the body by using a single-pass perfusion technique. The right iliolumbar vessels, common iliac vessels, and saphenous vein of the right hip were each ligated. The femoral vessels of the right leg were cannulated with vinyl tubing (i.d. 0.8 mm, o.d. 1.2 mm, Dural Plastics, Australia) and the inflow (arterial side) and outflow (venous side) cannulas were kept at the level of the thigh during the experiment. In this preparation, there was almost complete recovery of the perfusate in venous outflow (94.1±8.0%), and mixing of blood from the body was suppressed to 4.5±3.2%. The mean weight of the perfused muscle was 49.8±11.0 g.

Tyrode's solution (137 mM NaCl, 2.68 mM KCl, 1.80 mM $CaCl_2$, 11.9 mM $NaHCO_3$, 0.362 mM NaH_2PO_4, 0.492 mM $MgCl_2$, and 5.55 mM D-glucose) with bovine serum albumin (fraction V, Armour Pharmaceutical Co., U.K.) at a concentration of 4.7% (w/v) was used as the perfusate. The perfusate, maintained at 37 °C, was gassed with 95%O_2–5%CO_2 (pH 7.4) and pumped into the cannulated artery (1.66 ml/min). Test compounds were dissolved in dimethylsulfoxide (DMSO) and injected into the line of perfusion flow using a six-position rotary valve injector (type 50 Teflon rotary valves, Rheodyne, CA). Test samples (0.1 ml) were put in the flow as a pulse function by this procedure.

Sampling and Assay——The details of the sampling procedure were also in the previous report.[5] The outflow perfusate was collected at appropriate time intervals (at first 1—2 s, subsequently 10 s—2 min). In the case of Evans blue and MMC, the concentration in the supernatant was measured after centrifugation of the outflow perfusate for 15 min at 1500 rpm. The optical density of Evans blue was determined at 620 nm. MMC was determined by measuring antimicrobial activity against *Escherichia coli* B using a disc-plate method.[3,5] For propyl-MMC, samples were collected directly into 5 ml of ethyl acetate and shaken instantly in order to avoid regeneration of MMC. After centrifugation for 15 min at 3000 rpm, 4 ml of the ethyl acetate phase was removed and evaporated. The residue was dissolved in methanol and then assayed by high performance liquid chromatography (HPLC) (Trirotar, Jasco, Japan) in a reverse-phase mode. The stationary phase used was a Cosmosil $5C_{18}$ packed column (4.6×150 mm, Nakarai Chemicals, Japan). A mixture of methanol and distilled water (53:47) was used as the mobile phase. These procedures afforded almost complete recovery of propyl-MMC. The regenerated MMC was determined by bioassay from the residual effluent perfusate after extraction of propyl-MMC. It was confirmed that ethyl acetate did not disturb the MMC determination.

TABLE I. Structures and Physicochemical Properties of MMC and Propyl-MMC

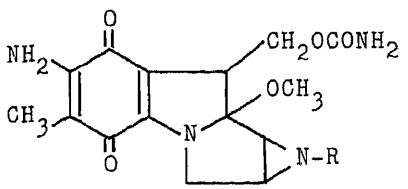

Compound	R	mp (°C)	PC_{oct}[a]	Solubility (mM)[b]		
				Water	Sesame oil	Hexane (×10³)
MMC	H	>270	0.414	2.73	0.018	0.234
Propyl-MMC	$COOC_3H_7$	203—207	32.7	0.333	0.104	<0.02

a) Partition coefficient between *n*-octanol and water. *b*) Determined at 25 °C.

***In Vitro* Determination of Regeneration of MMC from Propyl-MMC**——After the removal of blood by single-pass perfusion as described before, the thigh muscle of rabbit was homogenized with Tyrode's solution at 0—5 °C in a glass-Teflon homogenizer. Regeneration experiments were initiated by adding the stock solution. After 0, 0.5, 1, 2, and 4 h incubation at 37 °C, aliquots of samples were withdrawn and subjected for to HPLC analysis and bioassay.

Theoretical

Moment Analysis for Outflow Concentration–Time Curve

The first three (zero-th to second) statistical moment parameters (moments) for the outflow concentration–time curve are defined as follows[5]:

$$auc_i = \int_0^\infty C\,dt \tag{1}$$

$$\bar{t}_i = \int_0^\infty t \cdot C\,dt / auc_i \tag{2}$$

$$\sigma_i^2 = \int_0^\infty (t-\bar{t}_i)^2 \cdot C\,dt / auc_i \tag{3}$$

where t is time and C is the concentration of the substance normalized by expressing it as a fraction of the total injected amount in unit volume of outflow fluid (with dimensions of "% of dose/ml"). auc_i, $\bar{t}_i$, and σ_i^2 are the area under the outflow concentration–time curve, the mean transit time of the drug through the tissue, and the variance of the transit time, respectively. The moments defined by Eqs. 1—3 were calculated by using the linear trapezoidal formula and terminal phase extrapolation with a mono-exponential equation.[5,8] By introduction of the plate theory[9] and consideration of the partition between the mobile (perfusate) and stationary (tissue) phases[10] in the chromatography, the disposition parameters can be derived based on the well-stirred model[11-13] or the two compartment perfusion model.[13] Some of the disposition parameters which express the local disposition characteristics of the drug are calculated from the moments as follows:

$$F_i = auc_i / auc_{VRS} \tag{4}$$

$$k_i = (\bar{t}_i / \bar{t}_{VRS}) / F_i - 1 \tag{5}$$

$$\bar{t}_{el,i} = \bar{t}_i / (1 - F_i) \tag{6}$$

$$d_i = (\sigma_i^2)^{0.5} / \bar{t}_i \tag{7}$$

where auc_{VRS} and $\bar{t}_{VRS}$ are the area under the curve and the mean transit time of the vascular reference substance (VRS). These equations are derived based on the assumption that the elimination occurs from the equilibrium compartment, and not from the non-equilibrium compartment. In this theory, the non-equilibrium compartment does not necessarily correspond to the extravascular space. VRS is assumed not to distribute to extravascular tissue or to be eliminated. In this study, Evans blue bound to albumin was used as VRS. F_i (recovery ratio) represents the ratio of outflowed drug amount to input dose. k_i (tissue distribution ratio) equals the ratio of mass of drug in tissue to that in blood (perfusate) under steady-state conditions and corresponds to the capacity factor in a chromatographic system. $\bar{t}_{el,i}$ (mean elimination time) is the mean time value necessary to eliminate the drug and corresponds to mean residence time (MRT) in a whole-body recirculation system.[8] d_i (dispersion ratio) gives us information on mixing of the drug in the perfusion system. $d_i \geqq 1$ is a necessary condition for the calculation of Eqs. 4—6. The detailed theoretical background was reported in a previous paper.[5]

Deconvolution Analysis

The concentration–time curve of regenerated MMC after injection of propyl-MMC, $C_{P\to M}(t)$, can be defined as follows:

$$C_{P\to M}(t)=\int_0^t H_{reg.}(\tau)\cdot C_M(t-\tau)d\tau \tag{8}$$

where $H_{reg.}(t)$ is a time function of the regeneration rate (mg/min) from propyl-MMC to MMC and $C_M(t)$ is the MMC concentration–time curve after injection of MMC. In Eq. 8, it is assumed that regenerated MMC after injection of propyl-MMC behaves in the same way as MMC after its own injection. The Laplace transform of Eq. 8 is

$$C_{P\to M}(s)=H_{reg.}(s)\cdot C_M(s) \tag{9}$$

where $C_{P\to M}(s)$, $H_{reg.}(s)$, and $C_M(s)$ are corresponding transfer functions and s is the Laplace variable. Relationships between the transfer function and moments are defined as follows:

$$F_i=\lim_{s\to 0} C(s) \tag{10}$$

$$\bar{t}_i=\lim_{s\to 0} -\frac{d}{ds}\ln C(s) \tag{11}$$

$$\sigma_i^2=\lim_{s\to 0}\frac{d^2}{ds^2}\ln C(s) \tag{12}$$

The zero-th moment defined by the transfer function is the recovery ratio, F_i, that is derived from auc_i according to Eq. 4. Substitutions of Eq. 9 into Eqs. 10—12 yield

$$\begin{aligned} F_{P\to M}&=\lim_{s\to 0} C_{P\to M}(s)=\lim_{s\to 0} H_{reg.}(s)\cdot\lim_{s\to 0} C_M(s)\\ &=F_{reg.}\cdot F_M \end{aligned} \tag{13}$$

$$\begin{aligned} \bar{t}_{P\to M}&=\lim_{s\to 0} -\frac{d}{ds}\ln C_{P\to M}(s)\\ &=\lim_{s\to 0} -\frac{d}{ds}\ln H_{reg.}(s)+\lim_{s\to 0} -\frac{d}{ds}\ln C_M(s)\\ &=\bar{t}_{reg.}+\bar{t}_M \end{aligned} \tag{14}$$

$$\begin{aligned} \sigma^2_{P\to M}&=\lim_{s\to 0}\frac{d^2}{ds^2}\ln C_{P\to M}(s)\\ &=\lim_{s\to 0}\frac{d^2}{ds^2}\ln H_{reg.}(s)+\lim_{s\to 0}\frac{d^2}{ds^2}\ln C_M(s)\\ &=\sigma^2_{reg.}+\sigma^2_M \end{aligned} \tag{15}$$

where $F_{reg.}$ is the ratio of regeneration of MMC from propyl-MMC, and $\bar{t}_{reg.}$ is the mean regeneration time, which is the mean time value required for the regeneration process. $\sigma^2_{reg.}$ is the variance of the regeneration time. Equations 13—15 show essentially similar forms to those in the case of a whole-body recirculation system.[8,14]

The elimination process of propyl-MMC can be divided into regeneration of MMC (represented by symbols; $F_{reg.}$, $\bar{t}_{reg.}$, and $\sigma^2_{reg.}$) and sequestration as propyl-MMC. The following relationships are obtained.

$$F_P+F_{reg.}+F_{seq.P}=1 \tag{16}$$

where F_P and $F_{seq.P}$ are the ratios of recovered amount to outflowed perfusate and sequestrated amount as propyl-MMC to input dose. Elimination of regenerated MMC is also

divided into recovered and sequestrated fractions as follows:

$$F_{reg.}=F_{seq.M}+F_{P\to M} \tag{17}$$

where $F_{seq.M}$ is the sequestration ratio of regenerated MMC. Equations 13 and 17 give following relationship:

$$F_{P\to M}:F_{seq.M}=F_M:1-F_M \tag{18}$$

Results

Outflow Patterns and Moments

Figure 1 illustrates typical outflow concentration–time curves of propyl-MMC (○) and regenerated MMC (●) after injection of propyl-MMC. The whole concentration–time curve over 30 min is plotted on a semilogarithmic scale. The concentration of propyl-MMC rose rapidly to a peak, then fell in a manner described by a sum of exponentials. Table II lists their moments with those for VRS and MMC injection. The auc_M and auc_P were smaller than auc_{VRS}, suggesting the extraction of MMC and propyl-MMC in the muscle perfusion system. $\bar{t}_P$ and $\bar{t}_M$ were about threetimes and fourtimes of $\bar{t}_{VRS}$, respectively, indicating distribution of propyl-MMC and MMC into the extravascular space. The moments of regenerated MMC after injection of propyl-MMC showed a diminution in auc_i and increases in $\bar{t}_i$ and σ_i^2 due to the regeneration process, in comparison with MMC injected as itself.

In Vitro Experiments

In the muscle homogenate system, propyl-MMC showed a first-order elimination with remaining amounts of 79.3 ± 3.2, 77.6 ± 2.5, and 74.6 ± 1.8 (mean$\pm$S.D.) after 4 h, in 5, 10, and 20% tissue homogenate, respectively. The recovery as MMC was about 36% of the amount of degraded propyl-MMC at any homogenate concentration. The first-order elimination rate constant was obtained by the linear least-squares method for each tissue concentration. The tissue concentrations and obtained elimination rate constants showed a good correlation ($r=0.999$) and extrapolation to 100% tissue homogenate concentration gave a rate constant of $0.00287\,min^{-1}$.

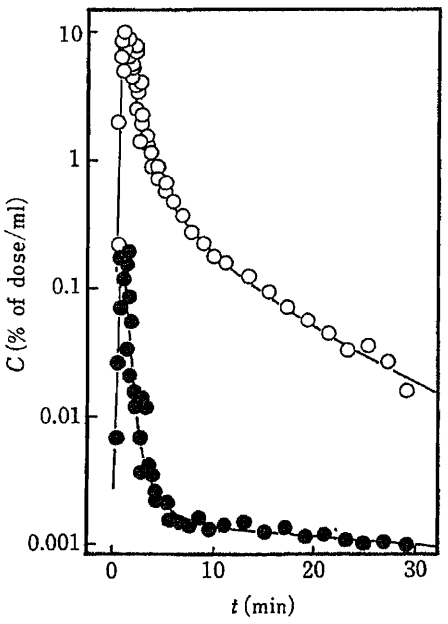

Fig. 1. Typical Outflow Concentration–Time Curves of Propyl-MMC and Regenerated MMC after Injection of Propyl-MMC

○, propyl-MMC; ●, regenerated MMC.

TABLE II. Moment Parameters (Moments) for VRS, MMC, Propyl-MMC, and Regenerated MMC after Injection of Propyl-MMC

	Moment parameters
Injection of VRS (6)	
auc_{VRS} (% dose·min/ml)	53.9±4.2
$\bar{t}_{VRS}$ (min)	1.11±0.11
σ^2_{VRS} (min²)	1.60±0.62
Injection of propyl-MMC (4)	
(a) Moments for propyl-MMC	
auc_P (% dose·min/ml)	18.2±1.7
$\bar{t}_P$ (min)	3.67±0.35
σ^2_P (min²)	30.4±6.1
(b) Moments for regenerated MMC	
$auc_{P\to M}$ (% dose·min/ml)	0.103±0.047
$\bar{t}_{P\to M}$ (min)	13.4±0.56
$\sigma^2_{P\to M}$ (min²)	252±283
Injection of MMC (5)	
auc_M (% dose·min/ml)	26.9±5.8
$\bar{t}_M$ (min)	4.05±0.19
σ^2_M (min²)	40.2±9.3

Each value is the mean±S.D. from the number of experiments in parenthesis.

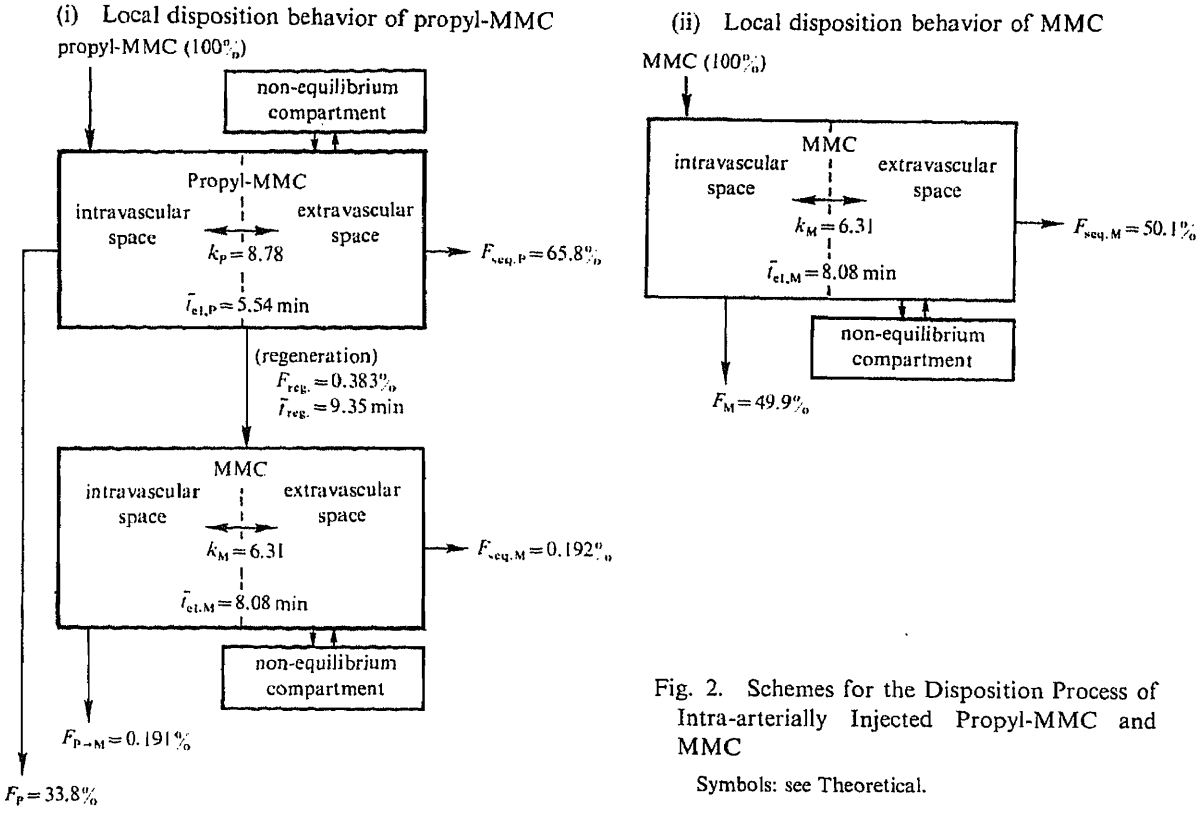

Fig. 2. Schemes for the Disposition Process of Intra-arterially Injected Propyl-MMC and MMC

Symbols: see Theoretical.

Construction of Local Disposition Profile of Propyl-MMC

After experimental determination of the moments of MMC, propyl-MMC, and regenerated MMC following injection of propyl-MMC, the secondary parameters were derived based on the present theory. Figure 2 illustrates a disposition profile of propyl-MMC in the muscle after intra-arterial bolus injection together with that of MMC. The pharmacokinetic behaviors of propyl-MMC and MMC were expressed with respect to the mean time necessary

for the subject process to proceed, and the relative contribution of each process. Propyl-MMC gave a larger tissue distribution ratio ($k_P=8.78$) than MMC ($k_M=6.31$). Most propyl-MMC molecules (more than 99.4%) were sequestrated as propyl-MMC but not recovered as MMC.

Dispersion Ratio

The dispersion ratios of VRS, MMC, and propyl-MMC were 1.12 ± 0.21, 1.56 ± 0.17, and 1.50 ± 0.12, respectively. These meet the necessary condition for calculation of Eqs. 4—6. Because the dispersion ratios were greater than 1, the existence of non-equilibrium compartments in the perfusion system was indicated for MMC and propyl-MMC. The dispersion ratio corresponding to regeneration of MMC from propyl-MMC was calculated by using $\bar{t}_{reg.}$ and $\sigma^2_{reg.}$. The value was calculated to be 1.56, but the large variance in $\sigma^2_{P\to M}$ makes further discussion of questionable value.

Discussion

In the present investigation, the local disposition characteristics of the MMC prodrug were elucidated mainly with regard to the regeneration process. Schemes representing the disposition behavior in the perfusion system were proposed for MMC and propyl-MMC. It was confirmed that lipophilic derivation produced a larger distribution and that rapid regeneration of the parent drug from the prodrug resulted in large local bioavailability of the parent drug, since the efflux rate was not so large.

Miyauchi *et al.* expressed the "apparent" intrinsic clearance in terms of the intrinsic clearances for the influx, efflux, and sequestration processes as follows.[15]

$$CL_{int,i}=\frac{CL_{int,seq}\times CL_{int,inf}}{CL_{int,seq}+CL_{int,eff}} \tag{19}$$

Equation 19 indicates that when $CL_{int,seq}\ll CL_{int,eff}$ is not attained, the influx rate into the extravascular space is largely reflected in the elimination rate from perfusate. When $CL_{int,seq}\ll CL_{int,eff}$ is attained, Eq. 19 can be reduced to $CL_{int,i}=CL_{int,seq}$, that is, the elimination rate corresponds to the sequestration rate.[15] Although irreversible binding to tissue components may occur, *in situ* elimination of propyl-MMC seems to include the distribution flux which represents drug movement from the intravascular space to the extravascular space. Further, a large part of the extraction ratio corresponds to the ratio of drug which is diffused into the extravascular space in a short time and will be recovered in outflow fluids according to an irreversible (non-linear) process. The dispersion ratio indicated the realization of finite mass transfer residence, but the mamillary compartment dose not correspond to the extravascular space.

k_i is related to the partition coefficient between perfusate and tissue, K, by $K=k_i\times\varepsilon$, where ε is the ratio of intravascular space volume to extravascular tissue space volume.[5] The value of ε is about 0.0384 ($=\bar{t}_{VRS}\cdot Q/$(volume of tissue$-\bar{t}_{VRS}\cdot Q$); Q is the perfusion flow rate), and thus the K values of propyl-MMC and MMC are 0.334 and 0.242, respectively. It is possible that the injection medium, DMSO, changes the partition balance between tissue and perfusate, but the difference between the physicochemical partition coefficient, PC_{oct}, and K suggests that the effective extravascular tissue volume is smaller than the virtual volume, especially in the case of propyl-MMC.

The most distinctive feature of the present analytical procedure is the application of statistical moment analysis to a single-pass perfusion system. Moment analysis was introduced into pharmacokinetics by Yamaoka *et al.*[8] and Cutler,[14] and it has many applications in pharmacokinetic calculations of model-independent parameters in whole-body recirculation systems. Concerning the impulse response of an open (single-pass) system

observed as a log-convex disposition curve, Weiss has recently proved that it has a mono-exponential terminal phase, and this supports the validity of the moment calculation against the outflow patterns.[16] In addition, since the moments are defined by transfer functions using Laplace transformation, network theory can also be applied to this analytical system.[12,13,17] In this report, one example of separation analysis of a subsystem from a macro system composed of several subsystems in series based on the network theory was presented. Another example was reported for subsystems in a parallel mode, and a general consideration of the effect of plasma protein binding on the organ uptake was presented for MMC, propyl-MMC, and other lipophilic derivatives.[7]

Acknowledgment The authors thank Professor Hitoshi Sezaki, Faculty of Pharmaceutical Sciences, Kyoto University, Kyoto, Japan, for his valuable suggestions and constructive discussions during this work. A part of this work was supported by a Grant-in-Aid for Scientific Research from the Ministry of Education, Science, and Culture, Japan.

References and Notes

1) G. Gregoriadis, *Nature* (London), **265**, 407 (1977); R. L. Juliano, "Drug Delivery Systems," ed. by R. L. Juliano, Oxford University Press, New York, 1980, p. 3.
2) M. Hashida, A. Kato, Y. Takakura, and H. Sezaki, *Drug Metab. Dispos.*, **12**, 492 (1984); Y. Takakura, S. Matsumoto, M. Hashida, and H. Sezaki, *Cancer Res.*, **44**, 2505 (1984).
3) H. Sasaki, M. Fukumoto, M. Hashida, T. Kimura, and H. Sezaki, *Chem. Pharm. Bull.*, **31**, 4083 (1983); H. Sasaki, E. Mukai, M. Hashida, T. Kimura, and H. Sezaki, *Int. J. Pharmaceut.*, **15**, 49 (1983).
4) M. Hashida and H. Sezaki, "Microspheres and Drug Therapy. Pharmaceutical, Immunological and Medical Aspects," ed. by S. S. Davis, L. Illum, J. G. McVie, and E. Tomlinson, Elsevier Biomedical Press, New York, 1984, p. 281; H. Sasaki, T. Kakutani, M. Hashida, and H. Sezaki, *J. Pharm. Pharmacol.*, **37**, 461 (1985); H. Sasaki, T. Kakutani, M. Hashida, T. Kimura, and H. Sezaki, *Chem. Pharm. Bull.*, **33**, 2968 (1985).
5) T. Kakutani, K. Yamaoka, M. Hashida, and H. Sezaki, *J. Pharmacokinet. Biopharm.*, **13**, 609 (1985).
6) T. Kakutani, Y. Suematsu, W. Y. Cheah, E. Sumimoto, and M. Hashida, *Chem. Pharm. Bull.*, **35**, 4898 (1987).
7) T. Kakutani, E. Sumimoto, and M. Hashida, *J. Pharmacokinet. Biopharm.*, in press.
8) K. Yamaoka, T. Nakagawa, and T. Uno, *J. Pharmacokinet. Biopharm.*, **6**, 547 (1978).
9) A. B. Littlewood, "Gas Chromatography. Principles, Techniques, and Application," 2nd ed., Academic Press, New York, 1970, p. 144.
10) L. R. Snyder and J. J. Kirkland, "Introduction to Modern Liquid Chromatography," 2nd ed., John Wiley and Sons, Inc., New York, 1979, p. 15.
11) M. Rowland, L. Z. Benet, and G. G. Graham, *J. Pharmacokinet. Biopharm.*, **1**, 123 (1973); K. S. Pang and M. Rowland, *J. Pharmacokinet. Biopharm.*, **5**, 625 (1977).
12) M. Weiss and W. Förster, *Eur. J. Clin. Pharmacol.*, **16**, 287 (1979).
13) M. Weiss, *J. Math. Biol.*, **15**, 305 (1982).
14) D. J. Cutler, *J. Pharm. Pharmacol.*, **30**, 476 (1978).
15) S. Miyauchi, Y. Sugiyama, Y. Sawada, K. Morita, T. Iga, and M. Hanano, *J. Pharmacokinet. Biopharm.*, **15**, 25 (1987).
16) M. Weiss, *J. Ther. Biol.*, **116**, 355 (1985); *idem*, *J. Pharmacokinet. Biopharm.*, **14**, 635 (1986).
17) R. L. Schoenfeld, *Ann. N. Y. Acad. Sci.*, **108**, 69 (1963); A. Rescigno and G. Segre, "Drug and Tracer Kinetics," Blaisdell, Massachusetts, 1966, p. 75.

[Chem. Pharm. Bull. 35(12)4915—4920(1987)]

Evaluation of *in Vitro* and *in Situ* Transdermal Absorption of Drugs in Pig and Rat Skin

JAN PŘÍBORSKÝ,*[,a,b] KOZO TAKAYAMA,[a] TSUNEJI NAGAI,[a] DANUŠE WAITZOVÁ,[b] and JIŘÍ ELIS[b]

Faculty of Pharmaceutical Sciences, Hoshi University,[a] Ebara-2-4-41, Shinagawa-ku, Tokyo 142, Japan and State Institute for Drug Control,[b] Srobarova 48, CS 100 41 Praha 10, Vinohrady, Czechoslovakia

(Received May 18, 1987)

The permeability characteristics of newborn pig skin and adult rat skin, either fresh or stored, to model drugs were examined and compared. Special attention was paid to the design to a new experimental system suitable for evaluation of skin permeability to various substances. Two types of model substances were used; insulin, a poorly absorbable substance with high molecular weight as a representative of peptide drugs, and brilliant blue, a low-molecular, relatively well absorbable substance. *In vitro* experiments performed with both substances in pig and rat gave comparable values of skin permeability. Maximum insulin concentration in the receiver solution was very similar in all experiments (164.5—180.5 μU/ml/24 h when Azone® was used and 136.5—178.0 μU/ml/24 h when *N*-methyl-2-pyrrolidone (NMP) was used as a penetration enhancer). The donor side concentration of insulin was 2.5 mg/ml.

The optimum concentrations of vehicle and penetration enhancer were 40.0% propylene glycol (PG) and 0.1% Azone® or 12.0% NMP, respectively. Brilliant blue experiments performed with the three skin preparations with 40.0% PG and 12.0% NMP gave similar values of the flux J_T and permeability P of 1.38—1.97 μg/cm²/h and 1.56×10^{-5}—2.22×10^{-5} cm/h, respectively. The concentration of brilliant blue in the donor compartment was 50 mg/ml. There were differences between the lag time in pig and rat skin experiments: about 3 h in the case of rat skin but 15 min in pig skin. In comparison to *in vitro* experiments, *in situ* studies gave much lower penetration of both test substances expressed as concentration in the receiver compartment. In the case of insulin with Azone® or NMP in the formulation, 30 times or 17 times lower concentration was found, and in brilliant blue experiments almost 5 times lower levels were observed. This new experimental system should be useful for examination of potential drug candidates as well as drug formulations for transdermal use.

Keywords——penetration enhancer; propylene glycol; insulin; brilliant blue; flux; permeability; lag time

Many papers have been published on *in vitro* transdermal absorption.[1-3] Various modifications of the Franz-type permeation cell have usually been used.[4-6] Such experiments usually take more than 24 h,[7,8] and the skin used is generally fresh or has been stored in a freezer.[9-11] In both cases, the skin is dead and some of its biological properties may be altered. Even so, it is assumed that the properties of the skin will remain unchanged throughout the experimental period (at least 24 h) in the permeation cell, which is usually in a bath at 37 °C. Under such conditions, where the skin is acting as a kind of membrane, the skin permeability can not be evaluated correctly. Nevertheless, such experiments are still of great importance for evaluation of the relative potency of new penetration enhancers, suitable drug selection and optimum formulation for transdermal absorption.

The aim of the present study was to compare the permeability characteristics of newborn pig skin and rat skin, either fresh or stored, with two model substances. A new experimental system was developed in which *in situ* full thickness skin is used throughout the experimental

period to maintain constant conditions.

Experimental

Materials——Bovine insulin used in this study was purchased from Sigma Chemical Company. Its specific activity was 23.5 U/mg. Azone® was kindly provided by Teijin Co., Ltd. Propylene glycol (PG) was purchased from Wako Pure Chemical Industries, Ltd., and *N*-methyl-2-pyrrolidone (NMP) and Brilliant blue FCF were from Tokyo Kasei Kogyo Co., Ltd. Other chemicals were of a standard analytical grade.

Formulations——Insulin (2.5 mg/ml) was dissolved in sodium citrate buffer (pH 3.0), then formulated into solutions containing either Azone® at concentrations from 0.0 to 0.5% or NMP from 0.0 to 20.0% (both previously dissolved in 40% PG). Brilliant blue was used as a 50.0 mg/ml solution formulated in 40.0% PG and 12.0% NMP. The same formulations were used in *in situ* experiments.

***In Vitro* Procedure**——For *in vitro* experiments, newborn male pig skin (Landrace female × Yorkshire male, F_1) from animals weighing 1020 ± 157 g, and skin of adult Wistar rats (185.0 ± 12 g) were used. The skin was taken from the abdominal region. The rats were shaved 24 h before the experiment and the next day the skin was taken. The skin was used either immediately or after storage for 30 d at −20 °C. It was mounted into Franz-type permeation cells[5] in which the volume of the receiver compartment was 15 ml. Saline was used as a medium in this compartment. The concentrations of drugs applied on the donor side were described above. The temperature of the bath was 37 °C, and the available surface area for penetration was 1.77 cm^2. Insulin samples were taken after 10 and 24 h and brilliant blue samples after 6, 12, 20 and 26 h. In the experiments comparing *in vitro* and *in situ* procedures, sampling was done after 10 h.

Animal Experiments——These experiments were performed on adult male Wistar rats (185.0 ± 10 g). The skin of these animals was prepared the same way as for *in vitro* experiments but the next day a transverse incision of approximately 3 cm was made in the lower abdominal region and an acrylate reservoir containing 3.0 ml of saline was applied under the skin, which was first separated from the subcutaneous tissue as well as major blood vessels, so that minor vessels and the capillary network remained. Residual vessels were slightly compressed after application of the acrylic reservoir and cover so that a limited blood supply persisted. The experiment was carried out under sterile conditions. The animals were kept throughout under pentobarbital anesthesia (0.5 ml/kg Nembutal injection, Abbott, containing 50.0 mg/ml of sodium pentobarbital). The formulations to be studied were applied on the concave portion of the skin surface whose visceral part was pressed into the acrylate reservoir (Fig. 1). To keep the solution on a limited area of skin surface (1.77 cm^2), a plastic ring with the same diameter as in the *in vitro* experiments was used. Samples were taken after 10 h.

Analytical Procedure——Insulin concentrations were measured by using the ELISA method (Insulin B-Test, purchased from Wako Pure Chemical Industries, Ltd.). Brilliant blue was estimated after centrifugation of the sample, by measuring the absorbance at 630 nm with a Hitachi 124 spectrophotometer. The calibration for brilliant blue was linear over the whole range of measured values.

Results

We compared newborn pig skin and fresh and stored rat skin using optimum concentrations of all substances in formulations according to our previous results.[12] Insulin was used as a peptide drug with low permeation ability. Brilliant blue experiments were used for counting fluxes and other characteristics of skin permeation of the two species. For prediction of differences between *in vitro* and *in vivo* experiments, a new method was introduced.

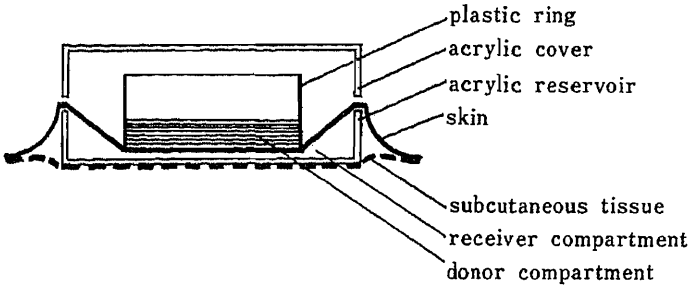

Fig. 1. Device for *in Situ* Transdermal Application of Drugs

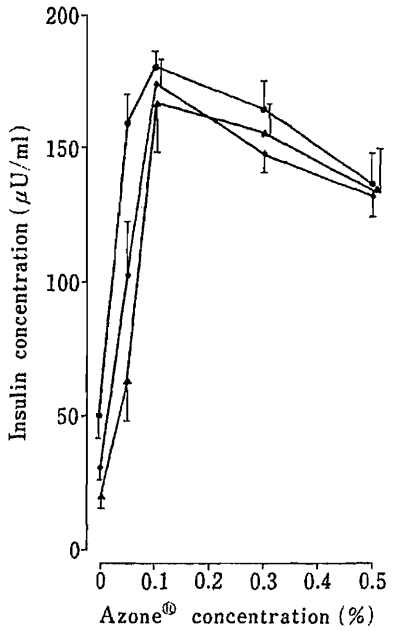

Fig. 2. Effect of Azone® on *in Vitro* Transdermal Absorption of Insulin

(▲) Pig skin, (●) fresh and (◆) stored rat skin. Dose 2.5 mg/ml. PG concentration 40%. Sampling time 24 h. Means ± S.E. (n = 5—6).

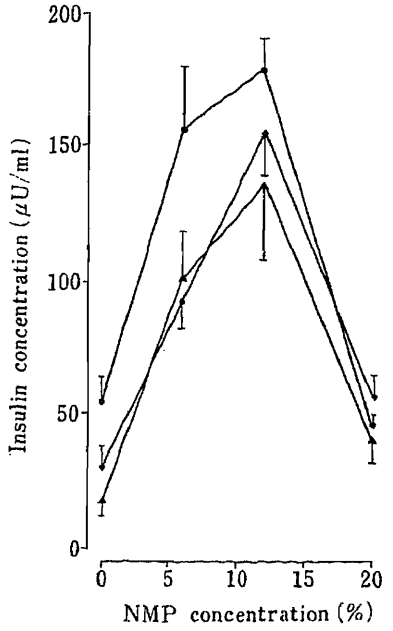

Fig. 3. Effect of NMP on *in Vitro* Transdermal Absorption of Insulin

(▲) Pig skin, (●) fresh and (◆) stored rat skin. Dose 2.5 mg/ml. PG concentration 40%. Sampling time 24 h. Means ± S.E. (n = 5—6).

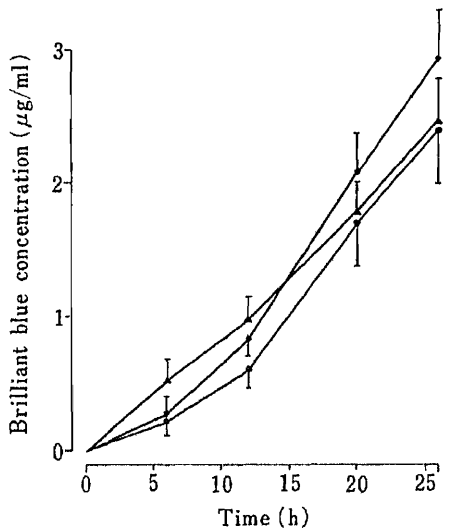

Fig. 4. Effect of NMP on *in Vitro* Transdermal Absorption of Brilliant Blue

(▲) Pig skin, (●) fresh and (◆) stored rat skin. Dose 50 mg/ml. NMP concentration 12%. PG concentration 40%. Means ± S.E. (n = 6).

TABLE I. Comparison of Lag Time, Flux and Permeability to Brilliant Blue in Newborn Pig Skin, Fresh (f) Rat Skin and after 30 d Storage (s)

	Lag time (t_L) (h)	Flux (J_T) ($\mu g/cm^2/h$)	Permeability (P) (cm/h)
Pig	0.25[a]	1.38	1.56×10^{-5}
Rat_f	2.85	1.53	1.73×10^{-5}
Rat_s	3.41	1.97	2.22×10^{-5}

a) $p < 0.01$ (*vs.* both rat experiments).

Figures 2 and 3 show insulin concentrations in the receiver compartment measured after 24 h *in vitro*, with Azone® and NMP was used as penetration enhancers, respectively. The curve shape is characteristic for each enhancer, and there were no significant differences in maximum concentrations of insulin between newborn pig skin and rat skin, either fresh or stored. It seems that the skin of both species has very similar permeation characteristics.

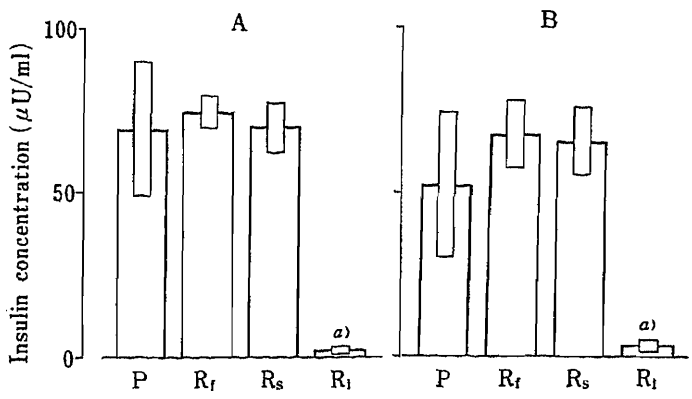

Fig. 5. Comparison of *in Vitro* and *in Situ* Transdermal Absorption of Insulin

A=Azone® (0.1%), B=NMP (12%) as a penetration enhancer. PG concentration 40%. Sampling time 10 h. P=pig, $R_{f,s,i}$=rat-fresh, stored, *in situ*. Means± S.E. (n=5—6). The permeated amount is significantly lower in *in situ* experiments than in *in vitro* systems (*a*) $p<0.01$).

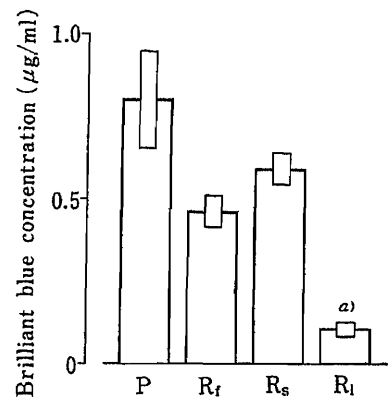

Fig. 6. Comparison of *in Vitro* and *in Situ* Transdermal Absorption of Brilliant Blue

NMP (12%) was used as a penetration enhancer. PG concentration 40%. Sampling time 10 h. P=pig, $R_{f,s,i}$=rat-fresh, stored, *in situ*. Means±S.E. (n=5—6). The permeated amount was significantly lower in *in situ* experiments than in *in vitro* systems (*a*) $p<0.01$).

(Maximum concentration of insulin in Azone® experiments was 164.5±24.1 μU/ml/24 h in pig skin, while the levels were 180.5±9.9 μU/ml/24 h in fresh rat skin and 172.4±15.3 μU/ml/24 h in the stored rat skin. In NMP experiments, the maxima were 136.5±45.7 μU/ml/24 h in pig skin, 178.0±18.5 μU/ml/24 h in fresh rat skin and 155.3±33.5 μU/ml/24 h in stored rat skin.) The donor side concentration of insulin was 2.5 mg/ml.

Further examinations carried out with brilliant blue (Fig. 4) confirmed the similarity of both types of the skin and also 30 d stored skin. The sampling was done after 6, 12, 20 and 26 h and indicated an almost linear increase of brilliant blue concentration in the receiver compartment during a 26 h experiment. In all three cases correlation coefficients were very high (r_{xy} was 0.999 in pig skin and 0.994 and 0.997 in rat skin experiments, respectively) and the slopes were similar. These correlation coefficients were calculated between 6 and 26 h, and demonstrate the linearity of the concentration increase. Table I summarizes the parameters of skin permeability. The only marked difference seems to be the duration of the lag time, which was approximately 15 min with pig skin, but about 3 h with both fresh and stored rat skin. Values of fluxes and permeabilities were approximately the same in all three cases.

There is usually a great difference between the results obtained *in vitro* and *in vivo*. This led us to develop the *in situ* method described above. The aim was on the one hand to eliminate some of the variables of *in vivo* experiments such as distribution, metabolism and elimination, and on the other hand to keep the skin alive throughout the experimental period. The skin in *in vitro* experiments may not maintain its properties during the experiment lasting 24 h or more in a bath at 37 °C. After completion of the *in situ* experiments carried out under sterile conditions, the animals were observed for two weeks. The healing of the wound occurred normally and we did not find any macroscopic signs of skin damage. The results of *in vitro* and *in situ* experiments with insulin after 10 h are compared in Fig. 5. Only the formulations containing the optimum concentration of Azone® (0.1%) or NMP (12%) selected based on the *in vitro* results were used. The difference between amount of permeated insulin *in vitro* and *in situ* for formulations containing Azone® or NMP was about 30 or 17 times, respectively. Brilliant blue also gave a lower permeability in the *in situ* skin experiment. The difference in amount of permeated brilliant blue was about 5 times (Fig. 6).

Discussion

Comparison of skin permeability in various species presents many problems. There is still no effective experimental system for predicting the suitability of a drug and its formulations for transdermal use in human skin. Differences or similarities in skin permeability between various species have been reported,[13] and also great differences in permeability in one species measured in various regions of the body.[14-16] Our comparison of two species (newborn pig and adult rat skin) indicated similar permeation ability. Of course such a result does not mean that pig and rat skin are similar. The influence of aging is another source of differences,[9,17] but the data are also controversial. The skin is most permeable in newborns and young individuals, while aging leads to a decrease in permeability. This led us to use newborn pig skin with relatively high permeability. The results proved that this type of skin is comparable with adult rat skin from the viewpoint of the permeability to insulin as well as to brilliant blue. The only difference in the brilliant blue experiments is in duration of the lag time which was more than 10 times longer in the rat skin than in the newborn pig skin. To exclude regional differences in permeability in one species (which may be in the range of two orders of magnitude[15]) we used only abdominal skin.

Another problem of *in vitro* experiments is that they are usually carried out for 24 h or more at 37 °C.[7] The skin is actually dead, and of course its properties may change and damage may occur. This could result in a higher permeability of the skin in *in vitro* systems, while under the same conditions in the *in situ* model the permeability is very low. In our model we use similar conditions to those used in permeation cells to obtain comparable results. This experimental system may be useful to examine potential drug formulation candidates, since several variables such as distribution, metabolism and elimination are excluded.

The most important part of the method is the preparation of the dermal part and removal of the major blood vessels to prevent drainage of the permeated substance. Small vessels that are not removed are slightly compressed when the acrylic reservoir and cover are applied. The capillary network is not affected and limited blood supply remains. By taking parallel samples from the systemic circulation and from the reservoir we showed that significant leakage into the blood-stream did not occur. As compared with the control group, we did not find any differences in blood concentrations of insulin. In the case of brilliant blue too, no differences between control and experimental animals were observed. To keep the sample on a restricted absorption surface (1.77 cm^2), it is necessary to attach a plastic ring on the skin surface.

Based on our experiments we can draw the following conclusions.

1. Newborn pig skin and the skin of adult rats have similar permeation characteristics. The data obtained in our experiments should have value as a basis for further studies of the relationships between experimental systems used for prediction of transdermal permeability.
2. The *in situ* experimental system should be useful for evaluation of potential drug and formulation candidates for transdermal application. The advantage is that the skin retains the properties of the living tissue throughout the experiment.

Acknowledgements This research was supported by a Special Research Grant from the Ministry of Science and Technology.

References

1) D. Mirejovsky and H. Takruri, *J. Pharm. Sci.*, **75**, 1089 (1986).
2) Y. Morimoto, K. Sugibayashi, K. Hosoya and W. I. Higuchi, *Int. J. Pharm.*, **32**, 31 (1986).
3) E. Touitou, *Int. J. Pharm.*, **33**, 37 (1986).
4) T. J. Franz, *J. Invest. Dermatol.*, **64**, 190 (1975).
5) E. W. Merritt and E. R. Cooper, *J. Controlled Release*, **1**, 161 (1984).

6) K. Tojo, M. Ghannam, Y. Sun and Y. W. Chien, *J. Controlled Release*, **1**, 197 (1985).
7) E. R. Cooper and B. Berner, "Methods in Skin Research," John Wiley & Sons, Ltd., 1985, pp. 407—432.
8) A. Hoelgaard and B. Mollgaard, "Advances in Drug Delivery Systems," Elsevier, Amsterdam, Oxford, New York, Tokyo, 1986, pp. 111—120.
9) R. L. Bronaugh, R. F. Stewart and M. Simon, *J. Pharm. Sci.*, **75**, 1094 (1986).
10) T. Ogiso, Y. Ito, M. Iwaki and H. Atago, *J. Pharmacobio-Dyn.*, **9**, 517 (1986).
11) K. Sugibayashi, K. Hosoya, Y. Morimoto and W. I. Higuchi, *J. Pharm. Pharmacol.*, **37**, 578 (1985).
12) J. Priborsky, K. Takayama, T. Nagai, D. Waitzova and J. Elis, Abstract of Papers, 107th Annual Meeting of the Pharmaceutical Society of Japan, Kyoto, April 1987, p. 842.
13) M. J. Bartek, J. A. La Budde and H. I. Maibach, *J. Invest. Dermatol.*, **58**, 114 (1972).
14) J. Hadgraft, *Int. J. Pharm.*, **16**, 255 (1983).
15) W. Schalla and H. Schaefer, "Dermal and Transdermal Absorption," W. V. G., Stuttgart, 1982, p. 56.
16) D. Dupuis, A. Rougier, C. Lotte, D. R. Wilson and H. I. Maibach, *J. Soc. Cosmet. Chem.*, **37**, 351 (1986).
17) R. H. Guy, *Therapeutic Research*, **3**, 1031 (1985).

[Chem. Pharm. Bull. 35(12)4921—4927(1987)]

Application of Interpolymer Complexation of Polyvinylpyrrolidone/Carboxyvinyl Polymer to Control of Drug Release[1)]

KOZO TAKAYAMA* and TSUNEJI NAGAI

Faculty of Pharmaceutical Sciences, Hoshi University, Ebara-2-4-41, Shinagawa-ku, Tokyo 142, Japan

(Received May 23, 1987)

Interpolymer complex formation of polyvinylpyrrolidone (PVP) with carboxyvinyl polymer (CP) was examined by turbidity measurement, a binding isotherm study and Fourier-transform infrared spectroscopy. The interpolymer complex of PVP with CP was found to be formed in the unit molecular ratio of 1 : 1 under ideal conditions, though the ratio of PVP in the solid complex was lower than 1 : 1 under practical conditions. Hydrogen bonding might be the driving force for the complexation, and the degree of hydrogen bonding was calculated to be about 40 to 50%.

The slowest dissolution rate of chlorpheniramine maleate from tablets, which consisted of a blend of PVP and CP was observed when the polymer combination ratio was 1 : 1. In the case of indomethacin, the longest lag time for the dissolution was observed at the polymer ratio of 1 : 1. Therefore, the drug dissolution behavior from PVP/CP tablets is dependent on the complex formation of PVP and CP.

Keywords——polyvinylpyrrolidone; carboxyvinyl polymer; interpolymer complexation; hydrogen bonding; chlorpheniramine maleate; indomethacin; controlled release

An interpolymer complex of polyvinylpyrrolidone (PVP) with carboxyvinyl polymer (CP), crosslinked polyacrylic acid, was recently reported to be applicable as a device for obtaining sustained release of drugs in the pharmaceutical field.[2,3)] However, there is still little information on the mechanism of this polymer–polymer interaction, though much is known about the PVP/polyacrylic acid complex.[4–6)] Hydrogen bonding between carbonyl groups of PVP and carboxyl groups of polyacrylic acid has been reported to be the main driving force for the complexation of PVP and polyacrylic acid. Since CP is a similar compound to polyacrylic acid, hydrogen bonding may be an important factor in the complexation of PVP and CP.

The purpose of the present study was to investigate the quantitative relationship between the mechanism of PVP/CP complex formation and the drug dissolution behavior from the polymer matrix, which consists of PVP and CP. Chlorpheniramine maleate (CPM) and indomethacin (IMC) were selected as model acid-soluble and alkali-soluble drugs, respectively.

Experimental

Materials——The polymers used are listed in Table I. PVP K-30 and PVP K-90 of extra pure reagent grade were purchased from Tokyo Kasei Industrial Co., Ltd. CP-I and CP-II marketed as "HIVISWAKO 105" and "HIVISWAKO 104" were supplied by Wako Pure Chemical Industries, Ltd. For the Fourier-transform infrared (FT-IR) study, CP-I and CP-II were used after being washed with chloroform and dried *in vacuo* at room temperature for 3 d. For the other studies, CP-I and CP-II were used without further treatment. CPM and IMC were purchased from Tokyo Kasei Industrial Co., Ltd., and Sigma Chemical Co., Ltd., respectively. Other chemicals were of reagent grade.

TABLE I. Polymers Used in This Study

Polymer	Mean molecular weight
Polyvinylpyrrolidone K-30 (PVP K-30)	40000
Polyvinylpyrrolidone K-90 (PVP K-90)	360000
Carboxyvinyl polymer I (CP-I)	1000000—1500000
Carboxyvinyl polymer II (CP-II)	2000000—3000000

Turbidity Measurement——PVP solution (2 ml; 0—0.02%) was mixed with CP suspension (2 ml; 0—0.02%) at 37 °C for 1 h to prepare the sample solution. Buffer solutions (pH 1.6—5.0), which consisted of 0.05 M H_3PO_4, 0.05 M NaCl and 0.05 M NaOH, were used to prepare the sample solutions. Total polymer concentration was fixed at 0.01% in all samples. The turbidity of each sample solution was determined at 600 nm, where there was no absorption due to the polymers in solution, using a Hitachi 124 spectrophotometer.

Binding Isotherm——PVP solution (2 ml; 0.2—1.0%) was mixed with CP suspension (2 ml; 0.5%). The mixture was then incubated at 37 °C for 48 h. After centrifugation for 20 min at 15000 rpm in a Hitachi SCR 20B centrifuge, PVP in the supernatant was determined by a ultraviolet (UV) absorption method[7] using a Shimadzu model LC-5A pump and a Hitachi model 638-41 UV monitor. Distilled water was used as the mobile phase. A 20 μl aliquot of sample solution was injected to the apparatus. The height of the UV absorption peak at 230 nm was measured for the determination of PVP. The relationship between PVP concentration and peak height showed good linearity.

Effect of pH and Ionic Strength on the Binding Amount of PVP to CP——PVP solution (5 ml; 1.2%) was mixed with CP suspension (5 ml; 0.2%). The mixture was then incubated at 37 °C for 48 h. After centrifugation for 20 min at 15000 rpm, PVP in the supernatant was determined by the same method as described above. In order to investigate the effect of pH on the binding amount of PVP, buffer solutions (pH 1.8—4.7), which consisted of 0.05 M H_3PO_4, 0.05 M NaCl and 0.05 M NaOH, were employed to prepare the polymer solutions. NaCl (0.1—0.4 M) was also added to the buffer solutions to examine the effect of ionic strength on the binding amount.

Preparation of the Solid Complex——PVP solution (111 ml; 0.1%) was mixed with CP suspension (72 ml; 0.1%). The sample solution was then incubated at 37 °C for 10 d. After the removal of water in the sample solution by the use of a rotary evaporator, the solid complex, which consisted of the two polymers in a combination ratio of 1 : 1 based on the unit molecular weight, was dried *in vacuo* for 3 d.

Infrared Absorption Spectroscopy——FT-IR spectra of PVP/CP solid complexes were measured using a Jasco model FT/IR-5 spectrophotometer (KBr disk method).

Preparation of Tablets for the Dissolution Study——Unless otherwise stated, flat-faced tablets of 150 mg weight (25 mg of CPM or IMC, 125 mg of the combination of PVP and CP) and 13 mm diameter were made by compressing the given amount of powder directly under 50 kg/cm^2 for 10 s using a Shimadzu hydraulic press for KBr tablets for IR spectroscopy.

Dissolution Test——A Toyama Sangyo model TR-5S3 dissolution tester was used at 100 rpm paddle speed with 300 ml of the dissolution medium at 37 °C. The dissolution media used were those described in JP XI as disintegration media No. 1 (pH 1.2) and No. 2 (pH 6.8). Aliquots (3 ml) of solution were taken at intervals and the volume was made up to the original volume by adding the dissolution medium. After adding an equal amount of 1 N H_2SO_4 to the sample solution, the amounts of CPM released in the medium of pH 1.2 were determined by UV spectrophotometry at 263 nm. The amounts of IMC released in the medium of pH 6.8 were determined similarly at 310 nm. Results are given as the mean values of three determinations.

Results and Discussion

Confirmation of Interpolymer Complex Formation

Figure 1 shows the turbidity as a function of weight ratio of PVP K-30/CP-II in the media of various pH values. Maximum turbidity was found at the weight ratio of 1 : 1 in the acidic medium (pH $\leqq$ 4). No solid complex formation was observed in the higher pH region. In order to examine further the complexation, the binding of PVP to CP was quantitatively analyzed by the application of Langmuir's equation:

$$C/M = 1/ab + C/a \quad (1)$$

where C is the equilibrium concentration of PVP, M is the binding amount of PVP to CP, a is the maximum binding amount and b is the apparent binding constant. The binding amount of

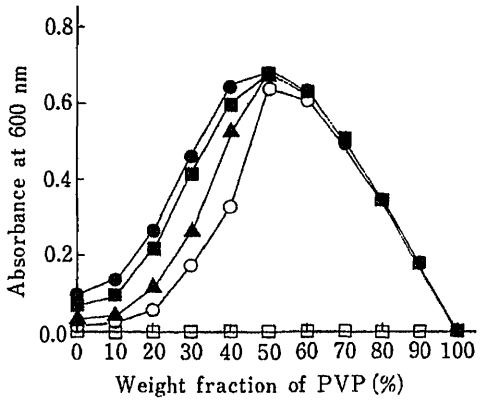

Fig. 1. Relationship between Polymer Combination Ratio and Turbidity in the PVP K-30/CP-II System (Total Polymer Concentration = 0.01%)

pH values: ●, 1.6; ■, 2.9; ▲, 3.4; ○, 4.1; □, 5.0.

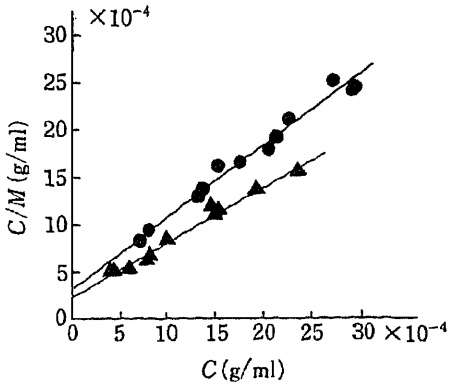

Fig. 2. Langmuir-Type Plots of PVP K-30 bound to CP-I and CP-II in Distilled Water at 37°C (Concentration of CP = 0.25%)

●, PVP K-30/CP-I; ▲, PVP K-30/CP-II.

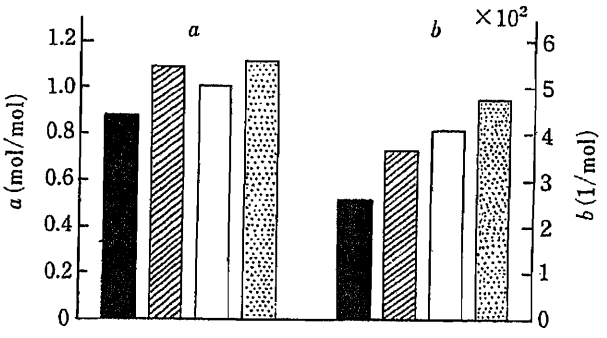

Fig. 3. Effect of Molecular Weight of Polymers on the Langmuir's Binding Parameters, *a* and *b*

■, PVP K-30/CP-I; ▨, PVP K-30/CP-II; □, PVP K-90/CP-I; ▦, PVP K-90/CP-II.

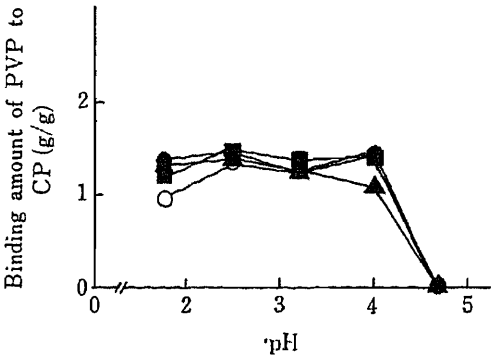

Fig. 4. Effect of pH on the Amount of PVP K-30 bound to CP-II at Various Sodium Ion Concentrations, $[Na^+]_i$, at 37°C

Values of $[Na^+]_i$: ●, 0.11—0.13 M; ▲, 0.21—0.23 M; ■, 0.31—0.33 M; ○, 0.41—0.43 M.

PVP to CP was determined by subtracting the equilibrium concentration of PVP from the initial concentration, since the solubility of PVP/CP complex is negligibly small. Good linearity of the Langmuir plot was observed in the case of PVP K-30, which bound to CP-I and CP-II, as shown in Fig. 2. In the case of PVP K-90, good linearity was also found. Figure 3 shows the effect of mean molecular weights of PVP and CP on the binding parameters, calculated from the values of intercept and slope in Fig. 2. The apparent binding constant, *b*, gradually increased with increasing molecular weight of both polymers. Therefore, the molecular size of the polymers is one of the significant factors in complex formation. On the other hand, the maximum binding amount, *a*, was almost independent of the molecular weight of the polymers. Interestingly, the *a* value was found to be about one in all sysfems. Therefore, the interpolymer complex could be formed with the unit molecular ratio of 1 : 1 under ideal conditions. However, the ratio of PVP in the solid complex actually obtained was a little lower than 1 : 1. This phenomenon might be due to the crosslinking of CP. Namely, the number of effective carboxyl groups, which can bind with PVP, seems to be limited because of the rigid structure of the CP molecule.

Figure 4 shows the effects of pH and ionic strength on the binding amount of PVP K-30 to CP-II. The complexation of PVP to CP was found to be a discontinuous function of pH

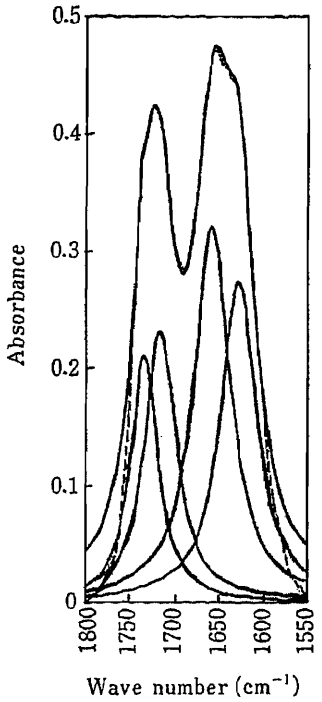

Fig. 5. FT-IR Spectra of PVP K-30/CP-II Complex

——, simulated; ------, observed.

TABLE II. Degree of Hydrogen Bonding in PVP/CP Interpolymer Complex (Unit Molecular Weight Ratio 1 : 1)

Complex	Hydrogen bonding (%) calculated based on	
	PVP	CP
PVP K-30/CP-I	38.2	44.7
PVP K-30/CP-II	43.4	51.3
PVP K-90/CP-I	45.5	47.9
PVP K-90/CP-II	43.8	51.0

between pH 4.0 and pH 4.7. A similar tendency was observed in the turbidity measurement as described above. On the other hand, no effect of the sodium ion concentration was observed, as shown in Fig. 4. Therefore, the dissociation of carboxyl groups of CP might be an important for the balance of complexation and decomplexation.

Next, the FT-IR spectrum of PVP/CP complex was determined. Figure 5 shows FT-IR spectra of PVP K-30/CP-II complex (unit molecular weight ratio 1 : 1) in the region of carbonyl absorption. Absorptions of carboxyl groups of CP and carbonyl groups of PVP each seem to be composed of two different kinds of peaks, which were separated by means of a computer simulation technique described by Kato *et al.*[8] Assignment of each IR peak was done as reported by Sasaki and Yokoyama.[5] From the left in Fig. 5, the first peak at 1740 cm^{-1} was assigned to the CP carboxyl groups bound with PVP by hydrogen bonding. The second one at 1720 cm^{-1} was assigned to the dimer carboxyl structure of CP. The third at 1670 cm^{-1} was assigned to the PVP carbonyl groups. The last peak at 1630 cm^{-1} was assigned to the PVP which was bound with CP by hydrogen bonding. The following equations were applied to determine the hydrogen bonding of PVP/CP complex:

$$HB_{CP} = 100\ A_{1740}/(A_{1740}+A_{1720}) \quad (2)$$

$$HB_{PVP} = 100\ A_{1630}/(A_{1630}+A_{1670}) \quad (3)$$

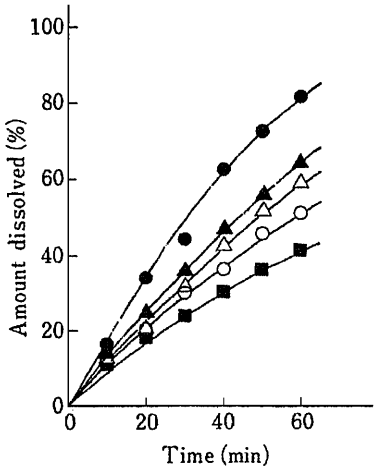

Fig. 6. Dissolution Profiles of CPM from PVP K-30/CP-II Polymer Matrix at pH 1.2 Determined by the Rotating Paddle Method (100 rpm, 37 °C)

Weight ratio of CPM/PVP K-30/CP-II: ●, 1/4/1; ▲, 1/3/2; ■, 2/5/5; ○, 1/2/3; △, 1/1/4.

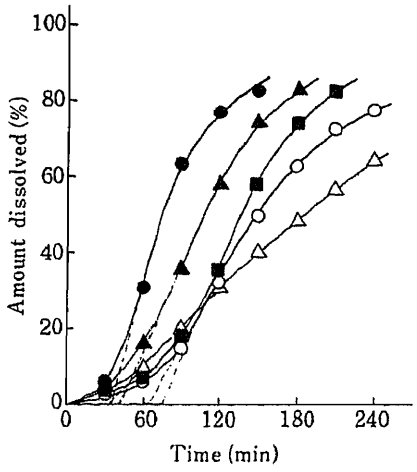

Fig. 7. Dissolution Profiles of IMC from PVP K-30/CP-II Polymer Matrix at pH 6.8 Determined by the Rotating Paddle Method (100 rpm, 37 °C)

Weight ratio of IMC/PVP K-30/CP-II: ●, 1/4/1; ▲, 1/3/2; ■, 2/5/5; ○, 1/2/3; △, 1/1/4.

where *HB* means the degree of hydrogen bonding (%), and *A* is the area of each simulated peak. The results are summarized in Table II. Degrees of hydrogen bonding were found to be about 40 to 50% and the value slightly increased with increasing molecular length of both polymers. In the case of the interpolymer complex between PVP and polyacrylic acid, more than 70% hydrogen bonding has been reported by Sasaki and Yokoyama.[5] The discrepancy in degrees of hydrogen bonding might be due to the crosslinking of CP. Namely, the activity of carboxyl groups of CP seems to be weaker than that in the case of polyacrylic acid, because of the rigid structure of the CP molecule.

Drug Release from PVP/CP Polymer Matrix

CPM was used as a model acid-soluble drug and IMC as a model alkali-soluble drug. Figure 6 shows the dissolution behavior of CPM from the tablet, which consists of a simple blend of PVP K-30 and CP-II in the dissolution medium of pH 1.2. The dissolution rate of CPM decreased gradually with increase of the amount of CP in the matrix up to the polymer ratio of 1 : 1. The slowest dissolution rate of CPM was observed when the polymer ratio was 1 : 1. After that, the dissolution rate of CPM increased with increase of CP. Therefore, the diffusion of CPM was considered to be controlled by the three-dimensional network structure, which was produced by the complex formation following water penetration into the matrix. The amount and density of the network structure in the matrix were considered to be a function of the polymer ratio.

The dissolution behavior of IMC was observed similarly in the dissolution medium of pH 6.8. A delay of dissolution was found in all samples and the longest lag time was observed at the weight ratio 1 : 1, as shown in Fig. 7. A similar tendency was observed in the case of solid dispersion form of IMC, as shown in Fig. 8. The solid dispersion form of IMC in PVP was prepared as described previously[9] and compressed to make tablets after mixing with CP. The dissolution rate of IMC in the steady state was found to be a linear function of time. It was not affected by the polymer ratio when the content of PVP was larger than 50%. The reason for the lag time, which was observed in Figs. 7 and 8, may be that the three-dimensional network structure was produced by complex formation following the penetration of the dissolution medium (pH 6.8) into the tablet. Though the pH value of the dissolution medium

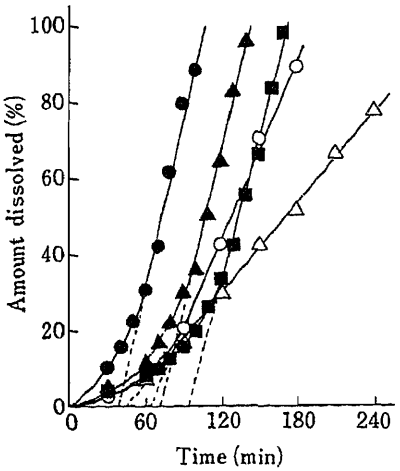

Fig. 8. Dissolution Profiles of IMC Solid Dispersions from PVPK-30/CP-II Polymer Matrix at pH 6.8 Determined by the Rotating Paddle Method (100 rpm, 37 °C)

Weight ratio of IMC/PVP K-30/CP-II: ●, 1/4/1; ▲, 1/3/2; ■, 2/5/5; ○, 1/2/3; △, 1/1/4.

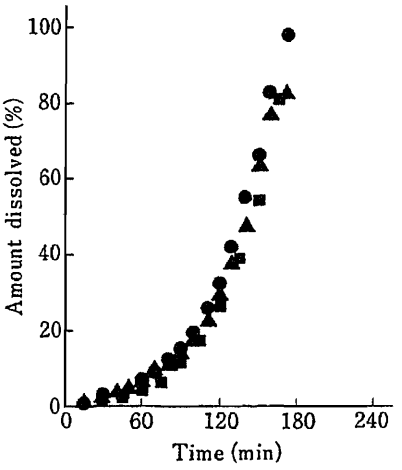

Fig. 9. Dissolution Profiles of IMC Solid Dispersions from PVPK-30/CP-II Polymer Matrix at pH 6.8 after Stirring at pH 1.2

Stirring time: ●, 0 min at pH 1.2; ▲, 30 min at pH 1.2; ■, 60 min at pH 1.2.

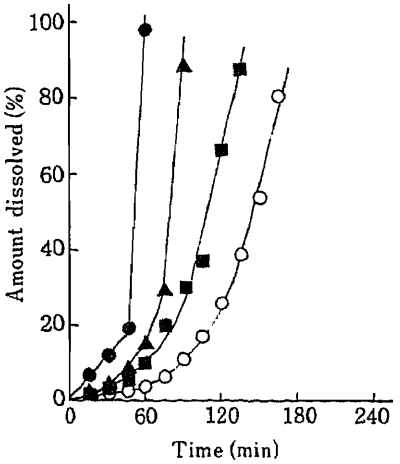

Fig. 10. Effect of Loading of Sodium Bicarbonate on Dissolution Profiles of IMC Solid Dispersions from PVP K-30/CP-II Polymer Matrix at pH 6.8 (100 rpm, 37 °C)

Amount of sodium bicarbonate: ○, 0%; ■, 7.7%; ▲, 14.3%; ●, 20.0%.

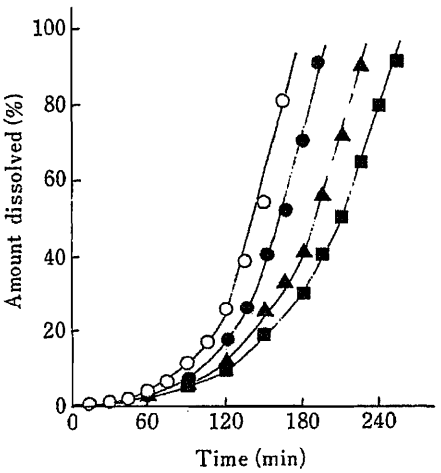

Fig. 11. Effect of Loading of Citric Acid on Dissolution Profiles of IMC Solid Dispersions from PVPK-30/CP-II Polymer Matrix at pH 6.8 (100 rpm, 37 °C)

Amount of citric acid: ○, 0%; ●, 7.7%; ▲, 14.3%; ■, 20.0%.

was higher than the critical pH for complexation, the pH value inside the polymer matrix could be low enough for the complexation owing to the acidity of CP. Figure 9 shows the effect of stirring the polymer matrix in the acidic medium of pH 1.2 on the subsequent dissolution of IMC at pH 6.8. No difference on the dissolution profiles of IMC was observed. Therefore, the three-dimensional network structure could be formed owing to the acidity of CP independently of the pH value of the dissolution medium in the initial dissolution stage. As a result, IMC was tightly held in the matrix in the initial dissolution stage. With the continuous penetration of the dissolution medium, the pH value in the matrix increased gradually. When the pH value in the matrix reached the critical pH for the decomplexation, the network structure disappeared and IMC was released readily.

Figure 10 shows the effect of sodium bicarbonate in the tablet on the dissolution of IMC. The dissolution of IMC was accelerated in direct relation to the amount of sodium bicarbonate in the polymer matrix. This is due to the acceleration of decomplexation in the polymer matrix. On the other hand, the dissolution of IMC was significantly delayed with the increase of citric acid loaded in the tablet, as shown in Fig. 11. The acceleration of complexation in the polymer matrix could account for this phenomenon. Therefore, the three-dimensional network structure, which was formed by the interpolymer complexation, could be controllable by loading acids or alkalis into the polymer matrix.

In conclusion, the complex formation of PVP and CP markedly affects the drug dissolution behavior. Specific properties of PVP/CP complex should be applicable to designing more precisely controlled drug release systems.

Acknowledgement This study was supported by a Grant-in-Aid for Scientific Research on Priority Areas, New Functionality Materials-Design, Preparation and Control, from the Ministry of Education, Science and Culture, 62604604. The authors would like to thank Mr. Toshiya Takahashi, Miss Yumiko Takinami, and Miss Tomoko Wakui for their assistance in the experimental work.

References and Notes

1) A part of this work was presented at the 107th Annual Meeting of the Pharmaceutical Society of Japan, Kyoto, April 1987.
2) N. A. Elgindy and M. A. Elegakey, *Sci. Pharm.*, **49**, 427 (1981).
3) M. A. Elegakey and N. A. Elgindy, *Sci. Pharm.*, **49**, 434 (1981).
4) E. Tsuchida, Y. Osada, and H. Ohno, *J. Macromol. Sci.-Phys.*, **B17**, 683 (1980).
5) N. Sasaki and T. Yokoyama, *Kobunshi Ronbunshu*, **41**, 9 (1984).
6) T. Tsutsui, H. Nakano, R. Tanaka, and T. Tanaka, *Kobunshi Ronbunshu*, **35**, 517 (1978).
7) H. Nogami, T. Nagai, and A. Kondo, *Chem. Pharm. Bull.*, **18**, 1185 (1970).
8) Y. Kato, K. Ando, and A. Nishioka, *Kobunshi Ronbunshu*, **32**, 200 (1975).
9) K. Takayama, N. Nambu, and T. Nagai, *Chem. Pharm. Bull.*, **28**, 3304 (1980).

[Chem. Pharm. Bull. 35(12)4928—4934(1987)]

Potentiating Effects of N^1,N^3-Diallyluracil, N^1,N^3-Diallylthymine and N^1,N^3-Diallyl-6-methyluracil on Pentobarbital-Induced Sleep and Diazepam-Induced Motor Incoordination

YUJI TATEOKA,[a] TOSHIYUKI KIMURA,[a] KAZUHITO WATANABE,[a] IKUO YAMAMOTO*,[a] and ING KANG HO[b]

Department of Hygienic Chemistry, School of Pharmacy, Hokuriku University,[a] 3, Ho Kanagawa-machi, Kanazawa 920-11, Japan and Department of Pharmacology and Toxicology, The University of Mississippi Medical Center,[b] 2500 North State Street, Jackson, Mississippi 39216, U.S.A.

(Received April 13, 1987)

N-Allyl derivatives of uracil (U), thymine (T) and 6-methyluracil (6-MU) were prepared, and their pharmacological activities (hypnotic activity and anticonvulsant activity against pentylenetetrazol (PTZ)-induced seizures) and interactions with three sedative-hypnotics [pentobarbital (PB), barbital (B) and diazepam (DZ)] were investigated in mice. N^1,N^3-Diallyluracil (DAU) alone exhibited hypnotic and anticonvulsant activities. None of the other allyl derivatives showed both pharmacological activities. As regards interactions, most of the compounds tested prolonged PB-induced sleep at either 80 or 160 mg/kg, i.p. Further, U, T, and 6-MU (160 mg/kg, i.p.) also prolonged the PB-induced sleeping time. DAU showed a prolonging effect on PB-induced sleep when given by intracerebroventricular (i.c.v.) injection. DAU, N^1,N^3-diallylthymine (DAT) and N^1-monoallyluracil (N^1-MAU) significantly prolonged the B-induced sleeping time at a dose of 160 mg/kg, i.p. Further, DAU and DAT (40 mg/kg, i.p.) enhanced DZ-induced motor incoordination. These results indicate that U and related compounds possess central nervous system (CNS)-depressant effects and DAU is the most potent among the *N*-allyl derivatives tested.

Keywords——N^1,N^3-diallyluracil; N^1,N^3-diallylthymine; N^1,N^3-diallyl-6-methyluracil; hypnotic activity; anticonvulsant activity; barbiturate-induced sleep; diazepam-induced motor incoordination

In previous studies,[1-6] we reported that allyl-substituted derivatives of barbiturates and related compounds exhibited various pharmacological activities in mice. *N*-Monoallylbarbital had more potent hypnotic activity than barbital (B).[2] Further, these allyl derivatives showed a potent synergistic effect on sedative hypnotic-induced narcosis. In contrast, *N*,*N'*-diallylpentobarbital apparently showed an antagonistic effect on B-induced sleep.[1,6] These results indicate that allyl-substituted barbiturates have multiple pharmacological activities.

It has been reported that uracil (U) and related oxypyrimidines exhibit some central depressant properties.[7-9] U shows a prolonging effect on hexobarbital-induced sleep and anticonvulsant activity against maximal electroshock seizures.[7,8] Krooth *et al.* have reported that pyrimidine bases increase the spontaneous activity at lower doses and decrease the activity at higher ones.[9] On the other hand, there is a report that U dose not affect the duration or frequency of wakefulness, slow wave sleep or paradoxical sleep at any dose in rats.[10] Since U and thymine (T) have an oxypyrimidine moiety, like the barbiturate, the structure–activity relationships of both compound groups are of interest. However, there has been no study on the pharmacological activity of *N*-allyl-substituted derivatives of U, T and 6-methyluracil (6-MU), although syntheses of some *N*-allyl compounds have been reported.[11-15] In order to reexamine the above findings and confirm the effect of *N*-allyl

substitution, we prepared these *N*-allyl compounds, and then systematically investigated their pharmacological activities.

Experimental

Animals——Male ddN mice weighing 22—28 g were used. Animals were housed under a normal light—dark cycle (7:00—19:00) at ambient temperature (23±1 °C). Food and water were given *ad lib.*

Chemicals and Preparation of *N*-Allyl Compounds——U, T and sodium B (Wako Pure Chemical Ind.), 6-MU (Nakarai Chemicals, Ltd.), sodium pentobarbital (PB, Tokyo Kasei Kogyo Co., Ltd.), diazepam (DZ, Yamanouchi Seiyaku Co., Ltd.) and pentylenetetrazol (PTZ, K & K Laboratories) were used. Preparation of *N*-allyl-substituted derivatives of U, T and 6-MU was carried out according to the reported method,[3] that is, each pyrimidine base was reacted with allyl bromide in acetone: 1 N NaOH (1:1, v/v). The physical and spectral data of the *N*-allyl compounds prepared are listed in Table I. Separation of N^1-monoallyl and N^3-monoallyl derivatives was performed by silica gel column chromatography with chloroform: isopropanol=97.5:2.5. Identification of N^1- and N^3-monoallyl derivatives was performed based on the shift (or lack of it) in the ultraviolet (UV) absorption maximum in basic solution and by comparing the values with those in the literature.[11—15]

Animal Experiments——All allyl compounds, U, T, 6-MU and DZ were suspended in 1% Tween 80–saline solution and the other drugs were dissolved in saline.

Hypnotic Activity [50% Hypnotic Dose (HD_{50})]: Allyl compounds were administered to each group of 6—10 mice at a dose of 500 or 640 mg/kg, i.p. and then the behavior of the treated mice was observed till 3 h after administration. Sleeping time was measured as the interval between loss and recovery of an effective righting reflex (considered to be recovery from a side position within 1 min[16]). The number of mice that lost the righting reflex was recorded for each dose, 400, 430, 460 and 500 mg/kg, i.p. of DAU, and the dose required to induce the effect in 50% of the animals (HD_{50} with 95% confidence limits) was determined.

Anticovulsant Activity [50% Effective Dose against PTZ-Induced Seizures ($PTZ\text{-}ED_{50}$)]: The anticonvulsant activity was evaluated in terms of the protection against PTZ-induced seizures, using a modification of the method described by Andrews *et al.*[16] Allyl compounds (250 mg/kg, i.p.) were administered to each group of 8 mice 20 min prior to the subcutaneous injection of PTZ, 120 mg/kg. The blocking of tonic-extensor convulsion was considered to be evidence of activity.

Acute Toxicity [50% Lethal Dose (LD_{50})]: The LD_{50} value for each compound tested was also determined. N^1,N^3-Diallyl-substituted compounds were administered at four different dosage levels. Mortality was observed for 3 d.

Effects on PB- and B-Induced Sleeping Time: The effects of allyl derivatives on PB-induced sleep were tested by two routes of administration [i.v. and intracerebroventricular (i.c.v.)]. All allyl derivatives and parent compounds (80 and 160 mg/kg=0.1 ml/10 g of body weight, i.p. and 200 μg/mouse=25 μl, i.c.v.) were injected 15 min prior to the administration of PB (40 mg/kg, i.p.). In the same way, allyl compounds were administered at a dose of 160 mg/kg, i.p. 15 min prior to the 300 mg/kg, i.p. injection of B. Barbiturate-induced sleeping time was measured. Control mice were injected with the 1% Tween 80–saline solution instead of test compounds. The i.c.v. administration was performed by the method of Haley and McCormick.[17]

Effects of N^1,N^3-Diallyluracil (DAU) and N^1,N^3-Diallylthymine (DAT) on DZ-Induced Motor Incoordination: Motor incoordination was measured according to the method previously reported.[1] DAU and DAT, 40 mg/kg, i.p. were administered to groups of ten mice 15 min prior to the 5 mg/kg, i.p. injection of DZ. The percentage of mice which fell off the rods within 30 seconds was recorded.

Statistical Analysis——HD_{50}, $PTZ\text{-}ED_{50}$, LD_{50} and their 95% confidence limits were calculated by the method of Litchfield and Wilcoxon.[18] Statistical significance was analyzed by using Student's *t*-test.

Results

Pharmacological Activity

Table II summarizes the pharmacological activities of each of the *N*-allyl-substituted derivatives alone. DAU showed some hypnotic and anticonvulsant activities. The HD_{50} and $PTZ\text{-}ED_{50}$ of DAU were 433 (406—462) mg/kg, i.p. and 259 (215—312) mg/kg, i.p., respectively. The onset time and duration of loss of righting reflex in the DAU-treated group were 5±1 min and 60±5 min (N=7/10), respectively, at a dose of 460 mg/kg, i.p. The $PTZ\text{-}ED_{50}$ for DAU was about 60% of its ED_{50} value. On the other hand, allyl compounds except for DAU exhibited neither loss of righting reflex nor anticonvulsant activity. The acute toxicity (LD_{50}, mg/kg, i.p.) of DAU, 560 (526—596), was lower than that of DAT, 375

TABLE I. Physical and Spectral Data for *N*-Allyl-Substituted Derivatives of U, T and 6-MU

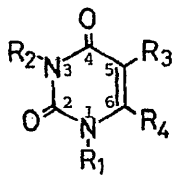

Compd.	R_1	R_2	R_3	R_4	Yield (%)	mp (°C) (Lit.)	Recryst. solvent	Formula	Analysis (%) Calcd (Found) C	H	N	UV λ_{max} nm (log ε) EtOH	pH 12	^{1}H-NMR δ (in $CDCl_3$)
N^1-MAU	$-C_3H_5$	H	H	H	36	100—103 (105—108)[11]	C_6H_6	$C_7H_8N_2O_2$	55.26 (55.64	5.30 5.29	18.41 18.35)	267 (4.00)	265 (4.14)	4.42 (2H, d, J=5 Hz, N^1-CH_2–), 5.37—5.58 (2H, m, =CH_2), 5.81 (1H, d, J=8 Hz, 5-H), 7.27 (1H, d, J=8 Hz, 6-H)
N^3-MAU	H	$-C_3H_5$	H	H	2	135—137 (133—134)[12]	C_6H_6	$C_7H_8N_2O_2$	55.26 (55.06	5.30 5.23	18.41 18.35)	261 (3.96)	286 (4.12)	4.53 (2H, d, J=5 Hz, N^3-CH_2–), 5.08—5.36 (2H, m, =CH_2), 7.09—7.18 (1H, m, 6-H), 10.48 (1H, br s, N^1H)
DAU	$-C_3H_5$	$-C_3H_5$	H	H	14	Oil[e]		$C_{10}H_{12}N_2O_2$	62.49 (62.32	6.29 6.27	14.57 13.97)	267 (3.93) 266[13] (3.97)		4.48 (2H, d, J=5 Hz, N^1-CH_2–), 4.63 (2H, d, J=5 Hz, N^3-CH_2–), 5.19—5.55 (4H, m, (=CH_2)$_2$), 5.86 (1H, d, J=6 Hz, 5-H), 7.37 (1H, d, J=6 Hz, 6-H)
N^1-MAT	$-C_3H_5$	H	$-CH_3$	H	28	97—99 (96—97)[14]	C_6H_6	$C_8H_{10}N_2O_2$	57.82 (57.53	6.07 6.00	16.86 16.84)	272 (4.01)	271 (3.88)	1.95 (3H, s, 5-CH_3), 4.42 (2H, d, J=6 Hz, N^1-CH_2–), 5.04—5.51 (2H, m, =CH_2), 5.68—6.20 (1H, m, –CH=), 7.12 (1H, s, 6-H)

N^3-MAT	H	$-C_3H_5$	$-CH_3$	H	6	174—175 (175—177)[12]	C_6H_6	$C_8H_{10}N_2O_2$	57.82 (57.70	6.07 6.08	16.86 16.83)	267 (4.09)	293 (4.24)	1.93 (3H, s, 5-CH_3), 4.63 (2H, d, J=7 Hz, N^3-CH_2–), 5.19—5.46 (2H, m, =CH_2), 5.79—6.19 (1H, m, –CH=), 7.17 (1H, d, J=5 Hz, 6-H), 10.53 (1H, br s, N^1H)
DAT	$-C_3H_5$	$-C_3H_5$	$-CH_3$	H	14	Oil[a]		$C_{11}H_{14}N_2O_2$	64.06 (63.48	6.84 6.82	13.58 13.86)	272 (4.03)		1.95 (3H, s, 5-CH_3), 4.42 (2H, d, J=6 Hz, N^1-CH_2–), 4.65 (2H, d, J=5 Hz, N^3-CH_2–), 5.02—5.52 (4H, m, (=CH_2)$_2$), 5.68—6.20 (2H, m, (–CH=)$_2$), 7.07 (1H, br s, 6-H)
N^1-MA-6-MU	$-C_3H_5$	H	H	$-CH_3$	10	174—175	$CHCl_3$–MeOH (9 : 1)	$C_8H_{10}N_2O_2$	57.82 (57.64	6.07 6.13	16.86 16.98)	265 (3.94)	267 (4.20)	2.25 (3H, s, 6-CH_3), 4.48 (2H, d, J=6 Hz, N^1-CH_2–), 4.99—5.35 (2H, m, =CH_2), 5.57 (1H, s, 5-H), 5.67—6.09 (1H, m, –CH=), 9.57 (1H, br s, N^3H)
N^3-MA-6-MU	H	$-C_3H_5$	H	$-CH_3$	10	175—179 (184)[15]	C_6H_6	$C_8H_{10}N_2O_2$	57.82 (57.61	6.07 6.06	16.86 16.77)	262 (4.09)	282 (4.20)	2.15 (3H, s, 6-CH_3), 4.51 (2H, d, J=6 Hz, N^3-CH_2–), 5.10—5.34 (2H, m, =CH_2), 5.59 (1H, s, 5-H), 5.66—6.10 (1H, m, –CH=), 10.64 (1H, br s, N^1H)
DA-6-MU	$-C_3H_5$	$-C_3H_5$	H	$-CH_3$	6	58—59	C_6H_{12}	$C_{11}H_{14}N_2O_2$	64.06 (64.12	6.84 6.95	13.58 13.74)	269 (4.27)		2.25 (3H, s, 6-CH_3), 4.45—4.64 (4H, m, (–CH_2–)$_2$), 4.99—5.37 (4H, m, (=CH_2)$_2$), 5.60 (1H, s, 5-H), 5.67—6.11 (1H, m, –CH=)

Abbreviations used are: MAU, monoallyluracil; DAU, N^1,N^3-diallyluracil; MAT, monoallylthymine; DAT, N^1,N^3-diallylthymine; MA-6-MU, monoallyl-6-methyluracil; DA-6-MU, N^1,N^3-diallyl-6-methyluracil; $-C_3H_5$, $-CH_2CH=CH_2$. *a*) Oily compounds were purified by column chromatography on silica gel.

TABLE II. Pharmacological Activities of *N*-Allyl-Substituted Derivatives of U, T and 6-MU

Compd.	HD_{50} (mg/kg, i.p.)	PTZ-ED_{50} (mg/kg, i.p.)	LD_{50} (mg/kg, i.p.)
U	None (640)[a]	>250	>640
N^1-MAU	None (640)	>250	>640
N^3-MAU	None (500)	>250	>500
DAU	433 (406—462)[b]	259 (215—312)	560 (526—596)
T	None (640)	>250	>640
N^1-MAT	None (640)	>250	>640
N^3-MAT	None (500)	>250	>500
DAT	None (550)	>250	375 (347—406)
6-MU	None (640)	>250	>640
N^1-MA-6-MU	None (640)	>250	>640
N^3-MA-6-MU	None (640)	>250	>640
DA-6-MU	None (480)	>250	425 (389—464)

a) The word "None" means that there was no loss of righting reflex even at the dose indicated in parentheses. *b*) The 95% confidence limits are shown in parentheses.

TABLE III. Effects of *N*-Allyl-Substituted Derivatives of U, T and 6-MU on PB- and B-Induced Sleep

Compd.	Sleeping time (min)			
	PB (40 mg/kg, i.p.)			B (300 mg/kg, i.p.)
	80 mg/kg, i.p.	160 mg/kg, i.p.	200 μg/mouse i.c.v.	160 mg/kg, i.p.
Control	21± 2 (30)		67± 5 (30)	106±20 (30)
U	33± 4[a] (10)	36± 5[b] (10)	64± 7 (10)	108±28 (20)
N^1-MAU	39± 6[b] (10)	70± 6[b] (10)	88±17 (10)	204±45[a] (12)
N^3-MAU	27± 3 (10)	29± 4 (10)	63± 5 (10)	81±19 (10)
DAU	113±10[b] (10)	297±26[b] (10)	112± 9[b] (10)	177±12[a] (12)
T	33± 4[a] (10)	47± 7[b] (10)	58± 7 (10)	103±21 (10)
N^1-MAT	66±12[b] (10)	107±12[b] (10)	79±15 (10)	121±34 (10)
N^3-MAT	33± 3[a] (10)	68± 4[b] (10)	71± 7 (10)	138±28 (10)
DAT	101±11[b] (10)	211±12[b] (10)	82±10 (10)	284±30[b] (10)
6-MU	18± 2 (10)	35± 5[a] (10)	57± 6 (10)	87± 9 (10)
N^1-MA-6-MU	27± 5 (10)	69±11[b] (10)	65± 6 (10)	93±19 (10)
N^3-MA-6-MU	38± 6[b] (10)	67± 5[b] (10)	67± 5 (10)	74± 5 (10)
DA-6-MU	94±15[b] (10)	107± 8[b] (10)	88±12 (10)	97±13 (10)

Compounds tested were administered 15 min prior to the injection of PB or B. Data are expressed as the mean±S.E. Numbers in parentheses represent numbers of animals used. *a*) Significantly different from the control ($p<0.05$). *b*) Significantly different from the control ($p<0.01$).

(347—406), or N^1,N^3-diallyl-6-methyluracil (DA-6-MU), 425 (389—464). The LD_{50} values of the other allyl compounds were larger than 500 or 640 mg/kg, i.p.

Potentiation of PB-, B- or DZ-Induced Depressant Activity

Table III shows the effects of *N*-allyl derivatives of U, T and 6-MU on PB- and B-induced sleep. DAU and DAT markedly prolonged the PB-induced sleeping time. The duration of sleeping time prolonged by DAU pretreatment was 14-fold greater than the control. DAU

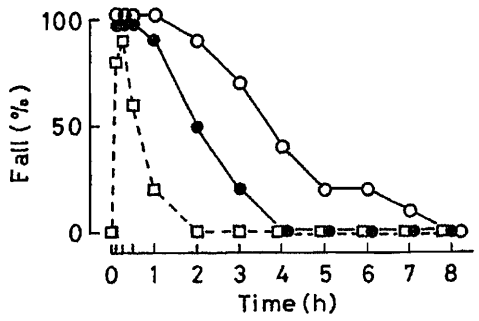

Fig. 1. Effects of DAU and DAT on DZ-Induced Motor Incoordination

DAU and DAT were administered i.p. 15 min prior to the i.p. injection of DZ. The control group was pretreated with 1% Tween 80–saline (vehicle). Ten mice were used for each group.
□---□, control (1% Tween 80–saline+DZ 5 mg/kg); ○—○, DAU 40 mg/kg+DZ 5 mg/kg; ●—●, DAT 40 mg/kg+DZ 5 mg/kg.

was the most potent compound as regards PB-induced sleep prolongation among the compounds tested. The other *N*-allyl-substituted compounds also prolonged PB-induced sleep at a dose of 160 mg/kg, i.p., except for N^3-monoallyluracil (N^3-MAU). The parent compounds, even, U, T and 6-MU (160 mg/kg, i.p.), significantly prolonged the sleeping time induced by PB. As a preliminary experiment, the time course (1, 15 and 30 min) of the effect of pretreatment with N^1-monoallyluracil (N^1-MAU) or DAU (200 μg/mouse, i.c.v.) on the PB (40 mg/kg, i.p.)-induced sleep was examined. Since the sleeping time of the DAU pretreated group was within the range from 110 to 120 min at all times examined (data not shown), the time of peak effect could not be determined. Thus administration of PB was set at 15 min after injection of *N*-allyl compounds. DAU only significantly prolonged the PB-induced sleeping time when given by i.c.v. injection. The other compounds did not show a prolonging effect on PB-induced sleep when given by i.c.v. injection, whereas DAT, N^1-MAU and DAU significantly prolonged the B-induced sleeping time, by 2.7-fold, 1.9-fold and 1.7-fold, respectively, as compared with the control. The mean sleeping time of mice pretreated with DAT was longer than with DAU. Interestingly, U, T and 6-MU did not exhibit any prolonging effect on B-induced sleep.

Figure 1 shows the effects of DAU and DAT, selected from among the allyl compounds, on the DZ (5 mg/kg, i.p.)-induced motor incoordination. Both DAU and DAT enhanced the effect of DZ at a dose of 40 mg/kg, i.p., although DAU or DAT alone did not induce apparent motor incoordination at the same dose. DAU was more potent than DAT.

Discussion

The results of the present study indicate that the introduction of two allyl groups onto N^1 and N^3 of the 2,4-dioxopyrimidine ring resulted in an increase of the depressant effect. *N*-Allyl-substituted derivatives of U seem to exhibit more potent depressant effects on the central nervous system (CNS) than N^1- and/or N^3-allyl-substituted derivatives of barbituric acid according to our previous data.[3] Recently, we have reported that N^3-benzyluridine exerted hypnotic activity when given by i.c.v. injection,[19] and that N^3-allyluridine and N^3-allylthymidine enhanced the drug-induced central depressant effect.[20] A compound that has two substituent groups at N^1 and N^3 of the U ring may generally possess a potent central depressant effect. The other *N*-allyl derivatives of U, T and 6-MU alone did not show loss of righting reflex or anticonvulsant activity. The acute toxicity of DAU was lower than that of DAT or DA-6-MU.

The interaction study of the *N*-allyl compounds with PB showed that the compounds tested (160 mg/kg, i.p.), except for N^3-MAU, significantly prolonged the PB-induced sleeping time. Upon i.c.v. administration, only DAU showed a significant potentiation of PB-induced sleep. This might be due to direct action of DAU on the CNS. The other allyl compounds did not show any significant prolonging effects on PB-induced sleep by i.c.v. injection. However,

DAT, N^1-MAU and DAU significantly prolonged the B-induced sleeping time. Since B is excreted unmetabolized,[21] an increase in its action could be due either to an enhanced penetration into the CNS or to alteration of neuronal sensitivity to the drug. The potentiation of DZ-induced motor incoordination by DAU and DAT also supports the hypothesis that both compounds have a direct depressant effect on the CNS.

N^1-Monoallyl-substituted derivatives of T, including U were more potent CNS depressants than the corresponding N^3-monoallyl-substituted derivatives. A methyl group at the 5 or 6 position of the U ring seems to be unnecessary for action on the CNS. It is of interest that the *N*-allyl compounds derived from endogenous substances such as U and T showed such potent pharmacological activities.

These results indicate that DAU and related *N*-allyl compounds have a CNS-depressant effect, and suggest that these compounds could prolong PB-induced sleep as a result of their depressant effect on the CNS.

References

1) I. Yamamoto, Y. Tateoka, K. Watanabe, T. Nabeshima, H. J. Fontenot and I. K. Ho, *Res. Commun. Chem. Pathol. Pharmacol.*, **50**, 209 (1985).
2) Y. Tateoka, I. Yamamoto, K. Watanabe and I. K. Ho, *Res. Commun. Chem. Pathol. Pharmacol.*, **52**, 17 (1986).
3) Y. Tateoka, T. Kimura, F. Yamazaki, K. Watanabe and I. Yamamoto, *Yakugaku Zasshi*, **106**, 504 (1986).
4) I. Yamamoto, Y. Tateoka, T. Kimura, F. Yamazaki, K. Hamajima, K. Watanabe and I. K. Ho, *Res. Commun. Chem. Pathol. Pharmacol.*, **54**, 191 (1986).
5) Y. Tateoka, T. Kimura, K. Watanabe, I. Yamamoto and I. K. Ho, *Chem. Pharm. Bull.*, **35**, 778 (1987).
6) I. Yamamoto, Y. Tateoka, K. Watanabe and I. K. Ho, *Life Sci.*, **40**, 1439 (1987).
7) D. G. Wenzel and M. L. Keplinger, *J. Am. Pharm. Assoc.*, **44**, 56 (1955).
8) D. G. Wenzel, *J. Am. Pharm. Assoc.*, **44**, 550 (1955).
9) R. S. Krooth, W. L. Hsiao and G. F. M. Lam, *J. Pharmacol. Exp. Ther.*, **207**, 504 (1978).
10) K. Honda, Y. Komoda and S. Inoué, *Report of the Institute for Medical & Dental Engineering*, **18**, 93 (1984).
11) L. Doub, U. Krolls, J. M. Vandenbelt and M. W. Fisher, *J. Med. Chem.*, **13**, 242 (1970).
12) R. L. Shone, *J. Heterocycle. Chem.*, **9**, 1175 (1972).
13) H. J. Minnemeyer, P. B. Clarke and H. Tieckelmann, *J. Org. Chem.*, **31**, 406 (1966).
14) T. Tanabe, K. Yamauchi and M. Kinoshita, *Bull. Chem. Soc. Jpn.*, **52**, 259 (1979).
15) S. Giambrone, *Chem. Abstr.*, **49**, 4662*i* (1955).
16) P. R. Andrews, G. P. Jones and D. Lodge, *Eur. J. Pharmacol.*, **55**, 115 (1979).
17) T. J. Haley and W. G. McCormick, *Br. J. Pharmacol.*, **12**, 12 (1957).
18) J. T. Litchfield and F. Wilcoxon, *J. Pharmacol. Exp. Ther.*, **96**, 99 (1949).
19) I. Yamamoto, T. Kimura, Y. Tateoka, K. Watanabe and I. K. Ho, *Chem. Pharm. Bull.*, **33**, 4088 (1985).
20) I. Yamamoto, T. Kimura, Y. Tateoka, K. Watanabe and I. K. Ho, *Res. Commun. Chem. Pathol. Pharmacol.*, **52**, 321 (1986).
21) E. W. Maynert and H. B. van Dike, *J. Pharmacol. Exp. Ther.*, **98**, 184 (1950).

[Chem. Pharm. Bull. 35(12)4935—4939(1987)]

Studies on Pharmacological Activation of Human Serum Immunoglobulin G (IgG) by Chemical Modification and Active Subfragments. VI. Anti-allergic Activity of Carboxamidemethylated Fc (CM-Fc) Fragment from Human Serum IgG

TSUTOMU MIMURA,*[,a] SUSUMU ITOH,[a] KAZUTAKE TSUJIKAWA,[a] HIROSHI NAKAJIMA,[a] YASUHIRO KOHAMA,[a] MASARU OKABE,[a] MASAKAZU IWAI,[b] TAKAO OHMURA[b] and KAZUMASA YOKOYAMA[b]

Faculty of Pharmaceutical Science, Osaka University,[a] Yamadaoka 1–6, Suita, Osaka 565, Japan and Central Research Laboratories, The Green Cross Corporation, Ltd.,[b] 2–1180–1, Shodai Ohtani, Hirakata, Osaka 573, Japan

(Received April 14, 1987)

Immunoglobulin G from human serum was digested with papain to give an Fc fragment, which was carboxamidemethylated [carboxamidemethylated Fc (CM-Fc), M.W. about 25000].

Types I, III and IV allergic reactions were significantly depressed by the administration of CM-Fc.

Keywords——carboxamide methylation; human IgG; carboxamidemethylated Fc; anti-allergic activity; passive cutaneous anaphylaxis; complement-dependent hemolysis; immuno-complex inflammatory model; Arthus reaction; delayed-type hypersensitivity

Coombs and Gell[1] classified allergic phenomena into four types, of which three (types I, II and III) are immediate-type, and one (type IV) is delayed-type. The former reactions are caused by humoral antibodies, while the latter is caused by a cellular antibody.

We have already reported that the carboxamidemethylated L chain[2] and the carboxamidemethylated H and L chains[3] show anti-ulcerogenic and anti-inflammatory activities, respectively.

In this paper, we describe the effect of carboxamidemethylated Fc (CM-Fc) on various allergic models.

Materials and Methods

Preparation of CM-Fc——According to Bennich and Turner,[4] 2% commercially available human serum immunoglobulin G (IgG) (Globulin-Midori) dissolved in 0.1 M sodium phosphate buffer (pH 6.75) containing 2 mM ethylenediaminetetra acetic acid (EDTA) and 10 mM cysteine hydrochloride (Nakarai Chem.) was digested with 0.02% papain (type III, Sigma). After 4 h, 150 μl of 0.5 M iodoacetamide (Wako Pure Chem.) was added to the reaction mixture. The mixture was then separated according to Nishioka *et al.*,[5] on a Sephadex G-100 column equilibrated with 10 mM phosphate-buffered saline (PBS, pH 7.2). The fraction containing Fab and Fc from Sephadex G-100 was separated by protein A–Sepharose CL-4B (Pharmacia Fine Chemicals) affinity chromatography, and the Fc fragment was purified. This fragment was reduced with dithiothreitol (Wako Pure Chem.) and carboxamidemethylated with iodoacetamide according to Korningsberg,[6] resulting in a carboxamidemethylated Fc fragment (CM-Fc). The molecular weight of CM-Fc was measured by polyacrylamide–sodium dodecyl sulfate gel electrophoresis according to Laemmli.[7]

Homologous Passive Cutaneous Anaphylaxis (PCA) in Rats——Dinitrophenylated ascaris extract (DNP-As) was prepared according to Eisen *et al.*,[8] and anti-DNP-As serum was raised in rats following the method of Tada and Okumura.[9] Male Wistar rats weighing 180—200 g had their backs shaved 24 h prior to experiments. Then 0.1 ml of anti-DNP-As serum, diluted four times with saline, was administered intradermally at three points in the left back, while 0.1 ml of saline was administered intradermally at three points in the right back. After 48 h, rats were intravenously injected with 1 ml of 0.5% Evans blue (Nakarai Chem.) in saline containing 4 mg of DNP-As. Thirty

minutes later, the rats were killed and skinned. The capillary permeability was expressed by multiplying the major and minor axes of the blue area. The sample was administered intraperitoneally 30 min prior to the injection of DNP-As.

Heterologous PCA in Guinea Pigs——Anti-egg albumin serum raised in the rabbit was prepared according to Eda *et al.*[10] Heterologous PCA was prepared according to the method reported by Harada *et al.*,[11] as improved upon by Ovary.[12] The male Hartley guinea pigs had their backs shaved 24 h prior to experiments. Then 0.1 ml of anti-egg albumin serum, diluted five hundred and twelve times with saline, was administered intradermally at two points in the left back, while 0.1 ml of saline was administered intradermally at two points in the right back. After 3.5 h, the guinea pigs were intravenously injected with 1 ml of 1% Evans blue in saline containing 5 mg of egg albumin (Nakarai Chem.). Thirty minutes later, the guinea pigs were killed and skinned. The capillary permeability was again expressed by multiplying the major and minor axes of the blue area. The sample was administered intraperitoneally 30 min prior to the injection of egg albumin.

Complement-Dependent Hemolysis——According to Mori *et al.*,[13] sheep red blood cells (SRBC; Handai Biken) were washed with gelatin veronal buffer (GVB), and suspended at 1.0×10^9/ml. Anti-SRBC serum, which was prepared according to Globsky,[14] was diluted 1600 times with GVB.

Five milliliters of GVB, 1 ml of the sample, 0.5 ml of SRBC suspension, 0.5 ml of anti-SRBC serum and 1 ml of the complement (from guinea pig serum, Handai Biken) were added, respectively. After incubation at 37°C for 90 min, the reaction was stopped on ice. Following centrifugation (3000 rpm × 10 min), the absorbance of the supernatant was measured at 540 nm. The result was expressed as the inhibition (percent) of hemolysis.

Immuno-Complex Inflammatory Model——According to Abe *et al.*,[15] male Balb/c mice (age 8 weeks) were immunized intravenously with 5×10^8 SRBC twice (day −19 and day −5). The right hind paw was inoculated with 2×10^8 SRBC to produce the immuno-complex (day 0). After 3 and 4 h, the amount of edema was recorded with a dial thickness gauge (Mitsutoyo Mfg. Co., Ltd.). The difference between the values just after and 3 or 4 h after the injection was calculated. The sample was administered intraperitoneally 30 min prior to SRBC injection.

Delayed-Type Hypersensitivity to Picryl Chloride——According to Tajima *et al.*,[16] male ddy mice weighing 20—30 g were immunized with 100 μl of 1% picryl chloride (Nakarai Chem.) solution in ethanol on the surface of the right ear. After 7 d, 100 μl of 1% picryl chloride solution in olive oil was applied to the surface of the left ear. Twenty-four hours later, the thickness of the left ear was measured with a dial thickness gauge, and the difference between the values before and after application was calculated. The sample was administered intraperitoneally 30 min before and 6 h after antigen challenge.

Delayed-Type Hypersensitivity to Methylated Bovine Serum Albumin——According to Baba *et al.*,[17] male ddy mice weighing 20—30 g were immunized subcutaneously with 0.2 ml of emulsion prepared from equal volumes of 0.25% methylated bovine serum albumin (MBSA, Sigma) in saline and Freund's complete adjuvant (Nakarai Chem.). After 6 d, 0.04 ml of 0.1% MBSA in saline was subcutaneously administered into the left hind paw of mice. Twenty-four hours later, the thickness of the foot pad was measured with a dial thickness gauge. The difference between the values immediately after and 24 h after the injection was calculated. The sample was administered intraperitoneally 30 min and 6 h after antigen challenge.

Statistics——Student's *t*-test was employed to assess the significance of differences between the mean values for the control group and the sample-administered groups.

Results

Type I Allergy

The effects of CM-Fc and Fc on homologous PCA in rats are summarized in Table I. CM-Fc significantly depressed the colored area at a dose of 20 mg/kg by 38.8%, while Fc showed no depression at the same dose.

The effect of CM-Fc on heterologous PCA in guinea pigs was also examined. CM-Fc at a dose of 20 mg/kg significantly depressed the colored area (27.4% inhibition; Table II).

Type II Allergy

The effects of CM-Fc and Fc on complement-dependent hemolysis are shown in Fig. 1. Fc inhibited hemolysis dose-dependently; the inhibition reached 40% at a dose of 100 μg/ml. On the other hand, CM-Fc did not inhibit hemolysis at all.

Type III Allergy

We examined the effects of CM-Fc and Fc using the immuno-complex inflammatory model for the active Arthus reaction. The maximum swelling of the hind pad was observed after 3 h. Fc at a dose of 20 mg/kg did not depress the pad swelling at the indicated times,

TABLE I. Effect of CM-Fc and Fc on 48 h PCA in Rats Mediated by IgE Antibody against DNP-As

Treatment	Dose (mg/kg)	Colored area[c] (mm^2)	% inhibition
Control[a]	—	30.4±4.1	—
CM-Fc[b]	10	30.8±5.8	0
	20	18.6±7.6[d]	38.8
Fc[b]	20	31.7±6.4	0

a) Saline. *b*) Sample was administered intraperitoneally 30 min before antigen challenge. *c*) All values represent the mean±S.E. ($n=8$). Significantly different from the control group: *d*) $p<0.01$.

TABLE II. Effect of CM-Fc on 3.5 h PCA in Guinea Pigs Mediated by IgG Antibody against Egg Albumin

Treatment	Dose (mg/kg)	Colored area[c] (mm^2)	% inhibition
Control[a]	—	191.3±14.6	—
CM-Fc[b]	10	205.4±32.9	0
	20	139.5±16.5[d]	27.4

a) Saline. *b*) Sample was administered intraperitoneally 30 min before antigen challenge. *c*) All values represent the mean±S.E. ($n=8$). Significantly different from the control group: *d*) $p<0.05$.

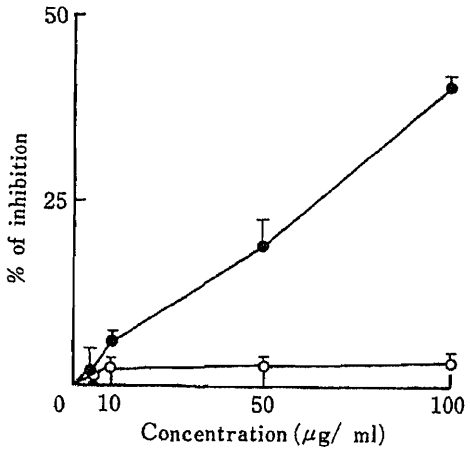

Fig. 1. Effects of CM-Fc and Fc on Complement-Dependent Hemolysis of SRBC (*in Vitro*)

Each point represents the mean±S.E. ($n=4$).
●, Fc; ○, CM-Fc.

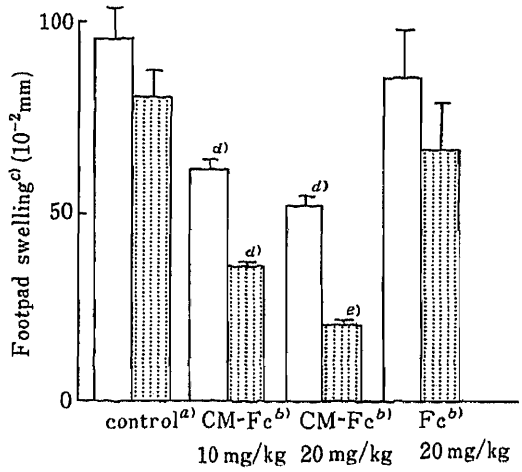

Fig. 2. Effects of CM-Fc and Fc on Complex-Mediated Hypersensitivity Induced by SRBC in Mice

a) Saline. *b*) Sample was administered intraperitoneally 30 min before SRBC injection. *c*) Each value is the mean±S.E. ($n=4$—5).
Significantly different from the control group: *d*) $p<0.05$, *e*) $p<0.01$.
□, 3 h; ▨, 4 h.

although CM-Fc at doses of 10 and 20 mg/kg significantly depressed the swelling (Fig. 2).

Type IV Allergy

As regards delayed-type hypersensitivity response to picryl chloride, CM-Fc significantly depressed the ear swelling at the dose of 20 mg/kg when the reagent was administered twice,

TABLE III. Effect of CM-Fc and Fc on Delayed-Type Hypersensitivity Response to Picryl Chloride in Mice

Treatment	Dose (mg/kg)	Ear swelling[c] ($\times 10^{-2}$ mm)
Control[a]	—	33.4±4.8
CM-Fc[b]	10	19.9±5.8
	20	17.5±3.8[d]
Fc[b]	20	36.7±8.4

a) Saline. *b*) Sample was administered intraperitoneally 30 min before and 6 h after antigen challenge. *c*) All values represent the mean±S.E. ($n=8$—9). Significantly different from the control group: *d*) $p<0.05$.

TABLE IV. Effect of CM-Fc and Fc on MBSA-Induced Hypersensitivity in Mice

Treatment	Dose (mg/kg)	Footpad swelling[c] ($\times 10^{-2}$ mm)
Control[a]	—	42.1±12.5
CM-Fc[b]	10	18.9± 3.4
	20	4.7±8.0[d]
Fc[b]	20	21.6± 8.0

a) Saline. *b*) Sample was administered intraperitoneally 30 min before and 6 h after antigen challenge. *c*) All values represent the mean±S.E. ($n=8$). Significantly different from the control group: *d*) $p<0.05$.

although Fc had no such effect (Table III).

The effects of CM-Fc and Fc on delayed-type hypersensitivity to MBSA are shown in Table IV. CM-Fc had a significant inhibitory capability at a dose of 20 mg/kg, and Fc slightly depressed the swelling at the dose of 20 mg/kg when the reagents were administered twice.

Discussion

Recently, we reported that bovine serum IgG L chain,[18] carboxamidemethylated Bence Jones protein[19] and human serum IgG L chain (Fr. I-L)[2] show anti-ulcerogenic activity based on their inhibition of gastric juice secretion. Moreover, Fr. I-L and Fr. I-H also had anti-inflammatory activity.[3] In this investigation, we prepared an Fc subfragment without the variable region for the purpose of obtaining a more homogenous structure from human serum IgG, and we obtained CM-Fc with a molecular weight of about 25000 (data not shown).

Coombs and Gell[1] classified allergic phenomena into four types. First, CM-Fc was examined for type I, an immediate allergy caused by an IgE antibody. Homologous PCA reaction, generally used as a type I allergic model, was depressed by CM-Fc, but not by Fc. Heterologous PCA was also depressed by CM-Fc.

Type II allergy is characterized by cell destruction resulting from a combination of the surface antigen of plasma membrane and its antibody, which depends on the complement.[20] CM-Fc did not inhibit complement-dependent hemolysis at all (Fig. 1), and also showed little inhibition of hypotonic hemolysis (data not shown). As Fc inhibited complement-dependent hemolysis, it was assumed that the complement-binding site was lost after carboxamidemethylation.

Opie[21] showed that type III allergy was due to antibody and antigen reacting in the tissue. Culbertson[22] and later Cannon and Marshall[23] demonstrated that the severity of this

phenomenon closely paralleled the level of precipitin in the blood. In the present experiments, we used the active Arthus phenomenon as a type III allergy model. CM-Fc significantly depressed this phenomenon at doses of 10 and 20 mg/kg. The Arthus phenomenon is divided into first and second stages characterized by slight and transient enhancement and strong and sustained enhancement of vascular permeability.[24] It was suggested that CM-Fc inhibited the latter stage to depress the Arthus phenomenon.

Type IV allergy is the phenomenon caused by lymphokines, which are released on contact of the antigen and sensitized T cells.[25] CM-Fc depressed the delayed-type hypersensitivities to both picryl chloride and MBSA. Therefore, we supposed that CM-Fc affected the cellular immune system.

Thus, CM-Fc is a potentially useful drug for three allergy types (I, III and IV) whereas Fc is not. This finding that anti-allergic activity was not acquired on carboxamidemethylation is consistent with our previous findings.[2,3,18,19] The next step will be a more detailed examination of the mechanism of action of CM-Fc.

Acknowledgement We are grateful to Miss Satoko Matsumoto and Miss Hiroko Azuma for their technical assistance.

References

1) R. R. A. Coombs and G. P. H. Gell, "Clinical Aspects of Immunology," 2nd ed., Blackwell Scientific Publ., Oxford, 1968, p. 575.
2) T. Mimura, T. Terada, M. Iwai, I. Kohda, S. Take, K. Maeda and S. Aonuma, *J. Pharmacobio-Dyn.*, **6**, 397 (1983); T. Mimura, M. Iwai, T. Terada, I. Kohda, K. Tsujikawa, K. Maeda and S. Aonuma, *ibid.*, **6**, 449 (1983).
3) T. Mimura, K. Tsujikawa, H. Nakajima, M. Okabe, Y. Kohama, M. Iwai and K. Yokoyama, *J. Pharmacobio-Dyn.*, **9**, 46 (1986); T. Mimura, K. Tsujikawa, H. Nakajima, S. Itoh, M. Okabe, I. Kohda and K. Yokoyama, *ibid.*, **9**, 799 (1986).
4) H. Bennich and M. W. Turner, *Biochim. Biophys. Acta*, **175**, 388 (1969).
5) K. Nishioka, K. Shimada and T. Mazaki, "Yakunitatsu Meneki Jikkenhoh," Kohdansha Scientific, Tokyo, 1984, p. 38.
6) W. Korningsberg, "Methods in Enzymology," XXV, Academic Press, New York, 1972, p. 185.
7) U. K. Laemmli, *Nature* (London), **227**, 680 (1970).
8) H. W. Eisen, S. Belman and M. E. Carsten, *J. Am. Chem. Soc.*, **75**, 4583 (1953).
9) T. Tada and K. Okumura, *J. Immunol.*, **106**, 1002 (1971).
10) A. Eda, H. Nagai and H. Wada, *Nippon Yakurigaku Zasshi*, **66**, 237 (1970).
11) M. Harada, M. Takeuchi and K. Katagiri, *Arerugi*, **15**, 1 (1966).
12) Z. Ovary, *Prog. Allergy*, **5**, 459 (1958).
13) T. Mori, Y. Osugi, K. Furuno, S. Takaku, T. Matsuno, S. Suzuki, K. Koyama, M. Shindo and Y. Takagaki, *Yakugaku Zasshi*, **95**, 1477 (1975).
14) M. M. Globsky, "Experimental Immunochemistry," 2nd ed., ed. by E. A. Kabat and M. M. Mayer, C. C. Thomas Publ., Springfield, Illinois, 1961, p. 133.
15) C. Abe, M. Tajino, M. Yoshida and Y. Shiokawa, *Ensho*, **1**, 738 (1981).
16) S. Tajima, E. Imai, K. Itoh and H. Nose, *Igakunoayumi*, **112**, 240 (1982).
17) M. Baba, T. Harada and S. Morikawa, *Acta Pathol. Jpn.*, **27**, 165 (1977).
18) T. Mimura, K. Kameda, T. Terada, I. Kohda, C. Tanaka and S. Aonuma, *J. Pharmacobio-Dyn.*, **5**, 301 (1982).
19) T. Mimura, I. Kohda, T. Terada, H. Tsujibo, H. Egawa and S. Aonuma, *J. Pharmacobio-Dyn.*, **5**, 125 (1982).
20) J. E. May and M. M. Frank, *J. Immunol.*, **108**, 1517 (1972).
21) E. L. Opie, *J. Immunol.*, **9**, 255 (1924).
22) J. T. Culbertson, *J. Immunol.*, **35**, 337 (1935).
23) P. R. Cannon and C. E. Marshall, *J. Immunol.*, **40** (1941).
24) E. E. Fischel, *Proc. Soc. Exp. Biol. Med.*, **6**, 537 (1947).
25) D. C. Dumonde, R. A. Wolstengrott, G. S. Panaya, M. Matthew, J. Morley and W. T. Howson, *Nature* (London), **224**, 381 (1969).

[Chem. Pharm. Bull. 35(12)4940—4945(1987)]

Studies on Pharmacological Activation of Human Serum Immunoglobulin G (IgG) by Chemical Modification and Active Subfragments. VII. Effect of Carboxamidemethylated Fc (CM-Fc) Fragment from Human Serum IgG on Lymphocytes and Macrophages

TSUTOMU MIMURA,*[,a] SUSUMU ITOH,[a] KAZUTAKE TSUJIKAWA,[a] HIROSHI NAKAJIMA,[a] YASUHIRO KOHAMA,[a] MASARU OKABE,[a] MASAKAZU IWAI,[b] TAKAO OHMURA[b] and KAZUMASA YOKOYAMA[b]

Faculty of Pharmaceutical Science, Osaka University,[a] Yamadaoka 1-6, Suita, Osaka 565, Japan and Central Research Laboratories, The Green Cross Corporation, Ltd.,[b] 2-1180-1, Shodai Ohtani, Hirakata, Osaka 573, Japan

(Received April 14, 1987)

The mechanism of the anti-allergic activity of carboxamidemethylated Fc (CM-Fc) was examined *in vitro*. CM-Fc had no effect on the proliferation of lymphocytes induced by concanavalin A (Con A), lipopolysaccharide (LPS), T cell-dependent mitogen or T cell-independent mitogen.

CM-Fc inhibited the activation of glycogen-stimulated guinea pig macrophages by FMLP and A23187, but not by phorbol 12-myristate 13-acetate (PMA).

Keywords——carboxamidemethylation; human IgG; carboxamidemethylated Fc; anti-allergic activity; Con A-induced proliferation; LPS-induced proliferation; glycogen-stimulated macrophage; lysosome enzyme; *N*-acetyl-β-D-glucosaminidase; lactate dehydrogenase

Despite various studies on antibody-producing mechanisms, the phenomenon is still poorly understood at the cellular level.

In previous papers, we have reported that the carboxamidemethylated L chain[1] has anti-ulcerogenic activity and that the carboxamidemethylated H and L chains[2] have anti-inflammatory activity. We also prepared carboxamidemethylated Fc (CM-Fc) from human immunoglobulin G (IgG) and showed that it has anti-allergic activity (types I, III and IV).[3] We now present data on the effect of CM-Fc on T and B lymphocytes, and macrophages, which are required for the antibody response to an antigen in intact animals.

Materials and Methods

Preparation of CM-Fc——As described in our previous paper,[3] 2% commercially available human serum IgG (Globulin-Midori) dissolved into 0.1 M sodium phosphate buffer (pH 6.75) containing 2 mM ethylenediaminetetra acetic acid (EDTA) and 10 mM cysteine-HCl (Nakarai Chem.) was digested with 0.02% papain (type III, Sigma). After 4 h, 150 μl of 0.5 M iodoacetamide (Wako Pure Chem.) was added to the reaction mixture, which was then separated on a Sephadex G-100 column which had been equilibrated with 10 mM phosphate-buffered saline (PBS, pH 7.2). Fab and Fc fractions from Sephadex G-100 were separated by Protein A-Sepharose CL-4B (Pharmacia, Fine Chemical) affinity chromatography, and Fc fragment was purified. The fragment was then reduced with dithiothreitol (Wako Pure Chem.) and carboxamidemethylated with iodoacetamide to yield carboxamidemethylated Fc (CM-Fc).

Culture of Murine Spleen Cells——According to Yanagihara *et al.*,[4] murine spleens were aseptically extracted from C57BL/6 male mice, aged 7 weeks, and cells were gently teased out with a slide glass into Hanks's balanced salt solution (HBSS, Nissui Pharmaceutical Co., Ltd.) in a small Petri dish. The cells were then dispersed by repeated aspiration with a Pasteur pipette and transferred to a tube, which was centrifuged three times at 1000 rpm for 10 min each. Cells were suspended at 5×10^7 in RPMI 1640 (Grand Island Biological Co.) containing 100 μg/ml streptomycin, 100 U/ml penicillin, 2.5 mM *N*-hydroxyethylpiperazine-*N'*-2-ethanesulfonate (HEPES) and 10% heat-

inactivated fetal calf serum (Takara Co., Ltd.). Viability of the cells was over 90% as determined by trypan blue staining.[5]

In the next step, we added 0.1 ml of cell suspension, 0.1 ml of sample, 0.7 ml of the medium and 0.1 ml of concanavalin A (Con A, Wako Pure Chem.) or lipopolysaccharide (LPS, *E. coli* 055:B5, Difco) at various doses to the Petri dish. This suspension was cultured under 5% CO_2 in air at 37°C for 72 h in Petri dishes (No. 3001, Falcon Plastics, Div. B-D Laboratories, Inc.).

Measurement of Intracellular Adenosine Triphosphate (ATP)—— After the culture, the celll suspension was centrifuged twice at 1000 rpm for 10 min. Then, 1 ml of HBSS was added to the pellet.

The measurement of intracellular ATP levels was performed by using the luciferin–luciferase bioluminescence method.[6] Specifically, according to the method reported by Ishizaka *et al.*,[7] 0.1 ml of cell suspension and 0.1 ml of ATP releasing buffer (Laboscience) were incubated at 37°C for 1 min, then 0.1 ml of luciferin–luciferase was added. The values of ATP were measured with a TD-4000 lumiphotometer (Laboscience).

Preparation of Macrophages——According to Nagaoka and Yamashita,[8] male guinea pigs weighing 400—500 g were fasted for 24 h then injected intraperitoneally with 100 ml of 0.17% glycogen (Sigma) in saline. The peritoneum was harvested 5 days after the injection. These cells were washed with phosphate-buffered saline without divalent cations after removal of contaminating erythrocytes by hypotonic treatment with 0.2% NaCl.[9]

The cells suspended in PBS were placed in Ficoll–Conray solution (D = 1.078 g/ml) and centrifuged at 2500 rpm for 20 min at room temperature. Cells obtained from the middle fraction were washed twice and suspended in HBSS containing 10 mM HEPES (Hanks-HEPES).

The purity of isolated cells was over 95% as determined by differential counting of macrophages stained with Giemsa, while the viability of cells was over 90% as determined by trypan blue staining.

Activation of Macrophages——According to Sasaki *et al.*[10] and Smolen and Weissman,[11] 0.1 ml of cell suspension, 0.1 ml of 50 μg/ml cytochalasin B (Sigma), 0.1 ml of sample and 0.6 ml of Hanks-HEPES were incubated at 37°C for 10 min, then 0.1 ml of 10^{-6} M *N*-formyl-L-methionyl-L-leucyl-L-phenylalanine (FMLP, Sigma), 10^{-7} M calcium ionophore (A23187, Sigma) or 2 μg/ml phorbol 12-myristate 13-acetate (PMA, Sigma) was added to the mixture and allowed to react for 15 min. The reaction was stopped on ice. After centrifugation (700 rpm × 10 min), aliquots of the supernatant were taken for standard determinations of *N*-acetyl-β-D-glucosaminidase (NAG) and lactate dehydrogenase (LDH) activities.

Enzyme Assay——According to Woolen *et al.*,[12] NAG was measured with *p*-nitrophenyl-N-acetyl-β-D-glucosaminide (Sigma) as a substrate. Incubation mixtures contained 0.2 ml of test solution and 0.2 ml of 5 mM substrate solution in 0.1 ml of 100 mM sodium citrate buffer containing 0.2 M NaCl (pH 4.5). After incubation for 1 h at 37°C, the reaction was terminated by adding 3 ml of 50 mM glycine–NaOH buffer (pH 10.4) containing 5 mM EDTA. The optical density was measured at 405 nm.

LDH activity was measured according to Schnyder and Baggiolini.[16] The reaction mixture, containing 0.2 ml of test solution, 0.2 ml of 0.1 M sodium phosphate–HCl (pH 7.5) and 0.1 ml of 0.8 mM nicotineamide adenine dinucleotide (NADH) (Boehringer Mannheim, Grade II), was incubated at 25°C for 1 min. Then 0.1 ml of 4 mM sodium pyruvate (Wako Pure Chem.) was added. LDH was assayed by determining the rate of oxidation of NADH at 340 nm using a UV-240 spectro-photometer (Shimadzu).

Statistics——Student's *t*-test was employed to assess the significance of differences between the mean values for the control group and the sample-added groups.

Results

Proliferation of Spleen Cells

The mitogenic activities of CM-Fc and Fc are shown in Fig. 1. There was no significant difference between CM-Fc at 2, 20 or 200 μg/ml, and the control. Fc also failed to inhibit the proliferation. Hydrocortisone, an immuno-suppressive drug, was significantly inhibitory at a concentration of 10 μg/ml (positive control).

When Con A (a T cell-dependent mitogen) was utilized, the maximum proliferation was seen at 2 μg/ml of Con A (data not shown). As shown in Fig. 2, CM-Fc (2-200 μg/ml) and Fc (200 μg/ml) slightly inhibited the proliferation induced by Con A (2 μg/ml) while hydrocortisone significantly inhibited it.

Next, the optimal concentration of LPS (a T cell-independent mitogen) was examined. The maximum proliferation was seen at 5 μg/ml of LPS (data not shown). CM-Fc did not inhibit the proliferation of spleen cells induced by 5 μg/ml of LPS and Fc only slightly inhibited it, but suppression was significant with hydrocortisone (Fig. 3).

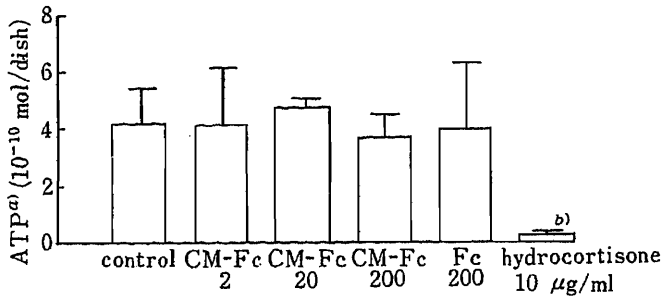

Fig. 1. Effects of CM-Fc, Fc and Hydrocortisone on Spontaneous Proliferation of Spleen Cells from Mice

a) Each value is the mean±S.E. ($n=3$).
Significantly different from the control group: *b*) $p<0.05$.

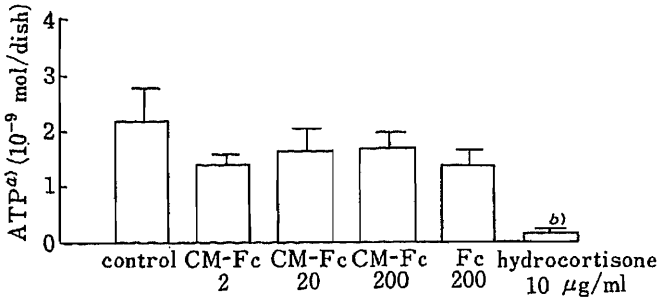

Fig. 2. Effects of CM-Fc, Fc and Hydrocortisone on Con A-Induced Proliferation of Spleen Cells from Mice

a) Each value is the mean±S.E. ($n=3$).
Significantly different from the control group: *b*) $p<0.05$.

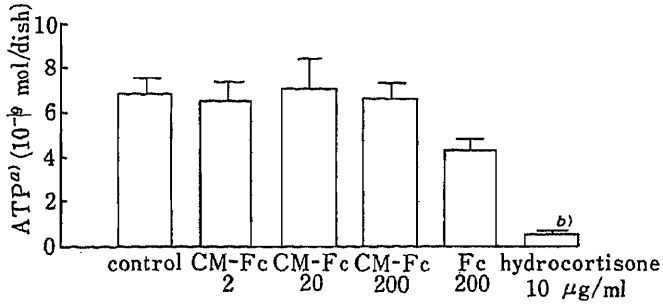

Fig. 3. Effects of CM-Fc, Fc and Hydrocortisone on LPS-Induced Proliferation of Spleen Cells from Mice

a) Each value is the mean±S.E. ($n=3$).
Significantly different from the control group: *b*) $p<0.01$.

Activation of Macrophages

The effects of CM-Fc and Fc on the release of the lysosomal enzyme (NAG) from FMLP-stimulated macrophages are shown in Fig. 4. The NAG activity was very low with non-stimulated macrophages, but when the macrophages were stimulated by FMLP, the NAG activity was about four times higher in the control. CM-Fc at a concentration of 50 μg/ml significantly inhibited the release of NAG, while Fc was not inhibitory. On the other hand, when the LDH activity, the cytoplasmic enzyme, was examined no significant effect was found.

CM-Fc at a concentration of 50μg/ml also significantly inhibited the release of NAG in A23187-stimulated macrophages, although Fc had no such effect. The LDH activity did not

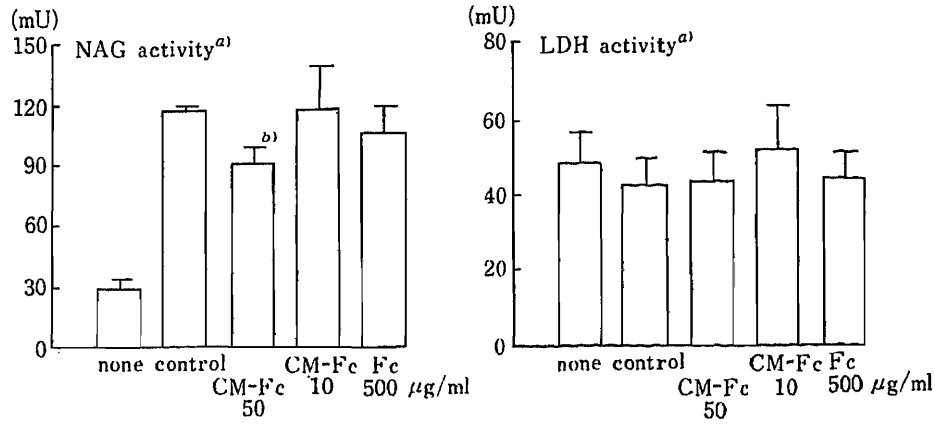

Fig. 4. Effects of CM-Fc and Fc on FMLP-Induced Releases of *N*-Acetyl-β-D-glucosaminidase (NAG) and Lactate Dehydrogenase (LDH) from Glycogen-Stimulated Macrophages in Guinea Pigs

Total activities (100%) of NAG and LDH (released by 0.1% Triton X-100) were 424.9±26.8 mU and 294.8±13.5 mU.
a) Each value is the mean±S.E. ($n=3$).
Significantly different from the control group: *b*) $p<0.05$.

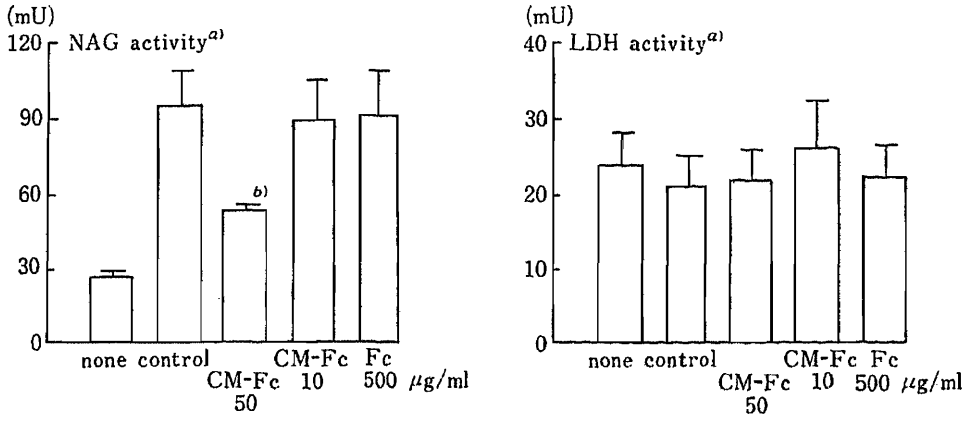

Fig. 5. Effects of CM-Fc and Fc on A23187-Induced Releases of NAG and LDH from Glycogen-Stimulated Macrophages in Guinea Pigs

Total activities (100%) of NAG and LDH (released by 0.1% Triton X-100) were 423.1±29.3 mU and 106.2±18.4 mU.
a) Each value is the mean±S.E. ($n=3$).
Significantly different from the control group: *b*) $p<0.05$.

change when A23187 or FMLP was used (Fig. 5).

Discussion

In the previous paper, we reported that carboxamidemethylated Fc (CM-Fc, M.W. 25000) has anti-allergic activity against types I, III and IV allergic responses.[3] In this paper, we describe the effects of CM-Fc on T and B lymphocytes and/or macrophages.

Using murine spleen cells, we studied the effect of CM-Fc on the proliferation of lymphocytes. Mitogens stimulate specific lymphocytes to synthesize the deoxyribonucleic acid (DNA), leading to morphological biochemical and physiological changes. CM-Fc and Fc were found to have no mitogenic activity in themselves, but hydrocortisone, an immunosuppressive drug, significantly inhibited the spontaneous proliferation of the spleen cells.

We next examined the proliferation of spleen cells utilizing Con A (a T cell-dependent mitogen) and LPS (a T cell-independent mitogen). Our results showed that CM-Fc did not affect T or B lymphocytes (Figs. 2 and 3).

Activated macrophages have been shown to secrete plasminogen activator,[14] collagenase[15] and an elastase-like enzyme,[16] in addition to lysozyme,[17] which is also secreted by nonactivated macrophages. Macrophages also selectively release β-glucuronidase, *N*-acetyl-β-D-glucosaminidase and other acid hydrolases when they are stimulated by undigestible particles,[18] lymphokines,[19] complement products[20] or A23187.[21] We stimulated macrophages with several macrophage-activating reagents and examined the release of lysosome enzyme as an index of activation. Our results demonstrated that CM-Fc inhibited the release of NAG when FMLP and A23187 were used as stimulators (Figs. 4 and 5), although not when PMA, a protein kinase C activator, was used (data not shown). Furthermore, we examined the cytotoxic activity, which was measured as LDH (the cytoplasmic enzyme) activity. CM-Fc had no cytotoxic activity by itself (Figs. 4 and 5).

Our results are consistent with those of Rosenslveich *et al.*,[22] who demonstrated that Con A did not affect lymphocyte proliferation in the absence of macrophages. Since CM-Fc slightly inhibited Con A-induced proliferation, it was supposed that CM-Fc suppressed lymphocyte proliferation mediated by macrophages.

Moreover, we presumed that CM-Fc would affect PI-response,[23,24] which occurs rapidly as soon as FMLP is added.[25] This causes an increase of intracellular Ca^{2+} and the activation of protein kinase C. Further, γ-interferon activates macrophages through the increase of intracellular Ca^{2+} and the activation of protein kinase C[26] and A23187 activates macrophages based on the influx of Ca^{2+}.[27] Thus, CM-Fc inhibited the increase of intracellular Ca^{2+} and/or the influx of extracellular Ca^{2+}. Consequently, we supposed that CM-Fc suppressed the activation of macrophages *via* an enhancement of cytoplasmic Ca^{2+}. Further work is planned to examine this.

Since we restricted ourselves in this study to glycogen-induced macrophages whose functions had already been activated in part, it will be necessary for us to employ resident macrophages of the peritoneum and the lung in future work.

Acknowledgement We are grateful to Miss Hiroko Azuma for her technical assistance.

References

1) T. Mimura, T. Terada, M. Iwai, I. Kohda, S. Take, K. Maeda and S. Aonuma, *J. Pharmacobio-Dyn.*, **6**, 397 (1983); T. Mimura, M. Iwai, T. Terada, I. Kohda, K. Tsujikawa, K. Maeda and S. Aonuma, *ibid.*, **6**, 449 (1983).
2) T. Mimura, K. Tsujikawa, H. Nakajima, M. Okabe, Y. Kohama, M. Iwai and K. Yokoyama, *J. Pharmacobio-Dyn.*, **9**, 46 (1986); T. Mimura, K. Tsujikawa, H. Nakajima, S. Itoh, M. Okabe, I. Kohda and K. Yokoyama, *ibid.*, **9**, 799 (1986).
3) T. Mimura, S. Itoh, K. Tsujikawa, H. Nakajima, Y. Kohama, M. Okabe, M. Iwai, T. Ohmura and K. Yokoyama, *Chem. Pharm. Bull.*, **35**, 4935 (1987).
4) Y. Yanagihara, T. Shida and H. Yoshii, *Nippon Yakurigaku Zasshi*, **78**, 439 (1981).
5) P. F. Kruse, Jr. and M. K. Palterson, Jr., "Tissue Culture, Methods and Applications," Academic Press, New York, 1973.
6) M. D. McElory and M. A. Deluca, "The Chemistry and Applications of Firefly Luminescence," Academic Press, New York, 1981; A. N. Corps, T. Pozzan, T. R. Hesketh and J. C. Metcalfe, *J. Biol. Chem.*, **255**, 10566 (1980).
7) A. Ishizaka, T. Sotooka and S. Matsumoto, *Nippon Rinsyo Menekigakkai Kaishi*, 7, 107 (1984).
8) I. Nagaoka and T. Yamashita, *Comp. Biochem. Physiol.*, **79B**, 147 (1984).
9) T. Yamashita, N. Imaizumi and S. Yuasa, *Cryobiology*, **16**, 112 (1979).
10) J. Sasaki, N. Tatewaki, N. Nose and H. Kyogoku, "Menekigaku Jikken Sosahou," Vol. XIII, Nippon Menekigakkai, Kanazawa, 1983.
11) J. E. Smolen and G. Weissmann, *Biochem. Pharmacol.*, **29**, 533 (1980).

12) J. W. Woolen, R. Heyworth and D. G. Walker, *Biochem. J.*, **78**, 111 (1961).
13) J. Schnyder and M. Baggiolini, *J. Exp. Med.*, **148**, 435 (1978).
14) J. C. Unkeless, S. Gordon and E. Reich, *J. Exp. Med.*, **139**, 834 (1974).
15) Z. Werb and S. Gordon, *J. Exp. Med.*, **142**, 346 (1975).
16) J. Schnyder and M. Baggiolini, *J. Exp. Med.*, **148**, 435 (1978).
17) S. Gordon, J. Todd and Z. A. Cohn, *J. Exp. Med.*, **139**, 1228 (1974).
18) P. Davies, R. C. Page and A. C. Allison, *J. Exp. Med.*, **139**, 1262 (1974).
19) R. Pantalone and R. C. Page, *J. Reticuloendothel. Soc.*, **21**, 343 (1977).
20) H. U. Schorlemmer and A. C. Allison, *Immunology*, **31**, 78 (1976).
21) T. Tokunaga, "Macrophage," Kodansha, Tokyo, 1986.
22) D. L. Rosenslveich, J. J. Farrar and S. Dougherty, *J. Immunol.*, **116**, 131 (1976).
23) Y. Nishizuka, *Trends Biochem. Sci.*, **9**, 163 (1984); *idem*, *Nature* (London), **308**, 693 (1984).
24) M. J. Berridge and R. F. Irrire, *Nature* (London), **313**, 315 (1984).
25) T. Hashimoto and Y. Homma, *Immunopharmacology & Therapy*, **2**, 78 (1984).
26) J. E. Meiel, D. O. Adams and T. A. Hamilton, *J. Immunol.*, **134**, 293 (1983).
27) K. Onozaki, T. Takenawa, Y. Homma and T. Hashimoto, *Cell Immunol.*, **75**, 242 (1983); J. D. Young, S. S. Ko and Z. A. Cohn, *Proc. Natl. Acad. Sci. U.S.A.*, **81**, 5430 (1984).

[Chem. Pharm. Bull. 35(12)4946—4952(1987)]

Effect of Sonication on the Dispersion State of Lipopolysaccharide and Its Pyrogenicity in Rabbits

TETSUO KOMURO,* TOSHIMI MURAI and HIRONOSHIN KAWASAKI

National Institute of Hygienic Sciences, Osaka, Hoenzaka 1-1-43, Higashi-ku, Osaka 540, Japan

(Received June 18, 1987)

The effect of sonication on the particle size of lipopolysaccharide (LPS) in aqueous media was studied, in order to examine the relation of particle size to pyrogenicity in rabbits, by the sucrose density gradient ultracentrifugation technique. LPS extracted from *E. coli* UKT-B according to the phenol/water method showed a polydispersed profile on the gradients, but after sonication for 3 min it formed a single peak in the lower density regions. From the results of electron micrographic observations, partial specific volume, viscosity and turbidity measurements, and density gradient data, it was revealed that sonication produced a decrease in the particle size of LPS. A more marked pyrogenicity in rabbits was observed in the LPS fractions in the lower density regions than in the higher ones, or in the fractions having smaller-sized particles of LPS than in the fractions having larger particles.

Keywords——lipopolysaccharide; LPS; LAL test; sonication; pyrogenicity

Introduction

Pyrogenicity is well known to be one of the fundamental biological activities elicited by lipopolysaccharide (LPS)[1,2] of gram-negative bacteria, and the biological activities of LPS, including pyrogenicity, are suggested to be greatly affected by the particle size, or state of dispersion,[3-11] since LPS extracted by the phenol/water method is usually considerably aggregated in aqueous media.[12,13] During our studies on the pyrogenicity of LPS preparations, we found that sonication for 2 or 3 min significantly enhanced their pyrogenicity in rabbits; a part of these results was reported at the 28th Symposium on Endotoxins in Japan.[14] This result suggests that sonication might disperse the aggregates of LPS into smaller and more uniform particles with an optimum size for manifesting biological activities in aqueous media, resulting in an enhancement of pyrogenicity. This phenomenon is noteworthy because the pyrogenicity of LPS was affected significantly by this physical procedure, which is fundamentally different from the action of surfactants such as sodium deoxycholate, which dissociate the aggregates of LPS mainly by chemical forces into subunits and simultaneously reduce the pyrogenicity.[6,9] In investigating what size of LPS particle is required for optimum biological activities, sonication seems to be a useful tool. This study was, therefore, undertaken to investigate in detail the dispersion state of LPS brought about by sonication in aqueous media by using the sucrose density gradient ultracentrifugation (SDGU) technique, in order to examine the relation of particle size of LPS to pyrogenicity and *Limulus* amoebocyte lysate (LAL) gelation activity.

Experimental

LPS——LPS was extracted from *E. coli* UKT-B according to the hot phenol/water method reported by Westphal *et al.*[15] Crude LPS was purified initially with 50% ethyl alcohol, twice, to yield semi-purified LPS and

further purified by ultracentrifugation in a Hitachi 55P-2 centrifuge (100000 × *g*, 2 h) until the ribonucleic acid content of the LPS preparation became negligible.

Sonication of LPS——LPS was suspended in sterilized, distilled water at the concentration of 1 mg/ml and sonicated for a definite period in an ice-bath using a Nihon Seiki ultrasonic generator, model US-3 (30 W/28 kHz).

SDGU Analysis of LPS——Linear density gradients having 4.5 ml of 5 to 40 or 2 to 16% (w/w) sucrose were prepared with a Hitachi gradient maker, model DGK-U. LPS was suspended in sterilized, distilled water at the concentration of 1 mg/ml; when necessary, the suspension was sonicated for a definite period, then 200 μl was layered onto the gradients. SDGU was performed at 100000 × *g* for 90 or 240 min at 4°C using a Hitachi swinging rotor, model RPS-40. Fractions of 200 μl were collected from the bottom of the tube through a needle inserted from above to yield 23 fractions, which were analyzed for LPS by the carbocyanine dye assay procedures described below. Sucrose was confirmed not to disturb this assay. Sucrose density of each fraction was measured with an Abbe refractometer (Atago Co., Ltd.).

Electron Micrographical Analysis of LPS——LPS samples for electron micrography were negatively stained with 3% phosphotungstic acid, pH 7.3, on carbon films and rendered hydrophilic by a glow discharge in air. Micrographs were recorded at an instrument magnification of 23000 (JEM-100U electron microscope, Nihon Denshi Co., Ltd).

Partial Specific Volume, Viscosity and Turbidity Measurements of LPS——Partial specific volume of LPS was measured by using a density column consisting of bromobenzene and xylene according to the usual method.[16] Relative viscosity of LPS was measured in the presence of 0.05 M NaCl at 20°C in an Ubbelohde-type viscometer. Turbidity experiments were performed by measuring the absorbance of LPS at 520 nm spectrophotometrically.

Chemical Analysis of LPS——LPS was determined colorimetrically by means of the carbocyanine dye reaction according to the method of Zey and Jackson.[17] Carbocyanine dye, 1-ethyl-2-[3-(1-ethylnaphtho[1,2*d*]thiazoline-2-ylidene)-2-methylpropenyl]naphtho[1,2*d*]thiazolium bromide, was obtained from Eastman Kodak Co.

Pyrogen Test of LPS in Rabbits——The pyrogenicity of LPS samples was tested in Japanese white male rabbits weighing about 3 kg in an air-conditioned room (temp. 24±1°C, relative humidity 55±5%). Not less than three animals were used in each experiment. LPS was fractionated by the SDGU technique described above and the fractions were assayed for LPS according to the carbocyanine dye method. Fractions were diluted with sterile saline to give a definite concentration of LPS. Rabbits were injected with 0.01 μg of LPS per kg of body weight intravenously and changes in rectal temperature were recorded automatically for 4 h. Maximum rectal temperature increase (ΔT_{max}) and fever index for 4 h (FI-4), representing the area under the fever curve for 4 h were determined as described previously.[14]

LAL Test of LPS——LAL tests were performed to detect LPS in test solutions semi-quantitatively.[18] The capacity of the endotoxins to cause gelation of the lysate from amoebocytes of *Limulus polyphemus* was estimated with the use of "Pre gel" (Seikagaku Kogyo Co., Ltd.) according to the usual method. Test solutions were made by serial tenfold dilution of samples containing LPS . When necessary, further twofold dilutions were made and endpoint dilution was recorded. The test results were scored as ++ (firm gel), + (loose gel) and − (slight flocculation).

Reagents——Standard ribonucleic acid (RNA) with known sedimentation coefficients (23, 16 and 5+6S) were purchased from Miles Laboratories Inc. All other reagents used in these experiments were of analytical grade and were purchased from commercial sources.

Results

Pyrogenicity and LAL Gelation Activity of LPS Fractionated by SDGU

Non-sonicated LPS was fractionated by the SDGU technique and the LPS content of each fraction was determined colorimetrically by application of the carbocyanine dye reaction. The results obtained are shown at the bottom of Fig. 1. Based on the amount of LPS determined in this way, a definite amount of LPS in each fraction was subjected to pyrogen test in rabbits and to the LAL test. Maximum rectal temperature increase and intensity of febrile response for 4 h were estimated and are represented in the middle of Fig. 1 as ΔT_{max} and FI-4, respectively. Stronger febrile responses in rabbits were observed in the LPS fractions in the lower density regions than in the higher density ones. This result agreed well with that of the LAL test as shown at the top of Fig. 1.

Dispersion Profile of LPS by SDGU

To clarify the effect of sonication on the particle size of LPS, the SDGU profile of LPS was investigated. LPS suspensions at the concentration of 1 mg/ml were sonicated for 1, 3, 10 or 30 min and the results obtained are shown in Fig. 2. In the case of non-sonicated LPS, LPS

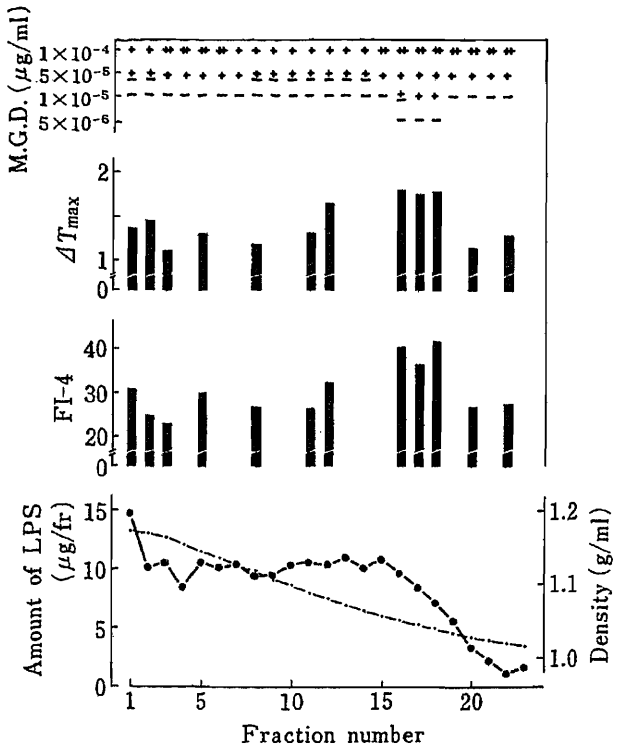

Fig. 1. Sucrose Density Gradient Ultracentrifugation Profile of LPS and Distribution Patterns of Pyrogenicity in Rabbits and LAL Gelation Activity

M.G.D., minimum gelation dose; FI-4, fever index for 4 h (representing area under the fever curve); ΔT_{max}, maximum increase in rectal temperature for 4 h. The linear density gradient was 5 to 40% (w/w) of sucrose. Centrifugation was done at 100000 × *g* for 90 min at 4 °C. The LPS dose in pyrogen tests was 0.01 μg/kg of body weight. Each bar indicates a mean of not less than three experiments.

was found to be distributed almost evenly throughout the gradient, suggesting the presence of various sizes of LPS particles in aqueous media. However, the SDGU profile of sonicated LPS was different from that of the non-sonicated LPS, that is, a peak appeared in the profile and the peak shifted gradually toward the lower-density regions with increased period of sonication. This suggests that larger particles of LPS became smaller under the influence of sonication. However, sonication for more than 10 min no longer caused a positional change of the peak except for a small decrease of the peak area and a corresponding increase in the amount near the top of the gradient.

Particle Size of LPS Sonicated for 3 min

The particle size of sonicated LPS (3 min) manifesting more potent pyrogenicity and LAL gelation activity as shown in Fig. 1, was estimated by using standard RNA with known sedimentation coefficients (S) of 23, 16 and 5+6S as markers. The result is shown in Fig. 3, suggests that LPS particles sonicated for 3 min have a definite size corresponding to standard RNA with a sedimentation coefficient of between 16 and 23 S.

Electron Micrography of LPS

The particle size of LPS was directly observed by electron micrography. The sizes of about 2000 particles of sonicated LPS were measured on the micrographs and compared with those of non-sonicated LPS as a control. The results obtained are presented in Table I, and some examples are shown in Fig. 4. It was revealed that non-sonicated LPS was variable in length, but that after 2 min of sonication, LPS particles with a length of more than 320 nm

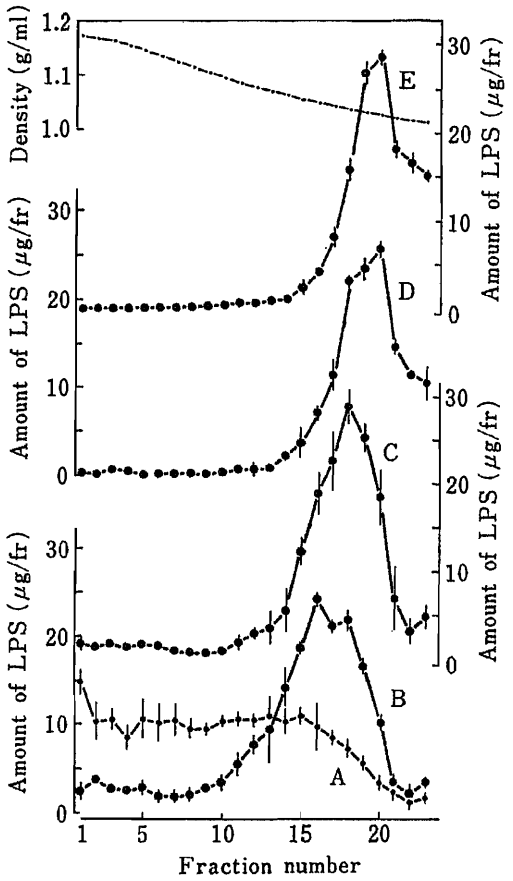

Fig. 2. Sucrose Density Gradient Profiles of Sonicated LPS

Sonication time: A, 0; B, 1; C, 3; D, 10; E, 30 min. The linear density gradient was 5 to 40% (w/w) of sucrose. Centrifugation was done at 100000 × *g* for 90 min at 4°C. Each point with bar indicates a mean ± S.D. of three experiments.
—·—, density; —●—, amount of LPS.

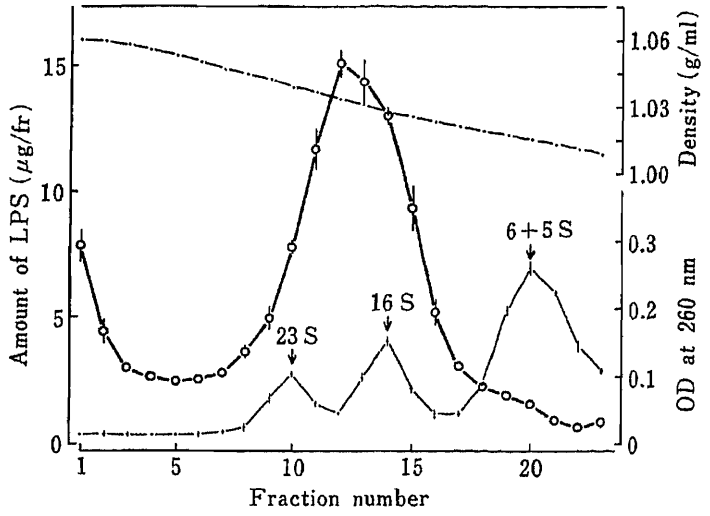

Fig. 3. Comparison of the Density Gradient Profile of Sonicated (3 min) LPS with That of Standard RNA

The linear gradient was 2 to 16% (w/w) of sucrose in water for LPS and in 15^{-1} M phosphate buffer solution, pH 7.0, for RNA. Centrifugation was done at 100000 × *g* for 240 min at 4°C. Each point with bar indicates a mean ± S.D. of three experiments.
—○—, amount of LPS; —·—, OD at 260 nm.

disappeared completely, while after 30 min of sonication, most particles fell within the range of less than 20 nm in length. These results demonstrate that the particle size of LPS was decreased by sonication.

Table I. Effect of Sonication on Particle Length of LPS

Range (nm)	Percentage of LPS particles sonicated for		
	0 min	2 min	30 min
0— 10	2.4	3.1	21.6
10— 20	13.5	19.3	61.2
20— 40	12.3	19.9	12.9
40— 80	18.1	30.4	4.0
80—160	24.0	25.9	0.0
160—320	13.8	1.5	0.0
320—	15.9	0.0	0.0

Based on micrographs of LPS sonicated for 2 or 3 min, the lengths of 2000 LPS particles were measured and the distribution pattern (percentage) was calculated.

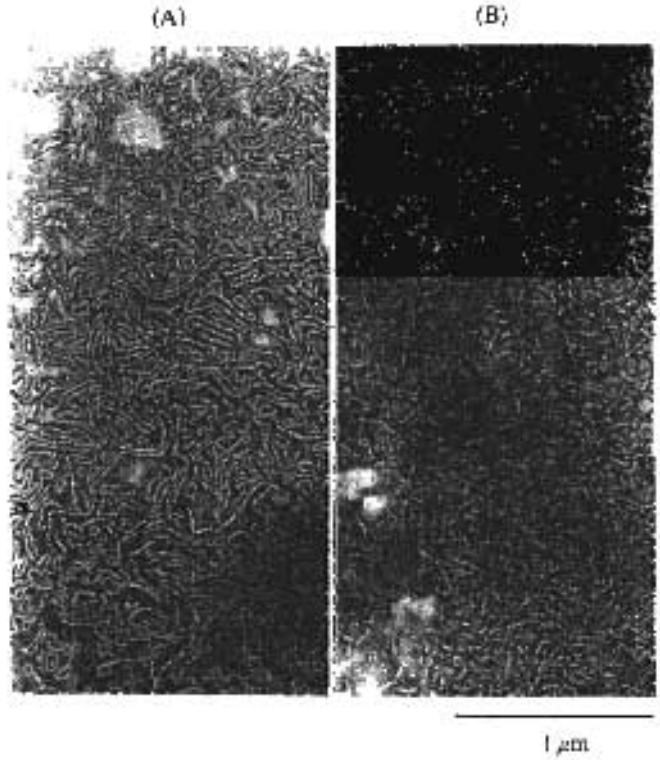

Fig. 4. Electron Micrographs of Negatively Stained Preparations of Phenol/Water-Extracted LPS from *E. coli* UKT-B

(A) Non-sonicated LPS. (B) sonicated (2 min) LPS

Partial Specific Volume, Viscosity and Turbidity of LPS

To clarify the effect of sonication on the particle size of LPS, some physicochemical properties were investigated. First, the partial specific volume of LPS was measured by using a density column consisting of bromobenzene and xylene. The value of the partial specific volume of non-sonicated LPS was approximately 0.717 ml/g, and did not change after sonication for 1, 2, 3, 5, 10 or 30 min.

Next, viscosity and turbidity changes of LPS induced by sonication were investigated. The results obtained are shown in Fig. 5. Sonication for a few minutes caused a remarkable fall in the viscosity of LPS, but the viscosity did not change on further sonication. A similar result was observed in the turbidity change of LPS as shown in Fig. 5. These results indicate

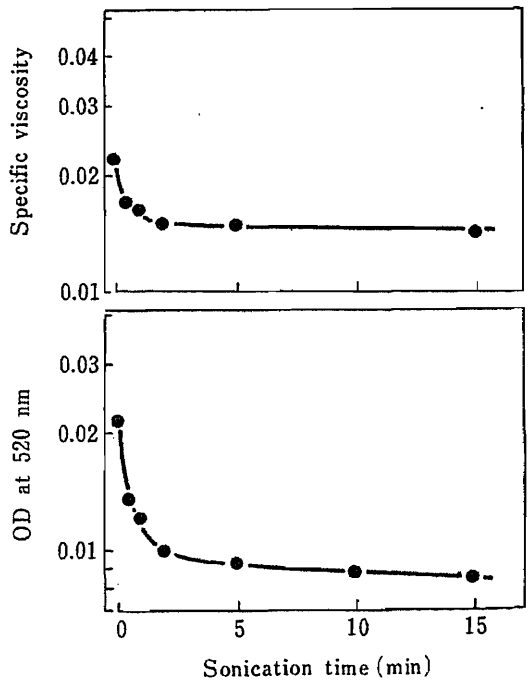

Fig. 5. Changes in the Viscosity and Turbidity of LPS Induced by Sonication

that the particle size of LPS was decreased by sonication.

Discussion

LPS of gram-negative bacteria is usually composed of two contrasting parts, a hydrophilic part and a hydrophobic part, and is therefore amphiphilic.[19,20] In spite of its favorable characteristics, it is only slightly soluble in water as well as in organic solvents. As pointed out previously,[21,22] this property has made the study of LPS difficult. In measuring not only physicochemical constants of LPS but also its biological activities, careful consideration must be given to the dispersion state of LPS in aqueous media. Our data indicated that the dispersion state of LPS in aqueous media was not always uniform in terms of the aggregate size, and our attention was, therefore, focused on the effect of sonication, which is most frequently used as a means to disperse or dissolve slightly soluble materials uniformly in aqueous media.[23,24]

Sonication caused a stepwise shift in the sedimentation profile of LPS on the sucrose gradient, which may not always directly reflect a decrease in the particle size of LPS. The change in sedimentation behavior observed in the present experiment is, however, considered to reflect a decrease in the particle size of LPS from the present results, *i.e.*, (1) that electron micrographic observations directly showed the decrease in the particle size of LPS by sonication, (2) that the partial specific volume of sonicated LPS was identical to that of non-sonicated LPS and (3) that the viscosity and turbidity of LPS were markedly decreased by sonication, and in addition, from other evidence that disaggregation of LPS lowers the sedimentation coefficient of LPS.[25,26] Based on these observations, studies of the dispersion state of LPS in aqueous media were carried out in order to examine the relation of particle size to biological activities of LPS. As shown in Fig. 2, sonication-induced disaggregation of LPS was demonstrated by SDGU. In other words, appropriate sonication made it possible for us to investigate LPS of limited size that retained the intact properties. Using this method, we found a potent pyrogenicity and LAL gelation activity of LPS in the lower density regions near 1.04 density on the sucrose gradient under the present experimental conditions, as shown

in Fig. 2, though this size is not the minimum that can be produced by the sonication (Fig. 2). These results strongly suggest that there might be a definite optimum particle size of LPS required for the manifestation of pyrogenicity in rabbits and for LAL gelation activity.

There are reports describing a reduction in pyrogenicity of LPS by a simple dissociation of LPS particles into subunits using surfactants such as sodium deoxycholate.[6,9] However, in those experiments LPS has not always remained in an intact state. That is, considering that LPS was treated with surfactants to reduce its particle size, there remains a possibility that active sites of LPS might be masked by forming a complex with surfactants,[2,11] resulting in a reduction of the pyrogenicity. To resolve this problem, it will be necessary to dissociate large particles of LPS into smaller ones without surfactants, or without undesirable modifications, and to isolate them for pyrogen test in rabbits.

The present experimental results showed that sonication decreased the particle size of LPS and that the most potent febrile response in rabbits was produced by smaller-particle-sized LPS in the lower density regions near 1.04 density on the sucrose gradient under the present experimental conditions. Sonication will be useful for studying the biological activities of LPS because it produces uniform-sized particles of LPS which show optimum activity and because smaller particles of LPS produced by sonication still retain the intact properties, probably without any modification except particle size.

References

1) R. J. Elin and S. M. Wolff, *Annu. Rev. Med.*, **27**, 127 (1976).
2) A. Nowotony, *Bacterial. Rev.*, **33**, 79 (1969).
3) B. S. Roberson and W. J. Cromartie, *J. Bacteriol.*, **84**, 882 (1962).
4) E. Ribi, W. T. Haskin, K. C. Milner, R. T. Anacker, D. B. Ritter, G. Goode, R. J. Trapani and M. Landy, *J. Bacteriol.*, **84**, 803 (1962).
5) K. C. Milner, K. Fukushi, W. T. Haskin, M. Landy, B. Malmgren and E. Ribi, *Bacteriol. Rev.*, **27**, 352 (1963).
6) E. Ribi, R. L. Anacker, R. Brown, W. T. Haskin, B. Malmgren, K. C. Milner and J. A. Rudbach, *J. Bacteriol.*, **92**, 1493 (1966).
7) F. C. McIntire, H. W. Sievert, G. H. Barlow, R. A. Finley and A. Y. Lee, *Biochemistry*, **6**, 2363 (1967).
8) D. F. Tarmina, K. C. Milner, E. Ribi and J. A. Rudbach, *J. Bacteriol.*, **96**, 1611 (1968).
9) D. F. Tarmina, K. C. Milner, E. Ribi and J. A. Rudbach, *J. Immunol.*, **100**, 444 (1968).
10) A. L. Jackson, *J. Bacteriol.*, **97**, 13 (1969).
11) F. C. McIntire, G. H. Barlow, H. W. Sievert, R. A. Finley and A. L. Yoo, *Biochemistry*, **8**, 4063 (1980).
12) J. W. Shands and P. W. Chun, *J. Biol. Chem.*, **255**, 1221 (1980).
13) O. Westphal and K. Jann, *Methods Carbohydrate Chem.*, **5**, 83 (1965).
14) S. Kanoh, Y. Ogawa, T. Komuro and H. Kawasaki, *Jpn. J. Med. Sci. Biol.*, **35**, 112 (1982).
15) O. Westphal, O. Lüderitz and F. Bister, *Z. Naturforshg.*, **7b**, 148 (1952).
16) Nihon Seibutsu Butsuri Gakkai (ed.), "Zoku Seibutsu Butsuri Gaku Kōza, Butsuri-teki Sokutei-hou II," Yoshioka Shoten, Tokyo, 1968, p. 209.
17) P. Zey and S. Jackson, *Appl. Microbiol.*, **26**, 129 (1973).
18) J. Levin, "Biochemical Applications of the Horseshoe Crab (Limulidate)," ed. by E. Cohen, Alan R. Liss, Inc., New York, 1978, p. 131.
19) J. M. Shands, J. A. Graham and K. Nath, *J. Mol. Biol.*, **25**, 15 (1967).
20) O. Westphal, *Int. Archs. Allergy Appl. Immunol.*, **49**, 1 (1975).
21) A. Nowotony, *Ann. N. Y. Acad. Sci.*, **133**, 586 (1966).
22) H. Beer, A. I. Braude and C. C. Brinton, *Ann. N. Y. Acad. Sci.*, **133**, 450 (1966).
23) L. Saunders, J. Perrin and D. Gammack, *J. Pharm. Pharmacol.*, **14**, 567 (1962).
24) D. Attwood and L. Saunders, *Biochem. Biophys. Acta*, **98**, 344 (1965).
25) C. Galanos and O. Lüderitz, *Eur. J. Biochem.*, **54**, 603 (1975).
26) K. A. Johnson, P. A. Ward, S. Goralnick and M. J. Osborn, *Am. J. Physiol.*, **88**, 559 (1977).

[Chem. Pharm. Bull. 35(12)4953—4959(1987)]

Isolation and Characterization of Protease Modified Ribonucleases from *Rhizopus* sp.

SACHIKO MINE,[a] EIJI WAKABAYASHI,[a] AKIHIRO SANDA,[b] YOSHIO TAKIZAWA,[b] KAZUKO OHGI[a] and MASACHIKA IRIE*,[a]

Department of Microbiology, Hoshi College of Pharmacy,[a] Ebara 2-4-41, Shinagawa-ku, Tokyo 142 and Faculty of Public Health, Azabu University,[b] Fuchinobe, Sagamihara, Kanagawa 229, Japan

(Received June 22, 1987)

In order to clarify the reason for the variation in specific activities of ribonuclease preparations from *Rhizopus* sp. ribonuclease (RNase Rh), low specific activity species (RNase Rh') were separated from native RNase Rh by DEAE Toyopearl 650 column chromatography and characterized. When RNase Rh' was subjected to gel electrophoresis in the absence of 2-mercaptoethanol, it gave a 24 kilodalton (kDa) protein band, but in the presence of the reducing agent it gave 17 and 7 kDa bands. These two peptides were separated by gel filtration and their NH_2-terminal amino acid sequences were determined. The results indicated that RNase Rh' was an enzyme species cleaved at about the 50th residue of native RNase Rh by proteases during the course of purification, but the two fragments were still covalently joined by S–S bridges. RNase Rh' retained about 70% of the native activity and has a similar conformation to the native enzyme.

Keywords——*Rhizopus*; ribonuclease; proteolytic modification; NH_2-terminal sequence

A base-nonspecific and adenylic acid-preferential ribonuclease (RNase Rh) has been purified by Tomoyeda *et al.*[1] and Komiyama and Irie[2] from *Rhizopus* sp. During the course of purification, we very often observed the presence of crystalline RNase Rh species having relatively low specific activity, about 70% of the highest one (327 unit/mg protein) (RNase Rh'). In this paper, we report that the RNase Rh preparation contained enzyme species modified by proteases at around the 50th residue from the N-terminal end of RNase Rh.

Materials and Methods

Reagents——Ribonucleic acid (RNA) used as a substrate was obtained from Kojin Co. Diethylaminoethyl (DEAE)-Toyopearl 650M was purchased from Toyo Soda (Tokyo). Marker proteins, ovalbumin, α-chymotrypsinogen, cytochrome c and insulin, were purchased from Sigma Chem. Co.

Enzyme Preparation——RNase Rh preparations from *Rhizopus* sp. were purified according to the method reported previously,[2] and further subjected to column chromatography on DEAE-Toyopearl 650M at pH 7.5.

Enzyme Assay——The standard assay used during purification was performed according to the previous paper[2] using RNA as a substrate. Enzyme solution (5—10 μl) was added to 2 ml of reaction mixture consisting of 50 mM acetate buffer (pH 6.0) and 0.25% RNA, and the reaction was performed at 37 °C for 1—5 min, then terminated by adding 1 ml of MacFadyen reagent.[3] An aliquot (0.3 ml) was diluted with 2 ml of deionized water, and the absorbancy at 260 nm was measured. The amount of RNase which produced an increase in absorbancy of 1.0 at 260 nm after a 5 min incubation was defined as one unit.

Protein Concentration——Protein concentration was estimated by measuring the absorbancy at 280 nm, taking that of a 0.1% solution as 1.0.

Polyacrylamide Gel Electrophoresis——Disc electrophoresis on polyacrylamide gel was performed by the method of Ornstein[4] and Davis[5] using pH 8.5 gel. Gel electrophoresis was performed at the current of 2.5 mA per tube for 1.5 h. Polyacrylamide gel electrophoresis in the presence of 0.1% sodium dodecyl sulfate (SDS) was performed according to the method of Shapiro *et al.*[6] using 7% polyacrylamide gel. Electrophoresis was carried out

for 4 h at 7 mA per tube. For both electrophoreses, approximately 20 μg of protein was applied per tube. The gels were stained with 0.025% Coomassie brilliant blue. Slab-gel electrophoresis was conducted using 12% polyacrylamide gel according to the method of Laemmli.[7]

Molecular Weight Determination——The molecular weights of RNase Rh′, and the peptides were estimated by gel filtration on Sephadex G-50 column (1.5 × 170 cm) equilibrated with 50 mM trimethylamine-acetate buffer (pH 8.0) containing 0.1 M NaCl according to Andrews.[8] Fractions of 1.3 ml each were collected. Marker proteins used were ovalbumin (MW 45000), α-chymotrypsinogen (MW 25700), cytochrome c (MW 12400) and insulin (MW 6000).

Amino Acid Analysis——Proteins and peptides were hydrolyzed in evacuated, sealed tubes with 6N HCl at 110 °C for 24 h. Analyses were performed by the method of Spackman *et al.*[9] with an amino acid analyzer (Nihon Denshi JLC-200A). Estimation of tryptophan content was performed by the method of Pajot.[10]

Automated Edman Degradation——A protein sample (about 0.3 μmol) was reduced and carboxymethylated in the presence of 8 M urea according to the method of Crestfield *et al.*[11] The reduced and carboxymethylated protein and peptides were subjected to automated Edman degradation[12] with a JEOL JAS 47K sequencer. Phenylthiohydrantoin (PTH)–amino acids were determined by high performance liquid chromatography (HPLC). HPLC was performed with JASCO Fine Sil C_{18-5} column (4.6 × 12.5 cm) equilibrated with solvent A (0.05% H_3PO_4 : acetonitrile = 90 : 10, v/v). PTH–amino acids were eluted with a concave gradient of solvent A and solvent B (0.1% H_3PO_4 : acetonitrile = 60 : 40, v/v) for 16 min at a flow rate of 2.0 ml/min, followed by elution with solvent B. An aliquot of the PTH–amino acid was subjected to isocratic elution on a column of Zorbax ODS (4.6 × 25 cm) with 12.5 mM acetate buffer (pH 4.5) containing 33% acetonitrile. PTH–amino acids were detected by measuring the absorbance at 254 or 315 nm (for dehydrothreonine and dehydroserine).

Circular Dichroism (CD) Spectrum——CD spectra were measured with a JASCO J-40 spectropolarimeter at 25 °C. The light path of the cell used was 0.5 or 0.05 cm. All data are expressed as molar ellipticity. Protein concentration was 10 μM.

Results

SDS Slab Electrophoresis of RNase Rh Preparation Having Low Specific Activity

The Specific activity of RNase Rh purified according to the previous paper[2] is about 237 unit/mg. However, we often observed RNase Rh preparations having low specific activity, such as 170—200 unit/mg. On disc electrophoresis at pH 8.5, such a preparation gave a single protein band at essentially the same location as RNase Rh having high specific activity. However, on 7% SDS disc electrophoresis in the presence of 2-mercaptoethanol, the low specific activity preparation gave two major bands and a very faint band having higher mobility (not seen in Fig. 1); one of the major bands had the same mobility as the high specific activity band and the other band showed slightly higher mobility. In order to estimate the molecular weight of the protein species involved in low specific activity preparation, it was subjected to 12% SDS slab electrophoresis in the presence of 2-mercaptoethanol. Two additional bands were seen, as well as a protein band having the same mobility as RNase Rh.

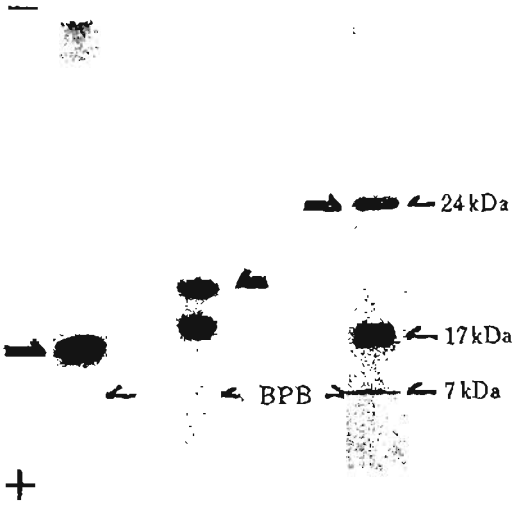

Fig. 1. Gel Electrophoreses of an RNase Rh Preparation Having Low Specific Activity (216 unit/mg)

Left column, disc electrophoresis at pH 8.5, in the absence of 2-mercaptoethanol; middle column, 7% SDS disc electrophoresis; right column, 12% SDS slab electrophoresis. Heavy arrows indicate the mobility of the native RNase Rh. The electrophoreses were performed as described in Materials and Methods.

The molecular weights estimated by electrophoresis of these three bands were 24, 17 and 7 kilodalton (kDa). Since 24 kDa is the molecular weight of the native RNase Rh, the other two bands might be due to the low specific activity species. The sum of these two bands coincides with that of native RNase Rh (24 kDa), and the presence of these two extra bands indicated the cleavage of RNase Rh, probably by proteases. The fact that we were not able to observe these two bands, 17 and 7 kDa in the absence of 2-mercaptoethanol indicated that the enzyme preparation having low specific activity consists of the 7 and 17 kDa species connected by S–S bridges. Hereafter, we designate this modified enzyme preparation as RNase Rh′.

Fractionation of Low Specific Activity RNase Rh′ by DEAE-Toyopearl Column Chromatography

The elution patterns on DEAE-Toyopearl 650M column chromatography of two enzyme preparations having specific activity 216 and 172 unit/mg are shown in Fig. 2a and 2b. In the former preparation, two RNase peaks appeared in addition to the major RNase peak corresponding to RNase Rh. In the latter preparation we observed a very small RNase Rh peak and two other enzyme peaks. SDS-slab electrophoresis of these two enzymes in the presence of 2-mercaptoethanol indicated the presence of the 17 kDa protein band and, thus they were RNase Rh′. By this step of purification, we could separate RNase Rh and RNase Rh′ species very effectively. In this work, we tried to characterize the major RNase Rh′

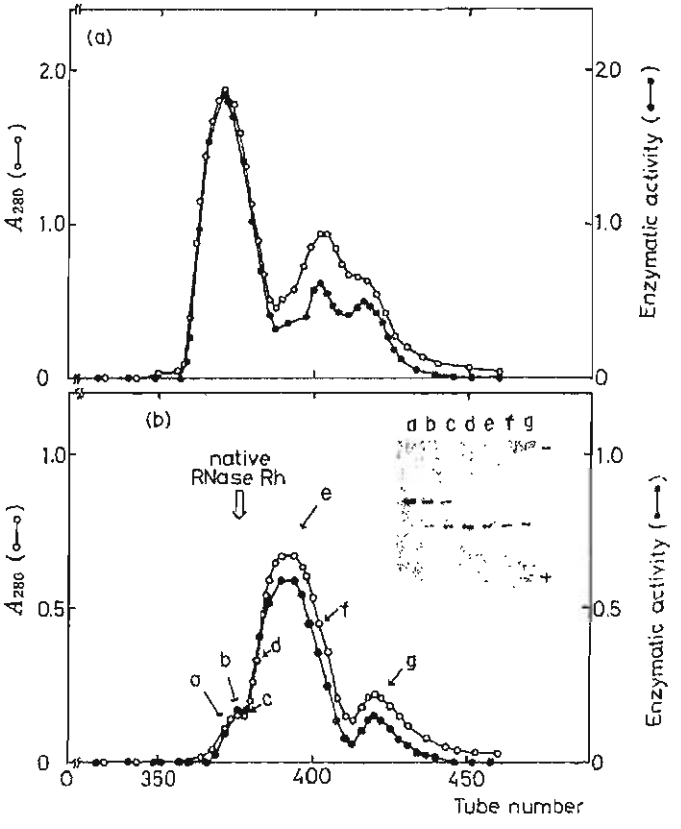

Fig. 2. DEAE-Toyopearl 650M Column Chromatography

(a) The enzyme preparation (specific activity 216 unit/mg) was applied to a column of DEAE-Toyopearl 650M (1.8 × 80 cm) equilibrated with 50 mM Tris-HCl buffer (pH 7.5). The enzyme was eluted with a linear gradient of NaCl from 0—0.2 M in the same buffer. Each 5.0 ml fraction was collected. ○, A_{280} (protein); ●, A_{260} (activity). The other experimental conditions were the same as described in Materials and Methods.

(b) The enzyme preparation (specific activity 172 unit/mg) was applied to the same column as in Fig. 2a. The other experimental conditions were the same as in Fig. 2a. The inset shows the results of slab electrophoresis of the fractions indicated by a—g.

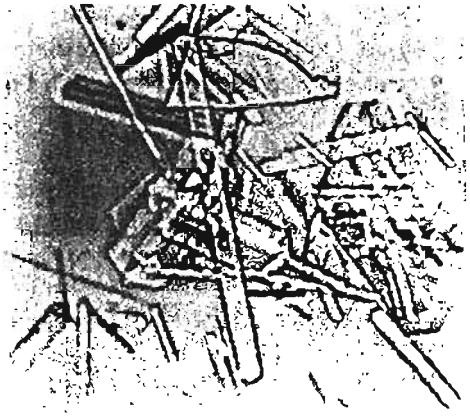

Fig. 3. Crystals of RNase Rh'

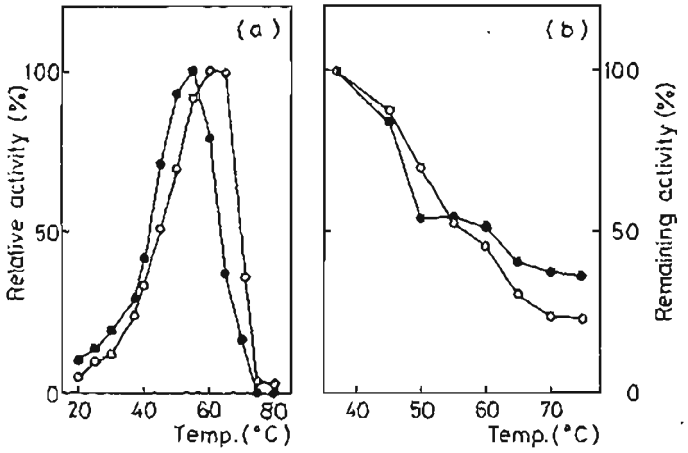

Fig. 4. Effect of Temperature on the Activities of RNase Rh and RNase Rh'

(a) Effect of temperature on the activities of RNase Rh and RNase Rh'. The enzymatic activities of RNase Rh and RNase Rh' (specific activity 172 unit/mg) were measured at the temperature indicated by use of the standard assay system except for the temperature. The ordinate shows percent of the maximum activity.

(b) Stability of RNase Rh and RNase Rh' to heating. The enzyme (60 μg) in acetate buffer (pH 5.0) was incubated at the indicated temperature for 5 min, then the enzymatic activity was measured at 37 °C. ○, RNase Rh; ●, RNase Rh'.

component which was eluted just after RNase Rh (specific activity, 160 unit/mg).

Crystallization of RNase Rh'

RNase Rh' thus obtained was concentrated to a small volume (several mg/ml), then dialyzed against deionized water. The crystalline materials formed after exhaustive dialysis were collected by centrifugation. The photograph of typical crystals is shown in Fig. 3.

Effect of Temperature on the Enzymatic Activity and Heat Stability of RNase Rh'

The effect of temperature on the enzymatic activity of RNase Rh' was studied at pH 5.0 and compared with that of RNase Rh. Although the optimum temperature of RNase Rh' was about 10 °C less than that of RNase Rh, the heat stabilities of the enzymes were comparable (Fig. 4).

CD Spectrum of RNase Rh'

The CD spectra of RNase Rh' and RNase Rh measured at pH 5.0 and room temperature were almost superimposable, indicating similarity in the gross conformation of both enzymes.

Amino Acid Sequences of 17 and 7 kDa Proteins

In order to estimate the locations of the 17 and 7 kDa proteins in RNase Rh, the two

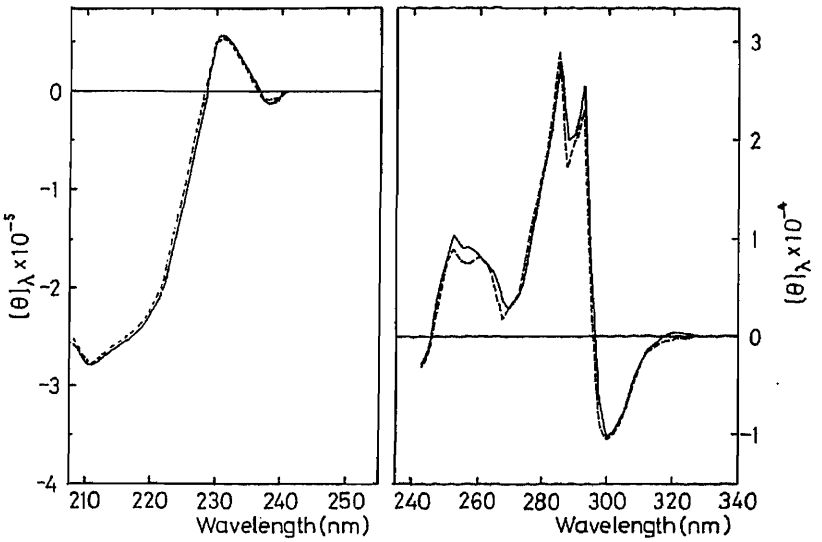

Fig. 5. CD Spectra of RNase Rh and RNase Rh'

——, RNase Rh; ----, RNase Rh'. The experimental conditions were the same as described in Materials and Methods.

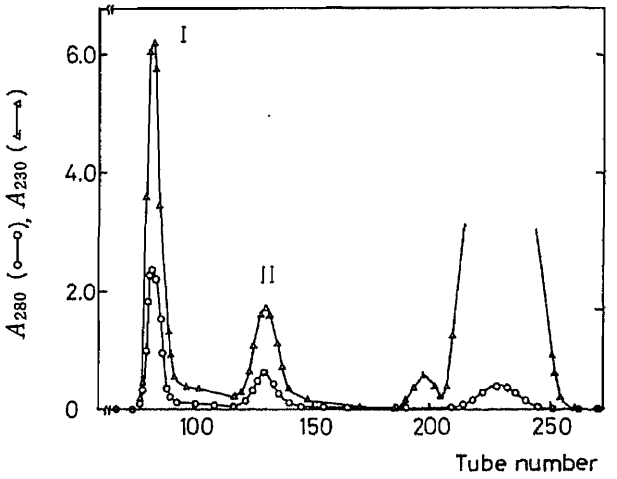

Fig. 6. Sephadex G-50 Column Chromatography of RCM RNase Rh'

RCM RNase Rh' (1.5 μmol) was applied on a Sephadex G-50 column (1.8 × 210 cm) equilibrated with 50 mM trimethylamine-acetate buffer (pH 8.0). Each 2.0 ml fraction was collected. The column was eluted with the same buffer. ○, A_{280}; △, A_{230}.

peptides were fractionated after reduced carboxymethylation of RNase Rh' by gel-filtration on a Sephadex G-50 column (Fig. 6). The high and low molecular weight components, component I and II, respectively, were pooled separately. The molecular weights of both components were estimated by gel filtration on Sephadex G-50 to be 17000 and 6—7000. The amino acid compositions of both components are shown in Table I. The sum of both components is very similar to the composition of the RNase Rh. The amino-terminal sequences of RCM RNase Rh, components I and II were determined by Edman degradation. The results are shown in Fig. 7. Since the N-terminal amino acid sequence of component II was the same as that of RNase Rh, it was concluded that component II corresponds to the NH_2-terminal 50 residues or so of RNase Rh, and component I is the C-terminal 160—170 residues of RNase Rh. It was concluded that RNase Rh' consists of the enzyme species cleaved at about 50 amino acid residues from the N-terminal. However, the two peptides are connected by S–S bridges so that the enzyme retained *ca.* 70% of the activity of the native RNase Rh.

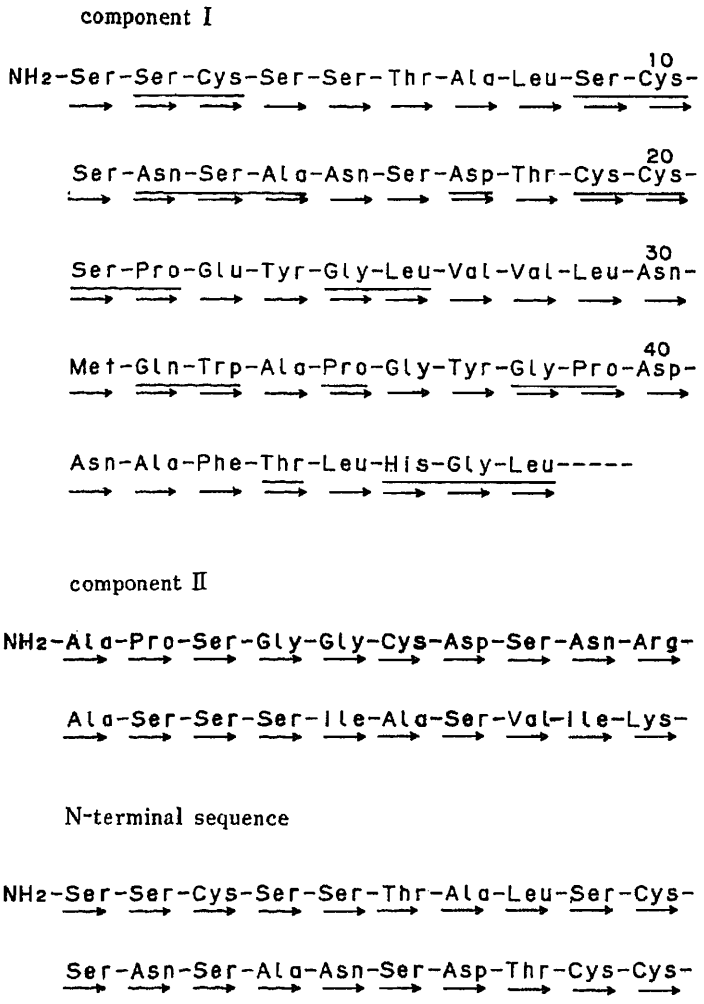

Fig. 7. N-Terminal Amino Acid Sequences of RNase Rh and Components I and II Derived from RNase Rh'

→ indicates each step of Edman degradation.

Discussion

RNase Rh', which has about 70% of the activity of native RNase Rh, has a very similar conformation to RNase Rh as judged from CD spectrum, and could be crystallized easily in spite of its proteolytic modification. The contribution of protease(s) to the formation of RNase Rh' is supported by the fact that when we prepared crude RNase Rh at room temperature instead of in a cold room, the yield of RNase Rh' increased markedly.

The evidence described here also indicated that the amino acid residues around the 50th position probably form a loop located at the surface of the molecule, being very susceptible to proteases during purification. This part of the molecule is probably far from the active site of RNase Rh. Component II of the minor RNase Rh' (the fraction between tube No. 420—450 in Fig. 2) gave the N-terminal sequence Gly–Gly–Cys–Asp–––. Thus the proteases also attack between 3rd and 4th amino acid residues from the N-terminal of component I as well.

These enzyme species are very useful for chemical modification studies of RNase Rh, because the site of a chemically modified group at the N-terminal part of the molecule could be easily determined after separation of this part. The application of this enzyme for chemical modification studies will be reported in a separate paper.

Table I. Amino Acid Compositions of Components I and II Obtained from RNase Rh′

Amino acid	RNase Rh (theoretical value)	RNase Rh′	
		Component I	Component II
		Residues/mol (nearest integer)	
CM-Cys	10	4.69 (5)	5.35 (5)
Asp	28	23.06 (23)	6.84 (7)
Thr	16	11.66 (12)	2.94 (3)
Ser	31	23.36 (23)	9.87 (10)
Glu	14	13.02 (13)	2.40 (2)
Pro	10	5.30 (5)	3.78 (4)
Gly	18	12.97 (13)	5.41 (5)
Ala	16	10.69 (11)	5.11 (5)
Val	11	8.68 (9)	1.82 (2)
Met	4	3.00[a] (3)	1.00[a] (1)
Ile	7	6.00 (6)	0.13
Leu	11	6.47 (6)	5.06 (5)
Tyr	17	15.11 (15)	2.13 (2)
Phe	6	4.80 (5)	1.06 (1)
His	3	2.22 (2)	1.31 (1)
Lys	9	8.04 (8)	1.37 (1)
Arg	4	3.85 (4)	0.07
Trp	5	2.86 (3)	1.77 (2)
Total	215	166	51

a) Assumed as Met 3.00 and 1.00 residues per mol for components I and II, respectively.

During the course of characterization, we determined the sequence of the NH_2-terminal 48 amino acid residues of RNase Rh. When this sequence is compared with that of the similar base non-specific and adenylic acid preferential RNase, RNase T_2 from *Aspergillus oryzae*,[13] several homologous sequences can be seen. They are underlined in Fig. 7.

Acknowledgement The authors thank Amano Pharmaceutical Co., Ltd., for the kind gift of the enzyme source Gluczyme.

References

1) M. Tomoyeda, Y. Eto, and T. Yoshino, *Arch. Biochem. Biophys.*, **131**, 191 (1969).
2) T. Komiyama and M. Irie, *J. Biochem.*, **70**, 765 (1971).
3) D. M. MacFadyen, *J. Biol. Chem.*, **107**, 297 (1934).
4) L. Ornstein, *Ann. N. Y. Acad. Sci.*, **121**, 321 (1964).
5) B. J. Davis, *Ann. N. Y. Acad. Sci.*, **121**, 404 (1964).
6) A. L. Shapiro, E. Vinevela, and J. V. Maizel, *Biochem. Biophys. Res. Commun.*, **28**, 815 (1967).
7) U. K. Laemmli, *Nature*, **227**, 680 (1970).
8) P. Andrews, *Biochem. J.*, **91**, 222 (1964).
9) D. H. Spackman, W. H. Stein, and S. Moore, *Anal. Chem.*, **30**, 1190 (1956).
10) P. Pajot, *Eur. J. Biochem.*, **63**, 263 (1976).
11) A. M. Crestfield, S. Moore, and W. H. Stein, *J. Biol. Chem.*, **238**, 622 (1963).
12) B. Blombäck, M. Blombäck, P. Edman, and B. Hessel, *Biochim. Biophys. Acta*, **115**, 371 (1966).
13) Y. Kawada and F. Sakiyama, Abstracts of Papers, The 34th Symposium on Protein Structure, Sendai, September 1985, p. 17.

Notes

[Chem. Pharm. Bull. 35(12)4960—4963(1987)]

One-Step Preparation of 1-Alkenyltriphenylphosphonium Perchlorates by Electrochemical Oxidation of Triphenylphosphine in the Presence of Alkenes

HIDENOBU OHMORI,* TOSHIKATSU TAKANAMI, and MASAICHIRO MASUI

Faculty of Pharmaceutical Sciences, Osaka University, 1-6 Yamadaoka, Suita, Osaka 565, Japan

(Received April 17, 1987)

Electrochemical oxidation of triphenylphosphine in dichloromethane at a graphite anode in the presence of olefins has been shown to be a convenient method for the preparation of 1-alkenyltriphenylphosphonium perchlorates under mild conditions.

Keywords——triphenylphosphine; 1-alkenyltriphenylphosphonium perchlorate; alkene; electrochemical oxidation; constant current electrolysis

Triphenylvinylphosphonium bromide (Schweizer's reagent)[1] and related 1-alkenylphosphonium salts are useful building blocks for the synthesis of carbocyclic[2] and heterocyclic[3] compounds, allylamines,[4] and 1,4-dienes.[5] Applications of 1-cycloalkenyltriphenylphosphonium salts to the synthesis of carbocyclic and heterocyclcic compounds and optically active organophosphorus compounds have also been reported.[6,7] However, the preparation of the phosphonium salts usually involves rather troublesome multistep procedures.[1,8,9] On the other hand, we found recently that electrochemical oxidation of triphenylphosphine (**1**) in the presence of olefins (**2**) can be an efficient method to prepare 1-alkenyltriphenylphosphonium salts (**3**)[10]: 1-cycloalkenyl derivatives (C_5—C_8) were obtained in 50—70% yields. This paper reports further examples of electrochemical preparation of **3** (Chart 1), including triphenylvinylphosphonium perchlorate (**3f**).

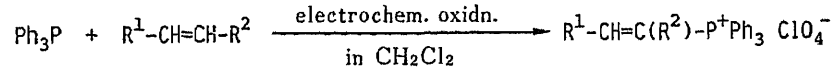

1 2 3

Chart 1

Results and Discussion

As described previously,[10] the phosphonium salt **3** was obtained by constant current electrolysis of a mixture of **1** and **2** in dry dichloromethane containing 2,6-lutidinium perchlorate ($LutClO_4$) in an undivided electrolysis cell. The results are shown in Table I.

Since the oxidation potentials of the olefins used are higher than that of **1**,[11] the process for the formation of **3** can be represented as shown in Chart 2 by analogy with the reactions of triphenylphosphine radical cation (**4**) with other nucleophiles.[12] $LutClO_4$ acts as a proton carrier, that is, it is reduced to the free base at the cathode and the latter accepts the proton liberated at the anode.

In the electrolysis with **2a**, **2c**, and **2d**, the phosphonium salts listed in Table I were

TABLE I. Electrochemical Preparation of 3[a]

Olefin 2 (amount (mmol))	Product 3[b]	Yield (%)[c]
a 1-Methylcyclohexene (15)	(2-Methylcyclohexen-1-yl)P^+Ph_3	41
b Cyclohexene (15)	(Cyclohexen-1-yl)P^+Ph_3	53[d]
c Styrene (3)	$C_6H_5CH=CH-P^+Ph_3$	79
d 4-Methylstyrene (3)	*p*-Me-$C_6H_4CH=CH-P^+Ph_3$	*ca.* 100
e 1,3-Cyclohexadiene (5)	(1,3-Cyclohexadien-1-yl)P^+Ph_3	92[e]
f Ethylene (saturated)	$CH_2=CH-P^+Ph_3$	30[f]

a) General procedure, see Experimental (amount of 1, 3 mmol). *b*) Counter anion, ClO_4^-. *c*) Isolated yield based on **1**. *d*) Quoted from ref. 10. *e*) Obtained as a crude product, see the text. *f*) At 0 °C, see Experimental.

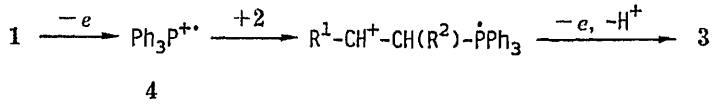

Chart 2

isolated, and no other compound derived from **1** and the olefins was obtained. The yield of **3a** was lower than that of **3b** under the same electrolysis conditions. In **2a** only one position is available for the attack of the radical cation **4** to give **3a**, that is, the 2-position, while **3b** will be formed by the reaction of **4** with **2b** at either of the two olefinic carbons. In the case of **2c** and **2d**, the radical cation **4** seems to attack preferentially at the position in the molecule with highest frontier electron density.[13] The proton nuclear magnetic resonance (^{1}H-NMR) spectra of **3c** and **3d**, which exhibit signals due to two vinyl protons with $J_{HH}=18$ Hz, suggest[14] that the phosphonium salts are *trans* isomers. Although the phosphonium salt **3e** was suggested, on the basis of spectroscopic data (see Experimental), to be the major component of the product isolated in the electrolysis with **2e**, it could not be separated from small amounts of impurities. When the product was treated with sodium hydroxide according to the known procedure,[9] (1,3-cyclohexadien-1-yl)diphenylphosphine oxide (**5e**) was obtained in 62% yield. In an attempt to prepare the phosphonium salts of the type, R–CH_2–$CH=CH-P^+Ph_3$ ClO_4^- (**3g**), electrolysis of **1** with 1-heptene was examined. An oily product mixture containing some phosphonium salt was obtained, but separation of the mixture into each component has not yet been achieved. In this case, treatment of the mixture with sodium hydroxide did not give the expected alkenyldiphenylphosphine oxide: Ph_3PO was isolated from the reaction.

The present results together with those reported previously[10] may suggest the possibility of preparing various 1-alkenyltriphenylphosphonium salts by electrochemical oxidation. However, further investigation is required to obtain the phosphonium salts **3g** and to improve the yield of the vinylphosphonium salt **3f**.

Experimental

All melting points are uncorrected. Infrared (IR) and ^{1}H-NMR spectra were measured with Nippon-Bunko A202, and Hitachi R-20 (60 MHz) or JEOL GX-400 (400 MHz) spectrometers, respectively. Constant current electrolysis was carried out using a Hokuto Denko HA-301 and HA-111 potentiostat/galvanostat.

Materials——$LutClO_4$ was prepared as described previously.[15] Dichloromethane was distilled from P_2O_5 and stored over molecular sieves. Other organic compounds were obtained from commercial sources and were purified by distillation or recrystallization.

General Procedure for the Preparation of 3——A 50 ml sample tube fitted with a silicon stopper was used as the electrolysis cell. A graphite plate anode (10.5 × 2 cm^2) and a stainless steel plate cathode (2.8 × 2 cm^2) were placed in

the cell at a distance of *ca.* 1 cm through the stopper. A solution of **1** (3 mmol) and **2** (amount, see Table I) in dry, deoxygenated CH_2Cl_2 (40 ml) containing 0.2 M $LutClO_4$, and anhydrous K_2CO_3 (3 g, suspended) were placed in the electrolysis cell. The system was subjected to electrolysis (20 mA; current density, *ca.* 1 mA/cm^2) at ambient temperature under an N_2 atmosphere until 2 F per mol of **1** (579 C, *ca.* 8 h) had been consumed: the N_2 gas was supplied from a balloon connected to the cell by a hypodermic needle. The electrolyzed solution, after the K_2CO_3 had been removed by filtration, was evaported to *ca.* 1—2 ml under reduced pressure. Water (100 ml) was added to the residue, and the mixture was extracted with $CHCl_3$ (50 ml × 4). The extracts were dried with anhydrous $MgSO_4$ and concentrated to *ca.* 5 ml under reduced pressure. The phosphonium salt **3** separated out when the residue was added dropwise to ether (100 ml) with stirring.

(2-Methy-1-cyclohexen-1-yl)triphenylphosphonium Perchlorate (**3a**): mp 178—180 °C (from CH_2Cl_2–ether). IR $\nu_{max}^{CHCl_3}$ cm^{-1}: 1590 (C=C), 1100 (ClO_4^-). NMR ($CDCl_3$) δ: 1.2—2.5 (11H, m), 7.5—8.2 (15H, m). *Anal.* Calcd for $C_{25}H_{26}ClO_4P$: C, 65.72; H, 5.74; Cl, 7.76. Found: C, 65.71; H, 5.73; Cl, 7.84.

(β-Styryl)triphenylphosphonium Perchlorate (**3c**): mp 189—190 °C (from CH_2Cl_2—AcOEt). IR $\nu_{max}^{CHCl_3}$ cm^{-1}: 1600 (C=C), 1100 (ClO_4^-). NMR ($CDCl_3$) δ: 7.17 (1H, dd, J_{PH}=23 Hz, J_{HH}=18 Hz), 7.40—7.45 (3H, m, H^m and H^p), 7.51 (1H, dd, J_{PH}=21 Hz, J_{HH}=18 Hz), 7.65—7.95 (17H, m, Ph_3P and H^o). *Anal.* Calcd for $C_{26}H_{22}ClO_4P$: C, 67.18; H, 4.77; Cl, 7.63. Found: C, 67.10; H, 4.71; Cl, 7.45.

[β-(4-Methyl)styryl]triphenylphosphonium Perchlorate (**3d**): mp 221—223 °C (from CH_2Cl_2–AcOEt). IR $\nu_{max}^{CHCl_3}$ cm^{-1}: 1600 (C=C), 1100 (ClO_4^-). NMR($CDCl_3$) δ: 2.46 (3H, s, CH_3), 7.14 (1H, dd, J_{PH}=23 Hz, J_{HH}=18 Hz), 7.35 (2H, br d, J=9 Hz, H^m), 7.41 (1H, dd, J_{PH}=21 Hz, J_{HH}=18 Hz), 7.6—8.0 (17H, m, Ph_3P and H^o). *Anal.* Calcd for $C_{27}H_{24}ClO_4P$: C, 67.72; H, 5.05; Cl, 7.40. Found: C, 67.94; H, 5.11; Cl, 7.17.

Electrolysis of **1** (786 mg) in the presence of **2e** (400 mg) followed by work-up as described above gave a crystalline solid as the product (1210 mg). The following spectral data, together with the ^{13}C-NMR spectra of vinyl- and allylphosphonium salts,[16] suggest that (1,3-cyclohexadien-1-yl)triphenylphosphonium perchlorate (**3e**) is the main component of the product. IR ν_{max}^{KBr} cm^{-1}: 1620 and 1585 (conjugated diene), 1100 (ClO_4^-). ^{1}H-NMR (CD_3CN) δ: 2.37—2.45 (4H, m), 6.23—6.27 (1H, m, H on C3), 6.42—6.48 (1H, m, H on C4), 6.71 (1H, dd, J_{PH}=20 Hz, J_{HH}=5.5 Hz, H on C2), 7.68—7.93 (15H, m, Ar). ^{13}C-NMR (DMSO-d_6) δ [J_{PC}(Hz), assignment]: 113.4 [84.7, C1], 146.5 [9.2, C2], 123.8 [16.0, C3], 136.8 [9.2, C4], 21.7 [8.4, C5 or C6], 22.9 [6.9, C6 or C5], 117.0 [89.3, P^+-C of Ph], 134.1 [10.7, *o*-C], 130.4 [13.0, *m*-C], 135.1 [3.1, *p*-C]. Treatment of the product (900 mg, *ca.* 2 mmol as **3e**) with NaOH in H_2O–EtOH according to the reported procedure[9] followed by column chromatography on silica gel [AcOEt–hexane (5:1)] gave (1,3-cyclohexadien-1-yl)diphenylphosphine oxide (**5e**) (351 mg, 62%): mp 139—140 °C (from hexane). IR $\nu_{max}^{CHCl_3}$ cm^{-1}: 1630 and 1600 (conjugated diene). NMR($CDCl_3$) δ: 2.2—2.4 (4H, m), 6.00—6.12 (2H, m), 6.38 (1H, br dd, J_{PH}=11 Hz, J_{HH}=3.5 Hz), 7.35—7.95 (10H, m). *Anal.* Calcd for $C_{18}H_{17}$ OP: C, 77.13; H, 6.11. Found : C, 76.86, H, 6.02.

Triphenylvinylphosphonium Perchlorate (3f)——Ethylene was bubbled through the solution of **1** (786 mg) in dry CH_2Cl_2 (40 ml) containing 0.2 M $LutClO_4$ and suspended K_2CO_3 for 30 min. The mixture was electrolyzed at 0 °C as described above. Work-up of the electrolyzed solution gave **3f** (350 mg): mp 134—136 °C (from CH_2Cl_2–ether). IR $\nu_{max}^{CHCl_3}$ cm^{-1}: 1590 (C=C), 1100 (ClO_4^-). NMR ($CDCl_3$) δ: 5.8—7.0 (3H, m), 7.3—8.0 (15H, m). *Anal.* Calcd for $C_{20}H_{18}ClO_4P$: C, 61.79; H, 4.67; Cl, 9.12. Found: C, 62.11; H, 4.63; Cl, 9.22.

Acknowledgement This work was supported in part by a Grant-in-Aid for Scientific Research (60570987) from the Ministry of Education, Science and Culture.

References and Notes

1) E. E. Schweizer and R. D. Bach, *J. Org. Chem.*, **29**, 1746 (1964).
2) R. Bonjouklian and R. A. Ruden, *J. Org. Chem.*, **42**, 4095 (1977); I. Kawamoto, S. Muramatsu, and Y. Yura, *Tetrahedron Lett.*, **1974**, 4223; A. T. Hewson, *ibid.*, **1978**, 3267; A. T. Hewson and D. T. MacPherson, *ibid.*, **1983**, 5807; A. G. Cameron and A. T. Hewson, *J. Chem. Soc., Perkin Trans. 2*, **1983**, 2979; M. E. Kuehne and R. J. Reider, *J. Org. Chem.*, **50**, 1464 (1985); and references cited therein.
3) E. E. Schweizer, *J. Am. Chem. Soc.*, **86**, 2744 (1964); E. E. Schweizer, S. D. Goff, and W. P. Murray, *J. Org. Chem.*, **42**, 200 (1977); E. Zbiral, *Synthesis*, **1974**, 775; K. B. Becker, *Tetrahedron*, **36**, 1717 (1980); J. V. Cooney, B. D. Beaver, and W. E. McEwen, *J. Heterocycl. Chem.*, **22**, 635 (1985); and references cited therein.
4) A. J. Meyers, J. P. Lawson, and D. R. Carver, *J. Org. Chem.*, **46**, 3119 (1981).
5) G. Just and B. O'Connor, *Tetrahedron Lett.*, **26**, 1799 (1985).
6) T. Minami, H. Sako, T. Ikehira, T. Hanamoto, and I. Hirao, *J. Org. Chem.*, **48**, 2569 (1983); T. Minami, Y. Taniguchi, and I. Hirao, *J. Chem. Soc., Chem. Commun.*, **1984**, 1046; T. Minami, T. Hanamoto, and I. Hirao, *J. Org. Chem.*, **50**, 1278 (1985); T. Minami, T. Chikugo, and T. Hanamoto, *ibid.*, **51**, 2210 (1986).
7) T. Minami, Y. Okada, Y. Taniguchi, R. Nomura, and I. Hirao, The 13th Symposium on Organic Sulfur and Phosphorus Chemistry, Hiroshima, 1985, Abstract p. 21; T. Minami, Y. Okada, R. Nomura, S. Hirota, Y. Nagahara, and K. Fukuyama, *Chem. Lett.*, **1986**, 613.

8) E. E. Schweizer and A. T. Wehman, *J. Chem. Soc.* (*C*), **1971**, 343; E. E. Schweizer, A. T. Wehman, and D. M. Nycz, *J. Org. Chem.*, **38**, 1583 (1973).
9) G. Saleh, T. Minami, Y. Ohshiro, and T. Agawa, *Chem. Ber.*, **112**, 355 (1979).
10) H. Ohmori, T. Takanami, and M. Masui, *Tetrahedron Lett.*, **26**, 2199 (1985).
11) The voltammetric peak potentials of **1** and **2** in acetonitrile (0.1 M $NaClO_4$) were as follows: **1**, 1.4; **2a**, 2.0; **2b**, 2.1; **2c**, 1.8; **2d**, 1.8; **2e**, 1.5 V *vs.* Ag wire (at a glassy carbon electrode, at 25 °C; voltage sweep rate, 50 $mV\,s^{-1}$).
12) H. Ohmori, K. Sakai, N. Nagai, Y. Mizuki, and M. Masui, *Chem. Pharm. Bull.*, **33**, 373 (1985) and references cited therein.
13) Simple molecular orbital calculation showed that the β position of the styrenes meets the requirement.
14) L. M. Jackmann and S. Sternhell, "Application of Nuclear Magnetic Resonance Spectroscopy in Organic Chemistry," 2nd ed., Pergamon Press, Oxford, 1969, pp. 301—304.
15) H. Ohmori, T. Takanami, H. Shimada, and M. Masui, *Chem. Pharm. Bull.*, **35**, 2558 (1987).
16) T. A. Albright, W. J. Freeman, and E. E. Schweizer, *J. Am. Chem. Soc.*, **97**, 2946 (1975) and references cited therein.

[Chem. Pharm. Bull. 35(12)4964—4966(1987)]

A One-Pot Isoquinoline Synthesis by Cyclodehydrogenation of *N*-Benzyl-α-alkylaminoacetals with Chlorosulfonic Acid: Formation of 3-Alkylisoquinolines[1)]

KAZUKO KIDO* and YASUO WATANABE

Daiichi College of Pharmaceutical Sciences, 22-1 Tamagawa-cho, Minami-ku, Fukuoka 815, Japan

(Received April 27, 1987)

A direct preparation of fully aromatized 3-alkylisoquinolines (**3e—p**), was achieved by cyclodehydrogenation with chlorosulfonic acid of *N*-benzyl-α-alkylaminoacetals (**2e—p**) which were prepared by addition of Grignard reagent to *N*-benzyliminoacetals (**1a—d**).

Keywords——*N*-benzyl-α-alkylaminoacetal; *N*-(3,4-dimethoxybenzyl)-α-alkylaminoacetal; *N*-(3-methoxybenzyl)-α-alkylaminoacetal; *N*-(4-methylbenzyl)-α-alkylaminoacetal; alkyl halide; 3-alkylisoquinoline; benzyliminoacetal; chlorosulfonic acid

In the previous paper,[2)] we reported a one-pot preparation of fully aromatized isoquinolines by the cyclodehydrogenation of benzylaminoacetals and α-alkylbenzylaminoacetals with chlorosulfonic acid($ClSO_3H$) without the use of any other oxidizing agent.

Now we wish to report a direct preparation of fully aromatized 3-alkylisoqunolines (**3**) by the cyclodehydrogenation with $ClSO_3H$ of *N*-benzyl-α-alkylaminoacetals (**2**), which were prepared by the addition of Grignard reagent to appropriate benzyliminoacetals (**1**).

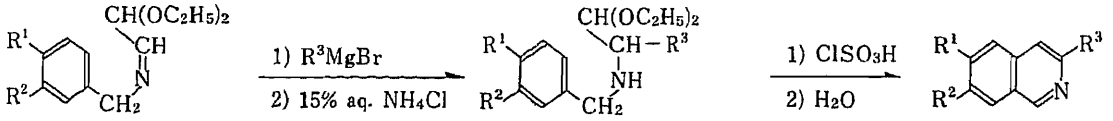

1a—d **2e—p** **3e—p**

a: $R^1=R^2=H$
b: $R^1=R^2=OCH_3$
c: $R^1=H$, $R^2=OCH_3$
d: $R^1=CH_3$, $R^2=H$

e: $R^1=R^2=H$, $R^3=CH_3$
f: $R^1=R^2=H$, $R^3=C_2H_5$
g: $R^1=R^2=H$, $R^3=n\text{-}C_3H_7$
h: $R^1=R^2=OCH_3$, $R^3=CH_3$
i: $R^1=R^2=OCH_3$, $R^3=C_2H_5$
j: $R^1=R^2=OCH_3$, $R^3=n\text{-}C_3H_7$

k: $R^1=H$, $R^2=OCH_3$, $R^3=CH_3$
l: $R^1=H$, $R^2=OCH_3$, $R^3=C_2H_5$
m: $R^1=H$, $R^2=OCH_3$, $R^3=n\text{-}C_3H_7$
n: $R^1=R^3=CH_3$, $R^2=H$
o: $R^1=CH_3$, $R^2=H$, $R^3=C_2H_5$
p: $R^1=CH_3$, $R^2=H$, $R^3=n\text{-}C_3H_7$

Chart 1

N-Benzyl-α-alkylaminoacetals (**2**) were treated with $ClSO_3H$ at $-10°C$ under a nitrogen atmosphere, then left to stand at room temperature for 72 h or heated 100 °C for 10 min. The crude base thus obtained was subjected to gas chromatography. Only one peak was recognized except for two cases (**2l**→**3l** and **2m**→**3m**).[3)] All of the known (**3e—h**, **k**, **n**, **o**) and new bases (**3i—j**, **3l**, **m** and **p**) obtained by this one-flask operation were shown be identical with the corresponding authentic specimens prepared by alternative well-known methods. Various spectral data, especially the ultraviolet (UV) absorption curves, of these bases were consistent with the fully aromatized structures.[4)] Yields of the products (**3**) based upon the

TABLE I. Physical, Spectral and Analysis Data and Yields of *N*-Benzyl-α-alkylaminoacetals (2e—p)

Substrate	bp (°C/mmHg)	Oxalate mp (°C) (from EtOH)	Formula	Analysis (%) Calcd (Found) C	H	N	MS (*m/z*) M^+	Yield (%)
2e	160—162/6 (94—96/0.4[b])	154—156						76
2f	132—135/5 (109—110/0.75[b])	133—134						74
2g[a]	183—184/5	108—109	$C_{16}H_{27}NO_2$	72.45 (72.31	10.19 10.18	5.28 5.22)	265	75
2h	230—233/6 (175/2[c])	130—131						74
2i	174—176/5 (160/0.2[c])	76—78						71
2j[a]	160—163/5	74—75	$C_{18}H_{31}NO_4$	66.46 (66.19	9.54 9.20	4.31 4.15)	325	70
2k[a]	165—169/5	148—149	$C_{15}H_{25}NO_3$	67.42 (67.13	9.36 9.12	5.42 5.21)	267	79
2l[a]	163—164/6	119—120	$C_{16}H_{27}NO_3$	68.32 (68.18	9.60 9.45	4.98 5.08)	281	76
2m[a]	163—165/6	110—111	$C_{17}H_{29}NO_3$	69.15 (68.86	9.38 9.48	4.75 4.85)	295	75
2n	135—136/6 (112—114/0.5[b])	140—141						77
2o	131—133/6 (108—110/0.4[b])	107—108						75
2p[a]	157—158/7	99—100	$C_{17}H_{29}NO_2$	73.12 (73.12	10.39 10.10	5.20 5.17)	279	75

a) New compounds. *b*) N. Vinot, *Bull. Soc. Chim. France*, **1960**, 617. *c*) P. Lejay and Cl. Viel, *Ann. Chim.*, **1977**, (2), 87.

substrates (**2**) were 3—72%.

In the previous paper[2] we proposed that $ClSO_3H$ not only plays the same role as sulfuric acid in the Pomeranz–Fritsch reaction but also can cause dehydrogenation.

Since the formation of 3-alkylisoquinolines is difficult or fails in the Pomeranz–Fritsch synthesis,[5] the Schlittler–Müller procedure[6] presented here in which $ClSO_3H$ is used as a cyclodehydrogenating agent presented here should be advantageous for one-pot syntheses of the fully aromatized 3-alkyl-isoquinolines from *N*-benzyl-α-alkylaminoacetals.

Physical and spectral data, yields and microanalyses of **2e—p** and **3e—p** are given in Tables I and II.

Experimental

Melting points were determined on a Yanaco micro melting point apparatus and are uncorrected. UV and mass spectra were taken on Jasco UVIDEC-505 and JEOL JMS-100 spectrometers. All solutions were dried over anhydrous $MgSO_4$.

Grignard Reaction of Benzyliminoacetals (1a—d): Formation of *N*-Benzyl-α-alkylaminoacetals (2e—p)——A benzyliminoacetal (**1a—d**, 20 mmol in 30 ml of Et_2O) was added to a Grignard reagent which was prepared from Mg (0.583 g, 24 mmol in 20 ml of Et_2O) and an alkyl halide (CH_3I, C_2H_5Br, *n*-C_3H_7Br, 24 mmol in 30 ml of Et_2O). The reaction mixture was decomposed with 15% aqueous NH_4Cl solution and the product was extracted with Et_2O. The extract was dried and distilled. Physical data, yields and elemental analyses are given in Table I.

Treatment of *N*-Benzyl-α-alkylaminoacetals (2e—p) with $ClSO_3H$: Formation of 3-Alkylisoquinolines (3e—p)—— An acetal (**2e—p**, 10 mmol) was added portionwise to $ClSO_3H$ (11.6 g, 100 mmol) at −10 °C with stirring under a

TABLE II. Physical, Spectral and Microanalytical Data and Yields of 3-Alkylisoquinolines (**3e—p**)

Base	mp (°C) or bp (°C/mmHg)	Picrate mp (°C) (from C_6H_6)	UV λ_{max}^{MeOH} nm (log ε)	Formula	High-resolution MS *m/z* (M^+) Calcd (Found)	Yield (%)
3e	63—64 (68[b])	203—204	217 (4.17), 247 (3.75), 253 (3.80), 259 (3.76), 312 (3.50), 326 (3.57)			72
3f	120—122/5	173—174 (171—172[b])	217 (4.74), 258 (3.65), 268 (3.64), 312 (3.48), 326 (3.58)			62
3g	131—132/5	160—161 (161[c])	221 (4.50), 260 (3.46), 271 (3.49), 313 (3.23), 327 (3.31)			60
3h	130—131 (132—133[d])	280—284 (dec.)	234 (4.50), 268 (3.42), 277 (3.39), 289 (3.26), 313 (3.21), 327 (3.18)			69
3i[a]	58—59	243—244	234 (4.50), 267 (3.54), 277 (3.39), 289 (3.38), 314 (3.37), 328 (3.38)	$C_{13}H_{15}NO_2$	217.1099 (217.1034)	66
3j[a]	67—68	198—199	231 (4.61), 265 (3.48), 277 (3.75), 289 (3.65), 315 (3.58), 328 (3.58)	$C_{14}H_{17}NO_2$	231.1255 (231.1250)	60
3k	65—66 (65—66[e])	233—234	224 (5.46), 257 (3.29), 265 (3.25), 333 (3.27), 344 (3.29)			18
3l[a]	56—57	199—202	224 (5.46), 256 (4.03), 264 (3.96), 332 (3.59), 343 (3.64)	$C_{12}H_{13}NO$	187.0994 (187.0945)	6
3m[a]	84—86	204—206	224 (5.52), 256 (4.00), 264 (3.94), 332 (3.62), 343 (3.64)	$C_{13}H_{15}NO$	201.1153 (201.1127)	3
3n	78—79	209—211 (193—195[b])	224 (4.78), 264 (3.31), 275 (3.34), 287 (3.20), 311 (3.24), 326 (3.34)			55
3o	35—36	208—209 (194—196[b])	223 (4.16), 264 (3.32), 275 (3.27), 288 (3.14), 310 (3.23), 326 (3.35)			51
3p[a]	45—46	194—196	223 (4.49), 264 (3.03), 275 (3.10), 287 (3.08), 310 (3.11), 324 (3.17)	$C_{13}H_{15}N$	185.1201 (185.1202)	47

a) New compounds. *b*) N. Vinot, *Bull. Soc. Chim. France*, **1960**, 617. *c*) J. M. Albahary, *Ber.*, **29**, 2391 (1890). *d*) T. Koyama, M. Toda, Y. Katsuse and M. Yamato, *Yakugaku Zasshi*, **90**, 11 (1970). *e*) R. B. Tirodkar and R. N. Usgaonkar, *Ind. J. Chem.*, **10**, 1060 (1972).

nitrogen atmosphere, then allowed to stand in the range from room temperature (for 72 h with reactive substrates such as **2h—p**) to 100 °C (for 10 min with the less reactive acetals such as **2e—g**). The reaction mixture was poured onto crushed ice. After extraction with Et_2O, the acidic solution was made alkaline with Na_2CO_3, and the product was extracted with CH_2Cl_2. The extract was dried, and the solvent was removed to give the product, which was distilled or recrystallized (from C_6H_6). Physical and spectral data, yields and microanalyses of the products are given in Table II.

Acknowledgement The authors are grateful to Miss Keiko Harada, Mr. Yōki Tasaki and Mrs. Ryōko Nakazono for mass spectral measurements and elemental analyses.

References and Notes

1) Part 6 in the series of "Halosulfonic Acid as a Cyclizing Agent for Isoquinoline Synthesis," part 5, K. Kido and Y. Watanabe, *Annual Report of Daiichi College of Pharmaceutical Sciences*, **14**, 1 (1983).
2) Part 3, K. Kido and Y. Watanabe, *Heterocycles*, **14**, 1151 (1980).
3) Chloro derivatives of the parent bases (**3l** and **3m**) were obtained as by-products in extremely low yield.
4) L. Hruban, F. Sântavý and Hegerová, *Collection Czech. Chem. Commun.*, **35**, 3420 (1970).
5) W. J. Gensler, "Organic Reactions," Vol. 6, ed. by R. Adams, John Wiley & Sons, Inc., New York, 1951, pp. 191—206.
6) E. Schlittler and J. M. Müller, *Helv. Chim. Acta*, **31**, 914 (1948).

[Chem. Pharm. Bull. 35(12)4967—4971(1987)]

1,4,7-Dioxaselenocines from 1,3-Oxaselenoles

KATSUHIDE MATOBA* and TAKAO YAMAZAKI

Faculty of Pharmaceutical Sciences, Toyama Medical and Pharmaceutical University, Sugitani, Toyama 930-01, Japan

(Received May 18, 1987)

The structure of the product from the reaction of diazomethane and 4,5,6,7-tetrahydro-4′,4′,6,6-tetramethylspiro[1,3-benzoxaselenole-2,1′-cyclohexane]-2′,4,6′-trione (I), which was prepared by the oxidation of dimedone with selenium dioxide, was proved by X-ray analysis to be 1,2,3,4,8,9,10,11-octahydro-3,3,10,10-tetramethyl-1,8-dioxodibenzo[*b*,*e*][1,4,7]dioxaselenocine (II). Several 1,3-oxaselenoles (IV) derived from bicyclo[3.3.1]nonane-2,4-diones (III) were treated with diazomethane in ether to give the corresponding dioxaselenocines (V) in good yields.

Keywords——β-diketone; bicyclo[3.3.1]nonane-2,4-dione; 3-oxaselenole; diazomethane; selenium dioxide; 1,4,7-dioxaselenocine; X-ray analysis

In our preliminary communication,[1] the product obtained from the reaction of diazomethane and 4,5,6,7-tetrahydro-4′,4′,6,6-tetramethylspiro[1,3-benzoxaselenole-2,1′-cyclohexane]-2′,4,6′-trione (I), which was prepared by the oxidation of dimedone with selenium dioxide (SeO_2), was suggested to be 1,2,3,4,8,9,10,11-octahydro-3,3,10,10-tetramethyldibenzo[*b*,*e*][1,4,7]dioxaselenocine-1,8-dione (II) on the basis of the elemental analysis, physical data, and some chemical reactions. To confirm the structure of compound II, we carried out an X-ray crystallographic analysis. In this paper, the results of the X-ray analysis and similar transformations of bicyclo[3.3.1]nonane-2,4-diones (III) are described.

The X-ray crystallographic analysis of compound II (Fig. 1) revealed that our earlier suggestion[1] was correct. The bond angles of C_6–Se, C_{4a}–O_5–C_6, C_6–Se–C_{7a}, and C_{11a}–O_{12}–C_{12a} are 113.2°, 119.3°, 99.8°, and 116.7°, respectively, and the bond lengths of C_6–Se and Se–C_{7a} are 1.95 and 1.91 Å, respectively.

This is the first example of the transformation of 1,3-selenoles to dioxaselenocines, and we therefore attempted to extend this reaction to the bicyclo[3.3.1]nonane system, which has been studied because of its interesting reactivity based on the fork-head interaction between C_3 and C_7. Bicyclo[3.3.1]nonane-2,4-dione (IIIa)[2] was treated with SeO_2 in dioxane to give an oxaselenole, 4′,5′,6′,7′,8′,9′-hexahydrospiro[3,7-methanocyclooctane-1,2′-5′,9′-metanocycloocta[1,2-*d*]-1,3-oxaselenole]-2,4′,8-trione (IVa) in a good yield; the product exhibited a characteristic pattern around the parent peak (*m*/*z* 380, base peak) due to the natural isotope abundance of Se in the mass spectrum (MS), and showed carbonyl stretching bands at 1730, 1705, and 1645 cm^{-1} in the infrared (IR) spectrum. Compound IVa was treated with an excess of diazomethane to give quantitatively an inseparable mixture of dioxaselenocines, *syn*- and *anti*-1,2,3,4,5,6,10,11,12,13,14,15-dodecahydro-2,6-methano-11,15-methanodicycloocta[*b*,*e*][1,4,7]dioxaselenocine-1,10-dione (Va and Va′), which showed a characteristic pattern of the parent peak centered at *m*/*z* 394 in the MS, the carbonyl and olefinic absorption bands at 1655, 1610, and 1580 cm^{-1} in the IR spectrum. The mixture exhibited two pairs of AB-type signals at δ 5.49—6.03 and 5.59—5.72 (4:1 in intensity) due to the C_8-protons in the nuclear magnetic resonance (NMR) spectrum. From an examination of a molecular model, the major product was suggested to be the *syn*-isomer (Va). In the *anti*-

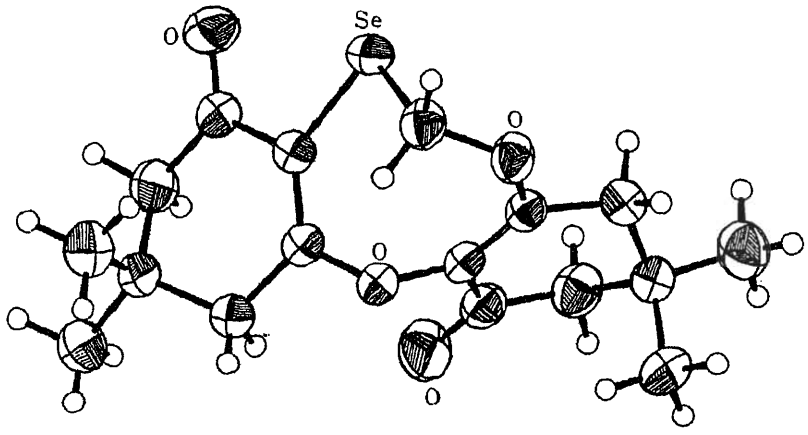

Fig. 1. ORTEP Drawing of the Molecule of Compound II

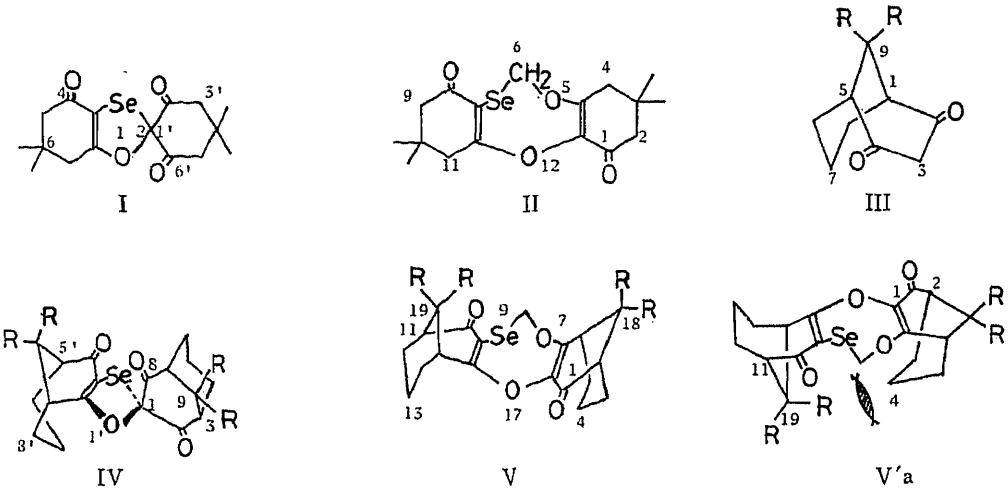

a: R=H b: R=OMe c: R-R=O

Chart 1

isomer (Va'), the dioxaselenocine ring is slightly distorted because of repulsion between the C_4- and C_{19}-methylene groups, and this distortion may affect the chemical shifts of the C_8-protons in Va'. This suggestion was confirmed by the result of a similar reaction using the 1,3-oxaselenolse obtained from 9,9-dimethoxybicyclo[3.3.1]nonane-2,4-dione (IIIb) or bicyclo-[3.3.1]nonane-2,4,9-trione (IIIc).

The product obtained by the oxidation of IIIb with SeO_2 was not crystallized and was treated with diazomethane to give pure 1,4,7-dioxaselenocine in a good yield; the product exhibited an AB-type signal at δ 5.53 and 6.04 in the NMR spectrum. From the chemical shift and an examination of a molecular model, this compound was suggested to be *syn*-1,4,7-dioxaselenocine (Vb). Compound Vb was hydrolyzed with diluted hydrochloric acid to give the 18,19-dioxo analogue of Va (Vc), which exhibited an AB-type signal (J= 10.6 Hz) due to the C_8-protons at δ 5.67 and 6.27 in the NMR spectrum.

Similarly, IIIc was oxidized with SeO_2 to give the 9,10'-dioxo analogue of IVa (IVc), but in poor yield.

Experimental

All melting points were taken on a Kofler block and are uncorrected. Thin layer chromatography (TLC) was

done on Merck precoated silica gel (SiO_2) plates. IR spectra were determined by using a JASCO IR-Al diffraction grating spectrophotometer; absorption data are given in cm^{-1}. NMR spectra were recorded in $CDCl_3$ on a JEOL FX-270 spectrometer with tetramethylsilane as an internal standard. The chemical shifts and the coupling constants (J) are given in δ and Hz, respectively. Ultraviolet (UV) spectra were obtained in $CHCl_3$ with a Hitachi 200-10 spectrophotometer, and absorption maxima are given in nm. Gas chromatography (GC) was carried out using a Shimadzu GC-6AM instrument with a stainless steel column (3 m/m × 3 m) packed with 5% SE-30. The nitrogen gas-flow rate was 40 ml/min. Mass spectra were measured with a JEOL D-200 (70 eV, direct inlet system). All solvents were removed under reduced pressure after drying of the solution over anhydrous Na_2SO_4.

4,5,6,7-Tetrahydro-4',4',6,6-tetramethylspiro[1,3-benzoxaselenole-2,1'-cyclohexane]-2'4,6'-trione (I)——A mixture of dimedone (3.8 g, 27 mmol) and SeO_2 (3.0 g, 27 mmol) in dioxane(50 ml) was stirred at 90°C for 20 h. The filtrate was concentrated and the residue was recrystallized from EtOH to give golden yellow prisms quantitatively. mp 167—169 °C (Lit.[3] 167 °C). TLC (CH_2Cl_2): Rf 0.3 (*cf.* dimedone: Rf 0.1). MS m/z (%): 358 (M^++2, 12), 356 (M^+, 58), 354 (M^+−2, 29), 352 (M^+−4, 11), 273 (M^+−83, 100), 83 ($(CH_3)_2C=CH-C\equiv O^+$, 59). IR (KBr): $\nu_{C=O}$ 1730, 1703, 1645, 1603. UV. λ_{max} (ε): 402 (141), 300 (3870), 250 (sh, 2300), 241 (2500). ^{1}H-NMR: 0.87 (3H, s, $C_{4'}$-Me), 1.15 (6H, s, C_6-Me), 1.21 (3H, s, $C_{4'}$-Me), 2.33 (2H, s, C_5-H), 2.63 (2H, s, C_7-H), 2.50, 3.02 (each 2H, d, J= 14.5, $C_{3'}$- and $C_{5'}$-H). ^{13}C-NMR: 25.3, 28.2, 29.9 (each q, Me), 30.4, 34.1 (each s, C_6 and $C_{4'}$), 38.7 (t, C_7), 50.0 (t, C_3 and $C_{5'}$), 50.9 (t, C_5), 92.9 (s, C_1 or C_2), 106.0 (s, C_{3a}), 169.9 (s, C_{7a}), 192.2 (s, C_4), 196.6 (s, $C_{2'}$ and $C_{6'}$). *Anal.* Calcd for $C_{16}H_{20}O_4$ Se: C, 54.09; H, 5.67. Found: C, 53.87; H, 5.63.

1,2,3,4,8,9,10,11-Octahydro-3,3,10,10-tetramethyldibenzo[*b*,*e*][1,4,7]dioxaselenocine-1,8-dione (II)——An excess of CH_2N_2 in Et_2O was added to a methanolic solution of I (0.48 g, 1.4 mmol). The crystalline solid obtained quantitatively after removal of the solvent was recrystallized from hexane to give pale yellow prisms. mp 108—109 °C. TLC (CH_2Cl_2): Rf 0.4. GC (250 °C): t_R 3.6 min. MS m/z (%): 372 (M^+−2, 16), 370 (M^+, 77), 368 (M^+−2, 37), 355 (M^+-CH_3, 49), 83 ($(CH_3)_2C=CH-C\equiv O^+$, 100). IR (Nujol): $\nu_{C=O}$ 1678, 1665 (C_1-carbonyl[4]), $\nu_{C=O}$ 1630, $\nu_{C=C}$ 1600. UV λ_{max} (ε): 300 (4200), 257 (13900), 240 (sh, 9500). ^{1}H-NMR: 1.10, 1.12 (each 6H, s, Me), 2.33, 2.35, 2.39, 2.92 (each 2H, s, CH_2), 5.78 (2H, s, C_6-H). ^{13}C-NMR: 27.8, 28.1 (each q, Me), 31.5, 32.0 (each s, C_3 and C_{10}), 43.6, 45.3 (each t, C_4 and C_{11}), 50.7, 50.9 (each t, C_2 and C_9), 67.4 (t, C_6), 114.1 (s, C_{7a}), 129.1 (s, C_{12a}), 161.6 (s, C_{4a}), 171.7 (s, C_{11a}), 193.8, 196.2 (each s, C_1 and C_8). *Anal.* Calcd for $C_{17}H_{22}O_4$ Se: C, 55.28; H, 6.00. Found: C, 55.24; H, 6.19.

4',5',6',7',8',9'-Hexahydrospriro[3,7-methanocyclooctane-1,2'-5',9'-methanocycloocta[1,2-*d*]-1,3-oxaselenole]-2,4',8-trione (IVa)——A mixture of bicyclo[3.3.1]nonane-2,4-dione(IIIa, 50 mg, 0.33 mmol) and SeO_2 (72 mg, 0.66 mmol) in dioxane (10 ml) was stirred overnight under reflux. The reaction mixture was filtered and the solid on the filter was washed with Et_2O. The combined filtrate was concentrated to give a yellow solid, which was purified through an SiO_2 column. The yellow oil obtained from the $CHCl_3$ eluate spontaneously solidified. IVa: yield,

TABLE I. Crystal Data for Compound II

Molecular formula	$C_{17}H_{22}O_4Se$
Molecular weight	369.35
Crystal system	Monoclinic
Space group	$P2_{1/n}$
Cell dimensions	
a	17.433 (3) Å
b	5.819 (4)
c	17.314 (6)
v	1720.0 (2) Å^3
z	4
D_X	1.426 g cm^{-3}
Final R value	3.3%

TABLE II. Bond Lengths (Å) for the Non-hydrogen Atoms

C(1)–O(13)	1.219 (3)	C(1)–C(2)	1.506 (4)	C(2)–C(3)	1.528 (4)
C(3)–C(4)	1.532 (3)	C(3)–C(14)	1.530 (4)	C(3)–C(15)	1.525 (4)
C(4)–C(4a)	1.499 (3)	C(4a)–O(5)	1.358 (3)	O(5)–C(6)	1.441 (3)
C(6)–Se(7)	1.949 (3)	Se(7)–C(7a)	1.913 (2)	C(7a)–C(8)	1.472 (3)
C(8)–O(16)	1.216 (3)	C(8)–C(9)	1.508 (4)	C(9)–C(10)	1.528 (4)
C(10)–C(17)	1.535 (4)	C(10)–C(18)	1.528 (5)	C(10)–C(11)	1.527 (3)
C(11)–C(11a)	1.498 (4)	C(11a)–O(12)	1.383 (3)	O(12)–C(12a)	1.401 (3)
C(12a)–C(1)	1.461 (3)	C(12a)–C(4a)	1.344 (3)	C(7a)–C(11a)	1.337 (3)

100 mg (80%). mp 232—234 °C (yellow prisms). IR (KBr): $\nu_{C=O}$ 1730, 1705, 1645, $\nu_{C=C}$ 1605. ^{1}H-NMR: 1.1—1.4 (1H, m), 1.4—2.0 (10H, m), 2.0—2.5 (5H, m), 2.60, 2.93, 3.03, 3.03 (each 1H, nearly s, bridgehead H). MS *m/z* (%): 380 (M^+, 100), 378 (M^+-2, 51), 352 (M^+-CO, 9), 298 ($M^+-C_4H_6CO$, 37), 269 ($M^+-C_6H_{11}CO$, 12), 256 (*m/z* 298 $-CH_2CO$, 53), 214 (*m/z* 256 $-CH_2CO$, 14), 55 ($C_2H_3CO^+$, 71). *Anal.* Calcd for $C_{18}H_{20}O_4Se$: C, 57.00; H, 5.31. Found: C, 56.78; H, 5.22.

***syn* and *anti*-1,2,3,4,5,6,10,11,12,13,14,15-Dodecahydro-2,6-methano-11,15-methanodicycloocta[*b*,*e*][1,4,7]dioxaselenocine-1,10-dione (Va)**——An excess of CH_2N_2 in Et_2O was added to a methanolic solution of IVa (90 mg). The crystalline solid obtained after removal of the solvent was recrystallized from hexane. *syn*- and *anti*-Va (4:1): yield, 93 mg. mp 128—132 °C. IR (Nujol): $\nu_{C=O}$ 1655, $\nu_{C=C}$ 1610, 1580. ^{1}H-NMR, *syn*: 1.4—2.0 (14H, m), 2.22, 2.50 (each 1H, d m, J=12.8, C_{18} or C_{19}-H), 2.57, 2.65, 2.69, 3.40 (each 1H, brs, bridgehead H), 5.49, 6.03 (each 1H, d, J=10.3, C_8-H), *anti*: 3.04(1H, brs, bridgehead H), 5.59, 5.72 (each 1H, d, J=10.1, C_8-H). MS *m/z* (%): 394 (M^+, 22), 392 (M^+-2, 10), 366 (M^+-CO, 8), 244 (IIIa+CSe, 100), 242 (51), 81 (SeH, 36), 69 ($C_3H_6CO^+$, 41).

TABLE III. Bond Agnles (°) for the Non-hydrogen Atoms

C(2)–C(1)–O(13)	122.17 (0.24)	C(12a)–C(1)–O(13)	121.08 (0.22)
C(2)–C(1)–C(12a)	116.71 (0.22)	C(1)–C(2)–C(3)	114.64 (0.22)
C(2)–C(3)–C(4)	107.73 (0.18)	C(3)–C(4)–C(4a)	114.13 (0.20)
C(4)–C(4a)–C(12a)	122.70 (0.20)	C(4)–C(4a)–O(5)	111.03 (0.19)
O(5)–C(4a)–C(12a)	126.26 (0.19)	C(4a)–O(5)–C(6)	119.26 (0.18)
O(5)–C(6)–Se(7)	113.23 (0.16)	C(6)–Se(7)–C(7a)	99.83 (0.11)
Se(7)–C(7a)–C(8)	113.16 (0.17)	Se(7)–C(7a)–C(11a)	127.35 (0.18)
C(8)–C(7a)–C(11a)	119.50 (0.22)	C(7a)–C(8)–O(16)	120.86 (0.24)
C(9)–C(8)–O(16)	122.21 (0.24)	C(7a)–C(8)–C(9)	116.83 (0.22)
C(8)–C(9)–C(10)	114.05 (0.24)	C(9)–C(10)–C(11)	108.35 (0.21)
C(10)–C(11)–C(11a)	113.92 (0.20)	C(7a)–C(11a)–C(11)	124.56 (0.21)
C(7a)–C(11a)–O(12)	122.42 (0.22)	C(11)–C(11a)–O(12)	112.87 (0.20)
C(11a)–O(12)–C(12a)	116.72 (0.18)	C(4a)–C(12a)–O(12)	122.71 (0.20)
C(4a)–C(12a)–C(1)	121.24 (0.20)	O(12)–C(12a)–C(1)	115.94 (0.20)

TABLE IV. Atomic Co-ordinates ($\times 10^5$) for Compound II with Estimated Standard Deviations in Parenthesis

Atom	*x*	*y*	*z*	*B*
C(1)	54544 (14)	−2255 (44)	27742 (13)	388 (5)
C(2)	46117 (15)	−9882 (47)	25815 (16)	443 (6)
C(3)	40148 (13)	9683 (43)	24782 (13)	372 (5)
C(4)	42027 (13)	24787 (49)	32172 (14)	385 (5)
C(4a)	50533 (11)	30772 (38)	34708 (11)	327 (5)
O(5)	51530 (9)	48964 (28)	39725 (9)	391 (3)
C(6)	58830 (14)	51459 (44)	45314 (15)	401 (6)
Se(7)	61741 (0)	24166 (5)	51762 (0)	426 (0)
C(7a)	69040 (11)	10608 (43)	46214 (13)	357 (5)
C(8)	74550 (13)	−5300 (47)	51105 (14)	404 (6)
C(9)	80592 (15)	−16589 (53)	47238 (16)	477 (6)
C(10)	83379 (13)	−1555 (47)	41119 (13)	408 (5)
C(11)	76210 (15)	6352 (60)	35098 (14)	456 (6)
C(11a)	69511 (13)	14026 (44)	38688 (13)	356 (5)
O(12)	64003 (9)	26687 (29)	33535 (9)	372 (3)
C(12a)	56239 (11)	18935 (40)	32297 (11)	335 (5)
O(13)	59771 (11)	−13402 (41)	25814 (13)	597 (5)
C(14)	40576 (18)	23748 (65)	17454 (16)	528 (7)
C(15)	31936 (15)	−473 (63)	24025 (20)	547 (8)
O(16)	73943 (11)	−9842 (43)	57810 (10)	592 (6)
C(17)	87917 (18)	19248 (63)	45164 (20)	556 (8)
C(18)	88780 (19)	−15136 (75)	36867 (19)	599 (9)

The 17,17,18,18-Tetramethoxy Analogue of Va (Vb)——A mixture of 7,7-dimethoxybicyclo[3.3.1]nonane-2,4-dione (IIIb, 212 mg, 1 mmol) and SeO_2 (222 mg, 2 mmol) in dioxane was treated under conditions similar to those used in the preparation of IVa. The product was not crystallized but was further treated with an excess of CH_2N_2 in Et_2O. Crude Vb obtained after removal of the solvent was purified by recrystallization from hexane. mp 200—202 °C. The yield was quantitative. ^{1}H-NMR: 1.2—2.1 (12H, m), 2.8—2.95 (3H, m, bridgehead H), 3.17, 3.20, 3.22, 3.23 (each 3H, s, OMe), 3.77 (1H, dd, J=3.8, 2.7, bridgehead H), 5.53, 6.04 (each 1H, d, J=10.3, C_8-H). MS m/z (%): 514 (M^+, 25), 483 (M^+-OMe, 9), 304 (IIIb+CSe, 100), 101 (methoxycyclohexenyl, 79). *Anal.* Calcd for $C_{23}H_{30}O_8$ Se: C, 53.81; H, 5.89. Found: C, 54.01; H, 5.89.

The 18,19-Dioxo Analogue of Va (Vc)——A 5% HCl solution (1 ml) was added to a mixture of Vb (100 mg) and Me_2CO (5 ml). The diluted solution was extracted with Et_2O. The residue obtained after removal of the organic solvent was recrystallized from Et_2O-hexane. mp 228—229 °C, yield: 80 mg (97%). ^{1}H-NMR: 1.5—2.4 (12H, m), 3.31, 3.31, 3.41, 4.15 (each 1H, br s, bridgehead H), 5.67, 6.23 (each 1H, d, J=10.6, C_8-H). MS m/z (%): 422 (M^+, 59), 258 (IVc+CSe, 75), 55 ($CH_2=CH-C\equiv O^+$, 100). *Anal.* Calcd for $C_{19}H_{18}O_6$ Se: C, 54.17; H, 4.31. Found: C, 54.44; H, 4.28.

The 9,10′-Dioxo Analogue of IVa (IVc)——A mixture of IIIc (166 mg, 1.0 mmol) and SeO_2 (287 mg, 2.6 mmol) in dioxane was treated in the usual manner. Crude IVc was recrystallized from EtOH (difficult to dissolve!). mp 261—263 °C. Yield: 61 mg (15%). ^{1}H-NMR: 1.4—2.15 (6H, m), 2.15—2.4 (3H, m), 2.51 (1H, d m, J=15.7), 2.6—2.8 (2H, m), 3.32 (1H, d like, J=4.7, bridgehead H), 3.59 (1H, dd, J=6.9, 3.1, bridgehead H), 3.65—3.71 (1H, m, bridgehead H), 3.75 (1H, dd, J=6.5, 3.3, bridgehead H). MS m/z (%): 408 (M^+, 26), 406 (14), 352 (M^+-2CO, 18), 324 (M^+-3CO, 27), 91 (50), 80 (71), 79 ($C_4H_5CO^+$, 100), 55 ($CH_2=CH-C\equiv O^+$, 94). *Anal.* Calcd for $C_{18}H_{16}O_6$ Se: C, 53.08; H, 3.96. Found: C, 52.85; H, 4.11.

X-Ray Analysis of Compound II——Intensity measurements were made with a Rigaku AFC 5R automatic 4-circle diffractometer using monochromated Cu-K_α radiation. Pale yellow single crystals of compound II for the X-ray study were obtained from hexane. The crystal data, intramolecular bond lengths (Å) and bond angles (°) for the nonhydrogen atoms, and atomic co-ordinates are given in Tables I, II, III, and IV, respectively.

Acknowledgement The authors thank Dr. C. Katayama of the analytical center of Rigaku Denki Co., Ltd., for the X-ray analysis, and Mr. M. Morikoshi and Mr. M. Ogawa for the measurements of ^{13}C-NMR spectra and elemental analyses, respectively.

References

1) K. Matoba and T. Yamazaki, *Heterocycles*, **20**, 1959 (1983) and references cited therein.
2) T. Yamazaki, K. Matoba, T. Itooka, M. Chintani, T. Momose, and O. Muraoka, *Chem. Pharm. Bull.*, **35**, 3453 (1987).
3) T. Laitalainen, T. Simonen, R. Kivekas, and M. Klinga, *J. Chem. Soc., Perkin Trans. 1*, **1983**, 333.
4) K. Matoba, K. Hamajima, and T. Yamazaki, *Yakugaku Zasshi*, **94**, 1459 (1974).

[Chem. Pharm. Bull. 35(12)4972—4976(1987)]

Purines. VI.[1] Reactions of 2-Chloro- and 2-(Methylsulfonyl)-9-phenyl-9*H*-purines with Nucleophiles

KEN-ICHI TANJI,* HARUMI KUBOTA, YUMI YAMAMOTO, and TAKEO HIGASHINO

School of Pharmaceutical Sciences, University of Shizuoka, 2-2-1 Oshika, Shizuoka 422, Japan

(Received May 18, 1987)

The reactions of 2-chloro-9-phenyl-9*H*-purine (**1**) with sodium methoxide, ethoxide, and phenoxide as *O*-nucleophiles, with butylamine and piperidine as *N*-nucleophiles, and with sodium methylsulfide as an *S*-nucleophile, afforded 2-methoxy- (**3a**), 2-ethoxy- (**3b**), 2-phenoxy- (**3c**), 2-butylamino- (**4a**), 2-piperidino- (**4b**), and 2-methylthio-9-phenyl-9*H*-purine (**5**), respectively. Compound **1** also reacted with ethyl cyanoacetate and phenylacetonitrile as *C*-nucleophiles in the presence of sodium hydroxide in dimethyl sulfoxide to give ethyl α-cyano-9-phenyl-9*H*-purine-2-acetate (**6a**) and α,9-diphenyl-9*H*-purine-2-acetonitrile (**6b**). However, **1** did not react with other active methylene compounds, ketones or potassium cyanide.

On the other hand, 2-(methylsulfonyl)-9-phenyl-9*H*-purine (**2**), prepared easily from **1**, smoothly reacted not only with active methylene compounds but also with ketones and potassium cyanide. When active methylene compounds, such as ethyl cyanoacetate and phenylacetonitrile, were used, **2** gave **6a** and **6b** in good yields. In the cases of ketones and potassium cyanide, the substitution reactions of **2** proceeded to give the corresponding 2-substituted 9*H*-purines (**7** and **8a—d**), as expected.

Keywords——2-chloro-9*H*-purine; 2-(methylsulfonyl)-9*H*-purine; nucleophilic substitution; nucleophile; synthesis

Recently we have reported that a chlorine atom[2] and a methylsulfonyl group[3] at the 6-position on the 9*H*-purine ring can be substituted with nucleophiles, resulting in the introducing of a carbon chain into the 6-position. On the other hand, little work has been reported on introducing a carbon chain into the 2-position of the 9*H*-purine ring. We examined the nucleophilic substitution of a chlorine atom and a methylsulfonyl group at the 2-position and succeeded for the first time in the introduction of functionalized carbons into the 2-position of the 9*H*-purine ring, giving the expected 2-substituted 9-phenyl-9*H*-purines (**5**, **6**, and **7**). In the present paper, we describe these results in detail.

Compound **1** was prepared by the substitution reaction of 5-amino-2,4-dichloropyrimidine with aniline, followed by cyclization of the resulting 5-amino-4-anilino-2-chloropyrimidine with ethyl orthoformate in acetic anhydride.

When a solution of **1** and sodium ethoxide in ethanol was refluxed for 1 h, 2-ethoxy-9-phenyl-9*H*-purine (**3b**) was obtained in good yield. Similar reactions of **1** with sodium methoxide and phenoxide under the same conditions gave 2-methoxy- (**3a**) and 2-phenoxy-9-phenyl-9*H*-purine (**3c**), respectively. When **1** was treated with butylamine and piperidine as *N*-nucleophiles, 2-butylamino- (**4a**) and 2-piperidino-9-phenyl-9*H*-purine (**4b**) were obtained, respectively. The reaction of **1** with sodium methylsulfide as an *S*-nucleophile in dimethylformamide (DMF) at 100 °C gave 2-methylthio-9-phenyl-9*H*-purine (**5**) in 90% yield.

Next, introduction of functionalized carbon substituents into the 2-position was investigated. Compound **1** reacted with ethyl cyanoacetate in the presence of sodium hydroxide in dimethylsulfoxide (DMSO) under the same conditions as those reported[2] for the

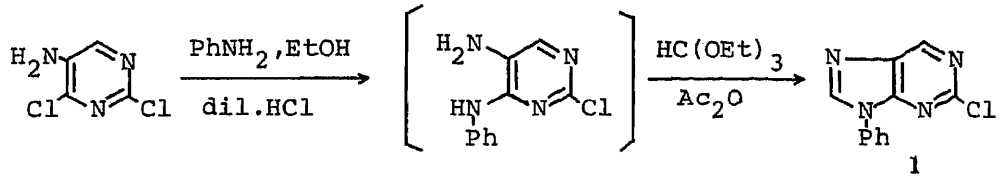

Chart 1

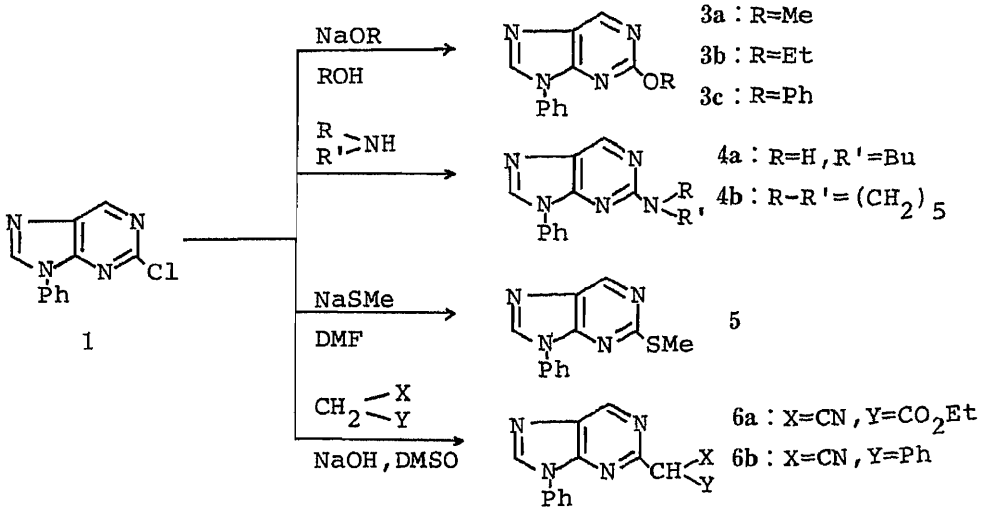

Chart 2

reaction of 6-chloro-9-phenyl-9*H*-purine, that is, heating at 100 °C for 1 h, to give ethyl α-cyano-9-phenyl-9*H*-purine-2-acetate (**6a**) in 29% yield. Similarly, **1** and phenylacetonitrile gave α,9-diphenyl-9*H*-purine-2-acetonitrile (**6b**) in 23% yield. However, when other active methylene compounds, ketones, and potassium cyanide were used, the desired products were not obtained. It appeared from the above results that the chlorine atom at the 2-position of the 9*H*-purine ring was less reactive to carbanions than that at the 6-position.

We have reported the nucleophilic substitution reactions of 2-(methylsulfonyl)-quinoxaline,[4] 1-(methylsulfonyl)phthalazine,[5] 4-(methylsulfonyl)cinnoline,[6] and 6-(methyl-sulfonyl)-9-phenyl-9*H*-purine[3] with carbanions and concluded that the methylsulfonyl group was replaced by carbanions more easily than the chlorine atom. In connection with such reactivity of the methylsulfonyl group, we examined the reaction of 2-(methylsufonyl)-9-phenyl-9*H*-purine (**2**) with carbanions.

2-Methylthio-9-phenyl-9*H*-purine (**5**) was oxidized with potassium permanganate in acetic acid to give **2** in 76% yield. Compound **2** smoothly reacted not only with active methylene compounds but also with potassium cyanide and ketones. Treatment of **2** with potassium cyanide in DMSO at 100 °C for 1 h afforded 9-phenyl-9*H*-purine-2-carbonitrile (**7**) in 74% yield, though the same reaction did not take place in the case of **1**.

Nucleophilic substitution reactions of **2** with active methylene compounds and ketones in the presence of potassium hydroxide in DMSO did not take place, but the reaction in tetrahydrofuran (THF) in the presence of sodium hydride instead of potassium hydroxide resulted in the formation of the desired products. Thus, when a solution of **2** and ethyl cyanoacetate in THF in the presence of sodium hydride was refluxed for 3 h, **6a** was obtained in 58% yield. Compound **2** and phenylacetonitrile also gave **7b** in 58% yield. Although the yields were low, the reaction of **2** with acetone and 2-butanone resulted in the formation of 1-(9-phenyl-9*H*-purin-2-yl)-2-propanone (**8b**) and 3-(9-phenyl-9*H*-purin-2-yl)-2-butanone

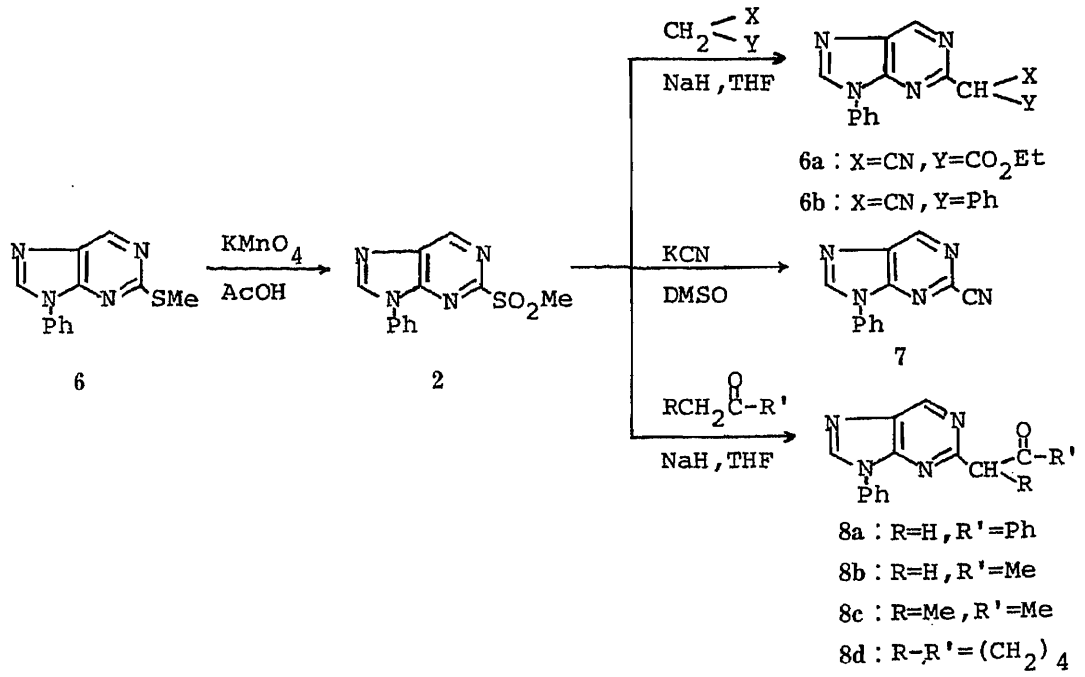

Chart 3

(**8c**). On the other hand, **2** smoothly reacted with acetophenone and cyclohexanone to give 2-(9-phenyl-9*H*-purin-2-yl)acetophenone (**8a**) and 2-(9-phenyl-9*H*-purin-2-yl)cyclohexanone (**8d**) in 62% and 63% yields, respectively.

We concluded that the chlorine atom and methylsulfonyl group at the 2-position were less reactive to carbanions than those at the 6-position in the 9*H*-purine ring, and the methylsulfonyl group was more reactive to carbanions than the chlorine atom at the 2-position in the 9*H*-purine ring. The substitution reaction of the methylsulfonyl group in **2** with nucleophiles is a useful method for the introduction of functionalized carbons into the 2-position of the 9*H*-purine ring.

Experimental

All melting points are uncorrected. Infrared (IR) spectra were measured with a Jasco IRA-1 grating IR spectrophotometer. Proton nuclear magnetic resonance (^{1}H-NMR) spectra were taken at 60 MHz and 23 °C with a Hitachi R-24 high-resolution ^{1}H-NMR spectrometer. Chemical shifts are expressed in parts per million (ppm) downfield from tetramethylsilane as an internal standard. The following abbreviations are used: s=singlet, d=doublet, t=triplet, q=quartet, m=multiplet, br=broad.

2-Chloro-9-phenyl-9*H*-purine (1)——A mixture of 5-amino-2,4-dichloropyrimidine (18 g, 0.11 mol), aniline (10.2 g, 0.11 mol), concentrated HCl (4.5 ml), EtOH (45 ml), and H_2O (290 ml) was refluxed for 1 h. The precipitate, 5-amino-4-anilino-2-chloropyrimidine, was filtered off. Yield, 14.5 g. A mixture of the crude 5-amino-4-anilino-2-chloropyrimidine (14.5 g, 0.066 mol), ethyl orthoformate (90 ml), and acetic anhydride (90 ml) was refluxed for 3 h. The EtOH was removed under reduced pressure. The residue was diluted with H_2O and the mixture was made alkaline with Na_2CO_3, and extracted with $CHCl_3$. The crude product was purified by SiO_2 column chromatography with $CHCl_3$ and recrystallized from benzene to give **1** as colorless needles, mp 169—170 °C. Yield, 10 g (64%). *Anal.* Calcd for $C_{11}H_7ClN_4$: C, 57.27; H, 3.04; N, 24.30. Found: C, 57.34; H, 3.10; N, 24.48. ^{1}H-NMR ($CDCl_3$) δ: 7.28—7.73 (5H, m, Ph), 8.23 (1H, s, C^8-H), 8.89 (1H, s, C^6-H).

2-Methoxy-9-phenyl-9*H*-purine (3a)——1) A mixture of **1** (0.5 g, 2.2 mmol), NaOMe (0.6 g, 11.1 mmol), and MeOH (20 ml) was refluxed for 1 h. The solvent was removed under reduced pressure. The residue was diluted with H_2O and extracted with $CHCl_3$. The crude product was purified by SiO_2 column chromatography with benzene and recrystallized from benzene to give **3a** as colorless needles, mp 110—112 °C. Yield, 0.42 g (86%). *Anal.* Calcd for $C_{12}H_{10}N_4O$: C, 63.70; H, 4.46; N, 24.77. Found: C, 63.49; H, 4.25; N, 24.64. ^{1}H-NMR ($CDCl_3$) δ: 3.95 (3H, s, OCH_3), 7.27—7.74 (5H, m, Ph), 8.47 (1H, s, C^8-H), 9.17 (1H, s, C^6-H).

2) A mixture of **2** (0.3 g, 1.1 mmol), NaOMe (0.3 g, 5.5 mmol), and MeOH (5 ml) was refluxed for 1 h. The solvent was removed under reduced pressure. The crude product was purified by SiO_2 column chromatography with benzene and recrystallized from benzene to give **3a**. Yield, 0.2 g (84%).

2-Ethoxy-9-phenyl-9*H*-purine (3b)——A mixture of **1** (0.2 g, 0.87 mmol), NaOEt (0.29 g, 4.3 mmol), and EtOH (15 ml) was refluxed for 1 h. The same work-up of the reaction mixture as described for **3a** gave **3b**, colorless needles from petroleum benzin–benzene, mp 117—121 °C. Yield, 0.17 g (82%). *Anal.* Calcd for $C_{13}H_{12}N_4O$: C, 64.98; H, 5.03; N, 23.32. Found: C, 65.50; H, 5.06; N, 22.93. ^{1}H-NMR ($CDCl_3$) δ: 1.48 (3H, t, J=7 Hz, $OCH_2C\underline{H}_3$), 4.48 (2H, q, J=7 Hz, $OC\underline{H}_2CH_3$), 7.27—7.81 (5H, m, Ph), 8.08 (1H, s, C^8-H), 8.85 (1H, s, C^6-H).

2-Phenoxy-9-phenyl-9*H*-purine (3c)——A mixture of **1** (0.2 g, 0.87 mmol), NaOPh (0.49 g, 4.3 mmol), and PhOH (5 ml) was heated at 100 °C for 3 h. The same work-up of the reaction mixture as described for **3a** gave **3c**, colorless needles from petroleum benzin–benzene, mp 130—131 °C. Yield, 0.23 g (92%). *Anal.* Calcd for $C_{17}H_{12}N_4O$: C, 70.82; H, 4.20; N, 19.44. Found: C, 70.73; H, 4.14; N, 19.38. ^{1}H-NMR ($CDCl_3$) δ: 7.15—7.70 (10H, m, N–Ph, O–Ph), 8.11 (1H, s, C^8-H), 8.78 (1H, s, C^6-H).

2-Butylamino-9-phenyl-9*H*-purine (4a)——A mixture of **1** (0.2 g, 0.87 mmol) and $BuNH_2$ (3 ml) was refluxed for 3 h. The excess $BuNH_2$ was removed under reduced pressure. The residue was diluted with H_2O and extracted with $CHCl_3$. The crude product was purified by SiO_2 column chromatography with $CHCl_3$ and recrystallized from petroleum benzin–benzene to give **4a** as yellow needles, mp 113—115 °C. Yield, 0.14 g (62%). *Anal.* Calcd for $C_{15}H_{17}N_5$: C, 67.39; H, 6.41; N, 26.20. Found: C, 67.36; H, 6.33; N, 26.20. IR ν_{max}^{KBr} cm^{-1}: 3280 (NH). ^{1}H-NMR ($CDCl_3$) δ: 0.74—1.16 (3H, m, $NCH_2CH_2CH_2C\underline{H}_3$), 1.32—1.84 (4H, m, $NCH_2C\underline{H}_2C\underline{H}_2CH_3$), 3.27—3.64 (2H, m, $NC\underline{H}_2CH_2CH_2CH_3$), 7.24—7.79 (5H, m, Ph), 7.89 (1H, s, C^8-H), 8.63 (1H, s, C^6-H).

9-Phenyl-2-piperidino-9*H*-purine (4b)——1) A mixture of **1** (0.2 g, 0.87 mmol) and piperidine (3 ml) was heated at 100 °C for 3 h. The same work-up of the reaction mixture as described for **4a** gave **4b**, yellow needles from petroleum benzin, mp 78—79 °C. Yield, 0.14 g (59%). *Anal.* Calcd for $C_{16}H_{17}N_5$: C, 68.79; H, 6.13; N, 25.07. Found: C, 68.48; H, 6.14; N, 24.97. ^{1}H-NMR ($CDCl_3$) δ: 1.45—1.85 (6H, m, $N<\underline{CH_2}_{\underline{CH_2}}>(\underline{CH_2})_3$), 3.62—4.05 (4H, m, $N<\underline{CH_2}_{\underline{CH_2}}>(CH_2)_3$), 7.33—7.78 (5H, m, Ph), 7.89 (1H, s, C^8-H), 8.70 (1H, s, C^6-H).

2-Methylthio-9-phenyl-9*H*-purine (5)——A mixture of **1** (10 g, 0.043 mol), 15% aqueous NaSMe (40.5 g, 0.086 mol), and DMF (50 ml) was heated at 100 °C for 3 h. The mixture was diluted with H_2O and extracted with benzene. The crude product was purified by SiO_2 column chromatography with benzene and recrystallized from benzene to give **5** as colorless needles, mp 136—138 °C. Yield, 9.5 g (90%). *Anal.* Calcd for $C_{12}H_{10}N_4S$: C, 59.48; H, 4.16; N, 23.13. Found: C, 59.70; H, 4.16; N, 23.45. ^{1}H-NMR ($CDCl_3$) δ: 2.55 (3H, s, SCH_3), 7.26—7.77 (5H, m, Ph), 8.08 (1H, s, C^8-H), 8.80 (1H, s, C^6-H).

2-(Methylsulfonyl)-9-phenyl-9*H*-purine (2)——A solution of $KMnO_4$ (4.7 g, 0.03 mol) in H_2O (50 ml) was added to a stirred solution of **5** (3.6 g, 0.015 mol) in AcOH (30 ml). The mixture was stirred for 1 h at room temperature, then sodium hydrogen sulfite was added, and the whole was extracted with $CHCl_3$. The crude product was purified by SiO_2 column chromatography with $CHCl_3$ and recrystallized from benzene to give **2** as colorless needles, mp 197—199 °C. Yield, 3.1 g (76%). *Anal.* Calcd for $C_{12}H_{10}N_4O_2S$: C, 52.55; H, 3.67; N, 20.43. Found: C, 52.15; H, 3.60; N, 20.34. IR ν_{max}^{KBr} cm^{-1}: 1142, 1306 (SO_2). ^{1}H-NMR ($CDCl_3$) δ: 3.31 (3H, s, SO_2CH_3), 7.27—7.74 (5H, m, Ph), 8.47 (1H, s, C^8-H), 9.17 (1H, s, C^6-H).

Ethyl α-Cyano-9-phenyl-9*H*-purine-2-acetate (6a)——1) A mixture of **1** (0.2 g, 0.87 mmol), NaOH (0.07 g, 1.74 mmol), ethyl cyanoacetate (0.2 g, 1.74 mmol), and DMSO (3 ml) was heated at 100 °C for 1 h. The mixture was diluted with H_2O and extracted with $CHCl_3$. The crude product was purified by SiO_2 column chromatography with $CHCl_3$ and recrystallized from benzene to give **6a** as colorless needles, mp 240 °C (dec.). Yield, 78 mg (29%). *Anal.* Calcd for $C_{16}H_{13}N_5O_2$: C, 62.53; H, 4.26; N, 22.79. Found: C, 62.75; H, 4.17; N, 22.79. IR ν_{max}^{KBr} cm^{-1}: 1650 (C=O), 2200 (CN). ^{1}H-NMR (CF_3COOH) δ: 1.40 (3H, t, J=6 Hz, $OCH_2C\underline{H}_3$), 4.32 (2H, q, J=6 Hz, $OC\underline{H}_2CH_3$), 7.50 (5H, m, Ph), 9.08 (1H, s, C^8-H), 9.14 (1H, s, C^6-H).

2) A mixture of **2** (0.3 g, 1.1 mmol), 50% NaH (in oil) (0.06 g, 1.2 mmol), ethyl cyanoacetate (0.14 g, 1.2 mmol), and THF (5 ml) was refluxed for 3 h. The solvent was removed under reduced pressure. The residue was diluted with H_2O and extracted with $CHCl_3$. The crude product was purified by SiO_2 column chromatography with $CHCl_3$ and recrystallized from benzene to give **6a**. Yield, 0.19 g (58%).

α,9-Diphenyl-9*H*-purine-2-acetonitrile (6b)——1) A mixture of **1** (0.5 g, 2.2 mmol), NaOH (0.25 g, 4.4 mmol), phenylacetonitrile (0.52 g, 4.4 mmol), and DMSO (8 ml) was heated at 100 °C for 1 h. The reaction mixture was worked up essentially in the same way as described for **6a** under item 1). The eluate with benzene–$CHCl_3$ (1 : 1) was recrystallized from petroleum benzin–benzene to give **6b** as colorless needles, mp 128—131 °C. Yield, 0.15 g (23%). *Anal.* Calcd for $C_{19}H_{13}N_5$: C, 73.29; H, 4.21; N, 22.50. Found: C, 73.40; H, 4.18; N, 22.41. IR ν_{max}^{KBr} cm^{-1}: 2240 (CN). ^{1}H-NMR ($CDCl_3$) δ: 5.44 (1H, s, $C\underline{H}<\underline{Ph}_{CN}$), 7.01—7.82 (10H, m, N–Ph, $CH<\underline{Ph}_{CN}$), 8.25 (1H, s, C^8-H), 9.02 (1H, s, C^6-H).

2) A mixture of **2** (0.2 g, 0.73 mmol), phenylacetonitrile (0.1 g, 0.88 mmol), 50% NaH (in oil) (0.04 g,

0.88 mmol), and THF (5 ml) was refluxed for 3 h. The same work-up of the reaction mixture as described for **6a** under item 1) gave **6b** (0.13 g) in 58% yield.

9-Phenyl-9*H*-purine-2-carbonitrile (7)——A mixture of **2** (0.2 g, 0.7 mmol), KCN (0.2 g, 3 mmol), and DMSO (3 ml) was heated at 80 °C for 1 h. The mixture was diluted with H_2O and extracted with $CHCl_3$. The product was recrystallized from benzene to give **7** as colorless needles, mp 164—165 °C. Yield, 0.12 g (74%). *Anal.* Calcd for $C_{12}H_7N_5$: C, 65.15; H, 3.19; N, 31.66. Found: C, 65.16; H, 3.11; N, 31.54. IR ν_{max}^{KBr} cm^{-1}: 2240 (CN). ^{1}H-NMR ($CDCl_3$) δ: 7.37—7.80 (5H, m, Ph), 8.48 (1H, s, C^8-H), 9.11 (1H, s, C^6-H).

2-(9-Phenyl-9*H*-purin-2-yl)acetophenone (8a)——A mixture of **2** (0.2 g, 0.73 mmol), 50% NaH (in oil) (0.04 g, 0.88 mmol), acetophenone (0.11 g, 0.88 mmol), and THF (5 ml) was refluxed for 1 h. The solvent was removed under reduced pressure. The residue was diluted with H_2O and extracted with $CHCl_3$. The crude product was purified by SiO_2 column chromatography with $CHCl_3$ and recrystallized from benzene to give **8a** as yellow needles, mp 164—165 °C. Yield, 0.14 g (62%). *Anal.* Calcd for $C_{19}H_{14}N_4O$: C, 72.60; H, 4.49; N, 17.83. Found: C, 72.68; H, 4.44; N, 17.67. IR ν_{max}^{KBr} cm^{-1}: 1635 (C=O). ^{1}H-NMR ($CDCl_3$) δ: 4.72 (1.14H, s, $CH_2C{=}O$), 6.31 (0.43H, s, $C\underline{H}{=}C{-}OH$), 7.25—8.05 (10H, m, N-Ph, PhC=O), 8.14 (0.43H, s, C^8-H), 8.21 (0.57H, s, C^8-H), 8.90 (0.43H, s, C^6-H), 9.04 (0.57H, s, C^6-H), 14.08—14.42 (0.43H, br, $CH{=}C{-}O\underline{H}$).

1-(9-Phenyl-9*H*-purin-2-yl)-2-propanone (8b)——A mixture of **2** (0.2 g, 0.73 mmol), 50% NaH (in oil) (0.04 g, 0.88 mmol), acetone (0.05 g, 0.88 mmol), and THF (15 ml) was refluxed for 1 h. The same work-up of the reaction mixture as described for **8a** gave **8b**, pale yellow needles from benzene, mp 100—103 °C. Yield, 24 mg (13%). *Anal.* Calcd for $C_{14}H_{12}N_4O$: C, 66.65; H, 4.79; N, 22.21. Found: C, 66.72; H, 4.82; N, 22.23. IR ν_{max}^{KBr} cm^{-1}: 1709 (C=O). ^{1}H-NMR ($CDCl_3$) δ: 2.24 (3H, s, $CH_3C{=}O$), 4.15 (2H, s, $CH_2C{=}O$), 7.26—7.75 (5H, m, Ph), 8.20 (1H, s, C^8-H), 9.00 (1H, s, C^6-H).

3-(9-Phenyl-9*H*-purin-2-yl)-2-butanone (8c)——A mixture of **2** (0.5 g, 1.8 mmol), 50% NaH (in oil) (0.1 g, 2 mmol), 2-butanone (0.15 g, 2 mmol), and THF (10 ml) was refluxed for 1 h. The same work-up of the reaction mixture as described for **8a** gave **8c**, pale yellow needles from benzene, mp 101—104 °C. Yield, 35 mg (7%). *Anal.* Calcd for $C_{15}H_{14}N_4O$: C, 67.65; H, 5.30; N, 21.04. Found: C, 67.22; H, 5.30; N, 20.73. IR ν_{max}^{KBr} cm^{-1}: 1710 (C=O). ^{1}H-NMR ($CDCl_3$) δ: 1.60 (3H, d, J=7 Hz, $C\underline{H}_3CH$), 2.15 (3H, s, $C\underline{H}_3C{=}O$), 4.20 (1H, q, J=7 Hz, $CH_3C\underline{H}$), 7.25—7.80 (5H, m, Ph), 8.25 (1H, s, C^8-H), 9.03 (1H, s, C^6-H).

2-(9-Phenyl-9*H*-purin-2-yl)cyclohexanone (8d)——A mixture of **2** (0.2 g, 0.73 mmol), 50% NaH (in oil) (0.04 g, 0.88 mmol), cyclohexanone (0.86 g, 0.73 mmol), and THF (5 ml) was refluxed for 1 h. The same work-up of the reaction mixture as described for **8a** gave **8d**, colorless needles from benzene, mp 138—139 °C. Yield, 0.14 g (63%). *Anal.* Calcd for $C_{17}H_{16}N_4O$: C, 69.85; H, 5.52; N, 19.16. Found: C, 69.50; H, 5.49; N, 19.05. IR ν_{max}^{KBr} cm^{-1}: 1640 (C=O). ^{1}H-NMR ($CDCl_3$) δ: 1.36—2.08 (4H, m, $C\underline{H}_2{<}^{CH_2{-}C}_{CH_2CH_2}{>}C{-}OH$), 2.08—2.80 (4H, m, $CH_2{<}^{C\underline{H}_2{-}C}_{CH_2C\underline{H}_2}{>}C{-}OH$), 7.28—7.85 (5H, m, Ph), 8.19 (1H, s, C^8-H), 8.89 (1H, s, C^6-H), 14.03—14.35 (1H, br, $CH_2{<}^{CH_2{-}C}_{CH_2CH_2}{>}C{-}O\underline{H}$).

References

1) Part V: T. Higashino, S. Yoshida, and E. Hayashi, *Chem. Pharm. Bull.*, **30**, 4521 (1982).
2) E. Hayashi, N. Shimada, and K. Watanabe, *Yakugaku Zasshi*, **99**, 205 (1979).
3) E. Hayashi and N. Shimada, *Yakugaku Zasshi*, **99**, 201 (1979).
4) *a*) E. Hayashi and T. Miyagishima, *Yakugaku Zasshi*, **87**, 826 (1967); *b*) *Idem*, *ibid.*, **88**, 1103 (1967); *c*) *Idem*, *ibid.*, **88**, 303 (1968).
5) *a*) E. Hayashi, T. Higashino, E. Ōishi, and M. Sano, *Yakugaku Zasshi*, **87**, 687 (1967); *b*) E. Hayashi and E. Ōishi, *ibid.*, **87**, 806 (1967); *c*) *Idem*, *ibid.*, **88**, 83 (1968).
6) *a*) E. Hayashi and T. Watanabe, *Yakugaku Zasshi*, **88**, 94 (1968); *b*) *Idem*, *ibid.*, **88**, 593 (1968); *c*) *Idem*, *ibid.*, **88**, 750 (1968).

[Chem. Pharm. Bull. 35(12)4977—4980(1987)]

An Efficient Method for Preparing *gem*-Dimethylcyclopropanes from *gem*-Dibromocyclopropanes

TAKASHI HARAYAMA,* HIDETO FUKUSHI, KAZUHIRO OGAWA, TETSUYA ARATANI, SATOSHI SONEHARA, and FUMIO YONEDA*

Faculty of Pharmaceutical Sciences, Kyoto University, Sakyo-ku, Kyoto 606, Japan

(Received May 27, 1987)

Reaction of *gem*-dibromocyclopropanes (**1**) with a higher-order organocuprate prepared from cuprous thiocyanate and methyllithium, followed by the addition of methyl iodide *in situ*, readily afforded dimethylcyclopropanes (**2**) in good to excellent yields regardless of the functional group in **1**.

Keywords——higher-order organocuprate; dibromocyclopropane; dimethylcyclopropane; substitution reaction; dibromocarbene

In connection with studies of the total synthesis of a class of natural products that contain the *gem*-dimethylcyclopropane ring system,[1] several methods for preparing *gem*-dimethylcyclopropanes have been developed, *e.g.* substitution of *gem*-dihalocyclopropanes with dimethylcopper lithium (Gilman's reagent),[2] addition of dimethylcarbene to olefins,[3] reaction of diphenylsulfonium isopropylide with conjugated carbonyl compounds,[4] and thermolysis of a pyrazolidine prepared by cycloaddition of dimethyldiazomethane to an olefin.[5] Although dimethylcopper lithium has usually been used for this purpose, the reaction is occasionally sluggish, requiring a long reaction time.[6-8] Recently, Lipshurtz *et al.* have reported that the higher-order organocuprates react readily and efficiently with inactive alkyl iodides and bromides, affording substitution products.[9-11] An application of the Lipshutz method to *gem*-dibromocyclopropane was attempted in order to develop an efficient method for preparing *gem*-dimethylcyclopropane, and we have already reported that reaction of the higher-order organocuprates with 8,8-dibromobicyclo[5.1.0]octane, followed by the addition of methyl iodide *in situ*, afforded the desired dimethylated compound in good yield.[12] Subsequently, we attempted an application of the present method to other *gem*-dibromocyclopropanes in order to examine its generality and usefulness. We describe here the results of this substitution reaction.[13]

gem-Dibromocyclopropanes (**1**) except **1c** were synthesized directly by reactions of the respective olefins with dibromocarbene prepared from bromoform and 40% sodium hydroxide solution in methylene chloride (method A) or from bromoform and potassium *tert*-butoxide in pentane (method B). The dibromo-silyl ether (**1c**) was synthesized by reaction of 1-cyclohexene-1-methanol with dibromocarbene (method A), followed by silylation with *tert*-butyldimethylsilyl (TBDMS) chloride. The yields are indicated in Table I. The structures of **1** were elucidated on the basis of their spectral data, and the stereostructure of **1b** will be discussed later. In a previous paper,[12] we reported that $Me_2Cu(CN)Li_2$ was more reactive than $Me_2Cu(SCN)Li_2$ in the reaction with dibromobicyclo[5.1.0]octane, yielding over-alkylated by-products. Therefore, the reactions of **1** with $Me_2Cu(SCN)Li_2$–MeI were examined. The results are listed in Table I, showing that reactions proceed smoothly to afford

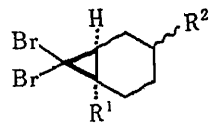

1a : R^1=H, R^2=α-COOMe
1b : R^1=H; R^2=β-COOMe
1c : R^1=$CH_2OTBDMS$, R^2=H
1d : R^1=OMe, R^2=H
1e : R^1=OMe, R^2=*tert*-Bu
1g : R^1=H, R^2= 
1h : R^1=H, R^2=CH_2OH
1i : R^1=H, R^2=CH_2OAc

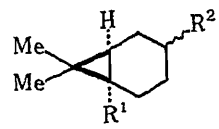

2a : R^1=H, R^2=α-COOMe
2b : R^1=H, R^2=β-COOMe
2c : R^1=$CH_2OTBDMS$, R^2=H
2d : R^1=OMe, R^2=H
2e : R^1=OMe, R^2=*tert*-Bu
2g : R^1=H, R^2= 
2h : R^1=H, R^2=CH_2OH
2i : R^1=H, R^2=CH_2OAc

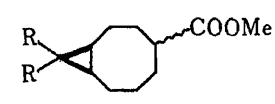

1f : R=Br
2f : R=Me

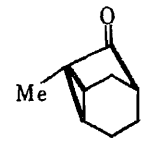

3

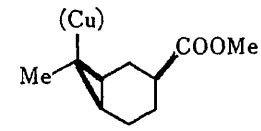

A

Chart 1

TABLE I. Yields of *gem*-Dibromocyclopropanes (**1**) and *gem*-Dimethylcyclopropanes (**2**)[a]

Products (Yield, %)		Method	Products (Yield, %)			
1a	(62)	A	**2a**	(91)		
1b	(34)		**2b**	(76)	**3**	(15)
1c[c]			**2c**	(75)		
1d	(91)	B	**2d**	(44)[d]		
1e[b]	(80)	B	**2e**[b]	(71)		
1f[b]	(51)	A	**2f**[b]	(73)		
1g[b]	(80)	A	**2g**[b]	(71)		
1h[b]	(40)	A	**2h**[b]	(85)		
1i[b]	(86)	A	**2i**[b]	(80)	**2h**[b]	(12)

a) Isolated yields. The compounds indicated by *b*) were inseparable mixtures (about 1 to 1.5 ratio). *c*) See Experimental. *d*) The low yield was assumed to be because of the high volatility of **2d**.

2 in a good yield regardless of the functional group, such as ester, acetate, alkyl ether, silyl ether, acetal, or hydroxy group. The structures of products were elucidated on the basis of their spectral data. Dimethylation of **1b** gave a small amount of the tricyclic ketone (**3**) produced *via* the metalated intermediate (A) along with the desired dimethylated compound (**2b**), indicating that **1b** is a *cis*-dibromide.[12]

In conclusion, the present method using $Me_2Cu(SCN)Li_2$–MeI is efficient for preparing the dimethyl compound (**2**) from the dibromo compound (**1**).

Experimental

The melting point of **1c** was determined with a Yanagimoto micro melting point apparatus, and is uncorrected. Compounds for which no melting point is given are oily. The infrared (IR) spectra (IR ν_{max}) were determined on a Shimadzu IR-400 spectrometer in chloroform. The proton nuclear magnetic resonance (^{1}H-NMR) spectra were obtained in chloroform-*d* at 200 MHz on a JEOL FX 200 instrument with chemical shifts being reported in parts per million downfield from tetramethylsilane as an internal standard (δ 0.0), and coupling constants in Hertz. Mass spectra (MS) were taken on a JEOL JMS 01SG-2 instrument (direct inlet) at 70 eV. All reactions were carried out under an atmosphere of argon. The reaction mixture was diluted with water and extracted with ether. The organic layer was washed with brine, dried over $MgSO_4$, and filtered, then the filtrate was concentrated to dryness *in vacuo*. Column chromatography was carried out on silica gel (Wakogel C-200) or Aluminum oxide 90 (Merck, activity II—III). Preparative thin layer chromatography (pTLC) was run on 20×20 cm plates coated with a 0.25 mm layer of Merck Silica gel GF_{254}.

General Procedure for Preparation of the Dibromides (1)——Method A: Bromoform (17 mmol), tributylamine (0.2 ml), and 40% aqueous sodium hydroxide (8 ml) were added successively to a solution of an olefinic compound

(3 mmol) in methylene dichloride (4 ml). The mixture was vigorously stirred under reflux for 2—6 h.

Method B: Bromoform (9 mmol) in pentane (5 ml) was added to a suspension of *tert*-BuOK (20 mmol) and an electron-rich olefin (5 mmol) in pentane (50 ml) at 0 °C. The reaction mixture was stirred for 2 h at 0 °C. Yields are given in Table I.

Methyl (1*RS*,3*SR*,6*SR*)-7,7-Dibromobicyclo[4.2.0]heptane-3-carboxylate (1a) and Methyl (1*RS*,3*RS*,6*SR*)-7,7-Dibromobicyclo[4.2.0]heptane-3-carboxylate (1b)——The residue in hexane was chromatographed on silica gel. Elution with hexane gave **1a**. IR: 1720 cm^{-1}. ^{1}H-NMR: 3.67 (3H, s, COOMe). MS Calcd for $C_9H_{12}Br_2O_2$: 309.9205 (M^+). Found: 309.9212. Successive elution with the same solvent gave **1b**. IR: 1720 cm^{-1}. ^{1}H-NMR: 2.48 (1H, dddd, J=14.4, 10.3, 4.4, 1.9 Hz, CH), 3.67 (3H, s, COOMe). MS Calcd for $C_9H_{12}Br_2O_2$: 309.9205 (M^+). Found: 309.9199.

(1*RS*,6*RS*)-(7,7-Dibromobicyclo[4.1.0]hept-1-yl)methoxy-*tert*-butyldimethylsilane (1c)——(7,7-Dibromobicyclo[4.1.0]hept-1-yl)methanol was synthesized from 1-cyclohexene-1-methanol in 50% yield according to method A. mp 104—105 °C (colorless plates from hexane). IR: 3580, 3430 cm^{-1}. ^{1}H-NMR: 3.67 (1H, d, J=11.7 Hz, CH_AH_BO), 3.86 (1H, d, J=11.7 Hz, CH_AH_BO). *Anal.* Calcd for $C_8H_{12}Br_2O$: C, 34.00; H, 4.28. Found: C, 33.83; H, 4.26. A mixture of the above dibromide (142 mg, 0.5 mmol), imidazole (102 mg, 1.5 mmol), and TBDMS chloride (91 mg, 0.6 mmol) in dimethylformamide (1 ml) was stirred at room temperature overnight. The residue in hexane was chromatographed on silica gel. Elution with hexane afforded **1c** (190 mg, 95% yield). IR: 1095, 840 cm^{-1}. ^{1}H-NMR: 0.06 (3H, s, Me), 0.08 (3H, s, Me), 0.91 (9H, s, *tert*-Bu), 3.67 (1H, d, J=10.1 Hz, CH_AH_BO), 3.75 (1H, d, J=10.1 Hz, CH_AH_BO). MS Calcd for $C_{14}H_{26}Br_2OSi$: 396.0120 (M^+). Found: 396.0122.

(1*RS*,6*RS*)-7,7-Dibromo-1-methoxybicyclo[4.1.0]heptane (1d)——The residue in hexane was chromatographed on silica gel and elution with hexane provided **1d**. IR: 1110—1070 cm^{-1}. ^{1}H-NMR: 3.47 (3H, s, OMe). MS Calcd for $C_8H_{12}Br_2O$: 281.9264 (M^+). Found: 281.9265.

7,7-Dibromo-4-*tert*-butyl-1-methoxybicyclo[4.1.0]heptane (1e)——The residue in hexane was chromatographed on aluminum oxide, and elution with hexane provided **1e**. IR: 1120—1080 cm^{-1}. ^{1}H-NMR: 0.82, 0.84 (total 9H, each s, *tert*-Bu), 3.46, 3.47 (total 3H, each s, OMe). MS Calcd for $C_{12}H_{20}Br_2O$: 337.9863 (M^+). Found: 337.9865.

Methyl 9,9-Dibromobicyclo[6.1.0]decane-4-carboxylate (1f)——The residue in hexane was chromatographed on silica gel. Elution with hexane afforded **1f**. IR: 1720 cm^{-1}. ^{1}H-NMR: 3.66, 3.67 (total 3H, each s, COOMe). MS Calcd for $C_{11}H_{16}Br_2O_2$: 337.9518 (M^+). Found: 337.9519.

2-(7,7-Dibromobicyclo[4.1.0]hept-3-yl)-1,3-dioxolane (1g)——The residue in hexane was chromatographed on aluminum oxide. Elution with hexane and 5% ether in hexane gave **1g**. IR: 1150—1120 cm^{-1}. ^{1}H-NMR: 3.84—3.94 (4H, m, OCH_2CH_2O), 4.58 (1H, d, J=4.4 Hz, CH). MS Calcd for $C_{10}H_{14}Br_2O_2$: 323.9363 (M^+). Found: 323.9378.

7,7-Dibromobicyclo[4.1.0]heptane-3-methanol (1h)——The residue in hexane was chromatographed on aluminum oxide. Elution with 20—50% ether in hexane gave **1h**. IR: 3600, 3430 cm^{-1}. ^{1}H-NMR: 3.32—3.52 (2H, m, CH_2O). MS Calcd for $C_8H_{12}Br_2O$: 281.9264 (M^+). Found: 281.9263.

3-Acetoxymethyl-7,7-dibromobicyclo[4.1.0]heptane (1i)——The residue in hexane was chromatographed on aluminum oxide. Elution with hexane and 10% ether in hexane provided **1i**. IR: 1730 cm^{-1}. ^{1}H-NMR: 2.04 (3H, s, COMe), 3.76—3.95 (2H, m, CH_2OAc). MS Calcd for $C_{10}H_{14}Br_2O_2$: 323.9363 (M^+). Found: 323.9363.

General Procedure for Reaction of Dibromides (1) with $Me_2Cu(SCN)Li_2$–MeI——Cuprous thiocyanate (345 mg, 2.84 mmol) dried under vacuum at 50 °C for 2 d was placed in a flamed-dried 30 ml two-necked flask, and dry ether (2 ml) was added. Methyllithium (5 ml of 1.1 M ether solution, 5.5 mmol) was added to the suspension at −78 °C and the mixture was gradually warmed to −10 °C over 30 min. Then, the mixture was cooled to −20 °C and a solution of a bromide (1) in dry ether (2.5 ml) and hexamethylphosphoric triamide (0.11 ml) was added to the mixture at the same temperature. The reaction mixture was stirred for 1—2 h and methyl iodide (1 ml) was added at −50 °C. After 10 min, the reaction mixture was quenched with saturated aqueous ammonium chloride at −50 °C and precipitates were filtrated off on a celite bed. The filtrate was extracted with ether and the organic layer was washed with 5% aqueous ammonia. Yields are given in Table I.

Methyl (1*RS*,3*SR*,6*SR*)-7,7-Dimethylbicyclo[4.1.0]heptane-3-carboxylate (2a)——Purification of the residue by pTLC (hexane : AcOEt = 6 : 1) gave **2a**. IR: 1725 cm^{-1}. ^{1}H-NMR: 0.65 (2H, m, 2 × CH), 0.93 (3H, s, Me), 0.98 (3H, s, Me), 3.66 (3H, s, COOMe). MS Calcd for $C_{11}H_{18}O_2$: 182.1308 (M^+). Found: 182.1309.

Methyl (1*RS*,3*RS*,6*SR*)-7,7-Dimethylbicyclo[4.1.0]heptane-3-carboxylate (2b) and (1*RS*,2*SR*,5*RS*,7*SR*)-7-Methyltricyclo[3.2.1.$0^{2,7}$]octan-6-one (3)——The residue was subjected to pTLC (hexane : AcOEt = 7 : 1). The upper zone gave **2b**. IR: 1725 cm^{-1}. ^{1}H-NMR: 0.46 (1H, ddd, J=9.2, 6.5, 2.4 Hz, CH), 0.75 (1H, ddd, J=9.2, 9.2, 5.5 Hz, CH), 0.96 (3H, s, Me), 0.99 (3H, s, Me), 3.65 (3H, s, COOMe). MS Calcd for $C_{11}H_{18}O_2$: 182.1307 (M^+). Found: 182.1310. The lower zone gave **3**. IR: 1725 cm^{-1}. ^{1}H-NMR: 1.21 (3H, s, Me). MS Calcd for $C_9H_{12}O$: 136.0888 (M^+). Found: 136.0887.

(1*RS*,6*RS*)-(7,7-Dimethylbicyclo[4.1.0]hept-1-yl)methoxy-*tert*-butyldimethylsilane (2c)——The residue in hexane was chromatographed on aluminum oxide. Elution with hexane afforded **2c**. IR: 1080, 840 cm^{-1}. ^{1}H-NMR: 0.01 (3H, s, Me), 0.02 (3H, s, Me), 0.38 (1H, dd, J=8.5, 2.0 Hz, CH), 0.89 (9H, s, *tert*-Bu), 0.99 (3H, s, Me), 1.08 (3H, s, Me), 3.41 (1H, d, J=10.0 Hz, CH_AH_BO), 3.58 (1H, d, J=10.0 Hz, CH_AH_BO). MS Calcd for $C_{16}H_{32}OSi$: 268.2222 (M^+). Found: 268.2206.

(1*RS*,6*RS*)-1-Methoxybicyclo[4.1.0]heptane (2d)——The residue in hexane was chromatographed on silica gel.

Elution with hexane gave **2d**. IR: 1140 cm^{-1}. ^{1}H-NMR: 0.68 (1H, dd, J=8.9, 2.0 Hz, CH), 0.99 (3H, s, Me), 1.16 (3H, s, Me), 3.24 (3H, s, OMe). MS Calcd for $C_{10}H_{18}O$: 154.1358 (M^+). Found: 154.1358.

4-*tert*-Butyl-1-methoxy-7,7-dimethylbicyclo[4.1.0]heptane (2e)——The residue in hexane was chromatographed on silica gel. Elution with hexane **2e**. IR: 1080 cm^{-1}. ^{1}H-NMR: 0.80, 0.82 (total 9H, each s, *tert*-Bu), 0.98, 0.99 (total 3H, each s, Me), 1.16, 1.17 (total 3H, each s, Me), 3.23, 3.25 (total 3H, each s, OMe). MS Calcd for $C_{14}H_{26}O$: 210.1984 (M^+). Found: 210.1978.

Methyl 9,9-Dimethylbicyclo[6.1.0]decane-4-carboxylate (2f)——Purification of the residue by pTLC (hexane: AcOEt=10:1) gave **2f**. IR: 1720 cm^{-1}. ^{1}H-NMR: 0.20—0.51 (2H, m, 2×CH), 0.93 (3H, s, Me), 1.01 (3H, s, Me), 3.65, 3.66 (total 3H, each s, COOMe). MS Calcd for $C_{13}H_{22}O_2$: 210.1620 (M^+). Found: 210.1627.

2-(7,7-Dimethylbicyclo[4.1.0]hept-3-yl)-1,3-dioxolane (2g)——The residue in hexane was chromatographed on aluminum oxide and elution with hexane afforded **2g**. IR: 1150 cm^{-1}. ^{1}H-NMR: 0.41—0.90 (2H, m, 2×CH), 0.93, 0.95 (total 3H, each s, Me), 0.98 (3H, s, Me), 3.79—4.00 (4H, m, OCH_2CH_2O), 4.57 (1H, d, J=4.9 Hz, CH). MS Calcd for $C_{12}H_{20}O_2$: 196.1463 (M^+). Found: 196.1469.

7,7-Dimethylbicyclo[4.1.0]heptane-3-methanol (2h)——The residue in hexane was chromatographed on silica gel. Elution with 5% ether in hexane provided **2h**. IR: 3620, 3440 cm^{-1}. ^{1}H-NMR: 0.42—0.91 (2H, m, 2×CH), 0.93, 0.94 (total 3H, each s, Me), 0.99 (3H, s, Me), 3.22—3.52 (2H, m, CH_2O). MS Calcd for $C_{10}H_{18}O$: 154.1358 (M^+). Found: 154.1355.

3-Acetoxymethyl-7,7-dimethylbicyclo[4.1.0]heptane (2i) and 2h——The residue in hexane was chromatographed on silica gel. Elution with 5% ether in hexane gave **2i**. IR: 1720 cm^{-1}. ^{1}H-NMR: 0.42—0.85 (2H, m, 2×CH), 0.93, 0.94 (total 3H, each s, Me), 0.98 (3H, s, Me), 2.05 (3H, s, COMe), 3.78—3.98 (2H, m, CH_2OAc). MS Calcd for $C_{12}H_{20}O_2$: 196.1463 (M^+). Found: 196.1467. Elution with 40% ether in hexane gave **2h**. This compound was identical with the alcohol (**2h**) on the basis of IR and ^{1}H-NMR spectral comparisons.

References and Notes

1) T. K. Devon and A. I. Scott, "Handbook of Naturally Occurring Compounds," Vol. II, Academic Press, New York and London, 1972.
2) G. H. Posner, "Organic Reactions," Vol. 22, ed. by W. G. Dauben, John Wiley and Sons, Inc., New York, 1975, p. 253 and references cited therein.
3) P. Fischner and G. Shaefer, *Angew. Chem., Int. Ed. Engl.*, **20**, 863 (1981).
4) E. J. Corey and M. Jautelat, *J. Am. Chem. Soc.*, **89**, 3912 (1967).
5) M. Saha, B. Bagby, and K. M. Nicholas, *Tetrahedron Lett.*, **27**, 915 (1986) and references cited therein.
6) M. D. Taylor, G. Minaskanian, K. N. Winzenberg, P. Santone, and A. B. Smith III, *J. Org. Chem.*, **47**, 3960 (1982).
7) E. J. Corey and G. H. Posner, *J. Am. Chem. Soc.*, **89**, 3911 (1967).
8) J. A. Marshall and J. A. Ruth, *J. Org. Chem.*, **39**, 1971 (1974).
9) B. H. Lipshutz, R. S. Wilhelm, J. A. Kozlowski, and D. Parker, *J. Org. Chem.*, **49**, 3928 (1984).
10) B. H. Lipshutz, J. A. Kozlowski, and R. S. Wilhelm, *J. Org. Chem.*, **48**, 546 (1983).
11) B. H. Lipshutz, R. S. Wilhelm, and J. A. Kozlowski, *Tetrahedron*, **40**, 5005 (1984).
12) T. Harayama, H. Fukushi, T. Aratani, K. Ogawa, T. Murata, and F. Yoneda, *Chem. Pharm. Bull.*, **35**, 1777 (1987).
13) T. Harayama, H. Fukushi, K. Ogawa, and F. Yoneda, *Chem. Pharm. Bull.*, **33**, 3564 (1985).

[Chem. Pharm. Bull. 35(12)4981—4984(1987)]

Constituents of the Seed of *Malva verticillata*. I. Structural Features of the Major Neutral Polysaccharide

NORIKO SHIMIZU and MASASHI TOMODA*

Kyoritsu College of Pharmacy, Shibakōen, Minato-ku, Tokyo 105, Japan

(Received May 29, 1987)

The major neutral polysaccharide, designated as MVS-I, was isolated from the seeds of *Malva verticillata* L. It was homogeneous on electrophoresis and gel chromatography. It is composed of L-arabinose: D-galactose: D-glucose in the molar ratio of 3:6:7. Methylation analysis, carbon-13 nuclear magnetic resonance, and periodate oxidation studies enabled elucidation of its structural features.

Keywords——*Malva verticillata*; seed; polysaccharide; MVS-I; arabinogalactoglucan; arabino-3,6-galactan moiety; component analysis; methylation analysis; structural feature

The seed of *Malva verticillata* L. (Malvaceae) is an Oriental crude drug (Japanese name, toukishi) used as a diuretic, laxative, and galactopoietic. The mucilages in this plant have been characterized,[1] but no study on the constituents of the seed has been reported so far. We have now isolated a pure neutral polysaccharide from the seeds of this plant. Its properties and structural features are reported here.

The seeds were homogenized and extracted with hot water. After addition of ethanol, the resulting precipitate was dissolved in water. After centrifugation, the supernatant was applied to a column of diethylaminoethyl (DEAE)-Sephadex A-25 (carbonate form). The eluate with water was purified by gel chromatography with Sephadex G-25, then applied to a column of Con A-Sepharose (Pharmacia Co.). The eluate from this with a phosphate buffer was dialyzed, concentrated and purified by gel chromatography with Sephadex G-25, then the eluate obtained was lyophilized.

The polysaccharide gave a single peak on gel chromatography with Cellulofine GCL-2000m. In addition, it gave a clear band on polyacrylamide gel disk electrophoresis. It had $[\alpha]_D^{24}$ $-13.9°$ (H_2O, $c=0.14$). Gel chromatography with standard pullulans gave a value of 77000 for the molecular weight. The polysaccharide is designated as MVS-I.

As component sugars of MVS-I, L-arabinose, D-galactose, and D-glucose were identified. Quantitative determination showed that the polysaccharide contained 16.1% arabinose, 39.4% galactose, and 44.5% glucose, and that their molar ratio was 3:6:7. No nitrogen was found in MVS-I. The nuclear magnetic resonance (NMR) spectrum and infrared (IR) spectrum of MVS-I showed no acetyl signal or absorption.

Methylation of the polysaccharide was performed with methylsulfinyl carbanion and methyl iodide in dimethyl sulfoxide.[2] The methylated product was hydrolyzed, and the hydrolyzate was converted into the partially methylated alditol acetates. Gas-liquid chromatography (GLC)-mass spectrometry (MS)[3] revealed derivatives of 2,3,5-tri-*O*-methyl-L-arabinose, 2,3-di-*O*-methyl-L-arabinose, 2,4,6-tri-*O*-methyl-D-galactose, 2,3,6-tri-*O*-methyl-D-galactose, 2,4-di-*O*-methyl-D-galactose, 2,3,4,6-tetra-*O*-methyl-D-glucose, and 2,4,6-tri-*O*-methyl-D-glucose as the products in a molar ratio of 3:3:2:6:4:1:13 from MVS-I.

The ^{13}C-NMR spectrum of MVS-I showed five signals due to anomeric carbons at δ 111.889, 110.108, 107.033, 105.845, and 105.225 ppm. The first two signals were assigned to

the anomeric carbons of α-L-arabinofuranose[4] and the signals at 107.033 and 105.845 to the anomeric carbons of β-D-galactopyranose residues.[5-7] The last signal was assigned to the anomeric carbons of β-D-glucopyranose.[5-7]

MVS-I was subjected to periodate oxidation followed by reduction with sodium borohydride.[8] The product from MVS-I contained galactose and glucose in a molar ratio of 6:13. No arabinose was found in the product. Most (93%) of the glucose residues survived after periodate oxidation, while the half of galactose residues were decomposed by this treatment.

Based on the accumulated evidence described above, it can be concluded that the minimal repeating unit of MVS-I is composed of seven kinds of component sugar units as shown in Chart 1.

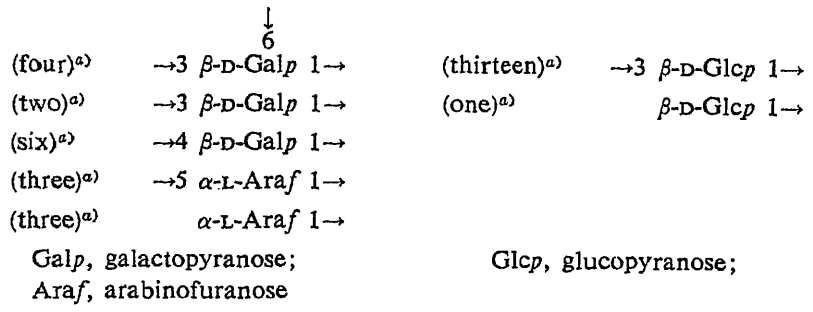

Chart 1. Component Sugar Residues in the Minimal Repeating Unit in the Structure of MVS-I

a) Number of residues.

It is conceivable that MVS-I contains arabino-3,6-galactan[9] moieties. Seeds of various plants, *i.e.*, *Coffea arabica*,[10] *Glycine max*,[11,12] *Brassica campestris*,[13] *Brassica napus*,[14] *Triticum aestivum*,[15] and *Raphanus sativus*[16] contain arabino-3,6-galactans. In contrast to these seed polysaccharides, MVS-I is essentially an arabinogalactoglucan. The ratio between arabinose and galactose is 1:2 in MVS-I, and the polysaccharide has 1,5-linked α-L-arabinofuranose units and 3,6-branched β-D-galactopyranose residues like typical arabino-3,6-galactans. In addition, it possesses 1,4-linked β-D-galactopyranose residues. The presence of such units is generally found in arabino-4-galactans.[17] Further, MVS-I possesses a characteristic glucan structure. All D-glucopyranose chains in MVS-I are β-1,3-linked in addition to having D-glucopyranose terminals. The results of detailed analysis of the sequence of structural units will be reported in subsequent papers.

Experimental

Solutions were concentrated at or below 40°C with rotary evaporators under reduced pressure. Optical rotations were measured with a JASCO DIP-140 automatic polarimeter. The ^{13}C-NMR spectrum was recorded on a JEOL JNM-GX 270 FT NMR spectrometer in heavy water containing acetone as an internal standard at 30 °C. IR spectra were measured with a JASCO IRA-2 infrared spectrophotometer. GLC was carried out on a Shimadzu GC-7AG gas chromatograph equipped with a hydrogen flame ionization detector. GLC-MS was performed with a JEOL JMS-GX 303 mass spectrometer.

Material——The material was imported from China, and its plant of origin was identified by cultivation in a botanical garden of this College.

Isolation of Polysaccharide——The seeds (200 g) were homogenized and extracted with hot water (2000 ml) under stirring for 1 h in a boiling water bath. After suction filtration, the filtrate was poured into two volumes of ethanol. After centrifugation and drying, the precipitate was dissolved in water (200 ml). The solution was applied to a column (5 × 78 cm) of DEAE-Sephadex A-25 (Pharmacia Co.). DEAE-Sephadex A-25 was pretreated as described in a previous report.[18] The column was eluted with water, and fractions of 20 ml were collected and analyzed by the

TABLE I. Relative Retention Times on GLC and Main Fragments in MS of Partially Methylated Alditol Acetates

	Relative retention time[a]	Main fragments (*m/z*)
1,4-Ac-2,3,5-Me-L-arabinitol	0.69	43, 45, 71, 87, 101, 117, 129, 161
1,4,5-Ac-2,3-Me-L-arabinitol	1.12	43, 87, 101, 117, 129, 189
1,3,5-Ac-2,4,6-Me-D-galactitol	1.29	43, 45, 87, 101, 117, 129, 161
1,4,5-Ac-2,3,6-Me-D-galactitol	1.42	43, 45, 87, 99, 101, 113, 117, 233
1,3,5,6-Ac-2,4-Me-D-galactitol	2.00	43, 87, 117, 129, 189
1,5-Ac-2,3,4,6-Me-D-glucitol	1.00	43, 45, 71, 87, 101, 117, 129, 145, 161, 205
1,3,5-Ac-2,4,6-Me-D-glucitol	1.35	43, 45, 87, 101, 117, 129, 161

a) Relative to 1,5-di-*O*-acetyl-2,3,4,6-tetra-*O*-methyl-D-glucitol. Abbreviations: Ac=acetyl; Me=methyl (*e.g.*, 1,4-Ac-2,3,5-Me-=1,4-di-*O*-acetyl-2,3,5-tri-*O*-methyl-).

phenol–sulfuric acid method.[19] The eluates obtained from tubes 9 to 49 were combined and concentrated, and half of the concentrate was applied to a column (5×78 cm) of Sephadex G-25. The column was eluted with water, and fractions of 20 ml were collected. The eluates obtained from tubes 27 to 32 were combined, concentrated and applied to a column (1.5×38 cm) of Con A-Sepharose (Pharmacia Co.). The column was equilibrated with 0.067 M phosphate buffer (pH 7) containing 0.15 M NaCl, 1 mM $MgCl_2$ and 1 mM $CaCl_2$, and kept at 4 °C. The column was eluted with the same buffer, and fractions of 10 ml were collected. The eluates obtained from tubes 4 to 10 were combined, dialyzed against distilled water and concentrated. The solution was applied to a column (5×81 cm) of Sephadex G-25. The column was eluted with water, and fractions of 20 ml were collected. The eluates obtained from tubes 28 to 31 were combined, concentrated and lyophilized. MVS-I was obtained as a white powder (yield, 100 mg from 200 g of seeds).

Gel Chromatography——The sample (3 mg) was dissolved in 0.05 M phosphate buffer (pH 7.5) containing 0.1 M NaCl and applied to a column (2.6×94 cm) of Cellulofine GCL-2000 m (Seikagaku Kōgyō Co.). Elution was carried out with the same buffer. Fractions of 5 ml were collected and analyzed by the phenol-sulfuric acid method. Standard pullulans having known molecular weights were run on the column to obtain a calibration curve.

Polyacrylamide Gel Electrophoresis——This was performed in an apparatus with gel tubes (4×130 mm each) and 0.005 M Tris–glycine buffer (pH 8.3) at 5 mA/tube for 40 min. Gels were stained by the periodate-Schiff (PAS) procedure. MVS-I gave a clear band at a distance of 4.2 cm from the origin.

Qualitative Analysis of Components——Hydrolysis and cellulose thin-layer chromatography (TLC) of component sugars were carried out as described in a previous report.[18] The configurations of component sugars were proved by GLC of trimethylsilylated α-methylbenzylaminoalditol derivatives.[20]

Determination of Components——The sample was hydrolyzed, reduced and acetylated as described in a previous report.[21] The derivatives were analyzed by GLC with a column (3 mm×2 m long spiral glass) packed with 3% OV 225 on Gaschrom Q (100 to 120 mesh) at 220 °C with a helium flow of 50 ml per min. Allose was used as an internal standard.

Methylation——This was performed with methylsulfinyl carbanion and methyl iodide in dimethyl sulfoxide as described in a previous report.[22] The methylation was repeated three times under the same conditions. Yield was 6 mg from 9 mg of the polysaccharide.

Analysis of the Methylated Products——The products were hydrolyzed with dilute sulfuric acid in acetic acid, then reduced and acetylated in the manner described in a previous report.[23] GLC-MS of partially methylated alditol acetates was performed with a fused silica capillary column (0.32 mm i.d.×30 m) of SP 2330 (Supelco Co.) and with programmed temperature increase of 4°C per min from 160 to 220 °C at a helium flow rate of 1 ml per min. The relative retention times of the products with respect to 1,5-di-*O*-acetyl-2,3,4,6-tetra-*O*-methyl-D-glucitol in GLC and their main fragments in the mass spectra are listed in Table I.

Periodate Oxidation——The polysaccharide (11.3 mg) was oxidized with 0.05 M sodium metaperiodate (6 ml) at 7 °C in the dark. The periodate consumption was measured by a spectrophotometric method.[24] The oxidation was completed after 3 d, and the maximal value of consumption was 0.46 mol per mol of anhydrosugar unit. The reaction mixture was successively treated with ethylene glycol (0.06 ml) at 7 °C for 1 h and sodium borohydride (60 mg) at 7 °C for 16 h, then adjusted to pH 5 by addition of acetic acid. The solution was dialyzed against distilled water. The non-dialyzable fraction was concentrated and applied to a column (2.6×92 cm) of Sephadex G-25. The column was eluted with water, and fractions of 10 ml were collected. The eluates obtained from tubes 19 to 22 were combined, concentrated and lyophilized. Yield, 8 mg.

Acknowledgement We are grateful to Misses T. Shimizu and N. Yoneda, for their technical assistance.

References

1) G. Racz and I. Mathe, *Farmacia* (Bucharest), **29**, 153 (1981) [*Chem. Abstr.*, **96**, 91535z (1982)].
2) S. Hakomori, *J. Biochem.* (Tokyo), **55**, 205 (1964).
3) H. Björndall, B. Lindberg, and S. Svensson, *Carbohydr. Res.*, **5**, 433 (1967).
4) J.-P. Joseleau, G. Chambat, M. Vignon, and F. Barnoud, *Carbohydr. Res.*, **58**, 165 (1977).
5) P. A. J. Gorin, "Advances in Carbohydrate Chemistry and Biochemistry," Vol. 38, ed. by R. S. Tipson and D. Horton, Academic Press, Inc., New York, 1981, pp. 37—72.
6) J. H. Bradbury and G. A. Jenkins, *Carbohydr. Res.*, **126**, 125 (1984).
7) K. Bock, C. Pedersen, and H. Pedersen, "Advances in Carbohydrate Chemistry and Biochemistry," Vol. 42, ed. by R. S. Tipson and D. Horton, Academic Press, Inc., Orland, 1984, pp. 193—214.
8) M. Abdel-Akher, J. K. Hamilton, R. Montgomery, and F. Smith, *J. Am. Chem. Soc.*, **74**, 4970 (1952).
9) A. E. Clarke, R. L. Anderson, and B. A. Stone, *Phytochemistry*, **18**, 521 (1979).
10) M. L. Wolfrom and D. L. Patin, *J. Org. Chem.*, **30**, 4060 (1965).
11) M. Morita, *Agric. Biol. Chem.*, **29**, 564 (1965).
12) T. Kikuchi, *Nippon Nōgeikagaku Kaishi*, **46**, 405 (1972).
13) I. R. Siddiqui and P. J. Wood, *Carbohydr. Res.*, **24**, 1 (1972).
14) O. Larm, O. Theander, and P. Aman, *Acta Chem. Scand., Ser. B*, **29**, 1011 (1975).
15) H. Neukom and H. Markwalder, *Carbohydr. Res.*, **39**, 387 (1975).
16) Y. Tsumuraya, Y. Hashimoto, and S. Yamamoto, *Carbohydr. Res.*, **161**, 113 (1987).
17) G. O. Aspinall, "Polysaccharides," Pergamon Press, Oxford, 1970, pp. 94—102.
18) M. Tomoda, S. Kaneko, M. Ebashi, and T. Nagakura, *Chem. Pharm. Bull.*, **25**, 1357 (1977).
19) M. Dubois, K. A. Gilles, J. K. Hamilton, P. A. Rebers, and F. Smith, *Anal. Chem.*, **28**, 350 (1952).
20) R. Oshima and J. Kumanotani, *J. Chromatogr.*, **259**, 159 (1983).
21) M. Tomoda, Y. Suzuki, and N. Satoh, *Chem. Pharm. Bull.*, **27**, 1651 (1979).
22) N. Shimizu, M. Tomoda, and M. Adachi, *Chem. Pharm. Bull.*, **34**, 4133 (1986).
23) M. Tomoda, K. Shimada, Y. Saito, and M. Sugi, *Chem. Pharm. Bull.*, **28**, 2933 (1980).
24) G. O. Aspinall and R. J. Ferrier, *Chem. Ind.* (London), **1957**, 1216.

[Chem. Pharm. Bull. 35(12)4985—4987(1987)]

Asymmetric Reduction of α-Methyl β-Keto Esters by Microbial Cells Immobilized with Prepolymer

HIROYUKI AKITA,*,[a] HIROKO MATSUKURA,[a] KENJI SONOMOTO,[b] ATSUO TANAKA,[b] and TAKESHI OISHI*,[a]

RIKEN (The Institute of Physical and Chemical Research),[a] 2-1, Hirosawa, Wako-shi, Saitama 351-01, Japan and Laboratory of Industrial Biochemistry, Department of Industrial Chemistry, Faculty of Engineering, Kyoto University,[b] Yoshida, Sakyo-ku, Kyoto 606, Japan

(Received June 5, 1987)

Asymmetric reduction of α-methyl β-keto esters using microbial cells immobilized by the prepolymer method was examined. It was found that by a proper selection of the prepolymer in the stage of immobilization, the chemical and optical yields were both improved appreciably in some cases compared to those obtained by reduction with the native microorganisms.

Keywords——microbial asymmetric reduction; immobilized yeast; α-methyl β-keto ester; α-methyl β-hydroxy ester; prepolymer method

Immobilization of biocatalysts is known to be effective for enhancing their stability and allowing easier isolation of the products. Entrapment techniques play a crucial role and still remain to be improved further. Immobilization with urethane (PU) or photo-crosslinkable

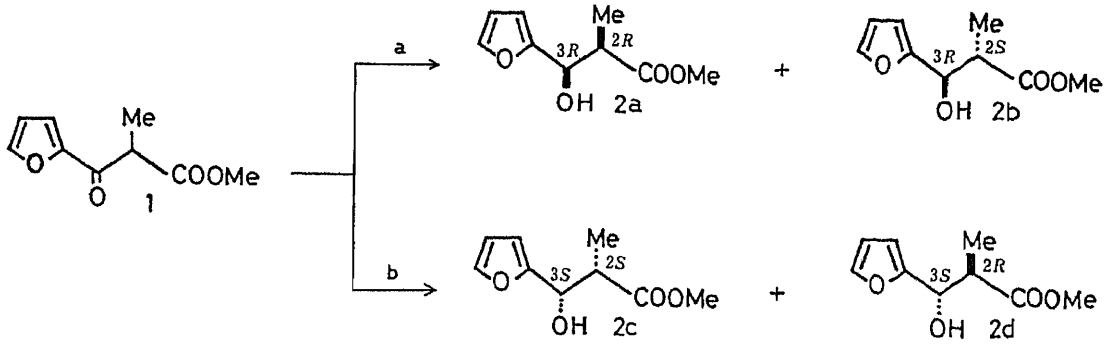

a, *Saccharomyces delbrueckii, Saccharomyces fermentati, Candida albicans*
b, *Kloeckera saturnus*

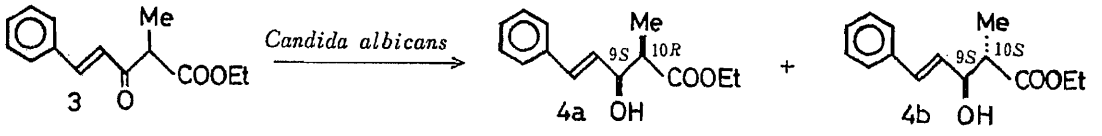

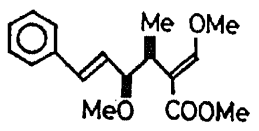

(−)-oudemansin A 5

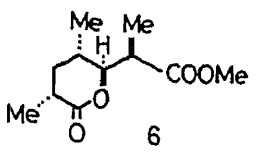

methyl ester of Prelog–Djerassi lactone

Chart 1

TABLE I

Entry	Substrate	Prepolymer	Total yield (%)	Products;	Optical purity (% ee)	*syn*/*anti*
With immobilized *Kloeckera saturnus*						
1[a]	1	None	29	**2c**; 68	**2d**; 46	47/53
2	1	PU-3	42	**2c**; 84	**2d**; 49	51/49
3[b]	1	PU-3	5	**2c**; 89	**2d**; 61	52/48
4	1	PU-6	58	**2c**; 84	**2d**; 66	49/51
5	1	ENT-4000	16	**2c**; 83	**2d**; 63	47/53
6	1	ENTP-4000	53	**2c**; 84	**2d**; 73	48/52
7[c]	1	ENTP-4000	66	**2c**; 81	**2d**; 64	49/51
With immobilized *Saccharomyces delbrueckii*						
8[a]	1	None	43	**2a**; 90	**2b**; 91	39/61
9	1	PU-6	33	**2a**; 56	**2b**; 74	41/59
10	1	ENT-4000	31	**2c**; 75	**2d**; 68	39/61
11[c]	1	ENT-4000	64	**2c**; 81	**2d**; 57	50/50
With immobilized *Saccharomyces fermentati*						
12[a]	1	None	21	**2a**; 84	**2b**; 86	40/60
13	1	PU-3	36	**2a**; 94	**2b**; 96	48/52
14	1	PU-6	9	**2a**; 95	**2b**; 97	42/58
15	1	ENT-4000	15	**2a**; 66	**2b**; 68	38/62
16	1	ENTP-4000	20	**2a**; 21	**2b**; 30	43/57
With immobilized *Candida albicans*						
17[a]	1	None	23		**2b**; >99	0/>99
18	1	ENT-4000	27	**2a**; 42	**2b**; 81	12/88
19[a]	3	None	45	**4a**; 97	**4b**; 97	78/22
20	3	PU-3	57	**4a**; 83	**4b**; >99	75/25
21	3	PU-6	64	**4a**; 96	**4b**; >99	75/25
22[c]	3	PU-6	79	**4a**; 95	**4b**; >99	70/30
23	3	ENT-4000	26	**4a**; >99	**4b**; >99	62/38
24[c]	3	ENT-4000	37	**4a**; 84	**4b**; >99	67/33

a) Solvent: usual liquid medium used previously.[2] *b*) Solvent: *n*-hexane saturated with water. *c*) The filtered, used, immobilized yeast cells were employed again after reactivation (see Experimental).

resin prepolymers (ENT and ENTP) has been developed by Fukui and Tanaka.[1] Although the advantages of this prepolymer method have already been shown in several cases, it is desirable to expand the scope of this method by testing it with various types of enzymatic reactions. Thus, we examined the effect of immobilization with these prepolymers on the previously reported yeast-promoted enantioselective reduction of α-methyl β-keto esters **1** and **3** to give the corresponding α-methyl β-hydroxy esters **2a**—**d**[2] and **4a**,**b**.[3] These compounds have been proved to be useful chiral synthons leading to bioactive natural products such as (−)-**5**[4] and **6**.[5]

Selected data on the present asymmetric reduction of **1** or **3** using immobilized yeasts are presented in Table I. Results obtained in the reduction with native yeasts are also shown for comparison.

The characteristic features of the present asymmetric reduction using immobilized yeasts are as follows: 1) By a proper selection of an effective prepolymer, both chemical yield and the optical purity were improved (entries 6, 7, 13, 21 and 22). 2) The immobilized yeasts can be used repeatedly (entries 7, 11, 22, and 24). In most cases, the enzymatic activity remains intact. 3) In some cases, the stereochemistry of the reduction is affected by the prepolymer used. In entries 10 and 11, products having opposite stereostructure are obtained. 4) Among the media so far examined, a 20% (w/v) sucrose solution was found to be the best in every

case. 5) The use of a water-miscible organic solvent such as dimethylsufoxide (DMSO), tetrahydrofuran (THF) or dioxane, or nonpolar organic solvents saturated with water, was shown to deactivate the immobilized microbial cells. Only in entry 3, *n*-hexane saturated with water could be used as the solvents, but the yield was poor.

Experimental

A typical immobilization procedure employed here is as follows. Thawed yeast cells (4 g) suspended in 1 ml of water were entrapped with 2 g of water-miscible urethane prepolymer, PU-3 or PU-6, by mixing continuously until gelation started. Thawed yeast cells (3.5 g) suspended in 1 ml of water were also immobilized with 3.5 g of photo-crosslinkable resin prepolymer (ENT-4000 or ENTP-4000) in the presence of a photosensitizer, benzoin ethyl ether (35 mg), under illumination with near-ultraviolet light (wavelength range, 300—400 nm; maximum intensity at 360 nm) for 3 min. The gel blocks thus formed were cut into small pieces (5 × 5 × 5 mm) and used for the reduction. A mixture of a substrate (**1** or **3**; 0.2—0.3 mmol) and immobilized microbial cells thus prepared in water-saturated organic solvents (100 ml) (benzene, *n*-hexane, *n*-heptane and isooctane) was shaken continuously at 30 °C for 3d. However, the starting material was recovered almost intact in every case except for entry 3. Thus, the reaction medium was changed to a sucrose solution (20 g/100 ml) and reduction was carried out under the same conditions as mentioned above. After completion of the reduction, the gel blocks were separated by filtration from the solution containing products. The immobilized cells thus recovered were washed with water and reactivated by shaking continuously in water (100 ml) in the presence of sucrose (20 g) at 30°C for one day, then used again (entries 7, 11, 22 and 24).

The structures and optical purities of **2a—d**,[2] **4a,b**[6] were determined after converting the compounds into the corresponding (+)-MTPA esters,[7] by comparison with authentic samples prepared previously.

References and Notes

1) S. Fukui and A. Tanaka, *Adv. Biochem. Eng/Biotechnol.*, **29**, 1 (1984).
2) *a*) H. Akita, A. Furuichi, H. Koshiji, K. Horikoshi, and T. Oishi, *Tetrahedron Lett.*, **23**, 4051 (1982); *b*) *Idem*, *Chem. Pharm. Bull.*, **32**, 1333 (1984).
3) H. Akita, H. Koshiji, A. Furuichi, K. Horikoshi, and T. Oishi, *Tetrahedron Lett.*, **24**, 2009 (1983).
4) H. Akita, H. Koshiji, A. Furuichi, K. Horikoshi, and T. Oishi, *Chem. Pharm. Bull.*, **32**, 1242 (1984).
5) S. F. Martin and D. E. Guinn, *Tetrahedron Lett.*, **25**, 5607 (1984).
6) NMR signals (400 MHz) due to the C-7 protons of the (+)-MTPA esters of all possible authentic *syn*- and *anti*-isomers **4** prepared by the use of native yeast of **3** are noted here, since these data were not given in the previous report (ref. 3). *syn*-(9*S*,10*R*) ester (**4a**); δ 6.736, d, J = 15.9 Hz, *syn*-(9*R*,10*S*) ester; δ 6.601, d, J = 15.9 Hz, *anti*-(9*S*,10*S*) ester (**4b**); δ 6.827, d, J = 15.9 Hz, *anti*-(9*R*,10*R*) ester; δ 6.745, d, J = 15.9 Hz.
7) *a*) J. A. Dale, D. L. Dull, and H. S. Mosher, *J. Org. Chem.*, **34**, 2543 (1969); *b*) J. A. Dale and H. S. Mosher, *J. Am. Chem. Soc.*, **95**, 512 (1973).

[Chem. Pharm. Bull. 35(12)4988—4989(1987)]

Chemistry of Amine-Boranes. XI.[1] A Convenient Synthesis of Dimethylamine-Borane

YASUO KIKUGAWA

Faculty of Pharmaceutical Sciences, Josai University, 1–1 Keyakidai, Sakado, Saitama 350–02, Japan

(Received June 8, 1987)

Dimethylamine-borane was synthesized in good yield from sodium borohydride and dimethylamine hydrochloride by using dimethoxyethane as a solvent.

Keywords——dimethylamine-borane; sodium borohydride; dimethoxyethane; synthesis

Amine-boranes are useful reagents which have many important laboratory and industrial applications.[2] In particular, dimethylamine-borane (DMAB) has been used widely as a reducing agent in chemical plating.[3] Commercially available DMAB is prepared by the reaction of diborane with dimethylamine at low temperature.[2a] DMAB is also prepared by other methods, such as reaction of lithium borohydride (LBH) with dimethylamine hydrochloride in ether,[2b,4] displacement of tetrahydrofuran (THF) with dimethylamine from THF-borane,[2b] or reaction of sodium borohydride (SBH) and dimethylamine in the presence of iodine.[5] We wished to prepare DMAB through a more convenient method.

It is generally accepted that ordinary amine-boranes can be prepared by the reaction of LBH with an amine hydrochloride in ether. The synthesis of pyridine-borane is exceptional, and can be successfully carried out by the reaction of SBH (instead of LBH) and pyridine hydrochloride in pyridine,[6] probably because both SBH and pyridine hydrochloride are comparatively soluble in pyridine. We have investigated the preparation of DMAB with SBH and dimethylamine hydrochloride by seeking a proper solvent. Many solvents were tested and the results were as follows: 1) DMAB was obtained in moderate but practically unsatisfactory yields in THF or dioxane. 2) Dimethylformamide (DMF) dissolves SBH and dimethylamine hydrochloride fairly well and DMAB was obtained in good yield; however, chromatography on a short silica gel column was needed to remove DMF completely. 3) Dimethoxyethane (DME) was revealed to be the best solvent not only for dissolving the reagents, but also because it could be easily removed by evaporation. Accordingly DMAB was obtained in good yield through a simple procedure.

Some secondary amine-boranes such as morpholine-borane or diethylamine-borane were also synthesized by using the combination of SBH, the amine hydrochloride and DME in yields of 71% and 55%, respectively. However, it is interesting to note that trimethylamine-borane could not be synthesized at all by the same procedure.

Experimental

All melting points are uncorrected. SBH was purchased from Morton Thiokol Ltd., Japan, Ventron Division.

DMAB——SBH (925 mg, 25 mmol) was added in small portions to a suspension of dimethylamine hydrochloride (2.24 g, 27.5 mmol) in DME (40 ml) under stirring. After 1 h, the reaction mixture was filtered and the filtrate was evaporated *in vacuo* to afford crude DMAB, mp 33°C (1.24 g, yield 84%), which was recrystallized from dichloromethane–hexane to give pure DMAB,[7] mp 36 °C (lit.[5] 36 °C).

References and Notes

1) Part X: Y. Kikugawa, *J. Chem. Soc., Perkin Trans. 1*, **1984**, 609.
2) *a*) H. C. Newsom, "Encyclopedia of Chemical Technology," 2nd ed., Vol. 3, ed. by Kirk-Othmer, Interscience Publishers, New York, 1964, pp. 728—737; *b*) R. A. Geanangel and S. G. Shore, "Preparative Inorganic Reactions," Vol. 3, ed. by W. L. Jolly, Interscience Publishers, New York, 1966, pp. 133—141; *c*) W. Büchner and H. Niederprüm, *Pure Appl. Chem.*, **49**, 733 (1977).
3) H. Narcus, *Plating*, **54**, 380 (1967); Y. Okinaka, *ibid.*, **57**, 914 (1970); K. Nihei, T. Ohsaka, and H. Sawai, *Denki Kagaku*, **44**, 402, 656 (1976).
4) H. Nöth and H. Beyer, *Chem. Ber.*, **93**, 931 (1960). It was claimed in the literature that SBH is also effective for the synthesis of amine-boranes; however, no experimental details were given. According to ref. 2*b*, LBH is used because it is more soluble in organic solvents than the other alkali metal borohydrides.
5) K. C. Nainan and G. E. Ryschkewitsch, *Inorg. Chem.*, **8**, 2671 (1969); *idem*, *Inorg. Synth.*, **15**, 122 (1974).
6) R. P. Barnes, J. H. Graham, and M. D. Taylor, *J. Org. Chem.*, **23**, 1561 (1958).
7) This was identified by mixed melting point determination with an authentic sample purchased from Morton Thiokol Ltd., Japan, Ventron Division.

[Chem. Pharm. Bull. 35(12)4990—4992(1987)]

The Synthesis of Lupin Alkaloids. II.[1] A Formal Synthesis of (±)-Sparteine

NORIYUKI TAKATSU, MASAYO NOGUCHI, SHIGERU OHMIYA, and HIROTAKA OTOMASU*

Faculty of Pharmaceutical Sciences, Hoshi University, 2-4-41 Ebara, Shinagawa-ku, Tokyo 142, Japan

(Received June 9, 1987)

2-Hydroxy-3-(2′-piperidyl)quinolizidine (**5**), an intermediate for the synthesis of (±)-leontiformidine (**1a**), was converted into (±)-sparteine (**7**) by a three-step procedure of oxidation, Mannich reaction and deoxygenation.

Keywords——lupin alkaloid; leontiformidine; sparteine; 8-oxosparteine; 2-hydroxyleontiformidine; 2-oxoleontiformidine; 3-(2′-piperidyl)quinolizidine; stereo-structure; Jones-oxidation

In the preceding paper,[1] we reported the total synthesis of two lupin alkaloids, leontiformidine (**1a**) and leontiformine (**1b**), using the 1,3-dipolar cycloaddition reaction of the enone (**2**) with 1-piperine 1-oxide (nitrone **3**) as a key reaction, as shown in Chart 1. Leontiformidine (**1a**) has a 3-(2′-piperidyl)quinolizidine structure, and another lupin alkaloid, sparteine (**7**), has a similar structure in which the C-1 and N-1′ positions are combined with a methylene group. Therefore, it seemed likely that 2-hydroxyleontiformidine (**5**), an intermediate for the preparation of **1a**, could be converted into **7** by a three-step procedure of oxidation, Mannich reaction and deoxygenation. This paper deals with the chemistry leading to (±)-**7** from **5**.

Chromic acid is generally used in the oxidation of amino alcohols to amino-carbonyl compounds. However, in the oxidation of **5**, epimerization at the C-3 must be considered, because the C-3 of **8** becomes an active methine carbon owing to the effect of the produced carbonyl group, and the 2-piperidyl group should take the thermodynamically stable equatorial form. To avoid epimerization at C-3 of **8**, various oxidations without the use of chromic acid were attempted. Under non-acidic conditions, Oppenauer oxidation and Moffatt oxidation did not occur, and the starting material was recovered. Swern oxidation gave a complicated mixture. Mild conditions using pyridinium chlorochromate (PCC) gave unsatisfactory results. Finally, Jones oxidation afforded **8** in 96% yield.

In order to confirm the stereochemistry of the product **8**, obtained under rather strongly acidic conditions, the reductive removal of the carbonyl oxygen was carried out. Wolff–Kishner reaction of **8** did not proceed, but the tosylhydrazone of **8** was reduced with $LiAlH_4$ to give **1a**, whose spectral data were identical with those of an authentic sample. Consequently, it was found that the stereo-structure at C-3 of **8** did not change during Jones oxidation.

Next, the Mannich reaction of **8** with HCHO was carried out. Under acidic conditions with HCl, the reaction did not occur. At pH 7—8 adjusted with AcOH, 8-oxo-sparteine (**9**) was obtained in 38% yield. The carbon-13 nuclear magnetic resonance (^{13}C-NMR) data of **9** were consistent with those of Bohlmann and Zeisberg.[2] Since **9** has already been converted to (±)-**7** by van Tamelen and Foltz,[3] this synthesis constitutes a formal synthesis of (±)-sparteine.

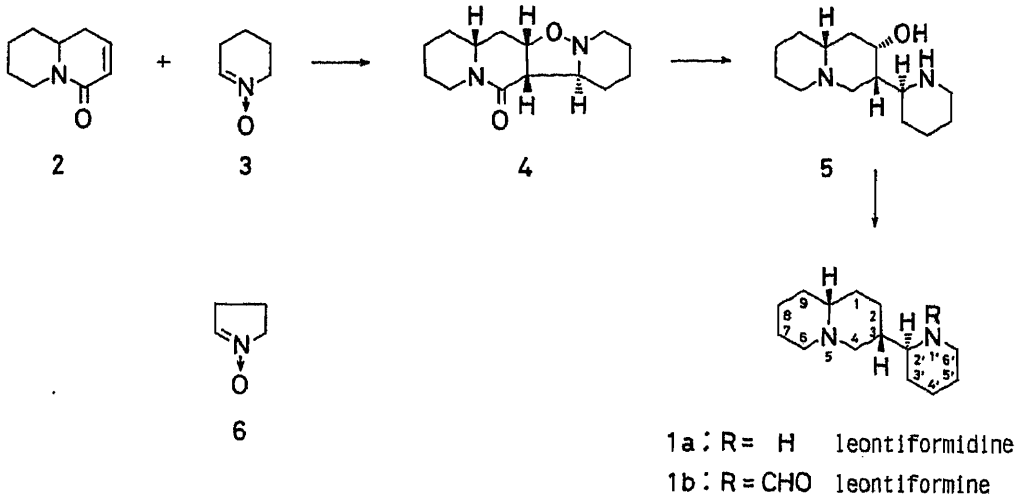

Chart 1

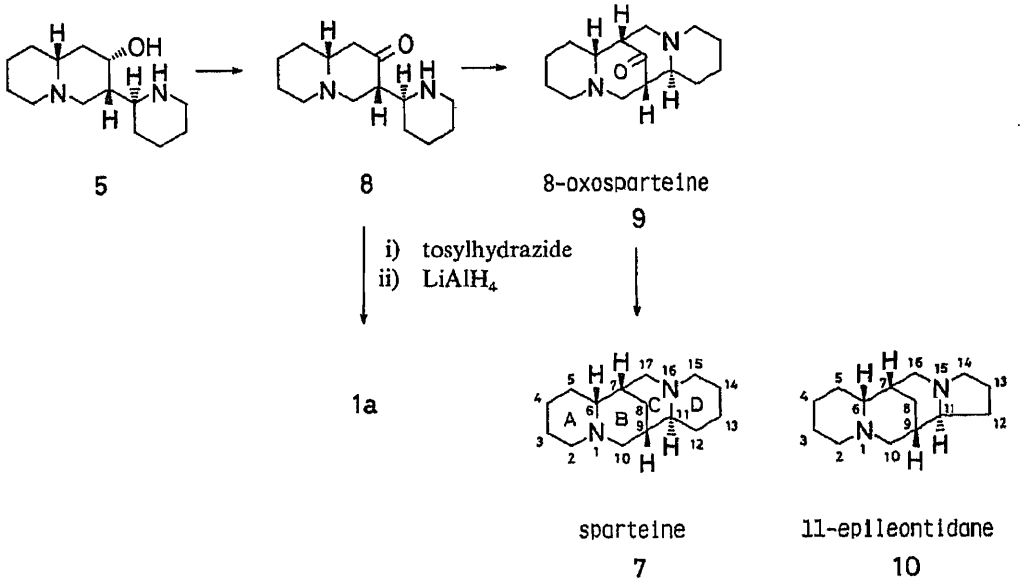

Chart 2

Thus, we have achieved a novel synthesis of sparteine, maintaining the stereo-structure from 2-hydroxyleontiformidine (**5**). This method should be applicable to the total synthesis of naturally occurring homologous alkaloids. For example, the quinolizidine-indolizidine alkaloid 11-epileontidane[4] has the structure **10**, in which the D-ring of sparteine (**7**) is replaced by a five-membered ring and the stereochemistry of chiral centers is the same as that of **7**. Accordingly, it is expected that the synthesis of **10** should be possible by using 1-pyrroline 1-oxide (**6**) instead of nitrone (**3**) in the foregoing procedures. The correctness of this assumption is now under investigation in our laboratory.

Experimental

Infrared (IR) spectra were measured with a Hitachi 215 spectrometer and MS with a JEOL JMS-D300 spectrometer. ^{1}H- and ^{13}C-NMR spectra were recorded on a JEOL JNM-GX 400 FT NMR with tetramethylsilane as an internal standard.

(±)-2-Oxoleontiformidine (8)——i) Oxidation of **5** with PCC: A solution of **5** (500 mg, 2.10 mmol) in dry CH_2Cl_2 (5 ml) was added to a stirred suspension of PCC (0.90 g, 4.18 mmol) and molecular sieves 3A powder (2.10 g) in dry CH_2Cl_2 (10 ml) at room temperature. Stirring was continued for 6 h, then water and K_2CO_3 were added and the solvent was evaporated off *in vacuo*. The residue was extracted with CH_2Cl_2 in a Soxhlet extractor for 12 h and the extract was evaporated *in vacuo*. The resulting product was chromatographed on silica gel with CH_2Cl_2–CH_3OH–28%NH_4OH (90 : 9 : 1) to give colorless crystals of **8**. Yield, 263 mg (53.0%).

ii) Jones Oxidation. Fresh Jones reagent (a mixture of CrO_3 5.34 g, H_2SO_4 4.6 ml, and water 8 ml make 20 ml) was added to a stirred suspension of **5** (200 mg, 0.84 mmol) in acetone (20 ml) to form a clear solution at 0°C. After being stirred for 2 h, the reaction mixture was warmed to room temperature and then stirred for a further 3 h. The resulting mixture was concentrated to half the initial volume, water and K_2CO_3 were added, and the solvent was evaporated off. The residue was extracted with CH_2Cl_2 in a Soxhlet extractor for 12 h, and the extract was concentrated to dryness. The solid obtained gave a single spot on thin layer chromatography (TLC). Yield, 190 mg, 96.1%. IR $\nu_{max}^{CCl_4}$ cm^{-1}: 3370(NH), 2930, 2850, 2800 (Bohlmann band), 1710 (C=O). ^{1}H-NMR ($CDCl_3$) δ: 2.66 (2H, m), 2.78 (1H, ddd, J=2.4, 7.2, 10.9 Hz), 2.96 (1H, m), 3.03 (1H, m), 3.16 (1H, dd, J=5.9, 11.2 Hz). MS *m/z*: 236(M^+), 152, 110, 98, 84 (base peak). High MS *m/z* 236.1887 (Calcd for $C_{14}H_{24}N_2O$: 236.1887).

(±)-Leontiformidine (1a) From the Tosylhydrazone of 8——A solution of **8** (50 mg, 0.21 mmol) and tosylhydrazide (47 mg, 0.25 mmol) in EtOH (70 μl) was heated at 90°C under an N_2 atmosphere for 20 h and then concentrated to dryness *in vacuo*. The residue was dissolved in dry tetrahydrofuran (THF) (2 ml) and this solution was added to a stirred suspension of $LiAlH_4$ (80 mg, 2.11 mmol) in dry THF under an N_2 atmosphere. The mixture was stirred for 12 h at ambient temperature, then the reaction was quenched by the addition of water. The insoluble material formed was filtered off and washed with CH_2Cl_2. The combined filtrate was dried and evaporated to give the residue, which was subjected to preparative TLC on silica gel with CH_2Cl_2–CH_3OH–28% NH_4OH (90 : 9 : 1) to give (±)-**1a** as a pale yellow syrup (34.3 mg, 73%). Spectral data of (±)-**1a** were consistent with those of an authentic sample.[1]

Mannich Reaction of 8: Formation of (±)-8-Oxosparteine (9)——A solution of **8** (190 mg, 0.80 mmol) and 35% formalin (64 μl, 0.81 mmol) in EtOH (0.5 ml) was adjusted to pH 7—8 with 50% AcOH and then heated at 110°C with stirring for 2 h. After the solution had cooled, the solvent was evaporated off *in vacuo* and then water, CH_2Cl_2 and K_2CO_3 were added and the whole was extracted with CH_2Cl_2. The organic layer was dried and evaporated *in vacuo* to give the residue, which was subjected to column chromatography on silica gel. Elution with CH_2Cl_2–CH_3OH–28%NH_4OH (90 : 9 : 1) afforded (±)-8-oxosparteine (**9**) as a pale yellow solid (74.3 mg, 37.2%). The spectral data of **9** were consistent with those reported by Bohlmann and Zeisberg.[2] IR $\nu_{max}^{CCl_4}$ cm^{-1}: 2935, 2855, 2803, 2770 (Bohlmann band), 1738, 1720 (C=O). ^{13}C-NMR ($CDCl_3$) δ: 23.32 (t), 23.65 (t), 25.41 (t), 25.52 (t), 29.86 (t), 34.90 (t), 51.88 (d), 54.39 (dd), 54.63 (d), 55.13 (dd), 55.92 (t), 62.16 (dd), 66.64 (d), 66.77 (d), 213.16 (s). MS *m/z*: 248 (M^+), 166, 165, 164, 152, 151, 150, 124, 110, 98 (base peak), 97, 96.

References

1) N. Takatsu, S. Ohmiya, and H. Otomasu, *Chem. Pharm. Bull.*, **35**, 891 (1987).
2) F. Bohlmann and R. Zeisberg, *Chem. Ber.*, **108**, 1043 (1975).
3) E. E. van Tamelen and R. L. Foltz, *J. Am. Chem. Soc.*, **82**, 2400 (1960).
4) A. D. Kinghorn, M. F. Balandrin, and L.-J. Lin, *Phytochemistry*, **21**, 2269 (1982).

[Chem. Pharm. Bull. 35(12)4993—4995(1987)]

Studies on *Cerbera*. V.[1] Minor Glycosides of 17α-Digitoxigenin from the Stems of Genus *Cerbera*

TATSUO YAMAUCHI,*[,a] FUMIKO ABE,[a] and ALFRED S. C. WAN[b]

Faculty of Pharmaceutical Sciences, Fukuoka University,[a] 8–19–1 Nanakuma, Jonan-ku, Fukuoka 814–01, Japan and Department of Pharmacy, Faculty of Science, National University of Singapore,[b] 10 Kent Ridge Crescent, Singapore 0511

(Received June 19, 1987)

17α-Digitoxigenin apiosyl-glucosyl-thevetoside and cellobiosyl-thevetoside were isolated, together with known biosides and triosides, from the stems of *Cerbera manghas* L.

Keywords——*Cerbera manghas*; *Cerbera odollam*; Apocynaceae; cardenolide; cardenolide apioside; 17α-digitoxigenin cellobiosyl-thevetoside

In the preceding paper, we described the isolation of glucos-3-ulosyl-thevetosides of 17α-digitoxigenin and 17α-tanghinigenin, and of cerleaside A (oleagenin α-L-thevetoside) from the air-dried leaves of *Cerbera manghas* L. and *C. odollam* GAERTN.[2] Cerleaside B (oleagenin β-D-glucosyl-(1→4)-α-L-thevetoside) was obtained from the fresh leaves of *C. odollam*, and a gentiotriosyl-thevetoside of digitoxigenin was isolated from the fresh leaves of *C. manghas*.[1] Since the oleagenin glycosides, cerleaside A[2] and cerleaside B,[1] formed part of the major glycosides in the leaves of *C. odollam*, we have examined the glycosides from the stems of the two species. This paper deals with the isolation of 17α-digitoxigenin glycosides composed of apiose, glucose and thevetose in the sugar moiety (**1**), cellobiosyl-thevetoside (**2**), and gentiobiosyl-thevetoside (**3**), along with other known biosides, glucosyl-thevetosides of digitoxigenin (**4**), 17α-digitoxigenin (**5**), tanghinigenin (**6**), 17α-tanghinigenin (**7**) and oleagenin (cerleaside B) (**8**), and triosides, gentiobiosyl-thevetoside of digitoxigenin (thevetin B) (**9**), tanghinigenin (**10**) and 2′-*O*-acetyl-thevetin B (**11**).[3]

Compound **1**, showing intermediate polarity between biosides and triosides on thin layer chromatography (TLC), was isolated as a solid from the stems of *C. manghas*. Since the negative fast atom bombardment (FAB)-mass spectrum (MS) afforded the $(M-1)^-$ peak at *m/z* 827 and $(M-C_5H_8O_4-1)^-$ peak at *m/z* 695, **1** was considered to be a trioside having a pentose as the terminal sugar. In the carbon-13 nuclear magnetic resonance (^{13}C-NMR) spectrum of **1**, the signals due to **5** were assignable; there was a downfield shift of C-6 of the glucose to which the terminal sugar is attached. The carbon signals of the pentose moiety observed at δ 111.1 (d), 80.3 (s), 77.8 (d), 75.0 (t), and 65.8 (t) and characteristic proton signals at δ 4.16 (2H, s), 4.34 and 4.56 (1H each, d, $J=9$ Hz) in the proton nuclear magnetic resonance (^{1}H-NMR) spectrum suggest the terminal pentose to be D-apiose.[4] After acid hydrolysis of **1** with 0.5 N H_2SO_4–50% dioxane, apiose, **5**, and **5**-anhydride were detected on TLC.

Compound **2** showed the same *Rf* value as **9** (thevetin B) on TLC. In the negative FAB-MS, the peaks of $(M-1)^-$, $(M-\text{hexose}-1)^-$, $(M-(2\times\text{hexose})-1)^-$, and $(\text{genin}-1)^-$ were observed at *m/z* 857, 695, 533 and 373, respectively, suggesting **2** to be a trioside composed of hexobiosyl-thevetose. The proton and carbon signals due to an aglycone moiety were assignable to 17α-digitoxigenin. Since **2** was hydrolyzed to **5** with β-glucosidase, and the signals due to the hexobiosyl moiety were identified as those of methyl β-cellobioside on the

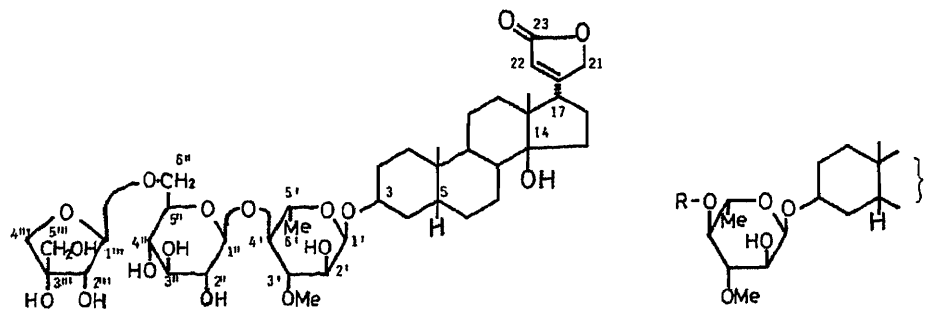

1

2 : R=—Glc$\overset{4\beta}{\leftarrow}$Glc

3 : R=—Glc$\overset{6\beta}{\leftarrow}$Glc

Chart 1

basis of the ^{13}C-NMR spectra,[5] **2** was determined to be 17α-digitoxigenin β-cellobiosyl-(1→4)-α-L-thevetoside.

Compound **3** was considered to be the 17α-isomer of **9** based on the ^{1}H- and ^{13}C-NMR spectra. The structure was confirmed by enzymic hydrolysis, yielding **5**.

Since the isolation of apiin, many glycosides having an apiosyl moiety have been reported. The occurrence of apiose in a cardenolide glycoside, **1**, is reported here for the first time. Compound **1** is named cerapioside. As with the glycosides from the leaves, the oleagenin glycoside was included among the major glycosides in the stems of *C. odollam*.

Experimental

Melting points, optical rotations, ^{1}H-NMR, ^{13}C-NMR and MS data were obtained as described in the preceding paper.[1] Column chromatography and TLC were conducted with the following solvent systems: solv. 1, $CHCl_3$–MeOH–H_2O (7:3:1, bottom layer); solv. 2, EtOAc–MeOH–H_2O (4:1:0.5); solv. 3, CH_3CN–H_2O. Spots on the TLC plate were detected by spraying diluted H_2SO_4 and heating the plate. High-performance liquid chromatography (HPLC) was run on a Waters ALC 200 equipped with a Radial Pack C_{18} column.

Isolation of 1, 2 and 3 from the Stems of *C. manghas*.——Air-dried stems of *C. manghas* L., cultivated in the greenhouse of Fukuoka University and harvested in Oct. 1986 (6 kg) were powdered and percolated with MeOH. The MeOH percolate was treated in the same manner as described in the preceding paper.[1] The bioside fraction was subjected to silica gel column chromatography with solv. 1 and solv. 2, reversed-phase column chromatography with RQ-1 (Fuji gel, solv. 3) and also HPLC (solv. 3) to isolate **1** (17 mg), **2** (6 mg), **3** (250 mg), **4** (85 mg), **5** (220 mg), **9** (200 mg), and **11** (7 mg).

Air-dried stems of *C. odollam* GAERTN. collected in Singapore in Feb. 1987 (1.2 kg), were treated in the same manner as described in the preceding paper[1] and the following glycosides were obtained; **3** (8 mg), **4** (25 mg), **5** (20 mg), **6** (80 mg), **7** (20 mg), **8** (13 mg), **9** (40 mg), and **10** (8 mg).

17α-Digitoxigenin β-D-Apiosyl-(1→6)-β-D-glucosyl-(1→4)-α-L-thevetoside (1) and Acid Hydrolysis of 1——A solid, $[\alpha]_D^{26}$ −60.3° (c=0.85, MeOH). Negative FAB-MS m/z: 827 ($C_{41}H_{64}O_{17}-1$)$^-$, 695 (M − apiose − 1)$^-$, 533 (695 − Glc)$^-$, 373 (aglycone − 1)$^-$. ^{1}H-NMR δ (ppm) (pyridine-d_5): 0.85, 1.19 (3H each, s, H-18, H-19), 1.80 (3H, d, J=6 Hz, H-6′), 3.42 (1H, t, J=9 Hz, H-17), 3.94 (3H, s, 3′-OMe), 4.16 (2H, s, H-5‴), 4.34, 4.56 (1H each, d, J=9 Hz, H-4‴), 4.71 (1H, d, J=2 Hz, H-2‴), 4.82, 4.97 (1H each, dd, J=18, 1 Hz, H-21a, b), 5.16 (1H, d, J=4 Hz, H-1′), 5.31 (1H, d, J=8 Hz, H-1″), 5.77 (1H, d, J=2 Hz, H-1‴), 6.12 (1H, d, J=1 Hz, H-22). ^{13}C-NMR δ (ppm) (pyridine-d_5): 30.3 (C-1), 26.8, 27.1 (C-2, C-6), 73.7, 73.6 (C-3, C-2′), 31.0 (C-4), 36.8 (C-5), 21.5 (C-7), 41.7 (C-8), 36.0 (C-9), 35.4 (C-10), 20.6 (C-11), 31.6 (C-12), 49.4 (C-13), 85.2 (C-14), 31.0 (C-15), 24.9 (C-16), 48.9 (C-17), 18.6, 18.5 (C-18, C-6′), 23.8 (C-19), 172.7 (C-20), 74.1 (C-21), 116.6 (C-22), 174.1 (C-23), 98.5 (C-1′), 85.3 (C-3′), 81.9 (C-4′), 67.5 (C-5′), 60.9 (3′-OMe), 104.9 (C-1″), 75.6 (C-2″), 78.3 (C-3″), 71.9 (C-4″), 76.9 (C-5″), 68.9 (C-6″), 111.1 (C-1‴), 77.8 (C-2‴), 80.3 (C-3‴), 75.0 (C-4‴), 65.8 (C-5‴). Compound **1** (3 mg) was refluxed with 0.5 N H_2SO_4–50% dioxane for 1 h, and the mixture was deacidified with IRA-410, and diluted with H_2O. The mixture was then extracted with BuOH. The BuOH extract was concentrated *in vacuo* and examined by TLC (solv. 1, *Rf* 0.65, 0.70) (**5**, 0.65; **5**-anhydride, 0.70). The H_2O layer was again evaporated to dryness *in vacuo* and the residue was examined by TLC (solv. 1, *Rf* 0.35, D-apiose: 0.35; solv. 2, *Rf* 0.45, D-apiose: 0.45).

17α-Digitoxigenin β-Cellobiosyl-(1→4)-α-L-thevetoside (2) and Enzymic Hydrolysis of 2——A solid, $[\alpha]_D^{24}$ −36.6° (c=0.25, MeOH). Negative FAB-MS m/z: 857 ($C_{42}H_{66}O_{18}-1$)$^-$, 695 (857-Glc)$^-$, 533 (695-Glc)$^-$, 373 (aglycone−1)$^-$. ^{1}H-NMR δ (ppm) (pyridine-d_5): 0.85, 1.19 (3H each, s, H-18, H-19), 1.63 (3H, d, J=6 Hz, H-6′), 3.42 (1H, t, J=9 Hz, H-17β), 3.95 (3H, s, 3′-OMe), 4.82, 4.97 (1H each dd, J=18, 1 Hz, H-21a, b), 5.18 (1H, d, J=3 Hz, H-1′), 5.19 (1H, d, J=8 Hz, H-1‴), 5.32 (1H, d, J=8 Hz, H-1″), 6.12 (1H, d, J=1 Hz, H-22). ^{13}C-NMR δ (ppm) (pyridine-d_5): 30.3 (C-1), 26.8, 27.1 (C-2, C-6), 73.7, 73.8 (C-3, C-2′), 31.0 (C-4, C-15), 36.8 (C-5), 21.5 (C-6), 41.7 (C-7), 36.0 (C-9), 35.4 (C-10), 20.6 (C-11), 31.6 (C-12), 49.3 (C-13), 85.2 (C-14), 24.9 (C-16), 48.9 (C-17), 18.5 (C-18, C-6′), 23.8 (C-19), 172.7 (C-20), 74.1 (C-21), 116.6 (C-22), 174.2 (C-23), 98.5 (C-1′), 85.3 (C-3′), 81.8 (C-4′), 67.3 (C-5′), 61.0 (3′-OMe), 104.9 (C-1″), 74.7 (C-2″), 76.5 (C-3″), 81.8 (C-4″), 76.3 (C-5″), 62.4 (C-6″), 104.6 (C-1‴), 75.2 (C-2‴), 78.4 (C-3‴), 71.6 (C-4‴), 78.2 (C-5‴), 62.5 (C-6‴). All signals of **2** taken in CD_3OD were in good agreement with those in the literature.[5] Compound **2** (5 mg) was dissolved in 20% EtOH (2 ml) and was shaken with cellulase (Sigma Chem. Co., Ltd.) (5 mg) at 38 °C for 5 h. The mixture was extracted with BuOH and the BuOH extract was examined by TLC and HPLC in parallel with authentic **5** [TLC: solv. 1, Rf 0.65 (**5**, 0.65). HPLC: solv. 30% CH_3CN–H_2O, 1 ml/min, t_R 7.6 min (**5**, 7.6 min)].

17α-Digitoxigenin β-Gentiobiosyl-(1→4)-α-L-thevetoside (3) and Enzymic Hydrolysis of 3——A solid, $[\alpha]_D^{28}$ −55.2° (c=1.3, MeOH). FAB-MS m/z: 881 $(M+Na)^+$. ^{1}H-NMR δ (ppm) (pyridine-d_5): 0.85, 1.19 (3H each, s, H-18, H-19), 1.78 (3H, d, J=6 Hz, H-6′), 3.42 (1H, t, J=9 Hz, H-17β), 4.82, 4.98 (1H each, dd, J=18, 1 Hz, H-21a, b), 5.12 (1H, d, J=3 Hz, H-1′), 5.13 (1H, d, J=8 Hz, H-1‴), 5.32 (1H, d, J=8 Hz, H-1″), 6.13 (1H, d, J=1 Hz, H-22). ^{13}C-NMR δ (ppm) (pyridine-d_5): 30.4 (C-1), 26.8, 27.1 (C-2, C-6), 73.7 (C-3, C-2′), 31.0 (C-4, C-16), 36.9 (C-5), 21.6 (C-7), 41.7 (C-8), 36.1 (C-9), 35.5 (C-10), 20.7 (C-11), 31.7 (C-12), 49.4 (C-13), 85.2 (C-14), 25.0 (C-16), 48.9 (C-17), 18.6 (C-18, C-6′), 23.9 (C-19), 172.9 (C-20), 74.1 (C-21), 116.6 (C-22), 174.2 (C-23), 98.5 (C-1′), 85.5 (C-3′), 81.4 (C-4′), 67.6 (C-5′), 61.0 (3′-OMe), 105.6, 104.8 (C-1″, C-1‴), 75.6, 75.2 (C-2″, C-2‴), 78.4 (×2), 78.3 (C-3″, C-3‴, C-5‴), 71.7, 72.1 (C-4″, C-4‴), 77.1 (C-5″), 70.8 (C-6″), 62.9 (C-6‴). Compound **3** (5 mg) was hydrolyzed with cellulase (5 mg) as described above. The BuOH extract showed the same Rf value and t_R as authentic **5** [TLC: solv. 1, Rf 0.65 (**5**, 0.65). HPLC: solv. 30% CH_3CN–H_2O, 1 ml/min, t_R 7.6 min (**5**, 7.6 min)].

Acknowledgements We thank Misses Y. Iwase and S. Hachiyama of Fukuoka University, for NMR and MS measurements. This work was supported by the JSPS-NUS Scientific Cooperation Programme.

References

1) Part IV: T. Yamauchi, F. Abe, and A. S. C. Wan, *Chem. Pharm. Bull.*, **35**, 4813 (1987).
2) T. Yamauchi, F. Abe, and A. S. C. Wan, *Chem. Pharm. Bull.*, **35**, 2744 (1987).
3) F. Abe and T. Yamauchi, *Chem. Pharm. Bull.*, **25**, 2744 (1977).
4) D. H. Ball, F. H. Bissett, I. L. Klundt, and L. Long, Jr., *Carbohydr. Res.*, **17**, 165 (1971); M. Nagai, M. Kubo, K. Takahashi, M. Fujita, and T. Inoue, *Chem. Pharm. Bull.*, **31**, 1923 (1983).
5) T. Usui, N. Yamaoka, N. Matsuda, K. Tuzimura, H. Sugiyama, and S. Seto, *J. Chem. Soc., Perkin Trans. 1*, **1973**, 2425; B. Gering and P. J. M. Wichtl, *Phytochemistry*, **26**, 753 (1987).

[Chem. Pharm. Bull. 35(12)4996—4999(1987)]

Occurrence of Bufogenin Conjugates in the Skin of Korean Toad[1)]

KAZUTAKE SHIMADA, JAI SEUP RO,[2)] CHIYOMI KANNO and TOSHIO NAMBARA*

Pharmaceutical Institute, Tohoku University, Aobayama, Sendai 980, Japan

(Received July 8, 1987)

The occurrence of two new bufogenin conjugates, desacetylcinobufagin 3-succinyl-L-arginine ester and cinobufagin 3-sulfate, together with two known gamabufotalitoxin homologs and resibufogein 3-sulfate, in the skin of Korean toad, *Bufo bufo gargarizans* CANTOR, is reported. Their structures were elucidated by degradative means and/or direct comparison with authentic samples. These bufogenin conjugates were assayed for inhibitory activity towards guinea pig heart Na^+, K^+-adenosine triphosphatase.

Keywords——*Bufo bufo gargarizans*; toad venom; bufogenin conjugate; desacetylcinobufagin 3-succinyl-L-arginine ester; cinobufagin 3-sulfate; Na^+,K^+-ATPase inhibition

In the previous paper of this series, we reported the isolation of cinobufagin 3-glutaryl-L-arginine ester together with seven known bufogenins and eight known bufotoxins from the dried body of Korean toad, *Bufo bufo gargarizans* CANTOR.[3)] The present paper deals with further studies on the isolation and characterization of bufogenin conjugates from the skin of Korean toad. The isolated conjugates were assayed for inhibitory activity towards guinea pig heart Na^+, K^+-adenosine triphosphatase (Na^+, K^+-ATPase; EC 3.6.1.3).

Twenty-six toads obtained in South Korea were sacrificed by freezing in dry ice, and the skins were immediately flayed off and extracted with ethanol. The ethanolic extract was concentrated *in vacuo* and the residue was subjected to column chromatography on silica gel. Further separation of bufogenin conjugates was effected by high-performance liquid chromatography (HPLC) using a reversed-phase column.

A new bufotoxin, mp 230—232 °C (dec.), $[\alpha]_D^{23}$ +18.9°, was isolated as a colorless amorphous substance. The compound gave negative ninhydrin and positive Sakaguchi tests. Upon hydrolysis with 6N hydrochloric acid, arginine was produced and identified by thin-layer chromatography (TLC). On being subjected to enzymic hydrolysis with a hog pancreas lipase preparation followed by methylation with diazomethane, the bufotoxin afforded desacetylcinobufagin 3-succinate methyl ester (**3b**), which was unequivocally characterized by direct comparison with an authentic sample.[4)] These findings together with the elemental analysis supported the assignment of the structure desacetylcinobufagin 3-succinyl-L-arginine ester (**4b**) for the new bufotoxin. The absolute configuration of arginine was defined by the substrate specificity of the enzyme used.[3)] Although the occurrence of desacetylcinobufagin 3-succinate (**2b**) in the skin of Japanese toad has previously been disclosed,[4)] this is the first reported isolation of **4b** from the toad venom. Gamabufotalin 3-adipoyl-L-arginine and -pimeloyl-L-arginine esters were also separated and characterized by direct comparison with authentic samples.[4)]

In addition, bufogenin 3-sulfates were separated by the chromatographic methods reported in the previous paper.[4)] Purification by HPLC on a reversed-phase column provided a new bufogenin sulfate as a colorless oily substance. The compound was positive with the

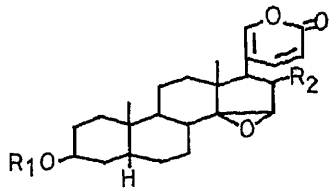

1: $R_1 = H$
2: $R_1 = CO(CH_2)_2COOH$
3: $R_1 = CO(CH_2)_2COOCH_3$
4: $R_1 = CO(CH_2)_2CONHCH(CH_2)_3NHCNH_2$ (COOH; NH)
5: $R_1 = SO_3Na$

a: $R_2 = H$
b: $R_2 = OH$
c: $R_2 = OAc$

Chart 1

TABLE I. Inhibition of Guinea Pig Heart Na^+,K^+-ATPase by Bufogenins and Their Conjugates

3-Substituent	Ouabain[a]	Genin		
		R[b]	DAC	C
	157±16.3	1480±240[c] (**1a**, 1.00)[d]	2490±210 (**1b**, 1.00)	79.1±3.48[7] (**1c**, 1.00)
suc-OH		>10000 (**2a**,[4] >0.15)	4250±350 (**2b**,[4] 0.59)	3100±550 (**2c**,[3] 0.03)
suc-L-Arg·OH		7300±670 (**4a**,[4] 0.20)	5030±270 (**4b**, 0.50)	292±19.6[7] (**4c**, 0.27)
SO_3Na		>10000 (**5a**,[5] >0.15)		4860±780 (**5c**, 0.02)

a) Reference compound. *b*) Abbreviations: R=resibufogenin, DAC=desacetylcinobufagin, C=cinobufagin, suc=$CO(CH_2)_2CO$-. *c*) Mean±S.E. ($\times 10^{-8}$ M, $n=3$). *d*) Figures in parentheses express the compound number listed in Chart 1 and the potency relative to the respective genin.

barium-rhodizonate reagent (sulfate ion). Upon hydrolysis in the usual manner, the sulfate yielded cinobufagin (**1c**), which was identified by HPLC and mass spectrometry. These data prompted us to synthesize cinobufagin 3-sulfate (**5c**), which proved to be identical with the natural product. Resibufogenin 3-sulfate (**5a**) was also isolated and identified by direct comparison with an authentic sample.[5]

In order to clarify the structure–activity relationship the isolated bufogenin conjugates and related compounds were tested for inhibitory activity towards Na^+, K^+-ATPase.[6] The molar concentrations of these compounds together with ouabain giving half-maximal inhibition (I_{50}) of Na^+, K^+-ATPase from guinea pig heart are listed in Table I. Among the bufogenins (**1a–c**) having the 14β,15β-epoxy structure, **1c** exhibited the most potent inhibitory activity. Bufogenin succinates (**2a–c**), succinyl-L-arginine esters (**4a–c**) and sulfates (**5a,c**) showed lower activity than the respective genin. These results are compatible with those presented in the previous report.[7]

Further studies on cardiac steroids in toad venoms are being conducted, and the details will be reported elsewhere.

Experimental

All melting points were taken on a micro hot-stage apparatus and are uncorrected. Optical rotations were measured with a JASCO DIP-4 automatic polarimeter. Mass spectral (MS) measurements were run on a Hitachi M-

52G spectrometer. Proton nuclear magnetic resonance (^{1}H-NMR) spectra were recorded using tetramethylsilane as an internal standard on a JEOL FX-100 spectrometer at 100 MHz. Abbreviations: s=singlet, d=doublet and dd=doublet of doublets. Silica gel HF_{254} and Silica gel 60 (70—230 mesh) (E. Merck AG, Darmstadt) were used for preparative TLC and column chromatography, respectively. A hog pancreas lipase preparation and other reagents were purchased from Sigma Chemicals Co. (St. Louis, MO) and Nakarai Chemicals Ltd. (Kyoto), respectively. HPLC was carried out on a Waters ALC/GPC 202 chromatograph equipped with an ultraviolet (UV) detector (280 nm) and a Develosil ODS-5 column (5 μm: 15 cm × 0.4 cm i.d.) (Nomura Chemical Co., Ltd, Seto) at a flow rate of 1 ml/min.

Extraction of Steroidal Components——Twenty-six toads (*Bufo bufo gargarizans* CANTOR) were collected in the middle zone of South Korea[8] and sacrificed by freezing in dry ice. The skins were immediately flayed off and extracted with EtOH (6 l) for 4 months. After removal of insoluble materials by filtration through a Celite layer, the filtrate was concentrated *in vacuo* below 50 °C to give a brown oily residue (9.67 g).

Isolation of Bufogenin Conjugates——The residue obtained was chromatographed on Silica gel 60 (37 cm × 2.5 cm i.d.) with AcOEt–MeOH (2 : 1) as an eluent. Further purification of the dried eluate by HPLC with CH_3CN–0.25% $(NH_4)_2CO_3$ (1 : 3) gave a new bufogenin sulfate (**5c**; 1 mg, t_R 11 min) as a colorless oily substance. Resibufogenin 3-sulfate (**5a**; 1 mg, t_R 9 min) was also obtained by HPLC in the same way. Its chromatographic behavior was identical with that of an authentic sample.[5] HPLC: CH_3CN–1.5% AcONa (pH 5.0) (1 : 3, t_R 14.5 min); tetrahydrofuran–1.5% AcONa (pH 5.0) (1 : 4, t_R 15.5 min).

Further chromatography on Silica gel 60 with AcOEt–MeOH (1 : 1) as described above gave a crude bufotoxin mixture, which in turn was purified by HPLC with MeOH–H_2O (5 : 4; t_R 10 min). Recrystallization of the dried eluate from MeOH-ether gave a new bufotoxin (**4b**) as a colorless amorphous substance (10 mg). Two known bufotoxin homologs were also obtained by HPLC with MeOH–H_2O (5 : 4); gamabufotalin 3-adipoyl-L-arginine ester (3 mg; t_R 3.5 min) and gamabufotalin 3-pimeloyl-L-arginine ester (3 mg; t_R 5.5 min). These bufotoxin homologs were identical with authentic samples with respect to ^{1}H-NMR spectra and chromatographic behavior.[9]

Structure Elucidation of Compound 4b——The compound showed the following physical and chemical properties: ninhydrin test, negative; Sakaguchi test, positive. mp 230—232 °C (dec.). $[\alpha]_D^{23}$ +18.9° (c=0.13, $CHCl_3$–MeOH (1 : 1)). *Anal.* Calcd for $C_{34}H_{48}N_4O_9 \cdot 3/2H_2O$: C, 59.71; H, 7.51; N, 8.19. Found: C, 59.79; H, 7.62; N, 7.87. ^{1}H-NMR ($CD_3OD/CDCl_3$)δ: 0.80 (3H, s, 18-CH_3), 1.00 (3H, s, 19-CH_3), 2.60 (4H, br s, $CO(CH_2)_2CO$), 3.58 (1H, s, 15α-H), 4.70 (1H, d, J=10 Hz, 16α-H), 5.08 (1H, br s, 3α-H), 6.20 (1H, d, J=10 Hz, 23-H), 7.25 (1H, d, J=2 Hz, 21-H), 8.02 (1H, dd, J=10, 2 Hz, 22-H). Compound **4b** (<1 mg) was heated with 6 N HCl (0.5 ml) in a sealed tube at 110 °C for 5 h. A portion of the resulting solution was subjected to two-dimensional TLC on Silica gel G (E. Merck AG) with $CHCl_3$–MeOH–17% NH_4OH (2 : 2 : 1) and phenol–H_2O (3 : 1) as developing solvents, and arginine was detected by means of the ninhydrin test.

Compound **4b** (1 mg) was dissolved in MeOH–1% NaCl (1 : 9) (2.5 ml) and incubated with a hog pancreas lipase preparation (1 mg) at 37 °C for 2 h. The incubation mixture was extracted with AcOEt. The organic phase was washed with H_2O, dried over anhydrous Na_2SO_4, and evaporated *in vacuo*. The residue was redissolved in MeOH (0.1 ml) and treated with an ethereal solution of CH_2N_2. After usual work-up, the crude product obtained was purified by preparative TLC with benzene–AcOEt (1 : 1) as a developing solvent. The adsorbent corresponding to the spot of *Rf* 0.23 was eluted with AcOEt to give **3b** (<1 mg) as a colorless amorphous substance. The product was identical with an authentic sample[4] with respect to MS and chromatographic behavior. MS *m/z*: 514 (M^+), 133, 115. HPLC: CH_3CN–H_2O (1 : 1, t_R 8.5 min). TLC: cyclohexane–acetone–$CHCl_3$ (10 : 3 : 3, *Rf* 0.33).

Structure Elucidation of Compound 5c——The compound showed a positive Ba^{2+}-rhodizonate test. An aqueous solution of **5c** (*ca.* 100 μg) was adjusted to pH 1.0 with 5% H_2SO_4, saturated with NaCl, and extracted with AcOEt (2 ml). The organic layer was allowed to stand at 37 °C for 2 h. The resulting solution was washed with 5% $NaHCO_3$ and H_2O, dried over anhydrous Na_2SO_4, and evaporated. The residue was identical with **1c** with respect to MS and chromatographic behavior. MS *m/z*: 442 (M^+). HPLC: CH_3CN–H_2O (2:1, t_R 6.5 min). Compound **5c** showed chromatographic behavior identical with that of a synthetic sample. HPLC: MeOH–1.5% AcONa (pH 5.0) (1 : 1, t_R 15.5 min), tetrahydrofuran–1.5% AcONa (pH 5.0) (1 : 4, t_R 19.5 min).

Synthesis of 5c——Compound **1c** (5 mg) in pyridine (2 ml) was treated with sulfur trioxide–pyridine complex (10 mg) under ice-cooling for 5 min and then at room temperature for 90 min. The reaction mixture was poured into ice-water (10 ml). The resulting solution was adsorbed on Amberlite XAD-2 resin (10 cm × 1.5 cm i.d.), washed with H_2O and then eluted with MeOH. The eluate was concentrated *in vacuo* and the residue in H_2O (0.5 ml) was passed through a Dowex 50W-X8 (Na^+ form) column (2.5 cm × 0.5 cm i.d.). After evaporation of the solvent, the desired compound was obtained as a colorless oily substance (**5c**, 3 mg). The compound showed a positive Ba^{2+}-rhodizonate test and its homogeneity was confirmed by HPLC with MeOH–0.5% $(NH_4)_2CO_3$ (5 : 4, t_R 8 min). ^{1}H-NMR ($CDCl_3/CD_3CD$) δ: 0.81 (3H, s, 18-CH_3), 0.98 (3H, s, 19-CH_3), 1.88 (3H, s, $OCOCH_3$), 2.85 (1H, d, J=10 Hz, 17α-H), 3.70 (1H, s, 15α-H), 4.72 (1H, br s, 3α-H, 5.45 (1H, d, J=10 Hz, 16α-H), 6.21 (1H, d, J=10 Hz, 23-H), 7.22 (1H, d, J=3 Hz, 21-H), 7.95 (1H, dd, J=10, 3 Hz, 22-H). On being subjected to solvolysis as described above, the compound gave **1c** as a sole product.

Assay for the Inhibition of Na^+, K^+-ATPase——The samples were tested for inhibitory activity towards Na^+,

K^+-ATPase (10 μmol Pi/mg protein) from guinea pig heart by the method described in the previous paper.[6] The concentration of a compound required for 50% inhibition was defined as the I_{50} value.

Acknowledgement The authors express their thanks to the staff of the central analytical laboratory of this Institute for elemental analyses and spectral measurements.

References and Notes

1) Part CCXXXV of "Studies on Steroids" by T. Nambara; Part CCXXXIV: H. Hosoda, R. Tsukamoto, M. Shishido, W. Takasaki and T. Nambara, *Chem. Pharm. Bull.*, **35**, 4856 (1987). In this paper deacetylcinobufagin-3-*O*-ylsuccinyl-L-arginine was named desacetylcinobufagin 3-succinyl-L-arginine ester. Other related compounds were also similarly expressed.
2) On leave from the College of Pharmacy, *Chung-Buk National University, Cheongju 310, Korea.*
3) K. Shimada, J. S. Ro, K. Ohishi and T. Nambara, *Chem. Pharm. Bull.*, **33**, 2767 (1985).
4) K. Shimada, Y. Fujii, E. Yamashita, Y. Niizaki, Y. Sato and T. Nambara, *Chem. Pharm. Bull.*, **25**, 714 (1977).
5) K. Shimada and T. Nambara, *Chem. Pharm. Bull.*, **27**, 1881 (1979).
6) K. Shimada, K. Ohishi and T. Nambara, *J. Pharmacobio-Dyn.*, **8**, 64 (1985).
7) K. Shimada, K. Ohishi, H. Fukunaga, J. S. Ro and T. Nambara, *J. Pharmacobio-Dyn.*, **8**, 1054 (1985).
8) Identification of the species was done by Dr. K. S. Lee, College of Pharmacy, Chung-Buk National University, to whom our thanks are due.
9) K. Shimada, M. Hasegawa, K. Hasebe, Y. Fujii and T. Nambara, *J. Chromatogr.*, **124**, 79 (1976).

[Chem. Pharm. Bull. 35(12)5000—5003(1987)]

One-Step Synthesis of a Cortisol Derivative for Radioiodination and Application of the ^{125}I-Labeled Cortisol to Radioimmunoassay

ATSUSHI SUGII,*,[a] NAOTAKE OGAWA,[a] TAKURO KAWANISHI,[a] TERUHISA UMEDA,[b] and TATSUO SATO[b]

Faculty of Pharmaceutical Sciences, Kumamoto University,[a] 5–1 Oe-honmachi, Kumamoto 862, Japan and Department of Internal Medicine III, Kumamoto University School of Medicine,[b] 1–1–1 Honjo, Kumamoto 862, Japan

(Received April 18, 1987)

A one-step synthesis of a cortisol derivative for radioiodination is presented. The radioimmunoassay for cortisol using the bridge heterologous ^{125}I-labeled antigen was more sensitive than that using a bridge homologous antigen. Cortisol levels in saliva and serum were easily determined by direct radioimmunoassay with the proposed ^{125}I-labeled antigen.

Keywords——cortisol; cortisol derivative one-step synthesis; ^{125}I-labeled cortisol; direct radioimmunoassay; saliva; serum

In radioimmunoassay (RIA) for haptens such as steroids and pharmaceuticals, ^{3}H- or ^{125}I-labeled haptens have been widely used. Gamma-emitting ^{125}I is preferred for labeling of the hapten because it is easy to count. When the hapten does not possess a suitable chemical structure for direct radioiodination, it has to be bound with an appropriate functional group such as an imidazole or phenolic moiety before radioiodination. In this case, a bridge exists between the hapten and the functional group. The difference in the chemical structure of the radiolabeled hapten from the original hapten molecule affects the sensitivity and specificity of the RIA.[1] The importance of the combination of antiserum and enzyme-labeled steroid have also been pointed out in enzyme immunoassay.[2]

Using cortisol as a hapten, we prepared ^{125}I-labeled antigens having a bridge homologous or heterologous to that of the immunogen. For the preparation of the bridge heterologous antigen, a new type of coupling reagent, which can be applied to an one-step synthesis of derivatives for radioiodination, is proposed. A direct RIA procedure for cortisol in saliva and serum is presented as an application of the ^{125}I-labeled bridge heterologous antigen.

Experimental

All unlabeled steroids were obtained from Sigma Chem. Co. (U.S.A.), Na^{125}I was a gift from Daiichi Radioisotope Laboratory (Japan) and [1,2,6,7-^{3}H]cortisol (100 Ci/mmol) was purchased from Amersham (England). All other reagents were of reagent grade and were used without further purification. (^{1}H-NMR) spectra were determined on a JEOL 60H spectrometer with tetramethylsilane as an internal standard.

Preparation of Antiserum against Cortisol——Cortisol-3-*O*-carboxymethyl-oxime (F3-CMO)[3] was conjugated to bovine serum albumin (BSA) according to the method of Erlanger *et al.*[4] (the number of cortisol molecules linked to one molecule of BSA was determined to be 20). The conjugate (1 mg) was dissolved in 0.5 ml of saline and emulsified with an equal volume of complete·Freund's adjuvant. A rabbit was given three booster injections subcutaneously at intervals of two weeks and thereafter injections once a month. Blood was collected 10 months after the initial injection and centrifuged at 2000 *g* for 10 min. The antiserum was stored at −20 °C. The titer was

approximately 20000.

Preparation of Coupling Reagent for Derivatization of Cortisol——3-(4-Imidazolyl)propionic Acid Hydrazide (IPH): Five grams of urocanic acid was dissolved in 72.4 ml of 0.5 N NaOH and catalytic reduction was carried out by using 0.5 g of a 10% palladium-on-charcoal catalyst for 2 h in the usual way. The reaction mixture was filtered and adjusted to pH 2 with concentrated HCl, and then concentrated under reduced pressure on a water bath. EtOH was added to the residue and the mixture was filtered. The filtrate was concentrated under reduced pressure and the residue, crude 3-(4-imidazolyl)propionic acid HCl, was esterified by heating to reflux with 50 ml of MeOH–HCl for 2 h. After removal of the excess HCl under reduced pressure, 7.2 g of 100% hydrazine hydrate was added and the whole was heated at 70°C for 2 h. The reaction mixture was concentrated to dryness in a rotary evaporator. EtOH was added to the residue and the mixture was filtered to remove hydrazine HCl. The filtrate was passed through an anion exchange resin column (Amberlite IR-45, OH form, 15 g, 1.5 × 20 cm) to remove HCl. The effluent was concentrated to dryness under reduced pressure and the residue was recrystallized from EtOH. Yield 0.8 g, mp 142 °C. ^{1}H-NMR (CD_3OD) δ: 2.31 (4H, m, $-CH_2CH_2-$), 6.49 (1H, s, imida 5H), 7.24 (1H, s, imida 2H). *Anal.* Calcd for $C_6H_{10}N_4O$: C, 46.74; H, 6.54; N, 36.34. Found: C, 46.77; H, 6.39; N, 35.78.

Preparation of Cortisol Derivatives——Cortisol-3-[3-(4-imidazolyl)propionic Acid] Hydrazone (F3-IPH): Cortisol (157 mg) and IPH (100 mg) were dissolved in 2 ml of MeOH and refluxed for 6 h. Purification by thin layer chromatography (TLC) (Kiesel-gel 60) using $CHCl_3$–MeOH–H_2O (24 : 7 : 1) as a developing solvent gave F3-IPH (37 mg, recrystallized from MeOH). mp 190°C. ^{1}H-NMR (CD_3OD) δ: 0.51 (3H, s, 18-CH_3), 1.09 (3H, s, 19-CH_3), 5.48 and 5.78 (1H, both s, 4-H, *anti*:*syn*=2 : 1), 6.47 (1H, s, imida 5H), 7.23 (1H, s, imida 2H). *Anal.* Calcd for $C_{27}H_{38}N_4O_5 \cdot 2H_2O$: C, 60.65; H, 7.92; N, 10.48. Found: C, 60.05; H, 7.72; N, 10.40. Cortisol-3-(O-carboxymethyl)oxime-histamine (F3-CMO-his) was prepared from F3-CMO, ethyl chloroformate and histamine according to the method of Allen and Redshaw.[1c]

Radioiodination of Antigens——Antigens were labeled with ^{125}I by the chloramine T procedure of Hunter *et al.*[5] Specific activity (according to the method of Morris[6]): F3-IPH-^{125}I, 700 Ci/mmol; F3-CMO-his-^{125}I, 100 Ci/mmol.

Standard Curves——Standard (cortisol) and antiserum were diluted in 0.1 M phosphate buffer (pH 7.4) containing 0.5% BSA. Radiolabeled antigens were diluted in 0.1 M phosphate buffer (pH 7.4). Radiolabeled antigen (*ca.* 10000 cpm, 0.1 ml) and diluted antiserum (0.1 ml) were added to a series of standard solutions (0.1 ml), and each mixture was incubated overnight at 4°C. After addition of 0.5 ml of dextran-coated charcoal, prepared by mixing dextran T 70 (50 mg) and Norit A (500 mg) in 100 ml of 0.1% gelatin at 4°C, the suspension was vortex-mixed and allowed to stand for 30 min at 4 °C, and then centrifuged at the same temperature for 15 min at 2000 *g*. The radioactivity in the precipitate or supernatant was measured in the usual way.

Direct RIA of Cortisol——The flow sheet of the direct assay is shown in Chart 1. Paired samples of saliva and blood were collected from normal, apparently healthy volunteers. In the study of analytical recovery of cortisol from serum or saliva to which had been added a known amount of cortisol, a 2.5 μl aliquot of normal human pooled serum (Nescol X, Chemo-Sero-Therapeutic Research Inst., Japan) or 0.1 ml of saliva was used. Free cortisol values in sera were determined by the equilibrium dialysis method[7] and the salivary cortisol level was determined by our IPH-RIA method presented here.

Results and Discussion

The structure of the immunogen, antigens, and related compounds are shown in Chart 2. Histamine or tyrosine methyl ester derivatives of steroids have been used as substrates for radioiodination of 3-carboxymethyloxime steroids,[1c,8] but their preparation involves several steps. Hydrazide derivatives of phenolic compounds have also been prepared and treated with steroid.[1d] Histamine forms mono-iodinated derivatives, whereas tyrosine methyl ester (TME) can form, in addition to the mono-iodo derivatives, di-iodinated TME derivatives which have a lower immunoactivity and are less stable.[9] Consequently, we used a histamine tracer. An antigen (F3-IPH) having a heterologous bridge was prepared by coupling cortisol with hydrazide derivatives of imidazole (IPH) and then radioiodinated. The F3-IPH-^{125}I derived from a new coupling reagent (IPH) had high specific activity. The hydrazide group can easily react with the conjugated ketone of cortisol and can subsequently be easily radioiodinated. An antigen (F3-CMO-his) having a bridge homologous structure to the immunogen was prepared by reaction of F3-CMO with histamine, and was derived to F3-CMO-his-^{125}I.

The standard curves for cortisol are shown in Fig. 1. The curve obtained using the radiolabeled bridge heterologous antigen (F3-IPH-^{125}I) was shifted to a region of lower concentration of cortisol and was more sensitive than the rediolabeled bridge homologous

sample or standard solution
+
BB-BSA
} total 0.2 ml
↓ mix
F3-IPH-^{125}I in BB, 0.1 ml
↓ mix
antiserum in BB-BSA, 0.1 ml
↓ mix and incubate overnight at 4°C
3% γ-globulin in BB, 0.1 ml
↓ mix
15% PEG in BB, 1 ml
↓ mix
centrifugation for 20 min at 4°C (2000 *g*)
↓
aspiration of supernatant
↓
counting (precipitation, bound)

BB: 0.5 M borate buffer (pH 8.6)
BB-BSA: 0.5% BSA in BB
PEG: polyethylene glycol 6000

Chart 1. Flow Sheet of IPH-RIA

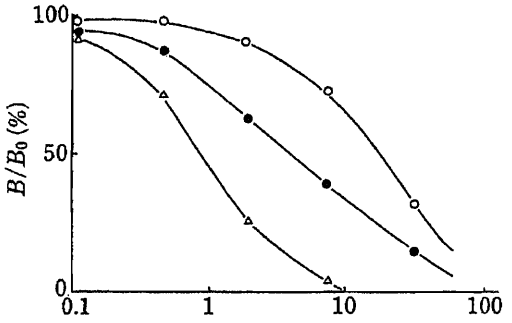

Fig. 1. Semi-logarithmic Standard Curves Obtained with Various Tracers for Cortisol RIA
○, ^{3}H-cortisol; ●, F3-CMO-his-^{125}I; △, F3-IPH-^{125}I.

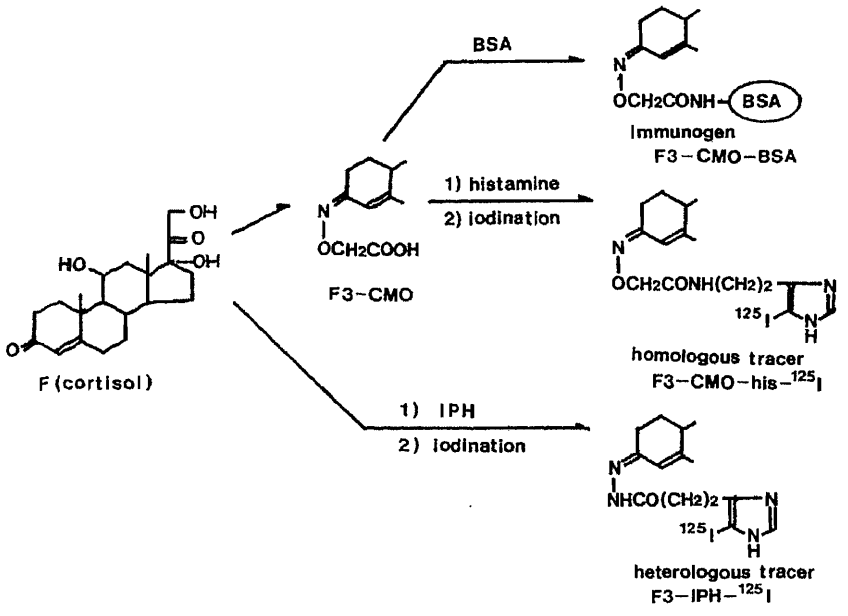

Chart 2

antigen (F3-CMO-his-^{125}I). ^{3}H-Cortisol, which has no bridge site, produced the least variation of B/B_0 (where B is the bound activity and B_0 is the activity bound in the absence of unlabeled cortisol) with the change in cortisol concentration.

The amount of cortisol in the samples (serum and saliva) was determined by using the bridge heterologous radiolabeled antigen (F3-IPH-^{125}I). The detection limit of the IPH-RIA for cortisol (according to the method of Ekins and Newman[10]) was 49 ng/dl. Tables I and II

TABLE I. Recovery of Cortisol Added to Normal Human Pooled Serum

Present	Cortisol (ng/tube) Added	Found	Recovery (%)
0.15	0.75	0.85	94.4
0.15	0.43	0.58	100.0
0.15	0.20	0.33	94.3
0.15	0.13	0.28	100.0
0.15	0.06	0.21	100.0
		Mean:	97.7

TABLE II. Recovery of Cortisol Added to Saliva

Present	Cortisol (ng/tube) Added	Found	Recovery (%)
0.31	1.73	1.99	97.5
0.31	0.79	1.14	103.6
0.31	0.40	0.71	100.0
0.31	0.15	0.47	102.1
0.31	0.09	0.41	102.5
		Mean:	101.1

show the recovery of cortisol added to serum and to saliva, respectively. The recovery was satisfactory. IPH-RIA can be used to determine cortisol in the presence of corticosteroid-binding globulin in serum without pretreatment of the sample. The concentration of cortisol in saliva is known to reflect the free cortisol level in serum, and determination of the cortisol level in the saliva, especially when it is difficult to draw blood from a vein, such as in children, seems to be very useful.[7b] The cortisol level in saliva is much lower than that in serum and saliva sometimes can not be collected in large amounts. Thus, it is important to determine the amount of cortisol in the smallest possible quantity of saliva. Free cortisol levels in serum determined by equilibrium dialysis were 7—14% of the concentration of total cortisol in serum. Salivary cortisol showed a good correlation with the values of serum free cortisol ($Y=1.731\ X+0.079\ \mu g/dl$, n, 10; r, 0.92; Y, serum free cortisol; X, salivary cortisol).

In conclusion, a new type of coupling reagent (IPH) could be applied to a one-step synthesis of a derivative for radioiodination. The IPH-RIA, which uses a bridge heterologous antigen, can be used to determine the cortisol level in serum and saliva with high sensitivity through a simple procedure using a small quantity of sample (serum 2.5 μl, saliva 100 μl).

Acknowledgement The authors wish to thank Miss Mari Maruyama of this faculty for her technical assistance.

References

1) *a*) E. H. D. Cameron, S. E. Morris, and B. Nieuweboer, *J. Endocrnol.*, **61**, XXXIX (1974); *b*) G. D. Nordblom, R. Webb, R. E. Counsell, and B. G. England, *Steroids*, **38**, 161 (1981); *c*) R. M. Allen and M. R. Redshaw, *ibid.*, **32**, 2335 (1978); *d*) C. Gomez-Sanchez, L. Milewich, and O. B. Holland, *J. Lab. Clin. Med.*, **89**, 902 (1977); *e*) M. Kojima, H. Sone, H. Ogawa, N. Nakazawa, and K. Tachibana, Japan. Patent 58-35520 (1983).
2) H. Hosoda, H. Yoshida, Y. Sakai, S. Miyairi, and T. Nambara, *Chem. Pharm. Bull.*, **28**, 3035 (1980).
3) A. H. Janosky, F. C. Schulman, and G. E. Wright, *Steroids*, **23**, 49 (1974).
4) B. F. Erlanger, F. Borek, S. M. Beiser, and S. Lieberman, *J. Biol. Chem.*, **228**, 713 (1957); *idem*, *ibid.*, **234**, 1090 (1959).
5) W. M. Hunter and F. C. Greenwood, *Nature* (London), **194**, 495 (1962); F. C. Greenwood, W. M. Hunter, and J. S. Glover, *Biochem. J.*, **89**, 114 (1963).
6) B. J. Morris, *Clin. Chim. Acta*, **73**, 213 (1976).
7) *a*) P. Robin, J. Predine, and E. Milgrom, *J. Clin. Endocrinol. Metab.*, **46**, 277 (1978); *b*) T. Umeda, R. Hiramatsu, T. Iwaoka, T. Shimada, and T. Sato, *Clin. Chim. Acta*, **110**, 245 (1981).
8) M. J. Hasler, K. Painter, and G. D. Niswender, *Clin. Chem.*, **22**, 1850 (1976).
9) S. L. Jeffcoate, "Radioimmunoassay of Steroid Hormones," 2nd ed., ed. by D. Gupta, Verlag Chemie, Weinheim, 1980, pp. 209—219.
10) R. Ekins and B. Newman, *Acta Endocrinol. Suppl.*, **147**, 11 (1970).

[Chem. Pharm. Bull. 35(12)5004—5009(1987)]

Determination of Chlorpromazine, Thiamine, Lincomycin, Ofloxacin and Theophylline by Ternary Complex Formation with Eosin and Palladium(II)[1)]

YOSHIKAZU FUJITA, ITSUO MORI,* KINUKO FUJITA, YOSHIHIRO NAKAHASHI and TAKESHI TANAKA

Osaka University of Pharmaceutical Sciences, 2-10-65, Kawai, Matsubara, Osaka 580, Japan

(Received May 26, 1987)

Color reactions among a drug, an organic dye and a metal ion were studied, and a simple and sensitive spectrophotometric method, without solvent extraction, has been established for the determination of some drugs by ternary complex formation with eosin and palladium(II) (probably involving an ion-association complex between ($Pd^{II}(drug)_n$) cation and eosin anion). Beer's law held up to *ca.* 2.0×10^{-5} M of each drug at 545 nm in the final volume of 10 ml, with apparent molar absorptivities of 5.7×10^4 l mol^{-1} cm^{-1} for chlorpromazine, 6.7×10^4 for thiamine, 5.5×10^4 for lincomycin, 4.0×10^4 for ofloxacin, and 3.5×10^4 for theophylline. The proposed method was applied to the determination of these drugs in pharmaceutical preparations. A fluorescence quenching method for the determination of these drugs by forming this ternary complex was also investigated for the purpose of enhancing the sensitivity of determination.

Keywords——spectrophotometry; fluorometry; ternary complex; eosin; palladium(II); chlorpromazine; thiamine; lincomycin; ofloxacin; theophylline

Of the methods available for enhancing the sensitivity of determination of organic compounds, the ion-pair complex formation system between an organic dye and an organic compound has often been used; suitable organic dyes[2)] are bromothymol blue, bromophenol blue, bromocresol green, methyl orange, tropaeolin OO, eosin, zincon, chromazurol S, tetrabromophenolphthalein ethyl ester, *etc.* These methods are complicated since they require an extraction procedure due to the formation of water-insoluble complexes. The addition of a surfactant or a water-micible organic solvent to avoid to any extraction procedure usually causes decomposition of the ion-pair complexes formed, and thus the organic compounds can not be determined any longer. In addition, these methods are not sensitive enough.

We have already reported[3)] some simple and sensitive spectrophotometric methods, which do not require any process of solvent extraction, for the determination of various organic compounds with an organic dye and a metal ion.

In this research, color reactions of various drugs by utilizing the ternary complex formation among an organic dye, a metal ion and an organic compound were studied in aqueous media, and then suitable conditions for the spectrophotometric determination of some drugs (chlorpromazine (CP), thiamine (TA), lincomycin (LCM), ofloxacin (OFLX) and theophylline (TP)) by using eosin and palladium (II) (Pd(II)) were established. The proposed method was applied to the assays of these drugs in pharmaceutical preparations. A fluorescence quenching method to determine these drugs was also investigated.

Experimental

Reagents and Apparatus——Standard aqueous solutions (1.0×10^{-3} M, M=mol l^{-1}) of CP, TA, LCM, OFLX

and TP were prepared by dissolving appropriate quantities of CP·HCl (Sigma Chemical Ltd.), TA·HCl (Wako Pure Co., Ltd.), LCM·HCl (Japan Upjohn Ltd.), OFLX (Daiichi Pharmaceutical Co., Ltd.) and TP (Tokyo Kasei Kogyo Co., Ltd.). Eosin and Pd (II) solutions were prepared as 2.0×10^{-3} M aqueous solutions, as described in the previous reports.[3] A 0.5% methylcellulose (MC) solution was prepared by dissolving MC (1500 cps, Kishida Chemical Co., Ltd.) in cold water. A buffer solution (pH 4.3) was prepared by mixing 0.2 M acetic acid and 0.2 M sodium acetate solutions. All other reagents and materials were of analytical grade, and were used without further purification. Deionized water was used. A Shimadzu model UV 240 spectrophotometer and a Shimadzu model RF-540 spectrofluorometer with 1.0-cm quartz cells were used. The pH measurements were made with a Hitachi-Horiba F-7 AD pH meter with a combination calomel glass electrode.

Standard Procedure for the Spectrophotometry——An aliquot of each drug solution (up to *ca.* 2.0×10^{-5} M) was transferred to a 10-ml calibrated flask. To this, 1.5 ml of a 0.5% MC solution, 3.0 ml of the buffer solution (pH 4.3), 0.75 ml of a 2.0×10^{-3} M eosin solution and 0.75 ml of a 2.0×10^{-3} M Pd(II) solution were added. The mixture was diluted to 10 ml with water, kept at 50 °C for 30 min, and then cooled for 5 min in water. The absorbance of the eosin–Pd(II)–drug solution (solution A) was measured at 545 nm against a similarly prepared eosin–Pd(II) solution (solution B).

Recommended Procedure for the Fluorometry——A sample solution containing up to *ca.* 7.5×10^{-6} M of each drug was placed in a 10-ml calibrated flask. To this solution, 1.5 ml of a 0.5% MC solution, 3.0 ml of the buffer solution, 0.5 ml of a 2.0×10^{-3} M eosin solution and 0.5 ml of a 2.0×1.0^{-3}M Pd(II) solution were added. The mixture was diluted to 10 ml with water and kept at 50 °C for 30 min. Solutions A and B were cooled to room temperature in water for 5 min, then the difference of relative fluorescence intensity between solutions A and B at 545 nm emission wavelength with excitation at 462 nm was measured.

Results and Discussion

On the addition of TA to the eosin–Pd(II) solution (solution B), a distinct difference of absorbance between the eosin–Pd(II)–TA solution (solution A) and solution B was observed at around 545 nm, and the absorbance difference of solution A against solution B was proportional to the concentration of TA. The absorbance of solution B at 545 nm was relatively low.

The effect of organic dyes was studied by measuring the difference of absorbance between organic dye–Pd(II)–TA or organic dye–Pd(II)–LCM and organic dye–Pd(II) solutions. Ion-association reagents such as eosin, phloxine, fluorescein, dibromofluorescein and bromophenol blue increased the absorbance of organic dye–Pd(II) solution, whereas chelating reagents such as *o*-hydroxyhydroquinonephthalein, pyrogallol red, zincon, chromazurol S and aluminon decreased its absorbance. Eosin was chosen on the basis of sensitivity.

The effect of metal ions was examined. Only Pd(II) was effective among various metal ions; Pd(II), iron(III), titanium(IV), zirconium(IV), aluminum(III), zinc(II), copper(II), manganese(II), silver(I), *etc.*

About 30 kinds of drugs were examined in the colored complex formation system with eosin and Pd(II). The results showed that compounds involving heterocyclic N-bases or S-bases were apt to form colored complexes. In this paper, suitable conditions for the determination of CP, TA, LCM, OFLX and TP are described.

Study of the Optimum Conditions for the Spectrophotometry

A maximum and constant absorbance of solution A against solution B was observed in the range of pH 3.8—4.5 with 3.0 ml of a 0.2 M acetic acid–0.2M sodium acetate buffer solution.

Solution A without surfactant was unstable and gave a precipitate. In order to solubilize and stabilize the colored complex, the use of various surfactants was tried. Cationic surfactants such as cetylpyridinium chloride depressed the colored complex formation due to the formation of an ion-pair complex between eosin and the cationic surfactant. MC (1500 cps), which is a nonionic and water-soluble polymeric surfactant, was found to be the best dispersion agent with respect to sensitivity.

The effect of the amounts of eosin and Pd(II) was examined by varying the molar ratio of

TABLE I. Sensitivities, Reproducibilities and Complex Compositions of Some Drugs in the Proposed Method

Drug	$\varepsilon^{a)}$ ($\times 10^4$)	R.S.D.[b)]	Mole ratio (Pd : eosin : drug)
CP	5.7	0.5	1 : 1 : 2
TA	6.7	1.0	1 : 1 : 2
LCM	5.5	0.8	3 : 3 : 1
TP	3.5	2.1	1 : 1 : 1
OPLX	4.0	2.1	1 : 1 : 1

a) Apparent molar absorptivity. *b*) Relative standard deviation ($n=5$).

eosin to Pd(II), the amounts of Pd(II) and CP being kept constant. A maximum absorbance was observed when the molar ratio of Pd(II) to eosin was approximately 1 : 1. Further, it was found that the eosin-to-Pd(II) ratio in the presence of a drug was 1 : 1. All further work was thus carried out with 1.5×10^{-5} M eosin and Pd(II) in the final volume, taking into consideration the determination limit of drugs.

The color development at room temperature was very slow, more than 24 h being required. The effects of temperature and time were examined by heating for 10—60 min at various temperatures (40, 50 and 60 °C); an almost constant absorbance was obtained at 50 °C for 25—60 min or at 60 °C for 20—50 min, followed by cooling to room temperature. As both of solutions A and B on heating at 60 °C formed jelly-like aggregates, which disappeared on cooling and agitating, the reproducibility was somewhat poor (the conditions are beyond the cloud point of MC[4)]). The absorbance of solution A against solution B kept at 50 °C for 30 min and cooled for 5 min in water remained constant for at least 24 h.

Calibration Curves and Nature of Ternary Complex

Under the standard procedure, calibration curves were prepared for CP, TA, LCM, OFLX and TP. Good linear relationship was obtained in the range up to *ca.* 2.0×10^{-5} M of each drug in the final volume of 10 ml. The apparent molar absorptivities (ε), the relative standard deviations (R.S.D., $n=5$) and the compositions of the ternary complexes obtained by the molar-ratio and continuous variation methods are listed in Table I.

Next, a study to establish the character of the ternary complex was performed. The acid dissociation properties of eosin in the presence of MC were determined spectrophotometrically[5)] at an ionic strength of 0.1 at 20 ± 0.1 °C. Eosin exists in any of the following forms, depending on the pH in aqueous solution:

$$H_3R^+ \overset{K_{a_1}}{\rightleftharpoons} H_2R \overset{K_{a_2}}{\rightleftharpoons} HR^- \overset{K_{a_3}}{\rightleftharpoons} R^{2-}$$

Where R denotes the undissociated parts of eosin. It was found that pK_{a1}, pK_{a2} and pK_{a3} in the presence of MC were -2.10, 2.85 and 4.95, respectively, and about 80% of eosin at pH 4.3 was estimated[6)] to be HR^-. Moreover, this ternary complex without surfactant was fairly well extracted into *n*-butanol (dielectric constant, 17.7[7)]), but got an insoluble film was formed at the interface of the two phases in methyl isobutylketone (13.1). The color development was remarkably depressed by the coexistence of small amounts of methanol or cationic surfactant. On the other hand, Shcherboy *et al.*[8)] reported a fluorometric method for the determination of Pd(II) with eosin and 1,10-phenanthroline (phen). On the addition of phen to solution B, the same colored complex ($\varepsilon \simeq 3.4 \times 10^4$) was produced. This reaction is based on the ion-association complex formation[9)] between $[Pd(phen)]^{2+}$ as a cationic component and eosin as an anionic counter-ion. From the results, it is deduced that the ternary complex formed in this

reaction system may be the ion-association complex between ($Pd^{II}(drug)_n$) cation and eosin anion.

Effect of Foreign Substances

The effect of foreign ions and substances on the determination of LCM or CP was examined. The following ions and substances caused no interference up to at least the concentrations indicated: 100-fold molar excess over LCM or CP of Ca(II), Mg(II), K(I), Na(I), fluoride, chloride, nitrate, sulfate, phosphate, glucose, lactose, succinate and urea; 10- to 20-fold molar excess of Cu(II), Co(II) and Zn(II). Fe(III), iodide, thiocyanate, tartrate, citrate, salicylate, ascorbate, glycine, caffeine, diphenhydramine and panthothenate interfere at 1- to 5-fold molar excess over LCM or CP. Human albumin caused positive errors. The interference of large amounts of Fe(III) could be removed by addition of fluoride ion solution. To overcome the effects of small amounts of positive interfering substances such as ascorbate, caffeine, diphenhydramine and pyridoxine, a standard addition method could be used. The results are summarized in Table II.

Application of the Proposed Method

The proposed method was applied to the determination of CP·HCl, TA·HCl, LCM·HCl, OPLX and TP in pharmaceutical preparations (tablet, capsule and injection). The content of a tablet or capsule was accurately weighed and ground in a mortar to a fine powder. The required amount of the powder was weighed, transferred into a 100-ml volumetric flask, diluted to the mark with water and filtered. An injection without pretreatment was transferred into a 100-ml volumetric flask and diluted to the mark with water. An appropriate amount of the sample solution was taken and assayed according to the standard procedure. The results obtained by the proposed method were in good agreement with those results of the other procedures, and recoveries were satisfactory (about 98—101%). The results are presented in Table III.

Study of the Fluorometry

As the formation of this ternary complex reduced the fluorescence of solution B, a fluorescence quenching method for the determination of these drugs was also investigated. The uncorrected fluorescence emission spectra of solutions A and B are shown in Fig. 1. On

TABLE II. Effect of Foreign Substances

Substance	Added[a]	Recovery of LCM (%)	Added[a]	Recovery of CP (%)
—	—	100.0	—	100.0
Fe(III), alum	2	115.6	2	127.8
Ca(II), chloride	100	100.0	100	100.0
I^-, potassium	2	88.0	2	88.7
$H_2PO_4^-$, potassium	100	100.0	100	100.0
Citric acid	2	86.5	5	91.0
Ascorbic acid	2	118.7	2	115.5
Glycine	5	83.5	10	91.5
Caffeine	2	116.3	2	127.6
Glucose	100	100.0	100	100.0
Pyridoxine	2	117.8	1	108.3
Diphenhydramine	2	116.3	1	107.6
Calcium pantothenate	2	97.3	5	90.0
Human albumin	(20 μg)	117.4	(10 μg)	105.2

LCM and CP, 1.0×10^{-5} M; eosin and Pd(II), 1.5×10^{-4} M; MC, 0.075%; reference, solution B.
a) Molar ratio (substance/LCM or CP).

TABLE III. Determination of Some Drugs in Pharmaceutical Preparations

Sample	Content (mg)[a,b]			Recovery[b] (%)
	Nominal amount	Present method	Other method	
CP·HCl tablet	10.0	9.90	9.89[d]	100.8
TA·HCl injection	1.0	1.02	1.01[e]	100.5
LCM capsule	250.0	253.4		99.1
OFLX tablet	100.0	103.5	102.8[f]	99.9
TP injection[c]	201.3	195.7	197.4[e]	98.4

a) Drug content, mg per 1 tablet, capsule or injection. *b*) Mean of 5 determinations. *c*) As aminophylline injection. *d*) Qnph–Pd(II) method, ref. 10). *e*) JP X method, ref. 11). *f*) UV method, ref. 11).

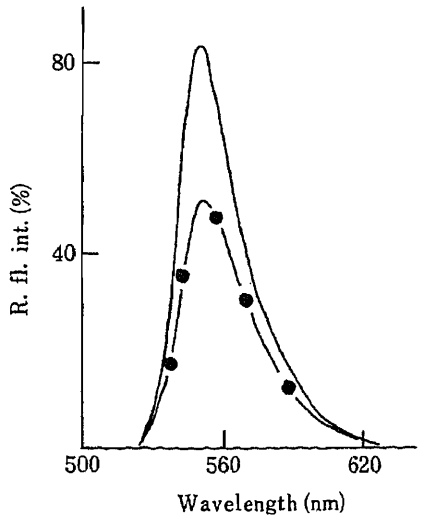

Fig. 1. Emission Spectra of Eosin–Pd(II) and Eosin–Pd(II)–CP Solutions under the Recommented Conditions

CP, 7.5×10^{-6} M; eosin and Pd(II), 1.0×10^{-4} M; MC, 0.075%; pH, 4.3; excitation wavelength, 462 nm. —●—, CP–eosin–Pd(II); ——, eosin–Pd(II).

the addition of CP to solution B, the relative fluorescence intensity (R. fl. int.) of solution B fell significantly, and the magnitude of the decrease was proportional to the concentration of CP.

In the development of the recommended procedure for the fluorometry, only the amounts of eosin and Pd(II) were studied, and the same conditions as for spectrophotometry were adopted for other reaction variables. The optimal amounts of eosin and Pd(II) were 1.0×10^{-4} M in the final volume of 10 ml. The calibration curves were linear in the range up to *ca.* 7.5×10^{-6} M of these drugs. The quenching effects decreased in the order TA > CP, LCM > TP > OFLX.

In conclusion, color reactions among various drugs, eosin and Pd(II) were examined, and spectrophotometric and fluorometric determinations of some drugs (CP, TA, LCM, OFLX and TP) were established by using ternary complex formation. The ternary complex formed in this reaction system was regarded as the ion-association complex between ($Pd^{II}(drug)_n$) cation and eosin anion. Compared with the conventional methods using organic dyes,[2,12] or metal ions[13] alone, the present method, which does not require an extraction procedure, has the advantages of simplicity, sensitivity and reproducibility. The present method should be useful and convenient for the simple determination and detection of various drugs for quality control and /or for screening tests, as well as for assay of pharmaceutical preparations.

Acknowledgement We are grateful to Japan Upjohn Ltd. and Daiichi Pharmaceutical Co., Ltd. for supplying

LCM·HCl and OFLX, respectively.

References and Notes

1) This paper is Part LXIII of a series entitled "Application of Xanthene Derivatives for Analytical Chemistry," Part LXII: I. Mori, Y. Fujita, K. Fujita, Y. Koshiyama and Y. Nakahashi, *Anal. Lett.*, accepted (1987). This work was presented at 106th and 107th Annual Meetings of the Pharmaceutical Society of Japan in Chiba, April 1986 and in Kyoto, April 1987.
2) *a*) M. Pesez and J. Bortos, "Colorimetric and Fluorimetric Analysis of Organic Compounds and Drugs," Marcel Dekker, Inc., New York, 1974; *b*) The Japan Society for Analytical Chemistry, "Bunseki Kagaku Binran," Maruzen Ltd., Tokyo, 1976; *c*) T. Inoue, "Iyakuhin Seizai No Bunseki," Chizinshoin, Ltd., Tokyo, 1978; *d*) T. Sakaguchi, "Yakuhin Bunseki Kagaku," Nankodo, Tokyo, 1978; *e*) W. Sadée and G. C. M. Beelen (M. Saito and Z. Tamura), "Drug Level Monitoring," Hirokawa Shoten, Tokyo, 1982; *f*) T. Sakai, *Dojin News*, **30**, 1 (1984); *g*) T. Mitsui, *Bunseki*, **1985**, 103.
3) *a*) Y. Fujita, I. Mori, S. Kitano, H. Kawabe and Y. Kamada, *Bull. Chem. Soc. Jpn.*, **57**, 1828 (1984); *b*) I. Mori, Y. Fujita, H. Kawabe and K. Fujita, *Bunseki Kagaku*, **34**, 648 (1985); *c*) I. Mori, Y. Fujita, H. Kawabe, K. Fujita, T. Tanaka and A. Kishimoto, *Analyst* (London), **111**, 1409 (1986); *d*) I. Mori, Y. Fujita and K. Sakaguchi, *Bunseki Kagaku*, **30**, 2599 (1982).
4) A. Kitahara, Y. Tamai, S. Hayano and I. Hara, "Surface Active Agents," Kodansha Scientific, Tokyo, 1981.
5) *a*) A. Albert and E. P. Sejesnt (T. Matsuura), "The Ionic Constants," Maruzen Co., Tokyo (1963); *b*) M. Shibata, M. Nakamizo and H. Kakiyama, *Nippon Kagaku Kaishi*, **1972**, 681.
6) H. Freiser and Q. Fernando (T. Fujinaga and E. Sekido), "Ionic Equilibria in Analytical Chemistry," Kagakudojin Ltd., Tokyo, 1977.
7) The Society of Synthetic Organic Chemistry, Japan, "The Pocketbook of Solvents," Ohme-sha, Tokyo, 1984.
8) D. P. Shcherbov, D. N. Lisitsina and I. D. Vredenskaya, *Org. Reagently Anal. Khim., Tezisy Dokl. Veses. Konf., 4th*, **2**, 129 (1976) [*Chem. Abstr.*, **88**, 15447*s* (1978)].
9) P. R. Haddad, *Talanta*, **24**, 1 (1977).
10) I. Mori, Y. Fujita and S. Kitano, *Bunseki Kagaku*, **32**, E1 (1983).
11) "Commentary of the Japanese Pharmacopoeia, Ed. X," Nankodo, Tokyo, 1981.
12) *a*) J. Lelijveld and H. Kortmann, *Bull. World Health*, **42**, 447 (1970); *b*) L. A. Roberts, *J. Pharm. Sci.*, **58**, 1015 (1969); *c*) S. Ogawa, M. Morita, K. Nishiura and K. Fujisawa, *Yakugaku Zasshi*, **85**, 650 (1965); *d*) U. R. Cieri, *J. Assoc. Off. Anal. Chem.*, **61**, 937 (1978); *e*) A. I. Zhebentyaev, *Khim.-Farm. Zh.*, **19**, 111 (1985) [*Chem. Abstr.*, **102**, 13791 (1986)].
13) *a*) M. Sawada, I. Motoyama, S. Yamada and Y. Kanaya, *Bunseki Kagaku*, **35**, T16 (1986); *b*) S. Tanabe and H. Taniguchi, *Bunseki*, **1985**, 879.

[Chem. Pharm. Bull. 35(12)5010—5014(1987)]

Centrifugal Partition Chromatography (CPC) as a Useful Method for Determination of Partition Coefficients between Octanol and Water

HIROSHI TERADA,*,[a] YASUTAKA KOSUGE,[b] NOBUYUKI NAKAYA,[b] WATARU MURAYAMA,[b] YOSHIAKI NUNOGAKI[b] and KAN-ICHI NUNOGAKI[b]

Faculty of Pharmaceutical Sciences, University of Tokushima,[a] Shomachi-1, Tokushima 770, Japan and Sanki Engineering Ltd.,[b] Imazato 2-16-10, Nagaokakyo, Kyoto 617, Japan

(Received May 27, 1987)

Centrifugal partition chromatographies (CPC) of three series of compounds, phenols, benzoic acids and *N*-phenylanthranilic acids, were performed with acetonitrile as a mobile phase and *n*-hexane as a stationary phase. Values for the partition coefficient (P_{cpc}) of these compounds were determined from the ratio of their concentration in the *n*-hexane phase to that in the acetonitrile phase, and they were compared with the partition coefficient between octanol and water determined by the shaking-flask method (P_{oct}). A significant linear relation was obtained between $\log P_{cpc}$ and $\log P_{oct}$ for each series of compounds up to $\log P_{oct}$ values of about 6, indicating that CPC is a very useful method for simple and accurate determination of P_{oct}.

Keywords——centrifugal partition chromatography (CPC); partition coefficient; high-performance liquid chromatography (HPLC); quantitative structure–activity relationship (QSAR)

In studies on the quantitative structure–activity relationship (QSAR), biological activity is generally expressed as a linear combination of parameters that represent the physical properties of the bioactive test compound. The hydrophobic property, generally expressed as the log of the partition coefficient between octanol and water ($\log P_{oct}$), is the major factor that influences drug action.[1)]

The standard method for determining $\log P_{oct}$ is the shaking-flask method. However, this method is tedious and requires relatively large amounts of pure samples and octanol. Furthermore, determination of $\log P_{oct}$ values of above 4 is very difficult, and requires the use of very rigorous experimental conditions.[2)] Thus, a more convenient method is required for determination of high $\log P_{oct}$ values. With recent improvements in techniques of high-performance liquid chromatography (HPLC), this procedure has become widely recognized as very efficient for determining high values of $\log P_{oct}$.[3)] Octadecyl silica (ODS) and glyceryl-coated controlled pore glass (gly-CPG) have been found to be useful stationary phases for HPLC, and with these stationary phases $\log P_{oct}$ values of up to 6 or more can be determined easily.[4)]

In the HPLC method, $\log P_{oct}$ is generally determined from the capacity factor k' of the test compound on the basis of the linear relation between $\log P_{oct}$ and $\log k'$. However, deviation of data points from this linear relation is sometimes observed.[4)] In view of these facts, an alternative method for simple determination of $\log P_{oct}$ is required.

Centrifugal partition chromatography (CPC) was recently developed based on counter-current chromatography (CCC): by application of centrifugal force fields during CCC, the chromatography can be performed very rapidly, simply and efficiently.[5)] CPC has mainly been used for separation of various compounds including natural products on a preparative scale.[6)]

However, it should be also useful for analytical purposes.

We studied the availability of CPC for determination of $\log P_{oct}$. As mentioned above, chromatography with the use of solid supports as in HPLC sometimes shows anomalous retention behavior even among compounds in a homologous series. Since CPC is based on the partition between two immiscible liquid phases without the use of any solid support, CPC is expected to be more efficient than HPLC for determining $\log P_{oct}$. In this study, we used *n*-hexane as a non-polar phase, and acetonitrile as a polar phase in the CPC. For determination of $\log P_{oct}$, performance of the CPC in the octanol–water system would be desirable, but our attempts were unsuccessful because of the high viscosity of octanol. Since CPC in the *n*-hexane–acetonitrile system is efficient for separation of organic compounds,[7] we used this chromatographic system as a first step to examine the availability of CPC for determination of $\log P_{oct}$. We found that $\log P_{oct}$ values of up to about 6 could be determined simply and rapidly with small amounts of sample compounds.

Experimental

Materials——3′-Substituted *N*-phenylanthranilates were kindly donated by Taisho Pharmaceutical Co. (Tokyo, Japan). Other reagents were obtained from either Wako Pure Chemical Industry (Osaka, Japan), or Nakarai Chemicals Co. (Kyoto, Japan). Test compounds were dissolved in the mobile phase at a concentration of 0.5—10 mg/ml, and 0.2 ml samples of the solutions were subjected to chromatography for determination of the $\log P_{oct}$ values.

Performance of CPC——CPC was performed at 25 °C in a centrifugal partition chromatograph, model CPC-LLN, Sanki Engineering Ltd.[5] The apparatus consisted of cartride-type micro-cells (total volume V_c=256.0 ml) on a centrifuge rotor. Chromatography was performed as follows. First the cartridges were filled with the solution used as the stationary phase, and then the mobile phase was introduced under centrifugation at a constant rate. The total volume of the stationary phase eluted before elution of the solvent front of the mobile phase was measured accurately. This volume corresponded to the volume of the mobile phase V_m, and the deviation in values was always within 1%. After elution of the mobile phase through the stationary phase for a certain period to achieve steady performance of the CPC, the sample solution was injected. The retention volume of the sample, V_e, was determined from the chromatogram recorded with a UV flow-cell monitor.

In this study, *n*-hexane was used as a stationary phase, and acetonitrile (CH_3CN) as a mobile phase. Each phase was saturated with the other phase before CPC. The flow rate of the mobile phase and V_m as well as V_e were determined in each run.

Determination of Partition Coefficient——The ratio of the concentration of test compounds in the nonpolar phase C_{NP} (*n*-hexane) to that in the polar phase C_{PP} (acetonitrile) corresponds to the partition coefficient in the CPC system. This value is referred to as P_{cpc}, and was calculated by the use of Eq. 1.

$$P_{cpc} = C_{NP}/C_{PP} = (V_e - V_m)/(V_c - V_m) \quad (1)$$

Results and Discussion

Figure 1 shows the chromatogram of 2,3,4,6-tetrachlorophenol obtained at a flow rate of 2.0 ml/min and rotation to be of 800 rpm. As described in the experimental section, the total volume of the separating cartridges V_c was fixed at 256.0 ml, the volume of the mobile phase V_m (=86.0 ml) was determined directly without using unretained compound, and only the retention volume of the test compound V_e (=115.3 ml) was measured from the chromatogram, as indicated in Fig. 1.

We performed CPC with acetonitrile-saturated *n*-hexane as a stationary phase, and *n*-hexane-saturated acetonitrile as a mobile phase, because the test compounds were sufficiently soluble in both solvents to give a measurable chromatogram. It is noteworthy that solubilization of the test compounds is a limiting factor in chromatographies. We carried out CPC with three series of compounds, phenols, benzoic acids and *N*-phenylanthranilates, and determined $\log P_{cpc}$ values according to Eq. 1. The values of V_m, V_e, and $\log P_{cpc}$ obtained are

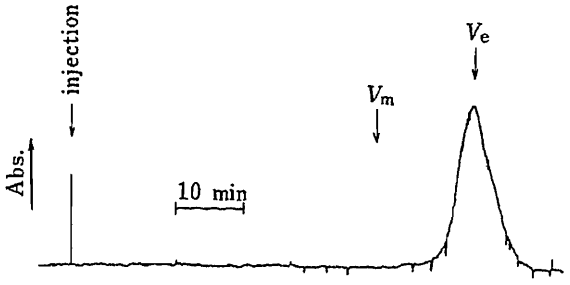

Fig. 1. Chromatogram of 2,3,4,5-Tetrachlorophenol

TABLE I. Chromatographic Data, and $\log P_{cpc}$ and $\log P_{oct}$ Values of Phenols, Benzoic Acids and *N*-Phenylanthlanilates

Compounds	V_m (ml)	V_e (ml)	$\log P_{cpc}$	$\log P_{oct}$ [a]
Phenols				
4-C_6H_5	83.5	93.1	−1.25	3.20
2,4-Cl_2	87.0	104.2	−0.99	3.08
2,4,6-Cl_3	84.0	107.6	−0.86	3.62
2,3,4,6-Cl_4	86.0	115.3	−0.76	4.10
2,3,4,5,6-Cl_5	85.5	121.3	−0.68	5.12
4-CN	86.0	89.3	−1.71	1.66
Benzoic acids				
3-Cl	87.5	95.3	−1.33	2.68
4-Cl	87.0	95.7	−1.29	2.65
3-CH_3	86.0	92.0	−1.45	2.37
4-NO_2	87.5	90.4	−1.76	1.83
4-CN	86.0	88.4	−1.85	1.56
N-Phenylanthranilates				
Not substituted	86.0	91.3	−1.51	4.36
3′-CF_3	86.5	97.6	−1.18	5.62
2′,3′-$(CH_3)_2$	86.5	98.3	−1.16	5.37
3′-NO_2	86.7	92.0	−1.50	4.57
3′-OH	87.0	90.0	−1.75	3.49
3′-OCH_3	86.8	91.3	−1.58	4.56
3′-$COCH_3$	86.5	90.2	−1.66	4.31

a) Cited from refs. 8 and 10.

summarized in Table I.

We next examined the relation of $\log P_{cpc}$ with $\log P_{oct}$. In all cases $\log P_{cpc}$ increased linearly with increase in $\log P_{oct}$. The linear relations could be expressed by Eq. 2.

$$\log P_{oct} = a + b \log P_{cpc} \tag{2}$$

For these three series of compounds the following relations shown as Eqs. 3—5 were obtained by least-squares calculation. In these equations n is the number of compounds, r is the correlation coefficient and s is the standard deviation. Values in parentheses under coefficients a and b are those of the 95% confidence intervals. These equations are highly significant by the F-test.

For phenols:

$$\log P_{oct} = 6.361 + 2.782 \log P_{cpc} \tag{3}$$
$$(1.602)\ (1.458)$$
$$n=6,\quad r=0.926,\quad s=0.487$$

For benzoic acids:

$$\log P_{oct} = 5.237 + 1.961 \log P_{cpc} \quad (4)$$
$$(0.502)\ (0.325)$$
$$n=5,\ r=0.995,\ s=0.059$$

For *N*-phenylanthranilates:

$$\log P_{oct} = 8.991 + 2.965 \log P_{cpc} \quad (5)$$
$$(1.591)\ (1.067)$$
$$n=7,\ r=0.950,\ s=0.242$$

From Eqs. 3—5 and Table I, it is concluded that values of $\log P_{oct}$ of up to about 6 can be determined by CPC. Of the compounds tested in this study, flufenamic acid (3′-trifluoromethyl-*N*-phenylanthranilic acid) had the highest $\log P_{oct}$ (5.62). The flow rate for CPC of flufenamic acid was 2.0 ml/min, and one run took less than 50 min. These chromatographic conditions afforded good resolution for accurate determination of V_e in a short period. Values of $\log P_{oct}$ of more than 6 could also be determined easily.

The regression analysis for all compounds resulted in a very poor correlation as shown in Eq. 6.

$$\log P_{oct} = 5.813 + 1.668 \log P_{cpc} \quad (6)$$
$$(2.313)\ (1.663)$$
$$n=18,\ r=0.468,\ s=1.158$$

However, the correlation between $\log P_{oct}$ and $\log P_{cpc}$ for compounds in the series of phenols and benzoic acids was highly significant as shown in Eq. 7, suggesting that the chromatographic behavior of phenols and benzoic acids are similar, while that of *N*-phenylanthranilates is different.

$$\log P_{oct} = 6.125 + 2.548 \log P_{cpc} \quad (7)$$
$$(0.795)\ (0.602)$$
$$n=11,\ r=0.953,\ s=0.348$$

The reason why *N*-phenylanthranilates showed such an "anomalous" behavior should be clarified in subsequent studies. The tendency for a six-membered ring formation by intramolecular hydrogen bonding between the carboxyl and amino groups of *N*-phenylanthranilates[8] may be related to the anomalous chromatographic behavior. Influences of chemical structure on the correlation have been observed in HPLC on an ODS stationary phase.[4,9] Furthermore, $\log P_{oct}$ values of up to about 6 have been determined by HPLC on an ODS-column.[3] Thus, the CPC method appears to be comparable in effectiveness to the HPLC method for determination of $\log P_{oct}$.

For improvement of the CPC procedure for determining $\log P_{oct}$ values, chromatographic conditions must be developed that to give a single correlation between $\log P_{cpc}$ and $\log P_{oct}$ for a wide variety of compounds in different chemical series. CPC is based on liquid–liquid partition, and the chromatographic mechanism involved is simpler than that in the case of HPLC. Furthermore, a wide variety of chromatographic conditions can be obtained by use of different combinations of stationary and mobile phases. Thus, further studies should lead to the development of suitable chromatographic conditions for determination of the $\log P_{oct}$ values of a wide variety of compounds.

In conclusion, CPC was found to be useful for determination of $\log P_{oct}$, when a calibration curve was drawn based on the linear relation between $\log P_{cpc}$ and $\log P_{oct}$ for compounds in the same chemical series as the test compounds. This method is as effective as HPLC, but is simpler.

References

1) C. Hansch and W. J. Dunn, III., *J. Pharm. Sci.*, **61**, 1 (1972); C. Hansch and J. M. Clayton, *ibid.*, **62**, 1 (1973).
2) N. El Tayer, H. van de Waterbeemd and B. Testa, *J. Chromatogr.*, **320**, 305 (1985); J. L. G. Thus and J. C. Kraak, *J. Chromatogr.*, **320**, 271 (1985).
3) R. Kaliszan, *J. Chromatogr.*, **220**, 71 (1981); J. E. Garst and W. C. Silsono, *J. Pharm. Sci.*, **73**, 1616 (1984).
4) K. Miyake and H. Terada, *J. Chromatogr.*, **240**, 9 (1982); C. Yamagami, H. Takami, K. Yamamoto, K. Miyoshi and N. Takao, *Chem. Pharm. Bull.*, **32**, 4994 (1984); K. Miyake, N. Mizuno and H. Terada, *ibid.*, **34**, 4787 (1986).
5) W. Murayama, T. Kobayashi, Y. Kosuge, H. Yano, Y. Nunogaki and K. Nunogaki, *J. Chromatogr.*, **239**, 643 (1982).
6) R. C. Bruening, E. M. Oltz, J. Furukawa and K. Nakanishi, *J. Am. Chem. Soc.*, **107**, 5298 (1985); T. Araki, Y. Kubo, T. Toda, M. Takata, T. Yamashita, W. Murayama and Y. Nunogaki, *Analyst*, **110**, 913 (1985).
7) H. Terada, Y. Kosuge, W. Murayama, N. Nakaya, Y. Nunogaki and K. Nunogaki, *J. Chromatogr.*, **400**, 343 (1987).
8) H. Terada, S. Muraoka and T. Fujita, *J. Med. Chem.*, **17**, 330 (1974).
9) H. Terada, *Quant. Struct.-Act. Relat.*, **5**, 81 (1986).
10) C. Hansch and A. J. Leo, "Substituent Constants for Correlation Analysis in Chemistry and Biology," Wiley, New York, 1979, pp. 67—336.

[Chem. Pharm. Bull. 35(12)5015—5019(1987)]

Formation of Fluorescent Substances in the Reaction of the Hydroperoxide Isomers of Methyl Linoleate and Amylamine

TOSHIHIRO IIO, KAZUAKI YODEN* and TOSHIKAZU TABATA

Showa College of Pharmaceutical Sciences, 1–8, Tsurumaki 5-chome, Setagaya, Tokyo 154, Japan

(Received May 1, 1987)

The formation of fluorescent substances through the reaction of degradation products of four geometrical isomers of methyl linoleate hydroperoxides with amylamine was studied. The 9- and 13-positional monohydroperoxide isomers having the *cis–trans* and *trans–trans* configurations were separated from autoxidized methyl linoleate by high performance liquid chromatography (HPLC) and their abilities to form fluorescent substances with amylamine in the presence of heme were compared. These four isomers produced the same fluorescent substances exhibiting excitation and emission maxima at 350 and 420 nm, respectively, and also showed the same abilities for fluorescence formation and the same elution profiles of fluorescent substances (FS-I and FS-II) on HPLC. This study proved that all four geometrical isomers were involved in the production of fluorescent substances upon reaction with amino compounds.

Keywords——lipid peroxidation; methyl linoleate; 9-hydroperoxide; 13-hydroperoxide; hydroperoxide geometrical isomer; fluorescence

Lipid peroxides have been suggested to play important biological roles in aging and in the etiology of cancer, and to produce toxic effects such as inactivation of enzymes, deoxyribonucleic acid (DNA) or various cell components.[1–3] It is well known that these lipid peroxides react with various amino compounds such as amino acids, proteins or DNA to form fluorescent pigments *in vivo* and *in vitro*.[4]

Although malondialdehyde has been considered to be involved in the formation of fluorescent pigments,[5,6] recent studies have suggested that the degradation products derived from hydroperoxides of linoleic acid or methyl linoleate (ML) are closely involved in fluorescence formation through reaction with amino compounds.[7–9] Moreover, these hydroperoxides are easily degraded by various types of catalyst such as heme compounds, metals or $FeCl_3$–cysteine.[10–12] It is also known that ML hydroperoxides (LOOH) obtained through autoxidation of ML mainly consist of 9-hydroperoxy-ML (9-LOOH) and 13-hydroperoxy-ML (13-LOOH) and that both of these are further autoxidized to complex mixtures of various oxidized products, generally termed secondary oxidative products (SP).[13,14]

We previously demonstrated that SP prepared from autoxidized ML also produced fluorescent substances similar to that of LOOH degraded by heme through reaction with amylamine.[15] This result suggested that the degradation products of both 9-LOOH and 13-LOOH formed by diverse catalysts and SP derived from LOOH during autoxidation are involved in fluorescence formation through reaction with amino compounds.

However, it was not clear which hydroperoxide of 9-LOOH and 13-LOOH was related directly to the formation of fluorescent substances. Therefore, in the present study, 9-LOOH, 13-LOOH and their two geometrical isomers were separated from LOOH by high performance liquid chromatography (HPLC) and their capacities for fluorescence formation were compared through reaction with amylamine after preincubation with heme.

Materials and Methods

Preparation of Four Hydroperoxide Isomers——ML (3 g), obtained from Tokyo Kasei Kogyo Co., Ltd., was autoxidized by stirring at 30°C for one week. Autoxidized ML was subjected to silica-gel column chromatography (2×40 cm; Wako gel C200, Wako Pure Chemical Industries Ltd.) and LOOH and SP were eluted with hexane–ethylether (7:3) and methanol according to the method of Terao and Matsushita.[16] An aliquot of each fraction was subjected to thin-layer chromatography (TLC: Silica-gel 60, Merck) developed with hexane–ethylether–acetic acid (60:40:1) and then each LOOH and SP fraction was evaporated under a nitrogen stream. 9-LOOH, 13-LOOH and their two corresponding geometrical isomers were separated by both normal- and reversed-phase HPLC according to the method of Chan and Levett.[17] Normal-phase HPLC was carried out on a silica-gel column (Si-5; 4×300 mm; Varian) with hexane–isopropanol (100:0.75) at a flow rate of 1 ml/min. Reversed-phase HPLC was carried out on a μ-Bondapak FFAA (3.9×300 mm; Waters) using methanol–water (70:30) at a flow rate of 0.8 ml/min. A ultraviolet (UV) detector (Lambda-Max model 480LC spectrophotometer; Waters) was used to monitor the effluent at 233nm. The UV absorption spectrum of each LOOH was measured with a Hitachi 200-10 spectrophotometer. The concentrations of the 9- and 13-positional isomers having the *cis–trans* and *trans–trans* configurations were estimated using molar absorbance values of 26000 (at 236 nm) or 28600 (at 233 nm).[18]

Each LOOH was reduced to the corresponding hydroxyl isomer with $NaBH_4$ in methanol and the electron ionization mass spectrum (MS) was measured with a JEOL D300 mass spectrophotometer. The ionization voltage was 30 eV. Gas-liquid chromatography (GC) was carried out using a glass column packed with 5% Silicon SE-52 on Celite 545 SK DMCS (Gasukuro Kogyo Inc.). The column temperature was 250°C.

Fluorescence Formation and Analysis——Each LOOH (500 nmol) was preincubated with heme (5 nmol) in 2 ml of methanol at 37 °C for 45 min. One milliliter of methanol containing amylamine (2 μmol) as a model amino compound was added to the preincubation mixture and then incubation was performed at 37 °C for 20 h for fluorescence formation. SP (1 mg) of ML was also incubated with amylamine (2 μmol) in 3 ml of methanol at 37°C for 20 h. Fluorescence spectra were measured with a Hitachi MPF-3 fluorescence spectrophotometer and the intensities were expressed as percentages of that of a quinine sulfate standard (0.1 μg/ml in H_2SO_4). HPLC of fluorescent substances was carried out on a μ-Bondapak FFAA (3.9×300 nm; Waters) using tetrahydrofuran–acetonitrile–water (15:40:55) at a flow rate of 1 ml/min. Fluorescence peaks were monitored with excitation and emission maxima at 350 and 420 nm with a Hitachi 650-10LC fluorescence spectrophotometer.

Preparation of Degradation Products from 13-LOOH with Heme——[1-^{14}C]13-Hydroperoxylinoleic acid was prepared from [1-^{14}C]linoleic acid (New England Nuclear) using soybean lipoxygenase (Sigma Chemical Co.) in 0.1 M borate buffer (pH 9.5).[19] The products were methylated with diazomethane and purified by TLC. [1-^{14}C]13-LOOH diluted with non-labelled 13-LOOH (1 μmol) was incubated with heme (10 nmol) in 4 ml of methanol at 37 °C for 45 min and the reaction mixture was passed through a Sep-pak Si cartridge (Waters) with hexane–ethyl ether (7:3) to separate heme compounds from the degradation products of 13-LOOH. The degradation products were subjected to reversed-phase HPLC on μ-Bondapak FFAA using acetonitrile–methanol–water (20:45:55) followed by methanol at a flow rate of 1 ml/min. The radioactivity in each fraction was measured with a liquid scintillation counter (Aloka; LSC-900). Seven major fractions were collected separately and the compounds extracted with chloroform–methanol (2:1) were used for fluorescence formation through reaction with amylamine. Analysis of their structures was carried out on the basis of UV absorption and GC-MS fragmentation data as described above.

Results and Discussion

LOOH prepared from autoxidized ML by silica-gel column chromatography was subjected to normal- and reversed-phase HPLC to separate the four geometrical isomers. The four purified isomers (A—D) were identified on the basis of the GC-MS fragmentation patterns of their corresponding hydroxy derivatives and UV absorption spectra according to the methods of Chan and Levett[17] and Lezerovich,[18] and the four hydroperoxy isomers were assigned the following structures: A, methyl 13-hydroperoxy-9-*cis*-11-*trans*-octadecadienoate (13-LOOH: c–t); B, methyl 13-hydroperoxy-9-*trans*-11-*trans*-octadecadienoate (13-LOOH: t–t); C, methyl 9-hydroperoxy-10-*trans*-12-*cis*-octadecadienoate (9-LOOH: t–c); D, methyl 9-hydroperoxy-10-*trans*-12-*trans* octadecadienoate (9-LOOH: t–t).

When LOOH, 9-LOOH (C+D) and 13-LOOH (A+B) were incubated with amylamine after degradation by heme, all of the hydroperoxides showed marked production of fluorescent substances having the same fluorescence intensities and fluorescence spectra with the same excitation (348—350 nm) and emission (415—420 nm) maxima (Table I). These

TABLE I. Fluorescence Formation through Reaction of Hydroperoxide Isomers with Amylamine

	Ex_{max}^{MeOH} (nm)	Em_{max}^{MeOH} (nm)	Fluorescence intensity (%)	Fluorescence peak height	
				FS-I (cm)	FS-II
LOOH	350	420	365.0	3.2	12.3
9-LOOH	350	418	349.0	3.6	12.7
13-LOOH	348	415	347.0	3.7	11.2
9-LOOH (t–t)	347	414	334.0	3.3	12.5
9-LOOH (t–c)	348	415	338.0	2.8	11.7
13-LOOH (t–t)	350	415	358.0	2.8	10.8
13-LOOH (c–t)	349	412	369.0	3.7	11.6
SP	345	415	980.0	14.8	23.7

Each of the LOOH isomers (500 nmol) was incubated with amylamine (2 μmol) at 37 °C for 20 h after preincubation with heme (5 nmol). SP (1 mg) were also incubated with amylamine (2 μmol) under the same conditions. Fluorescence intensities of reaction mixtures and fluorescence peak height of fluorescent substances were measured as described in Materials and Methods.

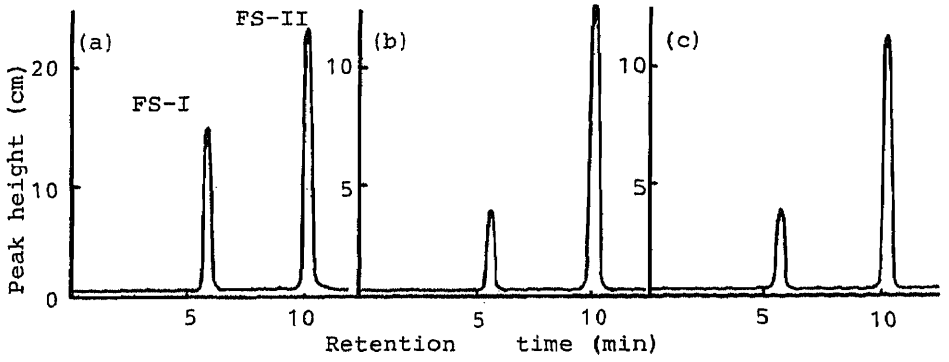

Fig. 1. High-Performance Liquid Chromatography of Fluorescent Substances Formed from Hydroperoxides with Amylamine

Fluorescent substances formed from SP (a), 9-LOOH (b) or 13-LOOH (c) with amylamine were separated on a μ-Bondapak FFAA column using the methods described in Materials and Methods.

LOOHs preincubated without heme, however, produced only small amounts of fluorescent substances.

Next, the four geometrical isomers (A—D) were incubated with amylamine under the same conditions as those described above, and the resulting fluorescent substances were analyzed. The spectra of the fluorescent substances derived from these isomers with amylamine after degradation by heme also showed the same excitation (347—350 nm) and emission (412—415 nm) maxima. Moreover, the fluorescence intensities of these reaction mixtures showed the same values (Table I).

The fluorescent substances produced from SP with amylamine in methanol were eluted at retention times of 6.0 min (FS-I) and 10.5 min (FS-II) on HPLC (Fig. 1a).[15] Similarly, 9-LOOH (Fig. 1b), 13-LOOH (Fig. 1c) and the four geometrical isomers also showed the same two fluorescence peaks.

These results indicate that the 9- and 13-positional isomers and their *cis–trans* and *trans–trans* configurations in LOOH have no influence on the ability to form fluorescent substances, and that moreover, a common compound with the basic structure essential for

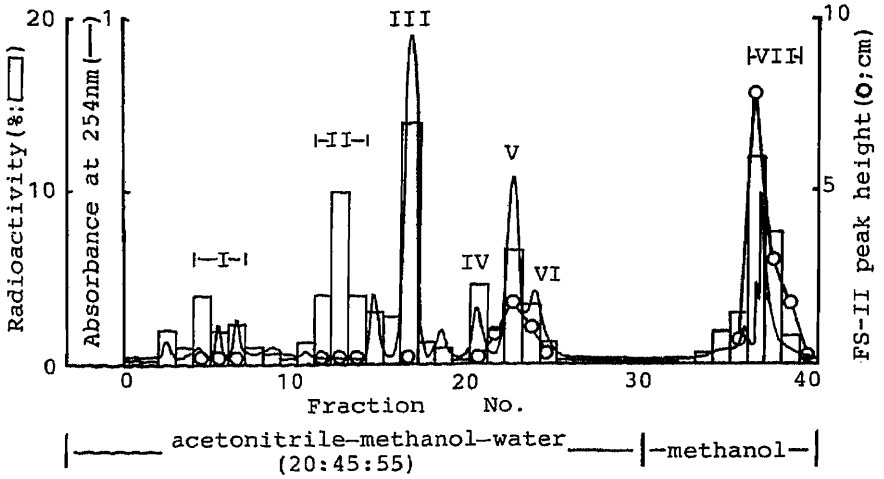

Fig. 2. Distribution of Products Derived from 13-Hydroperoxy Methyl Linoleate with Heme on HPLC

The products derived from 13-LOOH were subjected to HPLC on a μ-Bondapak FFAA column using acetonitrile–methanol–water (20:45:55) and methanol. The ability to produce fluorescence was measured by reaction of the effluent with amylamine (O). The effluent was also monitored for absorbance at 245 nm (——) and for radioactivity (□).

fluorescence formation may be produced by degradation of both 9-LOOH and 13-LOOH having *cis–trans* and *trans–trans* configurations. Chan *et al.* have shown that LOOHs interconvert thermally and that this thermal isomerization occurs by β-scission of peroxy radicals formed from LOOH.[20] Therefore, 9-LOOH: t–c and 13-LOOH: c–t may be converted, respectively, to 13-LOOH: t–t and 9-LOOH: t–t in the presence of heme at 37 °C.

For the purpose of separating the degradation products responsible for fluorescence formation, [1-^{14}C]13-LOOH (1 μCi: 1 μmol) was incubated with heme (10 nmol) at 37°C for 45 min and an aliquot of the reaction mixture was subjected to reversed-phase HPLC. As shown in Fig. 2, seven radioactive fractions were obtained. In order to identify the compounds present in the fractions, an appreciable amount of each was collected by HPLC with repeated injection. A combination of UV spectral analysis and GC-MS fragmentation of each compound established the following structures of the components present in fractions II—VI. Methyl 9-hydroxy-12,13-epoxylinoleate (II), methyl 9-keto-12,13-epoxylinoleate (III), methyl 13-hydroxylinoleate (IV), 13-LOOH (V) and methyl 13-ketolinoleate (VI) were the major degradative compounds present, as described previously by Hamberg[11a] and Dix and Marnett.[11b] However, we were unable to obtain sufficient data for the identification of the degradation products in fractions I and VII. When the fractions were examined to determine their potentials for fluorescence formation, the most marked formation of fluorescent substances was obtained from fraction VII through reaction with amylamine, two fluorescence peaks (FS-I and FS-II) being observed (Fig. 2). On the other hand, the other six major fractions showed only small amounts of fluorescent substances. These results suggest that none of these major degradation products (II—VI) was directly available for fluorescence formation.

Although the degradation products of LOOH produced by heme or SP consist of various oxidized products, when SP was also subjected to reversed-phase HPLC under the same conditions as those described above, the source responsible for fluorescence formation was eluted with methanol (data not shown).

From our results obtained in this study, it was apparent that the same fluorescent substances were formed from 9- and 13-LOOH in the presence of heme as were obtained from SP through reaction with amylamine. Furthermore, these results also indicate the possibility

that common sources available for fluorescence formation exist in the degradation products of 9- or 13-LOOH through reaction with heme and SP. With regard to the structure of the fluorescent substance, from the results of GC-MS fragmentation of purified FS-II formed from SP with amylamine, we suppose that the formation of FS-II may occur in the region of the 5 carbon atoms between the C9 and C13 positions in ML, involving a methyl ester group originating from ML (Iio *et al.*, unpublished data). However, the fine structures of these sources and the fluorescent chromophobic group remain to be clarified. Further studies will therefore be required in order to characterize the fluorescent substances and the sources responsible for fluorescence formation.

References

1) S. Hirai, K. Okamoto and M. Morimatsu, "Lipid Peroxides in Biology and Medicine," ed. by K. Yagi, Academic Press, New York, 1982, p. 305; R. L. Willson, "Free Radicals, Lipid Peroxidation and Cancer," ed. by D. C. McBrien and T. F. Slater, Academic Press, New York, 1982, p. 275.
2) B. N. Ames, M. C. Hollstein and R. Cathcart, "Lipid Peroxides in Biology and Medicine," ed. by K. Yagi, Academic Press, New York, 1982, p. 339; F. W. Summerfield and A. L. Tappel, *Arch. Biochem. Biophys.*, **233**, 408 (1984).
3) A. L. Tappel, *Fed. Proc. Fed. Am. Soc. Exp. Biol.*, **32**, 1870 (1973); S. Matsushita, *J. Agric. Food Chem.*, **23**, 150 (1975); M. S. Kanunga, "Biochemistry of Aging," Academic Press, New York, 1980, p. 79.
4) K. Kikugawa, *Adv. in Free Radical Biology & Medicine*, **2**, 389 (1986).
5) K. S. Chio and A. L. Tappel, *Biochemistry*, **8**, 2821 (1969).
6) K. Kikugawa, T. Maruyama, Y. Machida and T. Kurechi, *Chem. Pharm. Bull.*, **29**, 1423 (1981); K. Kikugawa, Y. Machida, M. Kida and T. Kurechi, *ibid.*, **29**, 3003 (1981); K. Kikugawa and Y. Ido, *Lipids*, **19**, 600 (1984).
7) H. Shimasaki, O. S. Privett and I. Hara, *J. Am. Oil Chem. Soc.*, **54**, 119 (1977).
8) K. Kikugawa, S. Watanabe and T. Kurechi, *Chem. Pharm. Bull.*, **32**, 638 (1984).
9) K. Fujimoto, W. E. Neff and E. N. Frankel, *Biochim. Biophys. Acta*, **795**, 100 (1984).
10) P. J. O'Brien, *Can. J. Biochem.*, **47**, 485 (1969).
11) *a*) M. Hamberg, *Lipids*, **10**, 87 (1975); *b*) T. A. Dix and L. J. Marnett, *J. Biol. Chem.*, **260**, 5351 (1985).
12) H. W. Gardner, D. Weisleder and R. Kleiman, *Lipids*, **13**, 246 (1978); H. W. Gardner and R. Kleiman, *Biochim. Biophys. Acta*, **665**, 113 (1981).
13) F. D. Gunstone, *J. Am. Oil Chem. Soc.*, **61**, 441 (1984); E. N. Frankel, *ibid.*, **61**, 1908 (1984).
14) K. Kanazawa, T. Mori and S. Matsushita, *J. Nutr. Sci. Vitaminol.*, **19**, 263 (1973); K. Kanazawa, E. Kanazawa and M. Natake, *Lipids*, **20**, 412 (1985).
15) T. Iio and K. Yoden, *Life Sci.*, **40**, 2297 (1987).
16) J. Terao and S. Matsushita, *J. Am. Oil Chem. Soc.*, **54**, 234 (1977).
17) H. W.-S. Chan and G. Levett, *Lipids*, **12**, 99 (1976).
18) A. Lezerovich, *J. Am. Oil Chem. Soc.*, **63**, 883 (1986).
19) M. O. Funk, R. Isaac and N. A. Porter, *Lipids*, **11**, 113 (1976).
20) H. W.-S. Chan, G. Levett and J. A. Matthew, *J. Chem. Soc., Chem. Commun.*, **1978**, 756.

[Chem. Pharm. Bull. 35(12)5020—5023(1987)]

Fluorometric Determination of Malonaldehyde in Oxidized Lipids

ATSUSHI IWATA and KIYOMI KIKUGAWA*

Tokyo College of Pharmacy, 1432-1 Horinouchi, Hachioji, Tokyo 192-03, Japan

(Received May 11, 1987)

Malonaldehyde contents in oxidized lipid samples were determined fluorometrically by applying the reaction reported by Sawicki *et al.* (*Anal. Chem.*, 35, 199 (1963)). This assay is based on the reaction of malonaldehyde with ethyl *p*-aminobenzoate in an acidic medium, followed by treatment with alkaline dimethylformamide to afford fluorescence. Time course studies of the malonaldehyde contents in methyl linoleate, soybean oil and sesame oil oxidized by the active oxygen method showed that the contents increased and subsequently decreased with increasing oxidation time. The malonaldehyde contents were always lower than those estimated by means of the thiobarbituric acid method.

Keywords——malonaldehyde; malonaldehyde dianil; fluorescence; oxidized lipid; fluorometric assay

Malonaldehyde is one of the secondary products formed during oxidation of polyunsaturated fatty acids.[1] Formation of the aldehyde has been regarded as significant because it is toxic,[2] carcinogenic[3] and mutagenic.[4] It readily reacts with proteins[5,6] and nucleic acids[7] to cause various biological and physicochemical alterations of the biopolymers. Determination of malonaldehyde in oxidized lipids has usually been performed by the thiobarbituric acid (TBA) method.[1,8] However, TBA is not specific to malonaldehyde but reacts with many other lipid oxidation products including monofunctional aldehydes.[9,10]

Sawicki *et al.*[11] reported that *p*-substituted aromatic amines react with malonaldehyde or tetramethoxypropane under acidic conditions to afford malonaldehyde dianils, which fluoresce on treatment with alkaline dimethylformamide (Chart 1).[12] This time, we determined

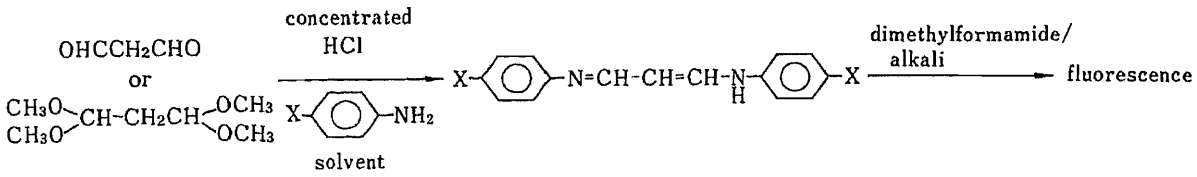

Chart 1

malonaldehyde contents in oxidized lipid samples by means of a procedure based on their reaction.

Experimental

Materials——Ethyl *p*-aminobenzoate, dimethylformamide (for spectroscopy), acetonitrile, dimethylsulfoxide (for spectroscopy) and tetra-*n*-propylammonium hydroxide (10% in water) were obtained from Wako Pure Chemical Industries, Ltd. Tetramethoxypropane (TMP) and methyl linoleate were the products of Tokyo Kasei Kogyo, Company, Ltd. Purified soybean oil was obtained from Showa-sangyo Company, Ltd. Japanese Pharmacopoeia grade sesame oil was used.

Analysis——Fluorescence spectra were measured with a 650-40 Hitachi fluorescence spectrophotometer with excitation and emission slit widths of 10 nm. Fluorescence spectra and intensities were not corrected. Oils (methyl

linoleate, soybean oil and sesame oil) were oxidized by means of the active oxygen method (AOM).[13] A 20-ml portion of each oil was placed in a tube and aerated with purified air at the rate of 2.3 ml/s and at 98°C. The peroxide values (POV) of the oxidized oils were determined according to Wheeler's method.[14] Determination of malonaldehyde by the TBA method was performed as described.[15] Thus, 1.0 mg of the sample was mixed with 1.0 ml of 0.5% TAB solution and 3.0 ml of 0.5% trichloroacetic acid, and the mixture was bubbled with nitrogen gas to remove oxygen. The mixture was then heated in a sealed tube at 60 °C for 90 min. The mixture was extracted with 3.0 ml of chloroform, and the absorbance at 532 nm of the supernatant was determined.

Fluorometric Determination of Malonaldehyde——A mixture of 2.0 ml of the solvent (dimethylformamide, acetonitrile or dimethy sulfoxide) containing the lipid sample (standard TMP or oxidized oil) and 1.0 ml of dimethylformamide containing 1.0% concentrated hydrochloric acid and 1.0% ethyl *p*-aminobenzoate. The mixture was heated at 100°C for 5 min. After cooling, 0.5 ml of 10% solution of tetra-*n*-propylammonium hydroxide was added. Fluorescence spectra and intensities were measured within 5 min. For measurement of malonaldehyde, control fluorescence intensities without the lipid sample were subtracted.

Results and Discussion

In order to apply Sawicki's reaction to the determination of malonaldehyde contents in oxidized lipid samples, a *p*-substituted aromatic amine that produces stable fluorescence and a solvent that dissolves oxidized lipid samples and does not disturb the formation of fluorescence are necessary.

Fluorescence produced by the reaction of TMP and ethyl *p*-aminobenzoate in dimethylformamide showed excitation maxima at 473, 488 and 496 nm and an emission maximum at 557 nm (Fig. 1A),[11] and the fluorescence remained stable at room temperature for at least 60 min. While the intensity of the fluorescence due to *p,p'*-sulfonyldianiline was higher,[11] it was less stable than that due to ethyl *p*-aminobenzoate. The calibration curve of the fluorescence intensities due to ethyl *p*-aminobenzoate in dimethylformamide (excitation at 496 nm and emission at 557 nm) was linear with respect to the amount of TMP up to 1.2 nmol.

Dimethylformamide could not dissolve lipid samples. Acetonitrile and dimethyl sulfoxide were adequate to dissolve methyl linoleate, soybean oil and sesame oil. The use of these solvents made the reaction mixtures containing lipid samples completely clear throughout the reaction. Fluorescence produced in the reaction of TMP and ethyl *p*-aminobenzoate in acetonitrile showed excitation maxima at 472, 482, 492 nm and an emission maximum at 547 nm (Fig. 1B solid curve): the emission maximum was shifted to shorter wavelength as compared to that of the fluorescence produced in dimethylformamide. In this case the calibration curve of fluorescence intensity (excitation at 472 nm and emission at 547 nm) was linear with respect to the amount of TMP up to 2.0 nmol. Fluorescence produced in the reaction of TMP and ethyl *p*-aminobenzoate in dimethyl sulfoxide showed excitation maxima at 473, 486, 496 nm and an emission maximum at 564 nm (Fig. 1C solid curve): the emission maximum was shifted to longer wavelength as compared to that of the fluorescence produced in dimethylformamide. In this case the calibration curve of fluorescence intensity (excitation at 496 nm and emission at 564 nm) was linear with respect to the amount of TMP up to 2.0 nmol.

Fluorescence development by monofunctional aldehydes such as acetaldehyde, 1-propanal, 1-butanal, 1-hexanal, 1-heptanal, 1-octanal, 2,4-hexadienal, 2,4-heptadienal and 2,4-decadienal was tested. Thus, 1.0 nmol of the aldehyde was reacted with ethyl *p*-aminobenzoate in acetonitrile. Only acetaldehyde and 1-propanal exhibited significant fluorescence with spectra similar to that of TMP. The fluorescence intensities of 1.0 nmol of acetaldehyde and 1-propanal were 1/100 and 1/200 of that of 1.0 nmol of TMP, respectively. Other aldehydes showed no significant fluorescence. The results indicate that formation of the fluorescence was selective to malonaldehyde. In order to determine the influence of unoxidized lipid samples on the fluorescence development, various amounts of TMP were reacted with ethyl *p*-aminobenzoate in the presence of 1.0 mg of unoxidized methyl linoleate

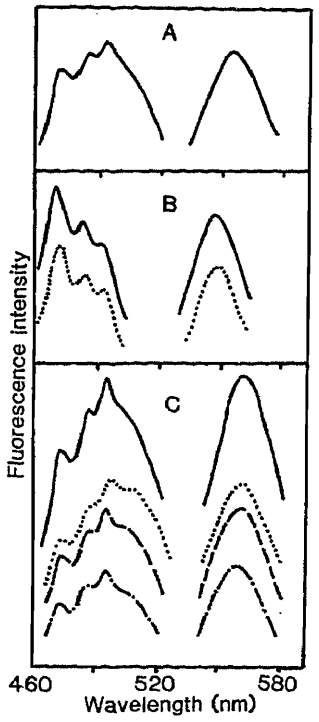

Fig. 1. Fluorescence Spectra of Alkaline Dimethylformamide-Treated Reaction Mixtures of TMP or Oxidized Lipid Samples and Ethyl *p*-Aminobenzoate in Dimethylformamide (A), Acetonitrile (B) and Dimethyl Sulfoxide (C)

The reaction conditions are described in Experimental. ——, 0.5 nmol of TMP; – – – –, 1.0 mg of oxidized methyl linoleate (POV: 1660 meq/kg); — —, 1.0 mg of oxidized soybean oil (714 meq/kg); and — — —, 1.0 mg of oxidized sesame oil (800 meq/kg).

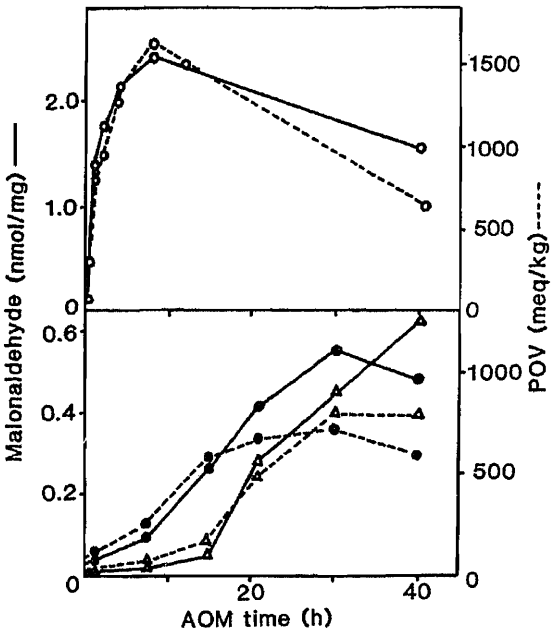

Fig. 2. Time Courses of the POV and the Malonaldehyde Contents Estimated by the Fluorometric Assay against the AOM Time of Methyl Linoleate (○), Soybean Oil (●) and Sesame Oil (△)

Oxidized methyl linoleate (0.4 mg), soybean oil (1.0 mg) and sesame oil (1.0 mg) were each dissolved in 2.0 ml of dimethyl sulfoxide and the solution was treated as described in Experimental. Fluorescence intensities of the reaction mixtures were estimated with excitation at 496 nm and emission at 564 nm. The malonaldehyde contents were determined from the calibration curves of standard TMP.

TABLE I. Comparison of the Malonaldehyde Contents in the Oxidized Oils Estimated by the Fluorometric Method and by the TBA Method

Sample (POV: meq/kg)		Malonaldehyde (nmol/mg oil)		Ratio (A/B)
		Fluorometric (A)[a]	TBA (B)[b]	
Methyl linoleate	(39)	0	0.35	0
	(1660)	2.5	5.8	0.43
Soybean oil	(31)	0.03	0.40	0.075
	(714)	0.56	1.15	0.49
Sesame oil	(9)	0	0	
	(800)	0.4	0.5	0.80

a) Malonaldehyde contents were estimated as described in the legend to Fig. 2. *b*) Malonaldehyde contents were estimated as described in Experimental.

or soybean oil in dimethyl sulfoxide. The fluorescence spectra and intensities were similar to those obtained in the absence of the oils, indicating that unoxidized lipid samples do not interfere with the formation of fluorescence.

Methyl linoleate, soybean oil and sesame oil were oxidized by the AOM.[13] Fluorescence

spectra of the reaction mixture of these oxidized oils with ethyl *p*-aminobenzoate in acetonitrile (Fig. 1B) or dimethyl sulfoxide (Fig. 1C) were identical to those of the reaction mixtures of TMP. The calibration curves of the fluorescence intensities in dimethyl sulfoxide were linear with respect to the amounts of the oxidized oils, methyl linoleate (POV: 1478 meq/kg), soybean oil (714 meq/kg) and sesame oil (800 meq/kg), up to 1.0 mg.

Time courses of the malonaldehyde contents in the AOM-oxidized methyl linoleate, soybean oil and sesame oil estimated by the above method employing ethyl *p*-aminobenzoate and dimethyl sulfoxide are shown in Fig. 2. The malonaldehyde contents in these oils increased and subsequently decreased with increasing oxidation time. The time course profiles were similar to those of peroxide values.

The malonaldehyde contents estimated by the above method were compared with those estimated by the TBA method with various oils and at different stages of oxidation (Table I). The values were always lower than those found by the TBA method. Since it has been shown that TBA reacts with not only malonaldehyde but also other secondary products of lipid oxidation,[9,10] this discrepancy may be reasonable. Determinations of malonaldehyde by the acid decomposition-acetylation-gas chromatographic (GC) method,[16] dansyl pyrazole-high performance liquid chromatographic (HPLC) method,[17] and direct HPLC method[18] have demonstrated that the malonaldehyde content oxidized lipid samples are lower than those obtained by use of the TBA method.

The fluorometric method originally reported by Sawicki *et al.*[11] may be useful for determination of malonaldehyde in oxidized fats and oils. This method may be more selective for malonaldehyde than the TBA method.

References

1) R. P. Bird and H. H. Draper, *Methods Enzymol.*, **105**, 299 (1984).
2) *a*) D. L. Crawford, R. O. Sinnhuber, F. M. Strout, J. E. Oldfield and J. Kaufmes, *Toxicol. Appl. Pharmacol.*, **7**, 826 (1965); *b*) K. D. Munkres, *Mech. Ageing Dev.*, **10**, 249 (1979).
3) R. J. Shamberger, T. L. Andreone and C. E. Willis, *J. Natl. Cancer Inst.*, **53**, 1771 (1974).
4) *a*) T. M. Yau, *Mech. Ageing Dev.*, **11**, 137 (1979); *b*) F. H. Mukai and B. D. Goldstein, *Science*, **191**, 868 (1976); *c*) R. J. Shamberger, C. L. Corlett, K. D. Beaman and B. L. Kasten, *Mutat. Res.*, **66**, 349 (1979); *d*) A. K. Basu and L. J. Marnett, *Carcinogenesis*, **4**, 331 (1983); *e*) *Idem*, *J. Cancer Res.*, **44**, 2848 (1984).
5) A. L. Tappel, "Free Radicals in Biology," ed. by W. A. Pryor, Vol. IV, Academic Press, New York, London, 1980, p. 1.
6) K. Kikugawa, *Advances in Free Radical Biology and Medicine*, **2**, 389 (1986).
7) See for instance, K. Kikugawa, K. Taguchi and T. Maruyama, *Chem. Pharm. Bull.*, **35**, 3364 (1987).
8) A. A. Barber and F. Bernheim, *Adv. Gerontol. Res.*, **2**, 355 (1967).
9) R. Marcuse and L. Johansson, *J. Am. Oil Chem. Soc.*, **50**, 387 (1973).
10) *a*) H. Kosugi and K. Kikugawa, *Lipids*, **21**, 537 (1986); *b*) H. Kosugi, T. Kato and K. Kikugawa, *Anal. Biochem.*, **165**, 456 (1987).
11) E. Sawicki, T. W. Stanley and H. Johnson, *Anal. Chem.*, **35**, 199 (1963).
12) K. Kikugawa and Y. Sugimura, *Chem. Pharm. Bull.*, **34**, 1794 (1986).
13) A. E. King, H. L. Roschen and W. H. Irwin, *Oil Soap*, **10**, 105 (1933).
14) D. H. Wheeler, *Oil Soap*, **9**, 89 (1932).
15) H. Kosugi and K. Kikugawa, *J. Food Sci.*, **50**, 1181 (1985).
16) E. N. Frankel and W. E. Neff, *Biochim. Biophys. Acta*, **754**, 264 (1983).
17) T. Hirayama, N. Yamada, M. Nohara and S. Fukui, *J. Sci. Food Agric.*, **35**, 338 (1984).
18) S. Csallany, M. D. Guan, J. D. Manwaring and P. B. Addis, *Anal. Biochem.*, **142**, 277 (1984).

[Chem. Pharm. Bull. 35(12)5024—5027(1987)]

Syntheses of 11-Substituted 3-Methyl-3,4,10,11-tetrahydro-1*H*,5*H*-pyrano[4,3-*b*][1,5]benzodiazepin-1-ones

KEIZO MATSUO,* IKUKO TANI, and KUNIYOSHI TANAKA

Faculty of Pharmaceutical Sciences, Kinki University, 3-4-1 Kowakae, Higashiosaka, Osaka 577, Japan

(Received July 22, 1987)

11-Substituted 3-methyl-3,4,10,11-tetrahydro-1*H*,5*H*-pyrano[4,3-*b*][1,5]benzodiazepin-1-ones were synthesized and tested for analgesic activity.

Keywords——pyranobenzodiazepinone; Mannich reaction; aminopyrine; analgesic activity; 3-hydroxy-5-methyl-2-penten-5-olide

In the course of our synthetic studies on biologically active compounds using dimedone, tetronic acids, and tetramic acids,[1] we reported that some 10-substituted 3,3-dimethyl-3,4,9,10-tetrahydro-1*H*-furo- and -pyrrolo[4,3-*b*][1,5]benzodiazepin-1-ones (**1** and **2**) showed analgesic activity as strong as that of aminopyrine in the phenylquinone writhing test in mice.[2] Namely, the extents of inhibition were 56.1% with **1a**, 61.0% with **1b**, and 68.3% with **2** at the dose of 50 mg/kg *p.o.*, while that of aminopyrine was 66.2%. The above observations prompted us to synthesize benzodiazepinone derivatives fused with other heterocyclic compounds in order to test their analgesic activity. We therefore synthesized 11-substituted 3-methyl-3,4,10,11-tetrahydro-1*H*,5*H*-pyrano[4,3-*b*][1,5]benzodiazepin-1-ones (**6**), which are isomers of **1**, and investigated the structure–activity relationships.

Synthesis of pyranobenzoidiazepinones (**6**) was performed by using a method similar to that employed previously for the preparation of furobenzodiazepinone derivatives (**1**).[3] Thus, the enaminolactones (**5a** and **5b**) were prepared by boiling a benzene solution of 3-hydroxy-5-methyl-2-penten-5-olide (**3**)[4] and an equimolar amount of 1,2-diaminobenzene (**4a**) or 1,2-diamino-4-chlorobenzene (**4b**) in 85.1 and 39.9% yields, respectively. When ethanol solutions

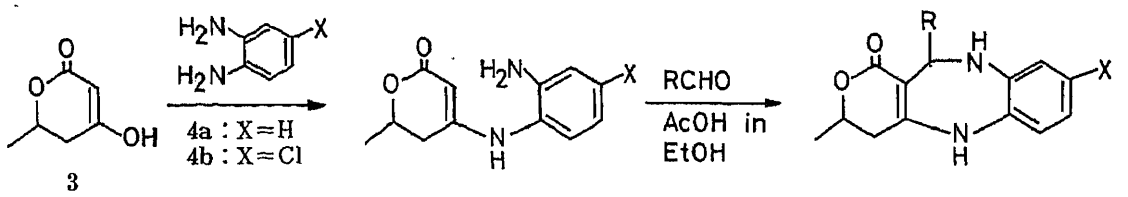

3

5a : X=H
5b : X=Cl

6a : X=H, R=C_6H_5
6b : X=H, R=2-ClC_6H_4
6c : X=H, R=4-$NO_2C_6H_4$
6d : X=H, R=3-$CH_3C_6H_4$
6e : X=H, R=2-pyridyl
6f : X=H, R=2-thienyl
6g : X=H, R=2-(5-nitro)furyl
6h : X=Cl, R=C_6H_5

1a : X=O, R=4-$NO_2C_6H_4$
1b : X=O, R=2-pyridyl
2 : X=NH, R=2-ClC_6H_4

Chart 1

TABLE I. Melting Points, Yields, and Elemental Analyses of **6**

6	R	X	mp (°C) (Recryst. solv.)	Yield (%)	Formula	Analysis (%) Calcd (Found)		
						C	H	N
a	C_6H_5	H	268—269 (MeOH)	92.4	$C_{19}H_{18}N_2O_2$	74.49 (74.68)	5.92 (5.89)	9.14 (9.18)
b	2-ClC_6H_4	H	259—260 (MeOH)	71.4	$C_{19}H_{17}ClN_2O_2$	66.96 (67.02)	5.03 (4.98)	8.22 (8.38)
c	4-$NO_2C_6H_4$	H	280—283 (MeOH)	70.7	$C_{19}H_{17}N_3O_4$	64.95 (64.95)	4.88 (4.88)	11.96 (11.94)
d	3-$CH_3C_6H_4$	H	265—268 (EtOH)	98.4	$C_{20}H_{20}N_2O_2$	74.98 (75.19)	6.29 (6.29)	8.74 (8.77)
e	2-Pyridyl	H	282—284 (MeOH)	91.8	$C_{18}H_{17}N_3O_2$	70.34 (70.46)	5.58 (5.61)	13.67 (13.64)
f	2-Thienyl	H	274—276 (MeOH)	95.7	$C_{17}H_{16}N_2O_2S$	65.36 (65.58)	5.16 (5.19)	8.97 (9.01)
g	2-(5-Nitro)furyl	H	300 (MeOH)	93.4	$C_{17}H_{15}N_3O_5$	59.82 (59.83)	4.43 (4.57)	12.31 (12.26)
h	C_6H_5	Cl	229.5—230.5 (EtOH)	49.2	$C_{19}H_{17}ClN_2O_2 \cdot C_2H_5OH$[a]	65.20 (65.50)	5.99 (6.02)	7.24 (7.53)

a) Exact Mass Calcd for $C_{19}H_{17}ClN_2O_2$: 340.0978. Found: 340.0982.

TABLE II. IR and ^{1}H-NMR Spectral Data of **6**

6	IR ν_{max}^{Nujol} cm^{-1}	^{1}H-NMR δ (J in Hz)[a,b]
a	3250, 1655, 1560, 1280, 1255, 1075, 1065, 1050, 960, 940, 865, 795	1.36 (3H, d, J=6, $CHCH_3$), 2.72 (2H, m, CH_2CH), 4.50 (1H, m, CH_3CH), 5.67 (1H, d, J=5, $CHNH$), 6.12 (1H, d, J=5, NH), 6.48—7.20 (9H, m, ArH), 8.83 (1H, brs, NH)
b	3380, 3290, 1640, 1610, 1550, 1280, 1255, 1210, 1055, 750	1.36 (3H, d, J=6, $CHCH_3$), 2.77 (2H, m, $CHCH_2$), 4.54 (1H, m, $CHCH_2$), 5.52 (1H, d, J=6, $CHNH$), 5.98 (1H, d, J=6, $CHNH$), 6.44—7.40 (8H, m, ArH), 9.03 (1H, NH)
c	3350, 3220, 1630, 1600, 1565, 1550, 1345, 1260, 1205, 1090, 1060, 825, 740	1.37 (3H, d, J=6, $CHCH_3$), 2.76 (2H, m, $CHCH_2$), 4.54 (1H, m, $CHCH_3$), 5.76 (1H, d, J=5, $CHNH$), 6.32 (1H, d, J=5, $CHNH$), 6.50—7.00 (4H, m, ArH), 7.42 (2H, d, J=8, ArH), 8.00 (2H, d, J=8, ArH), 9.00 (1H, s, NH)
d	3280, 1625, 1545, 1250, 1070, 1060, 950, 930, 795, 700	1.34 (3H, d, J=6, $CHCH_3$), 2.14 (3H, s, $ArCH_3$), 2.70 (2H, m, $CHCH_2$), 4.44 (1H, m, $CHCH_3$), 5.57 (1H, d, J=6, $CHNH$), 6.02 (1H, d, J=6, $CHNH$), 6.42—7.00 (8H, m, ArH), 8.73 (1H, brs, NH)
e	3320, 3250, 1640, 1555, 1270, 1070, 935, 755	1.35 (3H, d, J=6, $CHCH_3$), 2.68 (2H, m, $CHCH_2$), 4.50 (1H, m, $CHCH_3$), 5.39 (0.6H, d, J=6, $CHNH$), 5.66 (0.4H, d, J=6, $CHNH$), 5.97 (1H, brd, J=6, $CHNH$), 6.40—6.60 (3H, m, ArH), 6.76—7.06 (3H, m, ArH), 7.36—7.50 (1H, m, ArH), 8.30 (1H, m, ArH), 8.80 (1H, brs, NH)
f	3360, 3270, 1650, 1630, 1550, 1260, 1065, 750, 720	1.34 (3H, d, J=6, $CHCH_3$), 2.64 (2H, m, $CHCH_2$), 4.42 (1H, m, $CHCH_3$), 5.79 (1H, d, J=6, $CHNH$), 6.12 (1H, d, J=6, $CHNH$), 6.52—7.12 (7H, m, ArH), 8.79 (1H, brs, NH)
g	3330, 3220, 1635, 1610, 1545, 1275, 1090, 1055, 805, 790	1.34 (3H, d, J=6, $CHCH_3$), 2.68 (2H, m, $CHCH_2$), 4.51 (1H, m, $CHCH_3$), 5.41 (1H, d, J=6, $CHNH$), 6.15 (1H, d, J=4, ArH), 6.39 (1H, d, J=6, $CHNH$), 6.60—6.98 (4H, m, ArH), 7.32 (1H, d, J=4, ArH), 9.02 (1H, brs, NH)
h	3280, 1655, 1605, 1565, 1495, 1400, 1240, 1200, 1020, 950, 805, 700	1.34 (3H, d, J=6, $CHCH_3$), 2.67 (2H, m, $CHCH_2$), 4.46 (1H, m, $CHCH_3$), 5.61 (1H, d, J=6, $CHNH$), 6.36 (1H, d, J=6, $CHNH$), 6.48—7.16 (8H, m, ArH), 8.88 (1H, brs, NH)

a) Measured in DMSO-d_6. *b)* br, broad; d, doublet; m, multiplet; s, singlet.

of **5** and an equimolar amount of an aldehyde were stirred at room temperature in the presence of 2—3 drops of acetic acid overnight, the Mannich-type cyclization took place cleanly to give the corresponding 11-substituted 3-methyl-3,4,10,11-tetrahydro-1*H*,5*H*-pyrano[4,3-*b*][1,5]benzodiazepin-1-ones (**6a—h**). The generality of this reaction is illustrated by the good to excellent yields obtained in the reactions using aldehyde with a variety of electron-withdrawing and electron-releasing substituents on the phenyl group. Further, when the aldehydes had a heteroaromatic ring in place of the phenyl ring, the reaction also occurred in good yields.

The structures of **6** were assigned on the basis of elemental analyses, and infrared (IR) and nuclear magnetic resonance (NMR) spectral data. The IR spectra (Nujol) of **6** had absorptions at 3220—3380 cm^{-1} (NH stretching band) and at 1625—1655 cm^{-1} (lactone carbonyl). In the NMR spectra (in DMSO-d_6) of **6**, the C-11 methine proton signals were found to be coupled with the N-10 proton with the coupling constant of 6 Hz. Although it is possible for two isomers to exist regarding the configuration of the substituents at C-3 and C-11 of **6**, single isomers were isolated in all cases except **6e**, judging from the NMR spectra. In the case of **6e**, the methine proton signal appeared at δ 5.39 and 5.66 as a doublet in the integration ratio of 3:2. The stereochemistries of **6** were not determined.

For the analgesic activity test, the compounds **6c** and **6e** were selected, because they are isomers of **1a** and **1b**, which exhibited considerable activity, as mentioned above. The result of the test using the phenylquinone writhing method[5] showed that both **6c** and **6e** were much less active than the corresponding compounds **1a** and **1b** (the extents of inhibition of **6c** and **6e** were 18.2% and −1.1%, respectively, at the dose of 50 mg/kg *p.o.*).

These results indicated that the dimethyldihydrofuranone moiety is important for the appearance of the analgesic activity among these compounds in the series.[6]

Experimental

Melting points were determined on a Yanagimoto micro-melting point apparatus, model MP-S3, and are uncorrected. IR and ^{1}H-NMR spectra were measured with a Hitachi 260-30 infrared spectrometer and a JEOL JNM-FX 200 (200 MHz) spectrometer, respectively, using tetramethylsilane (TMS) as an internal standard. Mass spectra (MS) were measured with a JEOL JMS-HX 100 spectrometer.

3-(2-Aminoanilino)-5-methyl-2-penten-5-olide (5a)——A solution of 3-hydroxy-5-methyl-2-penten-5-olide (**3**)[4] (1 g, 7.8 mmol) and 1,2-diaminobenzene (**4a**) (0.844 g, 7.8 mmol) in benzene (25 ml) was stirred at reflux temperature, while water was removed as an azeotropic mixture. When no more water appeared, the precipitates that had formed were filtered off, washed with benzene, and recrystallized from ethanol to give 1.44 g (85.1%) of **5a** as colorless needles; mp 225—226 °C. IR ν_{max}^{Nujol} cm^{-1}: 3450, 3370, 3240, 1658, 1618, 1580, 1300, 1255, 1220, 1058, 1010, 820, 755. NMR (DMSO-d_6) δ: 1.30 (3H, d, J=6.5 Hz, CH_3CH), 2.50 (2H, m, $CHCH_2$), 4.30 (1H, s, =CH), 4.42 (1H, m, CH_3CHCH_2), 4.86 (2H, brs, NH_2), 6.57 (1H, dt, J=8, 2 Hz, ArH), 6.76 (1H, dd, J=8, 2 Hz, ArH), 6.90—7.04 (2H, m, ArH), 8.14 (1H, brs, NH). *Anal.* Calcd for $C_{12}H_{14}N_2O_2$: C, 66.04; H, 6.47; N, 12.84. Found: C, 65.90; H, 6.55; N, 12.63.

3-(2-Amino-4-chloroanilino)-5-methyl-2-penten-5-olide (5b)——A solution of **3** (2 g, 15.6 mmol), 1,2-diamino-4-chlorobenzene (**4b**) (2.97 g, 15.6 mmol) and a catalytic amount of *p*-toluenesulfonic acid monohydrate in benzene (50 ml) was stirred at reflux temperature as above. Recrystallization of the crude product from isopropanol afforded 1.574 g (39.9%) of **5b**; mp 199—202 °C. IR ν_{max}^{Nujol} cm^{-1}: 3470, 3340, 3160, 1620, 1580, 1300, 1245, 1205, 1005, 810. NMR (DMSO-d_6) δ: 1.31 (3H, d, J=6 Hz, $CHCH_3$), 2.46 (2H, m, $CHCH_2$), 4.26 (1H, s, CH=), 4.40 (1H, m, $CHCH_3$), 5.16 (2H, brs, NH_2), 6.50 (1H, dd, J=8, 2 Hz, ArH), 6.75 (1H, d, J=2 Hz, ArH), 6.89 (1H, d, J=8 Hz, ArH), 8.07 (1H, brs, NH). *Anal.* Calcd for $C_{12}H_{13}ClN_2O_2$: C, 57.04; H, 5.19; N, 11.09. Found: C, 57.10; H, 5.31; N, 11.06.

General Method for Syntheses of 11-Substituted 3-Methyl-3,4,10,11-tetrahydro-1*H*,5*H*-pyrano[4,3-*b*][1,5]benzodiazepin-1-ones (6a—g) and the 8-Chloro Derivative (6h)——An enaminolactone (**5**) (1.4 mmol) was dissolved in ethanol (15 ml). An equimolar amount of an aldehyde and 2—3 drops of acetic acid were added to the above solution, and the whole was stirred at room temperature overnight. Precipitates formed were filtered off and recrystallized from the appropriate solvent. Yields, melting points, microanalyses, and IR and NMR spectra data are listed in Tables I and II.

Acknowledgement The authors are grateful to Dr. Seiji Kuzuna, Medicinal Research Laboratories, Central Research Division, Takeda Chemical Industries Ltd., for analgesic activity testing.

References and Notes

1) *a*) K. Tanaka, K. Matsuo, Y. Nakaizumi, Y. Morioka, Y. Takashita, Y. Tachibana, Y. Sawamura, and S. Kohda, *Chem. Pharm. Bull.*, **27**, 1901 (1979); *b*) K. Matsuo, I. Kitaguchi, Y. Takata, and K. Tanaka, *ibid.*, **28**, 2494 (1980); *c*) K. Tanaka, K. Matsuo, A. Nakanishi, M. Jo, H. Shiota, M. Yamaguchi, S. Yoshino, and K. Kawaguchi, *ibid.*, **32**, 3291 (1984); *d*) K. Matsuo, M. Kimura, T. Kinuta, N. Takai, and K. Tanaka, *ibid.*, **32**, 4197 (1984); *e*) K. Matsuo and K. Tanaka, *Yakugaku Zasshi*, **104**, 1004 (1984); *f*) K. Matsuo, M. Ohta, and K. Tanaka, *Chem. Lett.*, **1985**, 291; *g*) K. Matsuo, M. Yoshida, M. Ohta, and K. Tanaka, *Chem. Pharm. Bull.*, **33**, 4057 (1985); *h*) K. Matsuo, M. Ohta, and K. Tanaka, *ibid.*, **33**, 4063 (1985).
2) K. Matsuo, S. Takada, J. Inoue, and K. Tanaka, *Yakugaku Zasshi*, **106**, 715 (1986).
3) K. Matsuo and K. Tanaka, *Chem. Pharm. Bull.*, **32**, 3724 (1984).
4) A. I. Scott, H. Guilford, and D. Skingle, *Tetrahedron*, **27**, 3039 (1971).
5) K. Tanaka, K. Matsuo, A. Nakanishi, T. Hatano, H. Izeki, Y. Ishida, and W. Mori, *Chem. Pharm. Bull.*, **31**, 2810 (1983).
6) The extent of inhibition of 10-(4-nitrophenyl)-3,4,9,10-tetrahydro-1*H*-furo[4,3-*b*][1,5]benzodiazepin-1-one in the same test was −3.5% at the dose of 50 mg/kg *p.o.*; K. Matsuo, T. Ohnishi, and K. Tanaka, unpublished result.

Communications to the Editor

[Chem. Pharm. Bull. 35(12)5028—5031(1987)]

STRUCTURE-ACTIVITY CONSIDERATION OF NOVEL ANTICANCER PLATINUM PYRIMIDINE "GREENS"

Takehiko Shimura,[a] Takenori Tomohiro,[a] Kiyoshi Maruno,[b] Yasuo Fujimoto[b] and Yohmei Okuno*,[a]

National Chemical Laboratory for Industry (NCLI),[a] Tsukuba 305, Japan and The Institute of Physical and Chemical Research,[b] Wako-shi 351, Japan

Platinum pyrimidine greens are very effective against L1210 cells, but the blues are inactive. A clear relationship between the activity and size of Pt-green molecules has been observed; smaller molecules with up to Pt-decanuclear complexes are much more active than larger ones. Formation of macrocells by the greens have been found for the first time with L1210 cells. The more active the green complex is, the denser is the population of the macrocells. These findings could be related to the membrane permeability.

KEYWORDS —— platinum uridine green; L1210 cell anticancer activity; macrocell formation; activity-molecular size relation; inactive platinum uridine blue

During the course of our extensive studies on antitumor platinum pyrimidine oligomer complexes,[1-5] we have discovered that the effect of platinum "green" species isolated by gel filtration as a minor product on the life span of mice bearing L1210 leukemia was exceedingly high.[1] In the earlier investigations,[6] the materials used for biological assays were not always sufficiently purified. Therefore, it is very probable that the activity of platinum blues reported so far has been caused by green species included in the samples. To test the assumption, efficient and selective synthesis of platinum greens was essential. This has been achieved very recently by the authors.[2,4] Since then we have been examining the structure-activity relationships using L1210 cells in tissue culture, and describe here the new results.

The platinum uridine greens investigated in this work have been prepared from aquated cis-diiododiammineplatinum(II)[7] and uridine treated with hydrogen peroxide as mentioned in a preceding paper.[4] Their molecular range from 8 to 28 as numbers of Pt in the molecule (platinum octamer to octacosamer). These are summarized in Table I, and the microanalytical data are given in the reference part.[8]

Biological activities were determined by examining the inhibition of growth of L1210 cells in tissue culture. The cells were cultured in the presence or absence of test samples (final concentration of 5 or 10 μg/ml) at 37 °C in

culture medium (GIBCO RPMI 1640) containing kanamycin and 10% of fetal bovine serum. The ratios of growth of the treated vs. control cells (initially employed 1 x 10^5 cells/ml, and grew to 1.4 x 10^6 cells/ml after 4 days) were determined. The bioassay results are also summarized in Table I.

Table I. Growth Inhibition of L1210 Cells in Tissue Culture by Platinum Uridine Greens

Sample[a]	Synthesis[b]	Molecular size Pt:Ud:NH_3[c]	Growth inhibition, % 5 μg/ml	10 μg/ml[d]	Ratio of macrocells[e]	Remarks[f]
1	A	10 : 6 : 20	78.0	92.8	-	-
2	"	11 : 6 : 22	59.2	93.7	-	-
3	"	11 : 9 : 20	-	77.1	0.43	84.1
4	B	10 : 8 : 19	-	84.8	1.34	91.3
5	"	9 : 4 : 16	-	99.3	3.0	99.8
6	A	11 : 8 : 21	-	91.6	2.05	97.3
7	B	8 : 5 : 15	-	99.2	3.25	99.8
8	A	13 : 13 : 20	32.4	68.3	-	-
9	B	14 : 14 : 23	12.3	51.9	-	-
10	"	13 : 12 : 23	20.9	69.2	-	-
11	"	16 : 16 : 28	-	35.5	-	-
12[g]	B	28 : 28 : 29	-	-1.9	0.0035	-1.5

a) Prepared in the same manner described in ref. 4. b) A: further details and microanalytical data are given in reference 8. B: synthesized in the previous work; see ref. 4. c) Calculated from elemental analysis results. d) Sample concentration used for the activity study. e) Ratios of macro- and normal-L1210 cells with a 10 μg/ml dose after 4 days at 37°C. See text. f) Growth inhibition at a 10 μg/ml dose determined excluding macrocells formed. See text. g) Pt-blue complex; prepared by air oxidation.

At a 10 μg/ml dose, platinum uridine greens were considerably active, but the corresponding blue material again clearly had no effect on the cell growth (actually, platinum blue sample had some promoting effect on the cell growth; 12 in Table I). These observations are thoroughly consistent with our earlier discoveries with *in vivo* experiments using CDF_1 mice.[1)]

It turned out that, among the green materials examined here, different preparations showed different activities; growth inhibition was distributed from 35.5 to 99.3% as shown in the Table. If we take molecular size into consideration, there seems to be a reasonable relation to the activity. Figure 1 shows the percentage of growth inhibition relative to molecule size (shown as numbers of platinum included). Clearly, smaller molecules are more active than larger ones. And molecules which contain up to 10 platinums (up to Pt-decanuclear complexes; see samples 1, 4-7) are the most effective against L1210 cells. To determine the best complex, related studies with lower molecules are currently in progress, which will be reported in detail later in a full paper. A wholly parallel tendency occurs with a smaller dose (5 μg/ml), though lesser efficiency resulted (Table I & Fig. 1).

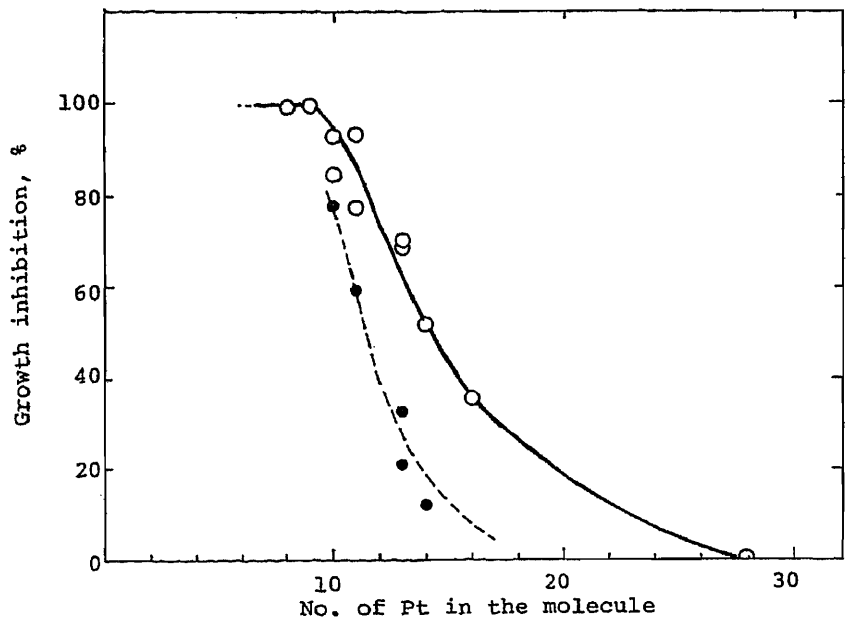

Fig. 1. A Relationship between Molecular Size and Activity against L1210 Cells in Tissue Culture
(○) with a 10 μg/ml dose. (●) with a 5 μg/ml dose.

There were considerable numbers of macrocells which were approximately twofold longer in diameter than the normal L1210 cells. The numbers of both cells were counted separately, and the ratios of macro- vs. normal-cells were calculated. The data are listed in Table I. Clearly the more active the material is, the denser is the population of the macrocells. For example, although almost no macrocells were detected in the presence of blue complex (sample 12), over three quarters of the surviving cells (even though only 0.7-0.8% of the cells survived compared with the control) were macrocells in the most efficient examples (see samples 5 and 7). In the last column of the Table I, growth inhibition determined excluding such macrocells are listed for reference.

Our present findings may be the first direct evidence of macrocell formation in animal cells with platinum greens. But two decades ago, formation of macrocells (up to 300 times larger than the normal bacteria) was reported in growth experiments with E. coli under electric fields using Pt-electrodes.[10]

Thus we have concluded that without doubt platinum uridine greens are active against L1210 cells, but that the corresponding blues are inactive. The activity differences recognized among the green complexes examined here are explainable by an evident relationship to the size of the molecules. Formation of macrocells has been perceived in the presence of Pt-greens for the first time with L1210 cells, which seems to be concerned with the mode of biological reactions. The above results may be related to the permeability of the membranes. This is one of the most important targets to be studied.

The authors are indebted to Dr. Tadashi Nakata for obtaining the microanalyses which were carried out at the Analytical Laboratory of The Institute of Physical and Chemical Research.

REFERENCES AND NOTES

1) Y.Okuno, K.Tonosaki, T.Inoue, O.Yonemitsu and T.Sasaki, Chem.Lett., 1986, 1947.
2) Y.Okuno, T.Inoue, O.Yonemitsu, T.Tomohiro and T.Laitalainen, Chem.Pharm. Bull., 35, 3074 (1987).
3) T.Tomohiro, T.Laitalainen, T.Shimura and Y.Okuno, Proceedings of the International Symposium on Activation of Dioxygen and Homogeneous Catalytic Oxidation, Elsevier, Amsterdam, in press.
4) T.Shimura, T.Tomohiro, T.Laitalainen, H.Moriyama, T.Uemura and Y.Okuno, submitted for publication.
5) T.Uemura, T.Tomohiro, K.Hayamizu and Y.Okuno, Chem.Phys.Lett., in press.
6) J.P.Davidson, P.J.Faber, R.G.Fisher,Jr., S.Mansy, H.J.Peresie, B.Rosenberg and L.VanCamp, Cancer Chemother. Rep. Part 1, 59, 287 (1975).
7) S. C. Dhara, Indian J. Chem., 8, 193 (1970).
8) Microanalysis results of platinum uridine greens synthesized in this work; For sample 1: Preparation condition and yield; [2°C, 3% H_2O_2, 0.1 M, 3 wk, 44.9%]; Anal. Calcd for $[Pt_{10}(C_9H_{11}N_2O_6)_6(NH_3)_{20}(OH)_2(H_2O)_6](SO_4)_8/8H_2O$: C,13.50; H,3.27; N,9.33; S,5.34; Pt[9],40.60; Found: C,13.42; H,3.18; N,9.15; S,5.25; Pt,40.48.
For 2: [2°C, 6% H_2O_2, 0.1 M, 3 wk, 17.4%]; Calcd for $[Pt_{11}(C_9H_{11}N_2O_6)_6(NH_3)_{22}(OH)_3(H_2O)_7](SO_4)_9/12H_2O$: C,12.38; H,3.33; N,9.09; S,5.51; Pt,40.97; Found: C,12.36; H,3.17; N,8.99; S,5.44; Pt,40.70.
For 3: [2°C, 1% H_2O_2, 0.1 M, 4 wk, 29.5%]; Calcd for $[Pt_{11}(C_9H_{11}N_2O_6)_9(NH_3)_{20}(OH)_3(H_2O)_3](SO_4)_7/8H_2O$: C,17.38; H,3.31; N,9.51; S,4.01; Pt,38.34; Found: C,17.21; H,3.19; N,9.50; S,3.94; Pt,38.47.
For 6: [40°C, 1% H_2O_2, 0.05 M, 48 hr, 50.1%]; Calcd for $[Pt_{11}(C_9H_{11}N_2O_6)_8(NH_3)_{21}(OH)_2(H_2O)_5](SO_4)_8/6H_2O$: C,15.87; H,3.24; N,9.51; S,4.71; Pt,39.38; Found: C,16.14; H,3.13; N,9.34; S,4.51; Pt,39.02.
For 8: [75°C, 1% H_2O_2, 0.1 M, 45 min, 19%]; Calcd for $[Pt_{13}(C_9H_{11}N_2O_6)_{13}(NH_3)_{20}(OH)_3(H_2O)_3](SO_4)_7/13H_2O$: C,19.93; H,3.40; N,9.14; S,3.18; Pt,35.97; Found: C,19.63; H,3.25; N,9.15; S,3.18; Pt,36.27.
9) Calculated from unburned ash.
10) B.Rosenberg, L.VanCamp and T.Krigas, Nature, 205, 689 (1965).

(Received October 16, 1987)

Communications to the Editor

[Chem. Pharm. Bull. 35(12)5032—5035(1987)]

SAMBACOLIGNOSIDE, A NEW LIGNAN-SECOIRIDOID GLUCOSIDE FROM *JASMINUM SAMBAC*

Takao Tanahashi,[a] Naotaka Nagakura,*[,a] Kenichiro Inoue,[b]
Hiroyuki Inouye,[b] and Tetsuro Shingu[c]
Kobe Women's College of Pharmacy,[a] Higashinada-ku, Kobe 658, Japan,
Faculty of Pharmaceutical Sciences, Kyoto University,[b] Sakyo-ku,
Kyoto 606, Japan, and Faculty of Pharmaceutical Sciences,
Kobe Gakuin University,[c] Nishi-ku, Kobe 673, Japan

The structure of a new secoiridoid glucoside, sambacolignoside (1), which had been isolated from *Jasminum sambac* (L.) Ait. together with seven new oligomeric iridoid glucosides and oleoside 11-methyl ester (2), was elucidated as 7-*O*-[(+)-1-hydroxypinoresinol-ß-D-glucoside-(7-6'")]-oleoside 11-methyl ester. This is the first example of a lignan linked secoiridoid glucoside.

KEYWORDS—*Jasminum sambac*; Oleaceae; sambacolignoside; lignan secoiridoid glucoside; oleoside 11-methyl ester; (+)-1-hydroxy-pinoresinol-1-ß-D-glucoside; COSY

Jasminum sambac (L.) Ait. (Japanese name, Matsurika) is an oleaceous shrub indigenous to Southeastern Asia, India and Arabia. Its flower is used to add fragrance to Jasmin tea. Recently, the secoiridoid glucosides, jasminin and sambacin were isolated from the leaves of this plant, together with several flavonoids.[1] As a part of our studies on the secoiridoids of the *Jasminum* plants,[2,3] we have performed a detailed survey of the MeOH extract of the fresh leaves of this plant and isolated a new lignan-secoiridoid glucoside, sambacolignoside (1), seven new oligomeric iridoid glucosides, and the known oleoside 11-methyl ester (2)[4,5] through a combination of several chromatographic methods. This paper defines the structure of the first glucoside, sambacolignoside (1).

Sambacolignoside (1) was obtained as a white powder, $C_{43}H_{54}O_{22}$ (positive ion FABMS m/z 923 $[M+H]^+$, negative ion FABMS m/z 921 $[M-H]^-$), $[\alpha]_D$ -97.1° (MeOH). It showed UV maxima (MeOH) at 233 and 280 nm (log ε 4.55 and 3.71) and IR bands (KBr) at 3435, 1730(sh), 1710, 1630, 1610(sh) and 1520 cm^{-1}.

As described below,[6] the ^1H-NMR spectrum of 1 indicated typical signals due to oleoside methyl ester, though the location of the carbomethoxy group was ambiguous. The spectrum further exhibited signals of a pair of 1,2,4-trisubstituted benzene protons and two aromatic methoxy groups. The bathochromic shift of the UV absorption maxima to 247 and 292 nm upon addition of NaOH revealed additionally the presence of aromatic hydroxy group(s). Moreover, irradiation of the methoxy singlets at δ 3.85 and 3.89 resulted in a 3.1% enhancement of the doublet (J=2.0 Hz) at δ 7.07 and a 4.2% increase of the doublet (J=2.0 Hz) at

δ 7.04, respectively. These findings demonstrated that the aromatic protons and methoxy substituents belong to two guaiacyl groups. This was further confirmed by ^{13}C-NMR spectral data (Table I).

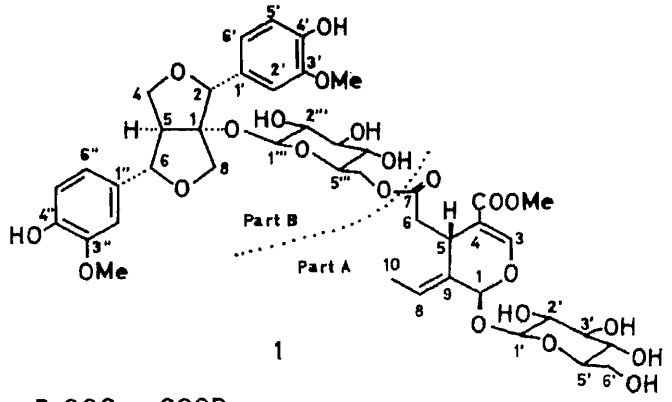

1

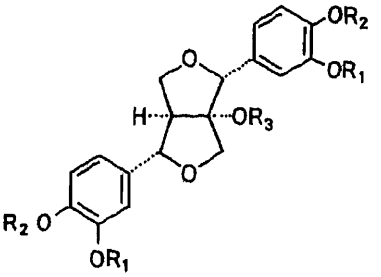

3: $R_1 + R_2 = CH_2$, R_3 =H

4: R_1=Me, R_2=R_3=H

5: R_1=Me, R_2=H, R_3=β-D-glucose

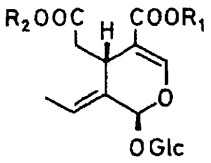

2: R_1=Me, R_2=H

6: R_1=R_2=Me

7: R_1=R_2=H

The ^{1}H-^{1}H COSY spectra (obtained in CD_3OD or CD_3OD-pyridine-d_5 (1:1) (Fig. 1)) and the ^{13}C-NMR spectrum of 1 indicated the presence of a 1-hydroxy-2,6-diguaiacyl-3,7-dioxabicyclo[3.3.0]octane ring skeleton and a glucose moiety in addition to the above described oleoside methyl ester moiety. The coupling constants of the signals due to protons on the dioxabicyclooctane ring were in good accordance with those of paulownin (3),[7] suggesting the same relative configuration of this ring in both 1 and 3. The lower field shift of the signal of C-1 in the lignan moiety of 1 in comparison with those of 3 and (+)-1-hydroxy-pinoresinol (4)[8] was accounted for by the glycosidation of the hydroxy group on this carbon. The β-linkage of glucose was deduced from the anomeric proton signal (δ 4.39, d, J=8.0 Hz).

All the above findings led us to the assumption that 1 is composed of oleoside methyl ester (part A) and (+)-1-hydroxypinoresinol-1-β-D-glucoside (5) (part B), the latter of which had recently been isolated from *Olea europaea* L. and *O. Africans* Mill. of the oleaceous family.[9] In fact, hydrolysis of 1 with 0.2 N NaOH afforded oleoside 11-methyl ester (2) and the above lignan glucoside (5). Formation of oleoside 11-methyl ester (2) from 1 indicated the linkage of the oleoside methyl ester moiety (part A) with the lignan glucoside moiety (part B) through the 7-carboxy group.

Finally, the attached position of oleoside 11-methyl ester (2) to the lignan glucoside (5) was determined by comparative studies of the ^{13}C-NMR signals of 1, 5, and oleoside dimethyl ester (6). The ^{13}C-NMR signals of 1 were in good accordance with the corresponding carbon signals of 5 and 6 except for shifts of signals due to C-5'" and C-6'" of the lignan glucoside moiety (part B) and the absence of the 7-methoxy carbon signal of the oleoside methyl ester moiety (part A). These differences can only be explained by the linkage of the 7-carboxy group of 2 to the 6'"-hydroxy group of 5. The downfield shift of ^{1}H-NMR signals due to 6'"-methylene protons of the part B also supported this conclusion. Thus, the

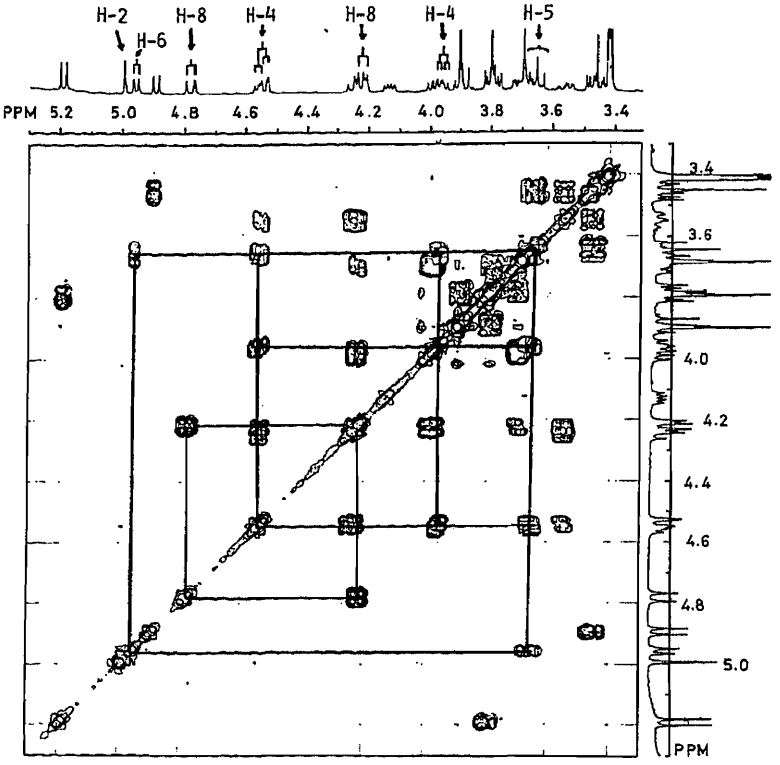

Fig. 1. ^{1}H-^{1}H COSY Spectrum of the 1-Hydroxy-2,6-diguaiacyl-3,7-dioxabicyclo[3.3.0]octane Ring of 1 in CD_3OD-pyridine-d_5(1:1)

Table I. ^{13}C-NMR Data for 1, 5 and 6 in CD_3OD

6		1		5	
Carbon	Part A	Part B			Carbon
1	95.2(d)	95.0(d)	99.2(s)	99.2(s)	1
3	155.1(d)	155.1(d)	89.4(d)	90.1(d)	2
4	109.4(s)	109.4(s)	72.1(t)	72.2(t)	4
5	31.8(d)	31.8(d)	60.4(d)	60.3(d)	5
6	41.0(t)	41.3(t)	87.6(d)	87.0(d)	6
7	173.5(s)	172.9(s)	73.8(t)	73.4(t)	8
8	124.8(d)	125.1(d)	128.8(s), 133.2(s)	128.2(s), 132.3(s)	1', 1"
9	130.6(s)	130.5(s)	113.8(d), 111.0(d)	114.2(d), 110.9(d)	2', 2"
10	13.6(q)	13.8(q)	148.5(s), 149.4(s)	148.7(s), 149.8(s)	3', 3"
11	168.6(s)	168.7(s)	147.4(s), 147.4(s)	148.2(s), 148.7(s)	4', 4"
OMe	51.9(q)	52.0(q)	115.4(d), 116.3(d)	115.5(d), 116.7(d)	5', 5"
	52.2(q)		122.1(d), 120.1(d)	122.5(d), 120.1(d)	6', 6"
			56.7(q), 56.7(q)	56.6(q), 56.6(q)	OMe
1'	100.9(d)	100.8(d)	100.1(d)	100.1(d)	1'"
2'	74.8(d)	74.8(d)*	74.9(d)*	74.9(d)	2'"
3'	78.4(d)	78.5(d)+	78.2(d)+	78.4(d)	3'"
4'	71.4(d)	71.6(d)	71.6(d)	71.3(d)	4'"
5'	77.9(d)	78.0(d)	75.2(d)	78.0(d)	5'"
6'	62.7(t)	62.8(t)	65.1(t)	62.6(t)	6'"

Values with the same superscript are interchangeable.

absolute structure of sambacolignoside was determined to be 7-O-[(+)-1-hydroxypinoresinol-1-ß-D-glucoside(7-6'")]-oleoside 11-methyl ester (1).

Oleoside (7) type secoiridoid glucosides are characteristic of oleaceaous plants, and several lignans and lignan glucosides have been isolated from plants of this family. Sambacolignoside (1) represents the first lignan linked secoiridoid glucoside.

ACKNOWLEDGEMENTS The authors are indebted to Prof. S. Nishibe, Higashi Nippon Gakuen University, for the gift of (+)-1-hydroxypinoresinol-1-ß-D-glucoside and to Mr. M. Morita, Kinki University, for MS measurements.

REFERENCES AND NOTES

1) S. A. Ross, S. M. El-Sayyad, A. A. Ali and N. E. El-Keltawy, Fitoterapia, 53, 91 (1982).
2) K. Inoue, T. Tanahashi, H. Inouye, F. Murai and M. Tagawa, Phytochemistry, 21, 359 (1982).
3) K. Inoue, T. Tanahashi and H. Inouye, Phytochemistry, 24, 1299 (1985).
4) In this experiment, neither jasminin nor sambacin has been isolated.
5) Though oleoside 11-methyl ester (2) or oleoside 7,11-dimethyl ester has erroneously been described as oleoside in some papers (e.g. R. T. LaLonde, C. Wong and A. I. Tsai, J. Am. Chem. Soc., 98, 3007 (1976); H. Tsukamoto, S. Hisada and S. Nishibe, Shoyakugaku Zasshi, 39, 90 (1985) or P. Gariboldi, G. Jommi and L. Verotta, Phytochemistry, 25, 865 (1986)); 7 represents the correct structure of the latter; cf. H. Inouye, T. Yoshida, S. Tobita, K. Tanaka and T. Nishioka, Tetrahedron, 30, 201 (1974).
6) ^{1}H-NMR (400 MHz, CD_3OD) of 1 δ : part A; 1.65(3H, dd, J=7.0 and 1.5 Hz, H_3-10), 2.38(1H, dd, J=14.5 and 9.0 Hz, H-6), 2.66(1H, dd, J=14.5 and 4.5 Hz, H-6), 3.66(1H, dd, J=12.0 and 6.0 Hz, H-6'), 3.67(3H, s, COOMe), 3.88(1H, dd, J=12.0 and 1.5 Hz, H-6'), 3.97(1H, dd, J=9.0 and 4.5 Hz, H-5), 4.82(1H, d, J=8.0 Hz, H-1'), 5.89(1H, br s(t-like), H-1), 6.07(1H, dq, J=0.8 and 7.0 Hz, H-8), 7.51(1H, s, H-3). Part B; 3.01(1H, t, J=8.0 Hz, H-2'"), 3.82(1H, dd, J=9.0 and 6.0 Hz, H-4), 3.85(3H, s, OMe), 3.89(3H, s, OMe), 3.96(1H, d, J=10.5 Hz, H-8), 4.04(1H, dd, J=12.0 and 6.5 Hz, H-6'"), 4.21(1H, dd, J=12.0 and 1.5 Hz, H-6'"), 4.36(1H, d, J=10.5 Hz, H-8), 4.39(1H, d, J=8.0 Hz, H-1'"), 4.48 (1H, dd, J=9.0 Hz and 8.0 Hz, H-4), 4.72(1H, s, H-2), 4.81(1H, d, J=5.5 Hz, H-6), 6.74(1H, d, J=8.0 Hz, H-5' or 5"), 6.80(1H, d, J=8.0 Hz, H-5" or 5'), 6.86(1H, dd, J=8.0 and 2.0 Hz, H-6' or 6"), 6.88(1H, dd, J=8.0 and 2.0 Hz, H-6" or 6'), 7.04(1H, d, J=2.0 Hz, H-2' or 2"), 7.07(1H, d, J=2.0 Hz, H-2" or 2').
7) A. S. R. Anjaneyulu, P. A. Ramaiah, L. R. Row, R. Venkateswarlu, A. Pelter and R. S. Ward, Tetrahedron, 37, 3641 (1981).
8) H. Tsukamoto, S. Hisada and S. Nishibe, Chem. Pharm. Bull., 32, 2730 (1984).
9) H. Tsukamoto, S. Hisada and S. Nishibe, Chem. Pharm. Bull., 33, 1232 (1985).

(Received October 21, 1987)

Communications to the Editor

[Chem. Pharm. Bull. 35(12)5036—5039(1987)]

STRUCTURES OF SARASINOSIDES A_1, B_1, AND C_1; NEW NORLANOSTANE-TRITERPENOID OLIGOGLYCOSIDES FROM THE PALAUAN MARINE SPONGE *ASTEROPUS SARASINOSUM*

Isao Kitagawa,*[,a] Motomasa Kobayashi,[a] Yoshihiro Okamoto,[a] Masayuki Yoshikawa,[a] and Yoshihiro Hamamoto[b]

Faculty of Pharmaceutical Sciences, Osaka University,[a] 1-6, Yamada-oka, Suita, Osaka 565, Japan and Suntory Institute for Biomedical Research,[b] Shimamoto-cho, Mishima-gun, Osaka 618, Japan

Nine new norlanostane-triterpenoid oligoglycosides (sarasinoside) were isolated from the Palauan marine sponge *Asteropus sarasinosum* and the structures of three major oligoglycosides named sarasinosides A_1 (7), B_1 (8), and C_1 (4) have been determined on the basis of chemical and physicochemical evidence including the x-ray analysis of the sapogenol.

KEYWORDS — sarasinoside A_1; sarasinoside B_1; sarasinoside C_1; norlanostane triterpenoid oligoglycoside; marine sponge; *Asteropus sarasinosum*; N-acetylglucosamine; N-acetylgalactosamine; X-ray analysis; ichthyotoxic activity; starfish fertilized egg development inhibition

In marine organisms, sea cucumber and starfish of echinoderm have been characterized to produce saponins.[1] Besides these echinoderms, only a limited number of marine organisms have been shown to contain glycosides. For example, pregnane- or cholestane-type steroidal monoglycosides or diglycosides from soft coral,[2] gorgonians,[3,4] or fish.[5] In search of biologically active marine natural products,[6] we have isolated nine new ichthyotoxic norlanostane-triterpenoid oligoglycosides named sarasinosides A_1, A_2, A_3, B_1, B_2, B_3, C_1, C_2, and C_3, from the Palauan marine sponge *Asteropus sarasinosum* and have elucidated their chemical structures.[7] This paper communicates the evidence consistent with the structures of sarasinosides A_1 (7), B_1 (8), and C_1 (4), which are specified as having one mole each of N-acetylglucosamine and N-acetylgalactosamine in their oligosaccharide moieties. This is the first isolation of triterpene oligoglycosides from marine organisms other than the sea cucumber.

The freeze-dried subject sponge (1.2 kg) was extracted with MeOH (r.t.). The extract was partitioned into a mixture of AcOEt and water and the water-soluble portion was then partitioned into a mixture of n-BuOH and water to afford the n-BuOH soluble portion (140 g). The n-BuOH soluble portion (20 g) thus obtained was subjected to silica gel column chromatography ($CHCl_3$-MeOH-H_2O) to furnish three saponin fractions: sarasinosides A (1.4 g), B (1.1 g), and C (0.3 g).[8] Each fraction was further separated by HPLC (ZORBAX-ODS, MeOH-H_2O) to afford major saponins: sarasinosides A_1 (7)(136 mg), A_2 (49 mg), and A_3 (80 mg) from A, sarasinosides B_1(8)(100 mg), B_2 (33 mg), and B_3 (67 mg) from B, and sarasinosides C_1 (4)(26 mg), C_2 (7 mg), and C_3 (20 mg) from C.

Sarasinoside A_1 (7), $C_{62}H_{100}O_{26}N_2 \cdot 2H_2O$,[9] mp 207-210°C, $[\alpha]_D^{25}$ -14° (MeOH), IR(KBr): 3370 (br), 1067 (br) cm^{-1}, showed a UV maximum at 237 nm (MeOH, ε=13500) ascribable to a conjugated enone moiety. Hydrolysis of 7 with 20% aq. H_2SO_4-MeOH

(1:1) yielded two isomeric sapogenols: 9, $C_{29}H_{46}O_2$, mp 124-127°C and 10, $C_{29}H_{46}O_2$, mp 153-155°C. Both possess a conjugated enone moiety in their side chains [9: IR (CCl_4) 1690, 1621 cm^{-1}, λ_{max} (MeOH) 236 nm (ε=12200), δ 6.06 (1H, s), 1.88, 2.14 (both 3H, s); 10: IR (CCl_4) 1688, 1618 cm^{-1}, λ_{max} (MeOH) 239 nm (ε=13300), δ 6.07 (1H, s), 1.89, 2.15 (both 3H, s)].

The ^1H NMR decoupling experiments (500 MHz) and the ^{13}C NMR analysis of 9 and 10, have led us to presume their norlanostane structures, which have been finally confirmed by the x-ray analysis of 10 with Δ^{14} (δ 5.13, m, 15-H), (Fig. 1).[10] ^{13}C NMR signals (d_5-pyr.) due to $\Delta^{8(14)}$ carbons of 9 were observed at δ_C 127.1 (s, C-8) and 141.8 (s, C-14),[11] whereas signals due to tetrasubstituted olefin carbons of sarasinoside A_1 (7) were observed at δ_C 127.5 (s) and 136.4 (s) assignable to C-8 and C-9.[11] Therefore, it has become evident that the aglycone of 7 has a Δ^8 moiety as depicted in 1, and acidic hydrolysis of 7 caused the double bond migration in the aglycone to furnish artifact sapogenols, 9 and 10, having a thermodynamically more favored double bond.[12]

The oligosaccharide moiety of sarasinoside A_1 (7) comprises 2 moles of glucose and 1 mole each of xylose, N-acetylglucosamine, and N-acetylgalactosamine,[13] which are connected by β-glycosidic linkages [δ 5.58 (d, J=8.6 Hz), 5.56 (d, J=8.5), 5.20 (d, J=7.6), 5.15 (d, J=8.6), 4.53 (d, J=8.2); δ_C 106.7, 105.5, 102.6, 102.2, 101.7, each d]. Enzymatic hydrolysis of sarasinoside A_1 (7) with crude hesperidinase provided A_1-pro-1 (2), $C_{42}H_{67}O_{11}N\cdot 2H_2O$, mp 171-174°C, $[\alpha]_D^{20}$ -20° (MeOH), and A_1-pro-2 (3), $C_{56}H_{90}O_{21}N_2\cdot 3H_2O$, mp 196-198°C, $[\alpha]_D^{20}$ -13° (MeOH). Methanolysis of fully methylated A_1-pro-1 (prepared with DMSO-NaH-CH_3I) liberated methyl 3,4-di-O-methylxylopyranoside,[14] thus the structure of A_1-pro-1 (2) has been elucidated. On the other hand, methanolysis of fully methylated A_1-pro-2 (3) liberated methyl 2,3,4,6-tetra-O-methylglucopyranoside and methyl 3-O-methylxylopyranoside.[14] Another enzymatic hydrolysis of sarasinoside A_1 (7) using β-glucosidase (Type II from almonds) gave A_1-pro-3 (5), $C_{54}H_{87}O_{21}N\cdot 2H_2O$, mp 189-192°C, $[\alpha]_D^{20}$ -25° (MeOH). Methylation followed by methanolysis of 5 liberated methyl 2,3,4,6-tetra-O-methylglucopyranoside, methyl 3,4,6-tri-O-methylglucopyranoside, and methyl 3,4-di-O-methylxylopyranoside.[14]

In the ^{13}C NMR spectra of A_1-pro-2 (3) and A_1-pro-3 (5), signals of C-6" in the N-acetylglucosamine moieties are observed at a lower field (δ_C 69.8 in 3, 69.6 in 5) than that in A_1-pro-1 (2) (δ_C 62.5) due to glycosidation shift.[16] Consequently, the structures 3 and 5 have been assigned as shown. In a similar manner, methylation analysis of sarasinoside A_1 (7) furnished methyl 2,3,4,6-tetra-O-methylglucopyranoside, methyl 3,4,6-tri-O-methylglucopyranoside, and methyl 3-O-methylxylopyranoside,[14] so that the structure of sarasinoside A_1 (7) has been determined.

Sarasinoside B_1 (8), $C_{61}H_{98}O_{25}N_2\cdot 2H_2O$, mp 197-199°C, $[\alpha]_D^{20}$ -16° (MeOH), showed the ^{13}C NMR spectrum which closely resembled the spectrum of sarasinoside A_1 (7) except for some signals due to the oligosaccharide moiety. Signals due to C-8 and C-9 were observed at δ_C 127.7 (s) and 136.4 (s), while acidic hydrolysis of 8 provided 9 and 10. Thus, the aglycone of 8 has been shown to be identical with that of 7. Sarasinoside B_1 (8) contains one mole each of glucose, N-acetylglucosamine, N-acetylgalactosamine, and two moles of xylose,[13] connected by β-glycosidic linkages [δ 5.56 (d, J=8.5 Hz), 5.43 (d, J=7.3), 5.21 (d, J=7.3),

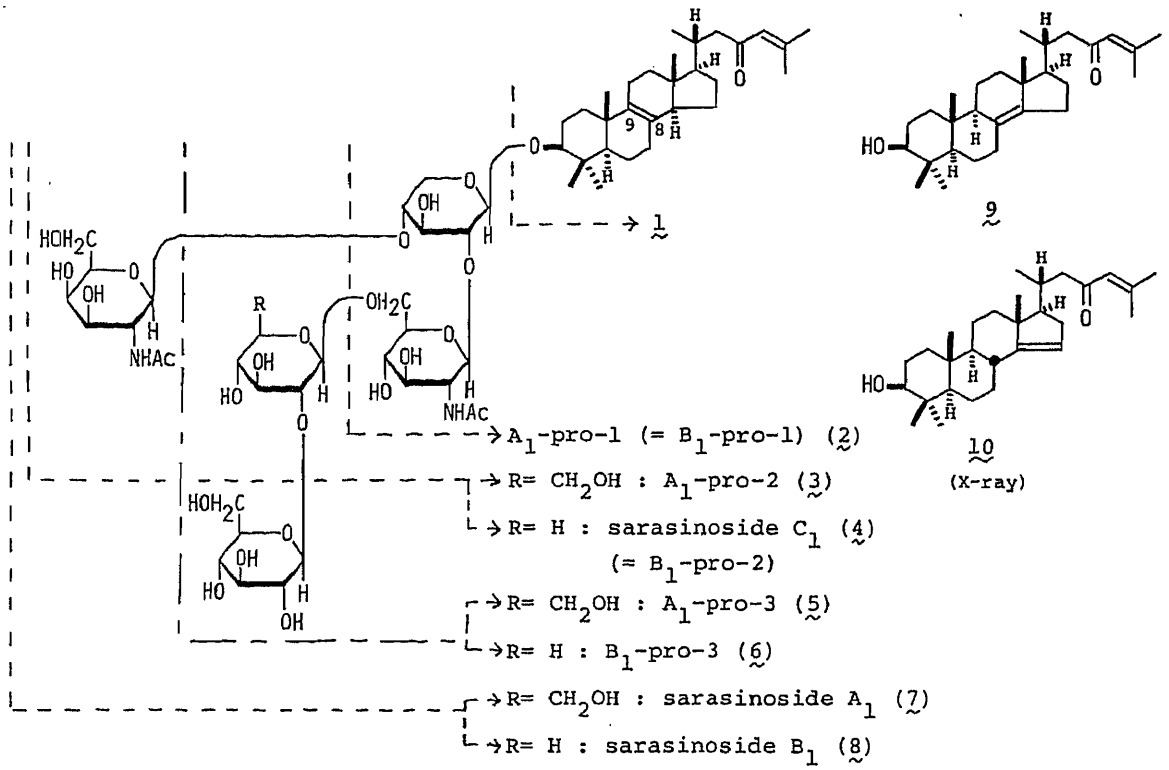

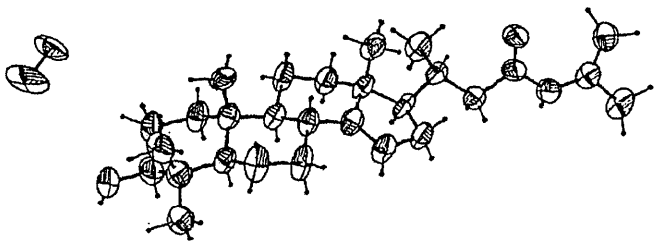

Fig. 1. Since the conformations of two crystallographycally independent molecules (A and B) are almost identical, the ORTEP drawing of the molecule B is shown here.

5.20 (d, J=8.2), 4.57 (d, J= 7.6); δ_C 106.7, 105.5, 103.2, 102.3, 102.0, each d]. Hydrolysis of sarasinoside B_1 (8) with crude hesperidinase furnished B_1-pro-1 (=A_1-pro-1) (2) and B_1-pro-2 (4), $C_{55}H_{88}O_{20}N_2 \cdot 2H_2O$, whereas hydrolysis using β-glucosidase afforded B_1-pro-3 (6), $C_{53}H_{85}O_{20}N \cdot 2H_2O$. Among these hydrolysates, B_1-pro-2 (4) was found to be identical with sarasinoside C_1 in all respects. Methylation analysis and ^{13}C NMR analysis of sarasinoside C_1 (4)(=B_1-pro-2), B_1-pro-3 (6), and sarasinoside B_1 (8), have finally shown that their structures are expressed as shown.

Among nine sarasinosides, the following biological activities have been found : ichthyotoxicity against killifish *Poecilia reticulata* [LD_{50} 0.39 μg/ml for 7, 0.71 μg/ml for 8, and inhibition against cell-division of fertilized eggs of the starfish *Asterina pectinifera*[17] [10 μg/ml for 7 and 8].

ACKNOWLEDGEMENT The authers are grateful to the Ministry of Education, Science, and Culture of Japan for the grant (No. 62470137). They are also indebted to Dr. N. Fusetani, the Univ. of Tokyo, and Mr. J. Tanaka, Ryukyu Univ., for biological tests.

REFERENCES AND NOTES

1) D.J.Burnell and J.W.ApSimon, "Marine Natural Products-Chemical and Biochemical Perspectives", Vol.V, P.J.Scheuer ed., Academic Press, New York, 1983, pp. 287-389.
2) M.Kobayashi, Y.Kiyota, S.Orito, Y.Kyogoku, and I.Kitagawa, Tetrahedron Lett., 25, 3731 (1984).
3) M.M.Bandurrage and W.Fenical, Tetrahedron, 41, 1057 (1985).
4) N.Fusetani, K.Yasukawa, S.Matsunaga, and K.Hashimoto, Tetrahedron Lett., 28, 1187 (1987).
5) K.Tachibana, M.Sakaitani, and K.Nakanishi, Tetrahedron, 41, 1027 (1985).
6) I.Kitagawa, N.K.Lee, M.Kobayashi, and H.Shibuya, Chem. Pharm. Bull., 35, 2129 (1987), and the preceding papers from our laboratory.
7) I.Kitagawa, M.Kobayashi, Y.Okamoto, M.Yoshikawa, and Y.Hamamoto, presented at the 29th Symposium on the Chemistry of Natural Products, Sapporo Aug., 1987. Symposium Paper pp. 568-575.
8) These three fractions respectively gave a single spot on ordinary thin-layer chromatogram.
9) The molecular compositions of compounds with the chemical formulae were determined by elemental analysis and/or high resolution mass spectrometry.
10) The crystals were recrystallized from AcOEt-MeOH: $C_{29}H_{46}O_2 \cdot CH_3OH$, colorless prisms, monoclinic, space group $P2_1$, a=33.941(4), b=7.421(2), c=11.161(2) Å, β=91.91(1)°, V=2809.7(8) Å^3, Z=4, Dc=1.08, μ=4.894 cm^{-1}. The x-ray diffraction intensity data from the crystal (0.4 x 0.2 x 0.4 mm) was obtained on a Rigaku AFC diffractometer equipped with a rotating anode x-ray generator (55 kV-200 mA), using graphite-monochromated Cu-Kα radiation (λ=1.5418 Å). A total of 4950 independent reflections with $2\theta \leq 126°$ were collected by the ω/2θ scanning mode. The structure was solved by the direct method MULTAN 78 (Main *et al.*, 1978). H atoms were determined by difference Fourier syntheses. The refinement was carried out by the block-diagonal least/squares method with anisotropic thermal parameters for non-H atoms and with isotropic thermal parameters for H atoms. The R factor was reduced to 0.075 using 4360 reflections with $|Fo| > 3\sigma(Fo)$. The determination of the structure was carried out on a microcomputer NEC PC-9801 VM2 using the automatic analysis program, developed by Katsube *et al.* The other computations were performed on PANAFACOM U-1200 II of Rigaku RASA-5RP system.
11) a) M.Tsuda, E.J.Parish, and G.J.Schroepfer Jr., J. Org. Chem., 44, 1282, 1290 (1979); b) E.Kho, D.K.Imagawa, M.Rohmer, Y.Kashman, and C.Djerassi, J. Org. Chem., 46, 1836 (1981).
12) L.F.Fieser and M.Fieser, "Steroids", Reinhold Pub. Corp., New York, 1959, p. 354.
13) Among methyl glycosides obtained by methanolysis, methyl 2-acetamido-2-deoxy-α-glucopyranoside [$[\alpha]_D^{20}$ +119° (H_2O)] and methyl 2-acetamido-2-deoxy-α-galactopyranoside [$[\alpha]_D^{20}$ +186° (H_2O)] were identified with authentic samples synthesized from N-acetyl-D-glucosamine and N-acetyl-D-galactosamine. Methyl glucoside and methyl xyloside liberated D-glucose and D-xylose by 5% aq. HCl hydrolysis.
14) The methylation affected N-methylation of N-acetylglucosamine and N-acetylgalactosamine moieties, so that methanolysis of fully methylated 2 and 3 facilitated cleavage of the N-acetamide linkage, and GLC analysis of methylated N-acetylglucosamine and N-acetylgalactosamine was without success. In order to identify the N-acetyl sugar moieties, fully methylated oligoglycosides were subjected to Hakomori's degradation method[15] and the resulting 3,4,6-tri-O-methyl-1,5-di-O-acetyl-2-deoxy-2-N-methylacetamidogalactitol and 3,4-di-O-methyl-1,5,6-tri-O-acetyl-2-deoxy-2-N-methylacetamidoglucitol were identified with synthesized authentic samples.
15) K.Stellner, H.Saito, and S.Hakomori, Arch. Biochem. Biophys., 155, 464 (1973).
16) a) R.Kasai, M.Suzuo, J.Asakawa, and O.Tanaka, Tetrahedron Lett., 1977, 175; b) K.Tori, S.Seo, Y.Yoshimura, and H.Arita, ibid., 1977, 179.
17) N.Fusetani, Y.Kato, K.Hashimoto, T.Komori, Y.Itakura, and T.Kawasaki, J. Nat. Prod., 47, 997 (1984).

ADDED IN PROOF (Nov. 22, 1987) After submission of this manuscript, one of the authors (I.K.) was informed by F. J. Schmitz, Oklahoma Univ. U.S.A. that his group has reached the same conclusion on the structure of their marine-sponge saponin named asteropin as the structure of sarasinoside A_1 (7) and their work will be submitted to J. Org. Chem.

(Received November 2, 1987)